NANOTECH FRANCE 2015

International Nanotechnology Conference
15 – 17 June 2015

Pôle Universitaire Léonard de Vinci, La Défense
Paris – France

Organizer

SETCOR Conferences & Events

www.sector.org

In Collaboration with

NanoSciences ILE-DE-FRANCE www.CnanoIDF.org

nanomedicine EUROPEAN TECHNOLOGY PLATFORM www.etp-nanomedicine.eu

NanoSaclay

SFNano Société Française de Nanomédecine French Society for Nanomedicine

IOP Publishing

cnrs

cea

Nanotech France 2015 Conference Program

Day 1 : June 15, 2015		
07:30 - 10:00	Registration + Welcome Coffee	Registration / Main Hall
10:00 - 12:30	Plenary Talks Session **Chairs:** Prof Corinne Chanéac, France and Prof. Dafiné Ravelosona - France	Amphitheatre H
12:30 - 14:00	Lunch Break + Exhibition + Poster Session I	Restaurant / Main Hall
14:00 - 16:00	Session I: Nanomaterials Fabrication/ Synthesis **Chairs:** Prof. Taeghwan Hyeon - Rep. of Korea and Prof Corinne Chanéac - France	Room 511
	Session II - A: Nanomaterials Characterization and Tools **Chairs:** Prof Christophe Petit - France and Dr Nicolas Tsapis- France	Room 508
	Session II - B: Nanomaterials properties **Chairs :** Dr Denis Morineau - France and Prof. Katsuyoshi Kondoh- Japan	Room 561
	Session II - C: Nanomaterials synthesis and properties **Chairs:** Dr Dafiné Ravelosona – France and Prof James Johnston- New Zealand	Room 412/413
16:00 - 16:30	Coffee Break + Exhibition + Poster Session I	Main Hall
16:30 - 18:45	Session I: Nanomaterials Fabrication / Synthesis **Chairs:** Prof Corinne Chaneac – France	Room 511
	Session II - A: Nanomaterials Characterization and Tools **Chairs:** Prof Christophe Petit - France and Dr Nicolas Tsapis- France	Room 508
	Session II - B: Nanomaterials Properties **Chairs** : Dr Denis Morineau - France and Prof. Katsuyoshi Kondoh - Japan	Room 561
	Session II - C: Nanomaterials Synthesis and Properties **Chairs:** Dr Dafiné Ravelosona – France and Prof James Johnston - New Zealand	Room 412/413

Day 2 : June 16, 2015		
08:30 - 10:30	Plenary Talks session **Chairs:** Prof. Nathalie Mignet – France, Prof Steve Rannard – United Kingdom and Prof Patrick Boisseau-France	Amphitheatre H
10:30 - 11:00	Coffee Break + Exhibition + Poster Session II	Main Hall
11:00 - 12:30	Session III: Nano Electronics **Chairs :** Dr Dafiné Ravelosona - France and Prof Jean-Luc Duvail - France	Room 412/413
	Session IV - A: Nanotech in Life Sciences & Medicine **Chairs:** Prof Nathalie Mignet – France, Prof Steve Rannard - United Kingdom and Prof Allan S. Hoffman USA	Room 511
	Session IV - B: Nanotech in Life Sciences & Medicine **Chairs:** Prof Frederic Chaubet, France and Dr Maria-Antonietta Buccheri - Italy	Room 508
	Session IV - C: Nanotech in Life Sciences & Medicine **Chairs :** Prof Patrick Boisseau - France and Prof Magnus Nyden - Australia	Room 561
	Nano MatEn 2015: Nanotech for Energy & Environment **Chairs:** Prof Roger Newman – Canada, Dr Sofoklis Makridis – Greece and Prof James Hill- Australia	Room 115/116
12:30 - 14:00	Lunch break + Exhibition + Poster session II	Restaurant / Main Hall
14:00 - 16:00	Session III: Nano Electronics **Chairs :** Prof Christos Christides – Greece, Prof Dao-Hua Zhang-Singapore and Prof James Johnston- New Zealand	Room 412/413
	Session IV - A: Nanotech in Life Sciences & Medicine **Chairs:** Prof Laurence Rozes – France, Prof Nathalie Mignet – France and Dr Alexandra Wittmar - Germany	Room 511
	Session IV - B: Nanotech in Life Sciences & Medicine **Chairs:** Prof Frederic Chaubet - France, Dr Maria-Antonietta Buccheri - Italy and Prof Vladimir Torchilin - USA	Room 508
	Session IV - C: Nanotech in Life Sciences & Medicine **Chairs :** Prof Patrick Boisseau - France and Prof Magnus Nyden - Australia	Room 561
	Workshop: Towards Horizon 2020 Call Priorities & Funding for Micro / Nano-Enabling Technologies	Room 115/116
16:00 - 16:30	Coffee break + Exhibition + Poster session II	Main Hall
16:30 - 18:45	Session III: Nano Electronics **Chairs :** Prof Christos Christides – Greece, Prof Dao-Hua Zhang-Singapore and Prof James Johnston- New Zealand	Room 412/413
	Session IV - A: Nanotech in Life Sciences and Medicine **Chairs:** Prof Laurence Rozes- France, Prof Nathalie Mignet- France and Dr Alexandra Wittmar - Germany	Room 511
	Session IV - B: Nanotech in Life Sciences and Medicine **Chairs:** Prof Frederic Chaubet - France, Dr Maria-Antonietta Buccheri- Italy and Prof Vladimir Torchilin, USA	Room 508
	Session IV - C: Nanotech in Life Sciences and Medicine	Room 561

	Chairs : Prof Steve Rannard - United Kingdom and Prof Magnus Nyden - Australia	
	Workshop: Towards Horizon 2020 Call Priorities & Funding for Micro / Nano-Enabling Technologies	Room 115/116

Day 3 : June 17, 2015		
08:30 - 10:30	Session IV - D: Nanotech in Life Sciences and Medicine / Nanosafety **Chairs:** Prof Karen Martinez- Denmark / Prof Hyunjoon Kong -USA	Room 511
	Nano MatEn 2015 : Nanotech for Energy and Environment **Chairs:** Prof Rajan Jose – Malaysia, Dr Sofoklis Makridis – Greece and Prof Guosheng Shao – United Kingdom	Room 412/413
	Session V: Other Nanoapplications **Chairs:** Prof Thierry Bastogne – France, Prof. Nathalie Mignet - France and Prof Raman Singh - Australia	Room 508
10:30 - 11:00	Coffee Break + Exhibition	Main Hall
10:30 - 13:00	Brokerage session / B to B Meetings	Main Hall
11:00 - 12:30	Session IV - D: Nanotech in Life Sciences and Medicine / Nanosafety **Chairs:** Prof Karen Martinez - Denmark and Prof Hyunjoon Kong - USA	Room 511
	Nano MatEn 2015 : Nanotech for Energy and Environment **Chairs:** Prof Rajan Jose – Malaysia, Dr Sofoklis Makridis – Greece and Prof Guosheng Shao - United Kingdom	Room 412/413
	Session V: Other Nanoapplications **Chairs:** Prof Thierry Bastogne - France, Prof. Nathalie Mignet - France and Prof Raman Singh - Australia	Room 508
11:30 - 14:00	Networking Cocktail + Closing Ceremony	Main Hall

15 June 2015
Advanced Nanomaterials: Synthesis / Fabrication, Characterization and Tools

Amphitheatre H

Session Chairs: Prof. Corinne Chanéac - France and Prof. Dafiné Ravelosona

07:30-10:00	**Registration + Welcome Coffee**	
10:00-10:40	New frontiers in the science of nanostructured materials for information technology **A. Fert**	**Prof. Albert Fert** (2007 Nobel Prize Physics), CNRS/Thales (UMR137) - **France**
10:40-11:20	State-of-the-Art in Metal Matrix Composites Reinforced with Carbon Nanotubes by Powder Metallurgy Process **K. Kondoh**	**Prof. Katsuyoshi Kondoh,** Osaka University **- Japan**
11:20-12:00	Designed Chemical Synthesis and Assembly of Uniform-sized Nanoparticles for Medical and Energy Applications **T.Hyeon**	**Prof. Taeghwan Hyeon**, Seoul National University - **Republic of Korea**
12:00-12:30	Nanomaterials for Biomedical and Green Chemistry Applications **J.Y. Ying**	**Prof. Jackie Y. Ying,** Institute of Bioengineering & Nanotechnology - **Singapore**
12:30-14:00	**Lunch Break + Exhibition + Posters session I**	

15 June 2015
Session I: Nanomaterials Fabrication / Synthesis

Room 511

Session Chairs : Prof. Taeghwan Hyeon - Rep. of Korea and Prof Corinne Chaneac - France

14:00-14:15	Hyperbranched-Polydendrons: A New Materials Platform for Advanced Polymer Technologies F L. Hatton, H. Rogers, A. Dwyer, L. M. Tatham, L. R. Tidbury, P. Chambon, A.Owen and **S. P. Rannard**	**Prof Steve Rannard**, University of Liverpool - **United Kingdom**
14:15-14:30	New geometric model for carbon nanocones incorporating curvature B.J. Cox and **J.M. Hill**	**Prof James M. Hill**, University of Adelaide - **Australia**
14:30-14:45	New Synthesis of Cobalt Nanoparticles with Tunable Size in Ionic Liquids **B. Morcos**, P.H. Haumesser and C.C. Santini	**Dr Bishoy Morcos**, CEA, LETI, Minatec Campus, Grenoble - **France.**
14:45-15:00	Intense visible emission from ZnO nanoparticles synthesized via co-precipitation and hydrolysis methods **Y. Zhu**, A. Apostoluk, B. Masenelli, P. Gautier, A. Valette and S. Danielle	**Ms Yao Zhu**, Institut national des sciences appliquées de Lyon – **France**
15:00-15:15	Influence of Processing Parameters on the Structure of Porous Metal Oxide-Cellulose Nanocomposites Prepared by Non-Solvent Induced Phase Separation **A. Wittmar** and M.Ulbricht	**Dr Alexandra Wittmar**, University Duisburg-Essen - **Germany**
15:15-15:30	Ultra-fast and controlled synthesis of Au-Iron Oxide hybrid nanocomposites using microfluidics **A.Larrea**, V.Sebastian, M. Arruebo and J.Santamaria	**Ms Ane Larrea**, University of Zaragoza – **Spain**
15:30-15:45	Atmospheric Pressure Plasma for Nanomaterials : Production of Tailored Metal, Oxide and Polymer coated nanoparticles by Discharge Filaments in Dielectric Barrier Discharges **J-P. Borra**, N. Jidenko, J. Hou and A. Weber	**Dr Jean-Pascal Borra**, CNRS-Paris-Sud University - **France**
15:45-16:00	Nanolithography using thermal scanning probes **S.M. Weber**	**Dr Stefan Weber**, SwissLitho AG - **Switzerland**
16:00-16:30	**Coffee Break + Exhibition + Poster session I**	

Session Chair: Prof Corinne Chaneac – France

16:30-16:45	A novel method for the preparation of poly(aminoacid) capped ultrasmall gold nanoclusters **I. Guryanov**, F. Polo, S. Antonello, F. Maran, E. V. Ubyivovk, E. Vlakh and T. Tennikova	**Dr Ivan Guryanov**, St.-Petersburg State University - **Russia**
16:45-17:00	First-principles calculations of two BN plus two C stripes BxCyNz selected nanotubes E. Ribas, M. J. Piotrowski, A. C. M Carvalho and **M. Machado**	**Dr Marcelo Machado**, Universidade Federal de Pelotas – **Brazil**
17:00-17:15	Control of inter (bi)metallic nanoparticular distances **F. Kameche**, A. Six, A.-T. Ngo, D. Kreher, F. Mathevet, A-J Attias, C. Salzemann, F. Charra and C. Petit	**Mr Farid Kameche**, 1 Sorbonne Universités, UPMC Univ Paris 06/ UMR 8233 - **France**
17:15-17:30	One pot microwave assisted synthesis of bisphosphonate alkene capped gold nanoparticles **R. Aufaure**, Y. Lalatonne, N. Lièvre, O. Heintz, L. Motte and E. Guénin	**Mr Romain Aufaure**, University Paris 13 - **France**
17:30-17:45	Electrodeposition of Gold Dendrites in the Presence of Aminosilane on FTO glass and Their Applications **N.Y .Hau** and S. P. Feng	**Ms Nga Yu Hau**, University of Hong Kong - **Hong Kong**

17:45-18:00	Novel Nano Rods of N-nicotinyl,N′,N″-bis(hexamethylenyl) Phosphorictriamide **N. Oroujzadeh**	**Dr Nasrin Oroujzadeh**, Iranian Research Organization for Science and Technology (IROST) - **Iran**
18:00-18:15	Cross-linked PAN-based thin-film composite membranes for non-aqueous nanofiltration **L. Pérez-Manríquez**, J. Aburabi'e, P. Neelakanda and K-V. Peinemann	**Ms Liliana Pérez-Manríquez**, King Abdullah University of Science and Technology (KAUST) -Thuwal - **Kingkom of Saudi Arabia**
18:15-18:30	Materials aspects of AlSi foams and AlSi + SiC composite foams joining **J. Nowacki**	**Prof Jerzy Nowacki**, West Pomeranian University of Technology- **Poland**
18:30-18:45	Nanofunctionalization of alginate and alginate/GelMA crosslinked hydrogels by nanoliposomes and 3D construct **R. Kadri**, B. Aliakbarian, L. Sanchez-Gonzalez, A. Tamayol, A.H. Najafabadi, A. Khademhosseini and E. Arab-Tehrany	**Ms Rana Kadri**, Lorraine University- **France**

15 June 2015 **Session II - A: Nanomaterials Characterization and Tools**		
Room 508		
Session Chairs: Prof Christophe Petit - France and Dr Nicolas Tsapis- France		
14:00-14:15	Simultaneous Topography and Electrochemical Imaging (SECM) **G. Kada**, S. Wu and C. Kranz	**Dr Gerald Kada**, Keysight Technologies GmbH - **Austria**
14:15-14:30	Copper nanoparticles: organization and stability **K. Ouadahi** and A. Courty	**Mrs Karima Ouadahi**, Pierre et Marie Curie University - **France**
14:30-14:45	Improved spectral imaging ellipsometry for nanoscale solid-liquid interface investigations **P. De Beule**	**Dr Pieter De Beule**, International Iberian Nanotechnology Laboratory, Braga - **Portugal**
14:45-15:00	Quantitative ellipsometric measurements of single micro-objects **D. Lyutov**, S. Hadjiiski, G. Tsutsumanova, S. Russev	**Mr Dimitar Lyutov**, University of Sofia – **Bulgaria**
15:00-15:15	blueDrive™ photothermal excitation for fast, reliable and quantitative AFM **A. Labuda**, J. P. Cleveland, N. Geisse, S. Hohlbauch, M. Kocun, R. Proksch, I. Revenko, M. Viani, D.A. Walters.	**Mr Julien Lopez**, Asylum Research, an Oxford Instruments Company, California - **USA**
15:15-15:30	On-chip characterization and sorting of engineered nanomaterial surface properties by real-time affinity monitoring **C. Desmet**, A. Valsesia, S. Muldur, V. Spampinato, G. Ceccone, P. Colpo and F. Rossi	**Dr Cloe Desmet**, European Commission Joint Research Centre, Institute for Health and Consumer Protection, Ispra - **Italy**
15:30-15:45	HPLC Optimization for Clotrimazole Assay in Microemulsion and Microemulsion-Based Gel **P. Boonme**, J. Kaewbanjong,T. Amnuaikit and E.B. Souto	**Dr Prapaporn Boonme**, Prince of Songkla University, Songkhla – **Thailand**
15:45-16:00	Structural characterization of DPPC nanosized liposomes by optical and cryoelectron microscopy: interactions with bovine serum albumin R. **Rachana**, J. Bellare and R. Banerjee	**Dr Rachana R**, JayPee Institute of Information Technology - **India**
16:00-16:30	**Coffee Break + Exhibition+ Poster Session I**	
Session Chairs: Prof Christophe Petit - France and Dr Nicolas Tsapis- France		
16:30-16:45	Nanometer scale characterizations of InGaN nanorods grown on GaN template **Y. El Gmili**, S. Sundaram, R. Puybaret, X. Li, P. L. Bonanno, C. Pradalier, P. L. Voss, J.P. Salvestrini and A. Ougazzaden	**Dr Youssef El Gmili**, UMI GeorgiaTech, CNRS2958 - **France**
16:45-17:00	Picodiagnostics of Nanomaterials Local Atomic Structure: X-Ray Absorption Spectroscopy and Computer Modeling Synergy **A. Soldatov**, A. Kravtsova, K. Lomachenko, M. Soldatov, A. Bugaev and O. Polozhentsev	**Prof Alexander Soldatov**, Southern Federal University of Russia - **Russian Federation**
17:00-17:15	Optical and Structural Characterizations of Phase Transition in Nanoscale Peroskite CH3NH3PbI3 **H. Wu**, W. Kong and Z. Ye	**Prof Huizhen Wu**, Zhejiang University - **China**
17:15-17:30	An Investigation of Sb2Te and Ge2Sb2Te5 Phase Change Memory Film Properties Deposited by Pulsed Laser Deposi-tion **S. E. Khansari** and M. Hoffman	**Mrs Sayedeh Emami Khansari**, University of New South Wales, Sydney - **Australia**
17:30-17:45	Advanced Transmission Electron Microscopy of Epitaxial-Enabled Morphology Controling ITO NWs **O.I. Lebedev**, S. Turner, Y. Shen and T. Wu	**Dr Oleg Lebedev**, CRISMAT Laboratory/UMR 6508/ CNRS ENSICAEN - **France**
17:45-18:00	Dynamic Characteristics of Carbon Nanotube Based Nano-composites with Atomic Vacancy and Stone-Wales Defects S.O. Gajbhiye and **S. P. Singh**	**Prof Satinder Paul Singh**, Indian Institute of Technology Delhi - **India**
18:00-18:15	Multi-scale characterization of chitosan-nanoemulsion blended film **R.R.A. Soares**, E.A. Tehrany, K. Delion, M. Guillemin, N.E. Amrani and W. Xu	**Mrs Raquel Soares**, ENSAIA, University of Lorraine - **France**

15 June 2015 Session II - B: Nanomaterials properties		
Room 561		
Session Chairs: Dr. Denis Morineau - France and Prof. Katsuyoshi Kondoh - Japan		
14:00-14:15	Identification of Ductility Function in Titanium Nitride Nanocoating Deposited on Polycarbonate-urethane of Ventricular Assist Device **A. Milenin**, M. Kopernik and S. Kąc	**Prof Andrij Milenin**, AGH University of Science and Technology - **Poland**
14:15-14:30	Diffusion of Proteins Through and Across Polyelectrolyte Multilayers **S.Pahal**, M.Varma and A.M.Raichur	**Mrs Suman Pahal**, Indian Institue of Science - **India**
14:30-14:45	Synthesis and Characterisation of Conjugated Polymer Nanoparticles for Fluorescence Imaging Applications **G. Redmond**	**Prof Gareth Redmond**, University College Dublin - **Ireland**
14:45-15:00	The Role of DC and PRC Current Densities on the Sliding Wear of Electrodeposited Nickel-Cobalt /CNT Composite Coatings R. Karslioglu and **H. Akbulut**	**Prof Hatem Akbulut**, Sakarya University - **Turkey**
15:00-15:15	Widely and Rapidly Switchable Wettability Through Short-Range Ordered-Disordered Transition and Redox Reaction **Y-H. Chang** and S-P. Feng	**Mrs Ya-Huei Chang**, University of Hong Kong - **Hong Kong**
15:15-15:30	Critical overview of polymer self-assemblies formation and characterization M. Dionzou, **C. Roux**, U. Till, B. Lonetti, J.-D. Marty, A.-F. Mingotaud, C. Mingotaud, P. Joseph, D. Goudounèche, B. Payré and M. Léonetti	**Dr Clément Roux**, Toulouse Unversity - **France**
15:45-16:00	Prediction of photothermal phase signatures from arbitrary plasmonic nanoparticles and experimental verification **O. Blum** and N.T. Shaked	**Mr Omry Blum**, Tel Aviv University - **Israel**
16:00-16:30	**Coffee Break + Exhibition + Poster Session I**	
Session Chairs: Dr. Denis Morineau - France and Prof. Katsuyoshi Kondoh - Japan		
16:30-16:45	In-Situ Thermally-reduced Graphene Oxide/Epoxy Composites: Thermal and Mechanical Properties **G. B. Olowojoba**, A. C. Taylor and A. J. Kinloch	**Dr Ganiu Olowojoba**, Imperial College London - **United Kingdom**
16:45-17:00	Tribological Behaviors of Yttria-Stabilized Zirconia (YSZ) Nanoparticles as Lubricant Additives **A. Sert** and D. Yılmaz Çakta	**Mr Abdullah Sert**, Eskisehir Osmangazi University - **Turkey**
17:00-17:15	Calcium phosphate super-balls synthesized in presence of gelatin and chitosan **J. Koetz** and I. Kovach	**Prof Joachim Koetz**, Potsdam University - **Germany**
17:15-17:30	NanoBuilding Blocks based-Hybrid organic-inorganic copolymers with Self-Healing Properties **L. Rozes**, F. Potier, A. Guinault, S. Delalande, C. Sanchez and F. Ribot	**Prof Laurence Rozes,** Sorbonne University, UPMC Univ Paris 06 /Collège de France/CNRS UMR 7574 - **France**.
17:30-17:45	Hybrid gold nanoparticles modified by oligopeptides for lead (II) ions interaction monitoring **J. Politi**, J. Spadavecchia, M. Iodice and L. de Stefano	**Dr Jane Politi**, Institute for Microelectronics & Microsystems, Naples, NRC - **Italy**
17:45-18:00	Characterization of Ferromagnetic Metal–Carbon Nanocomposites Prepared by Solid-Phase Pyrolysis of Metal-Phthalocyanines **A. Manukyan**, A. Mirzakhanyan, H. Gyulasaryan, R. Khachaturyan, E. Sharoyan	**Dr Aram Manukyan**, Institute for Physical Research/ NAS of Armenia - **Armenia**
18:00-18:15	Ambient scalable synthesis of surfactant-free thermoelectric metal chalcogenide nanostructures **C. Han**, Z. Li, W.L. Li, L.J. Zhang and S. X. Dou	**Mr Chao Han**, University of Wollongong - **Australia**
18:15-18:30	Effect of Temperature During Composite Materials Synthesis for the use as Gas Separators in Alkaline Water Electrolysers on their Ionic Conductivity and Oxygen Barrier Properties **J. Stojadinović**, G. Kasiribidhendi and F. La Mantia	**Dr Jelena Stojadinovic**, University of Bochum-Bochum - **Germany**
18:30-18:45	Effect of polystyrene nanocomposite prepared via Pickering emulsion polymerization on the mechanical properties of PP and EVA A.B. Moustafa, M.E. Abd El-Aziz, A.M Rabie and **H.A. Essawy**	**Prof Hisham Essawy**, National Research Center, Cairo - **Egypt**.

15 June 2015 Session II - C: Nanomaterials Synthesis and Properties		
Room 412/413		
Session chairs : Dr. Dafiné Ravelosona - France and Prof. James Johnston - New Zealand		
14:00-14:15	Kinetic Study of Functionalization of Carbon Nanomaterials **T.P. Dyachkova**, E.N. Tugolukov, I.V. Anosova and A.G. Tkachev	**Ms Tatyana Dyachkova**, Tambov State Technical University - **Russian Federation**
14:15-14:30	Single and Biphasic TiO2 nanotubes by Electrochemical Anodization **R.Savitha**, K. Nolan, A. Morrissey, R.Ravi Krishna, P.Selvam, R. Chetty	**Mrs Savitha Rangasamy**, Indian Institute of Technology, Madras - **India**.
14:30-14:45	3D Printed Hydrophobic and Antimicrobial Nanofunctionalised Surfaces **M. J. Cook**, L. Gilbertson, J. H. Johnston and T. Miller	**Ms Michelle Cook**, Victoria University of Wellington - **New Zealand**
14:45-15:00	Molecular dynamics simulation of glass formation and crystallization in binary PdNi and CuNi alloys. **M. Faruq**, A. Villesuzanne and G. Shao	**Mr Muhammad Faruq**, University of Bolton - **United Kingdom**
15:00-15:15	Graphene mediated synthesis of gold nanoparticles and its nanocomposite and their Applications P. C. Pandey and **Y. Pandey**	**Mr Yashashwa Pandey**, ,Indian Institute of Technology (BHU) - **India**
15:15-15:30	Preparation, morphological and AC electrical characterization of porous PEG/Polyaniline/Gold Nanowires composite. **M. Celentano**, R. Vecchione and P. A. Netti	**Dr Maurizio Celentano**, Napoli University - **Italy**
15:45-16:00	Low Pressure Chemical Vapor Deposition of Nickel Oxide Nanospheres as Anode for Lithium-ion Battery **L. Meda**, C. Arnold. A, J. He and A. Dangerfield	**Dr Lamartine Meda**, Xavier University of Louisiana - **USA**
16:00-16:30	**Coffee Break + Exhibition+ Poster Session I**	
Session chairs : Dr. Dafiné Ravelosona - France and Prof. James Johnston - New Zealand		
16:30-16:45	Morphology, Properties and Electrocatalytic Behaviour of Nanoporous Metals prepared by Electrolytic Dealloying of AgAuPt Alloys A. Vega and **R.C. Newman**	**Prof Roger Newman**, University of Toronto - **Canada**
16:45-17:00	Modulation of Active Sites in Supported Au38(SC2H4Ph)24 Cluster Catalysts: Effect of Atmosphere and Support Material **B.Zhang**, S.Kaziz, H.Li, M.G.Hevia, D.Wodka, C.Mazet, T.Bürgi and N.Barrabés	**Ms Bei Zhang**, University of Geneva - **Switzerland**
17:00-17:15	Tuning colloidal stability, MRI relaxivity and bioelimination of functional nanoparticles **A. Walter**, A. Garofalo, J. Taleb, P. Bonazza, C. Billotey, S. Laurent, L. Vander Elst, R. N. Muller, D. Felder-Flesch and S Begin-Colin	**Dr Aurelie Walter**, Ecole polytechnique fédérale de Lausanne **- Switzerland**
17:15-17:30	Parametric study on Fiber Bragg Grating for improvement of AE sensitivity **I. Kandas**, N. Shehata, E. Samir and H.A. Khater	**Dr Ishac Kandas**, Alexandria University - **Egypt.**
17:30-17:45	The Power of Heterogeneity: A Systems Approach to Complex Data in Materials Science **M. Nyden**, N, Williamson, M. Röding and T. Nann	**Prof Magnus Nyden**, University of South Australia, Adelaide - **Australia**
17:45-18:00	A facile route to synthesize rutile TiO2 nanorods arrays via hydrothermal method **M. Guo**, Y. Gao, Q. Deng, X. Xia and G. Shao	**Ms Meilan Guo**, University of Bolton - **United Kingdom**
18:00-18:15	The Effect of pH on Expanding Titanate Nanotubes & Their Use as a High Capacity Lithium-Ion Battery Electrode with High Rate Capability **A. Yürüm**, M. Yarali, E. Bicer and S. Alkan Gürsel	**Dr Alp Yurum**, Sabanci University, Istanbul - **Turkey**
18:15-18:30	Preparation of Graphene Encapsulated Silicon Nanoball by CVD using Metal Coating **H. Kim**, S. Park, I. Kang and H. Huh	**Mr Huijin Kim**, Korea Institute of Industrial Technology, Inha University - **Rep. of Korea**

16 June 2015		
Amphitheatre H		
Session Chairs: Prof. Nathalie Mignet - France, Prof. Steve Rannard – United Kingdom and Prof Patrick Boisseau - France		
8:30-9:10	The Early History of Nanocarriers as Drug Delivery Systems **A. S. Hoffman**	**Prof Allan S. Hoffman,** Bioengineering Department, University of Washington - **USA**
9:10-9:50	Nanomedicine for molecular imaging: interest of bimodality in preclinical studies **N. Mignet**	**Dr Nathalie Mignet**, CNRS - UMR8258/ Faculty of Pharmacy Paris- **France**
9:50-10:30	Nanotechnologies for the treatment of severe diseases **P. Couvreur**	**Prof. Patrick Couvreur,** University of Paris-Sud, Institut Galien, **France**
10:30-11:00	**Coffee Break + Exhibition + Poster session II**	

16 June 2015 Session III: Nano Electronics		
Room 412/413		
Session Chairs: Dr. Dafiné Ravelosona - France and Prof Jean-Luc Duvail - France		
11:00-11:15	Towards a force-displacement sensor based on vertical ZnO piezoelectric nanowires **E. León Pérez**, M. Mouis and E. Pauliac-Vaujour	**Mr Edgar Leon Perez**, CEA, LETI - **France**
11:15-11:30	Transport properties of nanoscale TFET by atomic scale simulations **U. Martinez Pozzoni**, T. Markussen, A. Blom and K. Stokbro	**Dr Umberto Martinez**, QuantumWise A/S - Copenhagen – **Denmark**
11:30-11:45	InAsSb based room temperature Infrared Photodetectors J. Tong, P. Ni and **D-H. Zhang**	**Prof Dao-Hua Zhang**, Nanyang Technological University – **Singapore**
11:45-12:00	Selective preconcentration within a nanoslit: one route for monitoring the biomolecule focusing front line. **F-D. Delapierre**, A-C. Louër, A. Pallandre and A-M Haghiri-Gosnet	**Dr François-Damien Delapierre**, LPN, CNRS, Marcoussis - **France**
12:00-12:15	Controlled Insulator to Metal transition in SiO2 –TiO2 nanocomposite containing silver nanoparticles **T. Das Gupta**, J. Corde, S. Perruchas, J-P. Boilot, A. Charles Rowe and T. Gacoin	**Mr Tapajyoti Das Gupta**, CNRS - Polytechnic School – Palaiseau – **France**
12:15-12:30	Surface-Dominated Transport and Enhanced Thermoelectric Figure of Merit in Topological Insulator Bi1.5Sb0.5Te1.7Se1.3 **T-C.Hsiung** and Y-Y. Chen	**Mr Te-Chih Hsiung,** National Taiwan University - **Taiwan**
12:30-12:45	Side-jump scattering in nanogranular Bi thin films **C. Christides** and P. Athanasopoulos	**Prof Christos Christides**, University of Patras - **Greece**
12:45-13:00	Light emission coupling from Carbon nanotubes in silicon photonic structures **C. Alonso-Ramos**, A. Noury, E. Durán-Valdeiglesias, W. Zhang, F. Sarti, Federico La China, H.C. Hoang, X. Le Roux, H. Yang, E. Cassan, N. Izard, A. Filoramo, V. Bezugly, M. Gurioli, L. Vivien	**Dr. Carlos Alonso- Ramos**, Univ Paris 11, **France**
12:30-14:00	**Lunch Break + Exhibition + Poster session II**	
Session III: Nano Electronics		
Room 412/413		
Session Chairs: Prof Christos Christides – Greece, Prof Dao-Hua Zhang-Singapore and Prof James Johnston- New Zealand		
14:00-14:15	Single-Molecule Switches Trigerred by Light,Chemical and Electrochemical Stimuli **N. Darwish**, A.C. Aragonès, T. Darwish, S. Ciampi and I. Díez-Pérez	**Dr Nadim Darwish**, University of Barcelona – **Spain**
14:15-14:30	Performance study of Phase Change Memory in Different Crossbar Architectures **N.H. El-Hassan**, T. N. Kumar and H. A.F.Almurib	**Ms Nemat H. El-Hassan**, University of Nottingham - **Malaysia.**
14:30-14:45	Synthesis of IV-VI Transition Metal Carbide and Nitride Nanoparticles using a Reactive Mesoporous Template for Electrochemical Hydrogen Evolution **N.S. H. Alhajri**, D.H. Anjum, M. N. Hedhili and K. Takanabe	**Ms Nawal Alhajri**, KAUST - **Kingkom of Saudi Arabia.**
14:45-15:00	Zinc doped InP colloidal quantum dots **N. Mordvinova**, A. Vinokurov, T Kuznetsova, S. Dorofeev and O. Lebedev	**Mrs Natalia Mordvinova**, Lomonosov Moscow State University – **Russia**
15:00-15:15	Micellar and Colloidal Dispersions of Conjugated Polymer Nanoparticles for Photoinduced Electron Transfer Applications **S. Wang** and G. Redmond	**Ms Suxiao Wang** University College Dublin - **Ireland**

15:15-15:30	Coupling between plasmonic response of supported gold particles and changes on TiO2 band gap **S. R. Islas**, R. Zanella and J. M. Saniger	**Ms Selene Islas,** Universidad Nacional Autónoma de México - **Mexico**
15:30-15:45	On Low Temperature Photoluminescence of Zinc-blende CdS and Au-CdS Nanocrystals **S. V. Kahane**, V. Sudarsan and S. Mahamuni	**Ms Shital Kahane**, SP Pune University - **India**
15:45-16:00	Nanoplasmonics in Inorganic Nanoparticles **T. Teranishi**	**Prof Toshiharu Teranishi**, Kyoto University - **Japan**
16:00-16:30	**Coffee Break + Exhibition + Posters session II**	
Session Chairs: Prof Christos Christides – Greece, Prof Dao-Hua Zhang-Singapore and Prof James Johnston- New Zealand		
16:30-16:45	MoS2 Transistors with Electrografted Organic Ultrathin Film as Efficient Gate Dielectric **H. Casademont**, L. Fillaud, X. Lefevre, R. Cornut, B. Jousselme and V. Derycke	**Mr Hugo Casademont**, CEA Saclay, IRAMIS / NIMBE (UMR 3685) / LICSEN - **France**
16:45-17:00	Nanoscale Magnetic Materials and Magnetic Nanodots for Spintronic Applications **S. Ghosh**	**Prof Santanu Ghosh**, Indian Institute of Technology Delhi- **India**
17:00-17:15	Polymer-Based Nanowires and Nanotubes: nanosources, wave-guiding **J.L. Duvail**, A. Garreau, J. Bigeon, N. Huby, B. Bêche, F. Massuyeau, A. Désert, S. Cordier, Y. Molard and E. Faulques	**Prof Jean-Luc Duvail,** University of Nantes - **France**
17:15-17:30	3D Simulation of DG-FinFET transistor with different channel materials and gate dielectrics **N. Boukortt**, B. Hadri, L. Torrisi, S. Patanè, A. Caddemi, and G. Crupi	**Mr Nour El Islam Boukortt**, University of Messina - **Italy**
17:30-17:45	Key Variable Components for Enhancing Charge Transfer at PbS Quantum Dots/Porphyrin Interfaces: From Quantum Confinement to Electrostatic Interaction **A. O. El-Ballouli**, E. Alarousu, O. M. Bakr and O. F. Mohammed	**Mrs Ala'a El-Ballouli**, King Abdullah University of Science and Technology (KAUST), Thuwal, **Kingdom of Saudi Arabia**
17:45-18:00	Room Temperature Synthesis and Characterization of Stable, Highly Luminescent PbS/CdS Core-Shell Quantum Dots with Emission Below 1100 nm **E. Durmusoglu**, P. Dagtepe, Y. Turker and H. Yagci Acar	**Mr Emek Goksu Durmusoglu**, Koc University, Istanbul - **Turkey**
18:00-18:15	PANI deposited carbon cloth as binder-free electrode for symmetric supercapacitor application M.V. Astakhov, R.R. Galimzyanov, A.A. Klimont, I.S. Krechetov, S.V. Stakhanova, O. V. Uryupina and **M. Kundu**	**Dr Manab Kundu**, National University of Science and Technology - **Russia Federation**
18:15-18:30	High performance photoconductive device for UV region fabricated using graphene- n-GaN nanowire hybrid structure on Si substrate S. Kang, **A. Mandal**, J.H. Chu, J-H. Park, S-Y. Kwon and C-R. Lee	**Dr Arjun Mandal**, Chonbuk National University - **Rep. of Korea**
18:30-18:45	Transparent and flexible electrodes based on metallic nanowire networks: New nanomaterials and operating stability. **A. Cabos**, C. Celle, A. Carella and J-P. Simonato	**Mr Anthony Cabos**, CEA-LITEN / DTNM / SEN / LSIN, Grenoble - **France**

16 June 2015 Session IV - A: Nanotech in Life Sciences and Medicine		
Room 511		
Session Chairs: Prof. Nathalie Mignet – France, Prof. Steve Rannard – United Kingdom and Prof. Allan S. Hoffman USA		
11:00-11:15	Emergence of Ag2S Quantum Dots and Their Magnetic Hybrid Structures as New Promising Bionanomaterials **H. Yagci Acar**, I. Hocaoglu, D. Asik, C. Grandfils, I. Ojea-Jimenez and F. Rossi	**Prof Havva Funda Yagci Acar**, Koc University, Istanbul - **Turkey**
11:15-11:30	Stimuli-sensitive combination nanopreparations of siRNA and chemotherapeutic drugs to treat multidrug resistant cancer **V. Torchilin**	**Prof Vladimir Torchilin,** Northeastern University, Boston - **USA**
11:30-11:45	Nanocapsules of perfluorooctyl bromide as theranostic agents: formulation and in vivo evaluation T. Boissenot, B. Larrat, A. Bordat, P. Calleja-Gonzalez, G. Giacalone, L. Mousnier, E. Fattal and **N. Tsapis**	**Dr Nicolas Tsapis**, Univ Paris-Sud, Institut Galien Paris-Sud, UMR CNRS 8612, LabEX LERMIT, Pharmacy Faculty - **France**
11:45-12:00	Formulation and evaluation of Rosuvastatin Calcium-loaded solid lipid nanoparticles **P. Shah**	**Dr Pranav Shah**, Uka Tarsadia University - **India**
12:00-12:15	A blueprint for modified siRNA-cationic peptide dendrimer based therapy of Type 2 diabetes through 'PTPN1' gene silencing **G. Kokil**	**Mr Ganesh Kokil**, The University of Queensland - **Australia**
12:15-12:30	Instability of Carbon Nanoparticles Interacting with Lipid Bilayers **D. Baowan**	**Dr Duangkamon Baowan**, Mahidol University, Bangkok - **Thailand**
12:30-14:00	**Lunch Break + Exhibition + Poster session II**	

16 June 2015 Session IV- A: Nanotech in Life Sciences and Medicine		
Room 511		
Session Chairs: Prof Laurence Rozes – France, Prof Nathalie Mignet – France and Dr Alexandra Wittmar - Germany		
14:00-14:15	Targeting of asymmetric amino acid-based cationic dendrimers to caveolae **P. Rewatkar**, H. S. Parekh and M. Parat	**Ms Prarthana Rewatkar**, Univ. of Queensland - **Australia**
14:15-14:30	Polymeric self-assemblies for photodynamic therapy: a critical approach U. Till, L. Gibot, B. Moukarzel, **A.F. Mingotaud**, M.P. Rols, M. Gaucher, F. Violleau, C. Chassenieux and P. Vicendo	**Dr Anne-Françoise Mingotaud**, IMRCP, Univ. Paul Sabatier, Toulouse - **France**
14:30-14:45	Biodegradable Nanoconstructs for Pharmacology: Development of Biomimetic Systems for Drug Delivery and Pathogen Blockage **T. Tennikova**, V. Korzhikov, I. Guryanov, V. Sharoyko and E. Vlakh	**Prof Tatiana Tennikova**, Saint-Petersburg State University, **Russian Federation**
14:45-15:00	Evaluation of Gelled Oil Nanoparticles as New Vehicles for Drug Delivery **B. Martin**, F. Brouillet, S. Franceschi-Messant and E. Perez	**Mr Baptiste Martin**, Toulouse University III- **France**
15:00-15:15	Bio-inspired catanionic vesicles as drug delivery systems: Study of the cell internalisation pathways P. Castagnos, C. Mauroy, J. Teissié, I. Rico-Lattes, A. C. Tedesco, M. P. Rols and **M. Blanzat**	**Dr Muriel Blanzat**, Paul Sabatier University, Toulouse - **France**
15:15-15:30	Novel Nano-Carriers for Controlled Pulmonary Drug Delivery **I. M. El-Sherbiny** and H. D. C. Smyth	**Prof Ibrahim El-Sherbiny**, Zewail City of Science and Technology - **Egypt**
15:30-15:45	Effect of Nanotube Materials on Encapsulation of Lysozyme **N. Thamwattana**	**Prof Ngamta Thamwattana**, University of Wollongong - **Australia**
15:45-16:00	Structure-directing star-shaped block copolymers: Supra-molecular vesicles for the delivery of anticancer drugs **C. Yang**, S. Qiong Liu, S. Venkataraman, S.J.Gao, X.T. Chia, J.L. Hedrick and Y.Y.Yang	**Dr Chuan Yang**, Institute of Bioengineering and Nanotechnology - **Singapore**
16:00-16:30	**Coffee Break + Exhibition + Posters session II**	
Session Chairs: Prof Laurence Rozes – France, Prof Nathalie Mignet – France and Dr Alexandra Wittmar - Germany		
16:30-16:45	Tunable release of dendritic fullerene-1 modulated by an electric field across a nanochannel membrane **G. Bruno, T. Geninatti**, R. L. Hood, D. Fine, G. Scorrano, J. Schmulen, S. Hosali, M. Ferrari and A. Grattoni	**Mr Giacomo Bruno**, Houston Methodist Research Institute - **USA**
16:45-17:00	Preparation of Hydrolysable Biocompatible Polymersomes for Drug Delivery **A.Azran-Gefen** and H.Bianco-Peled	**Mrs Gefen-Azran Adi**, Technion-Israel Institute of Technology - **Israel**.
17:00-17:15	Enhanced permeability througth the blood-brain barrier us-ing targeted solid lipid nanoparticles for brain drug delivery	**Ms Joana F. Queiroz**, University of Porto - **Portugal**

	J.F. Queiroz, A.R. Neves, S.A. Costa Lima and S. Reis	
17:15-17:30	Design of Magnetic Molecularly Imprinted Polymer for Controlled Release of Doxorubicin under Alternative Magnetic Field. **N. Griffete**, J. Fresnais, A. Bée and C. Ménager	**Dr Nebewia Griffete**, Pierre et Marie Curie University - **France**
17:30-17:45	BioConjugated Gold Nanoparticles for Enhaced Delivery and Cellular Uptakes **K. Rahme**, J. Guo, C. M. O'Driscoll and J. D. Holmes	**Dr Kamil Rahme**, Notre Dame University - **Lebanon**
17:45-18:00	Prednisolone-loaded pH-sensitive liposomes as an active targeting strategy for rheumatoid arthritis **V.M. Gouveia,** S. Lima, C. Nunes and S. Reis	**Ms Virgínia M. Gouveia**, University of Porto - **Portugal**
18:00-18:15	Rapid nanoformulation and cGMP preparation of antiretroviral drugs for oral HIV nanomedicine and human clinical dosing studies **M. Giardiello**, T. O. McDonald, P. Martin, N. Liptrott, M. Siccardi, A. Owen and S. Rannard	**Dr Marco Giardiello**, University of Liverpool - **United Kingdom**
18:15-18:30	Combined PTT & PDT cancer therapies mediated by hybrid carbon nanotubes and assessment of ultrasound elastography for monitoring tumor treatment **I Marangon**, A Andriola Silva, C Menard-Moyon, G Renault, N Luciani, A Bianco and F Gazeau	**Ms Iris Marangon**, Paris Diderot University - **France**

16 June 2015 **Session IV - B: Nanotech in Life Sciences and Medicine**		
Room 508		
Session Chairs: Prof. Frederic Chaubet - France and Dr. Maria - Antonietta Buccheri - Italy		
11:00-11:15	Penetration of mucoadhesive chitosan-dextran sulfate nanoparticles into the cornea **W. Chaiyasan**, W. Tiyaboonchai, S.P. Srinivas, S. Praputbut and U. Kompella	**Ms Wanachat Chaiyasan**, Naresuan University - **Thailand**
11:15-11:30	Magnetic nanoprobes with anti-HER2 single chain antibody fragments for active targeting of breast and ovarian cancers **C. Alric**, K. Hervé Aubert, N. Aubrey, E. Allard-Vannier, A. Di Tommaso, I. Dimier-Poisson and I. Chourpa	**Dr Christophe Alric**, University of Tours - **France**
11:30-11:45	Cellulose Nanocapsules of Metoprolol and its Metabolites Produced as New Products in Pharmaceuticals Recycling Processes **G.D. Souza**, D.H.E. Schiavon, C.B. Pelizaro and G.B. Teixeira	**Dr Gezimar Souza**, Accert Chemistry and Biotechnology.Inc - **Brazil**
11:45-12:00	Ph/temperature and Magnetic Field Responsive Doxorubicin Loaded NIPA Coated Superparamagnetic Nanoparticles for Targeted Cancer Therapy **R. Khodadust**, Y. Yar and H. Yagci	**Dr Rouhollah Khodadust**, Koc University - **Turkey**
12:00-12:15	Targeted polyethylene glycol gold nanoparticles for the treatment of pancreatic cancer: from synthesis to a proof-of-concept in vitro studies **J. Spadavecchia**, D. Movia, H. Moustaoui ,C. Moore, C.M. Maguire, S. Casale and A. Prina-Mello	**Dr Jolanda Spadavecchia**, Pierre et Marie Curie University/ CNRS - **France**
12:15-12:30	Oral insulin delivery and biodistribution of biopolymers-based nanoparticles **M.A. Lopes**, D.Aniceto, R. Seiça, F. Veiga and A.J. Ribeiro	**Ms Marlene A. Lopes**, Faculty of Pharmacy of University of Coimbra - **Portugal**
12:30-14:00	**Lunch Break + Exhibition + Poster session II**	

Session IV-B: Nanotech in Life Sciences and Medicine		
Room 508		
Session Chairs: Prof Frederic Chaubet - France, Dr Maria-Antonietta Buccheri - Italy and Prof Vladimir Torchilin, USA		
14:00-14:15	IONCs: a versatile tool for hyperthermia, imaging and controlled drug delivery **M.E. Materia**, P. Guardia, H. Kakwere, A. Sathya, M. Pernia, S. Nitti, G. Pugliese, L. Manna and T. Pellegrino	**Dr Maria Elena Materia,** Fondazione Istituto Italiano di Tecnologia - **Italy**
14:15-14:30	A Novel Wound Dressing Coated with Self-Assembling Peptide Nanofibrils as a Drug Carrier **R. Alazragi** and A. Aggeli	**Mrs Reem Alazragi**, University of Leeds - **United Kingdom**
14:30-14:45	Core-cone Structured Monodispersed Mesoporous Silica Manoparticles with Ultra-large Cavity for Protein Delivery **C. Xu**	**Mr Chun Xu**, University of Queensland - **Australia**
14:45-15:00	Impact of the Polyethylenimine Conjugation Mode on the Cell Transfection Efficiency of Silica Nanovectors **X. Wang**, S. Masse, G. Laurent, C. Hélary and T. Coradin	**Ms Xiaolin Wang**, Pierre et Marie Curie University - **France**
15:00-15:15	PEI – Starch Nanoparticles for siRNA based Gene Silencing Therapy for Cancer **B.B. Kandemir**, B. Özpolat, G.T. Köse and V. Hasırcı	**Ms Berke Bilgenur Kandemir**, Middle East Technical University, Ankara -**Turkey**
15:15-15:30	Synthesis of l-PEI and 2MPA Coated Biocompatible Silver Sulfide QDs as Transfection Vectors	**Ms Didar Asik**, Koc University-Istanbul - **Turkey**

	D. Asik ,F. Demir and H.Y. Acar	
15:30-15:45	The Role of Triblock Amphiphilic Copolymers for DNA Translocation Through Lipid Bilayers B. Rasolonjatovo, **C.Huin**, B.Pitard, J.Mathé, V.Bennevault-Celton, T.Le Gall, T.Montier, P.Lehn, H.Chéradame and P.Guégan	**Dr Cecile Huin**, University of Evry - **France**
15:45-16:00	Synthesis and Characterization of Folate-Targeted Poly(ethylene glycol) Coated Cationic Ag2S QDs for Tumor Targeted Gene Delivery **F. Demir,** R. Khodadust, D. Asik and H. Yagci Acar	**Mrs Fatma Demir Duman**, Koc University, Istanbul- **Turkey**
16:00-16:30	**Coffee Break + Exhibition + Posters session II**	
Session Chairs: Prof Frederic Chaubet - France, Dr Maria-Antonietta Buccheri - Italy and Prof Vladimir Torchilin - USA		
16:30-16:45	A Systemic Approach For Manipulating Geometries Of Nano Gold And Nano Silver in Synthesis for Controlling Vector Borne Diseases **S. Prakash**	**Prof Soam Prakash**, Dayalbagh Educational Institute, Dayalbagh - **India**
16:45-17:00	Influence of TiO2 and Al2O3 Addition on Mechanical Properties of Dental Zirconia **O. Agac**, A. Ozturk and J. Park	**Ms Ozlem Agac**, ATILIM University, Ankara - **Turkey**
17:00-17:15	Piezoresistive Strain Sensing Characteristics of Nano-carbon Composites G. R. Choi, H. K. Park, H. Huh, K. T. Lim, B. K. Choi, S. Y. Kim and **I. Kang**	**Prof Inpil Kang**, National University Busan - **Republic of Korea**
17:15-17:30	Plasmonic nanoparticle interaction with cell for photoacoustic cancer imaging **M. Ishihara**, T. Hirasawa, R. Sato and T. Teranishi	**Prof Miya Ishihara**, National Defense Medical College, Tokorozawa - **Japan**
17:30-17:45	Novel hybrid nanoparticles using upconversion luminescence for in vivo imaging **N. Francolon**, F. Leccia, E. Jouberton, D. Boyer, I. Miladi, Delphine Felder-Flesch, Sylvie Begin-Colin, L. Morel, E. Miot-Noirault, J-M. Chezal and R.Mahiou	**Ms Nadege Francolon**, Chemistry Institute of Clermont Ferrand - **France**
17:45-18:00	Efficient and Spatial-Selection Delivery of Quantum Dots in Live Cells by Gold Nanoparticle Medicated Photoporation **R. Xiong**, J. Demeestera, S. C. De Smedta and K. Braeckmans	**Mr Ranhua Xiong**, Ghent University - **Belgium**.
18:00-18:15	Nanoparticles functionalized with an antibody: toward an specific contrast agent of brain tumors by MRI **S. Richard**, M. Boucher, A. Herbet, Y. Lalatonne, S. Mériaux, D. Boquet and L. Motte	**Ms Sophie Richard**, CSPBAT /UMR CNRS 7244, Université Paris 13 University - **France**
18:15-18:30	Specificity and Sensitivity comparative study between phage PVP-S1 and monoclonal antibody as receptor in polydiacetylene vesicles for Salmonella colorimetric detection **T.V. de Oliveira**, N. de F.F.Soares, C.M. Carvalho, J. S. dos R. Coimbra, N. J. de Andrade, J. Azeredo, E. A. A. Medeiros and P. P. Freitas	**Dr Taíla Oliveira**, Federal University of Viçosa - **Brazil**
18:30-18:45	Nanoarchitectonics with Lipid and DNA Building Blocks: In situ Millisecond Time-Resolved SAXS Investigation B. Angelov, **A. Angelova**, M. Drechsler and S. Lesieur	**Dr Angelina Angelova**, CNRS UMR8612 Galien Institute- Paris Sud University- **France**

16 June 2015		
Session IV-C: Nanotech in Life Sciences and Medicine		
Room 561		
Session Chairs: Prof. Patrick Boisseau - France and Prof. Magnus Nyden - Australia		
11:00-11:15	A New Generation of Flower-Like Nanobiocatalyst for Superior Enzymatic Activity **I. Ocsoy**, N, Özdemir and B. Somturk	**Dr Ismail Ocsoy** Erciyes University - **Turkey**
11:15-11:30	Porous nanoparticles entrapped pipette tips for sensitive detection of bio-molecules **C. Lei**	**Ms Chang Lei,** University of Queensland - **Australia**
11:30-11:45	Ultrasensitive magnetic particles/DNAzymes based biosensors for clinical applications. **S. Persano**, G. Vecchio, P. Valentini and P.P.Pompa	**Mr Stefano Persano**, Istituto Italiano di Tecnologia - **Italy**.
11:45-12:00	Immobilization of pyranose 2---oxidase onto functionalized electrospun regenerated cellulose ultrafine fibers: anovel heterogeneous catalyst **W. Panatdasirisuk**, T. Vongsetskul, J. Sucharitakul, P. Chaiyen and P. Tangboriboonrat	**Ms Weerapha Panatdasirisuk**, Mahidol University, Bangkok - **Thailand**
12:00-12:15	Ultra-sensitive Silicon Nanowires for hormone detection **R. S. Forsyth**, R. M. Bigham, M. A. Mohd Azmi, Z. Tehrani, K. A. D. Walker and O. J. Guy.	**Ms Rhiannan Forsyth**, Swansea University - **United Kingdom**
12:15-12:30	Blocking Viral DNA Replication by Employing a Resonance Frequency Generated by Ag4O4 — A Real World Solution. **L. Mack**	**Dr Leigh Mack**, CIMTESES Foundation - **USA**
12:30-12:45	Synthesis and cytocompatability of functionalized multiwalled carbon nanotubes derivatives **A.A. Haroun**	**Prof Ahmed A. Haroun**, National Research Center, Cairo - **Egypt**

12:30-14:00	Lunch Break + Exhibition+ Poster session II

Session IV - C: Nanotech in Life Sciences and Medicine		
Room 561		
Session Chairs: Prof Patrick Boisseau - France and Prof Magnus Nyden - Australia		
14:00-14:15	Development of high sensitive devices using optical tweezers and diamond nanocrystals **J.R. Maze**, N. Figueroa, R. Gonzalez, N. Casanova,V. Waselowski, F. Sazunic, A. Chandía, F. Morales, L. Martinez, C. Wilson, A. Álvarez and M. Kogan	**Prof Jeronimo Maze**, Pontificia universidad Catolica - **Chile**
14:15-14:30	Versatile and easy to fabricate advanced surfaces to enhance the performance of DNA microarray detection **M.J. Bañuls**, D. González-Lucas, R. Puchades and A. Maquieira	**Dr Maria-Jose Bañuls** Politechnic University Valencia - **Spain**
14:30-14:45	DNA detection using Si-nanosandwich **A. Chernev**, N. Bagraev, L. Klyachkin, A. Emelyanov and M. Dubina	**Mr Andrew Chernev**, St. Petersburg Academic University - **Russia**
14:45-15:00	DNA Sensing at femtomolar level using microfluidic electro-chemical cell: advantages of carbon-based transducers B. Zribi, H. Korri-Youssoufi, A. Ouerghi, A. Cavanna, A. Madouri and **A-M Haghiri-Gosnet**	**Dr Anne-Marie Haghiri-Gosnet**, LPN / CNRS- Marcoussis - **France**
15:00-15:15	Selection of peptide motifs for the detection of small molecules in biotechnological applications **C. Di Natale,** C. Cosenza, P.L. Scognamiglio, E.Battista, F. Causa and P.A.Netti	**Ms Concetta Di Natale**, University of Naples - **Italy**.
15:15-15:30	Covalent functionalization of SWNT with ciprofloxacin for enhancing its antibacterial activity **M. Assali**, F.Abdallah, R. Khayyat and A.N. Zaid	**Dr Mohyeddin Assali**, An Najah National University - **Palestine**
15:30-15:45	High-aspect ratio nanostructures for cellular applications N. Buch-Månson, S. Bonde, K.R. Rostgaard, J. Bolinsson, J. Nygård and **K.L. Martinez**	**Prof Karen Martinez**, University of Copenhagen - **Denmark**
15:45-16:00	A Development of Microstrip Patch Antenna with Graphene and Titanium Dioxide For Orthopaedic Implants **N. Fugto**, S. Chaisiri, R. Kaewon and S. Sirivisoot	**Mr Nateetorn Fugto**, King Mongkut's University of Technology Thonburi - **Thailand**
16:00-16:30	**Coffee Break + Exhibition+ Posters session II**	
Session Chairs: Prof Steve Rannard - United Kingdom and Prof Magnus Nyden - Australia		
16:30-16:45	Nanoscale Modification of Natural Cell-derived Matrices for Tissue Engineering Applications **M.P. Hwang**, R. Subbiah and K. Park	**Mr Mintai Hwang**, Korea Institute of Science and Technology, Seoul – **Rep. of Korea**
16:45-17:00	Modular Assembly Gadolinium-Coated Nanoliposomes Enabling Detection of Ischemic Vasculature C. Smith, S. Zimmerman, Sanjay Misra and **H. Kong**	**Prof Hyunjoon Kong**, University of Illinois at Urbana-Champaign - **USA**
17:00-17:15	Pluronic F127 coated superparamagnetic nanoparticles for Human Umbilical Vein Endothelial Cell tracking via magnetic resonance imaging **B. Argibay**, R. Iglesias, M. Pérez-Mato,T. Sobrino, A. Beiras, J. Rivas, U. Himmelreich, J. Castillo, F. Campos	**Mrs Barbara Argibay Gonzalez,** Health Research Institute of Santiago de Compostela (IDIS), University Clinical Hospital Hospital **- Spain**
17:15-17:30	Preparation, Biological Activity and Mechanism of Action of Ag and AgBr Nanoparticles **P. Suchomel**, L. Kvitek, A. Panacek, R. Prucek, J. Hrbac, R. Vecerova and R. Zboril	**Mr Petr Suchomel**, Palacky University, Olomouc - **Czech Republic**
17:30-17:45	Preparation of Novel Selenium Nanoparticles with Strong In Vitro and In Vivo Anti-cancer Efficacy Using Tiger Milk Mushroom **K-H. Wong**	**Dr Ka-Hing Wong**, The Hong Kong Polytechnic University - **Hong Kong**
17:45-18:00	Conductive polypyrrole: a promising interface for attachment and proliferation of mammalian cells A.E. Fernández-Duke, B.E. Millán-Chiu, C. Arenas-Arrocena and **L.M. López-Marín**	**Dr Luz M. López-Marín**, Universidad Nacional Autonoma de Mexico - **Mexico**
18:00-18:15	An In Vitro Study of Osteoblast Behaviors on Graphene Oxide Electrodeposited on Anodized Titanium **P. Tanurat** and S. Sirivisoot	**Ms Pacharaporn Tanurat**, King Mongkut's University of Technology Thonburi - **Thailand**
18:15-18:30	STM Imaging of Yellow Fluorescent Protein under Ambient Condition **H.M.Yusoff**, I.I. Rzeznicka, H. Hoshi, S. Kajimoto, N.N. Horimoto, K.Sogawa and H. Fukumura	**Dr Hanis Mohd Yusoff**, Malaysia Terengganu University - **Malaysia**.

16 June 2015 NanoMatEn2015 : Nanotech for Energy and Environment		
Room 115/116		
Session Chairs : Prof Roger Newman - Canada, Dr Sofoklis Makridis - Greece and Prof James Hill - Australia		
11:00-11:15	Nanoparticles-based Plasmonic Organic Photovoltaic Devices for Enhanced Performance and Stability G. Kakavelakis, M. Krassas, M.M. Stylianakis, N. Vaenas, K. Savva, E. Stratakis and **E. Kymakis**	**Prof Emmanuel Kymakis**, Technological Education-al Institute (TEI) of Crete - **Greece**
11:00-11:30	Effect of halide-mixing on the electronic transmission in organometallic perovskites **G. Berdiyorov**, M. El-Amine Madjet, Fedwa El-Mellouhi, F. H. Alharbi and S. Kais	**Dr Golibjon Berdiyorov**, Qatar Environment and Energy Research Institute - Qatar Foundation - **Qatar**
11:00-11:45	One-pot Fabrication of Nb-doped TiO2 Photoanode for Dye-sensitized Solar Cells **Y-T. Huang**, Y-H. Chang, P. Zhai, N.Y. Hau and S-P. Feng	**Ms Yu Ting Huang**, University of Hong Kong - **Hong Kong**
11:45-12:00	Highly stable carbon nanofluids for solar thermal collectors **S. Mesgari**, N. Hjerrild and R. A. Taylor	**Dr Sara Mesgari Hagh**, University of New South Wales - **Australia**
12:00-12:15	Perovskite Solar Cell Modules built on Vertical TiO2 Nanorods with High Efficiency and Stability A. Fakharuddin, F. Di Giacomo, F. Matteocci, A.L. Palma, I. Ahmed, A. Di Carlo, T.M. Brown and **R. Jose**	**Prof Rajan Jose**, Malaysia Pahang University - **Malaysia**
12:15-12:30	The Development of Alumina Nanofluids-based ferro/ferricyanide Electrolyte and their Applications on Thermogalvanic Cells **C. Liu** and S-P. Feng	**Ms Chang Liu**, University of Hong Kong - **Hong Kong.**
12:30-12:45	Soft, Compressible and Interdigitated 3D Energy Storage Devices Built by Layer-by-Layer Assembly Inside Aerogels **A. Marais**, G. Nyström, E. Karabulut, L. Wågberg, Y.Cui and M. Hamedi	**Mr Andrew Marais**, Royal Institute of Technology KTH - Stockholm - **Sweden**
12:45-13:00	Numerial study of MAXI3 (X=Pb, Sn) perovskite based hetero-junction solar cells M. Guo and **G. Shao**	**Prof Guosheng Shao**, University of Bolton - **United Kingdom**
12:30-14:00	**Lunch Break + Exhibition + Poster session II**	

14:00-18:00	Workshop: **Towards Horizon 2020 call priorities & funding for Micro/Nano-enabling Technologies**
Room 115/116	

Speakers and Moderators:

- **Susan ANSON** (Karlruher Institut für Technologie, **Germany**)
- **Adrien BRUNET** (Karlruher Institut für Technologie, **Germany**)
- **Jérôme GAVILLET** (Commissariat à l'Energie Atomique et aux Energies Renouvelables, **France**)
- **Helmut LOIBL** (Fotec, **Austria**)
- **Lionel TENCHINE** (Pôle Européen de Plasturgie, **France**)
- **Todor Stefanov PETROV** (University of Birmingham, **United Kingdom**)

Welcome and Introduction about the 4M2020 initiative	**14:00 - 14:30**
4M2020 outline and intermediate results	**14:00 - 14:15**
Key Enabling Technologies (KETs) in advanced manufacturing - Nanotechnologies	**14:15 - 14:30**
Workshop Introduction and Sessions	**14:30 – 17 :45** **Including 30 mins coffee break**
Session 1 - Review and ranking of topics and products of high impacts for EU	
Session 2 - Key technologies and value chains	
Session 3 - Technical and non-technical bottlenecks	
Debriefing, Conclusion and Next Steps	**17:45 - 18:00**
Networking Cocktail	**18:00 - 19:30**

17 June 2015 Session IV-D: Nanotech in Life Sciences and Medicine / Nanosafety		
Room 511		
Session chairs: Prof Karen Martinez- Denmark / Prof Hyunjoon Kong-USA		
08:30-09:15	Nano- and Microfabricated Hydrogels for Regenerative Engineering **Ali Khademhosseini**	**Prof. Ali Khademhosseini**, Harvard-MIT's Division of Health Sciences and Technology (HST) / Brigham and Women's Hospital / Harvard Medical School - **USA**
09:15-09:30	SEEC Microscopy : An innovative optical technique for the live and label-free study of a enzymatic reaction in liquid A.Egea, **N.Médard**, M.Métivier and C.Vieu	**Dr Nicolas Médard**, Nanolane-Le Mans - **France**
09:30-09:45	Fe3-δO4 nanoparticles inhibit Clostridium difficile spore germination: an in vitro and in vivo study W-T. Lee, S-R. Wu, Y-N. Wu, Y-H. Chen, C-S. Yeh, P-J. Tsai and **D-B. Shieh**	**Prof Dar-Bin Shieh**, National Cheng Kung University - **Taiwan**
09:45-10:00	Biocompatibility of nano-vesicles derived from microbial cells: an assessment towards vaccine applications **B.E. Millán-Chiu**, A.O. Tinoco-Martínez, V.D. Compeán-García and L.M. López-Marín	**Dr Blanca.E. Millán-Chiu,** Universidad Nacional Autonoma de Mexico - **Mexico**
10:00-10:15	Identification of critical Monte Carlo simulation parameters in nanoparticles radiosensitization P. Retif, **T. Bastogne** and M. Barberi-Heyob	**Prof Thierry Bastogne**, University of Lorraine - **France**.
10:15-10:30	The spread of multi-wall carbon nanotubes to the room air as a result of their mixing in the fume hood E. Jankowska, T. Jankowski, W. Zatorski and P. Sobiech	**Dr Elzbieta Jankowska**, Central Institute for Labour Protection - **Poland**
10:30-11:00	**Coffee Break + Exhibition**	
11:00-11:15	The DaNa2.0 Knowledge Base Nanomaterials quality-approved and easy-to-understand information on current nanosafety research **C. Marquardt**, H.F. Krug, D. Kuehnel, F. Paul, C. Steinbach and K. Nau	**Dr Clarissa Marquardt**, Karlsruhe Institute of Technology (KIT) - **Germany**
11:15-11:30	In vitro study of lung surfactant-nanoparticle interactions for evaluating nanotoxicity **P. Lai**, W. Daear, M. Anikovskiy, R. Loebenberg and E.J. Prenner	**Mr Patrick Lai,** University of Calgary - **Canada**
11:30-11:45	Effect of Gold Nanoparticle Shape of Cellular Uptake and Toxicity **C. Carnovale**, V. Bansal, R. Shukla and G.Bryant	**Mrs Catherine Carnovale**, Royal Melbourne Institute of Technology - **Australia**
11:45-12:00	Genotoxicity and Mutagenicity Screening of Engineered Nanomaterials: **G. Vecchio**, M. Fenech, P.P. Pompa and N. Voelcker	**Dr Giuseppe Vecchio**, stituto Italiano di Tecnologia - **Italy**
12:00-12:15	Impact of ageing and protein remediation in the life-cycle of metal oxide nanoparticles in the organism **J. Volatron**, F. Carn, M. Hemadi, Y. Javed, D. Alloyeau and F. Gazeau	**Ms Jeanne Volatron**, Paris Diderot Universuty - **France**
12:15-12:30	Size and morphology dependence of gold nanorods and gold nanospheres in the nanotoxicological process: in vitro, in vivo and membrane models studies **J. Cancino**, P.M.P. Lins, V.S. Marangoni, J.C.F. Besson, M.E.C. Cancino, M.R.M. Natali ans V. Zucolotto	**Dr Juliana Cancino-Bernardi**, University of São Paulo - **Brazil**.
11:30-14:00	**Networking cocktail**	

17 June 2015 NanoMatEn2015 : Nanotech for Energy and Environment		
Room 412/413		
Session chairs: Prof Rajan Jose – Malaysia, Dr Sofoklis Makridis- Greece and Prof Guosheng Shao – United Kingdom		
8:30-8:45	Stability of organic solar cells using composites materials of inorganic nanostructures and polymers for efficient organic photovoltaics: time-resolved structural/morphological studies **B. Paci**, A. Generosi, M. Guaragno, V. Rossi Albertini, E. Stratakis and E. Kymakis	**Dr Barbara Paci,** ISM-CNR - **Italy**
8:45-9:00	Understanding Lithium solvation in ionic liquids from first principles molecular dynamics simulations **A. Kachmar** and M. Carignano	**Dr Ali Kachmar**, Qatar Environment and Energy Research Institute- Qatar Foundation - **Qatar**
9:00-9:15	Nanomaterials Impacts Across the Life Cycle: Case Study LCA on Organic Photovoltaic Solar Cells M. Tsang, G. Sonnemann, D. Bassani and **P. Garrigues**	**Mr Philippe Garrigues**, University of Bordeaux-CNRS - **France**
9:15-9:30	Sol-gel complex synthesis of biphasic anatase-brookite photocatalysts for hydrogen production **J. Drbohlavova**, V. Kasparek, K. Castkova, M. Kralova and J. Cihlar	**Dr Jana Drbohlavova**, Brno University of Technology - **Czech Republic**
9:30-9:45	Oxygen Electroreduction on Platinum Nanoparticles Deposited on D-glucose Derived Carbon **M. Taleb**	**Mr Masoud Taleb**, Tallinn University of Technology - **Estonia**
9:45-10:00	Fabrication of heterostructure between Tin oxides and TiO2 nanobelts for application in photocatalysis and gas sensing H. Liu and **G. Chen**	**Mr Guohui Chen**, Shandong University- **China**
10:00-10:15	Efficient and Stable Photo electrochemical Water-oxidation Performance of ZnO NRs with Ultrathin Cobalt Layer **N.K. Reddy**, S. Wahl, P. Bogdanoff and N. Pinna	**Dr Nandanapalli Koteeswara Reddy**, Humboldt University - **Germany**
10:15-10:30	New sensor for direct detection of pesticides in water by Raman spectroscopy coupled with enzymatic functionalized nanoparticles. **A. El Alami**, F. Lagarde, B. Mimouna and P. Daniel	**Ms Amal ALAMI**, Maine University, Le Mans - **France**
10:30-11:00	**Coffee Break + Exhibition**	
11:00-11:15	Graphene Coating and Nanocrystalline Alloy Structure: Novel Approaches for Remarkable Corrosion Resistance **R.K. Singh Raman**	**Prof Raman Singh**, Monash University - **Australia**
11:15-11:30	Characterization and application of multicomponent nanoparticles in the immobilization of heavy metals from water and liquid and solid mining tailings **L. Cumbal**, C. Bastidas and D. Delgado	**Prof Luis Cumbal**, Universidad de las Fuerzas Armadas - **Ecuador**
11:30-11:45	Characterization of Nanosized Metallic Sulfide Catalysts Obtained by Thermal Decomposition of Nanoemulsions **A.M. Quesada Perez**, S. Omani, A. Katrib and A. Bumajdad	**Dr Andres M. Quesada Perez**, Kuwait Institute for Scientific Research - **Kuwait.**
11:45-12:00	Surface Functionalization of TiO2 Nanoparticle and its Application for Biodiesel Production from Locally Sourced Used Cooking Oil **J. Gardy**, A. Hassanpour, X. Lai and M. Ahmed	**Mr Jabbar Gardy**, University of Leeds - **United Kingdom.**
12:00-12:15	Photopolymerization of Water-Soluble Acrylic Monomers Induced by PbS and CdS Nanoparticles **Y. Yar**, E. Buz and H. Yagci Acar	**Ms Yasemin Yar**, Koc University-Istanbul - **Turkey**
12:15-12:30	Design and synthesis of copper chalcogenide nanostructures for energy conversion and storage **X. Chen**, C. Han, Z. Li and S. Dou	**Mrs Xinqi Chen**, University of Wollongong- **Australia**
12:30-12:45	Reduced Carrier Recombination in PbS - CuInS2 Quantum Dot Solar Cells Z. Sun, G. Sitbon, T. Pons, A.A. Bakulin and **Z. Chen**	**Dr Zhuoying Chen**, ESPCI-ParisTech/CNRS/UPMC - **France**
11:30-14:00	**Networking Cocktail**	

17 June 2015 Session V: Other Nanoapplications		
Room 508		
Session Chairs: Prof Thierry Bastogne – France, Prof. Nathalie Mignet - France and Prof Raman Singh – Australia		
8:30-9:00	Nanotechnology in Food Packaging Industry: Opportunities and Challenges **V. Teixeira**	**Prof Vasco Teixeira, University of Minho - Portugal**
9:00-9:15	Nanotechnology: Promises and challenges for future **Akbar S. Khan**	**Dr. Akbar S. Khan**, Defense Threat Reduction Agency-Virginia- **USA**
9:15-9:30	Antimicrobial properties of graphene oxide and reduced graphene oxide **M. A. Buccheri**, S. Scalese, D. D'Angelo, F. Spanò, G. Compagnini, G. Rappazzo and V. Privitera	**Dr Maria-Antonietta Buccheri**, Consiglio Nazionale delle Ricerche (CNR) - **Italy**
9:30-9:45	Phosphonium Quat-Modified Nanoclays for In-Situ Polyester Nanocomposite Development: Optimisation of Modification for Particle Performance. **B.J. Naden** and L. Pilon	**Dr Benjamin Naden**, Pera Technology Ltd - **United Kingdom**
9:45-10:00	Efficient Design of Flexible and Low-cost Dual Band RFID inkjet printed antenna using silver nanoparticles ink A.M. Mansour, B.M. Hamza, **N. Shehata** and M. R. M. Rizk	**Dr Nader Shehata**, Alexandria University - **Egypt**
10:00-10:15	0D based resistive switching mechanism M. Paradinas, **Z. Konstantinovic**, S. Valencia, R. Abrudan, A. Pomar, F. Sandiumenge, Ll. Balcells, B. Martinez and C. Ocal	**Dr Zorica Konstantinovic**, Institut de Ciéncia de Materials de Barcelona, CSIC - **Spain**
10:15-10:30	Photocatalytic Silver/Silver Chloride Polymer Nanocomposites **E. W. Tate** and J. H. Johnston	**Mr Eldon Tate**, Victoria University of Wellington - **New Zealand**
10:30-11:00	**Coffee Break + Exhibition**	
11:00-11:15	Ammonia gas sensing properties of ZnO nanowires synthesized by thermal oxidation of Zn film B. Behera and **S. Chandra**	**Prof Sudhir Chandra**,Indian Institute of Technology, Delhi - **India**
11:15-11:30	Long-term corrosion protection by a nanocomposite thin PEA-TiO2-HMDSO coating **L. Ejenstam**, M. Tuominen, J. Pan, A. Swerin and P.M. Claesson	**Mrs Lina Ejenstam**, KTH Royal Institue of Technology - **Sweden**
11:30-11:45	Branched Polymer Nanoreactors for Catalysis by Design **V.O. Rodionov**, K.V. Bukhryakov and C. Mugemana	**Prof Valentin Rodionov**, KAUST, Thuwal, **Kingdom Saudi Arabia**
11:45-12:00	Novel Nanogold Coloured Wool Textiles, Aulana®, for Luxury Markets **J.H. Johnston** and K.A. Lucas	**Prof James Johnston**, Victoria University of Wellington - **New Zealand**
12:00-12:15	Nanotechnology for more Efficient Sustainable Buildings **R.B. Fouaad**	**Mr Ramy Fouaad**, Alexandria University - **Egypt**
12:15-12:30	Dynamic and Static Fluid Loss Characteristics and Rheological Properties of Nano-Based Drilling Fluids **Z. Vryzas**, O. Mahmoud, H. Nasr-El-Din and V. C. Kelessidis	**Mr Zisis Vryzas**, Texas A&M University at Qatar - **Qatar**
12:30-12:45	Surface-Bound Ligands Modulate Chemoselectivity and Activity of a Bimetallic Nanoparticle Catalyst V.O. Rodionov, **K.B. Vu** and K.V. Bukhryakov	**Dr Khanh B. Vu**, KAUST, Thuwal - **Kingdom of Saudi Arabia**
12:45-13:00	Effects of Nanotechnology Materials on Architectural Design- Applications, Possibilities and Future Trends **N.K.Parthenopoulou** and M.Malindretos	**Mrs Nikoleta Parthenopoulou**, Aristotle University of Thessaloniki - **Greece**
13:00-13:15	Synthesis, Characterization and Catalytic Performance of Supported Nickel Nanoparticles in Methane Steam Reforming M.J. Al-Marri, **S. Ali** and M. M. Khader	**Dr Sardar Ali**, Qatar University - **Qatar**
11:30-14:00	**Networking cocktail**	

15 June 2015
Posters Session I - A: Advanced NanoMaterials

N.	Title	Author/Affiliation/Country
1	One-step preparation of amylose and β-carotene nanoparticle inclusion microbeads using amylosucrase from Deinococcus geothermalis **C.A. Letona**, M-C. Lim and Y-R. Kim	**Mr Andres Letona**, Kyung Hee University – **Rep. of Korea**
2	Encapsulation of water molecules in cyclic peptide nanotube **P. Tiangtrong**, N. Thamwattana and D. Baowan	**Ms Prangsai Tiangtrong**, Mahidol University, Bangkok - **Thailand**
3	PDMS Surface Property Study and Sol-gel Modification Methods for the Immobilization of Unstable Enzyme **H. Bi**, A. C. Fernandes, F. Cardoso, M. Brito, S.I. Pinheiro Cardoso and P. Freitas	**Dr Hongyan Bi**, International Iberian Nanotechnology Laboratory - **Portugal**
4	New Methods for Creating Nanocomposites Based on Carbon Nanotubes and Graphene Nanoplatelets **E.A. Burakova**, A.V. Gerasimova, A.V. Melezhyk, A.G. Tkachev	**Dr Elena Burakova**, Tambov State Technical University, Tambov, **Russian Federation**
5	Preparation of Polybutadiene-Silica Nanoparticles via Differential Microemulsion Polymerization and their Hydrogenated Nanoparticles by Diimide Reduction **T. Tancharernrat**, G. L. Rempel and P. Prasassarakich	**Ms Thanyaporn Tancharernrat**, Chulalongkorn University - **Thailand**
6	Construction Copper-Based (I) Superstructures via Recrystallization **Y. Shang**, L. Guo and G. Y. Shang	**Dr Yang Shang**, Beihang University-Beijing - **China**
7	Bio-reduction of Graphene Oxide by Natural Products **E. Ozturk**, S. Şimsek and B. Ozbek	**Ms Elif Ozturk**, Yildiz Technical University - **Turkey**
8	Simple Synthesis of Magnetic Nanoparticles for same shape and size without Size separation **H.Y. Noh**, Y.J. Eom, M. Abbas and C.G. Kim	**Mr Heeyoon Noh**, Daegu Gyungbuk Institute of Science and Technology - **Rep. of Korea**
9	Acid hydrolysis to improve the production of Bacterial Cellulose Nanocrystals P. Paximada, E.A. Dimitrakopoulou, C. Fasseas and **I. Mandala**	**Dr Ioanna Mandala**, Agricultural University of Athens - **Greece**
10	High Pressure Laminates containing Fluorinated Polyhedral Oligomeric Silsesquioxanes **S. Magina**, D. Evtuguin, I. Portugal, J. Ferra and P. Cruz	**Mrs Sandra Magina**, CICECO - University of Aveiro, **Portugal**
11	Green Synthesis of Gold Nanoparticles by Using Peltophorum pterocarpum Flower Extracts M. Balamurugan, S. Kaushik and **S. Saravanan**	**Prof Saravanan Shanmugam**, Sona College of Technology - **India**
12	Stabilization metal nanoparticles by crown compounds with amine and hydroxyl groups in macrocyclic ring and studying their properties A.L.Shabanov, A.M.Maharramov, Z.O.Gakhramanova, M.A.Ramazanov, **U.A.Hasanova**, L.Z.Vezirova and F.V.Hajiyeva	**Prof Ulviyya Hasanova**, Baku State University - **Azerbaijan**
13	Novel Fractal Metamaterial subwavelength structure for sensors application **Y Trabelsi** , H Alkorre , J Stiens , M Kanzari and R Vouncks	**Mr Youssef Trabelsi**, National Engineering School of Tunisia (ENIT) - **Tunisia**
14	Combined Mechanical Disordering – Reactive Synthesis, Possible Method of Bulk Nanocrystalline Intermetallics Obtaining **R.L. Orban**, A. Lawley and M. Orban	**Prof Radu Liviu Orban**, Technical University of Cluj-Napoca - **Romania**
15	Effect of blending ratio of polymer layer on structural properties of polymer-coated mesoporous silica nanoparticles **Ş. Ünal** and B. Özbek	**Ms Sule Unal**, Yildiz Technical University -**Turkey**.
16	Targetting and Applications of Magnetic Nanoparticles P. Taparia and **S. Jindal**	**Mr Srijan Jindal**, Indian Institute of Technology, Roorkee - **India**
17	InxGa1-xN/GaN QDs by coaxial growth on non-polar n-GaN NW J.H. Park, J.K. Sim, D.Y. Um, T.S. Jang, **D.S. Lee** and C.R. Lee	**Ms Da som Lee**, Chonbuk National University - **Republic of Korea**
18	The Effect Of Assembly Conditions and Nanoparticle Condi-tions on Size, Morphology and Polydispersity Of Magnetic Nanoparticle Clusters **S.M. Martyn** and D.F. Brougham	**Ms Sarah Martyn**, Dublin City University - I**reland**
19	Polyurethane/GO Nanocomposites and Vapor Barrier properties **E. Yoo**, K. Shim and H. Huh	**Mr Eunsung Yoo**, Korea Institute of Industrial Technology, Seoul – **Rep. of Korea**
20	Fabrication of Electrospun Polyvinyl Alcohol / Polysaccharide Com-posite Nanofibers and their Prebiotic and Antibacterial Activities **W. Wahbi**, R. Siam and W. Mamdouh	**Mrs Walaa Wahbi,** The American University in Cairo - **Egypt**
21	Efficiency improvement in Dye Sensidized Solar Cells by Plasmonic effect of green synthesized Silver Nanoparticles **S.Saravanan**, R.Kato, M.Balamurugan, S.Kaushik and T.Soga	**Prof Saravanan Shanmugam**, Sona College of Technology - **India**

15 June 2015

Posters Session I - B: Nanomaterials Characterization / Properties and Tools

N.	Title	Author/Affiliation/Country
1	Study of chirality by High Resolution Optical Microscope of Si-CNT Prepared by Plasma Sputtering without catalyst **B.M. Mustafa**, A.M. Ezzat and M.M. Uonis	**Dr Bassam M. Mustafa**, Mosul University, Mosul - **Iraq**
2	Gas-Generating Theranostic Nanoparticles for Ultrasound Imaging and Photodynamic Therapy D. J. Park, K. H. Min and **S. C. Lee**	**Prof Sang Cheon Lee**, Kyung Hee University-Seoul - **Rep. of Korea**
3	The application of ultrasonic spectroscopy to the study of the gelation and chain relaxation properties of dually crosslinked hydrogels **K. Khouzami**, C. Branca, C. Crupi, S. Rifici, G. Ruello, U. Wanderlingh and G. D'Angelo	**Dr Khaoula Khouzami**, Messina University - **Italy**
4	New challenges in TiO2 nanoparticle characterisation and separation by Flow Field Fractionation **J. Omar,** A. Boix, C. von Holst	**Dr Jone Omar**, EC-JRC-IRMM - **Belgium**
5	Diamagnetism of Superparamagnetic Ni Nanoparticles Incapsulated in Carbon Shells A. Manukyan, A. Mirzakhanyan, **H. Gyulasaryan**, M. Farle and E. Sharoyan	**Mr Harutyun Gyulasaryan**, Institute for Physical Research of National Academy of Sciences **- Armenia**
6	Beryllium oxide nanowires and their optical properties for dosimetric applications **E. Pajuste**, G. Kizane, J. Prikulis and D. Erts	**Dr Elina Pajuste**, University of Latvia - **Latvia**
7	Computer microscopy of biological liquid dry patterns for medical diagnostics and modeling of their properties by dissipative dynamics methods **P. Lebedev-Stepanov**, M. Buzoverya, I. Shishpor and K. Vlasov	**Dr Peter Lebedev-Stepanov**, Photochemistry Center RAS - **Russian Federation**
8	Theoretical studies on electronic and magnetic properties of a two-dimensional Mn-Pc and Mn-TCNB monolayers **M. Mabrouk** and R. Hayn	**Ms Manel Mabrouk**, Aix-Marseille University/CNRS - **France**
9	Band Structure of ABA-Trilayer Graphene Superlattice un-der the Application of Periodic Kronig-Penney Type of Potential **S. Uddin** and K. S. Chan	**Mr Salah Uddin**, City University of Hong Kong - **Hong Kong**
10	Fabrication of transparent AZO/ZnO/ITO ReRAM devices and their switching characteristics depending on the deposition tem-perature of ZnO active layer **K. Y. Kim**, C. H. Cho, H. J. Kim, E. L. Shim and Y. J. Choi	**Mr Kyu Young Kim**, Sejong University, Seoul - **Republic of Korea**
11	Physico-chemical properties Fe-doped alumino-silicate nanotubes **E. Bahadori**, E. Shafia, S. Esposito, M. Armandi and B. Bonelli,	**Ms Elnaz Bahadori**, Politecnico di Torino **- Italy**
12	Nanostructured Polymer Matrix Composites for High Performace Engineering Applications **T. Turcsán** and L. Mészáros	**Mr Tamas Turcsan**, Budapest University of Technology and Economics - **Hungary**
13	Fatigue properties of basalt fiber and carbon nanotube reinforced hybridcomposites **J. Szakács** and L. Mészáros	**Mr Jozsef Szakács**, Budapest University of Technology and Economics - **Hungary**
14	The influence of redistribution ions in subphase at the properties langmuir monolayer **A.S. Chumakov**, A.V. Ermakov, V.P. Kim, I.A. Gorbachev and E.G. Glukhovskoy	**Mr Aleksei Chumakov**, Saratov State University - **Russian Federation**
15	Control possibility of separation surfactant from nanoparticles solution by Langmuir method **K.I. Kosolapova,** A.J.K. Al-Alwani and E.G. Glukhovskoy	**Ms Kristina Kosolapova**, Saratov State University - **Russian Federation**
16	Analyzing size dependence of thermal conductivity of suspended graphene with Null-Point Scanning Thermal Microscopy G. Hwang and **O. Kwon**	**Prof Ohmyoung Kwon,** Korea University-Seoul - **Republic of Korea**
17	Three---Arm Star Block---Copolymers: Enzyme---Inspired Catalysts for Oxidation of Alcohols in Water **C. Mugemana**, B.-T. Chen, K. V. Bukhryakov and V. Rodionov	**Dr Clement Mugemana**, KAUST – **Kingdom of Saudi Arabia**
18	Hydrophobic Material with Polymeric Shell G. Sugurbekova, **A.Seralin,** G.Demeuova and M.Baisariyev	**Mr Aidar Seralin**, Nazarbayev University - **Kazakhstan**
19	New Performances of Fluorescent Photosensitive Glass Ceramics for Petabyte Optical Disk 3D Written by Direct Laser Interaction **S. I. Jinga**, E. Pavel	**Prof Sorin JINGA**, "Politehnica" University of Bucharest - **Romania**
20	Iron Nanoparticles-Doped Water Treatment Residues for Arsenic Removal from Industrial Wastewater P. Sarntanayoot and **A. Imyim**	**Dr Apichat Imyim**, Chulalongkorn University-Bangkok-**Thailand**
21	Transfer and biotransformation of gold and silver nanoparticles through aquatic food chain **X. Zhao**, Qunfang Zhou and Guibin Jiang	**Dr Xingchen Zhao**, Chinese Academy of Sciences- **China**
22	Functionalization of textile materials by TiO2/RGO composites to enhance the photocatalytic degradation of Rhodamine B under light irradiation **V. Teixeira**	**Prof Vasco Teixeira**, University of Minho - **Portugal**

16 June 2015
Posters Session II - A: Nanotech in Life Sciences and Medicine

N.	Title	Author/Affiliation/Country
1	Assessment of protein aggregates in the presence of nanoscale vaccine adjuvants. **M.J.W. Johnston** and G.E. Frahm.	**Dr. Michael Johnston**, Biologics and Genetic Therapies Directorate, Health Canada- Ottawa- **Canada**
2	Kiteplatin Delivery by Hydroxyapatite Nanocrystals for the Treatment of Cancer. **N. Margiotta**, M. Lelli, V. Gandin, C.Marzano, S. Merli, S.Savino,N. Roveri, J.D. Hoeschele and G. Natile	**Prof. Nicola Margiotta**, University of Bari Aldo Moro, Bari - **Italy**
3	Self Micro-Emulsifying Drug Delivery Systems (SMEDDS) of Clove Oil for Fish Anesthesia **K. Janngeon**, S. Pikulkaew, W. Chaisri and S. Okonogi	**Ms Kantaporn Janngeon**, Chiang Mai University, Chiang Mai - **Thailand**
4	Development and characerization of bovine serum albumin nanoparticles of amphotericin B **D. B. Ludwig**, L. S. Pedroso, N. M. Khalil and R. M. Mainardes	**Mr Daniel Brustolin Ludwig**, State University of Midwest - **Brazil**
5	Curcumin-loaded Bovine Serum Albumine Nanoparticles: Development and evaluation of stability and antioxidant activity. **L. E. A. Camargo**,R. M. Mainardes and N. M. Khalil	**Mrs Luciana Camargo**, University of Midwest - **Brazil**
6	Silver Sub-nanometric Quantum Clusters as Potential Therapeutic Agents in Fight against Cancer **J.M. Blanco**, J. Calvo, E. Carbó Argibay, E.B. Alonso, F. Domínguez, M. A. López Quintela, and J. Rivasa,	**Mr Jose Blanco**, International Iberian Nanotechnology Laboratory - **Portugal**
7	Development of the nanoconjugate for liver fluke targeting **A.G.Pershina**, A.M.Demin, V.V.Ivanov, O.B. Shevelev, M.A. Uimin, K.V. Nevskaya, N.N. Shegoleva, A.S. Minin, A.E. Sazonov, V.P. Krasnov and L.M. Ogorodova	**Dr Alexandra Pershina**, Siberian State Medical University - **Russian Federation**
8	A Peptide-Based Drug Design to Overcome Major Challenges on Cancer Treatments **A. Sanchez**, A.D. Tinoco and L. Parham	**Ms Annelis Sanchez**, University of Puerto Rico - **Puerto Rico**
9	Superparamagnetic Iron Oxide Nanoparticles for Stem Cell Tracking by Magnetic Resonance Imaging **N. Guldris**, B. Argibay, Y.V. Kolen'ko, E. Carbó-Argibay, R. Iglesias, F.Campos, L.M. Salonen, M. Bañobre-López, J.Castillo and J. Rivas	**Ms Noelia Guldris**, International Iberian Nanotechnology Laboratory, Braga - **Portugal**
10	Phenylethyl Resorcinol in Nioesomes for Cosmetic formulation **J. Buruschat** and T. Amnuaikit	**Ms Janejira Buruschat**, Prince of Songkla University-Songkhla - **Thailand**
11	Nanostructured lipid carriers containing amazon natural lipids for the encapsulation of benzophenone-3 **P.A. Lima** and N. Durán	**Ms Paula Lima**, State University of Campinas (UNICAMP) - **Brazil**
12	Effect of phospholipid and ethanol concentrations on physical property of phenylethyl resorcinol loaded ethosome **T. Limsuwan**, P. Boonme and T. Amnuaikit	**Ms Tunyaluk Limsuwan**, Prince of Songkla University - **Thailand**
13	Clove Oil Loaded Nanoemulsions for Fish Anesthesia **S. Okonogi**, K. Janngeon, W. Chaisri and S. Pikulkaew	**Dr Siriporn Okonogi**, Chiang Mai University, Chiang Mai - **Thailand**
14	Optimization of in vitro conditions to treat cancer with magnetic hyperthermia **V. Vilas-Boas**, B. Espiña, Y. Kolen'ko, M. Bañobre-Lopez, V. Martins and F. Carvalho	**Ms Vania Vilas-Boas**, International Iberian Nanotechnology Laboratory (INL) - **Portugal**
15	Effective VEGF Binding to Au Nanocrystals with {111} Facets **J.H. Kim**, D.H. Jo, J.W. Hong, S.W. Han and J.H. Kim	**Prof Jeong Hun Kim**, Seoul National University Hospital - **Republic of Korea**
16	Toxicological Aspects of Graphene Oxide on Gill Cells of Adult Zebrafish (Danio rerio) **J. P. Souza**, I. M. M. Paino, F. Santos, P. F. M. Nogueira and V. Zucolloto	**Mrs Jaqueline Souza**, University of São Paulo - **Brazil**
17	Effect of Particle Size on Oral Absorption, Tissue Distribu-tion, and Excretion of Food Grade Titanium Dioxide and Silica Nanoparticles **M-R. Jo** and S-J. Choi	**Ms Mi-Rae Jo**, Seoul Women's University - **Republic of Korea**
18	Anti-angiogenic Effect of Gold and Silica Nanoparticles on Choroidal Neo-vascularization: Size Matters, Core does not **J. H. Kim**, D.H. Jo, Y. Piao, T.G. Lee, and J.H.Kim	**Dr Jin Hyoung Kim,** Seoul National University Hospital - **Republic of Korea**
19	Synthesis and surface modification of Fe3O4@SiO2@Au NPs as theranostic agents for Nanomedicine applications. **I. Monaco**, N. T. Hong, E. Locatelli and M. Comes Franchini	**Mrs Ilaria Monaco**, University of Bologna - **Italy**
20	Interactions of Zinc Oxide Nanoparticles with Dispersants: Cytotoxicity, Uptake, and Pharmacokinetics **S. J. Choi**	**Prof Soo-Jin Choi**, University of Seoul Women's University - **Republic of Korea**
21	Transdermal resveratrol nanoethosomes; Preparation, Op-timization; In-vitro, and In-vivo evaluation **H. Aldawsari** and K. Hosny	**Dr Hibah Aldawsari**, King Abdulaziz University, Jeddah - **Kingdom of Saudi Arabia**
22	Incorporation and release of gemcitabine prodrug in mesoporous silica nanoparticles	**Dr Barbara Stella**, University of Torino - **Italy**

	G. Berlier, A. Malfanti, I. Miletto, E. Bottinelli, D. Zonari, G. Blandino, **B. Stella** and S. Arpicco	
23	Visual Analysis of Water permeability in Aquaporin Z incorporated Giant Unilarmellar Vesicles **J-H. Lee**, H. Ryu, T-J. Jeon and Y-R. Kim	**Ms Jun-Hee Lee**, Kyunghee University - **Republic of Korea**
24	The production and the characterization of SPIO Nanoparticles for mediate tranfection of plasmid DNA **Z. Fohlerová**, D. Kovář and J. Hubálek	**Dr Zdenka Fohlerova**, CEITEC BUT - **Czech Republic**
25	Gold nanoparticle-based Immunoprecipitation (IP) sensor for Detection of Shiga toxin (Stx) from pathogenic Escherichia coli **K-B. Jeong**, J-H. Lee, M-C. Lim and Y-R. Kim	**Mr Ki-Baek Jeong**, Kyung Hee University, Yongin - **Republic of Korea**
26	Development of intelligent Drug Delivery Systems based on thermoresponsive gold nanoparticles **A. Cortijo Martín**, B. van Mele and G. Bruylants	**Mrs Ana Cortijo Martín**, Université libre de Bruxelles - **Belgium**
27	Development of a Mdm2 specific colorimetric biosensing platform using gold nanoparticles **M. Retout**, K. Bartik, Th. Doneux and G. Bruylants	**Mr Maurice Retout**, Université Libre de Bruxelles - **Belgium**
28	Enhanced Antibacterial Activity of Antibiotics in Combination with Silver Nanoparticles against Animal Bacteria **M. Smekalova**, V. Aragon, A. Panacek, L. Kvitek and R. Zboril	**Ms Monika Smékalová**, Palacky University in Olomouc - **Czech Republic**
29	The mechanisms for the radiosensitizing effects in high linear energy transfer radiation on colon cancer cells **E.H. Kim**, Y.K. Jeong, I. Cho, S.H. You, S.H. Cho and W-G. Jung	**Prof Eun Ho Kim,** Korea Institute of Radiological and Medical Sciences-Seoul- **Rep. of Korea**
30	Advantages and Obstacles of Using Microfluidic Based Immunoassay for the Detection of Cancer Biomarkers from Biofluids **R. Khnouf**, D. Karasneh, A. Elbetieha and B. Albiss	**Dr Ruba Khnouf**, Jordan University of Science and Technology, Irbid - **Jordan**
31	Efficient Encapsulation of Carboplatin Anticancer Molecule into Boron Nitride Nanotube : a Promising Drug Nanovector **M. El Khalifi**, E. Duverger, T. Gharbi, H. Boulhadour and F. Picaud	**Dr Mohammed El Khlalifi**, Université Franche-Comté University, Besançon - **France**
32	Atomistic binding energy and Coarse grained simulation studies to understand the structure and drug release activity of Vancomycin loaded Lipid Polymer Nanoparticles (LPNs) S.B. Vepuri, N. Seedat, R. Kalhapure, C. Mocktar, M. Soliman and **T. Govender**	**Prof Thirumala Govender**, University of KwaZulu-Natal, Durban - **South Africa**
33	Reliability, Availability, Maintainability and Safety Analysis for the Development of a Nano-material Plant **E. Davarpanah** and A. Carpignano	**Ms Elahe Davarpanah**, Politecnico di Torino - **Italy**
34.	Development of Liposomal Nanocarriers for Near-Infrared Dye: Preparation and Physico-Chemical Characterization **S. Koudelka**, J. Masek, R. Mikulik and J. Turanek	**Dr Stepan Koudelka**, St. Anne´s University Hospital Brno, Brno - **Czech Republic**
35	Improved Antimicrobial Activity of Electrospun Graphene-Chitosan/Gelatin Nanofibrous-Based Nanocomposite Scaf-folds **I.H. Ali**, A. Ouf, M.B. Taskin, J. Song, M. Dong, M. Chen, R. Siam and W. Mamdouh	**Ms Isra H. Ali**, The American University in Cairo- **Egypt**
36	Honey Chitosan Nanofibers Loaded With Natural Antimicrobials for Wound Dressing Applications **W.A. Sarhan** and H. M.E Azzazy	**Mrs Wessam Sarhan**, The American University in Cairo- **Egypt**
37	Doxorubicin loaded, pH-sensitive biodegradable naonogels and their bio-evaluation **P. Kumar**, N. Yadav, A. Chhikara and M. Chopra	**Mr Parveen Kumar**, University of Delhi-**India**
38	Increasing the efficiency of anticancer therapies using mono-dispersed chitosan nanoparticles **M.J. Masarudin**, S.M. Cutts, D.R. Phillips and P.J. Pigram	**Dr Mas Jaffri Masarudin,** Putra University - **Malaysia**
39	siRNA and miRNA-basedSNAs to target canonical and non-canonical Bcl-2 signaling in glioblastomas **A.Chalastanis**, F.M.Kouri, S.A.Jensen, Lisa A.Hurley and A.H.Stegh	**Dr Alexandra Chalastanis**, Northwestern University- **USA**
40	Nanosensors and nanomaterials for biomedicine **N.Casanova-M**, B. Céspedes, M Cisternas, N. Figueroa, R Gonzáles, A. Chandia, C. Contreras, R Segura, P. Conejeros, F. Morales, M. Kogan, C.A.M. Wilson, M.Favre, H. Bhuyan, A.R Alvarez, S.A.Hevia and JR Maze	**Dr Nathalie Casanova**, Pontificia Universidad Catolica - **Chile**

16 June 2015
Posters Session II - B: Nanoelectronics

N.	Title	Author/Affiliation/Country
1	Nanoscale Photonic Humidity Sensor Based on the Fluorescence Lifetime of BODIPY Dye Molecules S. Acikgoz, **H. Yungevis**, M.N. Inci and A. Sanyal	**Mr Hasan Yungevis**, Karamanoğlu MehmetBey University - **Turkey**
2	Silicon Carbide Tunable MEMS Resonator with Wide Operation Range **B. Svilicic**, E. Mastropaolo and R. Cheung	**Dr Boris Svilicic**, University of Rijeka - **Croatia**
3	High Mobility Materials For the Channel of DG Mosfet **S.Slimani** and B. Djellouli	**Ms Samia Slimani**, Mouloud Mammeri University (UMMTO) - **Algeria**
4	Lithium cobalt oxide thin films towards resistive memories **V.S.Nguyen**, Van Huy Mai, Alec Moradpour, Pascale Auban Senzier, Claude Pasquier, Kang Wang, …and Olivier Schneegans	**Mr Van Son Nguyen**, Paris-Sud University and UPMC**- France**
5	Tunable Luminescence Carbon nanoparticles From Carbohydrate Foodstuff **L. A. Adams**, K. Fagbenro-Owosheni, and A. Badejo	**Dr Luqman Adams**, University of Lagos, **Nigeria**
6	Modal parameter identification of perforated microplates from output data only **J. Lardiès**	**Prof Joseph Larides**, FEMTO-ST Institute - **France**
7	The Effect of 2-step Plasma Treatment for Single-walled Carbon Nanotube on Electrochemical Sensors **J.H. Kim**, K.B. Kim, C.W. Park and N.K.Min	**Mr Joon Hyub Kim**, Korea University-Chungnam – **Rep. of Korea**
8	Theoretical predictions of luminescence due to cyclosiloxanes in nanostructured Silicon Rich Oxide films employing the Global Reactions Model. N.D. Espinosa-Torres, J.A. Luna-López, **J.F.J. Flores-Gracia**, A.D. Hernández de la Luz, J. Martínez-Juárez and G. Flores-Carrrasco	**Dr Francisco Flores**, Benemérita Universidad Autónoma de Puebla - **Mexico**
9	Sensing Low Magnetic Field by Using Planar Hall Effect Sensor I. Song, S.H. Aiden Lee, **S.J. Kim** and C.G. Kim	**Mr Sung Joon Kim**, Daegu Gyungbuk Institute of Science and Technology (DGIST) – **Rep. of Korea**
10	Active plasmonics: Growing Gold Nanoparticles on a Flexible Substrate to enable simple mechanical control of their plasmonic coupling **U. Cataldi**, R. Caputo, Y. Kurylyak, G. Klein, M. Chekini, C. Umeton and T. Burgi	**Dr Ugo Cataldi**, University of Geneva - **Switzerland**
11	PU-RGO composites and its properties for thermal conductive adhesive **S. Choi**, S. Park and H. Huh	**Mr Sukhoon Choi**, Korean Institute of Industrial Technology(KITECH), Incheon - **Rep. of Korea**

16 June 2015

Posters Session II - C: Nano MatEn 2015 - Nanotech for Energy and Environment

N.	Title	Author/Affiliation/Country
1	Leaching of Nano-SiO2 from Municipal Solid Waste E.T. Sakallıoglu, M. Bakırdoven, I. Temizel, C.S.Uyguner- Demirel, **B. Demirel**, N.K. Copty, T.T. Onay and T. Karanfil	**Prof Burak Demirel**, Bogazici University, Institute of Environmental Sciences-Istanbul - **Turkey**.
2	The Role of Al2O3 and SiO2 Nanoparticles on the Cycleability of Li-Air Batteries with TEGDME-PEO/LiPF6 Electrolytes **A.Akbulut Uludağ**, M. Tokur, H. Algul, T. Cetinkaya, M. Uysal and H. Akbulut	**Mrs Ahsen Akbulut Uludag**, Sakarya University - **Turkey**
3	Transparent Hydrophobic Nanolayers on ETFESiOx Substrates for Solar Cells Encapsulation **G. Rossi**, P. Scarfato, L. Incarnato	**Dr Gabriella Rossi**, University of Salerno - **Italy**
4	Photovoltaic Response of Non-Toxic CuInS2 Quantum Dot based Conducting Polymer Composite Films **I. Singh**, J. Singh, A. Kumari, P.K. Rao and P.K. Bhatnagar	**Mr Inderpreet Singh**, University of Delhi- **India**
5	Benefits of a compact TiO2 layer for the elaboration of transparent TiO2 nanotubes array on conducting glass **A. Krumpmann** and A. Decroly	**Mr Arnaud Krumpmann**, University of Mons - **Belgium**
6	Study of LiFePO4 thin films as Li-ion battery cathode by in-situ electrochemical atomic force microscopy in aqueous electrolyte J. X. Wu and **G. Y. Shang**	**Prof Guangyi Shang**, Beihang University, Beijing - **China**
7	Textured fabrication of CdS/CdTe thin film PV cell with back contacts **M. Sridar Ilango** and S.K Ramasesha	**Mr Murugaiya Sridar Ilango**, Indian Institute of Science - **India**
8	Nonradiative Electron and Hole Relaxation Dynamics in Organometallic Halide Perovskites **M.E. Madjet,** F. El-Mellouhi, G. Berdiyorov, S. Ashhab, A. Akimov and S. Kais	**Dr Mohamed El-Amine Madjet**, Qatar Environment & Energy Research Institute, Qatar Foundation - **Qatar**
9	C-Nanotube Based Infrared Thermo-Voltaic Cells and Detectors T.Hosseini, N.Yavarishad and **N. Kouklin**	**Dr Nikolai Kouklin**, University of Wisconsin - **USA**
10	Natural Biodefensive Nanoparticles for Pest Control in Soy Culture **A.L. Santos**, V. Zucolotto, B.T.R. Rhein, I. Pezzopane and G.Rosa	**Dr Amanda Santos**, Nanomed Inc., São Carlos - **Brazil**
11	Sol-Gel Production and Electrochemical Characterization of Free-Standing Metal Oxide/MWCNT Nanocomposite Anodes for Li-Ion Batteries **H. Köse**, Ş. Karaal, A. O. Aydın, H. Akbulut	**Ms Hilal Kose**, Sakarya University - **Turkey**
12	The Effect of Different Solvent Combination of LiBF4 Electrolyte on Free-Standing SnO2/MWCNT Nanocomposite Anode Capacity for Li-ion Batteries **Ş. Karaal**, H. Köse, A. O. Aydın and H. Akbulut	**Mrs Seyma Karaal**, Sakarya University- **Turkey**
13	Photocatalytic Activities of ZnO and ZnO/ZnS Synthesized by Microwave-Hydrothermal Method **N. Güy**, Ş; Durmuş and M. Özacar	**Mrs Nuray Guy**, Sakarya University - **Turkey**
14	Polystyrene Micro/Nanofibers and its Application in the Removal of Crude Oil Spills **M. Alazab Alnaqbi**, A. Al Blooshi, Y. Greish and M. Mohsin	**Dr Mohamed Alazab Alnaqbi**, United Arab Emirates University, Al Ain - **United Arab Emirates**
15	Effects of biopolymer nano coils on sand dune stabilization and dust controlling **M. Aghaei Moghadam** and K. Zangeneh	**Mr Mostafa Aghaei**, Biopolynet Inc-Fredericton - **Canada**
16	Carboxymethyl-nanocellulose:a versatile raw-material in coating industry **A. Reis**, R. Duarte, J. Tedim, A. Caetano, A.P. Mendes de Sousa, J. Ataíde and D. Evtuguin	**Dr Ana Reis**, University of Aveiro - **Portugal**
17	Graphene Reinforced Concrete M.F. Craciun and **D. Dimov**	**Mr Dimitar Dimov**, University of Exeter - **United Kingdom**
18	Quantum Dot Sensitized Solar Cells with Cuprous Sulfide Counter Electrode N.M. Ferreira, C. Bernardo, I. Moura, P. J.G. Coutinho, A.G. Rolo, M. Vasi-levskiy, M. Pastor, F. Fernandes, V. Teixeira, J.O.Carneiro and **A. Samantilleke**	**Prof Anura Samantilleke**, Minho University - **Portugal**
19	Reduced graphene oxide on TiO2 nanorods and nanotubes photo-anode for solar hydrogen evolution **H. Kim and** B. L.Yang	**Mr Hyun Kim**, Kumoh National Institute of Technology, Geongbuk – **Rep. of Korea**
20	Silicon Nanowire as an Effective Absorber for Solar Cell Application: Fabrication and Numerical Simulation M. K. Hossain, **B. Salhi**, A. W. Mukhaimer and F. A. Al-Sulaiman	**Dr Billel Salhi**, King Fahd University of Petroleum and Minerals (KFUPM), Dhahran - **Saudi Arabia**
21	Environmentally Friendly Design of Tailor-Made Nano-porous Polymeric Gas Adsorbents **W.A. El-Mehalmey**, T. Madkour and R. A. Azzam	**Dr Worood El-Mehalmey**, American University in Cairo - **Egypt**
22.	Silica-based nanocoating and LDHs sensors for enhancement of paperboard barrier properties **V.M. Dias**, A. Kuznetsova, I. Portugal, J. Tedim, A.A. Yaremchenko and D. V. Evtuguin	**Dr Vânia Dias**, University of Aveiro-**Portugal**

Advanced Nanomaterials:
Synthesis / Fabrication, Characterization and Tools
Keynote Talks

New frontiers in the science of nanostructured materials for information technology

Albert Fert [1, 2]

[1] Unité Mixte de Physique CNRS/Thales, 1 av Fresnel, F91767 Palaiseau, France
[2] Université Paris-Sud, F91405 Orsay, France

Most of the recent advances in the information technologies (computing, communications) come from the creation of nanomaterials and nanostructures. I will review some of these recent advances and the next prospects in several fields of the information technologies:

- Information storage: from the magnetic storage in HDD to the perspective with spintronics and skyrmions.
- Nonvolatile magnetic memories.
- Ferroelectric memories and perspective for bio-inspired computing.
- Spintronics with graphene.

State-of-the-Art in Metal Matrix Composites Reinforced with Carbon Nanotubes by Powder Metallurgy Process

K. Kondoh
Osaka University, Joining and Welding Research Institute, Osaka, Japan

Abstract: Multi-wall carbon nanotube (MWCNT) is one of the effectively promising reinforcement materials to improve the mechanical properties such as hardness, strength, and Young's modulus of the composite materials. From a viewpoint of uniform dispersion of CNTs in matrix of the composites, two kinds of mixing processes were employed in this study; wet and dry mixing techniques. Regarding the former process, polar zwitterions generally have a high solubility in water, but a poor solubility in most organic solvents. 3-(N, N-dimethylstearylammonio) propanesulfonate, a typical linear zwitterionic surfactant used in this study, had both hydrophobic and hydrophilic groups. Electrostatic interactions, having larger attractive forces than the van der Waals forces between CNTs, occur at the hydrophilic because of the positive charge and negative charges on their headgroups. Therefore, the un-bundled CNTs are uniformly dispersed in the zwitterionic surfactant solution. The metal powders are dipped in this solution, and the composite powders coated with CNT films are prepared after removing the solution. Figure 1 shows a typical surface of metal powders coated with CNTs. The dry mixing process suggests that the high-energy ball milling equipment is employed to mix the metal powders with CNTs under the controlled atmosphere such as vacuum and argon gas. In general, CNTs have some mechanical damages during the dry mixing process, however, this process is remarkably cost-effective compared to the above wet process to disperse CNTs. By changing the sintering temperature, CNTs could be easily transferred to nano-scale carbides, which are also effective reinforcemnets of the composites. MWCNTs are mechanically mixed with pure aluminum (Al) powder by high-energy planetary ball milling (PBM) process, and shorted CNTs were dispersed inside and at the surface of Al powder. They were consolidated by SPS and followed hot extrusion. SPS was effective for complete reaction of CNTs with Al powder to synthesize Al_4C_3 nano-rods, which were dispersed in the matrix. The nano-dispersoids and grain refinement of α-Al caused the significant improvement of mechanical strength of pure Al matrix composites. TEM observation results of the Al_4C_3/Al composite are shown in Figure 2. In-situ nanorods had basal planes (001) of the hexagonal crystal paralleled to their axis direction. From the bright field TEM images and corresponding selected area diffraction (SAD) patterns, the nanorods were identified as single-crystal Al_4C_3. The nominal tensile stress-strain (S-S) curves shown in Figure 3 indicated yield strength and ultimate tensile strength of Al_4C_3/Al composites were attained to 307 MPa and 403 MPa, respectively. They are 90% and 78% enhanced compared with those of the reference pure Al material (162 MPa and 226 MPa) processed at same conditions, respectively.

Keywords: carbon nanotubes, powder metallurgy, composite material, reinforcements, aluminium, titanium, zwitterionic surfactant, dry mixing.

References:

Kondoh, K., Threrujirapapong, T., Umeda, J., Fugetsu, B, High-temperature properties of extruded titaniumcomposites fabricated from carbon nanotubes coated titanium powder by spark plasma sintering and hot extrusion, (2012), *Composites Science and Technology*, 72, 1291–1297.

Chen, B., Jia, L., Li, S., Imai, H., Takahashi, M., Kondoh, K, In Situ Synthesized Al4C3 Nanorods with Excellent Strengthening Effect in Aluminum Matrix Composites, (2014), *Advanced Engineering Materials*, 16, 972-975.

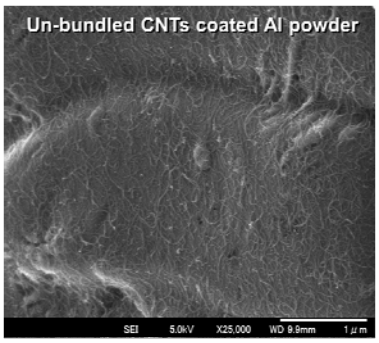

Figure 1: SEM observation on Al powder surface coated with un-bundled CNTs via wet mixing

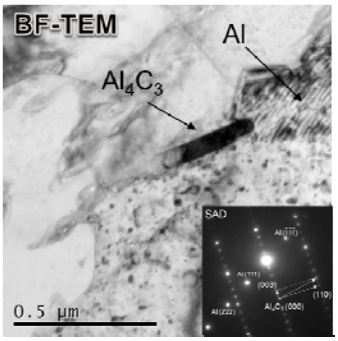

Figure 2: TEMobservation on Al_4C_3/Al composite and SAD pattern of typical $Al4C_3$.

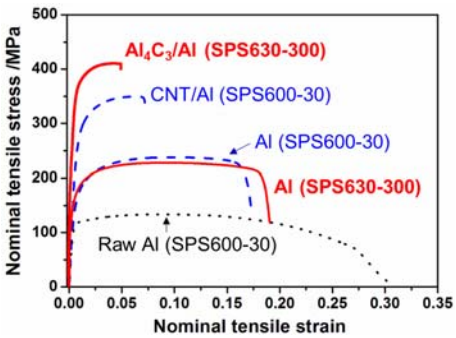

Figure 3: Tensile S-S curves of extruded Al composites reinforced with Al_4C_3 and CNT as well as pure Al by PM process.

Designed Chemical Synthesis and Assembly of Uniform-sized Nanoparticles for Medical and Energy Applications

Taeghwan Hyeon[1,2,*]
[1]Center for Nanoparticle Research, Institute for Basic Science (IBS), Seoul 151-742, Korea
[2]School of Chemical and Biological Engineering, Seoul National Universtiy, Seoul 151-742, Republic of Korea

Abstract: Over the last 10 years, our laboratory has focused on the designed chemical synthesis, assembly and applications of uniform-sized nanocrystals. In particular, we developed a novel generalized procedure called as the "heat-up process" for the direct synthesis of uniform-sized nanocrystals of many metals, oxides, and chalcogenides.

Recently our group has been focused on medical applications of various uniform-sized nanoparticles. Using 3 nm-sized iron oxide nanoparticles, new non-toxic MRI contrast agent was realized for high resolution MRI of blood vessels down to 0.2 mm. We demonstrated that ceria nanoparticles protect against ischemic stroke in an in vivo animal model. We reported the first successful demonstration of high-resolution in vivo three-photon imaging using biocompatible and bright Mn^{2+} doped ZnS nanocrystals. We fabricated tumor pH-sensitive magnetic nanogrenades composed of self-assembled iron oxide nanoparticles and pH-responsive ligands for theranostic application, enabling the visualization of small tumors of < 3 mm via pH-responsive T1 MRI and fluorescence imaging and superior photodynamic therapeutic efficacy in highly drug-resistant heterogeneous tumors. We synthesized tumor pH-sensitive nanoformulated triptolide coated with folate targeting ligand to treat hepatocellular carcinoma (HCC), which has one of the worst prognosis for survival as it is poorly responsive to both conventional chemotherapy and mechanism directed therapy.

We reported the large-scale synthesis of magnetite nanocrystals imbedded in a carbon matrix and hollow iron oxide nanoparticles. We demonstrated galvanic replacement reactions in metal oxide nanocrystals. When Mn_3O_4 nanocrystals were reacted with iron(II) perchlorate, hollow box-shaped nanocrystals of $Mn_3O_4/\gamma\text{-}Fe_2O_3$ ("nanoboxes") were produced. These iron oxide-based nanomaterials exhibited very high specific capacity and good cyclability for lithium ion battery anodes.

E-mail: thyeon@snu.ac.kr

Nanomaterials for Biomedical and Green Chemistry Applications

Jackie Y. Ying
Institute of Bioengineering and Nanotechnology, Singapore

Abstract: Nanocrystalline materials are of interest for a variety of applications. This talk describes the design and functionalization of nanocomposite materials for biological and chemical applications. Specifically, we have synthesized metallic, metal oxide and semiconducting nanocrystals for bioimaging, bioseparation, biosensing, theranostic, fuel cell and catalytic applications. These nanocrystals are ≤ 10 nm in size, and are surface modified to provide for high dispersion, biocompatibility, and water solubility. They are used as building blocks to create multifunctional nanocomposite particles with unique properties.

Nanoporous materials have also been developed with high surface areas and high porosities. We have synthesized nanoporous materials that are made of silica, transition metal oxides, and organic backbone. These systems can be tailored with a high density of functional groups either on the surface or in the framework of the materials. They demonstrated excellent properties as heterogeneous or heterogenized catalysts, providing high activity and recyclability. They are also useful as adsorbents for green chemistry applications.

Keywords: biomedical, nanomaterials, green chemistry, catalysts.

Session I: Nanomaterials Fabrication/ Synthesis

Hyperbranched-Polydendrons: A New Materials Platform for Advanced Polymer Technologies

F L. Hatton,[1] H. Rogers,[1] A. Dwyer,[1] L. M. Tatham,[2] L. R. Tidbury,[2] P. Chambon,[1] A.Owen,[2] S. P. Rannard[1]

[1] Department of Chemistry, University of Liverpool, Crown Street, L69 7ZD, UK

[2]Department of Molecular and Clinical Pharmacology, University of Liverpool, Block H, 70 Pembroke Place, Liverpool L69 3GF

Abstract: Complex polymer architectures often have functional benefits that are not achievable through simple or straightforward synthesis strategies such as self-assembly, tuneable surface interactions, phase separation and stimuli-responsive behaviour. Over recent years we have developed a highly flexible synthetic approach that offers complex polymer architectures through non-complex chemistry. Through the concerted propagation and branching of vinyl polymerisations initiated using dendron-derived initiators, very high molecular weight polymers bearing dendrons at one chain-end of each primary chain within a branched core can be generated [1]. These new architectures – hyperbranched Polydendrons – present considerable opportunities for advanced materials science. Our studies of branched polymer nanoprecipitation [2,3] and hyperbranched Polydendron nanoprecipitation have led to a platform approach allowing considerable synthetic flexibility. The formation of highly uniform nanoparticles which have the added benefits of being able to encapsulate small molecules whilst being salt stable have enabled studies as materials for nanomedicine. Pharmacological studies have shown a low cytotoxicity and the potential to also control the interactions with a range of cell types including accumulation in phagocytic and non-phagocytic cells and permeation through model gut epithelium [4]. Such permeation offers the long term potential for circulating nanoparticles after oral dosing; a major challenge for nanomedicines for chronic disease therapy. The flexibility and progress to date will be described in detail including initial results of these materials within a nanomedicine context.

Keywords: polymer architecture, controlled polymerization, dendrimers, nanomedicine, pharmacology, infectious diseases

References:

[1] F. L. Hatton, P. Chambon, T. O. McDonald, A. Owen, S. P. Rannard Hyperbranched polydendrons: a new controlled macromolecular architecture with self-assembly in water and organic solvents *Chem. Sci*., 2014, 5, 1844-1853.

[2] R. A. Slater, T. O. McDonald, D. J. Adams, E. R. Draper, J. V. M. Weaver, S. P. Rannard Architecture-driven aqueous stability of hydrophobic, branched polymer nanoparticles prepared by rapid nanoprecipitation *Soft Matter*, 2012,8, 9816-9827

[3] J. Ford, P. Chambon, J. North, F. L. Hatton, M. Giardiello, A. Owen, S. P. Rannard Multiple and Co-Nanoprecipitation Studies of Branched Hydrophobic Copolymers and A–B Amphiphilic Block Copolymers, Allowing Rapid Formation of Sterically Stabilized Nanoparticles in Aqueous Media *Macromolecules* 2015 DOI 10.1021/acs.macromol.5b00099

[4] F. L. Hatton, L. M. Tatham, L. R. Tidbury, P. Chambon, T. He, A Owen, S. P. Rannard Hyperbranched Polydendrons: A New Nanomaterials Platform With Tuneable Permeation Through Model Gut Epithelium *Chem. Sci.*, 2015, 6, 326-334

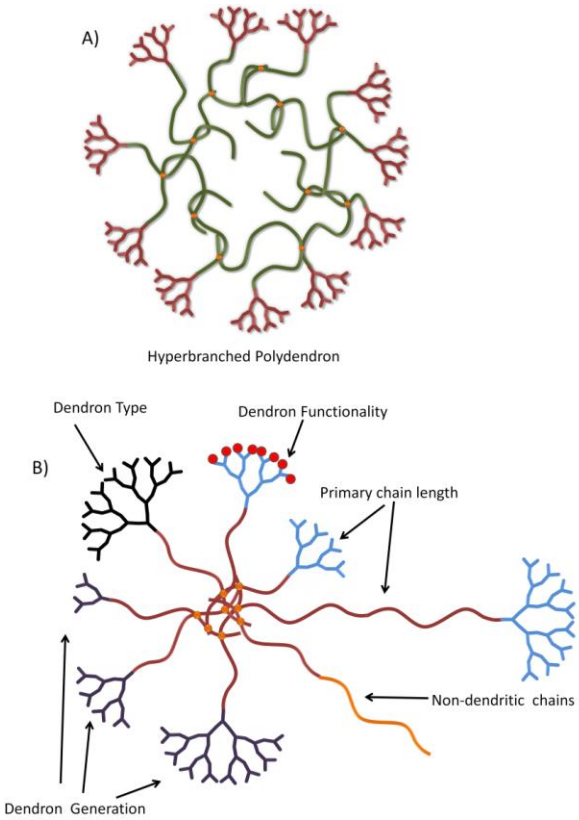

Figure 1: Schematic presentations of A) hyperbranched-polydendron, and B) Synthetic flexibility with the hyperbranched polymderon platform

New geometric model for carbon nanocones incorporating curvature

Barry J. Cox and James M. Hill*
Nanomechanics Group, School of Mathematical Sciences
University of Adelaide, SA 5005, Australia
*Corresponding author: Email jim.hill@adelaide.edu.au

Abstract: The conventional rolled-up model for carbon nanocones assumes that the cone is constructed from a rolled-up graphene sheet joined seamlessly, which predicts five distinct apex angles. This model completely ignores any effects due to the changing curvature and all bond lengths and bond angles are assumed to be those for the planar graphene sheet. Clearly curvature effects will become more important closest to the cone apex, and especially so for the cones with the smaller apex angles. For carbon nanotubes the present authors have proposed an exact polyhedral model that properly incorporates a hexagonal framework in which the bond angles and bond lengths are all assumed identical in the cylindrical configuration, and by necessity the sum of the bond angles is less than 360 degrees. In this talk we propose a corresponding model for carbon nanocones, but in this case it is not possible to produce a completely analogous model, since the cone structure does not have precise equality of all bond lengths and bond angles. The curvature changes along the length of the nanocone, and so too does the angle sum of the three bond angles at each carbon atom. Therefore, it is not expected that every point in the graphene lattice can be exactly congruent with all others. Here we derive an analytical expression for the cone radius applicable at any distance along the cone wall and we also derive an integral expression for the correction to the conical height, which goes some way towards accounting for the varying curvature of the cone wall. Predicted bond angles and bond lengths are shown to agree well with those obtained by relaxing the conventional rolled-up model using the LAMMPS software.

References

B. J. Cox and J. M. Hill,``Exact and approximate parameters for carbon nanotubes", Carbon, 45 (2007) 1453-1462.
B. J. Cox and J. M. Hill,``Geometric structure of ultra-small carbon nanotubes", Carbon, 46 (2008) 711-713.

Keywords: cone geometry; conventional rolled-up model; curvature effects; new geometric model.

New Synthesis of Cobalt Nanoparticles with Tunable Size in Ionic Liquids

Bishoy Morcos,[1,2,*] P.-H. Haumesser,[2] C. C. Santini[1]
[1] Université de Lyon, CNRS-UMR 5265, 43 Bd du 11 Novembre 1918, 69616, Villeurbanne Cedex, France.
[2] CEA–LETI-Minatec Campus, 17 rue des Martyrs, 38054 Grenoble Cedex 9, France.
bishoy.morcos@cea.fr

Abstract: Mono-dispersed metallic nanoparticles (NPs) represent a very interesting area of research owing to their special magnetic, electrical, optical and thermal characteristics. These unique properties originate from quantum effects as well as very high surface to volume ratio of such small particles. Cobalt (Co) NPs represent one of the most interesting metallic NPs because of their potential applications in catalysis, data storage, and magnetic fluids. They also find applications in the field of medication and diagnosis based on their unique magnetic properties. Co NPs are typically produced using either physical or chemical methods. As an example for physical synthesis, Co NPs can be prepared by direct current arc plasma evaporation method (Meng *et al.* 2012). The problem with such techniques is the lack of control on size for particles smaller than 100 nm (Balzani 2005). Chemical methods usually provide perfect control on size for nanoparticles that are very small up to 1 or 2 nm, *e.g.* the Co NP synthesis by chemical reduction of a selected Co organometallic precursor (1,5-cyclooctadiene)(cycloocta-dienyl) Cobalt (I), Co(COD)(COE) in the presence of ligand or polymer (Chaudret *et al.* 2007; Comesana-Hermo *et al.* 2014) or by thermal decomposition of Co carbonyl compounds requiring high temperature (Vollmer *et al.* 2011).

Ionic liquids (ILs) represent an important class of materials used to prepare metallic NPs. ILs not only act as solvents but also as stabilizing media because they possess high degrees of self-organization at the nano scale (Gutel *et al.* 2009; S. Campbell *et al.* 2013). Therefore, upon modifying the structure of either the anion or the cation, one can tune the size of the NPs (S. Campbell *et al.* 2013).

The aim of this work is to prepare metallic Co NPs with a narrow size distribution through the reduction of Co(COD)(COE) into metallic Co under H_2 using ILs as a solvent and stabilizing medium. NPs size is tuned by varying the experimental conditions or the IL nature (Figure 1). This reduction reaction is favored because it affords only volatile organic by-products easily removed from IL under vacuum, Eq. 1. The mechanism of NPs formation will be discussed as well the full characterization and magnetic properties of the Co NPs.

$$Co(\eta^3 - C_8H_{13})(\eta^4 - C_8H_{12}) \xrightarrow{H_2} Co + 2\,C_8H_{16} \qquad Eq.1$$

Keywords: Cobalt nanoparticles, Ionic liquid, Organometallic precursor.

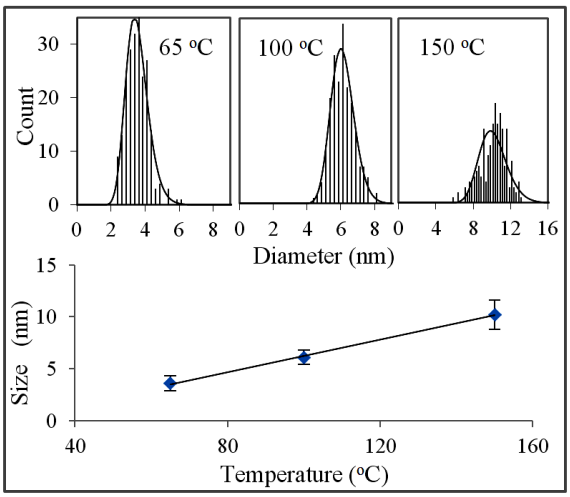

Figure 1: Histograms and size distribution of Co NPs determined from TEM images (200 particles measured) as a function of temperature. NPs were prepared by reduction of Co(COD)(COE) (0.05 M) in $C_1C_4Im\ NTf_2$ under 0.4 MPa H_2.

References:

Balzani, V. (2005) Nanoscience and Nanotechnology: A Personal View of a Chemist, *Small*, 1, (3) 278-283.

Chaudret, B., et al. (2007) Organometallic Nanoparticles of Metals or Metal Oxides, *Oil & Gas Science and Technology - Rev. IFP*, 62, (6) 799-817.

Comesana-Hermo, M., et al. (2014) Effect of a Side Reaction Involving Structural Changes of the Surfactants on the Shape Control of Cobalt Nanoparticles, *Langmuir*, 30, (15) 4474-4482.

Gutel, T., et al. (2009) Organized 3D-alkyl imidazolium ionic liquids could be used to control the size of in situ generated ruthenium nanoparticles?, *Journal of Materials Chemistry*, 19, (22) 3624-3631.

Meng, H., et al. (2012) Preparation of cobalt nanoparticles by direct current arc plasma evaporation method, *International Journal of Refractory Metals and Hard Materials*, 31, (0) 224-229.

S. Campbell, P., et al. (2013) Ruthenium Nanoparticles in Ionic Liquids - A Saga, *Current Organic Chemistry*, 17, (4) 414-429.

Vollmer, C., et al. (2011) Naked metal nanoparticles from metal carbonyls in ionic liquids: Easy synthesis and stabilization, *Coordination Chemistry Reviews*, 255, 2039-2057.

Intense visible emission from ZnO nanoparticles synthesized via co-precipitation and hydrolysis methods

Y. ZHU[1,*], A. APOSTOLUK[1], B. MASENELLI[1], P. GAUTIER[2], A. VALETTE[2], S. DANIELE[2]
[1]Université de Lyon, F-69000 Lyon, France and INL, CNRS, UMR 5270, INSA Lyon, Villeurbanne, France
[2]Université de Lyon, F-69000 Lyon, France and IRCE Lyon, CNRS, UMR 5256, F-69626 Villeurbanne France

Zinc oxide (ZnO) has a variety of intrinsic defects, thus it can provide a wide emission spectrum ranging from the blue to IR. The reported high yields of the defect luminescence of the ZnO in the visible [Tang *et al.*, 2010; Felbier *et al.*, 2014] have stipulated the interest in the application of ZnO in the energy down-shifting systems and in the white light sources. Because of the fact that the synthesis conditions can be easily modified, two different sol-gel methods (co-precipitation and hydrolysis) at room temperature were used to synthesize ZnO nanoparticles (NPs). The nanoparticles were chosen as due to their high surface/volume ratio they are expected to possess an increased quantity of the defects emitting in the visible (like oxygen vacancies and zinc vacancies for example). We report the influence of different synthesis parameters (the nature of the solvent, the presence of additives or a surfactant and the reaction time) on the visible emission spectrum and the photoluminescence (PL) efficiency of the synthesized ZnO NPs. In particular, the LiOH addition in a non-polar solvent such as ethanol in the co-precipitation method and the polyacrylic acid (PAAH) at 0.63 wt % in the hydrolysis method play an important role in the enhancement of the visible emission efficiency, which can be as high as 20 %. However, the ZnO NPs obtained using the PAA are hardly dispersible in any solvent, which limits their future applications and the incorporation in the functional thin layers. Using the PAAH and PAANa in the hydrolysis method, dispersible ZnO NPs with the photoluminescent external quantum efficiency (EQE) of 25 % were obtained (by mixing the PAAH and PAANa at 50:50), when the reaction time was 1 hour. By extending the reaction time to 24 hours, the ZnO NPs with PAAH and PAANa grafted on their surface precipitate from the solution and their luminescent external quantum efficiency (EQE) is increased to more than 50 % and with time it can even rise up to over 70 %. In addition, the lengths of PAAH and PAANa chains and the ratio between the content of the PAAH and PAANa also influence the visible emission spectrum and the luminescent EQE of ZnO NPs. It is found that the highest visible luminescent EQE was obtained for the ratio of PAAH and PAANa of 50:50 and if at least one of them had a short chain length. When higher ratio of PAAH to PAANa or a longer length of the PAAH or PAANa chains was used, the emission spectrum of the ZnO NPs blue shifted from green-orange to the blue range and the luminescent EQE decreased. This study facilitates further exploration of new techniques to attain intense visible emissions from ZnO NPs and also paves the way for depositing the ZnO NPs thin layers by a simple and low-cost sol-gel method.

References:

Tang X. S., Choo E. S. G., Li L., Ding J., Xue J. M. (2010), Synthesis of ZnO Nanoparticles with Tunable Emission Colors and Their Cell Labeling Applications, Chem. Mater., 22, 3383-3388.

Felbier P., Yang J., Theis J., Liptak R. W., Wagner A., Lorke A., Bacher G., Kortshagen U. (2014), Highly Luminescent ZnO Quantum Dots Made in a Nonthermal Plasma, Adv. Funct. Mater., 24, 1988-1993

Influence of Processing Parameters on the Structure of Porous Metal Oxide – Cellulose Nanocomposites Prepared by Non-Solvent Induced Phase Separation

A.Wittmar,[1,2,*] M.Ulbricht,[1,2]
[1]Lehrstuhl für Technische Chemie II, Universität Duisburg-Essen, 45141 Essen, Germany
[2]NETZ – NanoEnergieTechnikZentrum, 47057 Duisburg, Germany
alexandra.wittmar@uni-due.de

Abstract: The preparation of metal oxide – cellulose nanocomposites with a predefined pore structure and homogenous dispersion of nanoparticles in the polymer matrix is still a challenge. The main reason is the poor solubility of cellulose in common solvents due to its strong intra- and intermolecular hydrogen bonding.

Several ionic liquids (IL), and especially the imidazolium based chlorides and acetates, due to their ability to break the hydrogen bonds, proved to be attractive candidates for cellulose solubilisation and processing. Additionally, many hydrophilic ionic liquids have been found to be very good media for the preparation of nanoparticle dispersions (Wittmar *et al.*; 2013, 2014). The downside of this approach is given by the high viscosity of the ionic liquids themselves, and, as consequence, the high viscosity of the resulting polymer solutions. This slows down dramatically the phase separation process, leading to polymer films with relatively low porosity.

The aim of the present work is to address advantages and disadvantages of several preparation routes for metal oxide – cellulose nanocomposites, using IL as cellulose solvents, and to clarify the relationships between the preparation method and the resulting pore structure and nanoparticle distribution. The focus of the study is on the influence of the processing parameters and especially on the possibilities to increase the solvent – nonsolvent exchange rate during the phase separation process.

The complex influence of the temperature at which the phase separation process takes place was evaluated for cellulose solutions in 1-butyl-3-methylimidazolium acetate, in absence and presence of a polar co-solvent with the role to decrease casting solution viscosity. Furthermore, the co-solvents influence on the nanoparticle dispersibility in polymer matrix was evaluated.

Temperature and co-solvent addition improve polymer solubilization and help controlling the phase separation by facilitating the mass transport.

Keywords: ionic liquids, non solvent induced phase separation, cellulose-based nanocomposites, porous nanocomposites

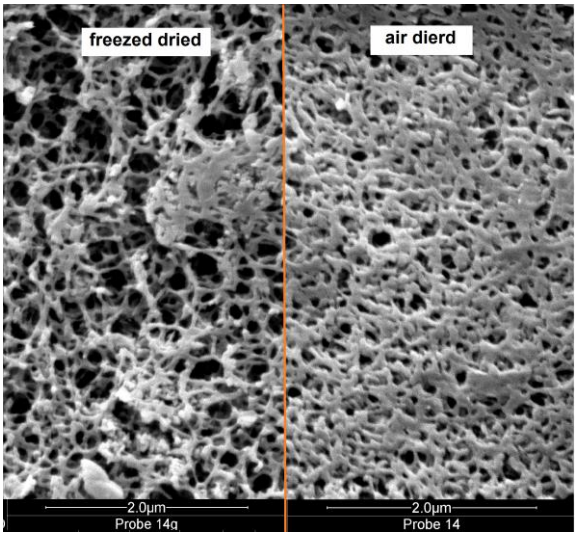

Figure 1: Electron microscopy images illustrating the important role played by the drying conditions onto the formation and consolidation of the porous structure of a cellulose acetate based nanocomposite prepared by phase separation from polymer solution in 1-buthyl-3- methylimidazolium acetate

References:

Wittmar A, Gajda M, Gautam D, Dörfler U, Winterer M, Ulbricht M, (2013) Influence of the cation alkyl chain length of the imidazolium-based room temperature ionic liquids on the dispersibility of TiO_2 nanopowders, *J. Nanopart. Res.* 15: 1463 - 1475

Wittmar A, Gautam D, Schilling C, Dörfler U, Meyer-Zayka W, Winterer M, Ulbricht M, (2014) Stable zinc oxide nanoparticles dispersions in ionic liquids, *J. Nanopart. Res.* 16: 2341 - 2355

Ultra-fast and controlled synthesis of Au-Iron Oxide hybrid nanocomposites using microfluidics

A.Larrea,[1*] V.Sebastian,[1,2] M.Arruebo[1,2], J.Santamaria[1,2]
[1] Department of Chemical Engineering. Institute of Nanoscience of Aragon (INA), University of Zaragoza, Zaragoza, Spain
[2] Research Center on Bioengineering, Biomaterials and Nanomedicine, CIBER-BBN, Madrid, Spain

Abstract: In recent years the production of nanocomposites involving magnetic and metallic elements has attracted much interest because of their potential applications such as drug delivery, tissue engineering, magnetic resonance imaging (MRI), cancer therapy, nanodiagnostics and catalysis (Sebastian et al., 2013).
Iron oxide nanoparticles are one of the magnetic nanoparticles widely used for biomedical applications, because of their low toxicity, chemical stability and biocompatibility (Calatayud *et al*., 2013). Moreover, the anchoring of gold nanoparticles to the surface of the iron oxide, improve their stability and increase their functionality, therefore the range of applications in which they can be used.
Precise control over the synthesis conditions and surface functionalization of magnetic nanoparticles is crucial because it governs their physicochemical properties, their colloidal stability and their biological behavior affecting their futures applications (Reddy *et al*., 2012).
Microfluidic systems are a powerful high-throughput tool to study and optimize a wide range of chemical reactions, and their use for the highly controlled nanoparticle synthesis have emerged in the last decade, offering multiple advantages over conventional synthesis method in which the reactor "batch" is used. These benefits include improvements in the crystallization process, good reproducibility and automation of the process. Laminar flow micro-reactors, however, are not enough suitable for the synthesis of nanoparticles with fast growth kinetics or where the presence of a specific reaction atmosphere is necessary. Segmented flow reactors are a good alternative, using an immiscible fluid (liquid or gas) to isolate the reagent segments. Key advantages of segmented flow include removing the dispersion, control of the reaction atmosphere and reduced reactor fouling (Nightingale *et al*., 2013).
We present a gas-liquid microreactor device as a powerful tool to fast synthesis of Au/iron oxide hybrid nanocomposites by controlling the reaction environment. We used a selected gas to form the iron oxide nanoparticles.Then, we have established a new approach to anchor the gold nanoparticles to the magnetic nanoparticles surface in a continuous fashion, a high yield and reproducible fabrication process. Pure and crystalline heterostructures (Au-Iron oxide nanoparticles), with magnetic and optic properties for use in biomedical and catalityc applications, were achieved in a time scale of 4 minutes. This reactor allows continuous flow and scale-up production keeping an excellent control over the synthesis.

Keywords: nanocomposites, magnetic nanoparticles, microfluidic reactors, segmented flow, continuous flow production, biomedical/catalityc applications.

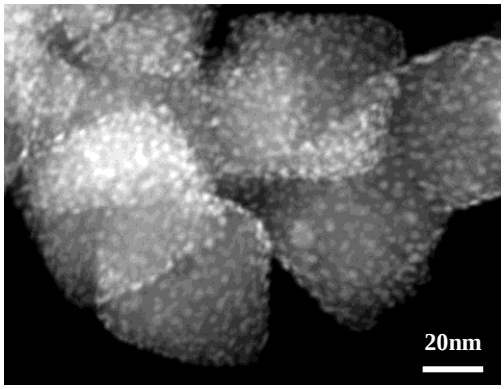

Figure 1: STEM-HAADF image of Au-Fe_3O_4 nanoparticles obtained using segmented flow microreactor

References:

Calatayud, M. P., Riggio, C., Raffa, V., Sanz, B., Torres, T. E., Ibarra, M. R., Goya, G. F. (2013). Neuronal cells loaded with PEI-coated Fe3O4 nanoparticles for magnetically guided nerve regeneration. *J.Mater. Chem. B*, *1*, 3607.

Nightingale, A. M., & Demello, J. C. (2013). Segmented flow reactors for nanocrystal synthesis. *Adv. Mater.*, *25*, 1813–21.

Reddy, L. H., Arias, J. L., Nicolas, J., & Couvreur, P. (2012). Magnetic nanoparticles: design and characterization, toxicity and biocompatibility, pharmaceutical and biomedical applications. *Chem. Rev.*, *112*, 5818–78.

Sebastian, V., Calatayud, M. P., Goya, G. F., & Santamaria, J. (2013). Magnetically-driven selective synthesis of Au clusters on Fe3O4 nanoparticles. *Chem. Commun*, *49*, 716–8.

Atmospheric Pressure Plasma for Nanomaterials : Production of Taylored Metal, Oxide and Polymer-coated nanoparticles by Discharge Filaments in Dielectric Barrier Discharges

J-P. Borra,[1*] N. Jidenko[1], J. Hou[2], A. Weber[2]
[1]*Laboratoire de Physique des Gaz et des Plasmas (CNRS –Université Paris Sud) F-91405*
Equipe Décharges Electriques et Aérosols, Supélec, France F-91192
[2]*Institute of Particle Technology, Technical University of Clausthal, Clausthal-Zellerfeld, Germany*

Abstract: This paper depicts a plasma process for the production of nano-particles in non-thermal atmospheric pressure. Such nanoparticles suspended in gases, also called aerosol with narrow size distribution are targeted for their size-dependant properties (Kodas and Hampden-Smith M. 1999).
Nucleated particles and subsequent 10-100nm agglomerates are produced in expanding vapors jets, usually produced by laser and spark discharges (1-100 mJ Gamaly, 2011 and Itina 2013).
Methods to induce non-thermal atmospheric pressure plasma filaments with lower energy per filament in (DBD 0.1-10µJ) are presented, in planar Dielectric Barrier Discharges with one or both electrodes covered by dielectric materials (alumina and polymers).
It is confirmed that the initial local vapor flux emitted from spots of interaction between plasma filaments and surfaces of different materials (Al_2O_3, Au, Ag, and Cu, Si, polymers) are reduced. Smaller primary particle density limits the local coagulation in the vapor plume (Borra et al.; 2015).Amorphous and crystalline pure metal primary nanoparticles with diameters below 5 nm are shown on Figure 1. Small agglomerates with diameters still below 5 nm are formed by agglomeration of these primary particles. Agglomeration happens at the end of the vapor jet expansion, as well as after the production during the transit between subsequent filaments in the DBD. The first step can be limited at reduced energy per filament by lowering the local vapor flux, while the second one depends on the transit time in the DBD.
Hence, such "low" energy plasma filaments (up to tens of µJ) efficiently lower the initial vapor flux to control the agglomeration. DBD were successfully tested for the production of tailored nanoparticles with tunable size and the same composition than the metal electrode. Similar results will be shown for oxides and polymer nanoparticles in bi-DBD.
Aerosol properties depend on the energy per filament and on materials properties. The energy yield of production (mol/J) is related to the inverse of melting enthalpies. The final size is controlled by plasma parameters and transit time in the DBD.
Hence, such plasmas can be used for the production of tailored particles with tunable size, composition and structure by plasma filaments to control the resulting properties of nano-powders and materials.

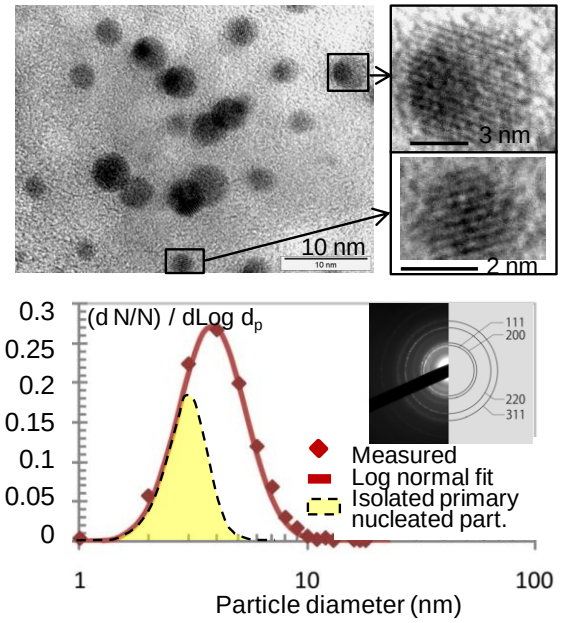

Figure 1: TEM micrograph, size distribution of gold particles (U_{pp}= 13 kV, g= 2.5 mm, transit time= 4 ms in N_2 Au-DBD with 1506 particles) with corresponding Small Angle Electron Difraction (SAED) figure of Au fcc crystalline structure.

This non-thermal plasma process may be used for nano-technologies, since it is performed at atmospheric pressure and can be used to reach size-dependant properties of nano-materials, without any precursor or solvent.

References:

Borra J.-P., et al (2015) Vaporization of metals into single-digit nanoparticles by non-thermal plasma filaments in DBD, *JAerosol Sc.*, **Vol. 79,** pp 109-125
Gamaly G.E. (2011) The physics of ultra-short laser interaction with solids, *Physics Reports* **508,** 91–243
Itina T.E., Voloshko A. (2013). Nanoparticle formation by laser ablation and spark discharges, *Appl. Phys B*, doi 10.1007//s00340-013-5490-6
Kodas T.T.& Hampden-Smith M.*Aerosol Processing of Materials* (New York: Wiley-VCH) (1999).

Nanolithography using thermal scanning probes

Stefan M. Weber
SwissLitho AG, Technoparkstrasse 1, CH-8005 Zurich, Switzerland

Abstract: We present a novel alternative to E-beam lithography in order to manufacture nanophotonic and nanoelectronic devices. The core of thermal scanning probe nanolithography (t-SPL) [1] is a heatable probe tip which is used for patterning and simultaneous inspection of nanostructures. The tip creates arbitrary, high-resolution nanostructures by local decomposition and evaporation of special resist materials. t-SPL is attractive due to the fact that no development and additional inspection steps are necessary in order to write nanostructures at 10 nm hp and even below. The direct 3D-writing capabilities that go beyond E-beam lithography use a closed-loop lithography scheme to reach a vertical resolution below 2 nm.

Since the proof-of-principle demonstrations of t-SPL in 2010 by IBM Research Zurich [2], the technology has seen tremendous progress. The breakthrough in patterning speed to match high-resolution Gaussian-beam E-beam lithography came in 2011 with patterning speeds up to 20 mm/s using only a single heated tip using resists like polyphthalaldehyde (PPA) [3]. In 2012, the high-speed imaging, in combination with the natural surface roughness of the polymer resist, was used to demonstrate position determination for stitching with 1 nm accuracy [4]. In 2014, a novel scheme employing the in-situ imaging and the detection of buried structures under the resist showed to be suitable for field overlays below 5 nm without the use of dedicated markers [5]. Compatibility with standard pattern transfer processes, like reactive ion etching, electroplating, or lift-off with a low line-edge roughness, and a resolution below 20 nm half-pitch [6] into semiconductors and metals has been recently demonstrated. Today, the first dedicated lithography systems for rapid prototyping applications based on this technology have been installed at universities in Europe and America by SwissLitho AG, a spin-off from ETH Zurich.

t-SPL also enables new possibilities for applications, e.g. for the fabrication of improved optical microcavities, or to create precisely defined Gaussian-shaped deformations in DBR mirrors where a strong lateral confinement while maintaining a cavity-Q of 10^5 is required [7]. Furthermore, the 3D-capabilities have been used to fabricate removable, 3D shape-matching traps for directed self-assembly, and the alignment and arbitrary placement of 25 nm x 80 nm-sized gold nanorods with 10 nm accuracy [8].

Thermal scanning probe nanolithography technology opens new possibilities for novel plasmonic-, nanophotonic- and nanoelectronic devices, in particular, where the accuracy of the distance between different functional parts of a device is crucial.

Keywords: 3D nanolithography, thermal scanning probe lithography, closed-loop lithography, pattern transfer, nanophotonics, plasmonics, nano-optics, micro-cavities, DBR mirrors, gold nanorods.

References:

[1] Garcia, R., Knoll, A. W., & Riedo, E. (2014) Advanced scanning probe lithography. *Nature nanotechnology*, 9(8), 577-587.

[2] Pires, D., et al., (2010). Nanoscale three-dimensional patterning of molecular resists by scanning probes. *Science*, *328*(5979), 732-735.

[3] Paul, P., et al., (2011). Rapid turnaround scanning probe nanolithography. *Nanotechnology*, 22(27), 275306.

[4] Paul, P., et al., (2012). Field stitching in thermal probe lithography by means of surface roughness correlation. *Nanotechnology*, *23*(38), 385307.

[5] Rawlings, C., et al., (2014). Nanometer control of the markerless overlay process using thermal scanning probe lithography. In *Advanced Intelligent Mechatronics (AIM), 2014 IEEE/ASME International Conference on* (pp. 1670-1675). IEEE.

[6] Wolf, H., et al., (2015). Sub-20 nm silicon patterning and metal lift-off using thermal scanning probe lithography. *Journal of Vacuum Science & Technology B*, *33*(2), 02B102.

[7] Ding, F., Stöferle, T., Mai, L., Knoll, A., & Mahrt, R. F. (2013). Vertical microcavities with high Q and strong lateral mode confinement. *Physical Review B*, *87*(16), 161116.

[8] Holzner, F., et al., (2011). Directed placement of gold nanorods using a removable template for guided assembly. *Nano letters*, *11*(9), 3957-3962.

A novel method for the preparation of poly(aminoacid) capped ultrasmall gold nanoclusters

I. Guryanov,[1,2,*] F. Polo,[3] S. Antonello,[3] F. Maran,[3] E. V. Ubyivovk,[4] E. Vlakh,[1,2] T. Tennikova,[1,2]
[1]St.-Petersburg State University, Laboratory of Biomedical Chemistry, St.-Petersburg, Russia
[2]Institute of Macromolecular Compounds RAS, St.-Petersburg, Russia
[3]University of Padova, Padova, Italy
[4]St.-Petersburg State University, Department of Physics, St.-Petersburg, Russia

Abstract: Nanoparticles (NPs) have an enormous potential for the construction and study of systems suitable for molecular recognition and self-assembly at the nanoscale. This is particularly true for possible applications in biomedicine, such as tissue engineering (Korzhikiov *et al.*; 2011), drug delivery (Becucci *et al.*; 2014), and medical diagnostics (Chikkaveeraiah *et al.*; 2012). In this contest, hybrid core/shell nanosystems based on gold nanoclusters capped with poly(aminoacids) could be particularly useful owing to their relatively easy preparation and functionalization, and the possibility of displaying bioactive molecular moieties in a controlled manner (Perego et al.; 2013). We have recently found that ultrasmall (1-1.6 nm) monolayer-protected Au_{144} nanoclusters (MPCs) easily undergo cellular uptake, show no toxicity, and once loaded with drugs display excellent properties as drug carriers (unpublished results). In this work we explored a novel method for assembling functionalized polymers on Au_{144} MPCs. The method consists in the direct polymerization of N-carboxyanhydrides using these MPCs as both supports and initiators of polymerization in order to create core/shell star-like platform as possible nanocarrier for different bioactive molecules (Scheme 1). To prepare gold nanoclusters containing free amino groups suitable to act as polymerization sites, the monolayer of preformed phenylethanethiolate-coated MPCs was modified via ligand place exchange using thiolated ligands carrying a Fmoc-protected amino-group. The number of exchanged ligands was calculated using NMR analysis. The so-obtained mixed monolayer gold nanoclusters were FMOC-deprotected and fully characterized by TEM, TGA, UV and electrochemistry, allowing us to verify that the gold core size was not affected by the above chemical steps. This communication will aslo describe the results obtained for the subsequent polymerization of N-carboxyanhydrides on the modified gold nanoclusters. The focus will be on the composition, structure, dispersity and stability of the so-prepared core/shell star-like nanostructures, as a function of the monomer to initiator ratio and the reaction temperature.

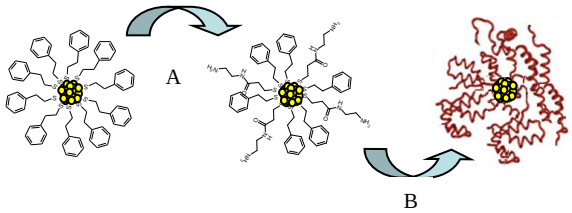

Scheme 1: Synthesis of core/shell star-like nanoparticles. (A) Ligand exchange reaction and preparation of the initiator of polymerization. (B) N-carboxyanhydride polymerization and polymer deprotection.

Keywords: gold nanoclusters, poly(aminoacids), N-carboxyanhydride, core/shell nanoparticles, biomaterials, polymerization, ligand exchange reaction, biomedical applications

References:

Korzhikov, V. A., Vlakh, E. G., Kasper, C., Tennikova, T. B. (2011) In vitro modeling of cell–scaffold interaction. *Rus. J. Bioorg. Chem.*, 37, 270–276

Becucci, L., Polo, F., Guidelli, R., Maran, F. (2014) Interaction of mixed-ligand monolayer-protected Au_{144} clusters with biomimetic membranes as a function of the transmembrane potential, *Langmuir*, 30, 8141-8151.

Chikkaveeraiah, B. V., Soldà, A., Choudhary, D., Maran, F., Rusling, J. F. (2012) Ultrasensitive nanostructured immunosensor for stem and carcinoma cell pluripotency gatekeeper protein NANOG, *Nanomedicine*, 7, 957-965.

Perego, D., Masciocchi, N., Guagliardi, A., Domìnguez-Vera, H. M., Gálvez, N. (2013) Poly(amino acid) functionalized maghemite and gold nanoparticles. *Nanotechnol.* 24, 075102

First-principles calculations of two BN plus two C stripes $B_xC_yN_z$ selected nanotubes

E. Ribas,[1] M. J. Piotrowski,[1] A. C. M Carvalho,[2] M. Machado[1*]
[1]Universidade Federal de Pelotas, Rio Grande do Sul, Brazil
[2]Universidade Federal de São Joal del Rei, Minas Gerais, Brazil

Abstract: Carbon boron nitride ($B_xC_yN_z$) nanotubes are realistic materials which are expected to present interesting properties associated with their stoichiometry, chirality, diameter, and atomic arrangement (Golberg *et al*., 2002). It is known that BCN nanotubes, with C and BN stripes parallel to the nanotube axis, possess high stability and that segregation of BN and C parts is favored (Zhang *et al.*, 2009; An *et al.* 2010). Finally, the different strain energies of the curved C and BN arcs in the nanotubes with parallely aligned stripes can generate ellipsoidal nanotubes (Machado *et al*., 2011). We report structural, energetic and electronic properties, via first-principles calculations, of armchair and zigzag BC_8N, BC_3N, $B_3C_4N_3$, and B_2CN_2 nanotubes composed by two diametrically opposed BN and C stripes. The eccentricity (*e*) was calculated for all studied systems and two different pattern were observed: distance between opposite C walls is (i) smaller or (ii) larger than the distance between opposite BN walls after geometric optimization. Higher *e* values (up to 0.52) were observed for the zigzag nanotubes, and this effect was attributed to the geometry of the nanotube and a so called *hinge* effect (Figure 1). Regarding the nanotubes stability, the order of importance was established as following: stoichiometry, number and type of chemical bonds, diameter, and cross section deformation. The band structure calculations revealed an energy gap ranging from zero to 1.2 eV. Projected density of states (PDOS) analysis have shown major contribution of C and N atoms at the highest occupied molecular orbital (HOMO) and C and B atoms at the lowest unoccupied molecular orbital (LUMO) for all systems. Finally, the local density of states (LDOS) calculations have shown that the HOMO (LUMO) for the armchair nanotubes is due to C atoms directly bonded to B (N) ones. On the other hand, for the armchair tubes, a diameter/stoichiometry dependence was observed. We understand that this study provides a better knowledge of this type of nanotubes. Also, new geometry configurations can be thought based on the alterations in the cross section of nanotubes, like triangular or squared shaped systems.

Keywords: carbon boron nitride, nanotubes, nanotechnology, first-principles calculations, cross section alteration.

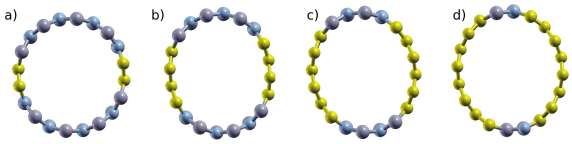

Figure 1: Pictorial scheme representing zigzag (10,0) nanotubes and the observed cross section alterations. The following stoichiometries are represented: a) B_2CN_2, b) $B_3C_4N_3$, c) BC_3N, and d) BC_8N.

References:

An., W., Turner, C. H. (2010) Linking Carbon and Boron-Nitride Nanotubes: Heterojunction Energetics and Band Gap Tuning, J. Phys. Chem. Lett. 1, 2269-2273.

Golberg, D., Dorozhkin, P., Bando, Hasegawa, M., Dong, Z.-C (2002) Semiconducting B-C-N nanotubes with few layers, Chem. Phys. Lett., 359, 220-228.

Machado, M., Kar, T., Piquini, P. (2011) The influence of the stacking orientation of C and BN stripes in the structure, energetics, and electronic properties of BC_2N nanotubes, Nanotechnology 22, 205706-205714.

Zhang, Z-Y., Zhang, Z., Guo, W. (2009) Stability and Electronic Properties of a Novel C-BN Heteronanotube from First-Principles Calculations, J. Phys. Chem. C 113, 13108-13114.

Control of inter (bi)metallic nanoparticular distances

F. Kameche[1,2*], A. Six[3,4], A.-T. Ngo[1,2], D. Kreher[3,4], F. Mathevet[3,4], A-J Attias[3,4], Caroline Salzemann, F. Charra[5], C. Petit[1,2]

[1] Sorbonne Universités, UPMC Univ Paris 06, UMR 8233, MONARIS, F-75005, Paris, France

[2] CNRS, UMR 8233, MONARIS, F-75005, Paris, France

[3] Sorbonne Universités, UPMC Univ Paris 06, UMR 8232, IPCM, F-75005, Paris, France

[4] CNRS, UMR 8232, IPCM, F-75005, Paris, France

[5] CEA/DSM/IRAMIS/SPEC, Centre de Saclay, F-91191 Gif-sur-Yvette Cedex, France

Abstract: Controlling the implementation of inorganic nanocrystals in bidimensionnal lattices, more particulary by controlling the distance between the nanoobjects is a real and present challenge in differents fields. For example, if magnetic nanoparticles are too close, we cannot change the magnetic moment of one nanoparticle but only a group of nanoparticle. With the high interest of nanoparticles developped during years, the chemical synthesis of nanoparticles is well known and well controlled. However, when deposited on a substrate, the interparticle distance are only directed by the surfactant. On the other hand, organic molecules can self-assemble on substrate like Highly Oriented Pyrollitic Graphite (HOPG) leading to 2D supramolecular networks (Bléger et al., 2007). If nanoporous networks are formed, they can be used at molecular sieves to trap guest molecules (Schull et al., 2006). Extending this results to trap nanoparticles is a good solution to have a real control of the nanocrystals organization.

Here, we first report the different ways to synthesize Pt and CoPt nanoparticles with a good control of size, shape and composition (Wikander et al.,2006; Demortière et Petit, 2007). These two materials are good candidates for catalytic applications. Moreover, CoPt is also known to possess magnetic properties (Demortière et Petit, 2007). Second, by using two kinds of organic matrices self-assembling into hexagonal or linear lattices we are able to fill nanopores with nanocrystals via simple drop casting.. and to control the type of 2D organization. Various microscopy techniques (electronic and scanning probe microscopy) have been used to characterize the nanoparticles and the self-assemblies,

Keywords: (Co)Pt nanoparticles, polyol synthesis, liquid-liquid phase transfert synthesis, self assembly at surfaces, TEM, SEM, STM, drop casting.

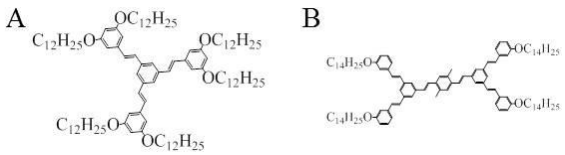

Figure 1: Molecule of (A) Tristilbene-3,5-C_{12} (TSB-3,5-C_{12}) and (B) 2C-C_{14}

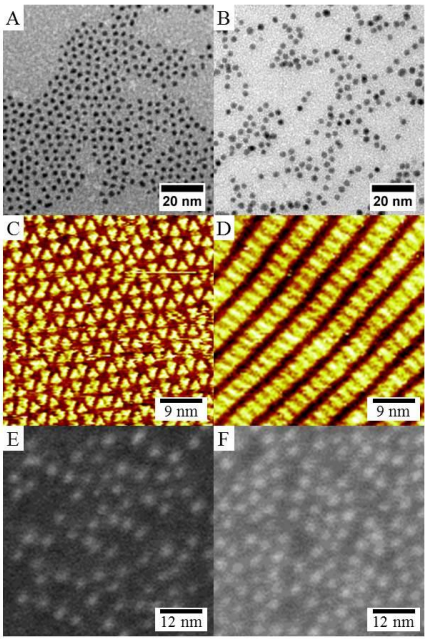

Figure 2: TEM images of platinum nanoparticles (A) and CoPt (B) synthesized via respectively liquid-liquid phase transfert and polyol process; . STM images of the self assembly on HOPG of (C) TSB-3,5-C_{12} and (D) 2C-C_{14}.SEM images of Pt nanoparticles deposited on HOPG (E) without and (F) with 2C-C_{14}.

References:

Schull, G., Douillard, L., Fiorini-Debuisschert, C., Charra, F., Mathevet, F., Kreher, D., Attias, A.-J. (2006), Single-Molecule Dynamics in a Self-Assembled 2D Molecular Sieve, *Nano Letters*, vol. 6, 1360-1363.

Wikander, K., Petit, C., Holmberg, K., Pileni, M.-P. (2006), Size Control and Growth Process of Alkylamine-Stabilized Platinum Nanocrystals: A Comparison between the Phase Transfer and Reverse Micelles Methods, *Langmuir*, 22, 4863-4868.

Demortière, A., Petit; C. (2007), First Synthesis by Liquid-Liquid Phase Transfer of Magnetic Co_xPt_{100-x} Nanoalloys, *Langmuir*, 23, 8575-8584.

Bléger, D., Kreher, D., Mathevet, F., Attias, A.-J., Schull, G., Huard, A., Douillard, L., Fiorini-Debuisschert, C., Charra, F. (2007) Surface Noncovalent Bonding for Rational Design of Hierarchical Molecular Self-Assemblies, Angew. Chem. Int. Ed., 46, 7404-7407

One pot microwave assisted synthesis of bisphosphonate alkene capped gold nanoparticles

Romain Aufaure,[1] Yoann Lalatonne,[1,2,*] Nicole Lièvre,[3] Olivier Heintz,[4] Laurence Motte[1] and Erwann Guénin[1,*]
[1]Université Paris 13, Sorbonne Paris Cité, Laboratoire CSPBAT, CNRS (UMR 7244), 74 avenue M. Cachin, 93017 Bobigny, France
[2]Department of Nuclear Medecine, Avicenne Hospital, Université Paris 13, Sorbonne Paris Cité, 125 rue de Stalingrad, 93009 Bobigny, France
[3]Université Paris 13, Sorbonne Paris Cité, UPRES 3410 Biothérapies Bénéfices et Risques, CNRS (UMR 7244), 74 avenue M. Cachin, 93017 Bobigny, France
[4]Université de Bourgogne, Laboratoire Interdisciplinaire Carnot de Bourgogne, CNRS (UMR 5209), 9 Avenue Alain Savary, BP 47870, 21078 Dijon Cedex, France

Abstract: Gold nanoparticles (GNPs) have proven to be a versatile platform for a large scope of applications, with potential use in numerous areas including: catalysis, optics and biology. Since the Turkevich study of 1951, the citrate capped GNPs are commonly used for a post functionalization by ligand exchange. Several molecules have been tested to replace citrate as reducing agent and stabilizer for one pot synthesis: carboxylic acids, amines, polysaccharides, thiophene derivatives and polymers.

Our project aims to develop new synthetic pathways for the direct synthesis of GNPs allowing easy access to functionalization. This is achieved by using synthesized (1-hydroxy-1-phosphonopent-4-enyl)phosphonic acid, presenting advantages of the well known bisphosphonate coating applied to colloidal gold instead of metal oxides (Figure 1). This molecules is bifunctional: Phosphonate group is able to both reduce gold(III) chloride and to coat the surface of the obtained GNPs. The terminal alkene group will remain inert during the NPs synthesis and will allow further chemoselective GNPs functionalization.

We have demonstrated the overall reaction mechanism and the interaction between our bisphosphonate compound and the gold surface by classical analytical chemistry techniques. Optimization of reaction pH has been assessed to yield homogeneous nanospheres of size ranging from 13-20 nm. Then reactions at the surface with the terminal alkene group have been characterized, confirming their chemoselective reactivity.

These new GNPs are also used as a building block for sized controlled covalent assemblies' preparation. The controlled size assemblies are water soluble and present specific optical properties shifting from blue to NIR absorption yielding to promising in vivo applications such as imaging probe and hyperthermia. We have also used similar phosphonated compound in a very recent work for hybrid nanostructures synthesis in aqueous media, enlarging the scope of applications.

Keywords: Gold nanoparticles, microwave, bisphosphonate, surface functionalization.

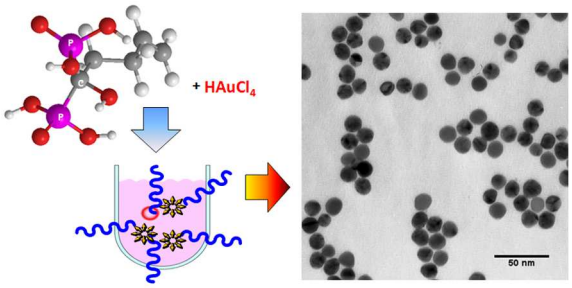

Figure 1: Microwave assisted synthesis of functionalized gold nanospheres.

Reference:

Aufaure, R., Lalatonne, Y., Lièvre, N., Heintz, O., Motte, L., Guénin, E. (2014), One pot microwave assisted synthesis of bisphosphonate alkene capped gold nanoparticles, *RSC Adv.*, 4, 59315

Novel Nano Rods of N-nicotinyl,N′,N″-bis(hexamethylenyl)Phosphorictriamide

Nasrin Oroujzadeh[1,*], Elham Delpazir[1]

[1]Institute of Chemical Technology, Iranian Research Organization for Science and Technology (IROST), Tehran, Iran

Abstract: Phosphoramides including -C(O)N(H)P(O)- moiety have received considerable attention due to their unique properties like anti-HIV, anti-HCV, antibacterial and anticancer drugs (Mehellou *et al*.; 2007). Nicotinamide, which is essential for the human body, plays a crucial role in biological oxidative chemistry (Mazzini *et al*.; 1995), (Magel *et al*.; 2001). With respect to the important properties and applications of phosphoramides and nicotinamide, we focused on phosphoramide compounds containing nicotinamide substituent group.

In this work, by using ultrasonic waves, nano particles (rods) of a new phosphoric triamide compound with formula $C_5H_5NC(O)NHP(O)(NC_6H_{12})_2$ were successfully synthesized (Figure1). After reaction between PCl_5 and nicotinamide and then one step oxidation, the product was reacted with proper amount of hexamethyleneimine in ultrasonic bath for 3 hours and then purified with solvent washing method. After that, the final purified product was fully characterized by SEM, (^{1}H, ^{13}C, ^{31}P) NMR, FT-IR and elemental analysis.

We expect this compound to show better biological activities than each of its ingredients. In addition, since nano scale materials have stronger and better properties due to their smaller size, we expect these new synthesized nano particles to show better biological and pharmacological activities in comparison to their macro size analogues; this subject is now under investigation with our team.

Keywords: Nano particles, Ultrasonic, Phosphoramide, Nicotinamide, Hexamethyleneimine.

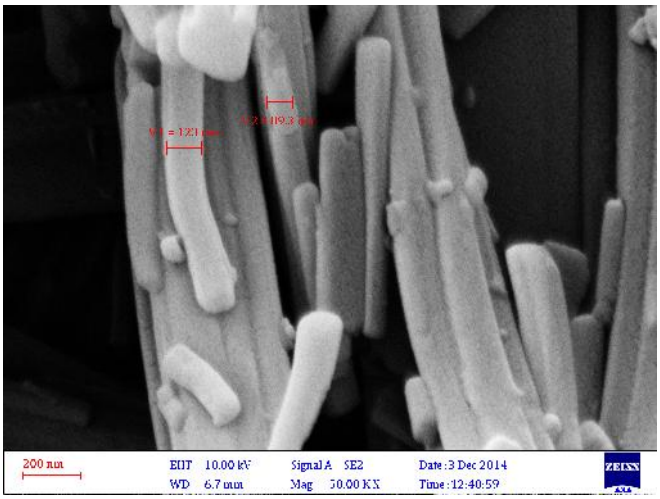

Figure 1: Morphology of the synthesized nano particles from SEM

References:

Magel, E.A., Hillinger, C., Wagner, T., Holl, W.(2001), Oxidative pentose phosphate pathway and pyridine nucleotides in relation to heartwood formation in Robinia pseudoacacia L , *Phytochem*, 57, 1061.

Mehellou, Y., McGuigan, C., Brancale, A., Balzarini, J. (2007), Design, synthesis, and anti-HIV activity of 2',3'-didehydro-2',3'-dideoxyuridine (d4U), 2',3'-dideoxyuridine (ddU) phosphoramidate "ProTide' derivatives, *Bioorg. Med. Chem. Lett.* 17, 3666.

Mazzini, S., Monderelli, R., Ragg, E., Scaglioni, L. (1995), Design, synthesis, and anti-HIV activity of 2',3'-didehydro-2',3'-dideoxyuridine (d4U), 2',3'-dideoxyuridine (ddU) phosphoramidate, *J. Chem. Soc. Perkins Trans* 2, 285.

Cross-linked PAN-based thin-film composite membranes for non-aqueous nanofiltration

Liliana Pérez-Manríquez, Jamaliah Aburabi'e, Pradeep Neelakanda, Klaus-Viktor Peinemann

Advanced Membranes and Porous Materials Center, King Abdullah University of Science and Technology (KAUST), 23955-6900 Thuwal, Saudi Arabia

Abstract: In this work, we present a new approach for the development of cross-linked PAN based thin film composite (TFC) membranes for non-aqueous application with perspectives toward new applications in harsh solvent environments.

The manufacturing method is easy to scale up. Polypropylene backed neat PAN membranes were fabricated by phase inversion process and cross-linked with hydrazine hydrate to get excellent solvent stability toward dimethylformamide (DMF). By interfacial polymerization a selective polyamide active layer was coated over the cross-linked PAN using N,N'-diamino piperazine (DAP) and trimesoyl chloride (TMC) as monomers. Permeation and molecular weight cut off (MWCO) experiments using various dyes were done to evaluate the performance of the membranes which showed excellent solvent stability toward DMF with a permeance of 1.7 L/m^2 h bar and a molecular weight cut-off of less than 600 Da.

Keywords:

Non-aqueous nanofiltration, Interfacial polymerization, Cross-linked Polyacrylonitrile.

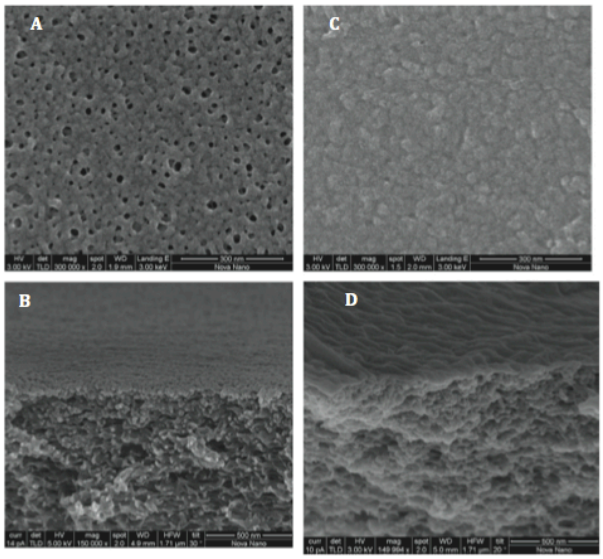

Figure 1. SEM pictures of surface and cross-section of the cross-linked PAN (A and B) and cross-linked PAN after surface modification with interfacial polymerization (C and D).

References:

Pérez-Manríquez,L;Aburabi'e,J; Neelakanda, P; Peinemann, K-V.Reactive & Functional Polymers 2014. doi:10.1016/j.reactfunctpolym.2014.09.015

Materials Aspects of AlSi + SiC Composites Foams Joining

J. Nowacki
Institute of Materials Science and Engineering
West Pomeranian University of Technology, Szczecin, Poland

Abstract: The cellular structure and unique properties of aluminum foams are the reason of their numerous applications and interests in respect of their joining (*Malekjafarian M. et al.*; 2012). The paper includes the characterization of the essence of microstructure, properties and application of aluminum and aluminum composite foams, the limitations, and possibilities of their joining. The aim of the research is the consideration of methods of welding, soldering and gluing AlSi foams and AlSi- SiC composite foams, and the joint structure. The possibility of joining AlSi9 foams and AlSi9-SiC composite foams using selected binding materials was confirmed, and higher tensile strength of the joint than the parent material was also ascertained. Preparing foam edges for joining requires that cutting products should be removed from its surfaces (Abolghasemi F. M. *et al.*; 2012). It is difficult on mickro and nano porous structures due to irregular shape of pores and limited access to them. Contrary to mechanical cleaning, chemical treatment yields satisfactory results. A varying size of soldering gap restricts uniform distribution of the solder and flux within the joint. The capillarity of the gap is much reduced or does not occur in the immediate vicinity of pores. In case of open pores, the flux penetrates into the foam, which means only a non-corrosive flux can be used. Foam porosity causes a substantial use of filler metal and flux as they escape deeper into the foam. Another essential restriction in Al foam soldering is lack of methodologies of testing the geometry of edges prepared for soldering, or that for testing mechanical properties. Besides, criteria for soldered joint acceptance are not available. Apart from problems resulting from foam structure, soldering aluminum is considered as a difficult process due to low melting point, high thermal conductivity and expansion, and a large shrinkage while aluminum cools down. A great affinity of aluminum for oxygen requires that aggressive fluxes be used to remove a layer of oxides Al_2O_3 from the specimen surface before soldering (Nowacki *et al.*; 2015). The process of Al foam flame brazing, due to non-uniform heating of macro-areas of a specimen, causes non-uniform distribution of brazing metal in the pores and foam structure strain due to partial melting of cell walls. This phenomenon does not occur in hot air soldering.

Keywords: Al foams joining, AlSi foams, microstructure and mechanical properties of AlSi foams joints, AlSi -SiC composite foams

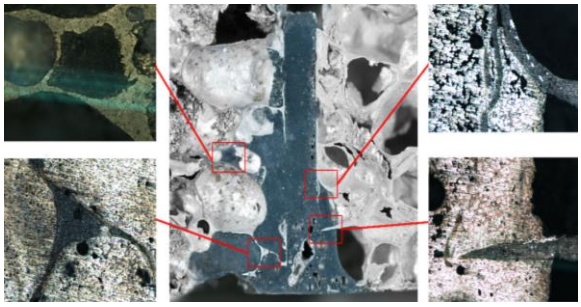

Figure 1: Al foam - Al foam brazed joint, Castolin FCW198 brazing metal, integrated macro- and micro- image

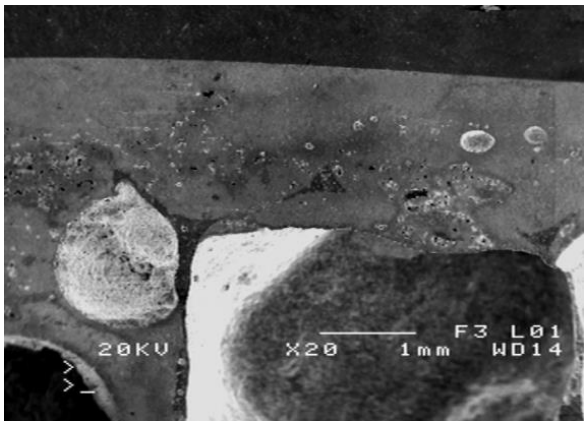

Figure 2: Al foam - Al sheet brazed joint, ZnAl22 brazing metal, macro- and micro- image. The microscopic image reveals melting and mixing of foam cell walls with filler metal and a visible pore not filled with liquid solder.

References:

Malekjafarian M., Sadrnezhaad S.K. (2012) Closed-cell Al alloy composite foams: Production and characterization, *Materials and Design* 42, 8–12

Abolghasemi F. M. Bordatchev E. V., Tutunea-Fatan O. R. (2012) An image-based methodology to establish correlations between porosity and cutting force in micromilling of porous titanium foams, *Int. J. Adv. Manuf. Technol*, 60, 841–851

Nowacki J. Moraniec K. (2015) Evaluation of Methods of Soldering AlSi and AlSi-SiC Particle Composite Al Foams, *J. of Materials Eng. and Perform.*
24, 426-433

Nanofunctionalization of alginate and alginate/GelMA crosslinked hydrogels by nanoliposomes and 3D construct

Rana Kadri[1], Bahar Aliakbarian[2,3], Laura Sanchez-Gonzalez[1], Ali Tamayol[2], Alireza Hassani Najafabadi[2], Ali Khademhosseini[2] and Elmira Arab-Tehrany[1,2]
Corresponding Author: elmira.arab-tehrany@univ-lorraine.fr
[1] Université de Lorraine, Laboratoire d'Ingénierie des Biomolécules, Nancy, France
[2] Center for Biomedical Engineering, Department of Medicine, Boston, USA
[3] Department of Civil, Chemical and Environmental Engineering (DICCA), University of Genoa, Via Opera Pia 15, 16145, Genova, Italy

Introduction

The hydrogels are 'soft' microscopic particles consisting of cross-linked polymeric molecules. They are valued for their functionality and ability to tune physical properties in industrial applications including controlled drug delivery, cosmetics, pharmaceuticals and tissue engineering. The overall goal of the proposed abstract is to functionalize the 3D hydrogel constructs from Alginate and GelMA by nano-liposome with and without active molecule (antioxidant).

Materials and Methods

The mixed solution of prepolymers was prepared in a way that the final alginate concentration was higher than 0.5% (w/v). The solution was directly injected in a beaker containing 2% $CaCl_2$ at a constant flow rate, where the fiber template was formed. A secondary crosslinking step was performed to create IPN fibers. The secondary crosslinking steps include UV exposure at 850 mW for GelMA, To functionalize the 3D hydrogel construct, the nanoliposome solution was prepared at 2% (w/w) marine lecithin with and without active molecule. The suspension was mixed for 4 h and then sonicated for 120 s (40 kHz, 40% of full power)[1]. 21,5 µl of prepared solution was added to hydrogels. The mechanical, biodegradability and morphological properties of functionalize and non-functionalize hydrogels were studied. We encapsulated the NIH 3T3 fibroblasts in this 3D scaffold and we functionalized this network by incorporation of nanoliposome. We assessed the viability of NIH 3T3 fibroblasts over time (7 days). All groups were made in triplicate (n=3).

Results

Figure 1a shows a morphological property of functionalized fiber fabricated from alginate:GelMA. The fiber was formed by wetspinning of the mixture in a $CaCl_2$ bath followed by 30 s UV illumination. We assessed the viability of NIH 3T3 fibroblasts during the fabrication process without nanoliposome (Fig. 1b). The results confirmed a high cellular viability after nanofunctionalization (Fig. 1c). The IPN fibers possess with nanoliposome has stronger mechanical characteristics in comparison to the hydrogel without nanoliposome. We showed by adding the nanoliposome from natural sources, the cells proliferation of NIH 3T3 increases.

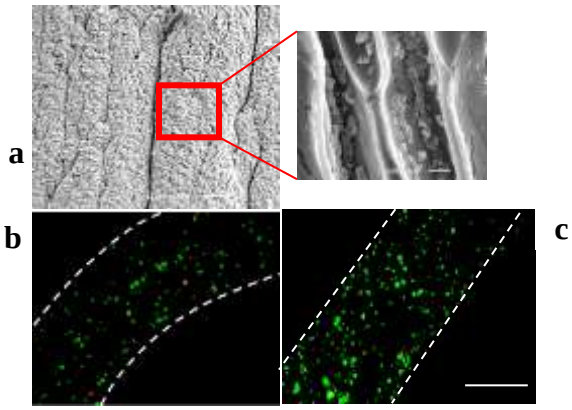

Fig. 1. (a) SEM images of 3D fiber; (b,c) cell viability during the fabrication process (green:live) with and without nanoliposome, respectively.

Discussion and Conclusions

A facile technique for fabricating hydrogel fibers is proposed which is compatible with a variety of hydrogels. The fabrication process does not affect cellular viability and activity. The presence of nano-soft particles (nanoliposome) from natural sources with and without active molecule improves the physico-chemical, mechanical and biological properties of 3D hydrogels.

References List references cited in text as

1. Arab Tehrany E., Kahn C. J.F., Baravian, C., Maherani B., Belhaj N., Wang X., Linder M. Colloids and Surfaces B. 95:75-81, 2012.

Session II - A: Nanomaterials Characterization and Tools

Simultaneous Topography and Electrochemical Imaging (SECM)

Gerald Kada[1], Shijie Wu[2], Christine Kranz[3]
[1]Keysight Technologies GmbH, Gruberstrasse 40, Linz, Austria
[2]Keysight Technologies Inc., 5301 Stevens Creek Blvd, Santa Clara, USA
[3]University of Ulm, Institute for Analytical Chemistry, Albert-Einstein-Allee 11, Ulm, Germany
gerald_kada@keysight.com

Abstract: Laterally resolved (electro)chemical information on a sample can be obtained with scanning electrochemical microscopy (SECM), where a biased ultra-microelectrode is scanned at a defined distance across the sample surface. However, conventional SECM suffers the lack of sufficient spatial resolution and the convolution of topography and electrochemical response due to the current-dependent positioning of the microelectrode.

Within the last decade several approaches have been reported, for directly integrating a micro- or nanoelectrode into an AFM probe. In order to maintain the functionality of both techniques, the integrated electrode is recessed from the end of the AFM tip. Consequently, the electrode is located at a defined distance to the sample surface, which is now defined by the length of the actual AFM tip. Thus, by applying a potential to this AFM-SECM probe and recording the Faradaic current related to electroactive surface processes, laterally resolved (electro)chemical information can be directly correlated to the topographical information obtained by the AFM measurement. So far, combining AFM with SECM required customized solutions, as no commercial SECM module for AFM systems was available and therefore the technology could only be used by a limited number of researchers.

Recently we have succeeded in bringing an SECM module onto a commercial AFM platform, providing a dedicated mount with integrated preamplifier for AFM-SECM probes and a bi-potentiostat, which allows to control the potential of the sample and the AFM tip-integrated electrode. This mechanism not only greatly minimizes the effort required for experimental setup, but also enables the capability of multifunctional imaging and surface modification with combined AFM-SECM modes. The advantage of the combined technique is that measurements are not limited to amperometry but can be extended to a multitude of electroanalytical techniques during AFM imaging. Several applications of this new SECM approach will be shown, starting from test structures up to redox-mediated membrane transport in cell membranes..

Keywords: scanning probe micoscopy, biosensors, electrochemistry, biorecognition

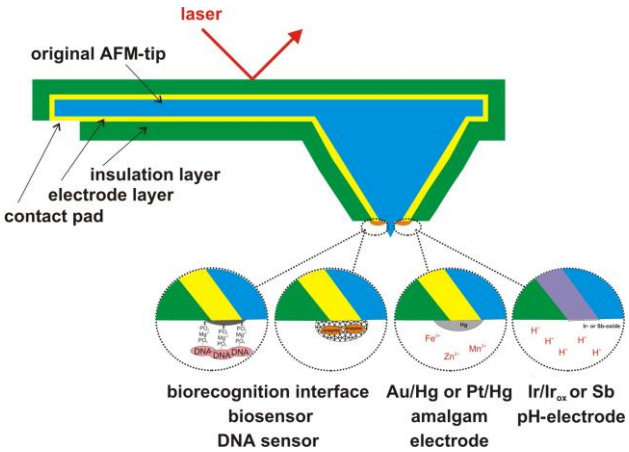

Figure 1: Applications of SECM using derivatized electrodes. Those electrodes can be modified with sensor layers or special electrode material for various nano-sensing opportunities in life science and material science.

References:

[1] C. Kranz, *Analyst*, **139** (2014) 336-352.
[2] J. V. Macpherson, P. R. Unwin, *Anal Chem*, **72** (2000), 276-285.
[3] C. Kranz, G. Friedbacher, B. Mizaikoff, A. Lugstein, J. Smoliner, E. Bertagnolli, *Anal Chem*, **73** (2001), 2491-2500.
[4] A. Kueng, C. Kranz, A. Lugstein, E. Bertagnolli, B. Mizaikoff, *Angew. Chem. Int. Ed*, **44** (2005), 3419-3422.
[5] C. Kranz, J. Wiedemair, *Anal Bioanal Chem*, **390** (2008), 239-243.
[6] S. Wu, *Keysight Technologies Datasheet* (2014), 5991-4525EN.

Copper nanoparticles: organization and stability

K. Ouadahi[1*], A. Courty[1]

[1]University of Pierre Marie Curie (UPMC), MONARIS laboratory, Paris, France

Abstract: Copper nanoparticles are of great interest because they are much cheaper than Ag or Au and they have very peculiar optical, electrical and thermal properties. Furthermore, nanosized Cu exhibits a prominent Localized Surface Plasmon Resonance (LSPR) in the visible range as Ag and Au. Nevertheless, a major drawback limiting the use of CuNPs is their tendency to oxidize. The literature on the synthesis of CuNPs of controlled size and shape is thus less developed than for Ag or AuNPs. In this context, we have developed a new synthetic route for spherical small copper nanoparticles (CuNPs) with size ranging from 3.5 nm to 11 nm and with an unprecedented associated monodispersity (<10%) (Courty *et al.* ; 2015). This synthesis is based on the reduction of an organometallic precursor ($CuCl(PPh_3)_3$) by ter-butylamine borane in presence of dodecylamine (DDA) at a moderate temperature (50 to 100°C). Because of their narrow size distribution, the CuNPs form long-range 2D and 3D organization at large scale. The wide range of CuNPs size is obtained by controlling the reaction temperature and DDA-to-copper phosphine salt ratio during the synthesis process (Figure 1). The addition of oleic acid (OA) after synthesis stabilizes the CuNPs (no coalescence) for several weeks under nitrogen atmosphere. We have studied their stability under air either in solution or after deposition on a solid substrate. We show that their organization induces greater stability against oxidation compared to the same nanocrystals when dispersed in solution. The present results are evidenced by transmission electron microscopy (TEM and HR-TEM), UV-Vis and IR spectroscopies and X-ray diffraction. The presentation focuses on the fabrication and the stability study of isolated or organized copper nanoparticles.

Keywords: copper nanoparticles, organization, optical properties.

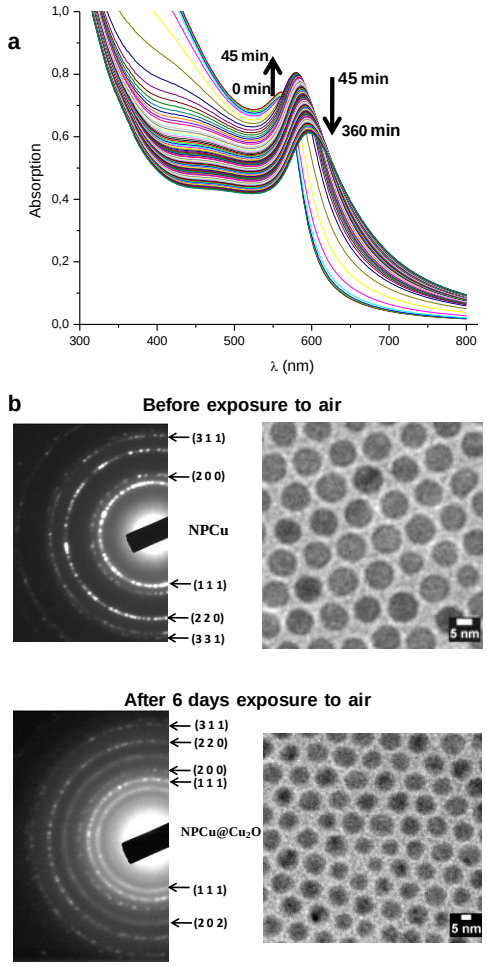

Figure 1: stability under air of copper nanoparticles: a) organized, b) isolated (dispersed in hexane)

References:

Ali Ben Aissa, M., Tremblay, B., Andrieux-Ledier, A., Maisonhaute, E., Raouafi, N., Courty, A., Copper nanoparticles of well-controlled size and shape: a new advance in synthesis and self-organization, *Nanoscale*, 2015, 7, 3189 – 3195.

Improved spectral imaging ellipsometry for nanoscale solid-liquid interface investigations

A. Miranda, P. A. A. De Beule
Applied Nano-Optics Laboratory, International Iberian Nanotechnology Laboratory, Braga, Portugal

Abstract: Ellipsometry is a widely applied technique for the characterization of thin films in nanotechnology (Azzam, 1977; Fujiwara 2005). We present an improved hardware design for spectroscopic imaging ellipsometry investigations at the liquid-solid interface (Figure 1) with vastly improved noise levels for ellipsometry angle determination (Figure 2). We achieve this by altering the illumination pathway of a commercial spectroscopic imaging ellipsometer (nanofilm_ep3_se – EP3, Accurion GmbH, Göttingen, Germany) consisting of a fibre coupled Xenon arc lamp ligh source with a customized white-light laser assembly comprising a supercontinuum fibre laser (EXB-6, NKT Photonics, Birkerod, Denmark) integrated with a multi-line diode laser system (IBeam Smart, Toptica Photonics, Gräfelfing, Germany) providing five laser lines between 350nm and 450nm. Further noise level reduction are obtained by the design of a new sample holder compatible with water dipping objectives (40x, CFI APO NIR, Nikon, Japan). We present and discuss newly obtained performance characteristics for spectroscopic imaging ellipsometry, whereby achieved noise level reductions allow for improved metrology of thin films at the solid-liquid interface. As an example, we apply our new set-up for the study of supported lipid bilayers.

Keywords: ellipsometry and polarimetry, thin films, optical constants, metrology.

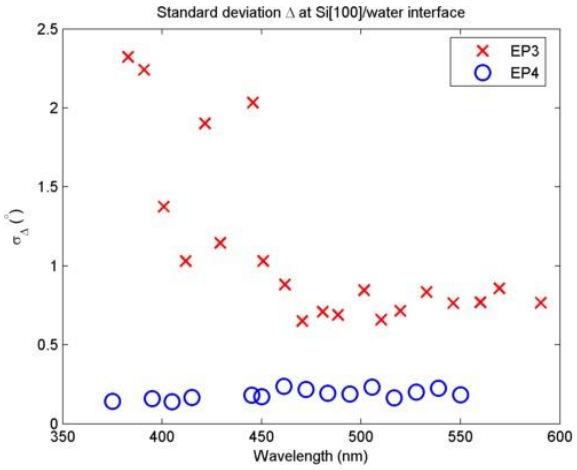

Figure 2: Standard deviation for ellipsometry Δ angle determination with spectroscopic imaging ellipsometry at a Si[100]/H_2O solid-liquid interface with a broadband Xe light source (EP3) and customized laser illumination system (EP4).

References:

Azzam, R. M. A., & Bashara, N. M. (1977). Ellipsometry and Polarizd Light. Amsterdam: *Elsevier Science Publishing Company, Inc*.

Fujiwara, H. (2005). Spectoscopic ellipsometry: principles and applications. Tokyo: *Maruzen Co. Ltd*

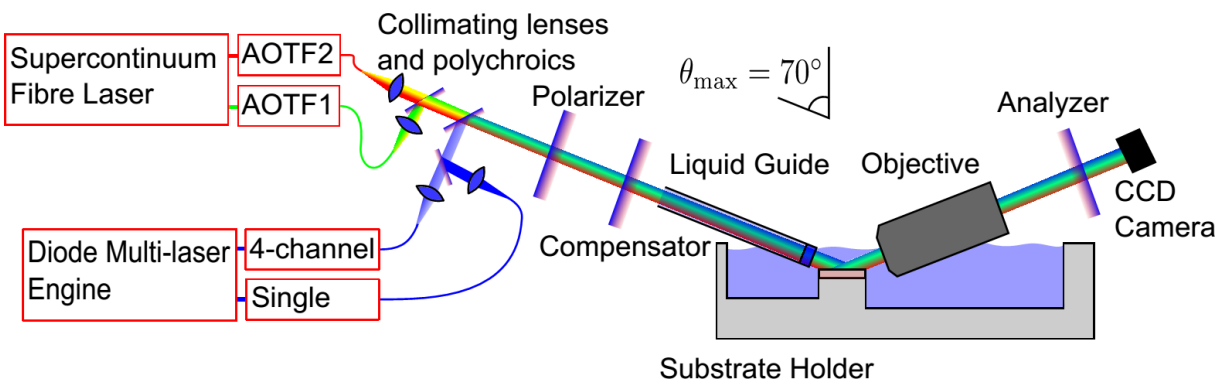

Figure 1: Spectroscopic imaging ellipsometry set-up (EP4) optimized for measurements at the solid-liquid interface.

Quantitative ellipsometric measurements of single micro-objects

D. Lyutov, S. Hadjiiski, G. Tsutsumanova, S. Russev
Department of Solid State Physics, Faculty of Physics, University of Sofia, 5 James Bourchier blvd., Sofia 1164, Bulgaria

Abstract: Ellipsometry is a well-known method for examination of bulk materials, solid state structures and thin films. It is very sensitive to the optical properties and structure of the sample in the direction normal to its surface. However, the conventional ellipsometry has low resolution in the sample surface plane. Several techniques can be used to improve the lateral resolution – focusing ellipsometry (Ye *et al.*, 2007), imaging ellipsometry (Asinovski *et al.*, 2008), scanning near field ellipsometry (Karageorgiev *et al.*, 2001). Although some of them allow quantitative measurements, their accuracy is lower than that of the conventional ellipsometry.

A technique for measurement of the ellipsometric angles of single micro-objects is presented. The experimental setup used allows only light reflected from the examined object to be detected. The sample is embedded in immersion oil and is sandwiched between a glass prism and a glass substrate (Figure 1). The influence of the diffraction effects on the optic response for micro-objects is addressed both theoretically and experimentally by means of comparison with macro objects with identical refractive index and thickness. The aim of this work is to demonstrate that ellipsometric measurements of micro-objects with accuracy comparable to that of the conventional ellipsometry are possible. Tests are made to estimate the repeatability, accuracy and the potential for local measurement of this ellipsometric configuration.

Keywords: ellipsometry, micro-objects, optical properties

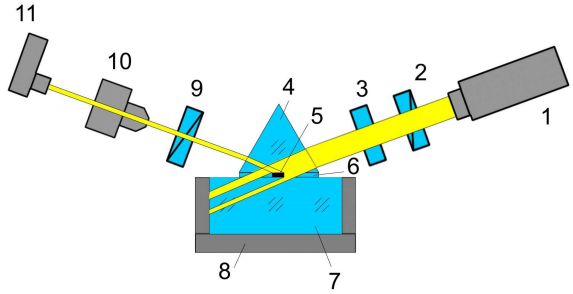

Figure 1: Scheme of the configuration of the ellipsometric device. 1- light source, 2 – polarizer, 3 – compensator, 4 – glass prism, 5 – examined micro-object, 6 – immersion oil, 7 – glass substrate, 8 – stage, 9 – analyzer, 10 – microscope optical system, 11 – photodetector

References:

Ye, S. H., Kwak, Y. K., Kim, S. H., Cho, H. M., Cho, Y. J., Chegal, W. (2007), Development of a focused-beam ellipsometer based on a new principle, *Aip Conf Proc*.931,69-73.

Asinovski, L., Beaglehole, D., Clarkson, M. T. (2008), Imaging ellipsometry: quantitative analysis, *Phys Status Solidi A*.205,4,764-771.

Karageorgiev, P., Orendi, H., Stiller, B., Brehmer, L. (2001), Scanning near-field ellipsometric microscope-imaging ellipsometry with a lateral resolution in nanometer range, *Appl Phys Lett*.79,11,1730-1732.

blueDrive™ photothermal excitation for fast, reliable and quantitative AFM

A. Labuda, J. P. Cleveland, N. Geisse, S. Hohlbauch, M. Kocun, R. Proksch,
I. Revenko, M. Viani, D.A. Walters.
Asylum Research, an Oxford Instruments Company, Santa Barbara, California, 93117.
aleks.labuda@oxinst.com

Since the advent of atomic force microscopy, cantilevers have predominantly been driven by piezo actuators for AC imaging and data acquisition. However, parasitic resonances of the AFM hardware, known as the "forest of peaks"[1], cause problems in all environments, ranging from viscous fluids[2], to water[3], air[4], and even vacuum[5].

AFM signals acquired with piezo-driven cantilevers reflect changes in the cantilever response *and* the piezo response. This reduces the accuracy of quantitative AFM studies, and may couple conservative and dissipative forces. Furthermore, it is well known that small high-frequency cantilevers enable faster AFM imaging; however, the forest of peaks prevents reliable cantilever tuning at high frequencies because piezo resonances tend to become more jagged and problematic as the drive frequency increases. The reliability of the AFM is also compromised because the forest of peaks changes with temperature and time, especially in liquids.

Photothermal excitation is a high frequency method for exciting a cantilever by heating/cooling the base of the cantilever. Photothermal excitation results in a repeatable and accurate cantilever transfer function that is time- and temperature-stable, resulting in stable imaging in liquids (see Figure) and dependable use for temperature-dependent studies. Because the driven transfer function represents the true cantilever transfer function, blueDrive ensures more accurate quantitative AFM experiments: the AFM signals stem from tip-sample interactions, rather than piezo resonances. Also, smaller cantilevers can be photothermally excited with large amplitudes for fast AFM imaging.

Our recent developments in perfecting photothermal excitation and its benefits to the AFM community will be discussed in this talk. To date, we have demonstrated reliable photothermal operation in air and fluid environments using a broad range of imaging techniques, such as AM-AFM (Tapping), FM-AFM, Contact Resonance, AMFM viscoelastic mapping.

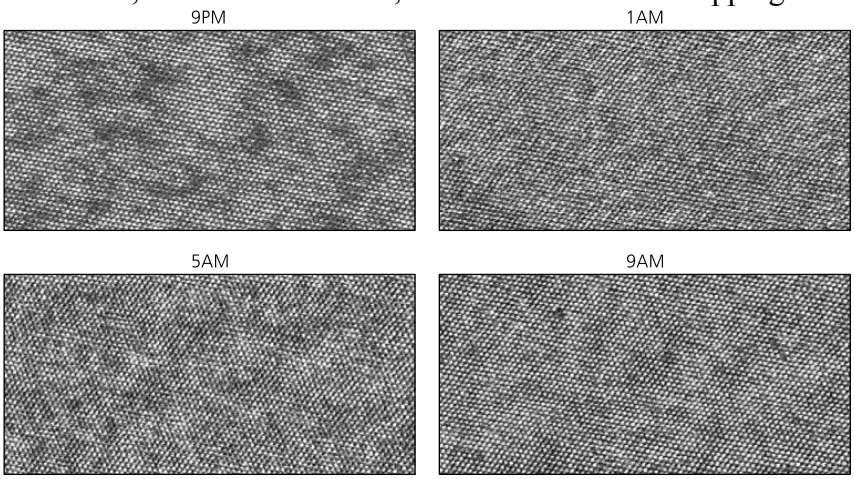

Figure: Unassisted overnight scan of the water/mica interface, measured by AM-AFM. Note the atomic resolution throughout the whole experiment, and point defect in the last image at 9AM.

References:
[1] T. E. Schaeffer, J. P. Cleveland, *et al*., J. Appl. Phys. **80**, 3622 (1996)
[2] A. Labuda, K. Kobayashi, Y. Miyahara, P. Grütter. Rev. Sci. Instrum. **83**, 053702 (2012)
[3] A. Labuda, K. Kobayashi, *et al*., AIP Advances **1**, 022136 (2011)
[4] R. Proksch and S. V Kalinin, Nanotechnology **21**, 455705 (2010)
[5] A. Labuda, Y. Miyahara, *et al*. Phys. Rev. B **84**, 125433 (2011)

On-chip characterization and sorting of engineered nanomaterial surface properties by real-time affinity monitoring

C. Desmet, A. Valsesia, S. Muldur, V. Spampinato, G. Ceccone, P. Colpo, F. Rossi
European Commission Joint Research Centre, Institute for Health and Consumer Protection, NanoBioScience Unit, Ispra, Italy.

Abstract: In the context of the extensive use of engineered nanomaterials (ENMs) in consumer products, industrial applications and nanomedicine, there is an important need of new methods for an exhaustive characterization of their physico-chemical properties. Among them, surface hydrophobicity is considered as an important property since it has a critical role in various processes such as protein adsorption, interaction with biological membranes or cellular uptake potentially related to an increase in toxicity, immune response, or haemolytic effect. Hence, it has been demonstrated that the ENMs hydrophobicity is a key factor to be controlled, in particular for nanomedicine applications [1,2,3].

Furthermore, the few existing processes dedicated to the full characterization of ENMs involve different techniques, which make it expensive and highly time-consuming. In this work we developed an inexpensive characterization process thanks to a disposable chip connected to an optical reader. The device proposed here enables the sorting of ENMs according to their hydrophobicity and surface charge, together with the characterization of their size and shape. The detection platform is based on the use of a micropatterned surface with tuned surface properties to bind ENMs selectively by hydrophobic forces and electrostatic interactions (Figure 1). The surface modifications were realized using different plasma coatings and layer-by-layer deposition of two types of polyelectrolytes, providing a broad range of combinations of surface hydrophobic groups and dissociable charged groups. The real-time absorption of ENMs on the differently functionalized microareas is monitored by a microscope-coupled camera, providing also ENMs characterization in terms of size distribution and shape. It gives information on the kinetics of adsorption, related to the affinity of the ENMs for the different surfaces. A microfluidic chamber coupled to a high-precision peristaltic pump enables the controlled dispensing of the ENMs on the detection platform. The key advantage of the device is the increase of the characterization throughput thanks to the all-in-one characterization process and the multiplexing that is able to replace the use of different methods and expensive equipment. In this way, the full characterization of ENMs could be expanded in all the areas covering nanomaterial-related applications.

Keywords: nanoparticles characterization, nanoparticles hydrophobicity, engineered nanomaterials, nanomedicine application.

References:

1. M. C. Jones *et al.* (2014) *Journal of Controlled Release*, 183, 94–104.
2. S. E. Mc Neil (2009) *Wiley Interdisciplinary Reviews: Nanomedicine and Nanobiotechnology*, 1, 264–271.
3. F. Shima *et al.* (2013) *Biomaterials*, 34, 9709-9716.

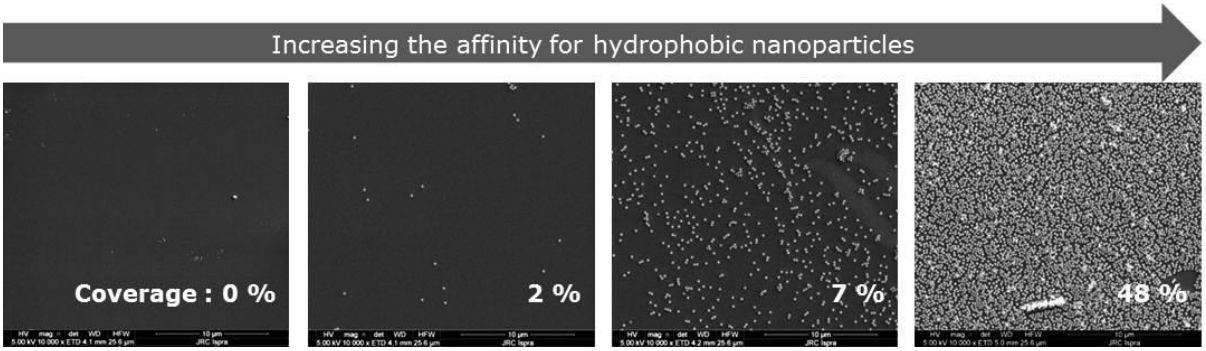

Figure 1. Hydrophobic particles sorting on surfaces with tuned properties (SEM images)

HPLC Optimization for Clotrimazole Assay in Microemulsion and Microemulsion-Based Gel

P. Boonme,[1,2*] J. Kaewbanjong,[1,2] T. Amnuaikit,[1] E.B. Souto[3]
[1]Department of Pharmaceutical Technology, Faculty of Pharmaceutical Sciences, Prince of Songkla University, Songkhla, Thailand
[2]Nanotec-PSU Center of Excellence on Drug Delivery System, Songkhla, Thailand
[3]Department of Pharmaceutical Technology, Faculty of Pharmacy, University of Coimbra, Coimbra, Portugal
*Corresponding author: prapaporn.b@psu.ac.th

Abstract:
Topical antifungal drugs are widely used to avoid systemic adverse effects and to directly deliver the drugs to the infection sites; however, conventional dosage forms have difficulty to effectively reach the target due to barrier function of the stratum corneum. Novel formulations such as microemulsions (MEs) and microemulsion-based gels (MBGs) are useful for topical drug delivery due to their skin penetration enhancement, production facilities and good appearance (Souto *et al*., 2011). To assay the drug concentration in these novel formulations, a quantitative analysis with high sensitivity has to be carried out. This study aimed to validate a high performance liquid chromatography (HPLC) method for fast measurement and quantification of clotrimazole loaded in a ME and a MBG. The HPLC method was modified from a previous report (Hoogerheide *et al*., 1981). In this study, a C18 column (5 μm, 150x4.6 nm) was used. A mixture of methanol and 0.025 M potassium dihydrogen phosphate (75:25 v/v) was a mobile phase. The flow rate was controlled at 1.0 ml/min. The injection volume was 10 μl and the wavelength detector was fixed at 254 nm. The data were integrated with the RF 10A (version 1.1) LC software program. Clotrimazole standard solutions were prepared at 0.3, 0.6, 0.9, 1.2 and 1.5 mg/ml in the mobile phase. Validation of the method was performed according to International Conference on Harmonisation (ICH) guidelines (Commission of European Communities, 1996). ME was prepared by simply mixing 20% w/w isopropyl palmitate, 20% w/w Tween 80, 20% w/w Span 80, 13.33% w/w isopropanol and 26.67% w/w water. Clotrimazole ME was prepared by dissolving 1% w/w the drug in ME. Clotrimazole MBG was prepared by adding 5% w/w fumed silica in clotrimazole ME (Kaewbanjong *et al*., 2014). Before assay, the 1 g clotrimazole ME was extracted with 10 ml absolute ethanol by vigorously shaking and filtering to obtain the HPLC sample. The 1 g clotrimazole MBG was extracted with 10 ml absolute ethanol by mixing in tightly closed container, heating the mixture at 50°C in water bath for 5 min, shaking to room temperature after removing from water bath, cooling in a methanol-ice bath for 15 min, centrifuging and collecting the supernatant. The residue in the centrifuge tube was repeatedly extracted with 10 ml absolute ethanol by the identical steps. The first and second extractions were mixed to obtain the HPLC sample (Hoogerheide *et al*., 1981). It was found that the retention time of clotrimazole was about 8.5 min and no interferences were observed. Calibration curve was in the linearity. Mean recoveries were 99.03-100.33% and mean coefficients of variation were 0.1298-0.6636% for intraday and 0.1366-1.1554% for interday. Limit of detection and quantification were calculated as 0.005 and 0.010 mg/ml, respectively. Drug concentration in the ME and MBG were 9.66±0.03 and 9.84±0.07 mg/g which were equal to 91.73±0.27% and 102.30±0.74% labeled amount, respectively. This analytical method was found to be suitable to determine clotrimazole concentration in both ME and MBG. However, the data of our preliminary study suggested that the extraction process had to be carefully performed to avoid alcohol loss via evaporation. Overall, it could be concluded that this modified HPLC method was optimized for quantitative assay of clotrimazole in novel formulations, i.e., ME and MBG. These formulations can be further used for treatment of skin fungal infection.

Keywords: clotrimazole, HPLC, ICH, microemulsion, microemulsion-based gel.

References:

Commission of European Communities. (1996) Validation of analytical procedures. *Proceedings of International Conference on Harmonisation (ICH)*.

Hoogerheide, J.G., Strusiak, S.H., Taddei, C.R., Townley, E.R., Wyka, B.E. (1981) High performance liquid chromatographic determination of clotrimazole in pharmaceutical formulations. *J. Assoc. Off. Anal. Chem.*, 64(4), 864-869.

Kaewbanjong, J., Amnuaikit, T, Boonme, P. (2014) Formulation and characterization of clotrimazole microemulsions and microemulsion-based gels. *Int. J. Nanosci.*, 13(4), 1440005.

Souto, E.B., Doktoraovava, S, Boonme, P. (2011) Lipid-based colloidal systems (nanoparticles, microemulsions) for drug delivery to the skin: materials and end-product formulations. *J. Drug Del. Sci. Tech.*, 21(1), 43-54.

Structural characterization of DPPC nanosized liposomes by optical and cryo-electron microscopy: interactions with bovine serum albumin

Rachana[1,2,*] J. Bellare[1], and R. Banerjee[1]
[1]Department of Biosciences & Bioengineering, Indian Institute of Technology Bombay, Powai, Mumbai, Maharashtra, India
[2]Department of Biotechnology, JayPee Institute of Information Technology, Sector-62, Noida, Utter Pradesh, India

Liposomes have been widely used for drug delivery. Whether, it is the case of studying the surfactant system of lungs or designing a liposomal drug delivery system, it is important to characterize liposomal preparations, ensuring their functionality. As, shapes, sizes and aggregation patterns of liposomes are correlated with their functions (Goerke, 1998), present study is an attempt to characterize the model liposomal preparations of dipalmitoylphosphatidyl choline (DPPC), morphologically and functionally (surface activity, *in vitro*), in presence and absence of, albumin and "blood serum", which may be present in the lung alveoli in case of: Adult Respiratory Distress Syndrome (ARDS) *etc*. (Holm et al, 1985; Rachana et al, 2004). Liposomes may also interact with various blood components while in systemic circulation during drug delivery, affecting their half-life and functionality. In the present study, bovine serum albumin (BSA) and serum were allowed to interact with DPPC liposomal preparations and were observed under optical and, cryo-TEM.Results have shown increase in size (from 50-100nm to ~200nm) and many morphological changes in their aggregation patterns such as: liposome engulfing, piling up (figure1) and rosette formation. No intact liposomal structures were observed on incubation with serum under optical microscope and very rare, 100-150nm liposomes were observed under cryo-TEM. Adsorption in the presence of albumin reflected an improvement in adsorption of DPPC liposome and the surface tension obtained at 1 sec of adsorption was reduced to 52.2 ± 0.9 mN/m,against 68mN/m (for pure DPPC) and to 49.8 ± 0.4 mN/m against 61 mN/m, after 30 min. However, if serum is also present at the site of delivery, the functionality of the liposomal preparation might be compromised and therefore, it should be carefully dealt with, while designing drug delivery system for diseases like, trauma induced ARDS.

Key words: Lung surfactant, DPPC liposomes, albumin and lung surfactant, nano liposomes

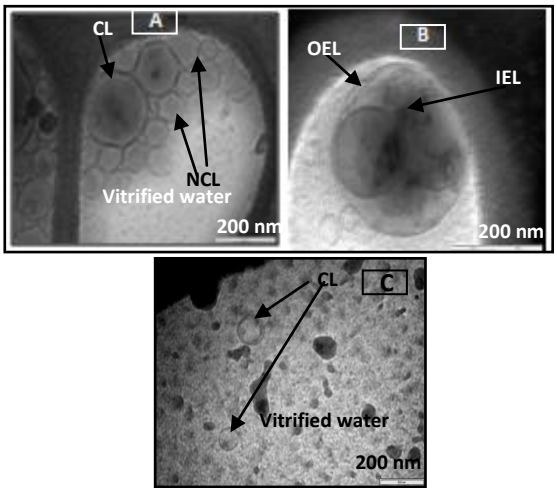

Figure 1: A: cryoTEM for Pure DPPC liposomes; B: With albumin, C: With serum, describing the morphological changes induced due to interaction of albumin with
DPPC liposomes. Albumin treatment causes an increase in size and engulfment of smaller liposomes by bigger liposomes (OEL = outer extended liposome, IEL = Inner engulfed liposome, CL = circular liposome, NCL = non circular liposome)

References:

Holm, B. A., Notter, R. H. and Finkelstein, J. H., (1985), Surface property changes from interactions of albumin with natural lung surfactant and extracted lung lipids, *Chem. Phys. Lipids*, 38, 287-298.

Goerke, J., (1998), Pulmonary surfactant: function and molecular composition, *BBA*, 1408, 79-89.

Rachana and R. Banerjee, (2004) , Interaction between hematological derivatives and dipalmitoylphosphatidylcholine: implication in Adult Respiratory Distress Syndrome,*Colloids Su*

Nanometer scale characterizations of InGaN nanorods grown on GaN template

Y. EL Gmili,[1*] S. Sundaram,[1] R. Puybaret,[1,2] X. Li,[1,2] P. L. Bonanno,[1,2] C. Pradalier,[1,2] P. L. Voss,[1,2] J.P. Salvestrini,[1] and A. Ougazzaden,[1,2]

[1]CNRS, UMI 2958 Georgia Tech - CNRS, 57070 Metz, France

[2]Georgia Institute of Technology, UMI 2958 Georgia Tech - CNRS, 57070 Metz, France

[3]Universite de Lorraine, Supelec, LMOPS, EA4423, 57070 Metz, France

Abstract: The tunability of the fundamental bandgap of indium gallium nitride (InGaN) across the full visible range spectrum has led to the development of a variety of optoelectronic devices including blue, green, red and white light-emitting diodes (Zhang *et al.*; 2011), blue and green laser diodes (Hsu *et al.*; 2012, and Zhang *et al.*; 2013), and solar cells (Matioli *et al.*; 2011, and Lang *et al.*; 2011). For this, thick, high-quality, and In-rich InGaN material is required. However, whatever the approach used (MQW, bulk layer), strain relaxation results in high density of dislocations, which usually act as nonradiative recombination centers and sources of leakage current paths in III-nitride thin films, and/or lead to phase separation. A possible solution to overcome this issue and prevent strain-related degradation of InGaN material is nano selective area growth (NSAG), which exploits 3D relaxation effects to release strain without creation of dislocations, leading to higher indium incorporation and thickness of the InGaN layer. It would also allow the reduction of the piezoelectric effect thanks to the growth along nonpolar or semipolar directions.

In this paper we study the NSAG of thick In-rich InGaN nanorods and nanostripes on GaN/Sapphire templates. First, a 100nm thick negative-tone resist is spin-coated on the GaN substrates by physical vapor deposition. The resist is patterned using an electron-beam lithography system. The part of the resist exposed to the electron beam cross-links into SiO_2. At last, TMAH etching treatment is used to open the nano-patterns (nano-holes and nano-stripes). The diameter of each circular opening is 100nm and the size of the stripe openings is $10x0.1\mu m^2$. A 150nm thick InGaN epilayer was then grown on these patterned templates using MOVPE.

As an example, Fig. 1 a) and b) show SEM images of perfectly selective InGaN nanostructures with excellent hexagonal shapes and smooth semipolar facets in nanorods and irregular triangular r-plane facet formation on the two elongated hexagonal pyramid in nanostripes. Fig. 1 c) shows cathodoluminescence (CL) measurements at low temperature (LT) in planar InGaN, and single InGaN nanostripe and nanorod, respectively. Single luminescence peak centered around 535nm was obtained for the InGaN nanorod instead of an emission peaks with two components for the planar InGaN, centered at 420nm and 520nm, and 464nm and 525nm for the nanostripe. For the whole set of structures, we can also notice a broad luminescence band centered around 590 nm which is attributed to the GaN defect band. In the planar InGaN, the presence of the two luminescence bands can be attributed to the presence of strained and relaxed InGaN sublayers (EL Gmili et al.; 2014), whereas the two luminescence bands observed in the nanostripe might be attributed to two different regions InGaN1 and InGaN2 due to different growth orientations. The indium content can be calculated according to the work of (Orsal et al.; 2014). The In content of the strained and fully relaxed sublayers of planar InGaN are 12% and 21%, respectively. In the nanostripe, the In composition of the two layers are 14% and 21%, whereas in the nanorod only one InGaN phase with 22% of In is revealed. For the same growth condition, the In incorporation in the nanorods is a little larger than in the nanostripes and almost twice as high as in planar InGaN. Further structural and optical characterization of these InGaN nanostructures will be presented.

Keywords: InGaN material, NSAG, SEM and CL.

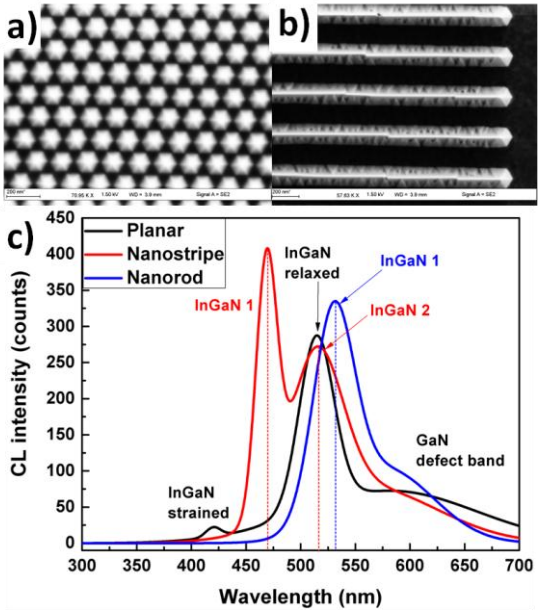

Figure 1: SEM images of InGaN nanostructure arrays grown on GaN/sapphire templates in a) circular opening and b) stripe opening, c) CL spectra at LT (77K) in planar InGaN, and single InGaN nanostripe and nanorod.

References:

Zhang, J., and Tansu, N. (2011), *J. Appl. Phys.*, 110. 113110.
Hsu, P.S., et al. (2012), *Appl. Phys. Lett.*, 100. 021104.
Zhang, J., and Tansu, N. (2013), *IEEE Photon. J.*, 5. 2600111.
Matioli, E., et al. (2011), *Appl. Phys. Lett.* 98. 021102.
Lang, J.R., et al. (2011), *Appl. Phys. Lett.* 98. 131115.
Orsal, G., et al. (2014), *Opt. Mater. Express.*, 4(5) , 6587.
EL Gmili, Y., et al. (2014), *Acta. Mater.* 61(17) , 6587.

Picodiagnostics of Nanomaterials Local Atomic Structure: X-Ray Absorption Spectroscopy and Computer Modeling Synergy

A. Soldatov,* A. Kravtsova, K. Lomachenko, M. Soldatov, A. Bugaev, O. Polozhentsev
Southern Federal University of Russia, Smart Materials Research Center, Rostov-on-Don, Russia

Abstract Method for extraction of 3D local atomic and electronic structure parameters on the basis of combination of x-ray absorption spectroscopy theoretical analysis including multidimensional fitting and ab-initio computer modeling is presented. Applications of this method to several families of nanoparticles including bare and doped by rare earth metals Fe3O4 nanoparticles for bio-medical applications, Cd and Zn chalcogenides based colloidal semiconductor quantum dots are presented. Nanoscale local atomic structure determines most of unique properties of novel nanostructured materials without long range order. To study its fine details one has to use both precise experimental methods (like x-ray absorption spectroscopy) and advanced theoretical simulations. Synergy of these two methods opens a route for picodiagnostics. The status of modern theoretical analysis of the experimental x-ray absorption spectra allows extracting atomic structure parameters with a precision of 1 picometer even for materials without long range order. This technique could be used in-situ and in time-resolved mode. The method for extracting of the 3D atomic structure parameters on the basis of advanced quantitative analysis of X-ray absorption near edge structure (XANES) has been tested for several different families of nanoparticles. The possibility to extract information on both bonding angles and bond lengths is demonstrated.

The results obtained by this method for some classes of nanostructured objects are presented: Bare and doped by rare earth metals Fe_3O_4 nanoparticles for bio-medical applications and Cd (Zn) chalcogenides based colloidal semiconductor quantum dots.

Recent ab initio quantum computer modeling of colloidal quantum dots based on CdS(Se) and ZnS(Se) as well as rare-earth metals-doped quantum dots made it possible to study the features of the atomic and electronic structure of semiconductor colloidal quantum dots of different size, and evaluate the effect of the impurity atoms [2]. Theoretical modeling also proved the sensitivity of XANES for verification of nanoscale atomic structure parameters determined by computer simulation for small quantum dots and to determine the parameters of the local environment of the impurity atoms inside the quantum dot.

In the same way the DFT computer modeling of Fe_3O_4 nanoparticles doped with rare-earth metal atoms and simulations of XANES for both initial and "relaxed" structures around impurity atoms inside the nanoparticle also shows the sensitivity of XANES for verification of nanoscale atomic structure parameters determined by computer simulation and thus, one find a way to determine the parameters of the local environment of the impurity atoms in the Fe_3O_4 nanoparticles of the basis of XANES fitting, proposed previously [1].

Keywords: picodiagnostics, local atomic structure, semiconductor quantum dots, magnetic nanoparticles, dopping, x-ray absorption spectroscopy, DFT simulations, biomedical applications.

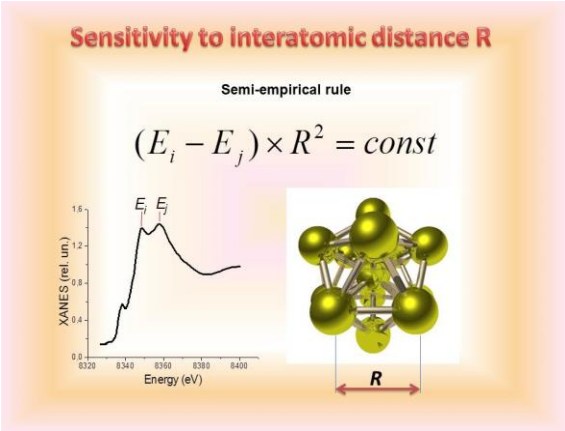

Figure 1. Illustration of high sensitivity of x-ray absorption spectroscopy to small variation of interatomic distances.

References:

1. Grigory Smolentsev, Alexander V. Soldatov (2007), FitIt: new software to extract structural information on the basis of XANES fitting, *Computational Materials Science*, 39 , 569-.

2. A.N. Kravtsova, K.A. Lomachenko, S.A. Suchkova, I.A.Pankin, M.B. Fayn, A.L.Bugaev, A.V. Soldatov, Dopped Quantum Dots of CdTe Family, *Bulletin of the Russian Academy of Sciences. Physic*s, 2015 , in Press

Optical and Structural Characterizations of Phase Transition in Nanoscale Peroskite $CH_3NH_3PbI_3$

Huizhen Wu,* Weiguang Kong, Zhenyu Ye
Department of Physics and State Key Laboratory of Silicon Materials,
Zhejiang University, Hangzhou, Zhejiang 310027, P.R. China
**E-mail:hzwu@zju.edu.cn*

Abstract: Organic-inorganic perovskites are newborn optoelectronic materials and show promising applications in both solar cells and lasers. A breakthrough on the methylammonium lead iodide ($CH_3NH_3PbI_3$, denoted as $MAPbI_3$) perovskite has been reported recently: the energy conversion efficiency of the hybrid perovskites photovoltaic devices reached ~19.3% (Zhou, 2014). Moreover, the $MAPbI_3$ has become even promising in application in lasing (Xing,2014). However, up to now little work regard to the the structure-dependent luminescence and the underlying physical mechanisms of this perovskite material has been reported. Little consensus was reached on optical transitions of band to band, defects and interface related effects because of insufficient experimental data. Besides, the previous studies mainly considered the optical properties of the $MAPbI_3$ in a single phase without analyzing the change of crystalline structures. Therefore, comprehensive understanding of the optical properties of $MAPbI_3$ is urgent in order to expand the fields of application for $MAPbI_3$. Moreover, it will help to improve the performance of perovskite-based solar cells.

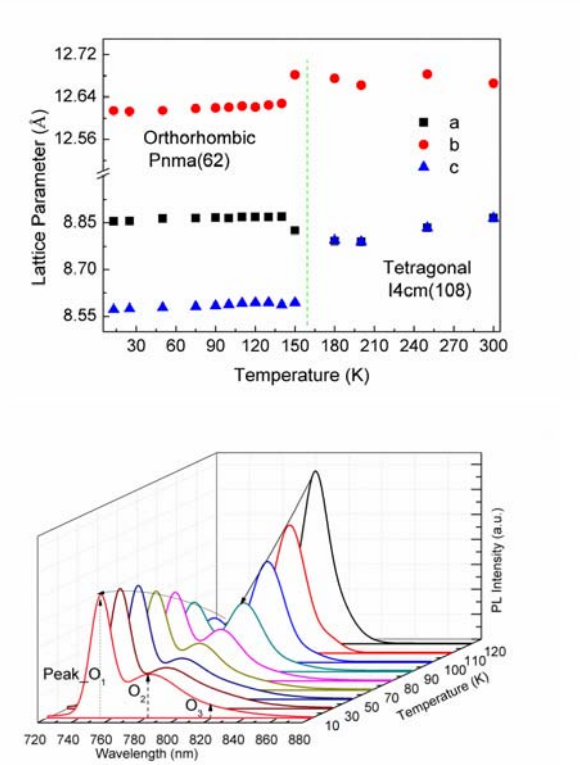

Figure 1: Refined lattice parameters determined by the low temperature XRD (Top). PL spectra of the $MAPbI_3$ perovskite-crystal at variable temperatures, the arrows indicate the evolution tendency of the luminescence intensity (Bottom).

In this work, phase transition in $MAPbI_3$ crystal is explored by the combination of variable-temperature X-ray diffraction (XRD) and steady photoluminescence (PL) with variable excitation power and time resolved PL. Variable temperature XRD results show phase transition of tetragonal-orthorhombic takes place at ~150K, instead, mixture of the two phases are still observable at 130K, which reveals the phase transition in $MAPbI_3$ is a gradual process. Steady and time resolved PL unambiguously reveals the existence of intermediate zone of the two phases. Two luminescence features observed in orthorhombic phase originate from free excitons and donor-acceptor pair (DAP) transitions, respectively. The observed DAPs are formed by the vacancies of iodine and lead in the orthorhombic phase. The phase transition phenomenon is further interpreted by time resolved PL characterization at low temperatures. Our results highlight the understanding of optical properties upon phase transition in $MAPbI_3$ and will be benefit to future optoelectronic devices.

Keywords: organic-inorganic perovskites, phase transition, x-ray diffraction, photoluminescence.

References:

Zhou, H., Chen, Q., Li, G., Luo, S., Song, T. B., Duan, H. S., Hong, Z. R., You, J.B., Liu,Y.S., and Yang,Y. (2014) *Science*, **345** (6196), 542-546.

Xing, G. C., Mathews, N., Lim, S. S., Yantara, N. X., Liu, F., Sabba, D., Gratzel, M., Mhaisalkar, S., and Sum, T. C. (2014), *Nature Materials*, **13** (5), 476-480.

An Investigation of Sb_2Te and $Ge_2Sb_2Te_5$ Phase Change Memory Film Properties Deposited by Pulsed Laser Deposition

S. Emami Khansari,[1] M. Hoffman,[1]
[1]School of Material Science and Engineering, University of New South Wales, Sydney, Australia

Abstract:
Phase change materials (PCMs) are promising candidates for the next generation of non-volatile memories. In this study, Sb_2Te and $Ge_2Sb_2Te_5$ (GST), as the two promising materials for phase change random access memory (PCRAM) application, were deposited by pulsed laser deposition (PLD). The effects of laser energy density and substrate temperature were investigated to obtain optimized deposition condition by reducing the size and number of the particulates as well as the obtaining closer stoichiometry to the targets.

The morphology and topography of the films' surface were studied by scanning electron microscopy (SEM) and atomic force microscopy (AFM). Energy dispersive spectrometry (EDS) was also used to identify the elemental composition of the deposited films and the crystalline structure of the films was investigated by x-ray diffraction (XRD) analysis. The results of SEM and AFM indicate that increase of laser energy density from14 mJ/cm^2 to 21 mJ/cm^2 substantially decreases the size and number of particulates in the surface of the Sb_2Te films as well as the roughness of the particulate free areas. However, in case of GST, the laser energy density does not significantly affect the size and number of the particulates on the surface.

XRD results show that Sb_2Te and GST films deposited at substrate temperature of 20℃ are amorphous; with increasing the substrate temperature the Sb_2Te films crystallize to a hexagonal structure with preferred orientation while the GST films first crystallize to a FCC structure and then with further increase of temperature the crystalline structure changes to hexagonal.

Keywords: phase change memory, pulsed laser deposition, $Ge_2Sb_2Te_5$, Sb_2Te

Advanced Transmission Electron Microscopy of Epitaxial-Enabled Morphology Controling ITO NWs

O .I.Lebedev,[1,*] S. Turner,[2] Y. Shen[3], T. Wu[4]
[1]Laboratoire CRISMAT,UMR 6508, CNRS ENSICAEN, F-14050 Caen, France
[2]EMAT, Department of Physics, University of Antwerp, B-2020 , Antwerpen, Belgium
[3]Division of Physics and Applied Physics, Nanyang Technological University, Singapore 637371
[3]Materials Science and Engineering, King Abdullah University of Science and Technology, Thuwal 23955, Saudi Arabia

Abstract: Controlling nanowire morphology in bottom-up synthesis and allowing the assembly of nanowires on planar substrates is of tremendous importance for device applications in electronics, photonics, sensing and energy conversion. To date, there has however been only limited success in reliably achieving these goals, hindering both the fundamental understanding of the growth mechanism and the integration of nanowires in real-world technologies. We will show an impact of the transmission electron microscopy (TEM) as an extremely versatile and powerful technique.

Novel dual-metal Au-Cu alloy nanoparticles were used as a catalyst for tin-doped indium oxide (ITO) nanowire growth. The enhanced mobility of the catalyst nanoparticles (NPs) enables *in situ* seeded growth of branched ITO nanowires (NWs) [1]. The dynamically tuned chemical potentials in the catalyst NPs selectively stabilize a rare cubic indium-tin-oxide phase (ISO), forming epitaxial heterojunctions within individual NW branches. This methodology of selecting phases and forming compositionally abrupt axial heterojunctions in NWs departs from the conventional synthesis routes, giving unprecedented freedom to navigate phase diagrams and promising novel nanomaterials and devices

Here we report that growth of planar, vertical and randomly oriented ITO nanowires can be realized on yttria-stabilized zirconia (YSZ) substrates via the vapor-liquid-solid (VLS) mechanism, by simply regulating the growth conditions, in particular the growth temperature. TEM and reciprocal space mapping experiments reveal the indispensable role of substrate-nanowire epitaxy in the growth of oriented planar and vertical nanowires at high temperatures, whereas randomly oriented nanowires without epitaxy grow at lower temperature [2]. Further control of the orientation, symmetry and shape of the nanowires was achieved through use of YSZ substrates with (110) and (111), in addition to (001) surfaces. Based on these insights, we succeeded in growing regular arrays of planar ITO nanowires from patterned catalyst nanoparticles.

Overall, our discovery of unprecedented orientation control in ITO nanowires advances the general VLS synthesis, providing a robust epitaxy-based approach towards rational synthesis of nanowires.

Keywords: ITO nanowires, advanced TEM, morphology control, phase stabilization.

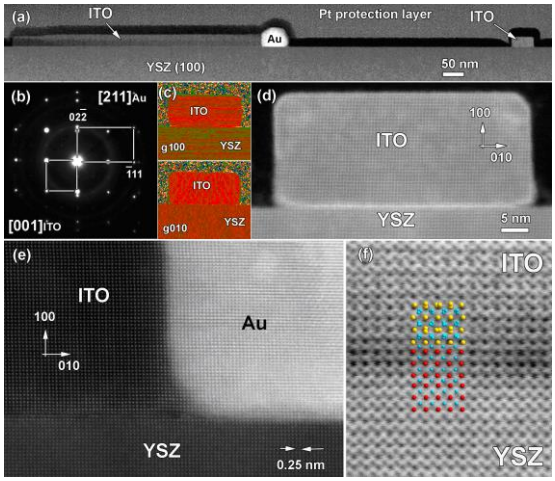

Fig.1 (**a**) Low-magnification STEM-HAADF image of the in-plane nanowires and (**b**) corresponding SAED pattern (**c**) GPA patterns along [100] and [010] directions. (**d**) HR STEM-HAADF cross-section image of ITO nanowire.(**e**) STEM-HAADF image of the tri-junctions of the ITO, YSZ and Au particle. (**f**) STEM-ABF image of ITO / YSZ interface with overlayed structural model

References:

[1] J.Gao, O.I.Lebedev, S.Turner, Y.F. Li, Y.H.Lu, Y.P.Feng, P.Boullay, W.Prellier, G.Van Tendeloo, T.Wu (2012) Selective phase stabilization and epitaxial axial heterojunctions in branched oxide nanowires *Nano Letters* **12(1)** 275-280
[2] Y. Shen, S.Turner, P.Yang, G.Van Tendeloo, O.I.Lebedev, T. Wu (2014) Epitaxy-Enabled Orientation Control in Tin-doped Indium Oxide Nanowires *Nano Lett.* **14** 4342-4351

Dynamic Characteristics of Carbon Nanotube Based Nano-composites with Atomic Vacancy and Stone-Wales Defects

Sachin O. Gajbhiye[1*] S. P. Singh[1]
[1]Department of Mechanical Engineering, Indian Institute of Technology Delhi,
Hauz Khas, New Delhi 110016, India

Abstract: A unique atomic structure of carbon nanotube unveils outstanding properties. This makes it potentially highly valued reinforcing material to strengthen composite materials. But, the presence of defects in the nanostructure substantially alters the material's properties. So, the static and dynamic characteristics of carbon nanotube based nanocomposites subjected to atomic vacancy and Stone-Wales defects are studied using nonlinear representative volume element. The carbon-carbon bond of nanotube is modeled using Tersoff-Brenner potential. The H110MA grade polypropylene is used as matrix material and its properties are tested in the laboratory which are further used to model it. The interaction between nanotube and polymer matrix is modeled using nonlinear spring elements in the presence of defects in reinforcing material. These interactions are represented by Lennard-Jones potential. The atomic vacancy and Stone-Wales defects are created in the atomic model of the nanocomposite material. In the designed representative volume element, the nanotube is surrounded by the matrix material from all direction as shown in Figure 1. It is observed that the presence of defect in the nano-structure significantly alter its static and dynamic characteristics when they are used alone but when it is dispersed in the matrix material the influence of defects in negligible.

Keywords: Carbon nanotube, Nanocomposites, Representative volume element, Atomistic vacancy defect, Stone-Wales defect, Tersoff-Brenner potential.

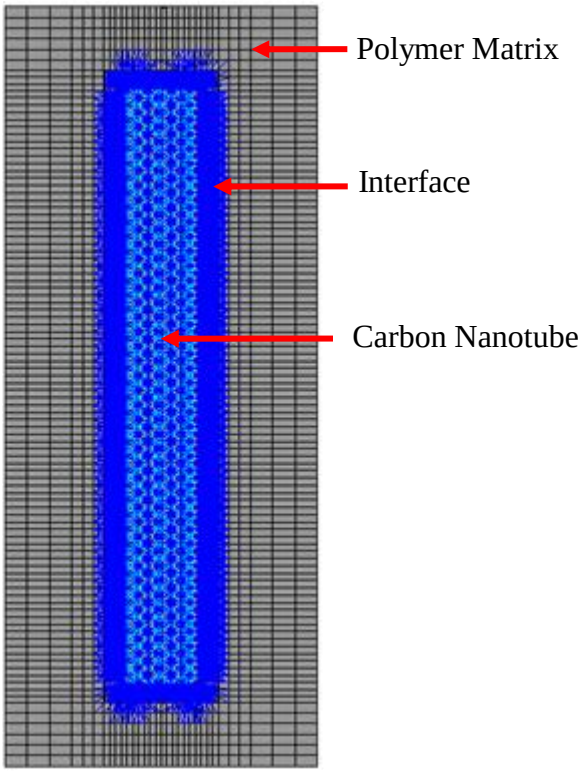

Figure 1. Representative volume element

Figure 1 shows the representative volume element of the nanocomposite material. The carbon nanotube is surrounded by the polymer matrix from all direction. Clearance is maintained amongst the carbon atoms of nanotube and polymer matrix which is equal to the equilibrium distance between carbon atoms of these two materials. The interface region is modelled using Lennard-Jones potential.

Multi-scale characterization of chitosan-nanoemulsion blended film

R.R.A. Soares*, M. C. Bourkaib, K. Delion, M. Guillemin, N.E. Amrani, W. Xu, E.A. Tehrany
Laboratory of engineering of biomolecules, ENSAIA, University of Lorraine, Nancy, France

Abstract: Edible films have recently received increased attention due to their various advantages including biodegradability and edibility. Among many materials that can be used to form edible films, chitosan is one of the most promising as it has a good film forming ability, which makes it suitable for use as a food packaging. Objective of this study is to functionalize the chitosan by adding the nanoemulsions from vegetable sources. After functionalization, physico-chemical, mechanical, morphological, chemical composition and structural properties of chitosan and chitosan/nanoemulsions blend films are studied. Various techniques are used to realize the multi-scale characterization of these films such as AFM, DMTA, WAXS, digidrom. The results show the wettability, mechanical, rheological, morphological and structural properties of chitosan were significantly affected by adding the nanoemulsions. Water contact angle of chitosan is decreased significantly by incorporation of lecithin. Decreasing of contact angle depends on lipid composition. We observe that mechanical property of chitosan changes by adding the nanoemulsions as plasticizer. We can conclude the incorporation of nanoemulsion as vector in chitosan develops a new matrix in food/packaging with an important role on physico-chemical properties. We can use the nanoemulsions to encapsulate the active molecules like as antioxidants and aromas compounds.

Keywords: nanofunctionalization, nanoemulsion, multiscale characterization, packaging application

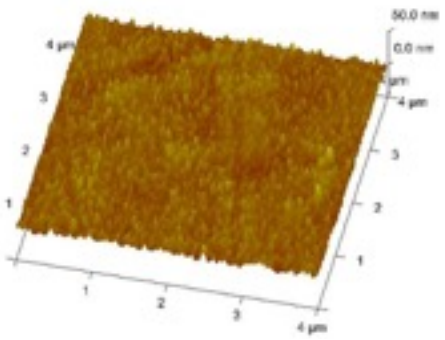

Figure 1. Figure illustrating the AFM image of chitosan.

References:

Imran M., Revol-Junelles A.M., Martyn A., Tehrany E.A., Jacquot M., Linder M., Desobry S. (2010) Active food packaging evolution: transformation from micro- to nanotechnology, *Critical Reviews in Food Science and Nutrition.*

Imran M., Revol-Junelles A. M., René N., Jamshidian M., Akhtar M. J., Tehrany E. A., Jacquot M., Desobry S. (2012) Microstructure and physico-chemical evaluation of nano-emulsion-based antimicrobial peptides embedded in bioactive packaging films, *Food Hydrocolloids.*

A. Seeboth, D. Lötzsch. (2003) Encyclopedia of Polymer Science and Technology, 3rd edition, John Wiley & Sons, New York.

Session II - B: Nanomaterials properties

Identification of Ductility Function in Titanium Nitride Nanocoating Deposited on Polycarbonate-urethane of Ventricular Assist Device

A. Milenin,[1] M. Kopernik,[1] S. Kąc,[1]
[1]AGH University of Science and Technology, Al. Mickiewicza 30, 30-059, Kraków, Poland

Abstract: The Polish left ventricular assist device (LVAD - RELIGA_EXT) will be made of thermoplastic polycarbonate-urethane (Bionate II) with deposited athrombogenic nano-coatings: gold (Au) and titanium nitride (TiN) (M.Kopernik *et al.*; 2014). The two scale solid numerical model developed in the Polish Artificial Heart Programme in Authors' FEM code was composed of a macro model of blood chamber and a micro model of TiN/Bionate II system (A.Milenin *et al.*; 2009). The input and validation data for the multiscale model was reached in tension test for Bionate II, nanoindentation test and inverse analysis for TiN. Due to the macro model validation, the results of a digital image correlation were compared with the FEM results computed on external surfaces of the blood chamber of LVAD (A.Milenin *et al.*; 2012).

However, a fracture occurrence has been observed on the boundary between the coating and the substrate in the LVAD. The FEA of stress and strain states in a micro and a macro scale models has confirmed the possibility of fracture (Figure 1). Consequently, the fracture criterion must be identified, what is the purpose of the present work. The tensile test in a micro chamber for the SEM has been performed in order to calibrate the fracture model of the TiN/Bionate II system for different thicknesses of deposited coating (Figure 2). Basing on experimental boundary conditions, the micro model of tension test has been developed in the Authors' FE code with implemented fracture criterion. The defined fracture criterion depend on effective strain and critical deformation function. The interpretation of micro tension test results has been done using the inverse algorithm. The FE models of tests were created for determination the conditions of fracture. The variation of values of critical deformation function in the test has been calculated in the stage of the test, in which the initiation of fracture has been occurred. The fracture parameter in each test has been computed. The difference between experimental and computed value of the fracture parameter at the moment of the fracture has been adopted as the objective function. The minimum of the objective function has been reached by a variation of the parameters of critical deformation function.

The micro scale model enriched with the fracture model enables the prediction of fracture and the comparison of different variants of macro and micro parameters of the LVADs.

Keywords: nanocoating, micro tension test, finite element method (FEM), fracture, ventricular assist device (VAD), titanium nitride (TiN).

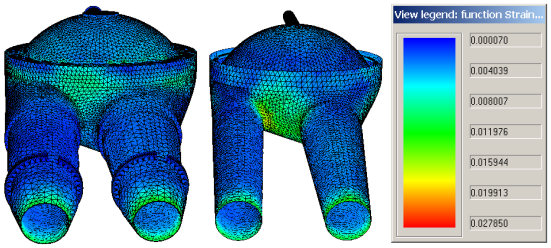

Figure 1: The distribution of strain intensity on external (left) and internal (right) surfaces of POLVAD-EXT chamber (temperature of chamber 25 C, P=37 kPa).

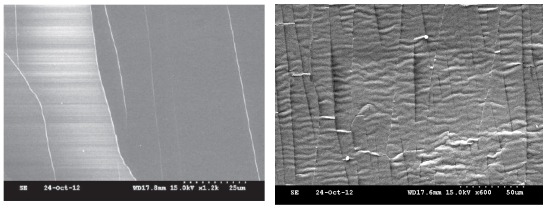

Figure 2: The SEM's image of 50 nm of TiN coating stretched 40 N (left) and 100 nm of TiN coating stretched 60 N (right) with fracture in TiN.

References:

A. Milenin and M. Kopernik, Multiscale FEM model of artificial heart chamber composed of nanocoatings, *Acta of Bioengineering and Biomechanics*, vol. 11, no. 2, pp. 13–20, 2009.

A.Milenin, M.Kopernik, D.Jurkojć, M. Gawlikowski, T. Rusin, M. Darłak, R. Kustosz, Numerical modelling and verification of polish ventricular assist device, *Acta of Bioengineering and Biomechanics*, 14/3 (2012) 49-57.

M. Kopernik, A. Milenin, S. Kąc, M. Wróbel, Stress-Strain analysis in TiN nanocoating deposited on polymer with respect to Au nanointerlayer // *Journal of Nanomaterials*, 2014, ID 813587, 1-12

Acknowledgements: Financial assistance from the Ministry of Science and High Education of Poland, project AGH no. 11.11.110.300 is acknowledged.

Diffusion of Proteins Through and Across Polyelectrolyte Multilayers

S.Pahal,[1] M.Varma,[1,2] A.M.Raichur[3]
[1]Centre for Nanoscience and Engineering, Indian Institue of Science, India
[2]Electrical Communication Engineering, Indian Institue of Science, India
[3]Materials Engineering, Indian Institue of Science, India

Abstract: Layer-by-layer assembly of polyelectrolytre multilayers (PEMs) is the most versatile approach for modifying surface as well as bulk properties of various substrates.This work explores the understanding of diffusion (lateral as well as transverse) of proteins across PEMs and how it can be modified by varying post assembly conditions. A weak PEM system has been selected as the model for these studies. Lateral diffusion studies are visualized by performing Florescence Recovery after Phtobleaching (FRAP) on these PEMs. FITC-labeled proteins have been used for these studies and lateral diffusion is measured by the bleached "hole filling" process as function of time. Transverse diffusion has also been studied by measuring the trasverse protein concentration distribution by using distance dependent fluorescence from fluorophores close to metal surfaces (Figure 1). Although Confocal laser scanning microscopy (CSLM) (Picart *et al.*, 2002) has been employed for diffusion studies across PEMs for the films having thickness in the range of micrometers, it is not suitable for probing PEMs thinner than around 500 nm. Therefore, X-ray photoelectron spectroscopy (XPS) (Jonathan *et al*, 2013) was recently utilized as a tool get transverse concentration profile of diffusing species in ultra-thin PEMs. Our protocol provides a simpler alternate approch to study the lateral diffusion as well as to extract the transverse concentration distribution in ultra-thin PEMs. This can be used a tool to understand the reservoir properties of PEMs and to get the detailed knowledge about the distribution and mobility of molecules acoss PEMs.

Keywords: Polyelectrolyte multilayers, layer-by-layer assembly, Fluorescence Recovery after Photobleaching (FRAP)

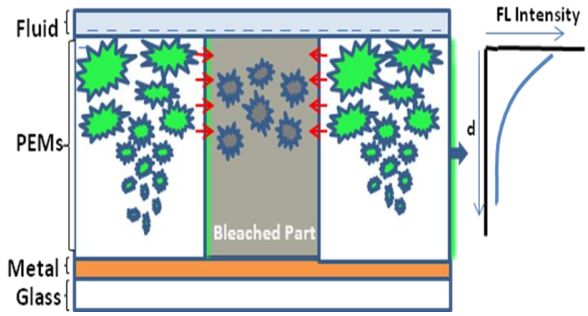

Figure 1: Schematic representing the overall approch for getting the detailed understanding of lateral as well as transverse diffusion across PEMs. Lateral diffusion is shown by movement of fluorphores from unbleached to bleached portion of PEMs and tranverse diffusion by the distance dependent fluorescence from FITC-labeled proteins in the PEM deposited on a metal surface. The temporal variation of fluorescnece intentsity can be fitted to extract the transverse distribution of fluorophores.

References:

Picart, C., Mutterer, J., Richert, L., Luo, Y., Prestwich, G. D., Schaaf, P., Voegel, J. C., Lavalle, P. (2002) Molecular basis for the explanation of the exponential growth of polyelectrolyte multilayers, *Proc. Natl. Acad. Sci. U.S.A.* 99, 12531-12535.

Jonathan, B. G., Michael, F. R., Robert, E. C.(2013) Depth-profiling X-ray photoelectron spectroscopy (XPS) analysis of interlayer diffusion in polyelectrolyte multilayers, *Proc. Natl. Acad. Sci. U.S.A*, 110,17, 6651–6656

Synthesis and Characterisation of Conjugated Polymer Nano-particles for Fluorescence Imaging Applications

G. Redmond,[1,]
[1]University College Dublin, School of Chemistry & Chemical Biology, Dublin, Ireland.

Abstract: Recent developments in materials synthesis, bio-conjugation methods and luminescence techniques have led to a rapid proliferation of novel fluorescence-based approaches to imaging in the life sciences. However, for high-resolution or long-time duration imaging applications, molecular dyes suffer from limitations of low brightness, poor photo-stability and fluorescence intermittency (blinking). Likewise, emissive nanoparticles, e.g., semiconductor quantum dots (Q-dots) and dye-loaded latex or silica beads, are also un-optimised. Q-dots often require an inorganic shell with a thick encapsulation layer for stability and biocompatibility, and many batches exhibit low emission rates, blinking, and significant fractions of "dark" particles. Dye-loaded beads have relatively large sizes with limited dye-loading concentrations due to problems of aggregation and self-quenching.

Consequently, we are exploring a potentially promising alternative based on highly fluorescent conjugated polymer materials which are already in use as active layers in polymer light-emitting devices, and, in conjugated polyelectrolyte form, as solar cells. Conjugated polymer materials exhibit a range of attractive properties, including high absorption cross-sections, radiative rates, and effective chromophore densities along with minimal levels of aggregation-induced fluorescence quenching. Using conjugated polymers as an emissive nanoparticle material also eliminates small dye molecules or heavy metal ions that could leach out into solution.

We have developed a range of conjugated polymer nanoparticles based on fluorene co-polymers. These polymers are surface functionalized with different molar ratios of polyethylene glycol. By varying the preparation conditions, different sizes of nanoparticles can be prepared, resulting in smaller (20-50 nm) nanoparticles, produced by a reprecipitation method, and larger (90-110 nm) particles, produced by a solvent exchange method. These particles exhibit high absorption cross-sections (10^{-13}-10^{-12} cm^2), high quantum yield (≈ 50%) and well-resolved, size-independent absorption and fluorescence spectra across a broad wavelength range. Single particle fluorescence imaging studies indicate much higher emission rates (≈ 10^8 s^{-1}) and little or no blinking as compared with typical results reported for single dye molecules and Q-dots. Analysis of single nanoparticle photo-bleaching trajectories for some particles indicates excellent photo-stability with almost 10^8 photons emitted per nanoparticle prior to irreversible photo-bleaching. Finally, nanoparticles were incubated with L929 murine aneuploid fibrosarcoma and MCF-7 human breast adenocarcinoma cell lines, fixed, and counter-stained with nuclear dyes. Subsequent fluorescence microscopic imaging indicated that nanoparticles are readily internalized by the cells; see Figure above. Further studies are in progress to understand processes of their trafficking and localization within various cell types.

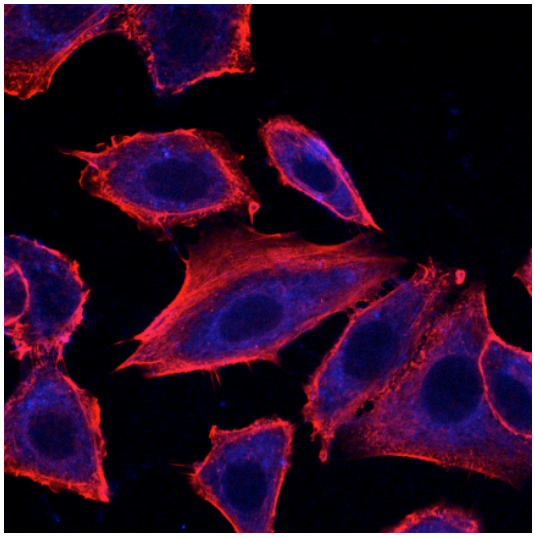

Figure: Polyfluorene nanoparticles (blue) in MCF-7 cells (red / phalloidin-TRITC).

Keywords: nanoparticles, colloidal dispersions, optical spectroscopy, fluorescence, non-blinking, photostability, brightness, cellular uptake.

The Role of DC and PRC Current Densities on the Sliding Wear of Electrodeposited Nickel-Cobalt /CNT Composite Coatings

Ramazan Karslioglu[1], Hatem Akbulut[1]
[1]Sakarya University, Engineering Faculty, Department of Metallurgical & Materials Engineering, Esentepe Campus, 54187, Sakarya/Turkey

Abstract: Surface properties are directly responsible for the performance of engineering materials because most of failures such as friction, wear, corrosion and fatigue often take place on the material surface. Electrodeposition technique is of great interest for industrial usage because it produces functional and protective coatings with low cost and easy control[1, 2]. In the Ni and Ni-Co metal matrix composites, when carbon nanotubes (CNTs) are selected as the third phase, because carbon nanotubes possess many remarkable properties such as high strength and elastic modulus, good flexibility, and unique conductivity[3].

In the present work, Nickel-Cobalt alloys and Nickel-Cobalt /Carbon nanotube composite coatings were prepared under direct current (DC) and pulse reverse current (PRC) methods. The microstructure of coatings was characterized by means of Scanning Electron Microscopy (SEM), X-Ray Diffraction (XRD) analysis and 3D profilometry facilities. One of the example showing co-deposition of MWCNTs with Ni,-Co is shown Fig. 1. The effect of current density and the current type on the co-deposited carbon nanotube content, microstructure and sliding wear properties were investigated. The results showed that the microstructure and performance of the coatings were greatly affected by current density, carbon nanotube content and the electrodeposition current type. Dispersion of the multiwalled carbon nanotubes (MWCNTs) into the Ni-Co matrix structure resulted in improving wear resistance performance of the Ni-Co electrodeposited coatings. This increment was attributed to the unique effect of the MWCNTs on load bearing ability and self lubrication between the friction surfaces. Introducing MWCNT into the Ni-Co matrix by co-electrodeposition resulted in wear mechanism change and decreased the real contact area since MWCNT dispersion causes to increase the surface roughness (Fig. 2). Among the studied electrodeposition techniques, PRC technique showed best features compared with the DC technique.

Keywords: Reverse Pulse electrodeposition; Ni-Co/MWCNT nanocomposites; surface roughness; reciprocating wear; wear mechanisms

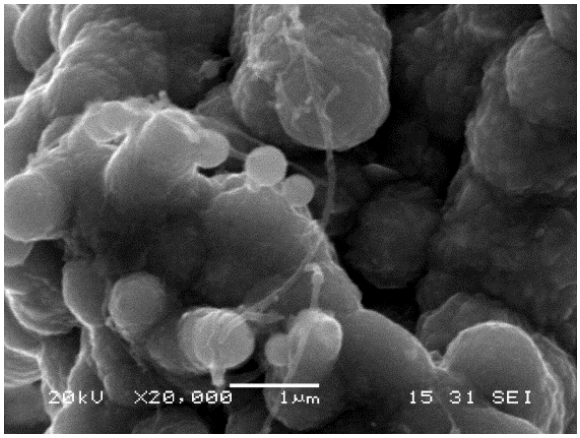

Fig.1. SEM surface structure of co-deposited Ni-Co/MWCNT composite.

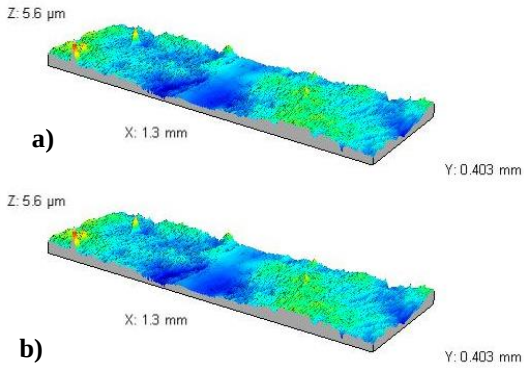

Fig. 2. 3D surface profilometry results of the a) Ni-Co and b) Ni-Co/MWCNT coatings after sliding test.

References:

1. F.Su, C. Liu, J. Guo, and P. Huang, Surface & Coatings Technology, Characterizations of nanocrystalline Co and Co/MWCNT coatings produced by different electrodeposition techniques, (2013), 217, 94-104.
2. L. Kodandarama, M. Krishna, H.N. Narasimha Murthy, and S.C. Sharma, Development and Characterization of Electrocodeposited Nickel-Based Composites Coatings, J. Materials Engineering and Performance, (2012), 21, 105-113.
3. L. Shia, C.F. Suna, P. Gao , F. Zhou, and W.M. Liu, Surface & Coatings Technology, Electrodeposition and characterization of Ni–Co–carbon nanotubes composite coatings, (2006), 200, 4870-4875.

Widely and Rapidly Switchable Wettability Through Short-Range Ordered-Disordered Transition and Redox Reaction

Ya-Huei Chang,[1*] Shien-Ping Feng[1]
[1] Department of Mechanical Engineering, The University of Hong Kong, Pokfulam Rd., Hong Kong

Abstract: As an earth-abundant semiconductor, nickel oxyhydroxide (NiOOH) has mainly been applied for electrochemical, electrochromic and optical devices. Our previous study first achieved its feasibility on wettability control from superhydrophilic to superhydrophobic via anodic plating and post chemical treatment to properly tune the porosity and surface energy.[1] However, the permanently chemical modification results in an irreversible wetting transition, thereby limiting its use for many cutting-edge applications. Some organic and inorganic materials have been found to intrinsically possess switchable nature by the change of composition, conformation, configuration, crystallization, morphology or vacancy recovery.[2] However, these existing wettability switchable materials show a sharp trade-off between the switching range and response time. Specifically, most flat organic materials offer rapid switch within several minutes but only small changes in water contact angles (WCAs < 40°), while smooth inorganic materials have inherently superior switching range (WCAs > 70°) but take several days upon dark storage.[3-5] In this work, without the needs of any chemical treatments, the as-deposited film of nanoporous NiOOH was alternatively exposed to environment chamber and ultraviolet (UV)/ozone, the WCAs could be able to quickly switch between superhydrophobic and superhydrophilic within 70 minutes over ten cycles. The switchable mechanism arises from a chemical redox reaction and short-range ordered-disordered transition (Figure 1) verified by HR-TEM, grazing incidence XRD and XPS. The rewritable two-dimensional (2D) microfluidic channels and wetting-contrast enhanced selective electroplating are demonstrated based on film properties of easily patternable, repairable and switchable wettability.[6]

Keywords: switchable wettability, short-range ordered-disordered transition, micropatterning, selective plating.

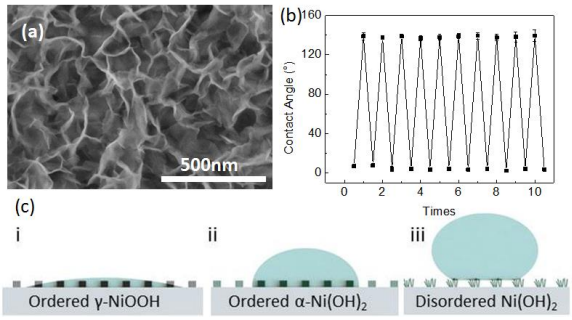

Figure 1: (a) Nanoporous structure of as-deposited NiOOH film through anodic plating. (b) Cycling test of NiOOH film alternatively exposed to environmental chamber and UV/ozone. (c) Schematic of the de-wetting mechanism resulting from the serial reactions of NiOOH/$Ni(OH)_2$ conversion and the defect-driven rearrangement of crystallographic orientation.

References:

1. Y.H. Chang, Y.T. Huang, M. K. Lo, C.F. Lin, C.M. Chen, and S.-P. Feng, "Electrochemical fabrication of transparent nickel hydroxide nanostructures with tunable superhydrophobicity/superhydrophilicity for 2D microchannels application," *J. Mater. Chem. A*, **2**, 1985, 2014.
2. B. Xin and J. Hao, "Reversibly switchable wettability," *Chem. Soc. Rev.*, **39**, 769, 2010.
3. N. Delorme, J. F. Bardeau, A. Bulou, and F. Poncin-Epaillard, "Azobenzene-Containing Monolayer with Photoswitchable Wettability," *Langmuir*, **21**, 12278, 2005.
4. S. Kidoaki, S. Ohya, Y. Nakayama, and T. Matsuda, "Thermoresponsive Structural Change of a Poly(N-isopropylacrylamide) Graft Layer Measured with an Atomic Force Microscope," *Langmuir*, **17**, 2402, 2001.
5. W. Sun, S. Zhou, P. Chen, and L. Peng, "Reversible switching on superhydrophobic TiO_2 nano-strawberry films fabricated at low temperature," *Chem. Commun.*, 603, 2008.
6. Y.H. Chang, N. Y. Hau, C. Liu, Y.T. Huang, C.C. Li, K. Shih, and S.P. Feng, "Short-Range Ordered-Disordered Transition of NiOOH/$Ni(OH)_2$ Pair Induces Switchable Wettability," *Nanoscale*, 2014.

Critical overview of polymer self-assemblies formation and characterization

M. Dionzou[1], C. Roux[1], U. Till[1,2], B. Lonetti[1], J.-D. Marty[1], A.-F. Mingotaud[1], C. Mingotaud[1], P. Joseph[3], D. Goudounèche[4], B. Payré[4], M. Léonetti[5]
[1] Toulouse Unviersity; IMRCP laboratory, CNRS UMR 5623, Toulouse, France
[2] Toulouse University, INPT – EI Purpan, Dpt Sciences Agronomiques et Agroalimentaires, Toulouse, France
[3] LAAS – CNRS, Toulouse, France
[4] Toulouse University, CMEAB, Faculté de Médecine Toulouse Rangueil, Toulouse, France

Abstract: Polymer vesicles, also called polymersomes, are increasingly assessed as drug nanovectors, owing to their ability to transport both hydrophilic and hydrophobic drugs (Messager et al.). A lot of published results in this domain uses an empirical approach to predict the self-assemblies' morphology. However, the rule linking the morphology to the hydrophilic fraction was mainly established on poly(ethyleneoxide-b-butadiene). Linked to our on-going studies on polymer self-assemblies for photodynamic therapy (Gibot et al., Till et al.), the work presented here aimed at cross-examining the methods of formation for polymersomes and pointing out the difficulties of characterization. Thus, a large variety of amphiphilic block copolymers containing first a poly(ethyleneoxide) block for the colloidal stability and the stealth in blood, and secondly various hydrophobic blocks, such as poly(ε-caprolactone), poly(D,L-lactide), poly(styrene), poly(butadiene) or poly(methylmethacrylate), were used, and their self-assembly examined. Different methods of formation will be examined, such as cosolvent addition, film hydration or electroformation. The influence of experimental parameters were assessed and critically compared with literature. This showed that although a general trend of morphology order vesicle – worm-like micelles – micelles is often observed, the limit between each area significantly varied depending on the polymers and for some cases, only micelles could be formed. Also, these self-assemblies being kinetically frozen, the influence of the fabrication method has been observed in some cases, as expected. Thus, selecting the right polymer and the right method of fabrication, either micelles or polymersomes with a size ranging from 15 to 1000 nm can be readily obtained. Regarding their characterizations, the work focused on routinely used dynamic light scattering and electron microscopy which enabled us to highlight difficulties that are often overlooked.

Keywords: Polymer vesicles, self-assemblies, light scattering, electron microscopy

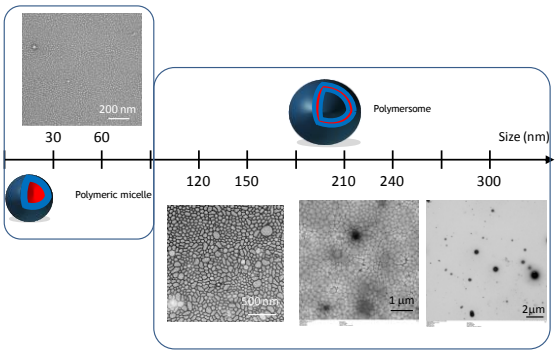

Figure 1: Range of polymer self-assemblies obtained in this study.

References:

L. Gibot, A. Lemelle, U. Till, B. Moukarzel, A.-F. Mingotaud, V. Pimienta, P. Saint-Aguet, M.-P. Rols, M. Gaucher, F. Violleau, C. Chassenieux, P. Vicendo (2014) "Polymeric micelles encapsulating photosensitizer: structure/ photodynamic therapy efficiency relation" *Biomacromolecules*, 15(4), 1443-1455

L. Messager, J. Gaitzsch, L. Chierico, G. Battaglia (2014), "Novel aspects of encapsulation and delivery using polymersomes" *Current Opinion in Pharmacology*, 18 (0), 104-111.

U. Till, M. Gaucher-Delmas, P. Saint-Aguet, G. Hamon, J.-D. Marty, C. Chassenieux, B. Payré, D. Goudounèche, A.-F. Mingotaud, F. Violleau (2014) "Asymmetrical Flow Field-Flow Fractionation with Multi-Angle Light Scattering and Quasi Elastic Light Scattering for characterization of polymersomes: comparison with classical techniques" *Analytical and Bioanalytical Chemistry*, 406(30), 7841-7853

Prediction of photothermal phase signatures from arbitrary plasmonic nanoparticles and experimental verification

O. Blum, N.T. Shaked
Department of Biomedical Engineering, Faculty of Engineering, Tel Aviv 69978, Israel

Abstract: We present a new approach for predicting spatial phase signals originated from photothermally excited metallic nanoparticles of arbitrary shapes and sizes. Heat emitted from the nanoparticle affects the measured phase signal via both the nanoparticle surrounding refractive index and thickness changes. Since these particles can be bio-functionalized to bind certain biological cell components, they can be used for biomedical imaging with molecular specificity, as new nanoscopy labels, and for photothermal therapy. Predicting the ideal nanoparticle parameters requires a model that computes the thermal and phase distributions around the particle, enabling more efficient phase imaging of plasmonic nanoparticles, and sparing trial and error experiments of using unsuitable nanoparticles. For the first time to our knowledge, using the proposed model, one can predict phase signatures from nanoparticles with arbitrary parameters. The proposed nonlinear model is based on a finite-volume method for geometry discretization, and an implicit backward Euler method for solving the transient inhomogeneous heat equation. To validate the model, we correlate its results with experimental results obtained for gold nanorods of various concentrations, which we acquired by a custom-built wide-field interferometric phase microscopy system.

Keywords: interferometric imaging, nanoparticles, digital holographic microscopy, plasmonics, phase measurement

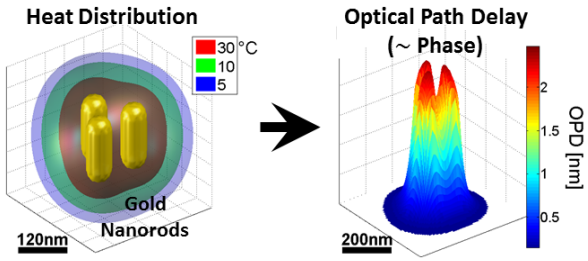

Figure 1: Prediction of Optical Phase Delay (OPD) from heat distribution map created by FVM model of nanoparticle heating

In-Situ Thermally-reduced Graphene Oxide/Epoxy Composites: Thermal and Mechanical Properties

G. B. Olowojoba,[1*] A. C. Taylor,[1] A. J. Kinloch[1]

[1]Mechanics of Materials Division, Department of Mechanical Engineering, Imperial College, London, UK

Abstract:
Graphene has excellent mechanical, thermal, optical, and electrical properties and this has made it a prime target for use as a filler material in the development of multifunctional composites for a variety of applications: electrostatic discharge, electrically conducting, touchscreen display, fire retardant coatings, lightweight materials with good barrier properties, targeted drug delivery applications, etc. However, challenges to overcome in order to take full advantage of the aforementioned properties of graphene include achieving good dispersion and good interfacial properties between filler and matrix. Several approaches aimed at achieving well-dispersed graphene in composites have been reported. In this work we report the thermal and mechanical properties of reduced graphene oxide/epoxy composites prepared via a scalable, environmentally-friendly and commercially-viable method. Transmission and scanning electron micrographs of the composites demonstrate that the reduced graphene oxide is well-dispersed throughout the composite. The composites also show good improvements in thermal conductivity and tensile modulus for relatively low loadings. These properties are compared with those of other commercially available graphene/reduced graphene oxide-based composites.

Keywords: Thermal reduction, graphene oxide, reduced graphene oxide, tensile modulus, thermal conductivity, glass transition temperature, dispersion.

Tribological Behaviors of Yttria-Stabilized Zirconia (YSZ) Nano-particles as Lubricant Additives

A. Sert,[1*] D. Yılmaz Çakta[2]
[1]Eskisehir Osmangazi University, Department of Mechanical Engineering, Eskisehir, Turkey
[2] Eskisehir Osmangazi University, Department of Metallurgical and Materials Engineering, Eskisehir, Turkey

Abstract:
Nanoparticles are used as additives in coatings or lubrication systems in order to prevent friction and wear of materials in industry. The new interest area of nanotribology shows that the lubricants with nano-particles have novel property in tribology, such as wear resistance, low friction coefficient, and high load capacity (Jiao *et al.*, 2011). ZrO_2 is one of the nanoparticles used for tribological consideration such as coatings (Yang *et al.*, 2011) and lubricant additives (Ma *et al.*, 2010). When zirconia doped with yttria, yttria-stabilized zirconia (YSZ) has good mechanical properties at high temperature and good chemical stability up to 1200 °C (Carpio *et al.*, 2015). Due to these properties, YSZ is a current material of choice for thermal barrier coatings.
The aim of this work is to enhance novel lubrication with different amount of YSZ nanoparticles (size<200nm) and characterization of tribological properties of AISI 4140 steel material in the lubricating system. Synthesized YSZ nanoparticles (Figure 1) are dispersed with different concentration (0.1%, 0.5% and 1.0% wt.) in synthetic engine oil (SAE10W40) and tribological test are conducted using ball-on-disc geometry (Figure 2). The morphology of worn surface are studied using scanning electron microscopy (SEM), the elemental analysis on the worn surfaces is also conducted with energy-dispersive X-ray spectroscopy (EDS) and the worn scar lengths are investigated using optical microscopy (OM). When the optimized concentration of nanoparticle additive is 0.5 wt.%, coefficients of friction is decreased about 12.6%. This research has uncovered a novel approach for minimizing energy loss by friction reduction and should benefit many sectors such as automobiles industry.

Keywords: nanoparticles, yttria-stabilized zirconia, lubricant additives, lubricant, friction, wear.

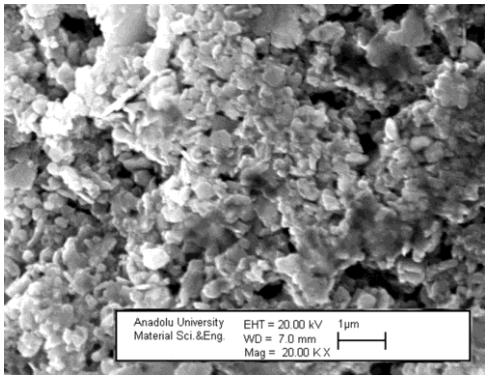

Figure 1: SEM image of the nano YSZ powder.

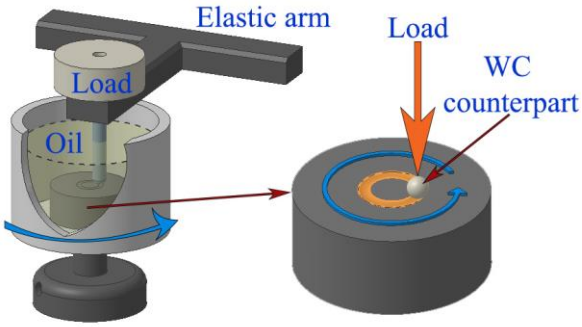

Figure 2: Figure illustrating the wear test device and the wear geometry.

References:
Jiao, D., Zheng, S., Wang, Y., Guan, R., Cao, B. (2011), The tribology properties of alumina/silica composite nanoparticles as lubricant additives, *Appl. Surf. Sci.*, 257, 5720-5725.

Yang, Y., Chen, W., Zhou, C., Xu, H., Gao, W. (2011), Fabrication and characterization of electroless Ni-P-ZrO_2 nano-composite coatings, *Appl. Nanosci.*, 1, 19-26.

Ma, S., Zheng, S., Cao, D., Guo, H. (2010), Anti-wear and friction performance of ZrO_2 nanoparticles as lubricant additive, *Particuology*, 8, 468-472.

Carpio, P., Borrell, A., Salvador, M.D., Gómez, A., Martínez, E., Sánchez, E. (2015), Microstructure and mechanical properties of plasma spraying coatings from YSZ feedstocks comprising nano- and submicron-sized particles, *Ceram. Int.*, 41, 4108-4117.

Calcium phosphate super-balls synthesized in presence of gelatin and chitosan

J. Koetz,* I. Kovach
Universität Potsdam, Institut für Chemie, Potsdam, Germany

Abstract: Calcified tissue of vertebrates can be identified as hybrid material, i.e. inorganic hydroxyapatite crystals bound by polymeric organics, arranged in a hierarchical structure. There are known different strategies to synthesize nanosized hydroxyapatite with diverse morphological structures.

Besides of hydroxyapatite many kinds of calcium phosphates are known. Calcium phosphates are classified by their Ca/P molar ratio. They can be converted into hydroxyapatite or used as Ca^{2+} ion resource.

Various biomineralization processes have been developed to stimulate bone formation in vitro. Here we present a precipitation procedure, where thin calcium phosphate platelets are formed at 90°C in presence of gelatin and chitosan. After heating up the hybridmaterial to 600°C the polymer components are burned out, and supramolecular flower-like ball structures are observed, shown in Figure 1.

By means of FT-IR spectroscopy, powder diffractometric and energy-dispersive X-ray (EDX) analysis in combination with high resolution scanning electron microscopy (HR-SEM) and high resolution transmission electron microscopy (HR-TEM), one can show that dicalcium phosphate and β-tricalcium phosphate (β-TCP) cristallites build up the inner structure of the card house balls.

Additionally experiments, i.e. polyelectrolyte titrations and Differential Scanning Calorimetric (DSC) investigations, show that polymer-polymer interactions between gelatin and chitosan are of special relevance for the formation of such open, porous ball structures. Based on these results one can conclude that electrostatic interactions between the two polymers are of minor importance in contrast to hydrogen bonding.

Keywords: biomineralization, bone formation, cement material in bone repair, β-tricalcium phosphate crystallites, open card house structure, super-balls,

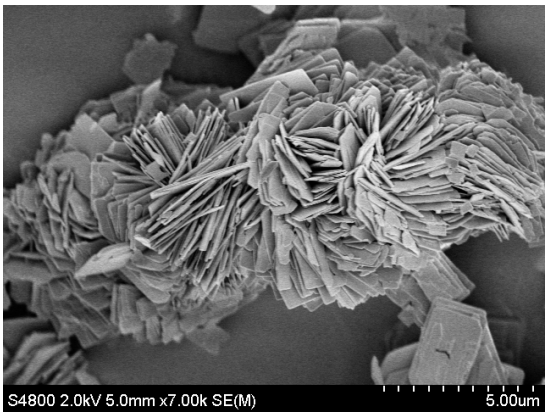

Figure 1: High resolution SEM micrograph of flower-like calcium phosphate balls

References:

Bleek, K., Taubert, A. (2013) New developments in polymer-controlled, bioinspired calcium phosphate meneralization from aqueous solution, *Acta Biometrialia, 9* , 6283-6321.

Sadat-Shojai, M., Khorasani, M-T., Dinpanah-Khoshdargi, E., Jamshidi, A. (2013) Synthesis methods for nanosized hydroxyapatite with diverse structures, *Acta Biometrialia, 9* , 7591-7621.

Nano-Building Blocks based-Hybrid organic-inorganic copolymers with Self-Healing Properties

L. Rozes[1,*], F. Potier[1], A. Guinault[2], S. Delalande[3], C. Sanchez[1], F. Ribot[1]
[1] Sorbonne Universités, UPMC Univ Paris 06, Collège de France, CNRS UMR 7574, Chimie de la Matière Condensée de Paris, F-75005, Paris, France
[2] Arts et Métiers ParisTech, CNRS UMR 8006, Procédés et Ingénierie en Mécanique et Matériaux, F-75013, Paris, France.
[3] PSA Peugeot Citroën, F-78140, Velizy Villacoublay, France.

Abstract: New dynamic materials, that can repair themselves after a strong damage, have been designed by hybridization of polymers with structurally well-defined nanobuilding units.
Hybrid elastomers have been elaborated from a common organic monomer, butyl acrylate, which was co-polymerized, under conventional thermally initiated free radical polymerization, with a difunctional organotin oxo-cluster, $[(BuSn)_{12}O_{14}(OH)_{16}](AMPS)_2$.
This well-defined nano-size cross-linker was selected because of the ionic interactions that the macrocation $[(BuSn)_{12}O_{14}(OH)_{16}]^{2+}$ exchanges with its two polymerizable counter anions (AMPS : Acrylamido-2-methyl-1-propanesulfonate).
The controlled design of cross-linked poly(*n*-butyl acrylate) (pBuA) has been performed by introducing a very low amount of the specific tin oxo-cluster. The non-covalent interactions (*i.e.* ionic bonds) developed at the hybrid interface play a double role. Such interactions are strong enough to cross-link the polymer, which consequently exhibits rubber-like elasticity behavior and labile enough to enable, after a severe mechanical damage, dynamic bond recombination leading to an efficient healing process at room temperature. In agreement with the nature of the reversible links at the hybrid interface, the healing process can be speed up considerably with temperature.
The healing efficiency was measured by a standard stress/strain tensile experiment. Recovery as high as 75% of the original elongation at break was observed. The dynamic nature of the cross-linking, has been studied by measuring the diffusion coefficient of the organotin oxo-clusters inside the swollen material.

Keywords: hybrid materials, polymer nanocomposites, sol-gel processes, DOSY NMR, self-healing properties.

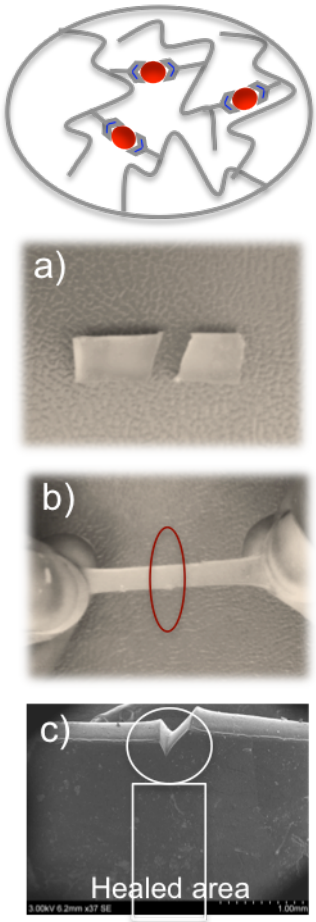

Figure 1: Illustrating of the crosslinking of poly(*n*-butyl acrylate) by nonobuilding blocks : $[(BuSn)_{12}O_{14}(OH)_{16}](AMPS)_2$ a) damaged sample b) healed sample c) healed area by SEM analysis.

References:

F. Potier, A. Guinault, S. Delalande, C. Sanchez, F. Ribot and L. Rozes, *Polymer Chemistry*, 2014, 5, 4474-4479

Hybrid gold nanoparticles modified by oligopeptides for lead (II) ions interaction monitoring

Jane Politi[1,2], Jolanda Spadavecchia[*3,4], Mario Iodice[1], Luca de Stefano[1]

[1]*Institute for Microelectronics and Microsystems, Unit of Naples-National Research Council, Italy*
[2]*Department of Chemical Sciences, University of Naples "Federico II", Naples Italy*
[3]*Sorbonne Universités, UPMC Univ Paris VI, Laboratoire de Réactivité de Surface, Paris, France.*
[4]*CNRS, UMR 7244, Laboratoire de Chimie, Structures et Propriétés de Biomateriaux et d'Agents Therapeutiques, Paris, France*

Abstract: Nanostructured materials have become increasingly popular due to their unique properties in development of novel biosensors. Therefore, more attention should be paid to find efficient synthesis methods to match the enlarging demand of gold nanoparticles. Several different solution synthesis methods have been employed to prepare gold nanoparticles, including biomolecule reduction of $HAuCl_4$, seed mediated synthesis at room temperature and polymer-assisted synthesis. Recently, the utility of nanomaterials for any application is strongly dependent upon their physicochemical characteristics and their interactions with surfaces modifiers (Spadavecchia *et al.*; 2014). Exchange of organic molecules on Au nanoparticles with PEG can indeed be performed to prepare biocompatible PEG-stabilized Au nanoparticles. Gold nanoparticles can interact with specifically sequenced peptides that can self-assemble on their surface. The polypeptides could induce or prevent aggregation of nanoparticles causing consequently the change of absorbance and, moreover, allow to interact with other metal ions i.e. Cd^{2+}, Ni^{2+}, Co^{2+}, Zn^{2+} etc. Lead is a widely used heavy metal in industrial applications (battery manufacture, paint, gasoline, etc.). Lead is toxic by ingestion and inhalation, and can seriously affect the gut and the central nervous system. Phytochelatins (PCs)oligopeptides have been widely studied because of their ability to chelate heavy metal ions in plants and fungi for detoxification mechanisms (Cobbett, 2000). We report here synthesis to prepare polymer-modified gold nanoparticles and gold nanorods using dycarboxylic PEG (DPEG) as stabilizer. A new kind of pegylated gold nanorods based assay to quantify lead-Phytochelatin 6 (PC_6) interactions in aqueous solution by using the proteins as bioprobes was developed (Politi *et al.*, 2015). These hybrids nanocomplexes are stable and biologically active: even if linked by adsorbed-gold interaction on the nanorods surface, the peptides are able to strongly bind the heavy metal ions with an affinity constant in the range of picomolar. The signal changes, i.e. variation of FT-SPR peak position, are important (more than 200 cm^{-1}) even at very low concentration (25 ppb) of metal ions: this result is very promising for development of sensitive and effective nanoparticle-based biosensor for quantifying lead (II) ions concentration in water (see Figure 1).

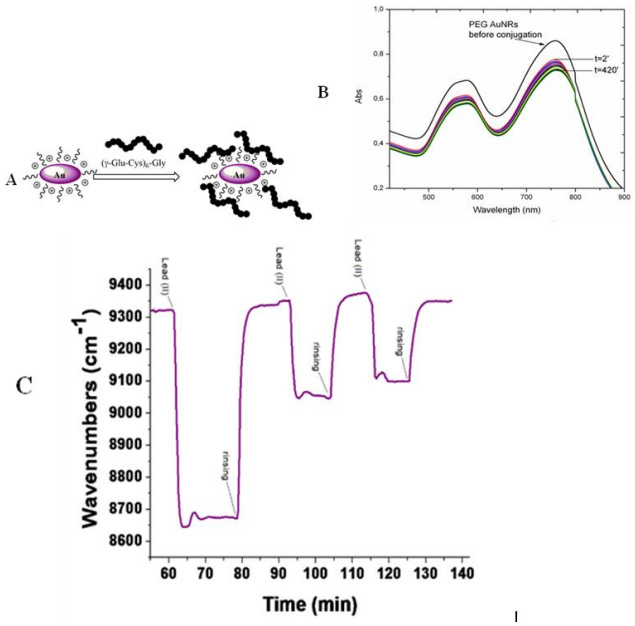

Figure 1. Schematization of oligopeptides self-assemblibg (A); UV-vis spectra of PEG gold nanorods during oligopeptides self-assembling (B); FT-SPR shifts of nanostructured surface as function of time of lead ions interaction (C).

Keywords: oligopeptides self-assembling, gold nanorods, lead ions detection.

References:

Cobbett, C.S.; (2000) Phytochelatin biosynthesis and function in heavy-metal detoxification. Current opinion in plant biology, 3, 211–216.

Politi, J., Spadavecchia, J.; Iodice, M.; De Stefano, L.; (2015**)** Oligopeptide–heavy metal interaction monitoring by hybrid gold nanoparticle based assay, *Analyst*, , 140, 149-155.

Characterization of Ferromagnetic Metal–Carbon NanocompositesPrepared by Solid-Phase Pyrolysis of Metal-Phthalocyanines

A. Manukyan,* A. Mirzakhanyan, H. Gyulasaryan, R. Khachaturyan, E. Sharoyan
Institute for Physical Research, NAS of Armenia, Laboratory of Solid State Physics, Ashtarak-2, Armenia

Abstract: We have synthesized a number of ferromagnetic metal–carbon nanocomposites (M/C, where M = Co, Ni, Fe), using solid-phase pyrolysis of metal-phthalocyanines. This reaction can be represented as (Manukyan *et al.*; 2012)

$$M(C_{32}N_8H_{16}) \xrightarrow[-8H_2,\,-4N_2]{T_{pyr},\,t_{pyr},\,p} M + 32C,$$

Where T_{pyr} is the pyrolysis temperature, t_{pyr} the pyrolysis time, and p_{pyr} the autogenic pressure in a reaction ampoule.

It is evident that the metal concentration in nanocomposites is about 3 at%. Changing the pyrolysis conditions, it is possible to prepare superparamagnetic and ferromagnetic nanoparticles with sizes from 5–10 nm to 200–300 nm in different carbon matrices. The structure, morphology and magnetic characteristics of nanocomposites were investigated by electron microscopy, X-ray diffraction, Raman spectroscopy and magnetometry. In particular, a transmission electron microscope image of Co/C nanocomposite is shown in Figure 1.

As seen, Co nanoparticles are embedded in the walls of multiwalled carbon nanotubes and in their ends, which leads to the bimodal size distribution (around 5 nm and 30 nm). From X-ray diffraction data it follows that Co nanoparticles have the fcc structure and the mean size of 15 nm. Raman spectra of samples contain "graphitic" G- and D-bands specific for carbon nanotubes. Magnetometry data show that Co nanoparticles have the saturation magnetization of 128 emu/g at 300 K, which is about 90% of magnetization of bulk cobalt, and the coercivity 380 Oe.
The structure and magnetic properties of Ni@C and Fe@C nanocomposites essentially differ from these of aforementioned compounds. In this case nanocomposites consist of metal nanoparticles coated by graphite-like shells (Ni@C and Fe@C), which prevent aggregation and oxidation of nanoparticles. The magnetic characteristics such as saturation magnetization and coercivity as well as the specific absorption rate (SAR) make these materials attractive for magnetic hyperthermia applications.

This work was supported by the SCS MES RA, within the framework of joint Armenian–Belarusian research project № 13RB–050 and the FP7 Project of the European Commission with Grant No. 608906 – NANOMAT–EPC.

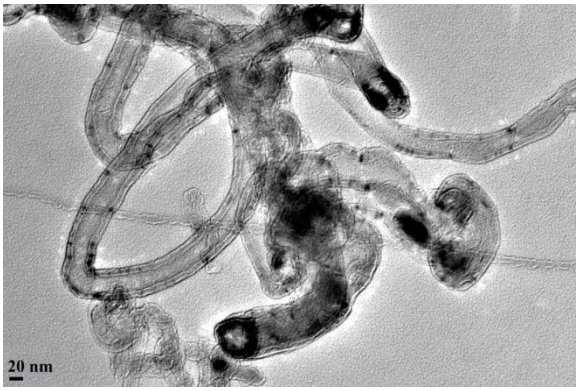

Figure 1: TEM image of cobalt nanoparticles embedded in the walls of multiwalled carbon nanotubes and in their ends.

Keywords: metal–carbon nanocomposites, metal-phthalocyanines, solid-phase pyrolysis, Co, Fe, Ni nanoparticles, ferromagnetism.

References:

Manukyan, A., Mirzakhanyan, A., Badalyan, G., Shirinyan, G., Fedorenko, A., Lianguzov, N., Yuzyuk, Yu., Bugaev, L., Sharoyan, E. (2012) Nickel nanoparticles in carbon structures prepared by solid-phase pyrolysis of nickel phthalocyanine, *J. Nanopart. Res.*, 14, 982-988.

Ambient scalable synthesis of surfactant-free thermoelectric metal chalcogenide nanostructures

C. Han,[1] Z. Li,[1,2,*], W.L. Li, [1] L. J. Zhang, [1] S. X. Dou[1]

[1] Institute for Superconducting and Electronic Materials, Australian Institute for Innovative Materials, University of Wollongong, Squires Way, North Wollongong, NSW 2500, Australia

[2] School of Radiation Medicine and Radiation Protection, Soochow University, 199 Ren Ai Road, Suzhou Industrial Park, Suzhou 215123, China

Email: zhenl@uow.edu.au; Tel: +61-2-42215163; Fax: +61-2-42215731

Abstract: Thermoelectric generators (TEG) / refrigerators (TER) can directly convert heat into electricity or vice versa. It is estimated that around 2/3 of energy produced is wasted as heat, and direct conversion of huge amount of waste heat into electricity by this green technology can significantly save on energy consumption and reduce carbon emissions because of its zero emissions and zero noise, excellent stability and reliability, and robust applicability.(Kraemer *et al.*, 2011) Only niche applications have been achieved, however, due to the limited number of high-performance thermoelectric (TE) materials. Among the different types of TE candidates, metal chalcogenides, especially lead and bismuth based selenides and tellurides, have been extensively investigated and applied in TE devices due to their excellent, reliable performance and lower cost in comparison with other candidates.(LeBlanc *et al.*, 2014) Their performance has been drastically improved through advanced nanoscience and nanotechnology in recent years. (Han *et al.*, 2014) Herein, a robust low-cost and high-efficiency ambient aqueous approach to the scalable synthesis of different surfactant-free nanostructured metal chalcogenides (M_aX_b, M = Cu, Ag, Sn, Pb, Bi; X = S, Se, Te; a = 1 or 2; and b = 1 or 3) has been developed (Figure 1). The effects of different reaction parameters, such as precursor concentration, precursor ratio, and amount of reducing agent, on the composition, size, and shape of the resultant nanostructures have been comprehensively investigated. This environmentally friendly approach is capable of producing large-scale metal chalcogenide nanostructures in a one-pot reaction for investigation of their thermoelectric properties towards conversion of waste heat into electricity. The results demonstrate that the thermoelectric properties of these metal chalcogenide nanostructures are strongly dependent on the types of metal chalcogenides, and their figure of merits are comparable with previous reports on their bulk and nanostructured counterparts. Recently, this roubust approach was extended to prepare CuAgSe ternary thermoelectric nanoparticles in a large scale.(Han *et al.* 2014) The resultant CuAgSe nanoparticles exhibit an interesting temperature-dependent reversible transition of metallic-n-p conductivity, accompanied by the transition of crystal structure from pure tetragonal phase, through a mixture of tetragonal and orthorhombic phases to cubic phase.

Keywords: ambient synthesis, metal chalcogenides, nanostructures, thermoelectric.

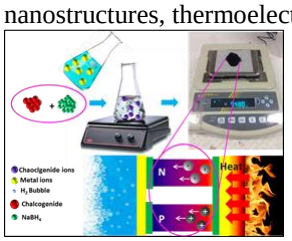

Figure 1: this Figure illustrating the two parts work that we are tempting to do: a general, scalable and low cost synthesized route for different nanostructured metal chalcogenides has been proposed and their thermoelectric performances will be tested.

References:

Kraemer, D., Poudel, B., Feng, H. P., Caylor, J. C., Yu, B., Yan, X., Ma, Y., Wang, X. W., Wang, D. Z., Muto, A., McEnaney, K., Chiesa, M., Ren, Z. F., Chen, G. (2011), High-performance flat-panel solar thermoelectric generators with high thermal concentration, *Nat. Mater.*, 10, 532-538.

LeBlanc, S., Yee, S. K., Scullin, M. L., Dames, C., Goodson, K. E. (2014), Material and manufacturing cost considerations for thermoelectrics, *Renew. Sustainable Energy Rev.*, 32, 313-327.

Han, C., Li, Z., Dou, S. X. (2014), Recent prigress on thermoelectric materials, *Chin. Sci. Bull.*, 59, 2073-2091.

Han, C., Sun, Q., Cheng, Z. X., Wang, J. L., Li, Z., Dou, S. X., Wang, L. Z. (2014), Ambient scalable synthesis of surfactant-Free thermoelectric CuAgSe nanoparticles with reversible metallic-n-p conductivity transition, *J. Am. Chem. Soc.*, 136, 17626-17633.

Acknowledgments

C. Han gratefully acknowledges the Chinese Scholarship Council (CSC) for his scholarship. Z. Li acknowledges support from the Australian Research Council (ARC) through the Discovery Projects DP130102699 and DP130102274. S. Dou is grateful for support from the Baosteel-Australia Research Centre (BARC) through the project BA110011 and from the ARC through the Linkage Project LP120200289.

Efect of Temperature During Composite Materials Synthesis for the use as Gas Separators in Alkaline Water Electrolysers on their Ionic Conductivity and Oxygen Barrier Propreties

J. Stojadinović,[1,*] G. Kasiribidhendi,[1] F. La Mantia,[1]
[1]University of Bochum, Dept. Chemistry and Biochemistry, Center for Electrochemical Sciences, Bochum, Germany

Abstract: Development of materials for the use in alkaline electrolyzers for gas separation has been directed towards surpassing the ionic conductivity, gas tightness, chemical, mechanical and thermal resistivity, life span, and cost effectiveness of the health hazardous asbestos and current state of the art Zirfon® separator [1].

Ionic conductivity of different gas separation membranes can be accurately determined by Electrochemical Impedance Spectroscopy with a four-electrode zero gap cell, while the use of the four-electrode non-zero gap cell coupled with a Mass Spectrometer enables the oxygen permeability assessment [2].

In order to gather better understanding of the separator materials' synthesis process, the interplay of the synthesis parameters and the electrochemical properties of the separator is studied here.

Temperature during synthesis was shown to have a significant influence on the ionic conductivity of developed separators. The effect of temperature on the morphology of the separators was investigated using X-Ray Diffraction and Scanning Electron Microscopy.

The understanding of the synthesis parameters interactions enables tuning of separators' ionic conductivity and oxygen permability, through the optimisation of the material fabrication.

Additionaly, it contributes towards broadening the material's application to systems other than alkaline electrolyzers, such as fuel cells and solar hydrogen generation.

Keywords: gas separation, synthesis temperature, ionic conductivity, oxygen permeability, X-Ray Diffraction.

References:

[1] P. Aerts, S. Kuypers, I. Genne, R. Leysen, J. Mewis, I. F. J. Vankelecom, P. A. Jacobs, Polysulfone-ZrO2 Surface Interactions. The Influence on Formation, Morphology and Properties of Zirfon-Membranes, *J. Phys. Chem.* B 110 (2006) 7425-7430.

[2] J. Stojadinović, S. Weiss, F. La Mantia, Effect of Electrochemical Cell Design on the Ionic Conductivity and Oxygen Permeation Determination of Gas Separators, *Electroch. Acta* 127 (2014) 153–158.

Effect of polystyrene nanocomposite prepared via Pickering emulsion polymerization on the mechanical properties of PP and EVA

A.B. Moustafa,[1] M.E. Abd El-Aziz,[1] A.M Rabie[2,] , H.A. Essawy[1*]
[1]Department of Polymers & Pigments, National Research Center, Dokki 12311, Cairo, Egypt
[2]Ain Shams University of Annaba, Chemistry Department, Cairo, Egypt

Abstract: Solid nanoparticles can be used as stabilizers for oil/water emulsions instead of the conventional surfactants. Emulsion polymerization of styrene, as an example of polymerizable oil, was started in the current study after ultrasonication of the monomer into the aqueous phase, with the aid of montmorillonite nanoparticles as solid particles stabilizer for the process. The imaging by a field emission scanning electron microscope (FESEM) equipped with energy dispersive X-ray (EDX) unit and transmission electron microscope (TEM) proved the formation of polystyrene/ montmorillonite nanocomposite as hybrid latex particles via Pickering mode of emulsification. The mechanical properties of polypropylene (PP) and ethylene-vinyl acetate copolymer (EVA) were studied after addition of various loadings (2, 4, 8, 12, and 14 wt%) of prepared polystyrene/ montmorillonite nanocomposite hybrids.

Keywords: Pickering emulsion, styrene, montmorillonite, polymerization, ethylene vinylacetate, polypropylene, reinforcement, mechanical properties.

Figure 1: Scheme demonstrates the synthesis of montmorillonite armored polystyrene latex via Pickering emulsion polymerization.

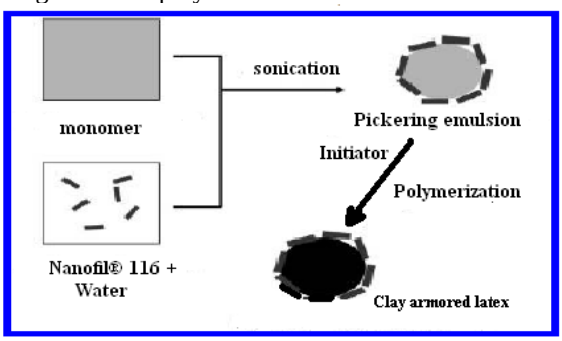

References:

Zhou, H., Shi, T., Zhou, X., (2013) Preparation of polystyrene/SiO_2 microsphere via Pickering emulsion polymerization: Synergistic effect of SiO_2 concentrations and initiator sorts, *Appl. Surf. Sci.*, 266, 33-38.

Moustafa, A.B., Abd El-Aziz, M.E., Emira, H.S., Rabie, A.M., Essawy, H.A. (2014), Emulsion polymerization of styrene using silica nanoparticles as solid stabilizer , *KGK*, 10, 47-53.

Lin, K., Yang, H., Petit, C. Lee, W. (2015), Magnetically controllable Pickering emulsion prepared by a reduced grapheme oxide-iron oxide composite, *J. Coll.Interf. Sci.*, 438,296-305.

Session II - C: Nanomaterials synthesis & properties

Kinetic Study of Functionalization of Carbon Nanomaterials

T.P. Dyachkova, E.N. Tugolukov, I.V. Anosova, A.G. Tkachev
Tambov State Technical University, Department "Technology and Methods of Nanoproducts Manufacturing", Tambov, Russian Federation

Abstract: Carbon-based nanomaterials are highly variable and possess unique physical properties. Presently, multi-walled carbon nanotubes (MWCNTs) and graphene nanoplatelets (GNPs) appear to be one of the most common and available materials. Nevertheless, their use in composite materials is often limited owing to a tendency to agglomerate. To improve the dispersibility in polymers and solvents, the surface of carbon nanomaterials can be functionalized by covalent attachment of various functional groups (Kharitonov *at all*, 2015) (hydroxyl, carboxyl, fluoride, amine, etc.). Functionalization is particularly valuable with respect to multilayered carbon nanostructures based on graphene, because tendency to agglomeration for this materials is especially strong because of large contacting surfaces.

The functional groups provide different kinds of interactions between the carbon nanostructures and polymer molecules: 1) electrostatic interaction; 2) hydrogen bond formation; and 3) covalent bond formation. Sometimes, the formation of composite polymer layers on the carbon nanomaterial surface can be observed due to such interactions. For instance, this may occur when modifying functionalized MWCNTs and GNPs with conducting polymers (polyaniline and polypyrrole).

Owing to the above-mentioned effects, functionalized MWCNTs- and GNPs-based composites are becoming more widely used in the manufacture of structural, building and electrode materials (Kondrashov *et al.*, 2013). This, in turn, raises the problem of obtaining functionalized and modified forms of carbon nanostructures in the industry. However, scaling processes of MWCNT and GNP functionalization requires a detailed study of the laws of their kinetics, determination of optimum technological regimes, providing production of materials with controlled characteristics (Dyachkova et al., 2013).

In this report, we present the results from a study on kinetic regularities of the carbon nanotube functionalization with liquid (nitric acid, potassium permanganate and hydrogen peroxide solutions) and gaseous (ozone, nitric acid and hydrogen peroxide vapors) oxidizing agents. It is shown that the gas-phase oxidation under optimum conditions allows obtaining materials with a high degree of functionalization with minimal consumption of reagents. It is proposed for the first time to use hydrogen peroxide vapor as oxidizing agent. It is demonstrated that in this case, the hydroxyl groups providing interactions with polar polymer matrices are mainly formed on the carbon nanotube surface. The optimum conditions for the carbon nanotube functionalization process in the hydrogen peroxide vapor were determined. The advantages of the proposed methods are the ease of implementation in the industry and the absence of environmentally hazardous waste.

Composites based on carbon nanomaterials modified with polyaniline (PANI) were obtained, and it was shown that preliminary functionalization of carbon surface with oxygen-containing functional groups improves the quality of nanocomposites obtained. With using this method, composites PANI/oxidized GNP and PANI/functionalized MWCNT were synthesized by of oxidative polymerization of aniline in presence of functionalized carbon nanomaterials. The kinetic regularities of the carbon nanostructure modification with polyaniline were studied. Besides, differences in temperature profiles of the oxidative polymerization reaction after modifying the pristine and oxidized MWCNTs and GNPs were disclosed. Influence of the morphology of original carbon nanomaterial, the degree of its pre-functionalization, medium acidity and molar ratio of reagents in the oxidative polymerization on the yield of PANI and electrical, thermal and electrochemical properties of composite materials was investigated. It was found that degree of polymerization and structure of PANI coatings are sensitive to the nature of functional groups on the surface of carbon nanotubes. Specific electrical resistance and capacitance properties of composites based on carbon nanotubes modified with PANI also depend on the conditions of oxidative polymerization.

The work was carried out within the framework of supporting the cooperation between Russian higher education institutions, state scientific institutions and organizations implementing complex projects on creation of high-tech production (RF Government Decree of April 9, 2010 No. 218; Contract of August 14, 2014 No. 02.G25.31.0123).

Keywords: multiwalled carbon nanotubes, graphene nanoplatelets, functionalization, oxidation, oxidative polymerization, nanocomposites.

References:

Kharitonov, A.P., Tkachev A.G., Blohin, A.N., Dyachkova, T.P., Maksimkin, A.A. Chukov, D.I. (2015) Reinforcement of epoxy resin composites with fluorinated carbon nanotubes, *Compos. Sci. Technol.*, 107, 162-168.

Kondrashov, S.V., Dyachkova, T.P., Bogatov, V.A., Mansurova, I.A., Marakhovskii ,P.S., Fokin, A.S. (2013) Utilization of carbon nanotubes for enhancing the heat resistance of epoxy binders, *Inorg. Mater. Appl. Res.*, 5, 394-399.

Dyachkova, T.P., Melezhyk, A.V., Gorsky, S.Yu., Anosova, I.V., Tkachev, A.G. (2013) Some aspects of functionalization and modification of carbon nanomaterials, *Nanosystems: Physics, Chemistry, mathematics*, 5, 605-621.

Single and Biphasic TiO_2 nanotubes by Electrochemical Anodization

R.Savitha,[1,2,*] Kieran Nolan,[2] Anne Morrissey,[3] R.RaviKrishna,[1] P.Selvam,[4] Raghuram Chetty[1]

[1] Department of Chemical Engineering, Indian Institute of Technology (IIT) Madras, Chennai, India.
[2] School of Chemical Sciences, Dublin City University (DCU), Dublin, Ireland.
[3] School of Biotechnology, Dublin City University (DCU), Dublin, Ireland.
[4] Department of Chemistry,IIT Madras, Chennai, India.
(*savitharangasamy@gmail.com)

Abstract: Titania (Titanium dioxide/TiO_2), is one of the most abundant elements and its application spans through various fields because of its chemical stability and specific photo induced properties. Utilization of TiO_2 in applications such as water splitting, solar cells, pollutant mineralization and disinfection needs high photocatalytic activity whereas in paints and cosmetics TiO_2 as a UV absorbent needs controlled photo reactivity (Carp *et al.*; 2004). There are four polymorphs of titania found in nature Anatase, Brookite, Rutile and Monocilinic. Among these Rutile is the most thermodynamically stable and Anatase has the most favourable kinetics. In certain systems, especially in photocatalytic degradation reactions, the presence of two phases (biphasic) for example, Anatase and Rutile, results in visible light activation of the catalyst for the production of reactive hydroxyl radicals. Thus the crystalline nature of TiO_2 decides its fate of utilization. Precise and controlled fabrication of titania nanoforms, to avail of high surface area is a key challenge in developing TiO_2 catalysts. One dimensional structures such as nanotubes and nanowires can be made as a mechanically stable three dimensional assembly with high surface area. Annealing of amorphous nanotubes (up to 500°C) crystallized into Anatase phase, and heat treated beyond 500°C, results in Anatase to Rutile transformation along with collapsing of nanotube morphology (Eder *et al.*; 2006).

In this work a simple and facile route to the synthesis of pure anatase and biphasic (Rutile+Anatase) nanotubes in powder form is proposed. This work focuses on nanotubes formation through rapid breakdown, electrochemical anodization with perchloric acid electrolyte and crystallization of the amorphous nanotubes through heat treatment. The effect of impurities present in the system, which causes early nucleation favoring rutile phase growth by introducing surface defects and oxygen vacancies, was also investigated. The nanotubes are morphologically characterized by Scanning and Transmission Electron Microscope; the crystalline phases are studied by X-ray diffraction pattern; optical properties by Diffusive Reflectance Spectroscopy (UV-DRS). Nitrogen adsorption-desorption (BET) studies were also carried out to estimate the porosity and surface area.

Preliminary experiments were conducted to examine the efficiency of these nanostructures for the photocatalytic degradation of Paracetamol and Famotidine in aqueous solutions.

Keywords: TiO_2 Nanotube, Electrochemical Anodization, Crystallization, Biphasic nanotube, Photodegradation.

References:

Carp, O., Huisman, C.L. & Reller, a., (2004), Photoinduced reactivity of titanium dioxide, *Progress in Solid State Chemistry*, 32, 33–177.

Eder, D., Kinloch, I. a & Windle, A.H., (2006), Pure rutile nanotubes. *Chemical Communications*, 30(13), 1448–50.

3D Printed Hydrophobic and Antimicrobial Nanofunctionalised Surfaces

M. J. Cook,[1*] L. Gilbertson,[2] J. H. Johnston,[1,3] T. Miller[2]
[1] Victoria University of Wellington, School of Chemical and Physical Sciences, New Zealand
[2] Victoria University of Wellington, School of Design, New Zealand
[3] The MacDiarmid Institute for Advanced Materials and Nanotechnology, New Zealand

Abstract: Superhydrophobic surfaces have been widely studied for many years, in order to determine their characteristics and create new surfaces with similar high water repellency. It has been determined that in addition to a chemical hydrophobicity (low surface energy), a surface roughness is also needed (Cassie & Baxter, 1944; Wenzel, 1936). This surface roughness is generally thought to require both a microstructure and an overlying nanostructure as observed on the superhydrophobic surface of the *lotus* leaf (Neinhuis & Barthlott, 1997). This required surface roughness has been produced in existing literature, using many different methods including solid freeform fabrication (Barahman & Lyons, 2011), etching, lithography and sol-gel (Celia *et al.*, 2013). Superhydrophobic surfaces are conventionally described as those with a static water contact angle of greater than 150°.

3D printing is a very useful fabrication method for producing 3D models with finely tuned physical forms. Fused Deposition Modelling (FDM) is the cheapest and easiest 3D printing technology, but has a comparatively low print resolution. It was thought to be unsuitable for printing superhydrophobic surfaces, as the necessary micro-scale dimensions of the surface roughness were difficult to achieve. In addition, the majority of FDM 3D printable materials are chemically hydrophilic or have too low viscosity to print the fine structures. Research by us has shown that by manipulating the build parameters of the 3D printer, carefully selecting the build material and subsequently chemically treating the 3D printed surfaces with a hydrophobic polymer, it is possible to produce close to superhydrophobic surfaces by FDM printing. The surfaces produced in this way have achieved contact angles of greater than 125° with a 10 µL water droplet. This provides a new method of fabricating water repellent surfaces and opens up new applications and possibilities for the design of consumer products.

The hydrophobic nature of such a surface can impart inherent bacteriostatic properties. This effect can be increased by incorporating silver nanoparticles onto the surfaces, as silver nanoparticles have been shown to have high antimicrobial activity (Morones et al., 2005). Using the technology of Johnston & Parry (2014) the 3D printed surface or initial polymer filament can be functionalized with silver nanoparticles to provide an effective antimicrobial surface without destroying the hydrophobicity of the surface. The paper presents the results of this study.

Keywords: surfaces, superhydrophobicity, antimicrobial, 3D printing, silver nanoparticles

References:

Barahman, M., Lyons, A. M. (2011), Ratchetlike slip angle anisotropy on printed superhydrophobic surfaces. *Langmuir*, 27, 9902-9909.

Cassie, A. B. D., Baxter, S. (1944), Wettability of Porous Surfaces. *Trans. Faraday Soc.*, 40, 546–551.

Celia, E., Darmanin, T., Taffin de Givenchy, E., Amigoni, S., Guittard, F. (2013), Recent advances in designing superhydrophobic surfaces. *J. Colloid Interface Sci*, 402, 1–18.

Johnston, J. H., Parry, M. (2014), New Generation Nanogold and Nanosilver Polymer Composites and Their Applications. *Proceedings NSTI-Nanotech 2014*, 1, 358-361. Washington, DC.

Morones, J. R., Elechiguerra, J. L., Camacho, A., Holt, K., Kouri, J. B., Ramírez, J. T., Yacaman, M. J. (2005), The bactericidal effect of silver nanoparticles. *Nanotechnology*, 16, 2346–2353.

Neinhuis, C., Barthlott, W. (1997), Characterization and Distribution of Water-repellent, Self-cleaning Plant Surfaces. *Ann. Bot.*, 79, 667–677.

Wenzel, R. N. (1936), Resistance of solid surfaces to wetting by water. *J. Ind. Eng. Chem.*, 28, 988–994.

Molecular dynamics simulation of glass formation and crystallization in binary PdNi and CuNi alloys.

Muhammad Faruq,[a] Antoine Villesuzanne,[a,b] and Guosheng Shao [a,c]

[a] Institute for Renewable Energy and Environmental Technologies, University of Bolton, Bolton BL35AB, UK

[b] CNRS, ICMCB, University of Bordeaux, F-33600 Pessac, France

[c] UK- China Centre for Multi-functional Nanomaterials, Zhengzhou University, Zhengzhou 450001, P.P. China

Abstract: Molecular dynamics (MD) using Quantum Sutton-Chen potentials were used to obtain an atomistic description of melting, glass formation and crystallization processes for Cu, Ni and Pd metals to study the PdNi and CuNi alloys. The thermodynamic and mechanical properties were calculated in the 0-2000K temperature range from the MD trajectories. The formation of amorphous Cu, Ni and Pd and their equimolar alloys by rapid quenching was investigated from MD at constant pressure and temperature (TPN ensemble). The structural properties were analyzed by means of pair distribution functions and volume *vs* temperature, at cooling rates ranging from 40 K/ps to 0.4K/ps. The relation between the cooling rate and glass transition temperature, or crystallization, was investigated. The radial distribution function agrees well with experimental results for amorphous phases. Upon cooling rates in the range from 5K/ps to 0.4K/ps, Cu, Ni, Pd metals and CuNi alloy form a crystalline structure while the PdNi alloy form a glass. A mismatch in atomic size (1.02 vs 1.134 ratio for CuNi and PdNi, respectively) appears to favor the glass formation.

Keywords: Molecular dynamics, Quantum Sutton-Chen potentials,Cu-Ni alloys, Pd-Ni alloys, Quenching rate,Glass formation.

Graphene mediated synthesis of gold nanoparticles and it nanocomposite and their Applications

P. C. Pandey, Yashashwa Pandey
Department of Chemistry, Indian Institute of Technology (BHU), Varanasi-221005, India

Abstract: The conversion of 3-Aminopropyltrimethoxysilane capped noble metal ions (Au^{3+} , Pd^{2+} , Ag^{+}) into respective nanopartcles in the presence suitable organic reducing agents constitute new route of metal nanoparticle synthesis justifying potential applications in many biomedical applications (Pandey et al, 2011, 2012).[1] The choice of organic reducing reagent precisely govern the dispersibility, nanogeometry, pH and salt tolerance of as synthesized nanoparticles for specific application[2-4]. Some of the organic reducing agent enable the formation of organic –inorganic hybrid during nanoparticle synthesis justifying enhanced catalytic activity of nanomaterial.[5] It was further investigated that the presence of graphene suspension along with reaction mixture facilitate the process of nanopparticles synthesis with significant change in electrocatalytic ability of the material. The presence of graphene allow nucleation site fo nanoparticles and results the formation of hybrid nanomaterial having potentiality for biocompatible thin film formation. This study will also permit us to discuss a new route of nanaoparticles synthesis justifying the micellar behavior of 3-APTMS that precisely control the practical usability of nanomaterial in biomedical applications..

Keywords: nanoparticle synthesis, organic-inorganic hybrid, electrocatalysis, silica-based nanomaterials, biomedical applications.

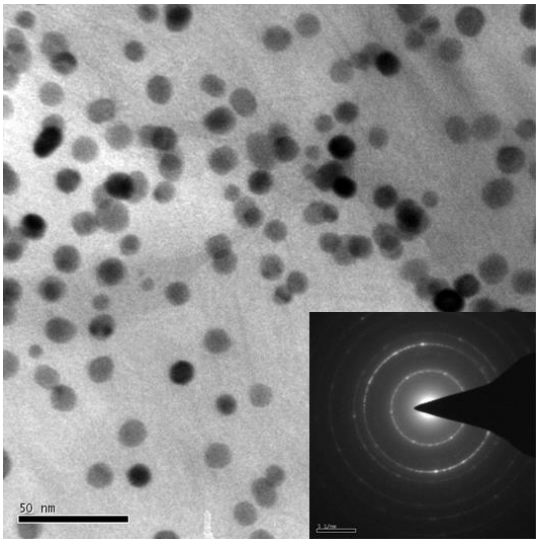

Figure 1: Figure illustrating the TEM image and respective diffraction pattern of graphene sheet that facilitate the 3-aminopropyltrimethoxysilane and formaldehyde mediated synthesis of gold nanoparticles.

References:

1. P. C. Pandey and D. S. Chauhan, *Analyst* 137, 376 **(2012)**.
2. P. C. Pandey, A. Pandey and G. Pandey, J. Nanosci. Nanotech. 14, 6606 **(2014)**
3. P. C. Pandey and G. Pandey, J. Nanosci.. Nanotech.**(2015)** (in press).
4. P. C. Pandey and Richa Singh, J. Nanosci.. Nanotech. 15, 5749 **(2015)**
5. P. C. Pandey and G. Pandey, J. Mater. Chemistry B. 2, 3383, **(2014).**

Preparation, morphological and AC electrical characterization of porous PEG/Polyaniline/Gold Nanowires composite.

M. Celentano[2], R. Vecchione[1], P. A. Netti[1,2]
[1]Center for Advanced Biomaterials for Health Care – IIT@CRIB, Istituto Italiano di Tecnologia – Largo Barsanti e Matteucci, Napoli, Italy
[2]Centro di Ricerca Interdipartimentale sui Biomateriali – CRIB, Università di Napoli Federico II, Napoli, Italy

Abstract: Heterogeneous conducting composites have been object of extensive studies in the last decades. The combination of conducting polymers with inorganic materials having different properties opens up new avenues for the development of innovative hybrid materials with interesting features.[1-4]
Polyanilines have been extensively studied in recent years due to many advantages among other conducting polymers such as low cost, easy synthesis, range of electrical conductivities and unique reversible proton doping-dedoping processes.[5]
At the same time, gold nanoparticles have been applied both in biology and in technology due to their tunable chemical-physical properties. Moreover, they can be easily conjugated with biological molecules.[6] Combination of organic and inorganic materials having biological moieties could be potentially applied in biosensor devices.[7]
We report the preparation of a new type of conducting organic-inorganic composite. In particular, conducting polyaniline in fiber form was dispersed into PEG porous matrix containing gold nanowires in network form.
The composite was characterized by TEM, SEM, ATR-FTIR and XPS. The AC electrical behavior was also studied. The relation among composition, morphology and AC electric response was taken into account.
Morphological and spectroscopic analysis have revealed that the gold nanowires were included only in the pores, while the hydrophobic polyaniline was dispersed in the PEG matrix. It was assumed that the more conductive phase were the pores, while the less conductive was ascribed to the PEG matrix. Results indicated that the PEG porous matrix conductivity was marginally affected if only gold nanowires networks or polyaniline were added. In the first case the pores filled by gold nanowire networks were electrically isolated, while in the second case the contribution to the electrical conductivity of PEG matrix was low due to the low amount and low intrisinc conductivity of polyaniline.
Newertheless, when both these two fillers were present in the matrix, at the same concentration of the previous cases, the percolation threshold was surpassed. Probably, the two fillers exerted a synergic effect on the AC conductivity. Indeed, the pores may be electrically interconnected through the polyaniline chains inside the PEG matrix.
In conclusion, high conductive heterogeneous composite with high porosity has been realized. This composite could be easly functionalizated with biological sensors and potentially applied as transduser in a biosensor device.

Keywords: heterogeneous composites, porous polymer matrix, gold nanoparticles, AC conduction, electron microscopy.

References:

[1] C.G.Wu, D.C. Degroot, H.O. Marcy, J.L. Schindler, C.R. Kannewurf, Y.J. Liu, W. Hirpo, M.G. Kanatzidis, *Chem. Mater.* 8 (1996) 1992.
[2] T.A. Kerr, H. Wu, L.F. Nazar, *Chem. Mater.* 8 (1996) 2005.
[3] E.R. Hitzky, P. Aranda, B. Casal, J.C. Galvan, *Adv. Mater.* 7 (1995)
180.
[4] W.J. Bae, K.H. Kim,W.H. Jo, Y.H. Park, *Macromolecules* 37 (2004) 9850.
[5] Trivedi, D. C., 1997. "Handbook of Conducting Molecules and Polymers", (ed.) by Nalwa, H. S., John Wiley and Sons 2:505.
[6] P. M. Tiwari, K. Vig, V. A. Dennis and S. R. Singh, *Nanomaterials*, 1, 31-63 (2011).
[7] T. A. Kumar , E. Capua , M. Tkachev , S. N. Adler, and R. Naaman, *Adv. Funct. Mater.*, 24(37), 5833-5840 (2014).

Low Pressure Chemical Vapor Deposition of Nickel Oxide Nanospheres as Anode for Lithium-ion Battery

L. Meda,[1*] C. Arnold. A,[1] J. He,[2] A. Dangerfield[3]
[1]Xavier University of Louisiana, Department of Chemistry, New Orleans, LA, USA
[2]Tulane University, New Orleans, LA, USA
[3]University of Texas at Dallas, Department of Materials Science and Engineering, Arlington, Texas, USA

Abstract: Low pressure chemical vapor deposition (LPCVD) of nickel oxide (NiO) nanospheres prepared directly on current collectors is ideal for studying the electrochemical properties because they are no interferences from additives. The direct growth of the materials onto current collectors provides faster mass and electron transport due to the improvement in conductivity across the interfaces and through the materials due to its nanosize. The microstructural characteristics of the as-prepared nanospheres were examined by high resolution transmission electron microscopy which showed that they were arranged randomly on the current collector. Selected area electron diffraction showed that the NiO is polycrystalline with the face-centered cubic crystal structure. The X-ray photoelectron spectroscopy showed that the as-prepared materials are pure NiO.

Aging of NiO electrodes were evaluated by cyclic voltammetry (CV) and charge-discharge measurements up to 140 cycles in the voltage range from 0.1 – 4.0 V versus Li/Li^+. After 140 cycles, a capacity of 1500 mAh/g was still observed. The expected capacity of NiO is 718 mAh/g, therefore 782 mAh/g is excess capacity. Both measurements revealed that the material is intact on the current collector. The LPCVD growth process creates very high surface area NiO which is one of the reasons for the overall improvement in electrochemical performances. However, high surface area introduces new challenges in the use of conversion reaction (equation 1a) for actual rechargeable batteries. This study will highlight the improvement in mass and electron transfer kinetics, but will also address the origin of the excess capacity observed in these systems due the high surface area of the NiO.

$$NiO + 2Li^+ + 2e^- \leftrightarrow Li_2O + Ni^0 \quad (1)$$

$$Li + LiPF_6/PC/DC/DMC \rightarrow \text{Li-Polymer} + Li_2CO_3 + LiF + LiO_2CO.R \quad (2)$$

$$\text{Li-Polymer} \leftrightarrow \text{Polymer} + Li \quad (3)$$

Keywords: nickel oxide, nanospheres, low pressure chemical vapor deposition, conversion reaction, electrochemical properties

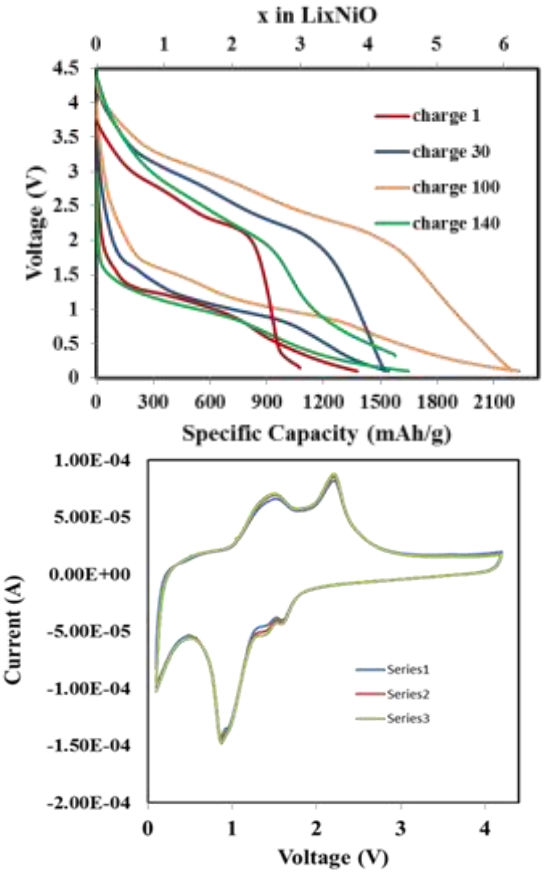

Figure1. (a) The galvanostatic discharge/charge performances of NiO nanospheres for 1st, 30th, 100th, 50th and 140th cycles at 1.5 C rate and (b) the CVs at 2nd and 130th cycles.

References:

Navulla, A., Stevens, G., Kovalenko, I., Meda, L. (2014), Reversible High Capacity in Hierarchical Columnar RuO_2 Nanoplates and Their Improved Performance in Lithium Ion Batteries, *J. Phys. Chem. C.*, 118, 13382−13386.

Varghese, B., Reddy, M. V., Yanwu, Z., Chang, S.L., Hoong, T.C., Rao, Subba, G.V., Chowdari, B.V.R., Wee, A.T.S., Chwee, T.L., Sow, C-R., (2008) Fabrication of NiO Nanowall Electrodes for High Performance Lithium Ion Battery, *Chem. Mater.*, 20, 3360-3367.

Morphology, Properties and Electrocatalytic Behaviour of Nanoporous Metals prepared by Electrolytic Dealloying of AgAuPt Alloys

Adrián Vega and Roger C. Newman
University of Toronto, Dept. of Chemical Engineering and Applied Chemistry
200 College St., Toronto, M5S 3E5, Ontario, Canada

Abstract: Nanoporous gold fabricated by electrolytic dealloying (selective dissolution) of Ag from an AgAu solid solution alloy has become a highly fashionable subject of research in the past decade. A high-profile book published by RSC and an inaugural conference held in Germany last summer have brought the subject to an even wider audience. Our own recent research has focused on the dealloying of ternary AgAuPt alloys with a low Pt content (1-3 at%) and systematic variation of the Au/Pt ratio, while maintaining 77 at.% Ag. Our published research, cited below, focused on the fundamental mechanisms of formation of the nanoporous materials and their response to heating in air or inert atmospheres (Pt co-segregates with O to the ligament surfaces in air, but desegregates in inert atmospheres). All ternary alloys gave a much more refined as-dealloyed morphology than the binary AgAu alloy, because Pt enriches at step edges, hindering the surface diffusion of gold. The smallest ligament size observed in our family of alloys is around 4 nm. Like all dealloyed materials, they show a bicontinuous morphology of ligaments and pores, with good mechanical integrity.

More recently, we have been examining the electrocatalytic properties of the dealloyed binary and ternary alloys. Alongside studies of methanol and ethanol oxidation, the Pt coverage of the nanosized ligaments has been probed by underpotential deposition (UPD) of hydrogen and UHV surface analysis. The UPD measurements show interesting variation from what is usually observed, which we attribute to the presence of isolated Pt atoms or very small clusters that do not have hollow sites with 3 Pt neighbours for H adsorption. These data require further analysis using a more sophisticated model than we have been using so far.

The kinetics of methanol and ethanol oxidation on the dealloyed AgAuPt materials are very rapid, and heat treatment in air to cosegregate Pt and O gives even faster kinetics (when expressed as true anodic current density; of course the porosity coarsens by surface diffusion when the material is heated at the necessary temperatures, $\geq$300ºC, so the true surface area is less).

In basic solution, carbonate yields are high for methanol and surprisingly high for ethanol. The latter result is under further investigation using a variety of analytical techniques. Studies in sulfuric acid are in progress.

The air-annealing process to segregate Pt can probably be optimized further, and even lower Pt contents in the starting alloy are of interest; however thermal coarsening of the porosity appears to accelerate below 1% Pt.

Further alloying is of interest in order to further stabilize the porous structure.

Keywords: nanoporous metals, electrolytic dealloying, electrocatalysis, surface segregation.

References:

Adrián A. Vega and Roger C. Newman, Nanoporous Metals Fabricated through Electrochemical Dealloying of Ag-Au-Pt with Systematic Variation of Au:Pt Ratio, *J. Electrochem. Soc. 2014 161(1): C1-C10.*

Adrián A. Vega and Roger C. Newman, Beneficial Effects of Adsorbate-Induced Surface Segregation of Pt in Nanoporous Metals Fabricated by Dealloying of Ag-Au-Pt Alloys, *J. Electrochem. Soc. 2014 161(1): C11-C19.*

Modulation of Active Sites in Supported $Au_{38}(SC_2H_4Ph)_{24}$ Cluster Catalysts: Effect of Atmosphere and Support Material

B.Zhang[1], S.Kaziz[2], H.Li[3], M.G.Hevia[4], D.Wodka[1], C.Mazet[3], T.Bürgi[1*], N.Barrabés[1*]
[1] Department of Physical Chemistry, University of Geneva, Geneva, Switzerland
[2] Department of Industrial Engineering, National High School of Engineers of Tunis, Tunisia
[3] Department of Organic Chemistry, University of Geneva, Geneva, Switzerland
[4] Institute of Chemical Research of Catalonia (ICIQ), Tarragona, Spain

Abstract: Thiolate-protected Au nanoclusters have fascinated chemists by offering well-defined and homogenous surface, which can be applied for catalytic reactions (Yamazoe *et al.;* 2014). Exposure of catalytically active gold sites on the cluster surface by thermal treatment and stabilization by supporting on metal oxides represent two effective methods to balance the catalytic activity and stability of Au nanoclusters in oxidation reactions (Shivhare *et al.;* 2013). $Au_{38}(SR)_{24}$ nanocluster bears intrinsically chiral features due to the arrangement of the protecting ligands on the surface of the cluster (Dolamic *et al.;* 2012), which makes it promising in enantioselective catalysis. We investigate the distinctly different interaction of $Au_{38}(SR)_{24}$ with two support materials Al_2O_3 and CeO_2 (Figure 1). The catalytic surfaces have been heated in different atmospheres and the removal of the thiolate ligands has been studied. Thermogravimetry (TG), Temperature programmed process coupled with mass spectrometer (TPRDO-MS) and X-ray absorption spectroscopy (XAFS) studies were performed to understand the desorption of thiol ligands depending on conditions and support material. Depending on the atmosphere and the support material the fate of the thiol ligands is different upon heating leading to metallic Au in the case of Al_2O_3 and to cationic Au with CeO_2. The thiolate removal seems to be a two-step procedure. The catalytic activity of these Au_{38} supported clusters was studied for the aerobic oxidation of cyclohexane. Conversion was higher for the gold clusters supported on CeO_2. Surprisingly, a significant amount of cyclohexanethiol was found, revealing the active participation of the thiolate ligand in catalytic reactions. The observation also indicates that breaking and formation of C-S bonds can be catalyzed by the gold clusters.

Keywords: Gold Cluster, catalyst, thiol ligand, thermal treatments, oxidation

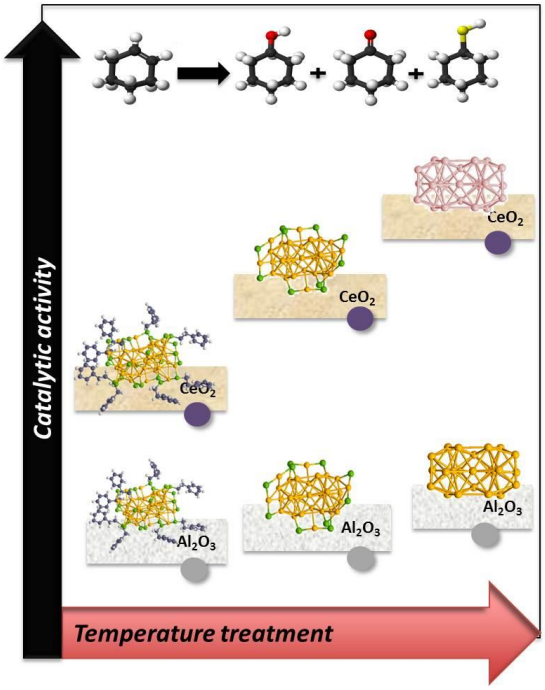

Figure 1: Figure illustrating the support and thermal pre-treatment effect on the modulation of $Au_{38}(SR)_{24}$ catalytic activity for cyclohexane oxidation.

References:

Yamazoe, S., Koyasu, K., Tsukuda, T. (2014) Nonscalable oxidation catalysis of gold clusters, *Acc. Chem. Res.*, 47,816-824.

Shivhare, A., Chevrier, M. D., Purves, W.R., Scott, W.J.R. (2013) Following the thermal activation of $Au_{25}(SR)_{18}$ clusters for catalysis by X-ray absorption spectroscopy, *J. Phys. Chem. C.*, 117,20007-20016.

Dolamic, I., Knoppe, S., Dass, A., Bürgi, T. (2012) First enantioseparation and circular dichroism spectra of Au_{38} clusters protected with achiral ligands, *Nat. Commun*, 3,798

Tuning colloidal stability, MRI relaxivity and bioelimination of functional nanoparticles

A. Walter,[1,2] A. Garofalo,[1] J. Taleb,[3,4] P. Bonazza,[3,4] C. Billotey[3,4], S. Laurent,[5] L. Vander Elst,[5] R. N. Muller[5], D. Felder-Flesch[1],S Begin-Colin,[1]

[1] Institut de Physique et Chimie des Matériaux de Strasbourg (IPCMS), UMR 7504, CNRS, Université de Strasbourg, 23, rue du Loess, BP 43, 67034 Strasbourg Cedex 2 (France).
[2] EPFL, Laboratoire de Technologie des Poudres, EPFL-STI-IMX-LTP Station 12 CH-1015 Lausanne, Suisse
[3] Laboratoire de Physico-Chimie des Matériaux Luminescents, UMR 5620 CNRS-UCBL, Université Claude Bernard Lyon1, 10 rue Ada Byron 69622 Villeurbanne cedex, France.
[4] Hospices Civils de Lyon - Service de Médecine Nucléaire Pavillon B, 5 place d'Arsonval, 69437 Lyon cedex 03, France
[5] General, Organic, Biomedical Chemistry; NMR and Molecular Imaging Laboratory
Université de Mons. 19 Avenue Maistriau, B-7000 Mons, Belgium; Center for Microscopy and Molecular Imaging (CMMI), 6041 Gosselies, Belgium

Abstract: Superparamagnetic iron-oxide nanoparticles (SPION) with appropriate functionalized surface have attracted a great deal of attention for their potential biomedical applications including magnetic resonance imaging (MRI) contrast enhancement, hyperthermia treatment, cell sorting, drug delivery, immunoassay and tissue repair. In all these applications, the tailoring of the SPION surface is mandatory not only to improve biocompatibility, solubility and stability but also to ensure a small particle size distribution (below 100 nm) after decoration and to preserve good magnetic properties, e.g. a high saturation magnetization. Furthermore, the steric hindrance of coating can affect the fate of NPs in biological system, such as cellular uptake and accumulation, circulation and clearance from body. Moreover, appropriate surface functionality is the perquisite for conjugating biomolecules to NPs for biomedical applications.

A dendritic approach as a coating strategy for the design of functional NPs is particularly interesting in the field of diagnostics (Figure 1). The appeal of such strategy is due to the unique properties of the dendritic structures which can be chemically tuned to reach ideal biodistribution or highly and efficient targeting efficacies. Indeed, dendrimers are macromolecules consisting of multiple perfectly branched monomers and this architecture makes them versatile constructs for the simultaneous presentation of receptor binding ligands and other biologically relevant molecules.

Keywords: SPION, Dendron, MRI, bioelimination, colloidal stability

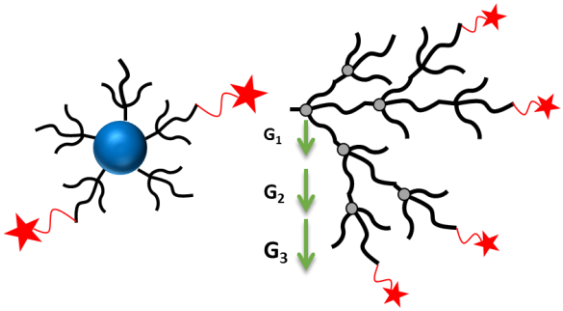

Figure 1: Figure illustrating the dendritic approach to functionalize NPs and dendritic coatings of generation 1(G1), 2 (G2) or 3 (G3)

We propose here to compare the effect of a linear ligand versus a dendritic coating of low generation (generation 1(G1), 2 (G2) or 3 (G3)) on the suspension stability, relaxivity properties and bioelimination of spherical SPION of 10 nm (NS10). NPs were synthesized by thermal decomposition and functionalized via a direct ligand exchange process.

The functionalization yielded nano-objects of 15 to 30 nm in size, stable in physiological media and showing both renal and hepatobiliary elimination.

The colloidal stability of functionalized NS10 has been evaluated in water and in different physiological media. NMRD profiles and relaxivity measurements highlighted the influence of the molecule architecture on the water diffusion close to the magnetic core thus influencing the relaxation properties at low magnetic field. Coupling of a fluorescent dye on the functionalized NS10 allowed investigating their biodistribution and highlighting urinary and hepato-biliary eliminations.

Parametric study on Fiber Bragg Grating for improvement of AE sensitivity

Ishac Kandas[1,2], Nader Shehata[1,2,3], Effat Samir[2], Hatem A. Khater[4]
[1]Department of Engineering Mathematics and Physics, Faculty of Engineering, Alexandria University, Egypt.
[2]Center of Smart Nanotechnology and Photonics (CSNP), Smart Critical Infrastructure (SmartCI) research center, Alexandria University, Egypt.
[3]Bradley Department of Electrical and Computer Engineering, Virginia Tech, United States.
[4]Naval Research & Development Department, Egypt.

Abstract: Recently, Fiber Bragg Gratings (FBGs) are attracting great attention in many applications such as underwater acoustic sensing. In this novel work, it is aimed to improve the sensitivity of FBG through analyzing relationship between the detected light power and the wavelength shift due to the applied pressure of the acoustic signal. The performance of various apodization profiles has been investigated. Among some selected apodization profiles, Cauchy profile has been proved to give the best performance. Then, by applying to different photodetectors, the results show that InGaAs detector type is more suitable than Ge one. At certain index modulation depth, a maximum wavelength shift is calculated for different lengths of FBG, after which there is no change would happen to the curve of light power and wavelength shift. These results could be applied in developing the sensitivity of acoustic sensors.

Fiber Bragg grating (FBGs) are becoming increasingly important in optical communication systems and sensing[1]. Many applications were recorded for FBGs. One of the most vital applications is sensing [2]. Either reflection spectrum or transmission one can be used as a sensing tool. For acoustic emission (AE) detection , Pizo-type sensor (PZT) can be used . Due to its many drawbacks [3], FBG becomes a promising sensor for AE. Simplicity, small size, multiplexing probability , high sensitivity [1, 3] make FBGs being better than PZT in sensing AE. The change on the pressure due to the AE would change the transmission or reflection spectrum. The shift in the FBG wavelength, λ_B is considered an indicator for the pressure change. The operational range and pressure sensitivity are the main targets to enhance the performance of FBG sensor.

First of all, the apodization profiles were tested to see which one will produce maximum sensitivity . The simulation uses uniform FBG of length 0.75 cm , and index modulation depth Δn of value 2×10^{-4}. Constant response of the photodector was
assumed. Also, constant intensity of the incident light (Fig. 1) .

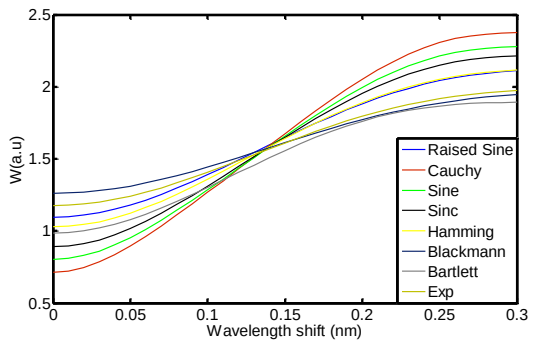

Fig. 1 The received intensity , W for different apodization profiles.

As shown , Cauchy profile is the best one as it provides the maximum slope.

Another analysis were done for different types of photodetectors at 1550 nm range . The used photdetectors are Ge, InGaAs. For all cases, the Cauchy profile is the best one. we compared the performance of the two photodetectors and the case of constant response (Fig.2). InGaAs is much better.

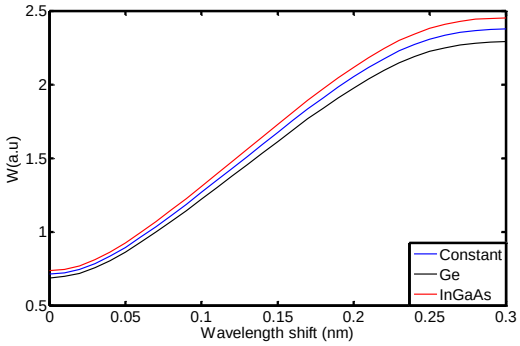

Fig.2 Response of different types of photodetectors.

It is important to calculate the maximum wavelength shift before saturation. Fig.3 shows the reflectivity for different FBG lengths.

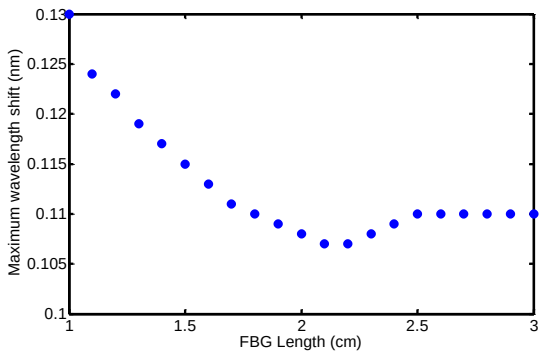

Fig.3 Maximum wavelength shift versus different lengths of FBG.

Keywords: Fiber Bragg Grating, apodization profile, photodetector, Acoustic sensor.

References:

[1] Graham Wild and Steven Hinckely, "Optical Fibre Gratings for Acoustic Sensors" Proceeding of 20th International Congress on Acoustic Sensors, ICA (2010).
[2] Xingjie Ni,Yong Zhao, JianYang, "Research of anovel fiber Bragg grating under water acoustic sensor" Sensors and Actuators A **138**, 76-80 (2007).
[3] Dae-Cheol Seo, Dong-Jin Yoon, IL-Bum Kwon and Seung-Suk Lee, "Sensitivity enhancement of fiber optic FBG sensor for acoustic" Proc. of SPIE Vol. 7294 729415:1-10 (2009).

The Power of Heterogeneity: A Systems Approach to Complex Data in Materials Science

M. Nyden,[1*] N, Williamson[1], M. Röding,[1] T. Nann[1]
[1]The Ian Wark Research Institute, Department of Information technology, engineering and the environment, University of South Australia, Adelaide, Australia

Abstract: Heterogeneity is here to stay – and will influence science even more in the future – partly because future raw materials are likely to originate from natural resources. It is a major challenge to science and technology to the point where it is difficult to consistently meet product quality standards.

We have developed a new method – a systems approach – to unlock the inherent potential of distributed data to create quantitative relationships between inputs/parameters and outputs/performances.

Previous work on quantitative correlation of distributed data is very limited[1]. The systems approach we have developed allows for the first time quantitative relationships from data that come in distributions of P(x), P(y) and P(z), rather than single values of x, y and z. It enables us to predict and optimise processes and materials and increase our fundamental understanding of heterogeneous materials. The goal is a 'grand unified theory' for dealing with distributed data, spectral data, temporal data, spatial data and more in all fields underpinned by distributed data.

Here we address effects of variable quality and heterogeneity of raw materials. More specifically we show the power of the systems approach for manufacturing of polydisperse catalytic particles and understanding relationships between diffusion and molecular weight of polymers in solution.

Keywords: Nanoscience, nanotechnology, material science, advanced manufacturing, processing, distributed data, polydispersity, heterogeneity, polymers, nanoparticles, diffusion, scaling.

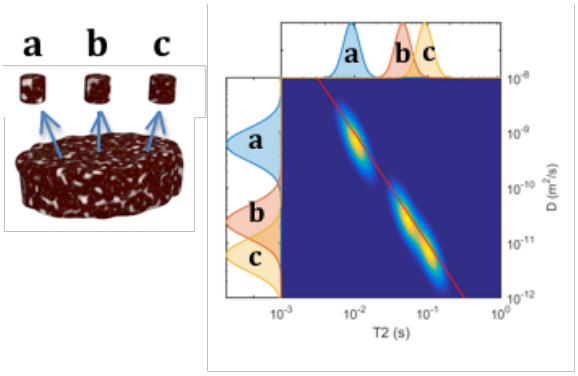

Figure 1 Six independent NMR relaxation and diffusion measurements represented on the x- and y-axes, from three subsamples a,b, and c of the same heterogeneous material, e.g. meat. Combined, the independent measurements are used to find the quantitative relationship (solid red line) between the parameters without performing time-consuming 2-d measurements (unpublished data).

References:

1. Oliva, J., Póczos, B., & Schneider, J. (2013). Distribution to distribution regression. In *Proceedings of The 30th International Conference on Machine Learning*, 1049-1057.

A facile route to synthesize rutile TiO_2 nanorods arrays via hydrothermal method

M. Guo[1, 2], Y. Gao[1], Q. Deng[3], X. Xia[1], G. Shao[2, 3*]
[1]Faculty of Materials Science and Engineering, Hubei University, Wuhan, 430062, P. R. China
[2]Institute for renewable energy and environmental technologies, University of Bolton, Bolton, BL3 5AB, UK
[3]UK-China Centre for Multifunctional Nanomaterials, Zhengzhou University, Zhengzhou 450001, China

Abstract: Hydrothermal method is a well-accepted sysnthesition method for its simple and low-cost procees as well as its rapid growth rate. Here highly-ordered, one-dimensional (1D) nanowires/nanorods arrays of rutile TiO2 were successfully grown on transparent, conductive glass substrate (FTO) by a hydrothermal method. Controllable length, diameter and density of the nanorod arrays (NRAs) were realized by adjusting hydrothermal conditions such as temperature, reaction time, concentration of reactants and type of solvent etc. The effect of these hydrothermal parameters on TiO2 nanofilms growth was discussed in detail. The density of nanorods can be adjusted by varying the volume ratio of ethanol/water, and the orientation and crystallinity of TiO2 nanofilms were enhanced with increasing dosage of ethanol. Samples with only ethanol as solvent displayed the best orientation and maximum thickness. Except for ethanol, other alcohol such as methanol, n-propanol and n-butyl were also used as solvent to investigate the role of alcohol type during hydrothermal process. It turned out that TiO2 nanofilms derived from all these alcohol solvents had the feature of morphology and single-crystal orientation similar to those prepared from ethanol. Furthermore, the areal density and degree of orientation of these samples reduced with decreasing molecular mass of the alcohol solvent. Films using ethanol as solvent possessed the optimal balance between orientation and surface morphology. Highly sensitive hydrogen sensors have been realised using self-assembled TiO_2 films.

Keywords: self-assembly, TiO2 thin films, Hydrogen sensing, hydrothermal synthesis

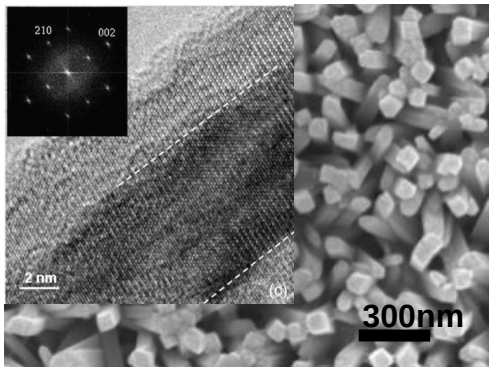

Figure 1: Morphology of typical rutile nanorod. The density of the nanorod varies with the volume ratio of ethano/water. HRTEM image exhibits high crystalinity of the nanorods, which contained clomnar subgrain boundaries. Inset shown corresponding FFT from the top subgrain.

The Effect of pH on Expanding Titanate Nanotubes & Their Use as a High Capacity Lithium-Ion Battery Electrode with High Rate Capability

A. Yürüm[1,*], M. Yarali[2], E. Bicer[3], S. Alkan Gürsel[2]
[1]Sabanci University Nanotechnology Research and Application Center, Istanbul, Turkey
[2]Faculty of Engineering and Natural Sciences, Sabanci University, Istanbul, Turkey
[3]Faculty of Pharmacy, Yeni Yuzyil University, Istanbul, Turkey

Abstract: Improvement of lithium-ion electrodes with high charge and discharge capacities is in high need especially for electronic devices and electric vehicles (Gong *et al.*, 2013). For that reaso, development of ion transport in the crystal structure is needed (Li *et al.*, 2013). The general idea is synthesizing nanometer scale particles. Reducing the particle size helps the ion diffusion in the structure (He *et al.*, 2014). Titanate nanotubes are promising materials because of their special morphology and high specific surface area. The nanotubes are formed by rolling-up of titanate nanosheets (Kasuga *et al.*, 1998). These titanates provide high rate capability and low volume expansion upon lithiation (Ren *et al.*, 2010). More importantly their tubular structure helps the transport of ions through the crystal. In this study, we synthesized titanate nanotubes and modified the interlayer distance by changing the pH. For the characterization XRD, SEM and BET (Figure 1) techniques were used. In addition, the effect of interlayer distance on energy capacity and rate capability was investigated. The shortest interlayer distance was observed at pH 4,5. Getting further away from this point, interlayer distances increased and this also increased the nanotube diameter. Conversely, specific surface area reaches its maximum value at pH 4,5. Potential-capacity profiles of TiO_2 nanoparticles showed distinct potential plateaus. Nevertheless, a very fast capacity drop was observed for TiO_2 particles. On the other hand, for titanates, broad peaks appear in CV measurements. For titanates capacities higher than 700 mAh/g were obtained. More importantly, titanates showed exceptional rate capabilities especially at wider interlayer distances due to higher mobility of ions in the structure (Figure 2). It was found that interlayer distance plays an important role in rate capability. However the material still needs some modifications to stabilize the capacity.

Keywords: expanded titanate nanotubes, pH, high capacity, high rate capability, Li-ion.

Acknowledgement. This study is supported by The Scientific and Technological Research Council of Turkey (TUBITAK): Project No. 113M575.

References:

Gong , Y. J., Yang, S. B., Liu, Z., Ma, L. L., Vajtai, R., Ajayan, P. M. (2013), Graphene-Network-Backboned Architectures for High-Performance Lithium Storage, *Adv. Mater.*, 25, 3979.

Li, L., Raji, A.-R. O., Tour, J. M. (2013), Graphene-Wrapped MnO_2–Graphene Nanoribbons as Anode Materials for High-Performance Lithium Ion Batteries, *Adv.Mater.*, 25, 6298.

He, M., Kravchyk, K., Walter, M., Kovalenko, M. V. (2014), Monodisperse Antimony Nanocrystals for High-Rate Li-ion and Na-ion Battery Anodes: Nano versus Bulk, *Nano Lett.*, 14, 1255.

Kasuga, T., Hiramatsu, M., Hoson, A., Sekino, T., Niihara, K. (1998), Formation of Titanium Oxide Nanotube, *Langmuir*, 14, 3160.

Ren, Y., Hardwick, L. J., Bruce, P. G. (2010), Lithium Intercalation into Mesoporous Anatase with an Ordered 3D Pore Structure, *Angew. Chem. Int. Ed.*, 49, 2570.

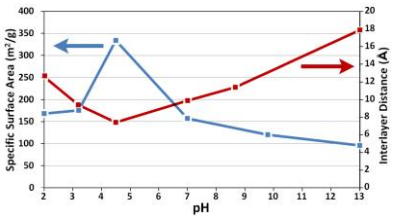

Figure 1: Surface area and interlayer distance values at various pH values: The shortest interlayer distance of 7,4 Å was observed at pH value of 4,5. Getting further away from this point, interlayer distances increased and this also increased the nanotube diameter. However, the highest specific surface area value of 334 m^2/g at was obtained at pH of 4,5.

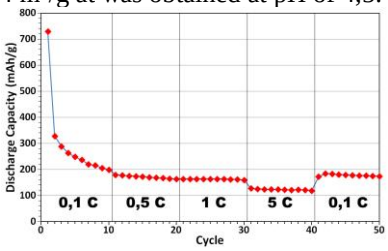

Figure 2: Rate capability test of titanate modified at pH 4,5: Potential-capacity profiles of TiO_2 (anatase) nanoparticles showed distinct potential plateaus at 1.7 and 2.2 V for discharging and charging, respectively. However, the capacity dropped from 254 mAh/g to 87 mAh/g in 10 cycles. Titanates show broad peaks appear in CV measurement. For titanates capacities as high as 750 mAh/g were obtained. More importantly, titanates showed exceptional rate capabilities especially at wider interlayer distances due to higher mobility of ions in the structure.

Preparation of Graphene Encapsulated Silicon Nanoball by CVD using Metal Coating

H. Kim,[1,2] S. Park,[2] I. Kang,[3] H. Huh[1*]
[1]Korea Institute of Industrial Technology, Thermochemical Energy System R&BD Group, Cheonan, Korea
[2]Inha University, Department of Chemistry, Incheon, Korea
[3]PuKyong National University, Division of Mechanical Engineering, Busan, Korea

Abstract: Concerning application of graphene, a lot of efforts have been made to improve performance of nanomaterials in many fields, such as electric and electronic devices. Some examples are preparation of 3-dimentional structure like nanoball or nanobubble by CVD process and hybridizing with silicone. These graphene-based materials are proven to be available for secondary battery, EMI and ACF in electronics. Especially, some research has shown that they were very effective to enhance safety and volumetric capacity when they were used as anode materials of secondary battery. Graphite or its compound with metal has been used as an anode material due to their high stability and reversibility, but it still has lower charge capacity. On the contrary, silicon is known as a material which increases the charge capacity to four times compared with carbon-based materials but it has lower stability and reversibility. For that reason, a few researchers just started to improve the charge capacity by hybridization of carbon-based material with silicon. In this study, we prepared a nanocarbon based material which had a new structure of graphene encapsulated silicon nanoball as an anode material which was applicable to high-capacity secondary battery. In order to form a graphene encapsulated silicon nanoball, metal coated silicon nanoballs was fabricated by electroless plating process. And then graphene was formed on surface of the resulting metal coated silicon nanoballs by CVD process. Finally, metal of the resulting materials was etched by hydrogen chloride. After etching process, the graphene encapsulated silicon nanoballs were formed a space between the silicon particle and the graphene, which can give more safety to volumetric change of anode during lithiation and delitiation when it applies to secondary betteries. Morphology of the graphene encapsulated silicon nanoball was observed by the field emission scanning electron microscope (FESEM) and the field emission transmission electron microscope (FETEM) to find core-shell structured nanoball. Spherical structure of graphene encapsulated silicon nanoball was investigated by the Raman, the X-ray Photoelectron Spectroscopy and the X-ray diffraction spectra to identify graphene layers on the surface of the inner silicon core.

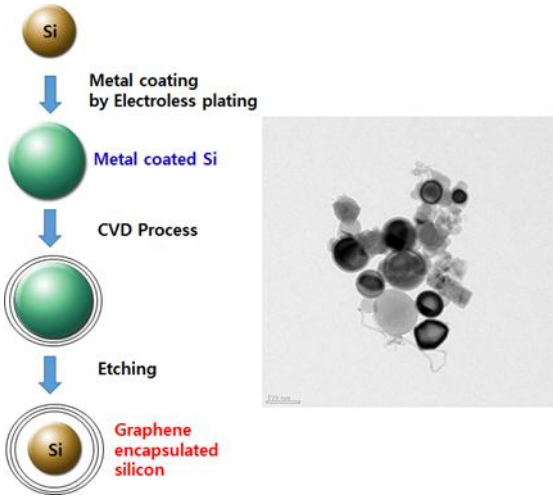

Figure 1. TEM image of graphene encapsulated silicon nanoball

Keywords: graphene, nanoball, silicon, encapsulate, CVD.

References:

Jung-Soo, L., Sun-I, K., Jong-chul, Y., Ji-Hyun, J. (2013) Chemical Vapor Deposition of Mesoporous Graphene Nanoballs for Supercapacitor, *Acs. Nano.* 7, 6047.

Seon-Mi, Y., Won Mook, C., Hionsuck, B., Hyeon-/jin, S., Inyong, S., Moon-Seok, K., Jung Jun, B., Hansu, K., Young Hee, L., Jae-young, C. (2012) Synthesis of Multilayer Graphene Balls by Carbon Segregation from Nickel Nanoparticles, *Acs. Nano.* 6, 6803.

Langli, L., Jinsong, W., Jiayan, L., Jiaxing, H., Vinayak P, D. (2014) Dynamics of Electrochemical Lithiation/Delithiation of Graphene-Encapsulated Silicon Nanoparticles Studied by In-situ TEM, *Scientific Reports*, 4, 3863.

Session III: Nano Electronics

Towards a force-displacement sensor based on vertical ZnO piezoelectric nanowires

E. León Pérez[1*], M. Mouis[2], E. Pauliac-Vaujour[1]
[1]CEA-LETI, Systems Department, F-38054 Grenoble, France
[2]IMEP-LAHC, Minatec, 3 Parvis Néel, 38016 Grenoble, France

Abstract: One-dimensional nanostructures offer a large range of potential applications in nano-electronics devices. For instance, ZnO piezoelectric nanowires (NWs) are promising elements for functionalities enhancement in nanodevices (Wang *et al.*, 2010), The implementation of these structures has been considered for high sensitivity sensors applications (Hichet *et al.*,2012) and the work presented here aims towards the full integration of these NWs within conventionnal silicon technologies in a more-than-Moore approach. In order to do so, a certain number of issues must be addressed: (i) pixel geometry, (ii) optimal pixel response collection, (iii) micro-fabrication and processing of specific materials (ZnO seed-layers) and (iv) controlled growth of NWs on processed chips.

We present the progress on finite element method (FEM) model of the full pixel architecture that provide valuable guidelines for optimal micro-fabrication. We report the parametric study of the piezo-response of one pixel as a function of the seed-layer thickness (t) and the electrode-NW spacing (d). It was found that the collection efficiency, i.e. the ratio of piezo-potentials in the electrodes and the NW, is higher for thinner seed-layers. For a perfect electrode-NW contact (d=0nm), collection efficiencies of about 60% are obtained for realistic seed-layer thicknesses (t~20nm). This value drops from 30% when electrode-NW contact is discontinued (few nm), emphasizing the small tolerance towards the contact spacing related to process variability.This study suggests the importance of fabrication variables and the nature of the seed-layers on the pixel response.
The impact of the seed-layers nature on the NWs features (e.g. average diameter, length and tilt angle) was investigated by carrying out NWs growth by hydrothermal method (Lincot *et al.*,2010) on different polycrystalline layers. We showed that chemical vapor deposited gallium-doped ZnO layers at 450°C are suitable, leading to µm long NWs and to 85 ± 23 nm and 165 ± 40 nm average diameter for template-free and localized growth (through 150nm holes spaced of 750nm), respectively.
It is shown that both FEM simulations and nanowires growth provide valuable insight for device guidelines and micro-fabrication.

Keywords: heterogeneous integration, nanowires, piezoelectricity, zinc oxide, nanodevice, simulation.

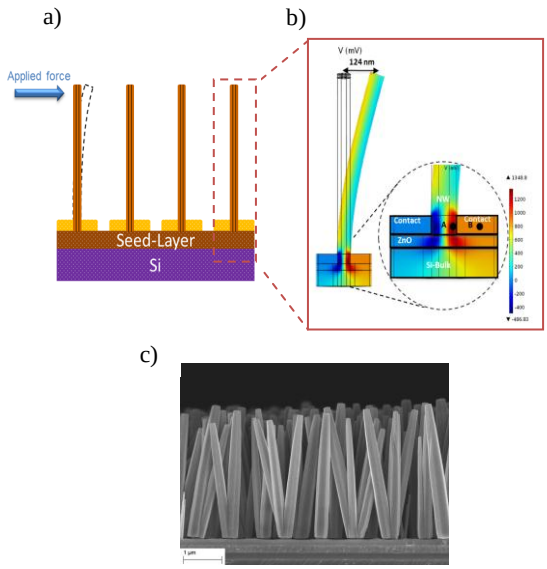

Figure 1: a) Schematic of the NW-based sensor; b) FEM simulation illustrating the mapping of the piezopotential of one pixel including one NW, two electrodes, the underlying ZnO seed-layer and a Si-substrate; and c) ZnO NWs obtained in a localized growth approach (through 150nm holes spaced of 750nm).

References:

Wang, Z. L. (2010), Piezopotential gated nanowire devices: Piezotronics and piezo-phototronics, *Nano Today, vol. 5, no.6, 540-552*.

Hinchet, R., Ferreira, J., Keraudy, J., Ardila, G., Pauliac-Vaujour, E., Mouis, M., Montès, L. (2012), Scaling rules of piezoelectric nanowires in view of sensor and energy harvester integration, *IEDM, 621-624*.

Lincot, D. (2010), Solution growth of functional zinc oxide films and nanostructures, MRS Bull., vol.35, 778-790.

Transport properties of nanoscale TFET by atomic scale simulations

U. Martinez Pozzoni, T. Markussen, A. Blom, K. Stokbro
QuantumWise A/S, Copenhagen, Denmark

Abstract: In this study we describe the transport characteristics of 2D-InAs tunnel field-effect transistors by means of atomic scale simulations. In particular, we compare results from density functional theory (DFT) using the Meta-GGA exchange correlation potential and tight-binding (TB) Hamiltonian. For the first time we show that the two methods give comparable results proving the predictive power of atomic scale simulations for this type of devices. Here, we describe the relevant theory and methodology employed. Moreover, we illustrate how one can easily modify all the important parameters of such nano devices to tune the corresponding transfer characteristic. For example, we can modify, at the atomic level, surface passivation, device geometry, doping concentration and doping regions (see figure 1a where the transfer characteristic of the 60 nm 2D-InAs p-i-n device with a 10-nm underlap region is shown), gate material (through work gate function tuning), and more. Results are analyzed in terms of I-V and transfer characteristics, real space density of states (band bending, see figure 1b), charge transfer, spectral current, effective potential across the device, as well as band structure and effective mass analysis of the nano structures employed. All calculations are performed with state of the art theories and methods as implemented in Atomistic Toolkit [1].
The research leading to these results has received funding from the European Community's Seventh Framework Programme (FP7/2007-2013) under Grant Agreement III–V-MOS Project No. 619326.

Keywords: tunnel field-effect transistor; density functional theory; tight binding Hamiltonian; InAs; atomic scale simulations;

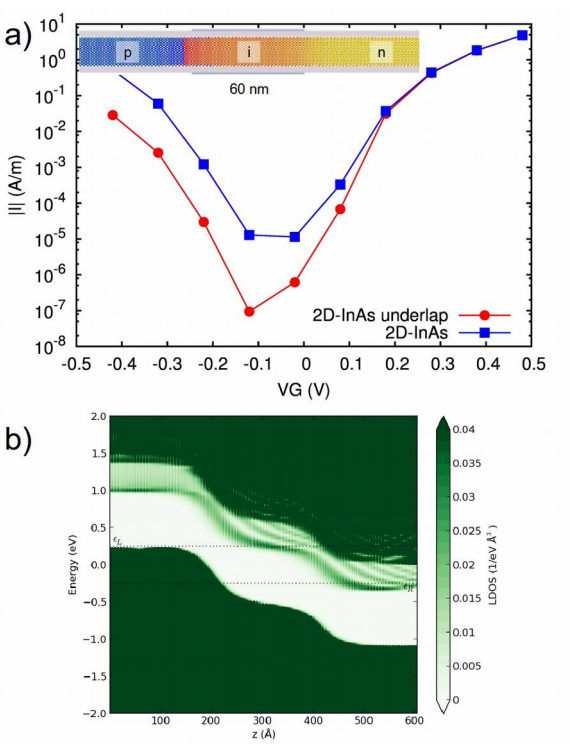

Figure 1: TFET atomistic simulation of a 2D-InAs p-i-n device: a) transfer characteristic of the device with a 20 nm and a 10 nm n-doped region, respectively. The source-drain bias is -0.5 V; b) projected local density of states across the 60 nm device

References:

[1] Atomistic Toolkit 2015, QuantumWise A/S (www.quantumwise.com)

InAsSb based room temperature Infrared Photodetectors

Jinchao Tong, Peinan Ni and Dao-Hua Zhang*

School of Electrical and Electronic Engineering,
Nanyang Technological University, Nanyang Avenue, Singapore 639798
Email: edhzhang@ntu.edu.sg

Abstract: InAsSb based semiconductors have been attracting more attention in the recent years as they are excellent materials for midwave infrared photodetectors which have wide applications over many areas [1-5]. One of the main features of the materials is the operation at near room temperature. In this paper, we present structural and optical properties of InAsSb epitaxial layers grown on GaSb substrates by molecular beam epitaxy and their photodetection performance. X-Ray Diffraction study shows that the ternary alloys operating at mid-wave infrared range can be made almost lattice-matched to the GaSb substrate. Photoluminescence measurements reveal that the energy band gap of the InAsSb materials follows the Bose-Einstein relation better than the Varshni law. Photoconductors fabricated with this material show spectral responses ranging from NWIR to MWIR at near room temperatures. The measured Johnson-noise limited detectivity is $\sim 1.4\times10^{8}\ \mathrm{cm\cdot Hz^{1/2}W^{-1}}$ at room temperature, and it can reach $\sim 1.1\times10^{9}\ \mathrm{cm\cdot Hz^{1/2}W^{-1}}$ by decreasing the temperature to 38 K.

Keywords: Infrared photodetector, InAsSb based, detectivity.

References:

[1] M. Razeghi, *Opto-Electron. Rev*., **6**, 155 (1998).

[2] D. H. Zhang, W. Shi, *Appl. Phys. Lett*., **73**, 1095 (1998).

[3] D. H. Zhang, W. Liu, Y. Wang, X. Z. Chen, J. H. Li, *Appl. Phys. Lett*. 93 (2008) 131107.

[4] Y. Wang, D. H. Zhang, X. Z. Chen, Y. J. Jin, J. H. Li, C. J. Liu, A.T. S. Wee, Sam Zhang and A. Ramam, *Appl. Phys. Lett*. 101 (2012) 021905.

[5] X. Z. Chen, D. H. Zhang, W. Liu, Y. Wang, J.H. Li, A.T.S. Wee and A. Ramam, *Electronics Letters*, 46 (2010) 787.

Selective preconcentration within a nanoslit: one route for monitoring the biomolecule focusing front line.

F-D. Delapierre,[1,*] A-C. Louër,[1] A. Pallandre,[1] A-M Haghiri-Gosnet[1]
[1]Laboratoire de Photonique et de Nanostructures, LPN/UPR20 CNRS, route de Nozay, 91460 Marcoussis, France

Abstract: Due to the electrical double layer, a nanometric restriction in a glass microchannel acts as a selective filter for ions under specific electric field and ionic strength. The unbalanced transport between anionic and cationic species in the microsystem leads to a polarization of the ionic concentrations (Zangle *et al.*, 2009). This polarization effect provokes variations of the local ionic flow which can be canceled at some specific locations where ions are collected. This phenomenon can be used to preconcentrate biomolecules before a separation step to improve the limit of detection. Numerical simulations (Plecis *et al.*, 2008) have shown that the localization, the intensity and the stability of the preconcentration vary depending on several parameters such as the electrophoretic mobilities, the channel surface charge, the bulk composition, the ionic force, the voltage or the height of the nanochannel etc. Four different preconcentration regimes, stable or unstable, can thus be defined depending on the position of the preconcentration front line. Our experiments have demonstrated the existence of these four regimes and our capabilities to travel in the regime diagram by varying the ionic force or the voltage. Tuning these parameters, preconcentration rates as high as 10^3 have been reached after 5 minutes. Moreover, by adding a hydrodynamic pressure flow (Figure 1) (Louër *et al.*, 2013), we are also able to stabilize unstable preconcentration regimes or adjust the localization of the preconcentration front line either on the anodic or on the cathodic side of the nanochannel (Figure 2) where it is required for further step of analysis.

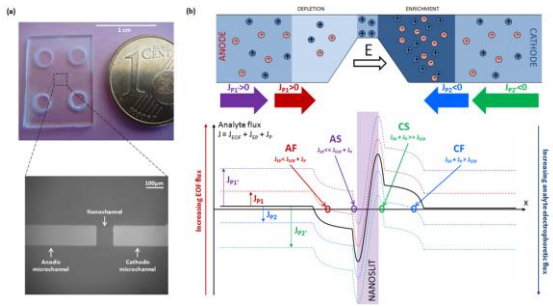

Figure 1: (a) General view of the whole pure-glass chip that integrates a 100µm-long and 150nm-deep nanochannel in a 1µm deep microchannel and (b) The mechanism of pressure-assisted preconcentration and separation. The local transport rate profile is represented in the MNM structure (flux of the analyte vs distance in the structure).

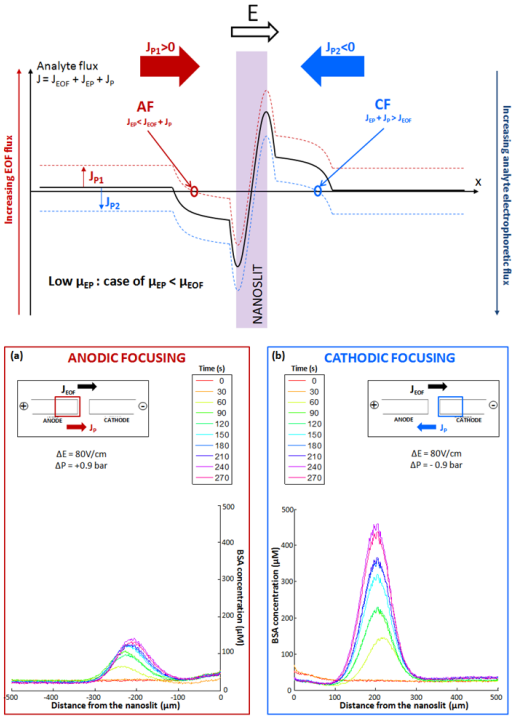

Figure 2: Two types of preconcentration for BSA: (a) Anodic Focusing (AF) when voltage and pressure are applied in the same way corresponding to an "anodic pressure" and (b) Cathodic Focusing (CF) when the two flows are opposite (case of a "cathodic pressure"). ΔE=80V/cm

Keywords: Electrophoretic flow, electroosmotic flow, ionic transport, electropreconcentration, nanochannel, nanofluidics.

References:

Zangle, T. A., Mani, A., Santiago, J. G. (2009), On the Propagation of Concentration Polarization from Microchannel-Nanochannel Interfaces Part II: Numerical and Experimental Study, *Langmuir*, 25, 3909-3916.

Plecis, A., Nanteuil, C., Haghiri-Gosnet, A. M., Chen, Y. (2008), Electropreconcentration with Charge-Selective Nanochannels, *Analytical Chemistry*, 80, 9542-9550.

Louër, A-C., Plecis, A., Pallandre, A., Galas, J-C., Estevez-Torres, A., Haghiri-Gosnet, A-M. (2013), Pressure-assisted selective preconcentration in a straight nanochannel, *Analytical Chemistry*, 85, 7948-7956.

Controlled Insulator to Metal transition in SiO_2 –TiO_2 nanocomposite containing silver nanoparticles

Tapajyoti Das Gupta1 , Joelle Corde1 , Sandrine Perruchas1 , Jean-Pierre Boilot1 , Alistair Charles Rowe1 ,Thierry Gacoin1

Ecole Polytechnique, Palaiseau, France

Abstract: Titanium dioxide is a well known semiconductor compound with exceptional dielectric, electronic and physico-chemical surface properties. These properties have been exploited in many applications such as white pigments, solar cells and photocatalysis, the latter being extensively studied for practical applications in decontamination or self cleaning devices [1]. The basic principle relies on the high redox activity of photogenerated carriers and radicals resulting from their reaction with adsorbed species at the surface of theoxide. Recently, our group developed nanostructured photocatalytic films based on the dispersion of preformed colloidal TiO nanoparticles into a surfactant template mesoporous silica binder. Such coatings were shown to exhibit exceptional self-cleaning properties. Recently, we investigated the potentiality of these film for the development of nanostructured metal-dielectric coating[2] obtained by the in-situ photoreduction of silver salts. Tunable silver volumic fraction up to 18% could be obtained by playing on the irradiation dose during the photoreduction process. Saturated films are near homogeneously filled over their entire thickness and exhibit metallic conduction properties with a conductivity of 40 S.cm properties of the nanocomposite films was also investigated, evidencing a critical volume fraction, φ^* ~ 13.1 %. The effect of mechanical stress on the electrical properties of the nanocomposite films was also investigated, evidencing a critical volume fraction, ϕ^* ~ 13.1 %, around which the resistance changes by orders of magnitude by applying a mechanical stress. It has long been recognized that the percolative insulator-to-metal in conducting metal composites is of potential use in sensor applications because the resistance of the material changes rapidly by many orders of magnitude with small variations in the conducting particle volume fraction, φ. However, fluctuations in the composite resistance also become large at the so-called critical volume fraction, φ^*, where percolation occurs. Here we show experimentally that, in consequence, the resulting intrinsic signal-to-noise ratio for strain detection is small at φ^*. The maximum signal-to-noise ratio is obtained slightly to the conducting, metallic side of the percolation threshold[3]. Ag/silica
nanocomposites should therefore be considered as a high sensitivity, low cost composite alternative to commercially available strain gages.
Finally, the photochromic properties of these films were investigated usingpost-synthesis irradiation of silver loaded films at different wavelengths [2].

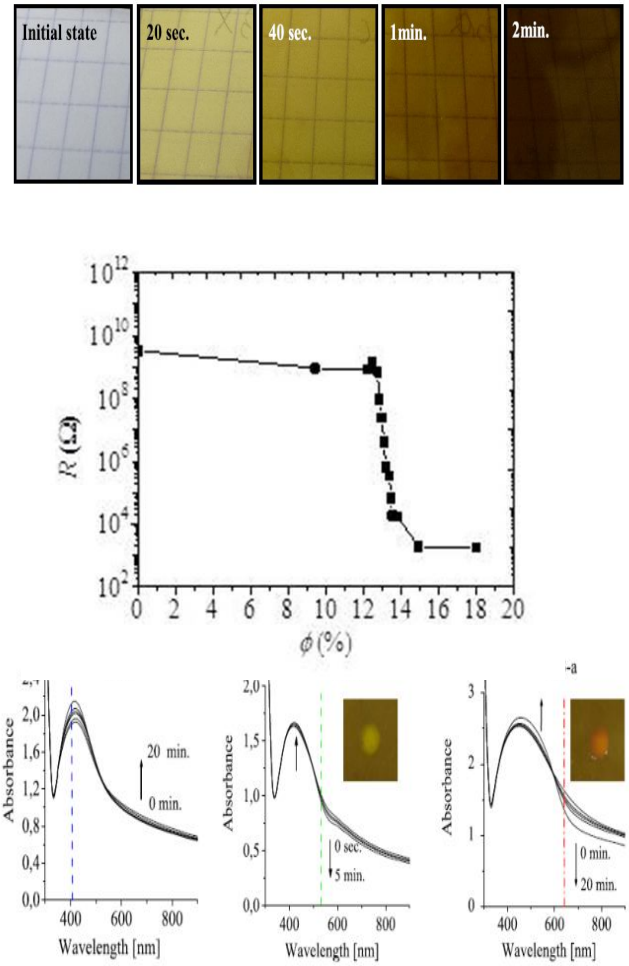

Figure (a).Images of the films subjected to different time of irradiation with UV lamp in the Ag^+ solution (b) Plots for the variation of resistance with volume fraction (c) Absorbance spectra (S1 8.2% vol; S2. 7% vol, S3 11 % vol) irradiated with laser beam at 405 nm, 532 nm and 633 nm respectively[2]

Significant changes in the plasmonic absorption spectra were explained as resulting from a local redistribution of the silver phase through irradiation.

Keywords: nanocomoposite, piezoresisitve material, photocatalysis, in-situ process, photochromic effect

References:

[1] A. Fujishima et al. J. Photochem. Photobiol. C 2000, 1, 1.
[2] J. Corde et al, Nanotechnology 23, 2012
[3] T. Das Gupta et al, Adv Funct Mater , 2014

Surface-Dominated Transport and Enhanced Thermoelectric Figure of Merit in Topological Insulator $Bi_{1.5}Sb_{0.5}Te_{1.7}Se_{1.3}$

Te-Chih Hsiung,[1,2,*] Yang-Yuan Chen [2]
[1] Department of Physics, National Taiwan University, Taipei 106, Taiwan.
[2] Institute of Physics, Academia Sinica, Taipei 11529, Taiwan.

Abstract: The recent discovery of topological insulators (TIs) has provided new route for producing low-dimensional relativistic electronic states. The exotic surface states of TIs have attracted the attention of scientists because of their fascinating physical properties and applicability in thermoelectric (TE) applications (Hsiung *et al.*; 2013, 2015).

Recently, the $Bi_{1.5}Sb_{0.5}Te_{1.7}Se_{1.3}$ (BSTS) system was confirmed to be a high-insulating bulk TI with high bulk resistivity because of the ordered occupation of Te/Se in the quintuple-layer unit, which substantially cancels the bulk carriers. In addition, the low-dimensional nanostructure with a high surface-to-volume ratio enables metallic surface conduction and TE transport properties to be efficiently probed. In this study, we selected BSTS nanowires as our target specimens and expect to observe the novel transport and TE properties therein.

We report an observation of an order of magnitude enhancement of the thermoelectric figure of merit (ZT=0.36) in topological insulator $Bi_{1.5}Sb_{0.5}Te_{1.7}Se_{1.3}$ nanowires at 300 K as compared with its bulk specimen (ZT=0.028). The enhancement was primarily due to an order of magnitude increase of electrical conductivity of the surface-dominated transport and thermally activated charge carriers in the nanowires. Magnetoresistance analysis revealed the presence of Dirac electrons and determined the Fermi level near the conduction band edge. This might be the first thermoelectric measurement of samples with a chemical potential in the gap of topological insulator without gate tuning and provides an opportunity to study the contribution of surface states to Seebeck coefficient and resistivity without concern for the complex effect of band bending.

Keywords: Topological insulators, thermoelectrics, nanowires, power factor, Shubnikov-de Haas oscillations

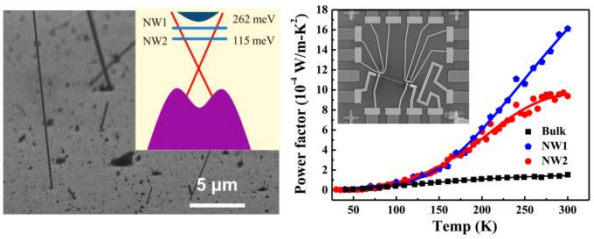

Figure 1: Thermoelectric transport measurements of topological insulator $Bi_{1.5}Sb_{0.5}Te_{1.7}Se_{1.3}$ nanowires reveal an enhancement of the thermoelectric figure of merit as compared with its bulk specimen.

References:

Hsiung, T. C., Chen, D. Y., Zhao, L., Lin, Y. H., Mou, C. Y., Lee, T. K., Wu, M. K., Chen, Y. Y. (2013) Enhanced surface mobility and quantum oscillations in topological insulator $Bi_{1.5}Sb_{0.5}Te_{1.7}Se_{1.3}$ nanoflakes, *Appl. Phys. Lett.* **103**, 163111

Hsiung, T. C., Mou, C. Y., Lee, T. K., Chen, Y. Y. (2015) Surface-Dominated Transport and Enhanced Thermoelectric Figure of Merit in Topological Insulator $Bi_{1.5}Sb_{0.5}Te_{1.7}Se_{1.3}$, *Nanoscale*, **7**, 518-523

Side-jump scattering in nanogranular Bi thin films

C. Christides,[1,*] P. Athanasopoulos,[1]
[1]Department of Computer Engineering & Informatics., University of Patras, Rion Patras 26504, Greece

Abstract: Nanogranular thin films of Bismuth with nominal thicknesses 15nm and 50nm were deposited by magnetron sputtering on Si(100)/SiN_x(100nm) substrates. Hall effect measurements between 5K and 300K reveal two conduction channels, and the observed curves (Fig.1a) of Hall resistivity $\rho_H(B)$ can be formulated as:

$$\rho_H(B) = \rho_H^{Surf} + R_\infty^{Bulk} \cdot B$$

where ρ_H^{Surf} is the intersection point with ρ_H-axis and R_∞^{Bulk} is the slope of $\rho_H(B)$ curve for B>3T, that is assigned to a bulk Hall coefficient: $R_\infty^{Bulk} \sim (e \cdot n_{eff})^{-1}$, with n_{eff} an effective carrier concentration. The temperature dependence (Fig.1b) of film resistivity ρ_{xx}(T,B=0) varies according a fitting function:

$$\rho_{xx}(T,B=0)=\rho_{xx}(5K,B=0)e^{-(\lambda T)^n}$$

that is related to a phase coherence length $L_\Phi(T) \sim T^{-n}$. Fig.1b shows the fitting curves and parameters to experimental data. A connection has been revealed among $\rho_H^{Surf}(T)$, $\rho_{xx}(T,B=0)$ and $R_\infty^{Bulk}(T)$, indicating that:

$$\rho_H^{Surf}(T,B=0) \sim \rho_{xx}^2(T,B=0) \sim R_\infty^{Bulk}(T) \sim (n_{eff})^{-1}$$

Fig.1c shows a scaling relationship: $\rho_H^{Surf} = a\rho_{xx} + \beta\rho_{xx}^2 = R_S$, that is expected in case of anomalous Hall coefficient R_S. Most important is the contribution of the side-jump term: $\rho_H^{Surf} \sim \rho_{xx}^2$, that is unlikely to be due to intrinsic mechanism inside non-magnetic Bi. The origin of a: $\rho_H^{Surf} \sim \rho_{xx}^2$, term can be attributed to extrinsic contribution from a combination of surface roughness plus electronic confinement inside grains (Zhou *et al.*; 2015), and metallic edge states (Takayama *et al.*; 2015) in nanogranular structure of Bi(15nm) and Bi(50nm) films.

Keywords: granular films, Hall effect, side-jump scattering, semimetallic conductance, surface states.

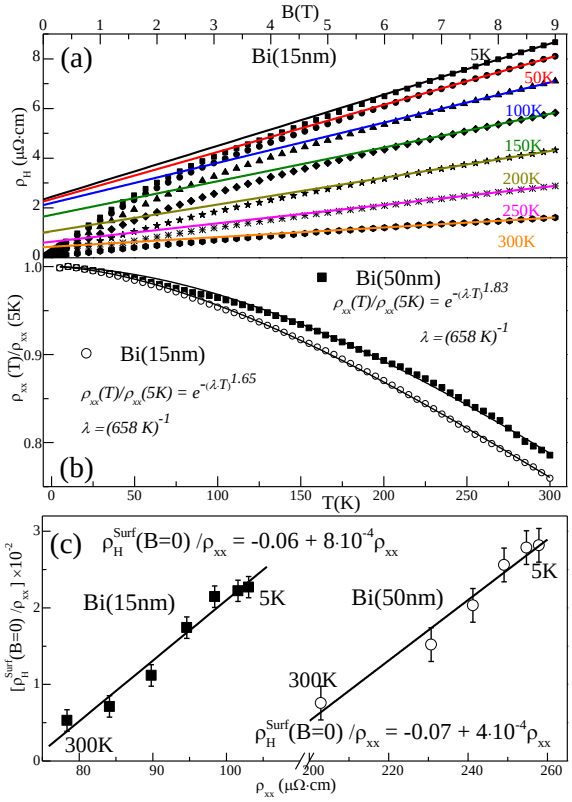

Figure 1: (a) Hall resistivity ρ_H(B) in Bi(15nm) film. (b) Normalized resistivity ρ_{xx}(B=0). (c) Scaling relationship between ρ_H(B=0) and ρ_{xx}(B=0):

The observed analogy (not shown here) of intersection points ρ_H^{Surf} (Fig.1a) and $\rho_{xx}^2(T,B=0)$ values (Fig.1b) to high-field slope values $R_\infty^{Bulk}(T)$ in $\rho_H(B)$ curves (Fig. 1a) is quite unusual and shows that the observed side-jump term cannot be attributed to magnetic susceptibility contributions that is reported in paramagnetic amorphous metals (Rhie *et al.*; 1993).

References:

Zhou, L., Grigoryan, V.L., Maekawa, S., Wang, X., Xiao, J., (2015) Spin Hall effect by surface roughness, *Phys. Rev. B* 91, 045407.

Takayama, A., Sato, T., Souma, S., Oguchi, T., Takahashi, T., (2015), One-Dimensional Edge States with Giant Spin Splitting in a Bismuth Thin Film, *Phys. Rev. Lett. 114, 066402.*

Rhie, K., Naugle, D.G., O, Beom-hoan, Markert, J.T., (1993) Side-jump effect in paramagnetic amorphous metals, *Phys. Rev. B* 48, 5973-5982.

Single-Molecule Switches Trigerred by Light,Chemical and Electrochemical Stimuli

Nadim Darwish* [a], Albert C. Aragonès, [a] Tamim Darwish, [b] Simone Ciampi [c] and Ismael Díez-Pérez [a]

[a] Departament de Química Física, Universitat de Barcelona, Diagonal 645, 08028 Barcelona, Spain and Institut de Bioenginyeria de Catalunya (IBEC) Baldiri Reixac 15-21, Barcelona, 08028 Spain
[b] Bragg Institute, Australian Nuclear Science and Technology Organisation (ANSTO), Locked Bag 2001 Kirrawee DC NSW 2232, Australia
[c] Intelligent Polymer Research Institute, University of Wollongong, Northfields Avenue, Wollongong, NSW 2522, Australia

Abstract: The concoction of chemistry, nanotechnology and electronics initiated what is known today as the field of Molecular Electronics, an intense emerging field that offers promise of replacing the current inorganic micro-sized electronics with nanoscale electronic platforms bearing active molecular components. In addition to their advantages in miniaturization, molecular electronic components provide enormous versatility to tune the electronic properties by the plethora of synthetic tailoring. Reversible single-molecule conductivity switching in response to external stimuli currently represents a major aim encouraged by the highly tunable switching capabilities offered by chemical backbones. Herin, we will present mutli-responsive single-molecule electrical switches based on incorporating phtochromic molecules between two metal electrodes using the scanning tunneling micrsocopy break-junction technique. A light pointer and/or a chemical signal can rapidly and reversibly induce the isomerization of bifunctional spiropyran derivatives in the bulk reservoir and consequently switch the electrical conductivity of the single-molecule device between a low and a high level.[1] In addition, we will present electrochemical switching of single anthraquinone molecules trigerred by electrochemical gating.[2] These studies contribute to the next limit of miniaturization of electronic components which is the realization of single-molecule electronics.

Keywords: molecular electronics, nano-scale electrical devices, single-molecule conductance, electrochemical gating, multi-responsive molecular switches, phot- and chemo-switches

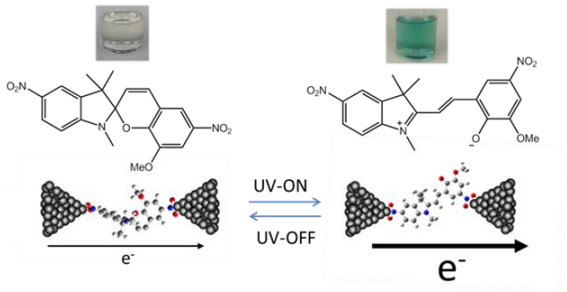

Figure 1: Figure illustrating an example of a single-molecule switching device based on the irradiation of UV-light[1].

References:

1- Darwish, N.; Aragones, A. C.; Darwish, T. A.; Ciampi, S.; Díez-Pérez, I.. Nano Letters 2014. DOI: 10.1021/nl5034599
2- Darwish, N.; Paddon-Row, M. N.; Gooding, J. J., Acc. Chem. Res. 2013, 47, 385-395.

Light emission coupling from Carbon nanotubes in silicon photonic structures

C. Alonso-Ramos[1], A. Noury[1α], E. Durán-Valdeiglesias [1], W. Zhang[1] , F. Sarti[2,3], Federico La China[2,3], H.C. Hoang[1], X. Le Roux[1], H. Yang[5], E. Cassan[1], N. Izard[1*], A. Filoramo[4], V. Bezugly[5],M. Gurioli[2,3] , L. Vivien[1+]

[1]Univ Paris 11, CNRS UMR 8622, Inst Elect Fondamentale (IEF), F-91405 Orsay, France
[2]Department of Physics, University of Florence, 50019 Sesto Fiorentino (FI), Italy
[3]European Laboratory for Non-linear Spectroscopy, 50019 Sesto Fiorentino (FI), Italy
[4] CEA Saclay, IRAMIS, NIMBE (UMR 3685), LICSEN, Bat. 125, F-91191 Gif-sur-Yvette, France
[5]Technische Universitaet Dresden, Institute for Materials Science, Dresden, Germany
[+] *Corresponding author: Laurent.vivien@u-psud.fr*

Abstract: The use of optics in microelectronic circuits to overcome the limitation of metallic interconnects is more and more considered as a viable solution. Numerous photonic building blocks compatible with CMOS fabrication tools have been developed. However, the integration of all these building blocks in the same chip is very complex and is not cost-effective due to the various materials used: Ge, Si and III-V. This drawback could be significantly overcome with the use of carbon nanotubes (CNTs). Indeed, CNTs are nanomaterials of particular interest in photonics thanks to their fundamental optical properties to emit, modulate and detect light in the wavelength range of silicon transparency. Here, we report on the comparison of the light emission coupling from CNTs into optical resonators including strip and slot ring resonators, photonic crystals and micro-disk. A theoretical and experimental analysis of the light interaction of CNTs according to the optical waveguide configurations will be carried out.

First, silicon waveguides were fabricated using classical Si process. CNTs embedded into a polymer layer were then deposited on the top of the waveguide. Figure 1 presents a theoretical comparison of the interaction between light and the strip and slot waveguide geometries, respectively.

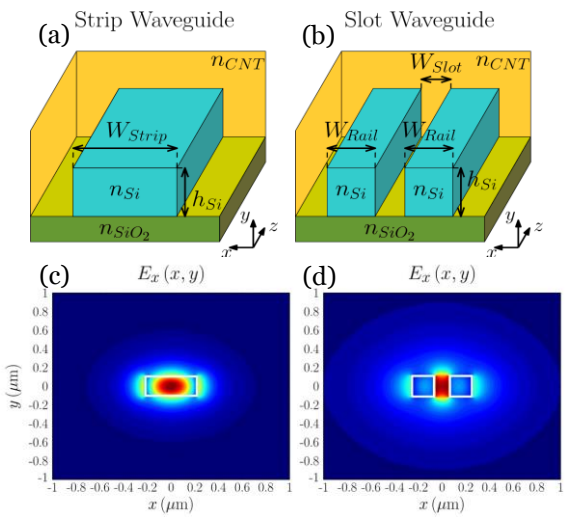

Fig. 1: Schematic views of strip waveguide (a) and slot waveguide (b). TE mode (Electric field E_x)of strip (c) and slot (d) waveguide.

As it can been seen, the optical mode in the slot waveguide is much more localized outside silicon (i.e. in the CNT layer), while for strip waveguide the mode is nearly confined inside silicon. In terms of light interaction with the CNT layer, slot waveguides are thus more promising to enhance the light coupling from CNTs. However, in terms of propagation loss, strip waveguides exhibit lower loss which induces better resonator behavior (i.e. higher Q-factors).

In conclusion, CNTs have some remarkable optical properties which could be exploited to develop a new kind of hybrid phtonics on silicon platform for a large range of applications including on-chip optical communications. We will present the latest results on the experimental demonstration of the light coupling from CNTs photoluminescence into a slot waveguide and its comparison under the same measurement conditions with a strip waveguide.

Acknowledgments
A. Noury acknowledges the Ministry of Higher Education and Research (France) for scholarship. This work has been supported by the European project FET CARTOON and by the ANR JCJC project "Ca (Re-) Lase !". The fabrication of the device was performed at the nano-center CTU-IEF-Minerve, which is partially funded by the 'Conseil Général de l'Essonne'. This work was partly supported by the French RENATECH network.

Keywords: Carbon nanotubes, silicon photonics, light emission, CMOS fabrication

Synthesis of IV-VI Transition Metal Carbide and Nitride Nanoparticles using a Reactive Mesoporous Template for Electrochemical Hydrogen Evolution

Nawal S. H. Alhajri[a], Dalaver H. Anjum[b], M. N. Hedhili[b] and Kazuhiro Takanabe[a,*]

[a] *Division of Physical Sciences and Engineering, KAUST Catalysis Center (KCC), King Abdullah University of Science and Technology (KAUST), 4700 KAUST, Thuwal, 23955-6900 Saudi Arabia.*
[b] *Advanced Nanofabrication, Imaging and Characterization core lab, King Abdullah University of Science and Technology (KAUST), 4700 KAUST, Thuwal, 23955-6900 Saudi Arabia.*

Abstract: Interstitial carbides and nitrides of early transition metals in Groups IV-VI exhibit platinum-like behavior which make them promising candidate to replace noble metals in a wide variety of reactions in particular electrocatalysis. Most synthetic methods used to prepare these materials lead to bulk or micron size powder which limit their use in catalytic applications. Attempts toward production of transition metal carbide and nitride nanoparticles in sustainable, simple and cheap manner have been rapidly increasing. In this paper we present a new approach to prepare nano-scale transition metal carbides and nitrides of group IV-VI by utilizing mesoporous graphitic carbon nitride (mpg-C_3N_4) that not only provides confined spaces for nanoparticles formation but also acts as a chemical source of nitrogen and carbon. In addition, our study shows that a whole class of transition metal carbide and nitride (IV-VI) nanoparticles with a size of 3 nm can be obtained in similar way directly through the reaction of mpg C_3N_4 with transition metal precursors under flow of N_2 at different temperatures while keeping the weight ratio constant at 1:1. The produced nanoparticles were characterized by XRD, CHN elemental analyses, TGA, nitrogen sorption, XPS, and TEM. These results confirmed that as moving from left to right (IV-VI) the transition metals have the tendency to form carbide rather than nitride.structure. The electrocatalytic activities of the produced samples were tested for hydrogen evolution reaction in acid media and the results demonstrated that molybdenum carbide nanoparticles exhibited the highest and most stable HER current in acidic media, with an onset potential of -100 mV vs. RHE, among the samples prepared in this study. This result is attributed to the sufficiently small particle size (8 nm on average) and accordingly high surface area (308 m^2 g^{-1}). The graphitized carbon layer on its surface formed by this synthesis may also function as an electronic bridge which will accordingly enhance the electronic conductivity and improve electron transfer reaction at the surface.

Keywords: transition metal carbide; transition metal nitride; nanoparticles; carbon nitride.

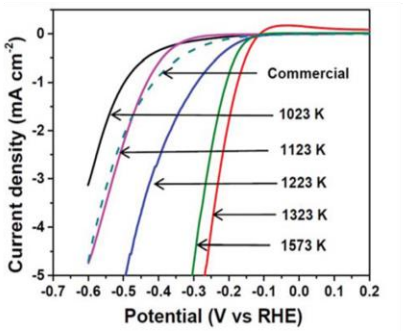

Figure 1: HER voltammograms of molybdenum carbide-carbon nanocomposites synthesized under different temperatures under N_2 flow and commercial Mo_2C.

References:

- Alhajri, N. S.; Yoshida, H.; Anjum, D. H.; Garcia-Esparza, A. T.; Kubota, J.; Domen, K.; Takanabe, K. *Journal of Materials Chemistry A* **2013**, *1*, 12606.
- Alhajri, N. S.; Anjum, D. H.; Takanabe, K. *Journal of Materials Chemistry A* **2014**, *2*, 10548.
- Garcia-Esparza, A. T.; Cha, D.; Ou, Y.; Kubota, J.; Domen, K.; Takanabe, K. *ChemSusChem* **2013**, *6*, 168.

Zinc doped InP colloidal quantum dots

N. Mordvinova*[1], A. Vinokurov[1], T Kuznetsova[1], S. Dorofeev[1], O. Lebedev[2]
[1] Lomonosov Moscow State University, Moscow, Russia
[2] CRISMAT, UMR 6508, CNRS-ENSICAEN-UCBN, 14050 Caen, France

Abstract: Quantum dots (QDs) have very wide scope of applications: in biomedicine, for the construction of photodetectors, solar cells, and electroluminescent devices among them the most interesting QD-LED displays. The II-VI QDs, for example CdSe and CdS, have been studied extensively, however have serious disadvantage – high toxicity of material, that's why another systems, such as A^3B^5-system, should be investigated. InP is a promising material for the creation of eco-friendly materials because it is more stable than II-VI materials and does not contain toxic elements, such as Cd, Hg, or Se. One of the ways to produce InP QDs is phosphine synthetic route, which allows to obtain QDs with narrow size distribution and good crystallinity but quite low photoluminescence intensity (Mordvinova *et al.*; 2014). This work is devoted to doping of InP QDs with zinc using gaseous phosphine as phosphorous precursor and myristic acid as stabylizer. We demonstrate how zinc affects the optical properties of QDs. We report the influence of different parameters (zinc amount, stabilizer, temperature and duration of synthesis) on luminescence wavelength and intensity. In addition we show that doping with zinc is accompanied with zinc-shell covering and is an effective way to improve optical properties of InP QDs.

Keywords: semiconductor nanocrystals, InP quantum dots, phosphine synthetic route, zinc doping, photoluminescence.

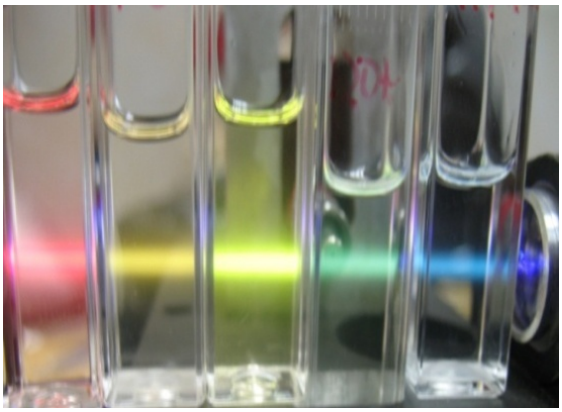

Figure 1: Luminescence of QDs with different mean diameters after postsyntetical treatment.

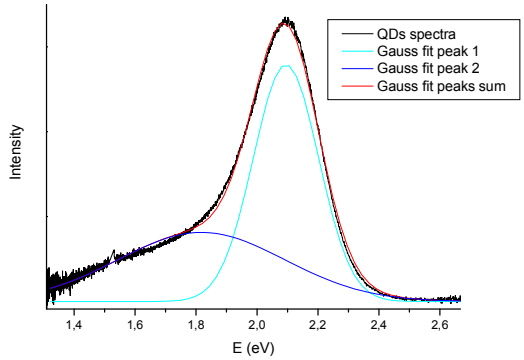

Figure 2: Typical luminescence spectra of Zn-doped QDs and its Gauss fitting.

References:

Natalia Mordvinova, Alexander Vinokurov, Sergey Dorofeev, Tatiana Kuznetsova, Konstantin Znamenkov, (2014), Phosphine synthetic route features and postsynthetic treatment of InP quantum dots, *Journal of Alloys and Compounds*, 582, 43–49.

Performance study of Phase Change Memory in Different Crossbar Architechtures

Nemat H. El-Hassan, T. Nandha Kumar and Haider A.F.Almurib
Department of Electrical and Electronic Eng.,
The University of Nottingham
Selangor, Malaysia.

Abstract: Resistive nonvolatile memories such as memristors, Magnetic Torque Junctions (MTJs) and Phase Change Memorys (PCMs) among others are considered as potentiall candidates for storage class memory, which is a new memory class presented to bridge the gab between high speed volatile memory and low dense power consuming nonvolatile memories. This class is expected to capture the desired qualities from both previous types to fulfill the growing demands of consumer electronics markt. PCM in particular poses most of desirable properties; including high density and scalabily, high operating speed, endurance and full CMOS compatibility (Nemat H. El-Hassan *et al.* 2014). Non-volatility of PCMs comes from the fact that the material exhibits a thermally induced phace change between at least two resistive states, and that the phase does not spontaneously reverse; therefore the material resistance is considered a memory element, and by placing a PCM in a crossbar architecture a very high density memory system can be achieved. Although the standard crossbar structure (Figure 1) offers high density, the sneak path (leakage) current issue effect the operation of PCM units, this effect is measured and compared between a standard nano-wire crossbar architecture and a new architechture suggested to mitigate sneak pathleakage current effects (T. Kumar *et al.* 2014). The leakage effects include operation delay, power loss and programming errors.

In this work we quantify the effects of sneak path current on a PCM based standard crossbar architechure and compare them to the modified architecture of (T. Kumar et al. 2014), in terms of; area overhead, power dissipation, delay time and reliability by using extensive simulation results and the PCM model presented by (Nemat H. El-Hassan et al. 2014)

Keywords: Phase Change; Chalcogenide; Non-Volatile Memory; Joule Heat, Crossbar, Leakage

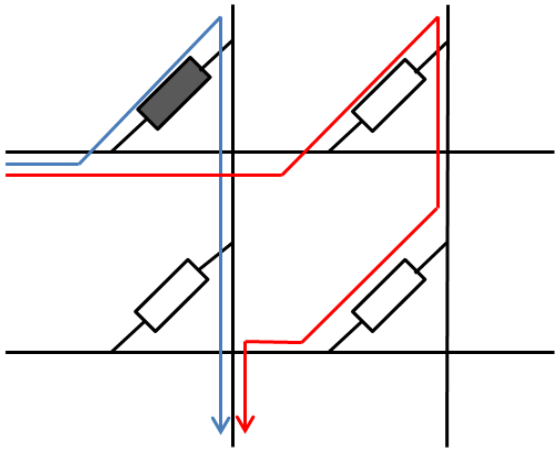

Figure 1 : Leakage currents in a crossbar architechture, the blue line is the current passing through the targeted cell (shaded), the red line is a possible leakage current path.

References:

T. Nandha Kumar, Haider A.F Almurib, Fabrizio Lombardi. (2014), A Novel Design of a Memristor-Based Look-Up Table (LUT) for FPGA In: *IEEE Asia Pacific Conference on Circuits & Systems*, 703-706.

Nemat H. El-Hassan, T. Nandha Kumar, and Haider Abbas F. Almurib. (2014), Improved SPICE Model for Phase Change Memory Cell, *5th IEEE International Conference on Intelligent and Advanced Systems*, 1- 6.

Micellar and Colloidal Dispersions of Conjugated Polymer Nanoparticles for Photoinduced Electron Transfer Applications

S. Wang, and G. Redmond,[1,]
[1]University College Dublin, School of Chemistry & Chemical Biology, Dublin, Ireland.

Abstract: We report on the preparation of aqueous dispersions of conjugated polymer nanoparticles based on poly(2-methoxy-5(2'-ethyl) hexoxy-phenylenevinylene) (MEH-PPV) by solubilisation of the polymer in the hydrophobic cores of F-127 micelles. As-prepared MEH-PPV micelles exhibit an average hydrodynamic diameter of 21 nm. Absorption, and photoluminescence excitation and emission spectral changes are observed on transfer of the conjugated polymer from a non-aqueous solvent to an aqueous micellar environment and are attributed to increased inter-chain interactions due to conjugated polymer chain collapse during encapsulation in the hydrophobic micellar cores; see Figure at right. When prepared in water, the micelles aggregate significantly over time. However, when prepared in buffer solution, the micelles exhibit good long-term collodial stability. When the MEH-PPV micelles are doped by the addition of controlled amounts of PCBM, the observed correspondence of photoluminescence emission quenching, quantum yield decreases, and emission lifetime shortening with increasing PCBM concentration indicates efficient photo-induced donor-to-acceptor charge transfer between MEH-PPV and the fullerenes in the cores of the micelles. This assignment is confirmed by transient absorption spectroscopic measurements that demonstrate that the MEH-PPV:PCBM micelles act as spatially confined donor-acceptor systems capable of successfully facilitating photo-induced charge carrier separation.

Also, we report on the preparation of aqueous dispersions of conjugated polymer nanoparticles based on the low band gap polymers APFO-3 and PCDTBT using a re-precipitation method in the absence of any surfactant additives. The resulting nanoparticle suspensions are stable over time, optically clear (not turbid), and present a characteristic purple colour associated with light absorption by the conjugated polymers. Dynamic light scattering measurements indicate average hydrodynamic diameters for the nanoparticles of approximately 36 nm (APFO-3) and 42 nm (PCDTBT). While polymer absorption and photoluminescence excitation spectra vary little on transfer from solvent solution to nanoparticle dispersion, the photoluminescence emission spectra of the nanoparticles are found to be significantly red-shifted and broadened, characteristic of increased inter-chain interactions due to conjugated polymer chain collapse in water during nanoparticle formation, resulting in the formation of a fraction of red-shifted aggregate species with energetic disorder. Likewise,

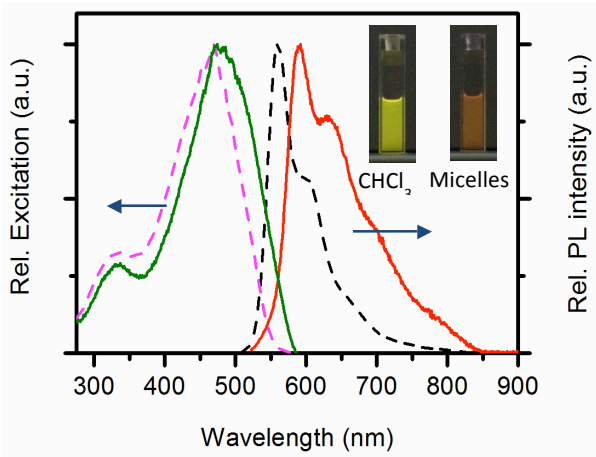

Figure: Fluorescence excitation and emission spectra acquired for MEH-PPV polymer chains dissolved in a good solvent ($CHCl_3$) and dispersed in an aqueous micellar format.

photoluminescence quantum yields and emission lifetimes decrease in the nanoparticle format, consistent with increased inter-polymer chain interactions in the nanoparticles providing more pathways for non-radiative decay of polymer excited states. Ensemble photobleaching studies indicate that the particles exhibit excellent photostabilities with nanoparticle death numbers being several orders of magnitude larger than those of typical organic dyes. Complementary single nanoparticle photoluminescence emission imaging studies highlight the multi-chromophoric nature of the polymer nanoparticles and confirm the favourable photostabilities associated with both the APFO-3 and PCDTBT nanoparticles. Finally, when the nanoparticles are doped by the addition of controlled amounts of PCBM, the observed correspondence of photoluminescence emission quenching, quantum yield decreases, and emission lifetime shortening with increasing PCBM concentration suggests efficient photo-induced donor-to-acceptor charge transfer between the conjugated polymers and the fullerenes dopants co-localised in the cores of the micelles illustrating the potential of these novel materials for application in future nanostructured bulk hetero-junction organic photovoltaic devices or in photocatalytic systems.

Keywords: nanoparticles, conjugated polymers, fullerenes, colloidal dispersions, optical spectroscopy, fluorescence, quenching, transient absorption, electron transfer, photovoltaics, photocatalysis.

Coupling between plasmonic response of supported gold particles and changes on TiO_2 band gap

S. R. Islas,[1*] R. Zanella,[1] J. M. Saniger ,[1]
[1]Materiales y Nanotecnología, Centro de Ciencias Aplicadas y Desarrollo Tecnologíco, UNAM, México, D.F.

Abstract: The supported gold nanoparticles in the visible light region exhibit a localized surface plasmon resonance (LSPR), and this defines the collective movement of conduction band electrons which is stimulated by irradiation of visible light (Garcia, 2012). Among the many factors that influence the LSPR of the Au NPs supported on TiO_2, and consequently its optical spectrum, those with higher relevance for this work are the size and shape of the NPs, the dielectric function of the surrounding NPs host and, more importantly, the gold NPs-support interactions.

The response plasmonic of the gold nanoparticles only has been used to study the metallic gold like the "ready to use" catalytic system (Zanella et al., 2004), while disregarding the influence of the activation process conditions on the final catalytic behavior. On the contrary, less studied how the nature of the gas used for thermal treatments can affect the metal-support interaction.

We study the processes of formation of gold nanoparticles *in situ* by means diffuse reflectance UV-visible spectroscopy. This study shown that this formation process in general is similar when is carried out in different atmospheres like Ar, N_2, H_2 and O_2, but the onset temperatures and final position of the plasmon band depends of the interaction between the atmosphere with the support. Moreover, it is possible attachment the changes in the band gap of the TiO_2 with the process of formation of plasmon absorption band of the gold nanoparticles. Both processes are coupled, probably mediated by charge transfer (Pacchioni G 2013, and Wang, Y.-G. et al. 2013).

Keywords: gold nanoparticles, resonance plasmon band, band gap, diffuse reflectance UV-Visible spectroscopy.

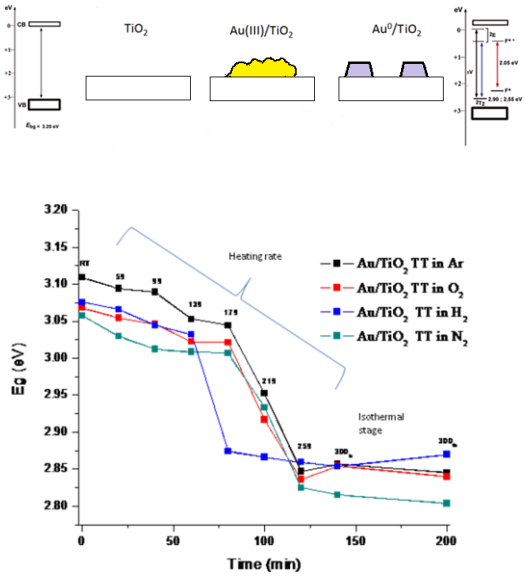

Figure 1: Figure illustrating as the changes on the supports band gap are attachment with the interaction between the gold nanoparticles and the conditions on the thermal treatment, which is by means of charger transfer process.

References:

Garcia, M. A. (**2012**), Surface Plasmons in Metallic Nanoparticles: Fundamentals and Applications. *J. Phys. D. Appl. Phys.*, *45*, 389501.

Zanella, R.; Giorgio, S.; Shin, C.; Henry, C. R.; Louis, C.,(**2004),** Characterization and Reactivity in CO Oxidation of Gold Nanoparticles Supported on TiO_2 Prepared by Deposition-Precipitation with NaOH and Urea., *222*, 357–367.

Pacchioni, G. (**2013)**, Electronic Interactions and Charge Transfers of Metal Atoms and Clusters on Oxide Surfaces. *Phys. Chem. Chem. Phys.*, *15*, 1737–1757.

Wang, Y.-G.; Yoon, Y.; Glezakou, V.-A.; Li, J.; Rousseau, R. (**2013)**, The Role of Reducible Oxide-Metal Cluster Charge Transfer in Catalytic Processes: New Insights on the Catalytic Mechanism of CO Oxidation on Au/TiO2 from Ab Initio Molecular Dynamics. *J. Am. Chem. Soc.*, *135*, 10673–10683.

Nanoplasmonics in Inorganic Nanoparticles

T. Teranishi*
Kyoto University, Institute for Chemical Research, Uji, Kyoto, Japan

Abstract: Localized surface plasmon polaritons, which are referred to simply as localized surface plasmons, are collective free carrier oscillations in nanoparticles (NPs) that are excited by incident light waves. At the NP surface, the localized surface plasmons exhibit enhanced near-field amplitudes, which are highly localized at the NP surface and decay rapidly in the dielectric surroundings. A very important aspect of localized surface plasmons is the localization of an enhanced electromagnetic field around the NPs with very high spatial resolution (subwavelength) as well as the generation of hot electrons (Teranishi *et al.*, 2011; Yang *et al.*, 2010; He *et al.*, 2012). Here I present the unique plasmonic properties of indium tin oxide (ITO) NPs (Kanehara *et al.*, 2009; Furube *et al.*, 2012) and non-stoichiometric copper sulfide nanodisks (Kanehara *et al.*, 2012; Chen *et al.*, 2015) in the near IR (NIR) region by changing the carrier (free electron or hole) density and structural anisotropy (Figure 1). In addition, as an example of plasmon-induced hot electron application, the visible-to-NIR plasmon-enhanced catalytic activity of palladium hexagonal nanoplates for the Suzuki coupling reactions is presented (Trinh *et al.*, submitted).

Keywords: localized surface plasmon, carrier density, electromagnetic field, hot electron injection, indium tin oxide, copper sulfide, palladium hexagonal nanoplate.

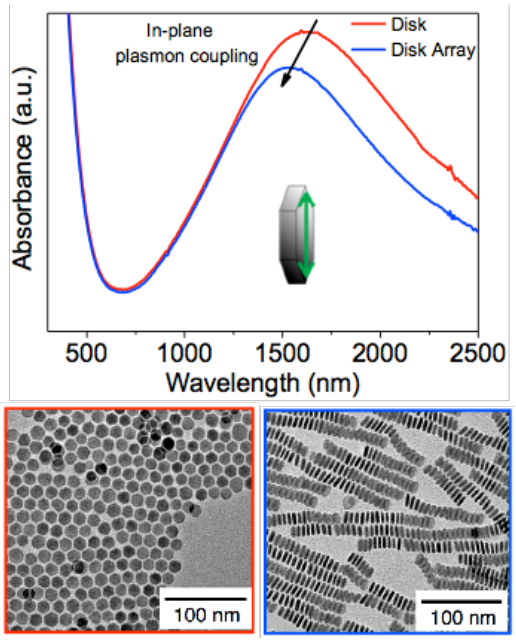

Figure 1: Change in localized surface plasmon resonance peak by aligning the Cu_7S_4 nanodisks in one dimension in $CHCl_3$

References:

Teranishi, T., Eguchi, M., Kanehara, M., Gwo, S. (2011) Controlled Localized Surface Plasmon Resonance Wavelength for Conductive Nanoparticles over the Ultraviolet to Near-Infrared Region, *J. Mater. Chem.,* 21, 10238-10242.

Yang, S., Kobori, H., He, C.; Lin, M.; Chen, H.; Li, C.; Kanehara, M., Teranishi, T., Gwo, S. (2010), Plasmon Hybridization in Individual Gold Nanocrystal Dimers: Direct Observation of Bright and Dark Modes, *Nano Lett.*, 10, 632-637.

He, C., Chen, H., Wang, C., Lin, M., Mitsui, D., Eguchi, M., Teranishi, T., Gwo, S. (2011), Far-Field Optical Imaging of a Linear Array of Coupled Gold Nanocubes at Visible Wavelengths: Direct Visualization of Dark Plasmon Modes, *ACS Nano*, 5, 8223-8229.

Kanehara, M., Koike, H., Yoshinaga, T., Teranishi, T. (2009), Indium Tin Oxide Nanoparticles with Compositionally Tunable Surface Plasmon Resonance Frequencies in the Near IR Region, *J. Am. Chem. Soc.*, 131, 17736-17737.

Furube, A., Yoshinaga, T., Kanehara, M., Eguchi, M., Teranishi, T. (2012), Electric Field Enhancement in NIR Two-Photon Absorption by Indium Tin Oxide Nanoparticle Film, *Angew. Chem. Int. Ed.*, 134, 816-819.

Kanehara, M., Arakawa, H., Honda, T., Saruyama, M., Teranishi, T. (2012), Large-Scale Synthesis of High-Quality Metal Sulfide Semiconductor Quantum Dots with Tunable Surface-Plasmon Resonance Frequencies, *Chem. Eur. J.*, 18, 9230-9238.

Chen, L., Sakamoto, M., Sato, R., Teranishi, T. (2015), Determination of a Localized Surface Plasmon Resonance Mode of Cu_7S_4 Nanodisks by Plasmon Coupling, *Faraday Dicuss.*, in press.

Trinh, T. T., Sato, R., Fujiyoshi, Y., Haruta, M., Kurata, H., Teranishi, T., Visible to Near-Infrared Plasmon-Enhanced Catalytic Activity of Pd Hexagonal Nanoplates for the Suzuki Coupling Reaction, submitted.

MoS_2 Transistors with Electrografted Organic Ultrathin Film as Efficient Gate Dielectric

H. Casademont,[1] L. Fillaud,[1] X. Lefevre,[1] R. Cornut,[1] B. Jousselme,[1] V. Derycke[1,*]
[1]CEA Saclay, IRAMIS / NIMBE (UMR 3685) / LICSEN, F-91191 Gif sur Yvette, France

Abstract: Two dimensional layered semiconductors, and in particular transition metal dichalcogenides such as molybdenum disulfide (MoS_2), have recently received increasing attention due to the combination of their unique electronic properties with their atomically thin geometry. Contrary to graphene, MoS_2 has a finite band gap of 1.2-1.9 eV (depending on the number of layers), thus complying with the requirements of digital electronic applications. To maximize the potential of MoS_2 as channel material in field effect transistors, it must be associated with an efficient gate dielectric.
Beside the mainstream CMOS technology, other fields such as large-area and/or printable electronics, sensors and display technologies could also benefit from the combination of 2D materials and new dielectrics, especially if these dielectrics present additional advantages in terms of mechanical flexibility, low temperature processes, conformability to structured substrates, cost and simplicity of equipment and processes, etc. In this respect, the development of *robust organic* nano-dielectrics and their combination with new semiconductors represent a high potential route.

In this context, we developed new dielectrics based on electrografted organic thin films on metallic electrodes. These dielectrics are produced at room temperature and under mild conditions. The process yields uniform films of nanometer thickness (4-8 nm range). In this work [1], we demonstrated the first transistors combining MoS_2 as channel material and an electrografted organic ultrathin film as gate dielectric. The transistors exhibit high I_{ON}/I_{OFF} ratio together with steep subthreshold slope as low as 110 mV/decade (Figure 1). Besides, the transfer characteristics of these transistors have no-hysteresis due to the hydrophobic and trap-free nature of our electrografted dielectric. The transistors reported in [1] were fabricated on rigid substrates and using mechanically exfoliated MoS_2. Their potential in large scale (based on CVD MoS_2) and flexible electronics will be discussed on the basis of our latest results.

Keywords: MoS_2 transistors, organic dielectrics, fluorinated diazonium salt, electrografting.

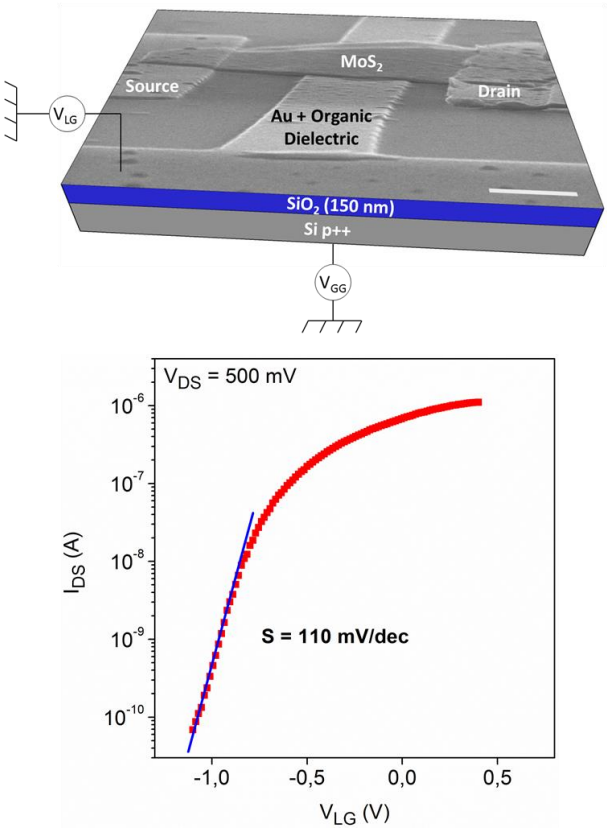

Figure 1: On top: Schematic representation and SEM image (scale bar = 500 nm) of a MoS_2 FET with an electrografted local-gate electrode. At the bottom: Transfer characteristic $I_D(V_{LG})$ measured at V_{DS} = 0.5 V and V_{GG} = 40 V of a MoS_2 FET with an organic dielectric thickness of 4 nm.

References:

[1] H. Casademont, L. Fillaud, X. Lefèvre, B. Jousselme, V. Derycke, submitted.

Nanoscale Magnetic Materials and Magnetic Nanodots for Spintronic Applications

Santanu Ghosh

Nanostech Laboratory, Indian Institute of Technology Delhi, New Delhi-16, India

Abstract: After the discovery of electron in 1911 by Robert Milikan in his famous 'Oil drop experiment', a new technology named 'Electronics' has changed the face of human civilisation. It will not be an exaggeration if the science and technology of the last century is named as an 'Era of electronics'. Starting with simple battery, galvanometer, vacuum diodes etc., now in almost all devices, equipments and home appliances, we have semiconductor based integrated electronic circuits. The saga continues till today. The entire electronics is based on a small physical quantity named as 'charge' of electron and its motion. The electron has another degree of freedom named as 'spin', which is basically an intrinsic angular momentum of an elementary particle. Although this physical entity was also discovered in early 20th century by Davisson and Germer, and theoretically interpreted by P. A. M. Dirac, we had to wait till 1986 to manipulate this in the motion of electron. This was possible because of a constant endeavour of materials scientists to grow low dimensional materials, down to few nm metallic multilayers. A concept of spin based electronics or 'Spintronics' has started with the discovery of giant magnetoresistance (GMR) by A. Fert and P. Grünberg in 1987. Since that, the scientist and technologists have realized this concept in various spin based devices, like 'spin valve', 'spin FET', 'magnetic RAM', GMR based data storage etc.

With the above introduction, and after depicting a short road map of spintronics, the following materials aspects, essential for spintronics will be addressed in this talk.

(A) Microstructure controlled RT-FM in Ni-ZnO films: Search for room temperature ferromagnetism (RT-FM) in wide band gap semiconductors has emerged as an important area of research from fundamental physics and possible applications in future spintronic devices. Room temperature ferromagnetism is observed in 200keV Ni^{+2} ions implanted with fluences of 6×10^{15} (2 % Ni) 8 $\times 10^{15}$ (3% Ni) and 2 $\times 10^{16}$ ions/cm^2 (7% Ni) on ZnO films grown on Si (100) substrate by vapour phase transport process. Experiments on this material indicate that exchange interaction between the charge carriers generated due to thermal effects of ion implantation and the localized spins of Ni is considered as main reason behind RT-FM.

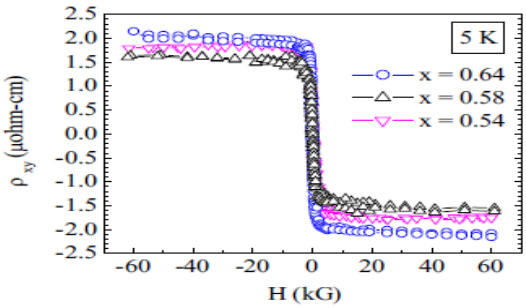

Figure 1: Extraordinary Hall effect of Ni nanoparticles embedded in thin silica matrix for highly sensitive magnetic field sensor

(B) Extra ordinary Hall effect (EHE) and tunnelling magnetoresistance (TMR) in nanogranular films: Magnetic metal nanoparticles (NPs) embedded in dielectric media is another important material to realize spin dynamics in a controlled manner. Size, shape, uniformity of NPs is the key issues in designing devices based on these materials. In this talk, a large hall coefficient based on anomalous Hall effect in Ni NPs embedded in thin SiO_2 matrix will presented. This will be followed by tunnelling magnetoresistance effect and role of Coulomb blockade in FeCo nanoparticles in thin SiO_2 matrix. Tailoring of nanoparticles shape by ion irradiation and a novel observation on electron emission from NPs will be discussed at the end.

Keywords: (i) Magnetic semiconductor, (ii) Exchange interaction, (iii) Microstructure, (iv) Transparent ferromagnetism, (v) Extra ordinary Hall effect, (vi) Tunneling magnetoresistance.

References:

J. App. Phys. 113, 183708 (2013), (ii) J. Appl. Phys. 111 (2012) 013715, (iii) Nanoscale Research Letter (NANO EXPRESS), 2011, 6: 155, (iv) J. Appl. Phys, 109 (2011), 073914, (v) J. Appl. Phys. 107 (2010), 113913, (vi) J. Appl. Phys. 107 (2010) 023901, (vii) J. Appl. Phys. 105 (2009) 033909, (viii) Vacuum 85 (2010) 139, (ix) Rad. Eff. And def. Sol. 163, (2008) 215.

Polymer-Based Nanowires and Nanotubes: nanosources, wave-guiding

J.L. Duvail,[1,*] A. Garreau,[1] J. Bigeon,[2] N. Huby,[2] B. Bêche,[2] F. Massuyeau,[1] A. Désert,[1] S. Cordier,[3] Y. Molard,[3] E. Faulques[1]
[1]Institut des Matériaux Jean Rouxel, UMR 6502 CNRS Université de Nantes, France
[2]Institut de Physique de Rennes, UMR 6251 CNRS Univeristé de Rennes-1, France
[3]Institut des Sciences Chimiques de Rennes, UMR 6226 CNRS Université de Rennes-1, France

Abstract: One-dimensional polymer-based nanostructures such as nanowires (NWs) and nanotubes (NTs) are nowadays intensively investigated since they promote enhanced properties, as well as new paradigms for electronic, optical, optoelectronic, and photonic devices (Garreau *et al.*, 2014).
Here, we propose a review of recent developments achieved in our group with collaborations on polymer-based nanowires and nanotubes. Various polymer-based NWs and NTs were synthesized by template strategies with advanced architectures designed for improving their functionality (waveguiding, color control of photoluminescence, photoconductivity and mechanical reinforcement,…). Both conjugated polymers (CPs) and photoresists containing photoactive species (transition metal compound clusters, single-walled-carbon nanotubes SWCNTs) were involved. The focus is made on the emerging strategies for understanding and controlling the behavior of charges, excitons and photons, as well as light propagation in sub-wavelength nanostructures.

First, an original design was realized to control accurately the color of photoluminescence in organic nanostructures (Garreau *et al.*, 2013). It consists in minimizing the role of charge and energy transfer mechanisms between two types of luminophores. This was achieved by an optimized spatial separation at the nanoscale with nanowires in a coaxial geometry: a green polymeric emitter shell (poly-para-phenylene-vinylene PPV) and a red phosphorescent emitter core ($[Mo_6Br_8F_6]^{2-}$ clusters@poly(methyl methacrylate) PMMA). In addition, the choice of luminophores was motivated to get a spectral separation, i.e. distinct color of PL emission, as well as no overlapping of their absorption and emission spectral range. Thus, it is possible to anticipate and to control simply the color of the emitted light on the chromaticity diagram as an interpolation of the CIE coordinates of each luminophore. This design make possible to reach a very sharp color change within 10 nm scale. Additionally, unique proportion equal typically to 1:1 for the green and red luminophores are required.

Second, we report light injection and sub-wavelength propagation in nanotubes made of SU-8, a photoresist used for integrated photonics. Nanotubes have been rarely investigated as waveguides. However, it is a very promising geometry for highly integrated photonic devices, as shown by theoretical simulation by finite domain time-dependent (FDTD) method (Bigeon *et al.*, 2014). The features of direct light injection and subwavelength propagation regime within nanotubes were determined. The injection into nanotubes of SU8 was successfully achieved by using polymer microlensed fibers with sub-micronic radius of curvature. The propagation losses into single SU8 nanotube were determined. The attenuation coefficient has been evaluated at 1.25 dB/mm by a cut-back method transposed to such nanostructures. The mechanisms responsible for losses in nanotubes were identified in view of FDTD theoretical support.

These recent advances in polymeric based NWs and NTs contribute to open new ways for the next generation of optoelectronic and photonic integrated devices.

Keywords: Nanowires, Nanotubes, Polymer, Nano-optoelectronics, Nanophotonics.

References:

Garreau, A. Duvail, J.L., (2014), Recent advances in optically-active polymer-based nanowires and nanotubes *Advanced Optical Materials*, 2, 1122-1140

Garreau, A., Massuyeau, F., Cordier, S., Molard, Y., Gautron, E., Bertoncini, P., Faulques, E., Wéry, J., Humbert, B., Bulou, A., Duvail, J.L. (2013), Color control in coaxial two-luminophore nanowires *ACS Nano* 7, 2977–2987

Bigeon, J., Huby, N., Duvail, J.L., Bêche, B., (2014), Injection and waveguiding properties in SU8 nanotubes for subwavelength regime propagation and nanophotonics integration *Nanoscale* 6, 5309-5314

3D Simulation of DG-FinFET transistor with different channel materials and gate dielectrics

N. Boukortt[1,2,*], B. Hadri[1], L. Torrisi[2], S. Patanè[2], A. Caddemi[3], and G. Crupi[3]
[1]Department of Electrical Engineering, University of Mostaganem, 27000 Mostaganem, Algeria.
[2]Dipartimento di Fisica e Scienze della Terra, University of Messina, 98166 Messina, Italy
[3]DICIEAMA Department, University of Messina, 98166 Messina, Italy.

Abstract:

This work investigates two different structures of double gate n-FinFET in 3-D with 8 nm gate length using SiGe and 3C-SiC in the channel region, respectively. In this work, the numerical simulation tool Atlas Silvaco was used to extract novel results concerning the electrical characteristics of the device. The influence of the gate work function and the gate dielectric on threshold voltage, subthreshold slope, transconductance, DIBL, leakage current, on current, and On/Off current ratio has been investigated. This study has been performed for four different gate dielectrics which are SiO_2, Si_3N_4, Al_2O_3, and ZrO_2. We observed that the best results are obtained when ZrO_2 is used as a gate oxide material.

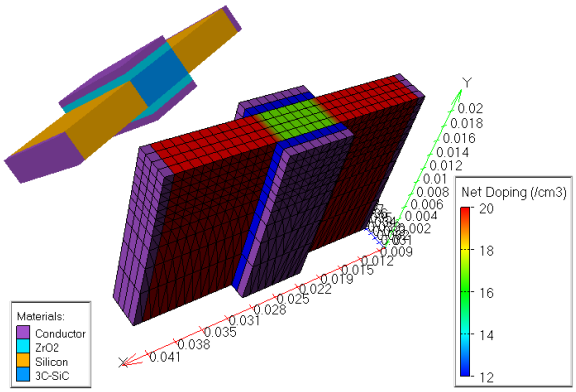

This figure illustrates the schematic structure used for our simulation. The FinFET technology is characterized by vertical silicon fins, fin length (L_g), fin height (H_{FIN}), and the silicon thickness (W_{FIN}) as shown in the figure. This study will also permit us to discuss about new multi-gate transistors (MuGFET) which enhance the performances of advanced microprocessors such as Intel Core new generation technology.

Keywords: Device scaling, Double gate MOSFET, FinFETs, High-k dielectric materials, 3C-SiC, Gate work function, Leakage current, Silvaco Software.

References:

Yakimova, R. Vasiliauskas, R. Eriksson, J. Syväjärvi, M. (2012), Progress in 3C-SiC growth and novel applications, *Mater S Forum*., 711, 3-10.

Raja, P. S. Joseph Daniel, R. Bino, N. (2012), Silicon Nanowire Based MOSFET Parameter Analysis, *IOSR-JECE.*, 3, 35-43.

Raja, P.S. Joseph Daniel, R. (2012), Effect of gate dielectric on threshold voltage of Nanoscale MOSFETS, *Int. J. Eng Res Dev*., 5, 93-104.

Shashank, N. Basak, S. Nahar, R. K. (2010), Design and Simulation of Nano Scale High-k Based MOSFETs with Poly Silicon and Metal Gate Electrodes, *Int.J. Adv Tech*., 1, 252-261.

Mohapatra, S. K. Pradhan, K. P. Sahu, P. K. (2014), Influence of High-k Gate Dielectric on Nanoscale DG-MOSFET, *Int. J. AST*., 65, 19-26.

Wong, H. Iwai, H. (2006), On the scaling issues and high-k replacement of ultrathin gate dielectrics for nanoscale MOS transistors, *Microelectron Eng*., 83, 1867-1904.

Kumar, M. Dubey, S. Kumar Tiwari, P. Jit, S. (2013), Analytical modeling and simulation of subthreshold characteristics of back-gated SSGOI and SSOI MOSFETs: A comparative study, *Curr. Appl. Phys*., 13, 1778-1786.

Lee, C. Ferain, I. Afzalian, A. Yan, R. Dehdashti Akhavan, N. Razavi, P. Colinge, J.-P. (2010), Performance estimation of junctionless multigate transistors, *Solid State Electron*., 54, 97-103.

Pradhan, K.P. Mohapatra, S.K. Sahu, P.K. Behera, D.K. (2014), Impact of high-k gate dielectric on analog and RF performance of nanoscale DG-MOSFET, *Microelectron. J*., 45, 144-151.

Rahimian, M. Orouji, A.-A. (2011), Nanoscale SiGe-on-insulator (SGOI) MOSFET with graded doping channel for improving leakage current and hot-carrier degradation, *Superlattices Microstruct*., 50, 667-679.

Key Variable Components for Enhancing Charge Transfer at PbS Quantum Dots/Porphyrin Interfaces: From Quantum Confinement to Electrostatic Interaction

A. O. El-Ballouli, E. Alarousu, O. M. Bakr and O. F. Mohammed

Solar and Photovoltaics Engineering Research Center, Division of Physical Sciences and Engineering, King Abdullah University of Science and Technology (KAUST), Thuwal, Kingdom of Saudi Arabia

Abstract: Quantum dot (QD) solar cells have emerged as a promising low-cost alternative to existing photovoltaic technologies (Pan *et al.*, 2013; Kamat *et al.*, 2013). Accordingly, understanding the interfacial charge transfer dynamics at different QD/electron-transporting material systems is necessary to optimize the solar cell performance by ensuring fast injection and separation processes, along with a long-lived charge separation state. Very recently, we have shown that only small-sized PbS QDs with a bandgap (E_g) > 1 eV can efficiently transfer electrons to phenyl-C_{61}-butyric acid methyl ester (PCBM) upon light absorption; as inferred from the ultrafast formation of the anionic species of PCBM (El-Ballouli *et al*., 2014). Nevertheless, it remains essential also to utilize larger-sized QDs efficiently for engineering multi-junction cells with broader energy harvesting capabilities; which cannot be achieved using PCBM as an electron accepting component. In this case, searching for an alternative electron accepting unit is crucial to harvest the light by large-sized PbS QDs. Here, we investigate the charge transfer and separation at PbS QDs/porphyrin interfaces using a combination of femto- and nanosecond broadband transient absorption (TA) spectroscopy and steady-state photoluminescence quenching measurements. Our results demonstrate that the ultrafast interfacial charge transfer between PbS QDs and porphyrin can be tuned by quantum confinement due to driving force variations, while maintaining the whole QD size range (E_g = 1.45-0.83 eV) effective for the electron transfer. Additionally, the charge transfer is tunable by the interfacial electrostatic interaction between the positively charged *meso* unit of porphyrin and negatively charged ligands capping the QDs. The work presented here will provide new key components to control the charge transfer processes at QD interfaces, and will thus advance both the design and the understanding of QD interfaces for solar energy technology and for other potential applications that principally rely on the interfacial dynamics such as light-emitting diodes and photocatalysis.

Keywords: semiconductor quantum dots, photovoltaics, interfacial charge transfer, ultrafast transient absorption spectroscopy.

References:

Pan, J.; El-Ballouli, A.; Rollny, L.; Voznyy, O.; Burlakov, V.; Goriely, A.; Sargent, E.; Bakr, O. (2013), Automated synthesis of photovoltaic-quality colloidal quantum dots using separate nucleation and growth stages, *ACS Nano*, 7, 10158–10166.

Kamat, P. (2013), Quantum dot solar cells: The next big thing in photovoltaics. *J. Phys. Chem. Lett.*, 4, 908-918.

El-Ballouli, A.; Alarousu, E.; Bernardi, M.; Aly, S.; Lagrow, A. P.; Bakr, O.; Mohammed, O. (2014), Quantum confinement-tunable ultrafast charge transfer at the PbS quantum dot and phenyl-C61-butyric acid methyl ester interface. *J. Am. Chem. Soc.*, 136, 6952-6959.

Room Temperature Synthesis and Characterization of Stable, Highly Luminescent PbS/CdS Core-Shell Quantum Dots with Emission Below 1100 nm

E. Durmusoglu,[1,*] P. Dagtepe,[2] Y. Turker,[3] H. Yagci Acar,[1]

[1] Koc University, Graduate School of Materials Science and Engineering, Rumelifeneri Yolu, Sarıyer, 34450 Istanbul, Turkey

[2] Kuantag A.Ş., Kısıklı Mahallesi Sarıgazi Caddesi No:65, Üsküdar, 34692 Istanbul, Turkey

[3] Koc University, Department of Chemistry, Rumelifeneri Yolu, Sarıyer, 34450 Istanbul, Turkey

Abstract: Semiconductor PbS and PbS/CdS core-shell quantum dots (QDs) have attracted a great attention due strong absorbance in the visible and emission in the near Infrared (NIR) region, mostly between 700-1600 nm. These optical properties make them a good candidate for applications such as luminescent tagging, sensors, photovoltaics and bio-imaging. Detectors used for the luminescence measurement or signal detection are actually important in terms of the sensitivity range, availability and cost. Relatively cheap and widely available silicon detectors work quite well up until 1100 nm. But, small size PbS QDs with emission below 1100 nm are scarce and are suffer from quenching. We successfully synthesized PbS QDs emitting below 1100 nm by using both lead oxide-thioacetamide and lead chloride-elemental sulfur precursor pairs with modifications to the most widely used Hines-Scholes (Hines *et al.*; 2006) and Cademartiri (Cademartiri et al.; 2006) methods.

In order to enhance the luminescence stability, we have grown a CdS shell around these small PbS crystals. Cation-exchange at room temperature was performed followed by annealing at higher temperatures for the formation of CdS shell and improvement of luminesence stability and intensity. CdS shell growth increased the luminescence intensity, stability over-time by reducing non-radiative events and reducing the surface defects. Moreover, blue shift in the emission maxima is observed with CdS deposition of the PbS which fits the emission to the sensitive range of Si-detectors.

We will discuss the influence of variables source of the PbS on the particle properties of PbS/CdS nanoparticles.

Keywords: NIR emission, lead sulfide, leadsulfide/cadmiumsulfide core-shell ,quantum dot, shell growth

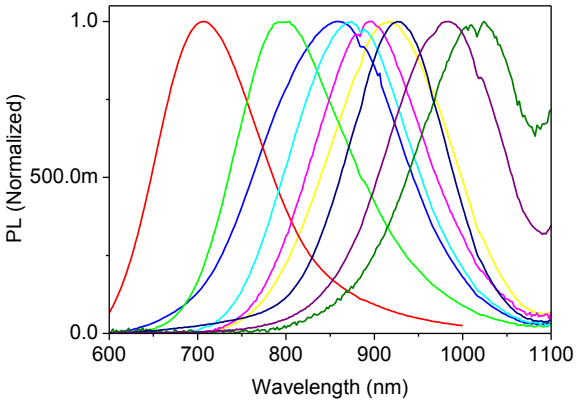

Figure 1: Emission spectrum of Different PbS/CdS quantum dots

References:

Hines, M.A., Scholes G.D., (2006). Synthesis of colloidal PbS nanocrystals with size tunable NIR emission, *Google Patents*, US 7118627 B2

Cademartiri, L., Bertolotti, J., Sapienza, R., Wiersma, D. S., von Freymann, G., & Ozin, G. a. (2006). Multigram scale, solventless, and diffusion-controlled route to highly monodisperse PbS nanocrystals. *The Journal of Physical Chemistry. B*, *110*(2), 671–3.

PANI deposited carbon cloth as binder-free electrode for symmetric supercapacitor application

M.V. Astakhov, R.R. Galimzyanov, A.A. Klimont, I.S. Krechetov, S.V. Stakhanova, O. V. Uryupina, M. Kundu*
National University of Science and Technology "MISIS", Moscow 119049, Russia

Abstract: In view of the current energy scenario and pursuit of alternative energy sources, supercapacitors (SCs) with excellent power density and superior cycling durability has positioned itself as the smartest choice for clean and efficient back up power sources and energy storage devices. The electrode material is one of the key components of a SC and to a large extent determines a SC's performance. Recently, in many reports, using nano-sized PANI with different microstructure deposited on carbon cloth a high value of gravimetric capacitance (F g^{-1}) with good cycle life has been reported (He *et al*.; 2013, and Bian *et al*.; 2012). In most of these cases, electrodes with low amounts PANI loading achieve very high gravimetric capacitance values with poor area-normalized capacitance values. But for real applications, achieving high gravimetric as well as area-normalized capacitance values is most crucial for their commercial success.

In this study, nano-structured PANI containing composite electrode based on Busofit T-040 carbon cloth (CC) with high specific surface area (900 m^2 g^{-1}) have been developed for symmetric supercapacitor devices by cost effective one step chemical polymerization of aniline. The carbon cloth consist of individual fibers of 7-8 μm diameter which are sufficiently tightly packed with random orientation (Fig. 1a). Such porous structure of carbon cloth is expected to facilitate the diffusion of electrolyte into the electrode material as well as to provide more channels for rapid ion transport. PANI uniformly deposited on the carbon surface as an individual granules whose diameter is about 30-50 nm (Fig. 1b).

The capacitive performance of CC as well as PANI/CC were characterized by the cyclic voltammetry (CV) and the galvanostatic charge-discharge in two-electrode configuration. PANI/CC demonstrates good electrochemical performance over carbon cloth in terms of weight-normalized and area-normalized specific capacitance. The weight-normalized and area-normalized specific capacitances for PANI/CC are 222 F g^{-1} and 6.66 F cm^{-2} respectively. Where as for CC these values are 120 F g^{-1} and 3.14 F cm^{-2}. The technological simplicity, easy to scale up and electrochemical performance of the PANI/CC demonstrate the significance of this work for industrial application.

Keywords: Supercapacitor, two electrode system, specific capacitance, chemical polymerization, polyaniline, carbon cloth.

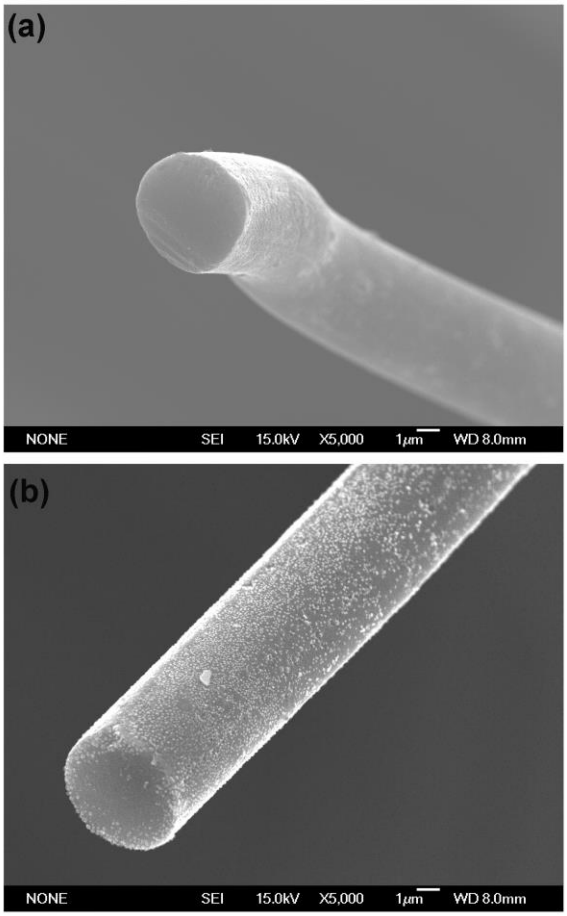

Figure 1: SEM images of CC (a) PANI/CC (b)

References:

He X., Gao B., Wang G., Wei J., Zhao C. (2013) A new nanocomposite: Carbon cloth based polyaniline for an electrochemical supercapacitor, Electrochim. Acta, 111, 210–215.

Bian L. J., Luan F., Liu S. S., Liu X. X. (2012) Self-doped polyaniline on functionalized carbon cloth as electroactive materials for supercapacitor, Electrochim. Acta, 64, 17–22.

High performance photoconductive device for UV region fabricated using graphene- n-GaN nanowire hybrid structure on Si substrate

San Kang,[1] Arjun Mandal,[1] Jae Hwan Chu,[2] Ji-Hyeon Park,[1] Soon-Yong Kwon,[2] and Cheul-Ro Lee [1]
[1]Semiconductor Materials Process Laboratory, School of Advanced Materials Engineering, Engineering College, Research Center for Advanced Materials Development (RCAMD), Chonbuk National University, Baekje-daero 567, Jeonju 561-756, Republic of Korea
[2]School of Materials Science and Engineering, Low Dimensional Carbon Materials Center, Ulsan National Institute of Science and Technology (UNIST), UNIST-gil 50, Ulsan 689-798, Republic of Korea

Abstract: This study demonstrates high performance photoconductive device to be operated in ultraviolet (UV) region consisting of graphene-n-GaN nanowire (NW) hybrid structure grown on silicon substrate with metal organic chemical vapor deposition (MOCVD) process. Raman spectroscopy and high-resolution transmission electron microscopy (HR-TEM) images confirmed the presence of monolayer graphene in the hybrid structure (Chu *et al.*, 2014). The graphene layer was not damaged after it was integrated with n-GaN NWs. The graphene layer had not only influenced the growth of defect-free, highly dense GaN NWs but also improved its material and crystalline qualities as confirmed from photoluminescence and X-ray diffraction (XRD) analyses. As a result, the graphene-n-GaN NWs hybrid structure under study represented a superior photoconductive channel with trap density much less than that of previously reported graphene-based photoconductive channels (Lee *et al.*, 2012). There was noticeable improvement in the photocurrent and photoresponsivity of the hybrid structure. Moreover, growth of the hybrid structure directly on silicon substrate and growth of n-GaN NWs without using metal-catalyst or droplet seeds added special importance to this study. Such simple, cost-effective and efficient photoconductive device involving graphene-n-GaN NW hybrid structure and utilizing the excellent electrical properties of graphene is undoubtedly a new proposal for GaN-based optoelectronics industry.

Keywords: GaN nanowires, graphene, photocurrent, photoresponsivity, ultraviolet photoconductive devices, metal organic chemical vapor deposition.

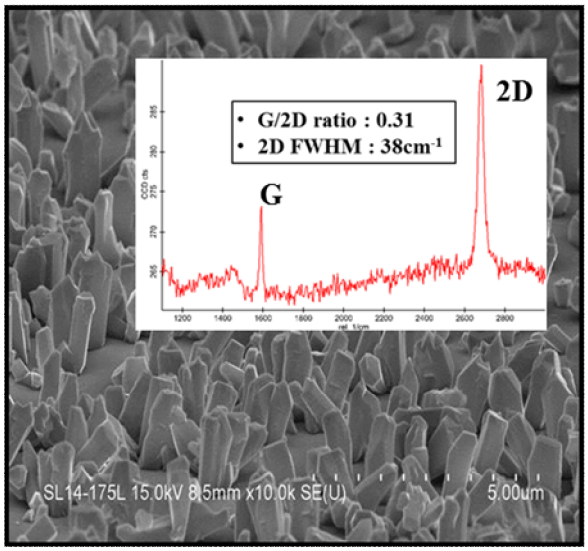

Figure 1: Field emission scanning electron microscopy (FE-SEM) image of graphene-n-GaN NW hybrid structure. FE-SEM image shows highly dense n-GaN NWs. Inset shows Raman spectroscopy of the underlying graphene layer.

References:

Chu, J. H., Kwak, J. S., Kim, S. D., Lee, M. J., Kim, J. J., Park, S. D., Choi, J. K., Ryu, G. H., Park, K. B., Kim, S. Y., Kim, J. H., Lee, Z. H., Kim, Y. W., Kwan, S. Y. (2014), Monolithic graphene oxide sheets with controllable composition, *Nat. Comm.*, 5, 3383.

Lee, H. W., Heo, K., Park, J. S., Park, Y. G., Noh, S. G., Kim, K. S., Lee, C. H., Hong, B. H., Jian, J., Hong, S. H. (2012), Graphene–nanowire hybrid structures for high-performance photoconductive devices, *J. Mater. Chem.*, 22, 8372-8376.

Transparent and flexible electrodes based on metallic nanowire networks: New nanomaterials and operating stability.

A. Cabos[1], C. Celle[1], A. Carella[1], J-P. Simonato[1]
[1]CEA-LITEN / DTNM / SEN / LSIN, 17 rue des Martyrs, 38054 Grenoble, France.
Corresponding author: anthony.cabos@cea.fr

Abstract: Transparent conductive thin films are widely used in technologies like solar cells, light-emitting diodes, and display technologies. The fabrication of transparent conductive films is currently realized with thin films of transparent conductive oxides (TCOs), and in particular indium tin oxide (ITO). The as-made ITO transparent conductors suffer from limitations like costly fabrication process and brittleness. The use of solution-processable nanomaterials, and especially metallic nanowires, appears as a promising alternative since it affords a large random two dimensional nanowire area, low-cost deposition method with high performances [1]. Among metals, silver is the more mature process, copper has merely the same properties, with another advantage, price and abundance of its.

Thanks to polyol (or hydrothermal for copper) process, metallic nanowire are synthesized in our laboratory, silver nanowire have a mean length of 10µm and a mean diameter of 60nm and copper nanowire a mean length of 128 µm and a mean diameter of 166nm (Figure 1) [2].Their dimension confers them a high aspect ratio and dispersed randomly in a substrate, threshold of percolation can be reached. Dispersed nanowires lead to a transparent and flexible electrode. Many printing techniques are available to make those electrodes in order to integrate into devices such as thermal film heater, thermochromics display or touch sensor [3] [4]. Thanks to the use of spray coating, flexible electrodes have excellent performance (i.e. R□<20Ω/□ at T>90%), and moreover infrared go also through the electrode [1].

Figure 1: SEM pictures of silver nanowire networks for transparent flexible electrode.

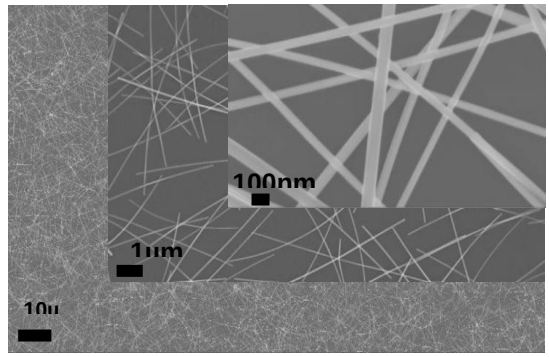

The study will be focused on stability of electrode under various stresses (electrical, environmental). Results are very promising because after three years, electrodes are stable under ambient air. More details will be given on the stability of those electrodes in operating conditions and their reaction at different stresses. Part of the study will also deal with other nanomaterials, synthesis, their performance and their stability under different environments.

Keywords: Organic, flexible and printed electronics / metallic nanowire/ transparent electrode

References:

[1] D. Langley, G.Giusti, C. Mayousse, C. Celle, D. Bellet, J.-P. Simonato, Nanotechnology, 24, 452001 (2013)
[2] C. Mayousse, C. Celle, A. Carella , J.-P. Simonato, Nano Research, 7(3) : 315-324 (2014)
[3] Celle, C., Mayousse, C., Moreau, E., Basti, H., Carella, A., & Simonato, J.-P. Nano Research, 5(6), 427–433. (2012)
[4] Mayousse, C., Celle, C., Moreau, E., Mainguet, J.-F., Carella, A., & Simonato, J.-P. (2013) 24(21), 215501.

On Low Temperature Photoluminescence of Zinc-blende CdS and Au-CdS Nanocrystals

Shital V. Kahane,[1] V. Sudarsan,[2] Shailaja Mahamuni[1]
[1]Department of Physics, SP Pune University, Ganeshkhind, Pune, India
[2]Chemistry Division, Mod Labs, Bhabha Atomic Research Centre, Trombay, Mumbai, India

Abstract: Optical studies are carried out on chemically prepared (Lin *et al*., 2006) zinc-blende CdS and core-shell Au-CdS nanocrystals (NCs) using low temperature photoluminescence (PL) spectroscopy. Contrary to the reported literature primarily discussing defect related emission in CdS, the enhancement in band edge photoluminescence intensity by 1.5 times is observed in Au-CdS core-shell NCs compared to bare CdS. Low temperature photoluminescence spectroscopic measurements reveal splitting of band edge luminescence into very sharp and narrow lines (Figure 1). PL features, as expected, clearly reveal red-shift with an increase in the temperature. Measured energy values of narrow lines fit well with the empirical Varshni equation (Hoang *et al*., 2006) revealing bulk like temperature dependence of the band gap and an intrinsic nature of CdS. The feature located at 2.96 eV (Fx), and having the highest intensity is attributed to the near band edge emission or free exciton. The feature 2.91 eV (difference of 50 meV) is due to optical phonon replica (Fx-LO) of free exciton while the one at 2.86 eV (difference of 100 meV) is Fx-2LO replica. Feature A (3.02 eV) represents the emission from second excited state ($1P_{3/2}$-$1p_e$) of CdS while B (3.10 eV) is the emission from third excited state ($1S_{1/2}$-$1s_e$) (Kim *et al.,* 2013). Shell of zinc-blende CdS on cubic Au NCs was formed. Core-shell Au-CdS NCs are studied with the aid of low temperature PL measurements. Emission from second ($1P_{3/2}$-$1p_e$) and third ($1S_{1/2}$-$1s_e$) excited state remains unaffected, while phonon replicas are perturbed in Au-CdS NCs due to change in lattice parameter along with electron-phonon interaction.

Keywords: Zinc-blende CdS nanocrystals, Au-CdS core shell nanocrystals, chemical method, low temperature photoluminescence, splitting of band edge emission, Varshni equation, optical phonons.

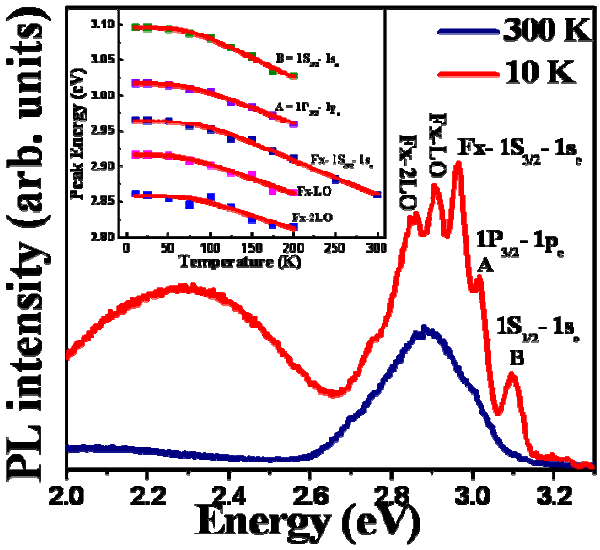

Figure 1: Room and low temperature (10 K) phototluminescnec spectra of CdS nanocrystals. Inset shows temperature dependence PL emission peaks of CdS QDs. Solid squares indicates experimental data while curve indicates calculated result using Varshni equation.

References:

Lin, H., Chen, Y., Wu, J., Wang, D., Chen, C. (2006) Carrier transfer induced photoluminescence change in metalsemiconductor core-shell nanostructures, *Appl. Phys. Lett.,* 88, 161911-3.

Hoang, T., Titova, L., Jackson, H., Smith, L., Yarrison-Rice, J., Lensch, J., Lauhon, L. (2006) Temperature dependent photoluminescence of single CdS nanowires, *Appl. Phys. Lett.*, 89, 123123-3.

Kim, Y., Jang, D. (2013) Direct observation of valence band splitting using room temperature photoluminescence of CdSnhollow submicrospheres *Chem. Commun.,* 49, 8940-8942.

Session IV : Nanotech in Life Sciences & Medicine

The Early History of Nanocarriers as Drug Delivery Systems

Allan S. Hoffman

Bioengineering Department, University of Washington, Seattle, WA 98195 USA

Abstract: Nano-scale drug delivery systems (NDDS) are very special. NDDS are special because they are usually targeted to specific cells in specific tissues or organs. They are also special because most of them are focused on cancer chemotherapy. The size scale of these NDDS ranges from a few nm up to several hundreds of nm. In recent years, the number of FDA-approved NDDS has grown significantly.

There are many different types of NDDS, and many of them may also be PEGylated (conjugated with PEG molecules). **Table 1** lists the different nanocarriers. Most of these systems are composed of water-soluble and hydrophilic synthetic polymers, although they may be combined with hydrophobic components. The liposome is a different kind of nanocarrier; it is a small aqueous vesicle enclosed by a lipid bilayer made of phospholipids.

Table 1: Examples of Nanocarriers

Liposomes
PEGylated Liposomes
Polymer-drug Conjugates
PEGylated Drugs
Antibody-drug Conjugates
Polycation-nucleic acid Complexes (Lipoplexes and Polyplexes)
PEGylated Lipoplexes and Polyplexes
Polymeric Micelles
PEGylated Polymeric Micelles
Albumin-drug Nanoparticles
Drug NPs, Nanogels, Nanotubes
Dendrimer-drug Nanoparticles
Polymersomes

A nanocarrier may be conjugated to a drug, (eg, PEGylation) or it may be complexed ionically to a drug of the opposite charge, (eg polyplexes and lipoplexes) or it may physically entrap a drug (eg, liposomes). It may also be biologically ("actively") targeted to specific cells using monoclonal antibodies or peptide ligands, or physically ("passively") targeted to tumors via leaky blood vessels (EPR effect). The molecular weight (or size) and biodegradability of the nanocarrier are both very important to its eventual clearance from the body after delivering the drug.

There are three key discoveries / developments that have helped to bring NDDS into the clinic. They are 1) PEGylation 2) active targeting and 3) passive targetting (EPR). The history of these technologies will be described, and this talk will continue as a review of the early history of the types of nanocarriers listed in Table 1.

Historical References:

- A Abuchowski, JR McCoy, MC Palczuk, T van Es, and FF Davis, (1976) J Biol Chem 252, 3582-3586.
- FF Davis, (2002) Adv Drug Del Revs, 54, 457-458.
- AD Bangham, RW Horne, AM Glauert, JT Dingle, JA Lucy, (1962) Nature 196 , 952–955.
- Y Barenholz, (2012) J Contr Rel, 160, 117-134.
- P Couvreur, B. Kante, M. Roland, and P. Speiser, (1979) J Pharm Sci, 68, 1521–1524.
- JJ Marty, RC Oppenheim, and P Speiser, (1978) Pharm Acta Helv, 53, 17-23.
- R Duncan, (2009) Adv. Drug Del. Rev., 61, 1131–1148.
- G Wu and C Wu, (1987) J Biol Chem, 262, 4429-4432.
- A Harada and K Kataoka, (1995) Macromol, 28, 5294-5299.
- J Kreuter, Pharm Acta Helv, (1983) 58, 196.
- Y Matsumura and H Maeda, (1986) Cancer Research, 46, 6387-5392.
- MD Pierschbacher and E Ruoslahti, (1984) Nature, 309, 30-3.
- H Ringsdorf, (1975) J Pol Sci, Symposium 51, 135-153.
- AS Hoffman, (2008) *J Contr Rel*, 132, 153–163.

Nanomedicine for molecular imaging: interest of bimodality in preclinical studies

B-T Doan,[1] G. Ramniceanu,[1] J. Seguin[1], M. Bessodes[1], D. Scherman[1], F. Lux[2], O. Tillement[2], N. Mignet[1*]
[1]Unité des Technologies Chimiques et Biologiques, Department of Nanomedicine for imaging and therapy, Université Paris Descartes, CNRS UMR8258, INSERM U1022, Chimie Paristech, Paris, France
2 Institut Lumière Matière, Université Lyon 1, France
*Nathalie.Mignet@parisdescartes.fr

Abstract: Nanoparticles have potentials in imaging in particular as enhanced contrast agent for techniques with low sensitivity, such as MRI or Ultrasound imaging. They also have a role to play in bimodal imaging. Indeed, thanks to their possible functionalization, various chromophores or contrastophor can be linked to the surface or within the core to provide new properties or to allow obtaining a high number of valuable informations in preclinical studies, while highly reducing the number of animals. Few examples of the interest of bimodal agents in preclinical evaluation will be shown. First, the conception of a protein scaffold targeting the Asialoglycoprotein receptor (Chaumet-Riffaud et al. 2010). A radioactive label provide quantitative informations on the liver function while an optical label will provide evidence on the specificity of the targeting. A second example will concern tumor imaging thanks to integrin targeting. A bimodal silica based scaffold allowed to approach within the same experiments the kinetic by optical imaging and a relative quantitative estimation using MRI (Ramniceanu et al. 2015). Another example from gaz microbubbles. These agents enhanced the ultrasound imaging signal however to follow the excipients and approach their elimination profile, optical imaging can provide some additional informations (Manta et al. 2015).

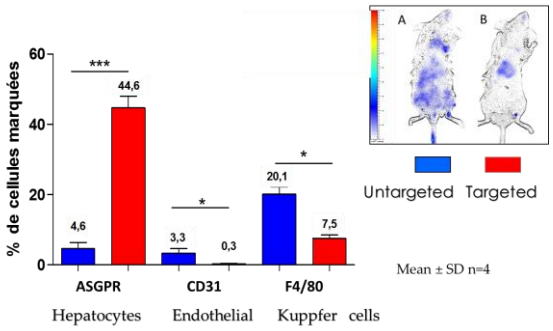

Figure 1: Figure illustrating the distribution of targeted and untargeted protein. The radioactive labeling gives the quantitative informations on the amount of the tracer in the various organs. The addition of an optical tracer will allow demonstrating the specificity of the signal at the cellular level, using immunohistology or flow cytometry on preleved organs and dissected cells.

Keywords: Targeted nanoparticles, Integrin targeting, Asialoglycoprotein receptor, Silica nanoparticles (AGUIX), protein scaffold, molecular imaging, MRI, optical imaging.

References:

Chaumet-Riffaud, P., Martinez-Duncker, I., Marty, A. L., Richard, C., Prigent, A., Moati, F., Sarda-Mantel, L., Scherman, D., Bessodes, M., and Mignet, N., (2010) Synthesis and application of lactosylated, 99mTc chelating albumin for measurement of liver function, *Bioconjug Chem 21*, 589-96.

Ramniceanu G., Doan, B-T., Seguin, J, Lux, F., Tillement, O., Mignet, N. (2015) Bimodal imaging ot integrin targeting in a colon tumor mice model, *in preparation.*

Manta, S., Renault, G., (2015) Pharmacokinetic of positively charged and pegylated microbubbles by dual modality: ultrasound and optical imaging, *In preparation.*

Nanotechnologies for the treatment of severe diseases

Patrick COUVREUR
University of Paris-Sud, Institut Galien, UMR CNRS 8612, 5 rue J-B Clément F-92296
Chatenay-Malabry - France

Even if new molecules are discovered to treat severe diseases, the clinical use and efficacy of conventional chemotherapeutics is hampered by the following limitations: (i) drug resistance at the tissue level due to physiological barriers (non cellular based mechanisms), (ii) drug resistance at the cellular level (cellular mechanisms), and (iii) non specific distribution, biotransformation and rapid clearance of the drugs in the body. It is therefore of importance to develop nanodevices able to overcome these limitations.

This will be illustrated by two nanomedicine platform developed in the laboratory: the design of biodegradable nanoparticles loaded with doxorubicin for the treatment of the resistant hepatocarcinoma (a nanomedicine currently in phase III clinical trials) (1) and the “squalenoylation” (2), a technology that takes advantage of squalene's dynamically folded conformation to link this natural and biocompatible lipid to anticancer (3), antimicrobial (4) or neuroprotective compounds (5) in order to achieve the spontaneous formation of nanoassemblies (100–300 nm) in water, without the aid of surfactants. The design of “multidrug” nanoparticles combining in the same nanodevice chemotherapy and imaging (ie., “nanotheranostics”) or various drugs with complementary biological targets will be also discussed (6). Finally, it will be shown that the construction of nanodevices sensitive to endogenous (ie. pH, ionic strenght, enzymes etc.) or exogenous (ie., magnetic or electric field, light, ultrasounds etc.) stimuli may allow the spatio-temporal controlled delivery of drugs and overcome resistance to current treatments (7).

References

1. L. Barraud et al., J. Hepatology, 42, 736-743 (2005)
2. P. Couvreur et al., Nano Letters, 6, 2544-2548 (2006)
3. A. Maksimenko et al., Proceedings of the National Academy of Science, 111 (2) E217-E226 (2014)
4. N. Semiramoth et al., ACS Nano, 6, 3820-3831 (2012)
5. A. Gaudin et al., Nature Nanotechnology, 9, 1054-1063 (2014)
6. A. Maksimenko et al., ACS Nano, 8, 2018-2032 (2014)
7. S. Mura et al., Nature Materials, 12, 991-1003 (2013)

Emergence of Ag_2S Qunatum Dots and Their Magnetic Hybrid Structures as New Promising Bionanomaterials

H. Yagci Acar[123], I. Hocaoglu[1], D. Asik[1], C. Grandfils[4], Isaac Ojea-Jimenez[5], François Rossi[5]
[1]*Koc University, Graduate School of Materials Science and Engineering, Istanbul, Turkey*
[2]*Koc University, Department of Chemistry, Istanbul, Turkey*
[3]*KUYTAM, Koc University, Surface Science and Technology Center, Istanbul, Turkey*
[4]*Centre Interfacultaire des Biomatériaux (CEIB), University of Liège (ULg), Chemistry Institute, B6c, Allée du 6 août, 11, B-4000 Liège (Sart-Tilman), Belgium*
[5]*Institute of Health and Consumer Protection, European Commission Joint Research Center, Ispra-21027, Italy*

Abstract: Nanobiomaterials offer nano-solutions for bioapplications. Nanoparticles are very important class of nanomaterials that are utilized biotechnology and medicine. Best example that found commercialization is probably superpramagnetic iron oxide used as contrast agent. A unique class of nanoparticles is semiconductor quantum dots that provide size tunable emission behavior in addition to broad absorabce and narrow emission window. This offers a trenedous advantage as a fluorophore, yet, QDs can be taioled as drug/gene delivery vehicles with suitable coatings and receptor specific tags. Yet, most of the studied QDs are cadmium based and pose significant toxicity. There are many attempts such as core/shell structures, PEGylation etc to decrease the toxicity yet, excitation in the UV and emission in the visible region pose significant limitation to the relatively unsafe exciatation wavelengths, limited penetration depth and autofluoresence of the tissue in the visible region. Therefore, QDs that can be excited in the visible and emitting in the NIR region is highly desirable. Ag_2S with bandgap energy of 0.9 eV and very high cytocompatability offer a great potential in realization of practical QDs for medicine and biotechnology(Hocaoglu *et al, 2012;* Hocaoglu *et al, 2014).*

Aqueous synthesis of Ag_2S QDs that emit in the medical window (700-900nm) with different surface coatings and the highest quantum yields reported in the literature (6 to 150 % with respect to NIR Dye) will be discussed. Cytototoxicity and hemocompatability of such particles will also be discussed showing their great potential as biomaterials. These NIR QDs will be demonstrated as strong optical imaging agents in the in vitro cell studies (Figure 1).

Another group of desired and popular nanomaterials are multifunctional hybrid nanoparticles. We will discuss the synthesis of magnetic and luminescent hybrid nanoparticles (Figure 2) composed of SPIONs and Ag_2S NIRQDs, discuss their hemo and cyctocompatibility as well as their optical and magnetic properties.

Overall, we will demonstrate Ag2S with variety of surface coatings, with good optical properties and very good cyto/hemocompatability as a new QD platform for medicine and bioapplications.

Keywords: Ag_2S, Near-infrared, magnetic, luminescent, hybrid, hemocompatibility, cytocompatibility, optical imaging

Figure 1: Cellular uptake and localization of Ag_2S QDs by NIH/3T3 mouse fibroblast cells (200 µg/mL QD, 24h incubation). (A) Fluorescence, (B) Transmission and (C) Overlay channels of confocal micrograph. The scale bar represents 20 µm. (excitation at 532nm)

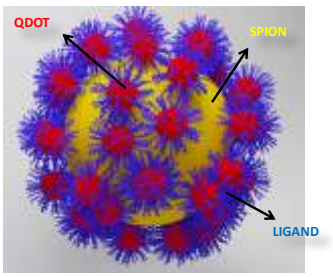

Figure 2: Schematic representation of a hybrid nanoparticle.

References:

Hocaoglu, N. Cizmeciyan, R. Erdem, C. Ozen, A. Kurt, A. Sennaroglu, H. Yagci Acar*, "Development of Highly luminescent and Cytocompatible Near-IR-Emitting Aqueous Ag_2S Quantum Dots", *Journal of Materials Chemistry*, **22,** 14674-14681, 2012.

Hocaoglu, F. Demir, O. Birer, A. Kiraz, C. Sevrin, C. Grandfils, H. Yagci Acar, " Emission Tunable, Cyto/hemocompatable, Near-IR-Emitting Ag_2S Quantum Dots by Aqueous Decomposition of DMSA", *Nanoscale*, 2014,**6**, 11921-11931.

Stimuli-sensitive combination nanopreparations of siRNA and chemotherapeutic drugs to treat multidrug resistant cancer

Vladimir Torchilin
Center for Pharmaceutical Biotechnology and Nanomedicine, Northeastern University, Boston, MA 02115, USA

Abstract: Tumor therapy, especially in the case of multidrug resistant cancers, could be significantly enhanced by using siRNA down-regulating the production of proteins, which are involved in cancer cell resistance, such as Pgp or survivin. Even better response could be achieved is such siRNA could be delivered to tumors together with chemotherapeutic agent. This task is complicated by low stability of siRNA in biological surrounding. Thus, the delivery system should simultaneously protect siRNA from degradation. We have developed several types of lipid-core polymeric micelles based on PEG-phospholipid or PEI-phospholipid conjugates, which are biologically inert, demonstrate prolonged circulation in the blood and can firmly bind non-modified or reversibly-modified siRNA. Additionally, these nanopreparations can be loaded into their lipidic core with poorly water soluble chemotherapeutic agents, such as paclitaxel or camptothecin. In experiments with cancer cell monolayers, cancer cell 3D spheroids, and in animals with implanted tumors, it was shown that such co-loaded preparations can significantly down-regulate target proteins in cancer cells, enhance drug activity, and reverse multidrug resistance.

In order to specifically unload such nanopreparations inside tumors, we made them sensitive to local tumor-specific stimuli, such as lowered pH, hypoxia, or overexpressed certain enzymes, such as matrix metalloproteases. Using pH-, hypoxia-, or MMP2-sensitive bonds between different components of nanopreparations co-loaded with siRNA and drugs, we were able to make the systems specifically delivering biologically active agents in tumors, which resulted in significantly improved therapeutic response.

References

- Torchilin VP. Multifunctional, stimuli-sensitive nanoparticulate systems for drug delivery. Nat Rev Drug Discov. 2014;13(11):813-27
- Jhaveri A, Deshpande P, Torchilin V. Stimuli-sensitive nanopreparations for combination cancer therapy. J Control Release. 2014;190:352-70.
- Zhu L, Perche F, Wang T, Torchilin VP. Matrix metalloproteinase 2-sensitive multifunctional polymeric micelles for tumor-specific co-delivery of siRNA and hydrophobic drugs. Biomaterials. 2014;35(13):4213-22.
- Zhu L, Wang T, Perche F, Taigind A, Torchilin VP. Enhanced anticancer activity of nanopreparation containing an MMP2-sensitive PEG-drug conjugate and cell-penetrating moiety. Proc Natl Acad Sci U S A. 2013;110(42):17047-52.
- Perche F, Biswas S, Wang T, Zhu L, Torchilin VP. Hypoxia-targeted siRNA delivery. Angew Chem Int Ed Engl. 2014;53(13):3362-6

Nanocapsules of perfluorooctyl bromide as theranostic agents: formulation and in vivo evaluation

T. Boissenot,[1] B. Larrat,[2] A. Bordat,[1] P. Calleja-Gonzalez,[1] G. Giacalone,[1] L. Mousnier,[1] E. Fattal,[1] N. Tsapis,[1]
[1]Univ Paris-Sud, Institut Galien Paris-Sud, UMR CNRS 8612, LabEX LERMIT,
Faculté de Pharmacie, Châtenay-Malabry, France
[2] CEA/DSV/I2BM/Neurospin, Gif-sur-Yvette, France

Abstract: The need to detect cancer at its early stages, as well as, to deliver chemotherapy to targeted site motivates many researchers to build theranostic platforms which combine diagnostic and therapy. Among imaging modalities, ultrasonography and MRI are widely available, non invasive and complement each other. Both techniques often require the use of contrast agents.
We have developed nanocapsules of perfluorooctyl bromide as dual contrast agent for both imaging modalities. The soft, amorphous polymer shell provides echogenicity, while the high-density perfluorinated liquid core allows detection by ^{19}F MRI. We have used a shell of poly(lactide-co-glycolide) (PLGA) since this polymer is biodegradable, biocompatible and can be loaded with drugs. These capsules were shown to be efficient *in vitro* as contrast agents for both ^{19} F MRI and ultrasonography. In addition, for *in vivo* applications a poly(ethyleneglycol) (PEG) coating promotes stability and prolonged circulation. Being stealth, nanocapsule can accumulate passively into implanted tumors by the EPR effect.A anti-cancer drug paclitaxel was encapsulated within the PEGylated capsules with the goal of triggering its release upon the application of ultrasound. Capsule surface can also be decorated with RGD moieties to actively target integrins overexpressed on tumor neovessels. We will present nanocapsule formulation and characterization, and will show promising in vivo results obtained for both ultrasonography and ^{19} F MRI, as well as the efficacy of the formulation on xenograft tumors in mice.

Keywords: Nanocapsules, Theranostic, ^{19}F MRI, ultrasonography.

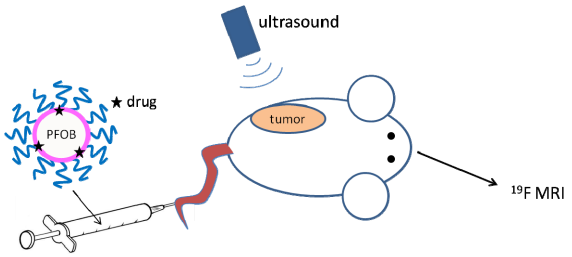

Figure 1: Schematic representation of our objectives

References:

Pisani, E., Tsapis, N., Galaz, B., Santin, M., Berti, R., Taulier, N., Kurtisovski, E., Lucidarme, O., Ourevitch, M., Doan, B.T., Beloeil, J.C.; Gillet, B., Urbach, W., Bridal, S.L., Fattal, E. (2008) Perfluorooctyl Bromide Polymeric Capsules as Dual Contrast Agents for Ultrasonography and Magnetic Resonance Imaging, *Adv. Funct. Mat.,* 18(19), 2963-2971.

Diou, O., Tsapis, N., Giraudeau, C., Valette, J., Gueutin, C., Bourasset, F., Zanna, S., Vauthier, C., Fattal ,E. (2012) Long-circulating perfluorooctyl bromide nanocapsules for tumor imaging by ^{19}FMRI, *Biomaterials*, 33(22), 5593-5602.

Diou, O., Fattal, E., Delplace, V., Mackiewicz, N., Nicolas, J., Mériaux, S., Valette, J., Robic, C., Tsapis N. (2014) RGD decoration of PEGylated polyester nanocapsules of perfluorooctyl bromide for tumor imaging: influence of pre or post-functionalization on capsule morphology. *Eur. J. Pharm. Biopharm.*, 87(1), 170-177.

.

Formulation and evaluation of Rosuvastatin Calcium-loaded solid lipid nanoparticles

Kruti A. Dhoranwala[1], Pranav Shah[1,*], Shailesh Shah[1]
[1]Maliba Pharmacy College, Uka Tarsadia University,
Gopal Vidyanagar, Bardoli-Mahuva Road, Dist: Surat, Gujarat, India

Abstract: Rosuvastatin Calcium is an anti-hyperlipidemic drug which is sparingly soluble in water and possesses low oral bioavailability (20%). The aim of this investigation was to design and evaluate solid lipid nanoparticles (SLNs) of Rosuvastatin Calcium. The SLNs were prepared by high pressure homogenization using glyceryl monostearate as lipid carrier and poloxamer-188 as surfactant. A two factor, three level (3^2) full factorial design was applied to study the effect of independent variables i.e. amount of glyceryl monostearate (Y1) and % concentration of poloxamer-188 (Y2) on dependent variables i.e. Particle size and % entrapment efficiency (%EE). Particles size, %Entrapment efficiency, zeta potential, drug content, *in vitro* drug release and particles morphology are evaluated for SLNs. The experimental results of optimized batch (batch A10) exhibited particle size 529.6nm with PDI of 0.506. %EE was found to be 48.90 ± 1.85% and drug release was found to be 97.41 ± 1.48 % in 36 hours. Accelerated stability studies showed no significant change in the mean particle size and %EE after storage at 40°C/75% RH for the period of three months. The developed formulation may be absorbed via the lymphatic route thereby avoiding hepatic first pass metabolism. This may lead to improvement in bioavailability, reduction dose and dose related side effects etc.

.

Figure 1: Figure illustrating solid lipid nanoparticle

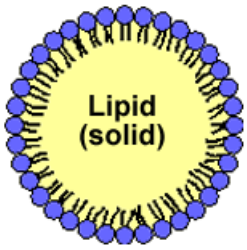

References:

Porter, C.J.H., Charman, W.N. (2001), Intestinal lymphatic drug uptake: an update. *Adv. Drug Deliv. Rev.* 50, 61–80.

Charman, W.N., Porter, C.J.H. (1996), Lipophilic prodrugs designed for intestinal lymphatic transport. *Adv. Drug Deliv. Rev.* 19, 149–169.

Das, S., Ng Wai, N.K., Kanaujia, P., Kim, S., Tan, R.B. (2011), Formulation design, preparation and physicochemical characterizations of solid lipid nanoparticles containing a hydrophobic drug: effects of process variables. *Colloids and Surfaces B: Biointerfaces.* 88(1), 483-489.

Chalikwar, S.S., Belgamwar, V., Talele, V., Surana, S.J., Patil, M.(2012), Formulation and evaluation of Nimodipine-loaded solid lipid nanoparticles delivered via lymphatic transport system. *Colloids and Surfaces B: Biointerfaces*. 97, 109– 116.

A blueprint for modified siRNA-cationic peptide dendrimer-based therapy of Type 2 diabetes through *'PTPN1'* gene silencing

G. Kokil[1*], T. Pereira[2], R. Veedu[3,4], J. Wengel[4], G. Ramm[2], H.S. Parekh[1]
[1]School of Pharmacy, The University of Queensland, Brisbane, Australia
[2] The Hepatic Fibrosis Group, QIMR Berghofer Medical Research Institute, Brisbane, Australia
[3]School of Chemistry and Molecular Biosciences, The University of Queensland, Brisbane, Australia
[4]Nucleic Acid Centre, University of Southern Denmark, Campusvej 55, Odense M 5230 Denmark

Abstract: In 2014, the WHO reported that over 347 million individuals worldwide were affected by diabetes mellitus (DM), of which T2DM accounted for ~90% of all cases. The T2DM-affected population mainly comprises individuals where insulin resistance (IR) and pancreatic β-cell dysfunction are the key drivers of the disease, with a complex interrelationship responsible for initiating its pathogenesis. Genome-wide association studies have identified >40 susceptible genes closely associated with T2DM. One of those genes, *PTPN1* encodes for tyrosine phosphatase-1B (PTP-1B) protein. Documented evidence firmly supports the role of PTP-1B in T2DM and obesity through negative regulation of insulin as well as leptin signalling (Koren *et al.*; 2007). At the genetic, molecular, biochemical and physiological levels, PTP-1B has proven beyond reasonable doubt to be a valid target for correcting the key underlying cause of T2DM i.e. insulin resistance. To-date the pursuit of traditional drug-based therapies against PTP-1B have been plagued with issues of "drugability"; this has meant that siRNA-based approaches (through PTP-1B silencing) are a highly attractive therapeutic proposition towards combating insulin resistance in T2DM patients.

Of the various nucleic acid modifications reported, sugar modifications resulting in locked nucleic acids (LNA) and unlocked nucleic acids (UNA) (Figure 1) have gained considerable interest (Veedu *et al.*; 2010). Our current research demonstrates superior stability (**Figure 2**) and gene silencing ability of LNA/UNA-modified siRNA towards the PTP-1B gene, over their unmodified counterparts (**Figure 3b**). Furthermore, effective delivery of these modified siRNAs using hybrid chemical carrier systems (vesicular and non-vesicular) is also under investigation (Shah *et al.*; 2014). Unmodified siRNA specific to rat PTP-1B (commercially sourced) and LNA/UNA-modified siRNA's were synthesized and annealed. Studies were performed on a rat hepatoma cell line (H4IIE) with PTP-1B expression and insulin resistance induced using tumor necrosis factor-α (TNF-α), palmitic acid and tunicamycin. We used RT-PCR and western blot to assess PTP-1B mRNA and protein levels, and a significant (30%) increase in PTP-1B mRNA expression was observed at 180 min post-incubation with TNF-α (**Figure 3a**). Our finding indicate that insulin resistance is being invoked, and forms the basis of evaluating the effects of our modified siRNA delivered using chemical carrier systems. It is expected that modified siRNA-based therapeutics when combined with appropriately engineered carrier systems will create the next generation of gene-based treatment strategies for T2DM.

Keywords: T2DM, PTP1B, siRNA, LNA, dendrimer.

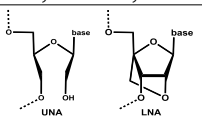

Figure 1: Chemical structure of LNA and UNA.

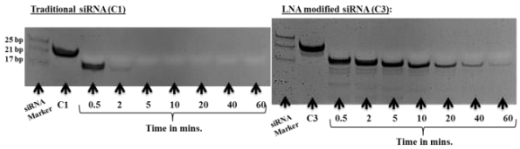

Figure 2: Stability of LNA modified siRNA against its traditional counterpart incubated in 1 mg/mL RNase A @ 37 °C.

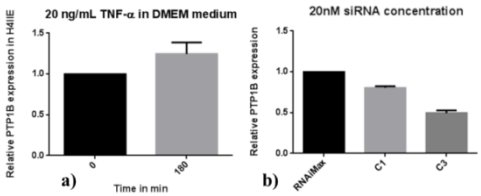

Figure 3: a) Relative expression of PTP1B mRNA in H4IIE cell line incubated with 20 ng/mL of TNF-α for 3 hr. **b)** Comparative gene silencing efficiency between C1 and C3.

References:

Koren, S., Fantus, I. G. (2007), Inhibition of the protein tyrosine phosphatase PTP1B: potential therapy for obesity, insulin resistance and type-2 diabetes mellitus, *Best Pract. Res. Clin. Endocrinol. Metab.*, 21(4), 621-40.

Veedu, R. N., Wengel, J. (2010), Locked nucleic acids: promising nucleic acid analogs for therapeutic applications, *Chem. Biodiversity*, 7, 536-42.

Shah, N., Parekh, H., Steptoe R. (2014), Asymmetric peptide dendrimers are effective linkers for antibody-mediated delivery of diverse payloads to B Cells in vitro and in vivo, *Pharm. Res.*, 31(11), 3150-60.

Instability of Carbon Nanoparticles Interacting with Lipid Bilayers

D. Baowan,[1*] B.J. Cox,[2] J.M. Hill[2]
[1]Department of Mathematics, Faculty of Science, Mahidol University, Rama VI Rd., Bangkok, Thailand
[2]Nanomechanics Group, School of Mathemtaical Sciences, University of Adelaide, Adelaide, SA, Australia

Abstract: Due to the large number of possible applications of nanoparticles in cosmetic and medical products, the possible hazards of nanoparticles in the human body are a major concern. A worst-case scenario is that nanoparticles might cause health issues such as skin damage or even induce diseases such as cancer. As a first step in the study of the toxicity of nanoparticles, we investigate here the energy behaviour of three distinct carbon nanoparticles interacting with a lipid bilayer; namely nanotubes, nanocones and fullerenes. We determine the energy behaviour of these nanoparticles interacting with a lipid bilayer using the Lennard-Jones potential together with the continuous approximation, which assumes that a discrete atomic structure can be replaced by a surface of uniform atomic density. First, the equilibrium spacing between the two layers of a bilayer is predicted to be 3.36Å. For an assumed circular hole in the lipid bilayer, a relation for the molecular interaction energy is determined, involving the circular hole radius, and the perpendicular distance of the nanoparticle from the hole (Fiugre 1). For each nanoparticle, the relation between the minimum energy location and the hole radius b is found, and for example, for the fullerene, for $b > 6.81$Å, the nanoparticle relocates from the surface of the bilayer to the interior, and as the hole radius increases further moves to the centre of the bilayer, remaining there for increasing hole radii. When the system has no external forces, the nanoparticle will not penetrate through the lipid bilayer but rather remains encased between the two layers.

Keywords: mathematical model, Lennard-Jones potential function, continuous approximation, lipid bilayer, carbon nanoparticles.

References:

Colvin, V.L. (2003) The potential environmental impact of engineered nanomaterials, *Nat. Biotechnol.*, 21, 1166-1170.

Thomas, T., Thomas, K., Sadrieh, N., Savage, N., Adair, P., Bronaugh, R. (2006) Research strategies for safety evaluation of nanomaterials, part VII: Evaluating consumer exposure to nanoscale materials, *Toxicol Sci*. 91, 14-19.

Baowan, D., Cox, B.J., Hill, J.M. (2012) Instability of C_{60} fullerene interacting with lipid bilayer, *J. Mol. Model*, 18, 549-557.

Baowan, D., Peuschel, H., Kraegeloh, A., Helms, V. (2013) Energetic of liposomes encapsulating silica nanoparticle, *J. Mol. Model*, 19, 2459-2472.

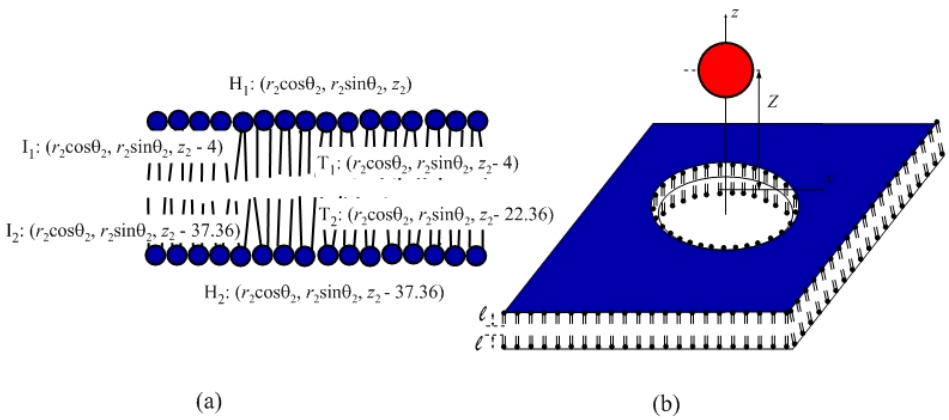

Figure 1: Model for (a) structural dimensions of lipid bilayer where H_1 and H_2 represent upper and lower head groups, I_1 and I_2 denote upper and lower intermediate layers and T_1 and T_2 are upper and lower tail groups and (b) a hole in bilayer.

Targeting of asymmetric amino acid-based cationic dendrimers to caveolae

P. Rewatkar*, H. S. Parekh, M. Parat
School of Pharmacy, Pharmacy Australia Centre of Excellence, The University of Queensland, Australia

Abstract: Caveolae are plasma membrane subdomains ranging from 50-100 nm in diameter. They are abundant in many mammalian cells and are rich in lipids such as glycosphingolipids and cholesterol. They participate in endocytosis, transcytosis, and numerous signal transduction events (Parat; 2009). Membrane proteins of the caveolin family, and cytoplasmic proteins of the cavin family are essential for caveola formation. Gene disruption of either caveolin-1 or cavin-1 (also known as PTRF i.e. polymerase I and transcript release factor) results in caveola deficiency.

Cationic, amino acid-based dendrimers (Parekh *et al.;* 2011) are highly branched chemically-derived gene-vectors developed to transport cargo with therapeutic potential such as pharmacological agents or genetic material, across the plasma membrane. We prepared a panel of cationic dendrimers and investigated whether they use caveola as a route of internalization. We further evaluated the role of cationic charge density and head group chemistry in promoting dendrimer endocytosis via caveolae. Cell-based studies were performed using wild type (WT) or caveolin-1 gene-disrupted i.e. caveola-deficient (KO) mouse embryo fibroblasts. Cells were exposed to biotinylated peptide dendrimers for 12h and internalization was detected after fixation, using Cy3-streptavadin and fluorescence imaging. Nuclei were stained using 4',6-diamidino-2-phenylindole (DAPI). The number of dendrimer-containing red cells per field was counted and expressed as % of the total number of cells per field. Furthermore, to confirm internalization of dendrimers, time dependent kinetics of internalization was performed.

There was a statistically significant difference in entry of cationic dendrimers between WT and KO cells. Internalization was not abolished in KO cells, suggesting that other routes of entry also participate in dendrimer endocytosis **(Figure 1)**. We further unveiled differences between dendrimers with varying charge density and head group chemistry **(Figure 2)**. In addition, significantly increased uptake for WT cells was observed in a time course study at the earliest time point (1 min) for a 16+ charged Arginine dendrimer.

Our results show, using a molecular approach, that (i) caveolae mediate at least in part the entry of cationic dendrimers in cells and (ii) dendrimer structure can be modified to promote caveolar endocytosis.

Keywords: Caveolae, endocytosis, drug delivery, dendrimer

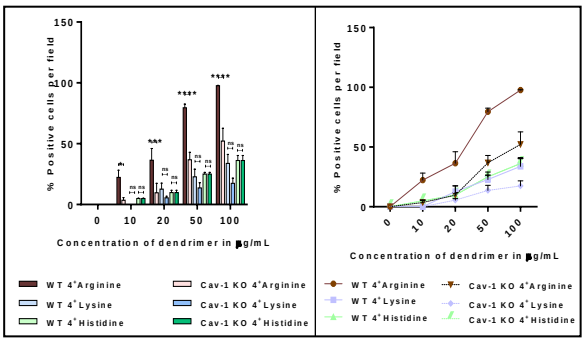

Figure 1: Caveolae participate in binding and internalization of tested dendrimers
Fibroblasts isolated from wild type or caveolin-1 knockout mice were tested for biotinylated 4 charged cationic dendrimer binding and internalization. The cells were treated with dendrimers for 12 h. Results are reported as % positive cells per field. N=3 separate experiments. *p<0.05, **p<0.01, ***p<0.001, ****p<0.0001.

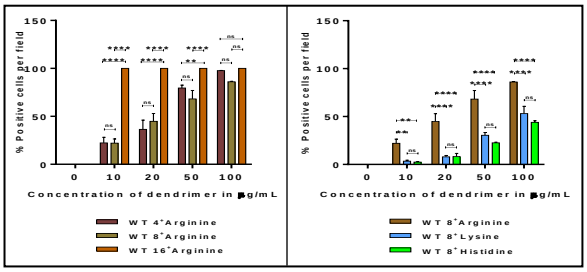

Figure 2: Dendrimer head group, charge density and generation modulate cellular entry
Fibroblasts isolated from wild type mice were tested for biotinylated 4, 8 and 16 charged cationic dendrimer surface binding and internalization. The cells were treated with dendrimers for 12 h. Results are reported as % positive cells per field. N=3 separate experiments. **p<0.01, ****p<0.0001, ns, not significant.

References:

Parat, M. (2009) The biology of caveolae: achievements and perspectives, *Int. Rev. Cell. Mol. Biol.*, 273, 117-162.

Shah, N., Steptoe R., Parekh H. (2011) Low-generation asymmetric dendrimers exhibit minimal toxicity and effectively complex DNA, *J. Pept. Sci.*, 17(6), 470-8.

Polymeric self-assemblies for photodynamic therapy: a critical approach

U. Till[1,2,3], L. Gibot[1], B. Moukarzel[2], A.F. Mingotaud[2*], M.P. Rols[1], M. Gaucher[3], F. Violleau[3], C. Chassenieux[4] and P. Vicendo[2]

[1] Equipe de Biophysique Cellulaire, IPBS-CNRS UMR 5089, 205 Route de Narbonne, BP 64182, 31077 Toulouse Cedex, France;

[2] Université de Toulouse; UPS/CNRS; IMRCP, 118 route de Narbonne, F-31062, Toulouse Cedex 9, France;

[3] Université de Toulouse, Institut National Polytechnique de Toulouse – Ecole d'Ingénieurs de Purpan, Département Sciences Agronomiques et Agroalimentaires, UPSP/DGER 115, 75 voie du TOEC, BP 57611, F-31076 Toulouse Cedex 03, France;

[4] LUNAM Université, Université du Maine, IMMM UMR CNRS 6283 Département PCI, Avenue Olivier Messiaen, 72085 Le Mans Cedex 09, France

Abstract: The work presented here suggests a new approach in the critical development of polymeric nanovectors for photodynamic therapy (PDT) against cancer. Whereas hundreds of studies quickly jump forward from formation of self-assemblies to biological application without having a thorough examination of the vector solution, we suggest having a parallel assessment of formation/characterization of the nanovectors and biological activity. This is possible by first using a careful physical chemistry characterization of the vectors by both batch techniques (light and neutron scattering, electron microscopy, atomic force microscopy) and Asymmetrical Flow Field-Flow Fractionation (AsFlFFF) coupled to adequate detectors (refractometry, light scattering). This enables us to have a deep knowledge of the solution of the vectors regarding purity, size and zeta potential. The case of both polymeric micelles and polymersomes will be presented, using poly(ethyleneoxide-b-ε-caprolactone), poly(ethyleneoxide-b-D,L-lactide) and poly(ethyleneoxide-b-styrene). Self-assemblies exhibiting size range of 20-200 nm will be shown.

The work clearly shows the possible presence of different populations of nanovectors in some cases. For each new vector, its ability to carry a photosensitizer (Pheophorbide a) for PDT is examined. The activity in PDT either in 2D and 3D cell culture will be presented and compared on different batches, in link with the purity analysis. Here again, it becomes highly recommended to develop a critical approach considering in vitro analyses, since differences of efficiencies are clearly observed depending on the vectors and the 2D or 3D culture type.

Keywords: Polymeric micelles, self-assemblies, Asymmetrical Flow Field-Flow Fractionation, light scattering, photodynamic therapy, spheroids

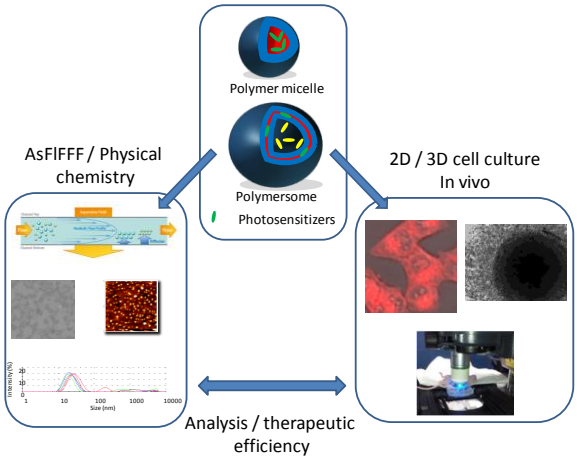

Figure 1: Process of nanovectors development for PDT. The therapeutic efficiency is systematically linked to a thorough characterization of the vector solution, including its purity.

References:

L. Gibot, A. Lemelle, U. Till, B. Moukarzel, A.-F. Mingotaud, V. Pimienta, P. Saint-Aguet, M.-P. Rols, M. Gaucher, F. Violleau, C. Chassenieux, P. Vicendo (2014) "Polymeric micelles encapsulating photosensitizer: structure/ photodynamic therapy efficiency relation" *Biomacromolecules*, 15(4), 1443-1455

U. Till, M. Gaucher-Delmas, P. Saint-Aguet, G. Hamon, J.-D. Marty, C. Chassenieux, B. Payré, D. Goudounèche, A.-F. Mingotaud, F. Violleau (2014) "Asymmetrical Flow Field-Flow Fractionation with Multi-Angle Light Scattering and Quasi Elastic Light Scattering for characterization of polymersomes: comparison with classical techniques" *Analytical and Bioanalytical Chemistry*, 406(30), 7841-7853

Biodegradable Nanoconstructs for Pharmacology: Development of Biomimetic Systems for Drug Delivery and Pathogen Blockage

T. Tennikova,[1,2,*] V. Korzhikov,[1,2] I. Guryanov,[1,2] V. Sharoyko,[1] E. Vlakh [1,2]
[1]Institute of Chemistry, Laboratory of Biomedical Chemistry, Saint-Petersburg State University, Saint-Petersburg, Russian Federation
[2]Institute of Macromolecular Compounds, Russian Academy of Sciences, Saint-Petersburg, Russian Federation

Abstract: The urgent task of modern care of public health is developing completely brand-new, "smart" drug formulations that can provide a superior therapeutic efficacy with a minimum of side effects. Moreover, the research in this direction might able to achieve the unexpected decisions when choosing therapy for various, including widespread and extremely dangerous, diseases. In particular, biodegradable nanocontainers with stipulated physical and chemical (particle size, size distribution, degradation rate of chemical bonds defined by a structure of polymer) characteristics of nanoparticles, as well as biological (biomimetic) properties of their surface, which smoothly invaded in the natural processes of human body, enable to provide such results.

The aim of presented research is design and synthesis of special biologically functionalized nanoconstructs based on nanoparticles of various chemical nature, including those modified with biofunctional gold nanoclusters, which have been recently developed in our team. The methods of biological functionalization of nanoparticle surface for addressed drug delivery to specified biological targets with properties of blocking the pathogens of various origins to facilitate their rapid clearance from the body by phagocytosis are developed.

The proposed nanoconstructs and means of their medical application certainly can be transferred to the pharmaceutical industry.

Reducing the risk of side effects due to the accurately designated molecular targets and reduction of time for therapy determine the social significance of the results and may have significant economic benefits.

Application of the unique information of the multifunctional Biobank SPbSU and bioinformatics tools for searching of specific sequences of natural biopolymers in order to select the optimal complementary pairs and *in silico* modeling of highly specific intermolecular interactions allowed functionalization of nanoconstructs to develop the new personalized approaches to diagnosis and treatment of various diseases (hepatitis C, diabetes of 1 and LADA types, AIDS, different types of cancer, etc.).

Keywords: biodegradable polymer nanoparticles, surface biofunctionalization, biomodels, ligand-research interactions, biomimetics, drug delivery, pathogen blockage, socially significant deseases

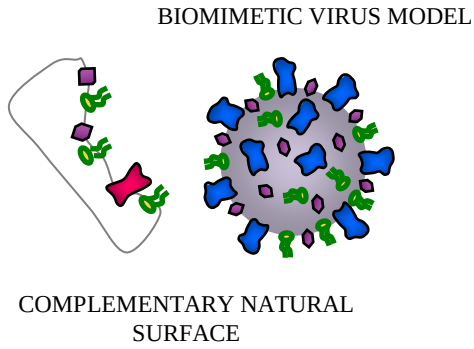

Figure 1: Figure illustrating the algorithm of nanoconstructs based on biodegradable drug-containing (inside) nanoparticles provided by multifunctional ligands both to address the carriers to corresponding natural receptors and to bind the pathogens in a bloodstream.

References:

Korzhikov, V., Litvinchuk, E., Tennikova T.B. (2015) Different approaches for surface modification of PLA nanoparticles with polyvinylsaccharides, *Bioconjugate Chem.*, In Press

Guryanov, I, Sharoyko, V., Tennikova T., (2015) Receptor-ligand interactions, their functions in biological systems and practical application in biomedicine, REVIEW ARTICLE, *ChemBioChem*, In Press.

Korzhikov, V., Polyakov, D., Shavlovsky, M., Tennikova, T. (2015) Directed phagocytosis of PLA-nanoparticles with functionalized surface, *ChemMedChem*, In Press

Korzhikov, V., Roeker, S., Vlakh, E., Kasper, C., Tennikova, T. (2008) Synthesis of multifunctional polysaccharide containing controllable amount of biospecific ligands, *Bioconjugate Chem.*, 19, 617-625.

This research is financially supported by Russian Scientific Foundation (grant #14-50-00069).

Evaluation of Gelled Oil Nanoparticles as New Vehicles for Drug Delivery

Baptiste Martin,[1] Fabien. Brouillet,[2] Sophie Franceschi-Messant,[1] Emile Perez[1]
1- *Laboratoire des Interactions Moléculaires et Réactivité Photochimique (IMRCP), UMR 5623 CNRS, Université Paul Sabatier, 31062 Toulouse, France*
2- *Ecole Nationale Supérieure des Ingénieurs en Arts Chimiques et Technologiques (CIRIMAT-ENSIACET) 4 allée Emile Monso - BP44362, 31030 Toulouse cedex 4 – France*

**Corresponding author.* Email address: martin@chimie.ups-tlse.fr

Abstract: In recent years, a growing interest has emerged in the development of semi-solid colloidal careers for the delivery of water-insoluble drugs. Solid lipid Nanoparticles (SLN) and Nanostructured Lipid Careers (NLC) are example of such systems. Their preparation consists of a hot emulsification over the melting temperature of the solid lipids and freezing at room temperature to form an aqueous dispersion of solid particles. However, crystallization occurring in the lipid matrix leads to significant drug expulsion during storage, and the formed objects also present a low biodisponibility because of a solid in solid encapsulation.

As an alternative to SLN, we propose the use of an original family of organogel nanoparticles, obtained through a smilar process. Organogels are semi-solid materials in which an organic solvent (e.g., vegetable oil) is entrapped in the three-dimensional fibrous network formed by self-aggregation of a low molecular mass organic gelator (12-Hydroxystearic acid). The preparation process of the gelled oil nanoparticles is based on the sol-gel phase transition of the organogel obtained by hot emulsification (T°>T°gel) in presence of an aqueuous solution of stabilizing agent (Polyvinylalcohol 80), leading to a stable semi-solid dispersion after cooling (T°<T°gel), (Figure 1).

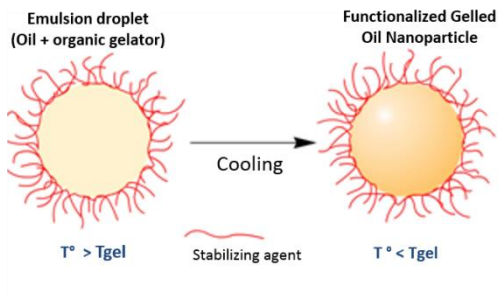

Figure 1: Concept of the elaboration of the gelled nanoparticle aqueous dispersion.

In a first part, we will present the preparation and the characterization of the aqueous dispersions of the gelled oil particles. Then we will evaluate the encapsulation properties and delivery of the prepared systems using different drugs and models, varying their hydrophobicity and pKa (indomethacin, ibuprofen, ketoconazole, efavirenz, Nile red).

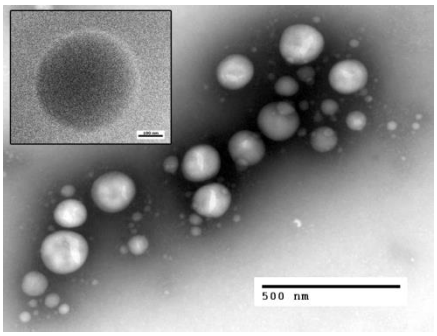

Figure 2: TEM micrograph showing organogel particles made of soybean oil and HSA as gelator

Encapsulaton efficiency studies showed an impressive drug loading of 99% and no significant drug leakage during storage.

In vitro dialysis release experiments showed different kinetic profiles in comparison with control buffer solutions, underlying the importance of the drug solubility in the gelled oil and its possible ionisation in water. The results obtained have enabled us to evaluate the drug delivery capabilities of these gelled particles and their possible use in different pharmaceutical pathways (oral or skin).

Keywords: Organogels, Gelled Nanoparticle, Aqueous dispersion, Drug delivery

References:

Kirilov P., Lukyanova L., Fransechi-Messant S., Perier V., Perez E., Rico-Lattes i (2008) A new type of colloidal dispersions based on nanoparticles of gelled oil, *Colloids Surf., B.*, 328, 1-7

Boudier A., Kirilov P., Franceschi-Messant S., Belkhelfa H., Hadioui L., Roques C., Perez E., Rico-Lattes I. (2010), Evaluation of stabilized gelled soya bean oil nanoparticles as new hydrophobic reservoirs, *J. Microencapsul*., 27, 682-692.

Bio-inspired catanionic vesicles as drug delivery systems: Study of the cell internalisation pathways

P. Castagnos[1], C. Mauroy[1,2], J. Teissié[2], I. Rico-Lattes[1], A. C. Tedesco[3], M. P. Rols[2], M. Blanzat[1*]
[1]IMRCP, UMR CNRS 5623, Université P. Sabatier, 118 route de Narbonne, 31062 Toulouse, France
[2]IPBS, UMR 5089 CNRS, Université Paul Sabatier, 205 route de Narbonne, 31077 Toulouse, France
[3]Departamento de Quımica, Laboratorio de Fotobiologia e Fotomedicina, FFCLRP, Universidade de São Paulo, Ribeirão Preto, Brazil

Abstract: The cell membrane is a selective barrier that regulates the transfers of drugs into the cell. During the last forty years, a number of drug delivery systems have been developed to control drug release profile, absorption and distribution, with a view to improving efficacy and safety. The direct release of active molecules inside the cytoplasm is often considered as the most efficient and the safest mechanism for drug delivery. This promising strategy, which can proceed through membrane fusion between suitable carriers and the cell membrane, is not straightforward and it has raised important research and developments for the design of synthetic delivery systems.

Among drug delivery systems, catanionic vesicles, made of cationic and anionic surfactants, have appeared as powerful candidates for pharmaceutical applications because they are relatively cheap and easy to use (Soussan *et al.*, 2009). Using labelled vesicles made of a sugar-based catanionic surfactant, the work reported here aims at exploring the mechanisms of their internalisation into cells. The study was performed on different cell types using confocal laser scanning microscopy and flow cytometry, and confirmed the contribution of endocytotic and fusion processes with the plasma membranes of cells (Boudier *et al.*, 2011; Mauroy *et al.*, 2014). We confirmed the ability of sugar-derived catanionic vesicles to fuse with lipidic membranes using pure lipidic systems (Mauroy et al. 2012).

Finally, to validate the great potential of catanionic vesicles for further applications as drug delivery systems, examples of use of this catanionic system will be presented (Castagnos *et al.*, 2014).

Keywords: drug delivery, catanionic vesicles, membrane fusion, endocytosis, glycolipids, biomedical applications.

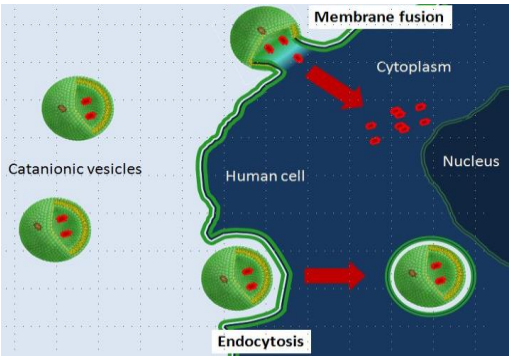

Figure 1: Figure illustrating the versatile cellular uptake mediated by catanionic vesicles

References:

E. Soussan, S. Cassel, M. Blanzat, I. Rico-Lattes (2009), Drug delivery by soft matter: Matrix and vesicular carriers. *Angew. Chem. Int. Ed.*, 48, 274-288.

A. Boudier, P. Castagnos, E. Soussan, G. Beaune, H. Belkhelfa, C. Menager, V. Cabuil, L. Haddioui, C. Roques, I. Rico-Lattes, M. Blanzat (2011), Polyvalent catanionic vesicles: Exploring the drug delivery mechanisms. *Int. J. Pharm.*, 403(1-2), 230-236.

C. Mauroy, P. Castagnos, J. Orio, M.C. Blache, I. Rico-Lattes, J. Teissie, M.P. Rols, M. Blanzat (2014), Versatile cellular uptake mediated by catanionic vesicles: simultaneous spontaneous membrane fusion and endocytosis. *Molecular Pharmaceutics*, DOI: 10.1021/mp500458f.

C. Mauroy, P. Castagnos, M.C. Blache, J. Teissie, I. Rico-Lattes, M.P. Rols, M. Blanzat (2012), Interaction between GUVs and catanionic nanocontainers: new insight into spontaneous membrane fusion. *Chem. Commun.*, 48 (53), 6648-6650.

P. Castagnos, M.P. Siqueira-Moura, P. Leme-Goto, E. Perez, S. Franceschi, I. Rico-Lattes, A.C. Tedesco, M. Blanzat (2014), Catanionic vesicles charged with chloroaluminium phthalocyanine for topical photodynamic therapy. In vitro phototoxicity towards human carcinoma and melanoma cell lines. *RSC Adv.*, 4, 39372-39377.

Novel Nano-Carriers for Controlled Pulmonary Drug Delivery

I. M. El-Sherbiny[1,*], H. D. C. Smyth[2]
[1]Zewail City of Science and Technology, Center for Materials Science, 6th October City, 12588 Giza, Egypt;
[2]Division of Pharmaceutics, College of Pharmacy, University of Texas at Austin, Austin, TX 78712, USA
Presenting author: ielsherbiny@zewailcity.edu.eg

Abstract: A substantial body of research has focused recently onto pulmonary drug delivery as a well-accepted treatment for many lung diseases. This work was aiming to develop and *in-vitro* evaluate new series of carriers for controlled pulmonary drug delivery. The developed carriers systems combine the benefits of nanoparticles (NPs) and respirable/swellable microparticles while avoiding their shortcomings. The carriers are based on PEG-grafted-chitosan (PEG-g-CS) copolymer and ionotropically crosslinked with sodium tripolyphosphate (STPP) and/or Sodium hyaluronate (HAs) in form of hydrogel NPs. The drug-loaded hydrogel NPs were then used to develop respirable/swellable 2-5 microns size microparticles (MPs) through controlled spray drying of an aqueous suspension of the NPs and lactose as excipient. The particle size was determined by laser diffraction and dynamic light scattering. Surface morphology was investigated by AFM and SEM. An *in-vitro* aerosolization study was performed with the aid of a next generation impactor, NGI. Dynamic swelling, *in-vitro* biodegradation, particle's density, and moisture contents were also determined. In addition, *in-vitro* release profile of the loaded drug was investigated in simulated body fluids. The *in-vivo* investigation of the encapsulated drug was also performed using the insufflation method. The average sizes of the prepared crosslinked PEG-g-CS NPs and the MPs were found to be 83.2±2.4 nm and 4.1±0.03 µm, respectively. The NPs-MPs carriers showed high swelling within few minutes, low aerodynamic density (0.2±0.03 g/cc), moisture content of 4.1-9.0%, good *in-vitro* biodegradation, high drug loading capacity exceeding 93%, and a promising sustained drug release both *in-vitro* and *in-vivo*. In conclusion, the developed NPs-MPs systems are very promising and could be utilized as potential carriers for sustained delivery of various drugs to the lung.

Keywords: Nanoparticles, microparticles, swellable, lung, pulmonary, drug delivery

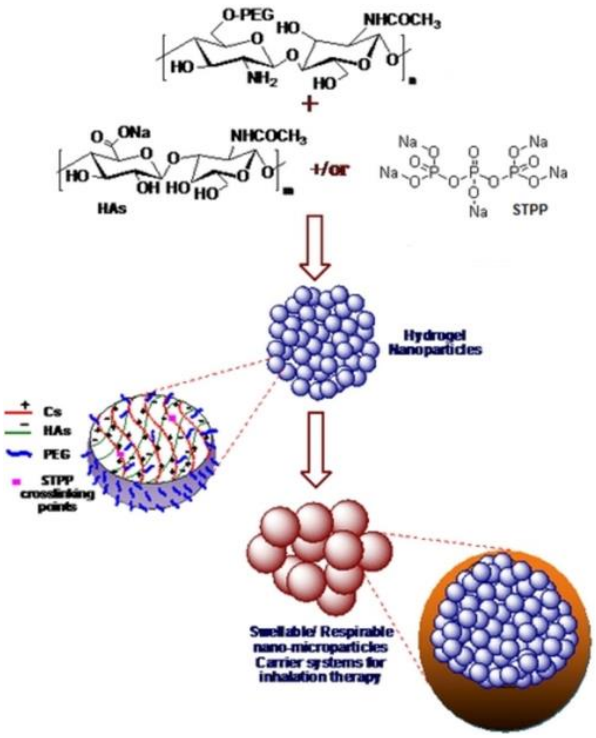

Figure 1. An illustration of the developed polymeric NPs-in-MPs as pulmonary carrier systems.

Effect of Nanotube Materials on Encapsulation of Lysozyme

N. Thamwattana[1*]
[1]School of Mathematics and Applied Statistics, University of Wollongong,Wollongong, NSW 2522, Australia

Abstract: Lysozyme is an enzyme often used in biochemical and pharmaceutical engineering and food industries as an antibacterial agent. Immobilization of lysozyme by encapsulating in a nanotube has much interest due to the enhanced property in ambient condition. Experimentally, various types of nanotubes have been proposed as a host for lysozyme. Here, we model the interaction between lysozyme and various types of nanotubes in order to compare the effectiveness of different nanotube materials. Based on the van der Waals interaction, which we model using the Lennard-Jones potential and a continuum approach, we find that different types of nanotubes have very little effect on the minimum radius (b_0) that will allow the acceptance of the lysozyme molecule and also on the critical radius (b_{cr}) that will maximise the interaction among the lysozyme molecule and the tube. However, while carbon, silicon, boron nitride and silicon carbide nanotubes possess similar energy profiles, the energy level of titania nanotube is much smaller than other tubes. This lower level of energy implies that to expel the lysozyme from the titania nanotube would require less amount of energy compared to other types of nanotubes. Based on this result, it may be said that titania nanotube has more potential for the delivery of lysozyme molecule. Since b_0 and b_{cr} for the titania nanotube are the smallest, less amount of material is needed to create the titania nanotube that allow the acceptance of the lysozyme or to generate the tube that gives optimum interaction. Following titania nanotube are carbon, boron nitride, silicon carbide and silicon nanotubes, ranging in order of the smallest to the largest b_0 and b_{cr}. For a titania nanotube, we also consider the electrostatic effect on its interaction with a lysozyme molecule by using the Coulomb potential. We find that the electrostatic energy dominates the interaction between the lysozyme and the titania nanotube. When the net charge of lysozyme is positive, we find that the smallest radius of the titania nanotube that will accept the lysozyme molecule is b_0 = 18.55 Å, noting that the radius of the lysozyme is 18.54 Å. This reduces from b_0 = 21 Å when we only consider the van der Waals energy. For the case when the lysozyme has negative net charge, the lysozyme molecule cannot enter the titania nanotube as the repulsive energy dominates. Results presented here can be extended to guide experiments to determine appropriate type of nanotube materials for effective molecular storage.

Keywords: Boron nitride nanotubes, carbon nanotubes, silicon nanotubes, silicon carbide nanotubes, titania nanotubes, lysozyme, Lennard-Jones potential, Coulomb potential, continuum approach

Structure-directing star-shaped block copolymers: Supra-molecular vesicles for the delivery of anticancer drugs

Chuan Yang[1], Shao Qiong Liu[1], Shrinivas Venkataraman[1], Shu Jun Gao[1], Xin Tian Chia[1, 2], James L. Hedrick[3], and Yi Yan Yang[1,*]

[1]Institute of Bioengineering and Nanotechnology, 31 Biopolis Way, The Nanos, #04-01, Singapore 138669

[2]School of Biological Sciences, Nanyang Technological University, 60 Nanyang drive, Singapore 637551

[3]IBM Almaden Research Center, 650 Harry Road, San Jose, California 95120, USA

Abstract: Amphiphilic polycarbonate/PEG copolymer with a star-like architecture was designed to facilitate a unique supramolecular transformation of micelles to vesicles in aquous solution for the efficient delivery of anticancer drugs. The star-shaped amphipilic block copolymer was synthesized by initiating the ring-opening polymerization of trimethylene carbonate (TMC) from methyl cholate through a combination of metal-free organo-catalytic living ring-opening polymerization and post-polymerization chain-end derivatization strategies. Subsequently, the self-assembly of the star-like polymer in aqueous solution into nanosized vesicles for anti-cancer drug delivery was studied. DOX was physically encapsulated into vesicles by dialysis and drug loading level was significant (22.5% in weight) for DOX. Importantly, DOX-loaded nanoparticles self-assembled from the star-like copolymer exhibited greater kinetic stability and higher DOX loading capacity than micelles prepared from cholesterol-initiated diblock analogue. The advantageous disparity is believed to be due to the transformation of micelles (diblock copolymer) to vesicles (star-like block copolymer) that possess greater core space for drug loading as well as the ability of such supramolecular structures to encapsulate DOX. DOX-loaded vesicles effectively inhibited the proliferation of 4T1, MDA-MB-231 and BT-474 cells, with IC50 of 10, 1.5 and 1.0 mg/L, respectively. DOX-loaded vesicles injected into 4T1 tumor-bearing mice exhibited enhanced accumulation in tumor tissue due to the enhanced permeation and retention (EPR) effect. Importantly, DOX-loaded vesicles demonstrated greater tumor growth inhibition than free DOX without causing significant body weight loss. The unique ability of the star-like copolymer emanating from the methyl cholate core provided the requisite modification in the curvature to generate vesicles of high loading capacity for DOX with significant kinetic stability that have potential for use as an anti-cancer drug delivery carrier for cancer therapy.

Keywords: Star-like polycarbonate; Vesicles; Doxorubicin; Biodistribution; Anti-tumor activity.

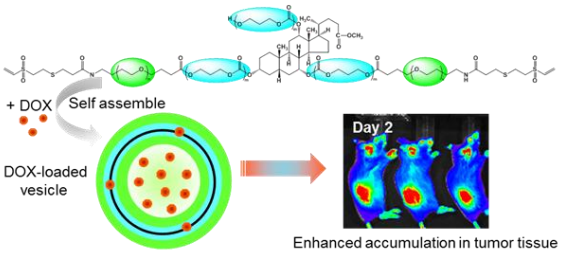

Figure 1: Star-like polycarbonate/PEG block copolymer has been synthesized and assembled into vesicles for anticancer drug delivery. When injected into 4T1 tumor-bearing mice, DOX-loaded vesicles demonstrated greater anti-tumor efficacy than free DOX.

References:

A.B.E. Attia, C. Yang, J.P.K. Tan, S.J. Gao, D.F. Williams, J.L. Hedrick, Y.Y. Yang, The effect of kinetic stability on biodistribution and anti-tumor efficacy of drug-loaded biodegradable polymeric micelles, Biomaterials 34 (2013) 3132-3140.

C. Yang, A.B.E. Attia, J.P.K. Tan, X.Y. Ke, S.J. Gao, J.L. Hedrick, Y.Y. Yang, The role of non-covalent interactions in anticancer drug loading and kinetic stability of polymeric micelles, Biomaterials 33 (2012) 2971-2979.

Tunable release of dendritic fullerene-1 modulated by an electric field across a nanochannel membrane

Giacomo Bruno[1,2,*], Thomas Geninatti[1,3,*], R. Lyle Hood[1] , Daniel Fine[1] , Giovanni Scorrano[1] , Jeffrey Schmulen[1] , Sharath Hosali[4] , Mauro Ferrari[1] , and Alessandro Grattoni[1]
[1]Nanomedicine Department, Houston Methodist Research Institute (HMRI), Houston, TX, USA
[2] Electronic Department, Politecnico di Torino, Turin, Italy
[3]College of Materials Science and Engineering, University of Chinese Academy of Sciences, Beijing, China
[4]Nanomedical System, Inc., Austin, TX, USA
*equal contribution

Abstract: Future progress in drug delivery technologies will require precise temporal and volumetric control of therapeutic release. Chronotherapies based on aligning treatment administration with circadian rhythms have been demonstrated as more effective for several chronic pathologies (Youan 2010), such as colorectal cancer (Li et al. 2013), rheumatoid arthritis (To et al. 2011), and hypertension (Hermida et al. 2011), among others. Here we present a silicon membrane with hundreds of thousands of nanochannels fabricated with sub-nanometer precision using sacrificial etching techniques. While no electric field was applied (configuration A in Fig. 1) zero order transport was observed across 5.7 nm nanochannel membranes. The temporal, reproducible control of the dendritic fullerene-1 (DF-1) was established by application of a low potential (1.5 V) across two platinum electrodes positioned on either side of the membranes (configuration B, Fig. 1). Conductance measurements were performed in order to demonstrate that the interruption was attributable to Ionic Concentration Polarization (ICP) at the interface between the membrane's micro- and nanochannels (Kim et al. 2009), even in concentrated solutions (≤ 1 M NaCl). Due to its low power consumption (100 nW), one envisioned goal of this technology is creation of an implantable and remotely controllable system for personalized, telemedical therapeutic administration.

Keywords: Nanochannel membrane, Controlled drug delivery, Chronotherapy, Active release, Ionic concentration polarization, Electrokinetic transport, Telemedicine, Personalized medicine.

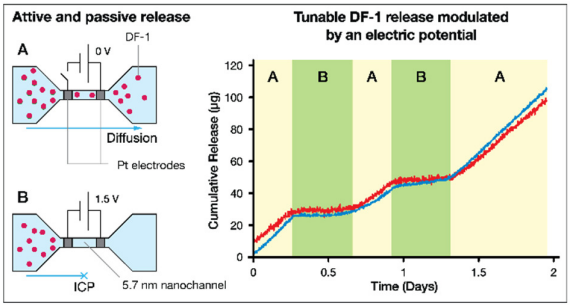

Figure 1: Figure illustrating two replicates of the cumulative release of dendritic fullerene-1 (DF-1) tuned by a passive release (configuration A) and an active release (configuration B) phase across a membrane containing hundreds of thousands 5.7 nm nanochannels.

References:

Hermida, R. C., D. E. Ayala, J. R. Fernandez, F. Portaluppi, F. Fabbian, and M. H. Smolensky. (2011). Circadian rhythms in blood pressure regulation and optimization of hypertension treatment with ACE inhibitor and ARB medications. Am J Hypertens 24 (4):383-391.

Kim, P., S. J. Kim, J. Han, and K. Y. Suh. (2009). Stabilization of ion concentration polarization using a heterogeneous nanoporous junction. Nano Lett 10 (1):16-23.

Li, X. M., A. Mohammad-Djafari, M. Dumitru, S. Dulong, E. Filipski, S. Siffroi-Fernandez, A. Mteyrek, F. Scaglione, C. Guettier, F. Delaunay, and F. Levi. (2013). A circadian clock transcription model for the personalization of cancer chronotherapy. Cancer Res 73 (24):7176-7188.

To, H., H. Yoshimatsu, M. Tomonari, H. Ida, T. Tsurumoto, Y. Tsuji, E. Sonemoto, N. Shimasaki, S. Koyanagi, H. Sasaki, I. Ieiri, S. Higuchi, A. Kawakami, Y. Ueki, and K. Eguchi. (2011). Methotrexate chronotherapy is effective against rheumatoid arthritis. Chronobiol Int 28 (3):267-274.

Youan, B. B. (2010). Chronopharmaceutical drug delivery systems: Hurdles, hype or hope? Adv Drug Deliv Rev 62 (9-10):898-903

Preparation of Hydrolysable Biocompatible Polymersomes for Drug Delivery

A.Azran-Gefen, H.Bianco-Peled
Department of Chemical Engineering, Technion-Israel Institute of Technology.

Abstract: The desire to understand molecular self-assembly and to explore potential applications motivates the study of self-assembly principles, theories, properties and structures of the assemblies. Block copolymer chains aggregate into various morphologies according to different contributions to the free energy of the system. The most common morphologies are spherical and cylindrical micelles, and polymeric vesicles, termed polymersomes. Polymersomes are hollow spheres with sizes ranging from tens of nanometres to tens of micrometres, typically having a hydrophobic wall and hydrophilic internal and external coronas. Polymersomes have been studied vastly in the last decade and new types of drug delivery systems based on their unique properties have been reported. Yet, only few studies dealt with biocompatible and biodegradable polymersomes. A better understanding of the formation mechanisms of polymersomes and of the relation between nanostructure and properties are still required. Therefore, in this work will investigate the self-assembly of block copolymer aggregates with emphasis on polymersomes. This research will deal with the formation of polymersomes from two types of biocompatible and biodegradable block copolymers, poly(ethylene oxide)-b-poly(ε-caprolactone) (PEO-b-PCL) and poly(ethylene oxide)-b-poly(lactic acid) (PEO-b-PLA). The study of the relation between aggregates morphology and preparation techniques include variation of experimental parameters and evaluating their effect on the formed structures. The main tools that used in the research are size and structure characterization using light and X-ray scattering techniques and electron microscopy. Further experiments would be conducted in order to explore the usage of the polymersomes carriers as drug delivery vehicles for three model drugs of different hydrophilicity. Three types of block copolymer aggregates have been produced and and characterization of structure has been conducted. In order to allow a rational design of polymersomes, insights into the formation and properties of biocompatible polymersome systems are needed. Therefore, the overall goal of this research is to establish a better understanding of biocompatible block copolymer systems with an emphasis on systems that lead to formation of polymersomes

Keywords: polymersomes, PEO-PCL, hydrolysis, drug delivery.

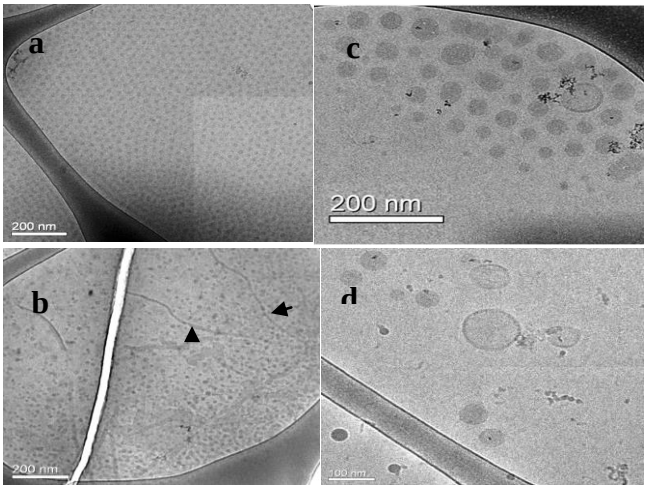

Figure 1: cryo-TEM micrographs of OLA2 (a) , OCL1(b) and OCL2 (c,d). The copolymers differ by their hydrophilic fraction,f

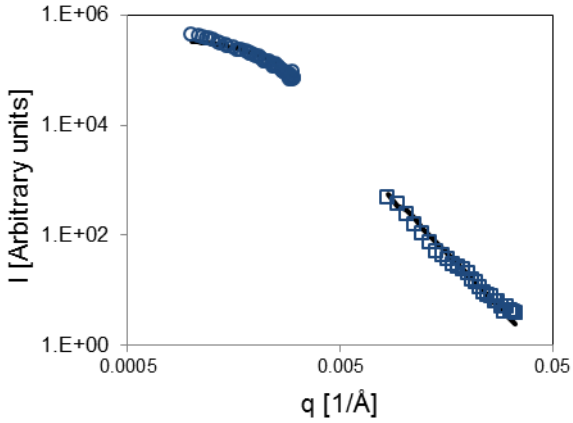

Figure 2: SLS (O) and SAXS (□) data for PEO-PCL 0.1%wt. The line represents the best fit model

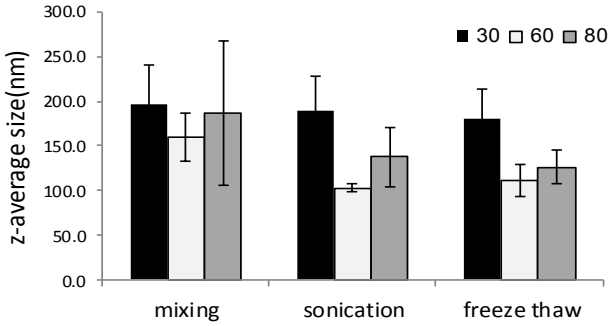

Figure 3:-average size of aggregate dispersions throughout the preparation process at different temperatures

Enhanced permeability througth the blood-brain barrier using targeted solid lipid nanoparticles for brain drug delivery

Joana Fontes Queiroz[1*], Ana Rute Neves[1], Sofia A. Costa Lima[1] and Salette Reis[1]

[1] UCIBIO, REQUI*M*TE, Department of Chemical Sciences, Faculty of Pharmacy, University of Porto, Portugal
[*]fontes_joana@hotmail.com

Abstract: The challenging of cross the blood-brain barrier (BBB) and reach the brain in a therapeutic concentration is the Holy Grail for effectively treat and cure brain diseases. In fact, more that 98% of all the potential new drug for the treatment of brain diseases are unable to cross the BBB. Here, nanotechnology can be an important tool to improve the specificity and permeability of drugs in the BBB. In this context the aim of this work was the development of a new delivery system to direct drugs to the brain, by functionalizing solid lipid nanoparticles (SLNs) with apolipoprotein E (ApoE) molecules, aiming to enhance their binding to low-density lipoprotein (LDL) receptors overexpressed on the BBB endothelial cells.

SLNs were successfully functionalized with Apo E, by two distinct strategies which took advantage of the strongest known non-covalent interaction between biotin and avidin. The functionalization of SLNs with ApoE was demonstrated by infrared spectra and fluorimetric assays. Transmission electron microscopy (TEM) images revealed spherical nanoparticles, dynamic light scattering (DLS) gave a Z-average under 200 nm, polydispersity index below 0.2 and zeta potential between -10 mV and -15 mV. A stability study revealed that these characteristics remained unchanged for at least 6 months. In vitro cytotoxic effects were evaluated by MTT and LDH assays in the hCMEC/D3 cell line, a human BBB model, and revealed no toxicity up to 1.5 mg/ml of formulation solid amount for 4 hour of incubation. The enhanced permeability of functionalized SLNs was evaluated in transwell devices cultured with hCMEC/D3 monolayers and it was found a 1.5-fold increase in the permeability of functionalized SLNs when compared with non-functionalized ones.

The different molecular mechanisms of endocytosis and transcytosis processes were also studied in order to clarify the transport pathways of the nanoparticles through the BBB. It was used flow cytometry system (FCS), confocal laser scanning microscopy (CLSM) and fluorimetric assays with tracers and different pathway inhibitors. The transport of SLNs across the hCMEC/D3 monolayer was found through a transcellular but not a paracellular route. Functionalized SLNs exhibited higher intracellular uptake compared with non-functionalized ones and were found to enter cells through a specific clathrin-mediated mechanism, related to the expression of LDL receptors on BBB.

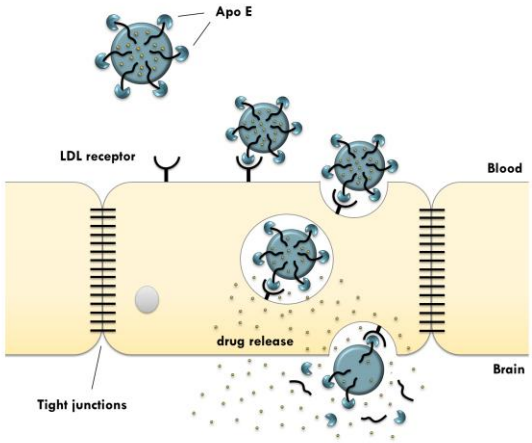

Figure 1: Schematic representation of the proposed mechanism of Apo E - functionalized SLNsuptake in brain (not to scale).

These novel ApoE-functionalized SLNs resulted in dynamic stable systems capable of being used for an improved and specific brain delivery of drugs through the BBB.

Keywords: Blood-brain barrier, drug-delivery, nanotechnology, solid lipid nanoparticles, functionalization, apolipoprotein E.

Acknowledgments: This work received financial support from the European Union (FEDER funds through COMPETE) and National Funds (FCT, Fundação para a Ciência e Tecnologia) through project Pest-C/EQB/LA0006/2013. The work also received financial support from the European Union (FEDER funds) under the framework of QREN through Project NORTE-07-0124-FEDER-000067. To all financing sources the authors are greatly indebted.

Design of Magnetic Molecularly Imprinted Polymer for Controlled Release of Doxorubicin under Alternative Magnetic Field.

N. Griffete,[1*] J. Fresnais,[1] A. Bée[1], C. Ménager[1]
[1]Sorbonne Universités, UPMC, University Paris 06, UMR CNRS 8234, PHENIX, Paris, France

Abstract: Magnetic nanoparticles (MNPs) have attracted considerable attention for magnetic targeting and hyperthermia applications owing to their ability to generate heat when exposed to an alternative magnetic field (AMF) without penetration depth limit. Novel magnetic materials for therapeutic agents release based on thermosensitive polymers or vesicles have been developed. In this case, the approach was to induce an increase of permeability of the vector by heat dissipation under AMF excitation. Another way to release drug is to use hyperthermia to break bond between superparamagnetic iron oxide nanoparticles and the target in presence of oscillating magnetic fields. Recently, multifunctional ligands linked to iron oxide nanoparticles took benefits from local heating of nanoparticle's surface to release a fluorophore on demand. Our approach is motivated by these last developments, i.e. to use local heating as the key parameter to trigger drug release.
We synthesised an innovative magnetic delivery nanodevice for targeted cancer therapy showing active control over drug release by using hyperthermia effects. Our material, wich combines the drug controlled release ability of non thermosensitive Molecularly Imprinted Polymers (MIP) with magnetic properties of iron oxide nanoparticles, allows the control release of doxorubicine.

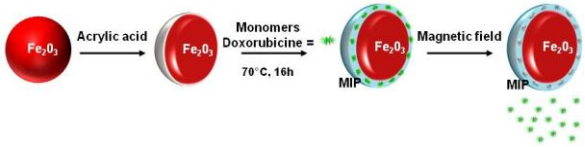

Scheme 1. Multistep synthesis of Fe_2O_3@DOX-MIP via a subsequent grafting of an acrylic acid compound and the growth of the polymer at 60°C. By applying an AMF, the doxorubicin is released.

Upon AMF exposure, the bonds between the MIP and the doxorubicin are broken and the molecule is released without any significant heating of the medium. These materials offer great promise for the doxorubicin release under alternating magnetic field but moreover we think that this approach can be expanded to other polymers or molecules. Using Magnetic molecularly imprinted polymers for drug delivery under AMF is a major advance in the development of multifunctional targeted drug delivery technologies and may become important theranostic tools in nanomedicines for in vitro and in vivo applications.

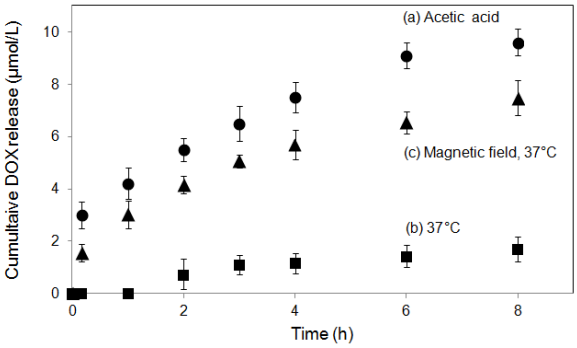

Figure 1: Influence of an AMF on the release kinetics of Fe_2O_3@DOX-MIP nanoparticles at (a) after acidic treatment, (b) 37°C without magnetic field and; (c) under alternative magnetic field (335 kHz, 5A), 37°C in µmol/L.

Keywords: hybrid nanomaterials, hyperthermia, alternative magnetic field, molecularly imprinted polymer, controlled release, biomedical applications.

References:

N'Guyen, T. T. T., Duong, H. T. T., Basuki, J., Montembault, V., Pascual, S., Guibert, C., Fresnais, J., Boyer, C., Whittaker, M. R., Davis, T. P., Fontaine, L. (2013) Functional Iron Oxide Magnetic Nanoparticles with Hyperthermia-Induced Drug Release Ability by Using a Combination of Orthogonal Click Reactions, *Angew. Chem. Int. Ed.*, 52, 14152-14156.

Griffete, N., Li, H., Lamouri, A., Redeuilh, C., Chen, K., Dong, C. Z., Nowak, S., Ammar, S., Mangeney C. (2012), Magnetic nanocrystals coated by molecularly imprinted polymers for the recognition of bisphenol A, *J. Mater. Chem.*, 22, 1807-1811.

Béalle, G., Lartigue, L., Wilhelm, C., Ravaux, J., Gazeau, F., Podor, R., Carrière, D., Ménager, C. (2014), *Phys. Chem. Chem. Phys.*, 16, 4077-4081.

BioConjugated Gold Nanoparticles for Enhaced Delivery and Cellular Uptakes

.

K. Rahme,[1,2,3*] J. Guo,[4] C. M. O'Driscoll,[4] J. D. Holmes[2,3]

[1] Department of Sciences, Faculty of Natural and Applied Science, Notre Dame University (Louaize), Zouk Mosbeh, Lebanon

[2] Materials Chemistry and Analysis Group, Department of Chemistry and the Tyndall National Institute, University College Cork, Cork, Ireland

[3]Centre for Research on Adaptive Nanostructures and Nanodevices (CRANN), Trinity College Dublin, Dublin 2, Ireland

[4] Pharmacodelivery group, School of Pharmacy, University College Cork, Cork, Ireland

Abstract: Gold nanoparticles (Au NPs) have demonstrated promising properties for enhanced cellular interaction including; size and shape dependent optical properties originated from the surface plasmon resonance band, a low cytotoxicity and an ease of bioconjuguation (Khlebtsov et al; 2010). Moreover, the nanoscale nature of Au NPs provides opportunities to interact with biomolecules (i.e. antibodies, nucleotides, peptides, proteins) and living cells. Therefore, Au NPs have received considerable attention for a wide range of applications in optoelectronics, diagnostics, thermal therapy, drug and gene delivery and have contributed to the advancement of bionanotechnology (Tiwari et al; 2011; Alkilany et al; 2011). A key challenge to applications of Au NPs in drug delivery is *in vivo* instability as unmodified Au NPs are subject to aggregation in the physiological environments prior to arrival at the site of action. Attachment of neutral polymers such as polyethylene glycol (PEG) has been shown to increase the biological stability of NPs. However, attachment of PEG can also dramatically decease the cellular uptake of NPs (Pozzi et al; 2014). To overcome this issue, PEGylated Au NPs can be conjugated with bioactive targeting ligands to facilitate site-specific delivery via ligand-receptor mediated endocytosis. In this study proteins (ApoE, BSA and Transferrin) were grafted onto Au NPs through an ethylene glycol linker. Transferrin (Tf) was shown to enhance cellular uptake of Au NPs relative to untargeted Au NPs (Figure 1). In addition, in this presentation we will also show that cationic AuNPs were synthesised by conjugation of L-cysteine methyl ester hydrochloride and large branched polyethylenimine. These NPs also have potential for enhanced cellular uptake and siRNA delivery.

Keywords: gold nanoparticles, polyethylene glycol, protein, drug delivery, cellular uptake, biomedical applications.

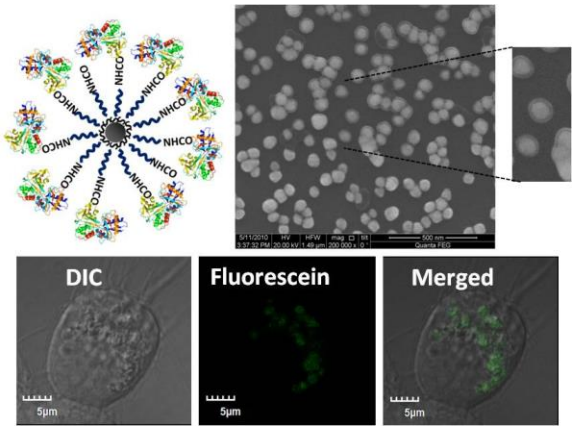

Figure 1: Schematic illustrating the final nanparticle structure with an ethylene glycol and protein coating (up left), SEM image showing the nanopartilces surrounded with an organic layer (up right). Intracellular distribution of fluorescein-labelled AuNPs-Tf in prostate cancer (PC3) cells following 24h post-transfection (lower images). These TEM images, left to right represented Differential interference contrast (DIC), fluorescein, and merged images of DIC and fluorescein.

References:

Khlebtsov, N.G., Dykman L.A. Optical properties and biomedical applications of plasmonic nanoparticles (2010) *J.Quant. Spectrosc. Ra.* 111, 1–35.

Tiwari, P. M., Vig, K., Dennis, V. A. Shree R., Singh S. R. (2011) Functionalized Gold Nanoparticles and Their Biomedical Applications *Nanomaterials, 1*, 31-63.

Alkilany, A. M, Murphy, C. J. (2011) Toxicity and cellular uptake of gold nanoparticles: what we have learned so far? *J. Nanopart. Res*., 12, 2313–2333.

Pozzi. D., Lagana. A., et al. (2014) Effect of polyethyleneglycol (PEG) chain length on the bio–nano-interactions between PEGylated lipid nanoparticles and biological fluids: from nanostructure to uptake in cancer cells, *Nanoscale*, 6, 2782-2792.

Prednisolone-loaded pH-sensitive liposomes as an active targeting strategy for rheumatoid arthritis

Virgínia M. Gouveia[1*], Sofia Lima[1], Cláudia Nunes[1] and Salette Reis[1]
[1]ICETA/UCIBIO/REQUIMTE, Department of Chemical Sciences, Faculty of Pharmacy, University of Porto, Portugal
[*]virginia.mgouveia@gmail.com

Abstract: Rheumatoid arthritis (RA) is a chronic systemic inflammatory and autoimmune disease mainly characterized by the progressive inflammation of the synovial tissue of the body joints, destruction of cartilage and further bone erosion. Currently available treatment options include non-steroidal anti-inflammatory drugs, glucocorticoids and disease modifying anti-rheumatic drugs, either used as monotherapy or in combination therapy.

In this project we focus on the use of glucocorticoids, namely prednisolone, which is one of the most used by the physicians once RA is diagnosed, due to its rapid effect in suppressing the characteristics inflammation of RA. However, these therapeutic agents are associated with severe side effects resultant from limited selectivity and widespread biodistribution of drug molecules into non-target tissues. In order to overcome the drawbacks of conventional therapy, the aim of the following project was to design pH-sensitive liposomes as suitable drug delivery nanosystems for the treatment of RA. Although these liposomes are stable at physiological pH, they undergo rapid liposomal destabilization under acidic conditions as those presented in endosomes of target cells.

In addition to the pH sensitivity, the extension of liposomes binding and internalization were enhanced either with polyethylene glycol-folic acid (PEG-FA) or hyaluronic acid (HA). By this means that designed pH-sensitive liposomes will, firstly by the PEGylation of liposomes, improve long-circulating times; secondly by the coupling with specific targeting conjugates, enable high binding to over-expressed target cell receptors, hence ensuring cell uptake; and thirdly by using decreased endosomal pH values, trigger and control the release of drug. Thus, the design of targeted pH-sensitive liposomes for the treatment of RA, aims to improve the therapeutic efficiency and efficacy of prednisolone, due to liposomes ability to mediate a specific and controlled release of the drug molecules into target cells, while limiting adverse off-target unwanted effects.

The *in vitro* performance of the designed pH-sensitive liposomes was evaluated through the physicochemical characterization, in terms of encapsulation efficiency, drug loading capacity, size, size distribution, zeta potential and TEM analyses underline a difference in the targeted pH-sensitive liposomes from the non targeted ones. Addicionally, drug release studies were performed mimicking both physiologic (pH 7.4) and acidic (pH 5.0) conditions. Finally, *in vitro* cellular studies were carried out to evaluate both cell viability and cytotoxicity character of designed liposomal formulations, using MTT and LDH assays. And, cell uptake kinetics and mechanism were assessed by flow cytometry, showing that synthethised targeting conjugates specifically improved the uptake by target cells.

This project proves that the selectivity and stability of the designed pH-sensitive liposomes increases the bioavailability of the drug molecules at the site of inflammation, once the liposomes specifically internalize into the target cells, where is trigger controllably the release of drug. Therefore, pH-sensitive liposomes have a huge potential as drug delivery systems to enhance the therapeutic efficiency of prednisolone, minimizing the well-know deleterious side effects in the treatment of RA.

Keywords: rheumatoid arthtitis, pH-sensitive liposomes, prednisolone, folic acid, hyaloronic acid.

Knowledgements: This work received financial support from the European Union (FEDER funds through COMPETE) and National Funds (FCT, Fundação para a Ciência e Tecnologia) through project Pest-C/EQB/LA0006/2013. The work also received financial support from the European Union (FEDER funds) under the framework of QREN through Project NORTE-07-0124-FEDER-000067. To all financing sources the authors are greatly indebted. CN also acknowledge the FCT for financial support through the Post-Doc Grant (SFRH/BPD/81963/2011).

Rapid nanoformulation and cGMP preparation of antiretroviral drugs for oral HIV nanomedicine and human clinical dosing studies

M. Giardiello,[1] T. O. McDonald,[1] P. Martin,[2] N. Liptrott,[2] M. Siccardi,[2] A. Owen,[2] S. Rannard[1]
[1]Department of Chemistry, University of Liverpool, UK
[2]Department of Molecular & Clinical Pharmacology, University of Liverpool, UK

Abstract: The first planned in-human clinical dosing studies for oral dosed nanomedicines for HIV are discussed. The global increase in patients surviving with HIV has given rise to greater demand for anti-retroviral drugs (ARVs). Oral dosage of ARV drugs is extremely desirable for HIV patients due to patient adherence and the need for long term daily dosing over prolonged periods. Herein, a strategy for the progression from small laboratory scale to industrial cGMP manufacturing scales of solid drug nanoparticles (SDNs) is demonstrated. A novel emulsion templated, freeze drying method was used to prepare more than of 4500 ARV SDNs for material evaluation.[1] Subsequently, pharmacological testing of more than 450 nanodispersions was carried out which demonstrated significant pharmacokinetic enhancement with respect to non-nanoformulated ARVs.[2] A large amount of both physical and pharmacokinetic data were collected from less than 4.5 g of ARVs.

Lead SDNs were progressed towards novel emulsion spray-drying synthesis. With the use of an industrially relevant Niro Mobile Minor spray dryer, establishment of scale was achieved leading to large scale production of viable powders for loading into capsules for oral dosage to healthy volunteers for clinical trial studies. Physical characterization *via* PXRD show the dry powders obtained to be amorphous. Upon addition of water (1 mg/mL) powders easily dispersed showing SDN particle size of approximately 250 nm, determined by DLS. Stability testing of aqueous nanodispersions showed SDN particles to remain stable for several hours as well as stable to acid and basic conditions. Storage stability studies were also conducted on the produced bulk powder as well as the clinically prepared drug powder capsules under three temperature and humidity regimes and monitored by HPLC yielding long term storage stability data.
Documentation and MHRA approval has been applied for and granted and as such clinical development and human clinical trial dosage for the first oral dosed nanomedicine for ARV therapy against HIV is imminent.

Keywords: Human clinical trial, Solid Drug Nanoparticles, HIV, Antiretroviral drugs, industrial scale up.

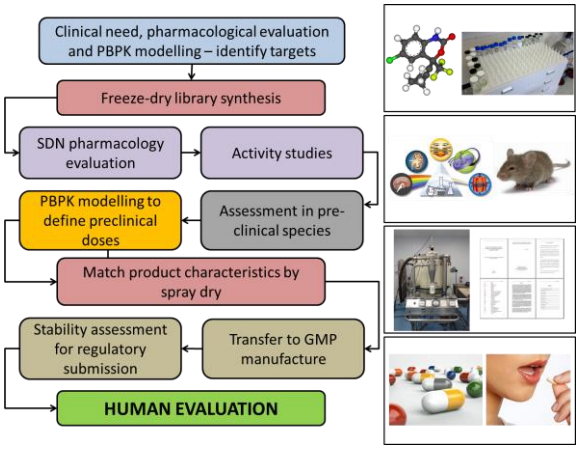

Figure 1: Strategy showing progression from small laboratory scale SDN production through to both *in vitro* and *in vivo* pharmacological analysis followed by industrial scale up and finally through to human clinical dosing studies.

References:

1. Zhang, H., Wang, D. Butler, R., Campbell , N. L., Long, J., Tan, B., Duncalf, D. J., Foster, A. J., Hopkinson, A.,Taylor, D., Angus, D., Cooper, A. I., Rannard, S. P. (2008) Formation and enhanced biocidal activity of water-dispersable organic nanoparticles. *Nat. Nanotechnol*. 3, 506 – 511.

2. McDonald, T., Giardiello, M., Martin, P., Siccardi, M., Liptrott, N. J., Smith, D., Roberts, P., Curley, P., Schipani, A., Khoo, S. H., Long, J., Foster, A. J., Rannard, S., P. and Owen, A. (2014) Antiretroviral Solid Drug Nanoparticles with Enhanced Oral Bioavailability: Production, Characterization, and In Vitro–In Vivo Correlation. *Adv. Healthcare Mater.*, 3, 400 – 411.

Combined PTT & PDT cancer therapies mediated by hybrid carbon nanotubes and assessment of ultrasound elastography for monitoring tumor treatment

I Marangon[1], A Andriola Silva[1], C Menard-Moyon[2], G Renault[3], N Luciani[1], A Bianco[2], F Gazeau[1]
[1]Laboratoire Matière et Systèmes Complexes (MSC), CNRS-UMR 7057, Université Paris Diderot, France
[2]Institut de Biologie Moléculaire et Cellulaire, CNRS-UPR 9021, Strasbourg, France
[3]Plateforme Paris Descartes Imagerie du Petit Animal, Institut Cochin

Abstract: Nano-composites combining multiple functionalities in one single nano-object hold a lot of promises for controlled drug delivery and targeted therapy [1].

In this work carbon nanotubes (CNTs) were functionalized with a therapeutic agent, namely a photosensitizer (mTHPC) already approved in clinical practice for photodynamic therapy (PDT). The aim is to couple the intrinsic properties of CNTs as efficient drug vector and potent photothermal agent with those of the photosensitizer and so benefit from the action of a double light-activated therapy i.e. photothermal therapy (PTT) and PDT.
The first part of this study consisted in quantifying the internalization of drug-loaded CNTs by tumor cells, intracellular release of mTHPC and the absence of intrinsic dark toxicity. Then, we investigated *in vitro* the biologic effects of the distinct therapies and highlighted their combined effects. For this, tumor cells were illuminated either by a 808 nm near-infrared laser radiation (to mediate PTT and local intracellular heating) or by 650 nm laser radiation in order to excite the photosensitizer and thus trigger ROS production. Through different approaches, we studied cell viability, apoptotic cascade and gene expression and demonstrated that each treatment impacts the cell by distinct mechanisms leading to synergistic effect.

The photothermal therapy was also tested *in vivo* on epidermoid carcinoma xenografts implanted in mice. This study had a dual objective: evaluate the therapeutic efficacy of the PTT mediated by CNTs by monitoring the tumor regression and assess the utility of ultrasound elastography to provide mechanical properties of tumor tissue. Indeed, on one hand, the tumor stiffness has been shown as a predictive marker of tumour malignancy. On the other hand, thermal therapy has been associated with local damage on the tumor extracellular matrix with impact on tumor solid stress. Therefore the stiffness of the tumors was monitored throughout the period of the treatment using shear wave elastography. Two distinct types of heating were experimented: moderate hyperthermia (temperature of the tumor monitored at 43°C - 45°C for 20 min, repeated twice) and thermal ablation (50°C for 3 min, repeated twice). We aimed to determine the best compromise between overheating limitation, thermal damage and outcome on tumor progression. It appeared a dramatic decrease of the tumor stiffness for tumors responding favorably to the treatment compared to the others. This non-invasive and non-ionizing imaging technique may allow correlating the effects of hyperthermia on tumor tissues with the evolution of their mechanic properties but also with pathological features. The final objective is to enlarge the use of ultrasonic elastography as a tool for non-invasive personalized monitoring of therapy.

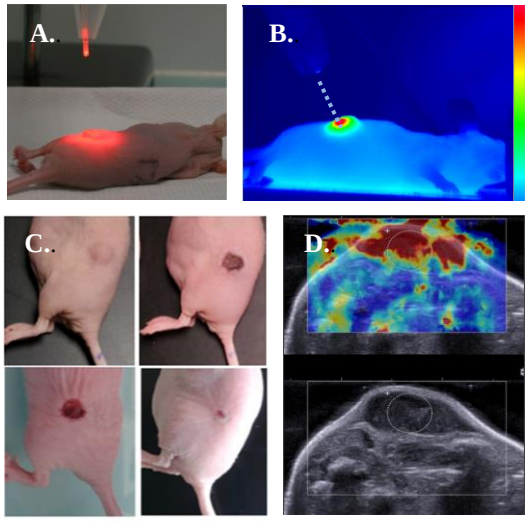

Keywords: cancer treatment, carbon nanotubes, photodynamic and photothermal therapies, elastography

Figure 1: (A) Tumor treatment by laser illumination (B) Thermographic infrared camera photograph of a mouse under laser illumination (laser beam in dotted line): right scale represents the color code for surface temperature (C) Tumor regression (before treatment, and at +1, 8, 12 days) (D) Tumor imaging (top) shear wave elastography : monitoring of the tumor stiffness (bottom) conventional ultra-sonography.

Reference [1] Z.Liu et al., Carbon materials for drug delivery & cancer therapy, Materials Today, 2011, 316-323

Penetration of mucoadhesive chitosan-dextran sulfate nanoparticles into the cornea

W. Chaiyasan,[1*] W. Tiyaboonchai,[1] S.P. Srinivas,[2] S. Praputbut,[1] U. Kompella, [2]
[1]Naresuan University Technology, Faculty of Pharmaceutical Science, Phitsanulok, Thailand
[2]Indiana University, School of Optometry, Bloomington, Indiana, United States
[3]University of Colorado, Pharmaceutical Sciences, Denver, CO, United States

Abstract: Nanoparticles-based drug/gene delivery has been reported for potential therapeutic management of various ocular surface and corneal disorders. In this study, we have examined the efficiency of mucoadhesive chitosan-dextran sulfate nanoparticles (CDNs) penetration across the cornea at the microscopic level by using porcine eyeball as a model. CDNs were produced by polyelectrolyte complexation of the positively charged chitosan and negatively charged dextran sulfate. CDNs were labeled with fluorescein isothiocyanate by reaction of the amino groups of chitosan and the isothiocyanate groups of FITC. Specifically, we have employed a custom-built confocal scanning microfluorometer (CSMF) for record the depth of fluorescence across the cornea. CSMF, equipped with a water-immersion objective (Zeiss 40x; 0.75 NA and wd = 1.2 mm), was employed to quantify the penetration dynamics of SRB. The output of a white LED, which was modulated at 10 kHz, was filtered through an interference filter (565 + 10 nm) and led to the excitation port of the CSMF. The FITC fluorescence (475 nm) and scattered light passing through a parfocal exit slit positioned in the eyepiece were detected by two photomultiplier tubes (R928 Hamamatsu) coupled to two lock-in amplifiers. All measurements were performed with eyeballs held underneath the objective on a precision and motorized XYZ linear translation stage (Newport). FITC-labeled CDNs (FCDNs) was applied onto the porcine cornea for 1.5 and 6 hours with and without intact epithelium. After the experiments, each cornea sample was separated and observed under fluorescence microscopy to confirm the removal of the corneal epithelial layer. Moreover, FCDNs were exposed to primary porcine corneal epithelial cells (PCE) for 30 and 120 min to investigate the cellular uptake mechanism. Meanwhile, the PCE were stained with LysoTracker Red to visualize their appearance in the late endosomes. FCDNs showed a spherical shape with a mean particle size of < 400 nm with positive surface charge. Instillation of FCDNs on the whole cornea with epithelium-intact over 1.5-6 hours led to a peak in fluorescence close to the scatter peak corresponding to the superficial epithelium, while instillation on the bare stroma showed higher fluorescence from deeper layers of the stroma (Figure 1). FCDNs could be endocytosed by PEC via clathrin-dependent pathway and also found in the late endosome/lysosome compartments. Based on the results, it can be concluded that the research into the penetration of mucoadhesive CDNs into the cornea has been very successful. This strategy can be used to deliver drugs payloads to corneal epithelium using CDNs.

Keywords: chitosan-dextran sulfate nanoparticles, mucoadhesive, cornea, custom-built confocal scanning microfluorometer.

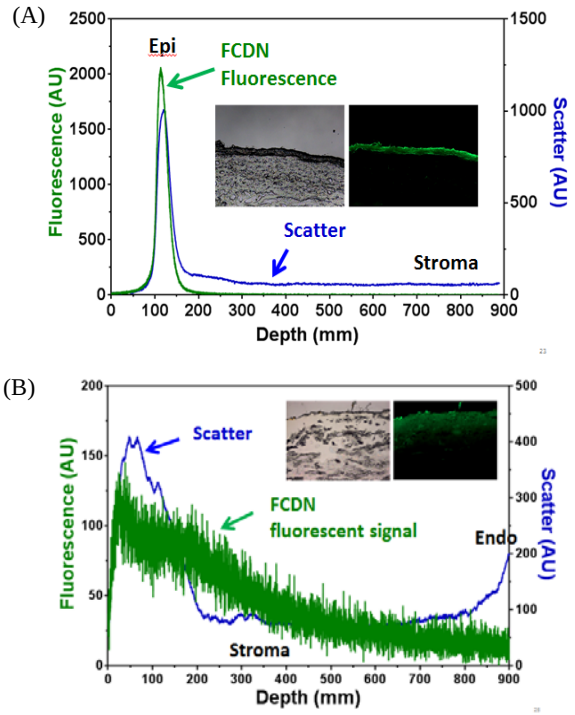

Figure 1: Penetration of FCDNs across the epithelial surface (A) and into stroma (B) after 1.5 hours using CSMF to measure depth-resolved fluorescence. The insert pictures showed the histologically of cornea after experimenting.

Magnetic nanoprobes with anti-HER2 single chain antibody fragments for active targeting of breast and ovarian cancers

C. Alric,[1,*] K. Hervé Aubert,[1] N. Aubrey,[2] E. Allard-Vannier,[1] A. Di Tommaso[2], I. Dimier-Poisson[2], I. Chourpa[1]

[1]Nanomédicaments et Nanosondes, EA6295, Faculté de Pharmacie, Université François Rabelais, Tours, France
[2]Immunologie Parasitaire Vaccinologie et Biothérapie Anti-Infectieuse, IPVBAI, UMR1282 Université-INRA, ISP, Faculté de Pharmacie, Université François Rabelais, Tours, France

Abstract: Polyethylene glycol (PEG)-coated superparamagnetic iron oxides nanoparticles (SPIONs) are known as attractive platforms for anticancer theranostic nanomedicine combining magnetic resonance imaging, drug delivery and hyperthermia functions (Gautier *et al*., 2013; Hervé *et al*., 2008; Liu *et al*., 2011). The major challenge for all the injectable nanomedicines consists in improving their ability to target efficiently the disease cells while preserving their stealthyness relatively to the immune system of the body. The conjugation of antibodies to nanoprobes is intended to insure cancer cells targetting: for instance, anti-HER2 antibody Herceptin® is known to specifically recognise breast and ovarian cancer cells (Colombo *et al*., 2012). However, the conjugation of whole antibody (MW~150 kDa) to nanomedicines induces several drawbacks that limit the efficiency of cancer targeting: poor control of functionnalisation geometry, decreased colloidal stability *in vitro* and stealthyness *in vivo*. To overcome these drawbacks, it is possible to decorate nanomedicines with a scFv fragment (MW ~27 kDa), i.e. the smallest functional antigen-binding domain of the antibody (Vigor *et al*, 2010). In the present study, we describe synthesis and characterization of new generation of magnetic nanoprobes: SPION-PEG functionalised with recombinant scFv of Herceptin®. The physico-chemical properties of our SPION-PEG-scFv were assessed by atomic absorption, fluorescence and photon correlation spectroscopies. The presence of scFv fragments was analyzed both qualitatively and quantitatively, by means of optical spectroscopy. According to the analysis data, our SPION-PEG-scFv nanoprobes combined several advantages such as: (i) regio-specific covalent binding of the scFv to the PEG external surface of nanoprobes; (ii) small and regular size (hydrodynamic diameter of ca. 100 nm); (iii) nearly neutral surface insuring good colloidal stability and stealthyness. From the biological point of view, the scFv-nanoprobes were immunoreactive as it was shown by ELISA and immunofluorescence methods. In addition, absence of the Fc constant domain should reduce the nanoprobes immunogenicity – this will be studied in the very close future.

Keywords: SPIONs, scFv fragment, anti-HER2, nanoprobes, diagnostic, targeting, cancer.

Acknowledgments:

We acknowledge financial support from Région Centre (project NCIS) and Ligue Nationale contre le Cancer.

References:

Gautier, J., Allard-Vannier, E., Hervé-Aubert, K., et al., (2013) Design strategies of hybrid metallic nanoparticles for theragnostic applications, *Nanotechnology*, 24, 432002.

Hervé, K., Douziech-Eyrolles, L., Munnier, E., et al., (2008) The development of stable aqueous suspensions of PEGylated SPIONs for biomedical applications, *Nanotechnology*, 19, 465608.

Liu, D.; Wu, W.; Ling, J.; Wen, S.; Gu, N.; Zhang, X. (2011) Effective PEGylation of Iron Oxide Nanoparticles for High Performance in Vivo Cancer Imaging. *Adv. Funct. Mater., 21*, 1498–1504.

Colombo, M.; Corsi, F.; Foschi, D.; Mazzantini, E.; Mazzucchelli, S.; Morasso, C.; Occhipinti, E.; Polito, L.; Prosperi, D.; Ronchi, S.; *et al.* (2012) HER2 Targeting as a Two-Sided Strategy for Breast Cancer Diagnosis and Treatment: Outlook and Recent Implications in Nanomedical Approaches. *Pharmacol. Res.*, 62, 150-165.

Vigor, K. L.; Kyrtatos, P. G.; Minogue, S.; Al-Jamal, K. T.; Kogelberg, H.; Tolner, B.; Kostarelos, K.; Begent, R. H.; Pankhurst, Q. A.; Lythgoe, M. F.; *et al.* (2010) Nanoparticles Functionalized with Recombinant Single Chain Fv Antibody Fragments (scFv) for the Magnetic Resonance Imaging of Cancer Cells. *Biomaterials*, 31, 1307-1315.

Cellulose Nanocapsules of Metoprolol and its Metabolites Produced as New Products in Pharmaceuticals Recycling Processes

Gezimar D. Souza,[1*] Daniela H. E. Schiavon,[1] Claudia B. Pelizaro[1], Gabriela. B. Teixeira[1]
[1] ACCERT CHEMISTRY AND BIOTECHNOLOGY INC. Rua Alfredo Lopes, 1717, sala 7E, São Carlos – SP, Brazil
*gezimar@accert.com

Abstract: Accert Chemistry and Biotecnology Inc. has been developing different processes for recovering expired pharmaceuticals and out-of-date medicines. Strategies include development of bioprocess using microorganisms and enzymes to promote specific reactions in active pharmaceutical ingredients (API) and then generate degradation products standards (DPS) or active metabolites (AM). Herein, cellulose nanocapsules containing metoprolol and some of its active metabolites have been prepared by emulsion–solvent evaporation method[1]. Metoprolol is a beta-blocker that affects the heart and blood flow through arteries and veins[2]. Different conditions were applied (temperature, rotation, nanoparticules concentration, API, DPS or AM concentration) and the results indicated API, DPS or AM concentration does not significantly influence the size of the nanocapsules, which are extremely affected by the employed producing method (from 250 nm to 900 nm). Nanoparticles sizes were determined by scanning electron microscopy (SEM) and encapsulation efficiency was determined by ultra-high performance liquid chromatography coupled with ultraviolet detector (UHPLC-UV). The results suggest that efficient process for recovering expired pharmaceuticals or out-of-date medicines can be achieved by generating cellulose nanocapsules. Such kinds of processes are of desired since cellulose is a widely used excipient in pharmaceutical products. Therefore, using such approach pharmaceuticals recycling can be a very good way of producing new pharmaceuticals products or formulations.

Keywords: pharmaceutical recycling, cellulose nanocapsules, metoprolol, new pharmaceutical products, metabolites.

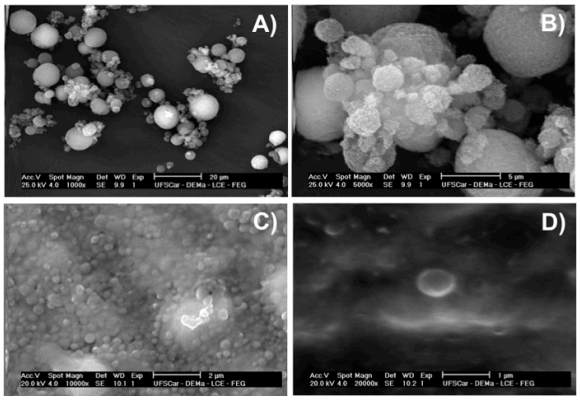

Figure 1: SEM of examples os nanocapsules obtained.

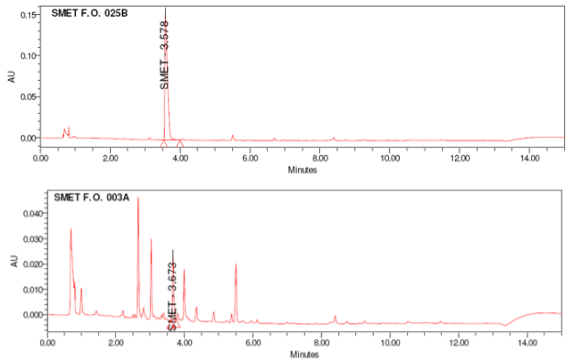

Figure 2: UHPLC-UV of metoprolol (above) and metoprolol after a biorreaction using enzymes (bellow). Such samples were encapsulated with cellulose.

References:

1. Zhao, J., Zhao, X., Jiang, Z., Li, Z., Fan, X., Zhu, J., Wu, H., Su, Y., Yang, D., Pan, F., Shi, J. (2014) Biomimetic and bioinspired membranes: preparation and application. *Progress in Polymer Science*, 39(8), 1668-1720.

2. Guengerich FP. (2001) Common and Uncommon Cytochrome P450 Reactions Related to Metabolism and Chemical Toxicity. *Chemical Research in Toxicology*. 14, 611-650.

Ph/temperature and Magnetic Field Responsive Doxorubicin Loaded NIPA Coated Superparamagnetic Nanoparticles for Targeted Cancer Therapy

Rouhollah KHODADUST[1#] , Yasemin YAR[1], Havva YAGCI ACAR[1]
[1]*Department of Materials Science and Engineering, Koc University, Turkey*
[#]*Corresponding author: rkhodadust@ku.edu.tr*

Abstract:

"Intelligent" materials which are able to respond to external stimuli, represent one of the most exciting and immerging class of materials that can be applied for biomedical application. Poly(N-isopropylacrylamide) (PNIPAAm), seems as the most suitable of this group for biomedical applications (Ward et al 2011). This is because of the fact that lower critical solution temperature LCST of PNIPAM is around 32°C which is close to the body temperature (37°C) (Shimizu et al 2010). Superparamagnetic nanoparticles (SPIONs), another important group of "Intelligent" materials, have gained great attention in the fields of nanomedicine due to being biocompatible, biodegradable, facilely tunable, and superparamagnetic and thus controllable by an external magnetic field (Mok et al 2013).In this study, in order to improve the delivery and therapeutic properties, NIPAM polymer, a potent system for hyperthermia therapy was combined with superparamagnetic core which resulted in the combination of non-contact (Magnetic force) and contact (pH and Temprature) forces. We tried to design this polymeric nanocarrier more applicable as drug delivery system by increasing the LCST from 32°C to mild hyperthermia temperatures about 42°C. In order to investigate the in vitro thermo-chemosensitisation characteristics of our nanoparticles for drug delivery applications, doxorubicin, one of the most widely used anticancer drugs, was loaded on newly synthesized pH/temperature and magnetic field responsive NIPA-Fe_3O_4 nanoparticles. Thermo-chemosensitisation paved the way for increased antineoplastic drug accumulation in tumors and enhanced drug cytotoxicity. The characterization of nanoparticles was studied. Then loading efficiency was optimized and the release studies performed at different temperatures (25˚C, 37˚C, 42˚C) and pH (7.4, 5.6) (Figure1). Then cell cytotoxicity of the complex compared with free form of doxorubicin. Finally time and temperature dependent cell internalization and drug release of the complex was studied using life time inverted florescent microscopy (Figure2). Results demonstrated that the prepared complex can be a potent delivery system especially for targeted cancer therapy.

Keywords: Cancer; PNIPAAm ; superparamagnetic; Doxorubicin; biocompatible; biodegradable; targeted cance therapy;

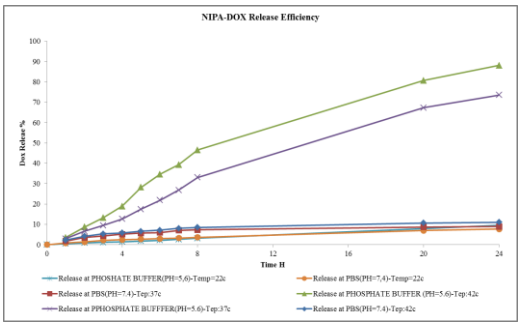

Figure 1. Release of doxorubicin from NIPA-Fe3O4 Nanoparticles at pH 5.6 and pH 7.4 with three different temperature as 22˚C, 37˚C and 42˚C.

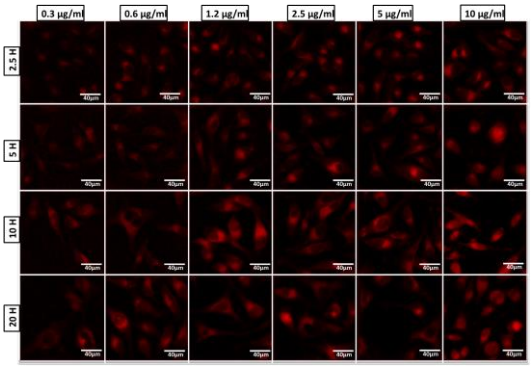

Figure 2. Uptake of doxorubicin loaded NIPA-Fe3O4 Nanoparticles by Hela Cells. Confocal laser microscopy image of Hela cells incubated together with doxorubicin loaded NIPA-Fe3O4 Nanoparticles with different concentration (0.3, 0.6, 1.2, 2.5, 5 and 10 µg/ml) of doxorubicin contents at different time points (2.5h, 5h, 10h and 20 h) at 37˚C.

References:

Ward, M.A.; Georgiou, T.K. Thermoresponsive terpolymers based on methacrylate monomers: Effect of architecture and composition. J. Polym. Sci. Part A 2010, 48, 775-783.

Shimizu, K.; Fujita, H.; Nagamori, E. Oxygen plasma-treated thermoresponsive polymer surfaces for cell sheet engineering. Biotechnol. Bioeng. 2010, 106, 303-310.

Mok, H., & Zhang, M. (2013). Superparamagnetic iron oxide nanoparticle-based delivery systems for biotherapeutics. Expert opinion on drug delivery, 10(1), 73-87.

Targeted polyethylene glycol gold nanoparticles for the treatment of pancreatic cancer: from synthesis to a proof-of-concept *in vitro* studies.

Jolanda Spadavecchia[1 2] Dania Movia[3], Hanane Moustaoui[2] ,Caroline Moore[3], Ciaran Manus Maguire[3], Sandra Casale[1], Adriele Prina-Mello[3,4]

[1]*Sorbonne Universités, UPMC Univ Paris VI, Laboratoire de Réactivité de Surface, 4 place Jussieu, F-75005 Paris, France.*
[2]*CNRS, UMR 7244, Laboratoire de Chimie,Structures et Propriétés de Biomateriaux et d'Agents Therapeutiques, Paris, France.*
[3]*AMBER centre and CRANN institute, Trinity College Dublin, Ireland*
[4] *Department of Clinical Medicine, School of Medicine, Trinity College Dublin, Ireland*

Abstract: Gold nanoparticles (AuNPs) are attracting considerable interest as viable biomedical materials, and research into them is growing due to their unique physical and chemical properties (Movia et al , 2014;Cui et al 2008).
Here we report the synthesis of doxorubicin-loaded PEGylated AuNPs (DOX-PEGAuNPs) by a simple one-step method, and their further functionalization with an anti-potassium channel monoclonal antibody (mAb) by terminal carboxylic acid groups for their future application in the treatment of pancreatic cancer. The mAb efficiently recognizes a specific antigen expressed on the membrane of pancreatic cancer cells, with positive effects on the drug delivery efficiency. The relevance and major interest of the so-obtained nanoparticles in the presence of terminal carboxylic acid groups at their surface, as confirmed by infrared X-Ray Diffraction (XRD), and X-ray Photoelectron Spectroscopy (XPS), and Polarization Modulation-Reflection-Adsorption-Infrared-Spectroscopy (PM-IRRAS), in addition to the surrounding PEG chains, is essential to avoid non-specific protein adsorption (Spadavecchia et al 2014). In parallel, biocompatibility, as well as the therapeutic efficacy, were evaluated in Proof-of-Concept (PoC) *in vitro* studies by means of a high throughput technique (namely, flow cytometry analysis) (Figure 1). Data gathered from this study may have further applications for the safe design of nanostructures to be applied for therapeutic purposes in the treatment of cancer.

Keywords: PEG Gold Nanoparticles, Doxorubicin, Mab; cancer, PM-IRRAS, biomedical applications.

Acknowledgment:
This project was partially supported by EU FP7 QualityNano Infrastructure project (grant number: 262163).

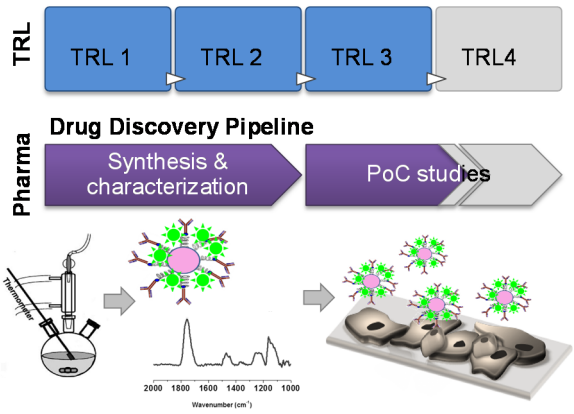

Figure 1: Technology Readiness Level (TRL) for pharmaceutical products development.

References:
D. Movia, V. Gerard, C. Manus Maguire, N. Jain, A. P. Bell, V. Nicolosi, T. O'Neill, D.Scholz, Y.Gun'ko, Y. Volkov, A.Prina-Mello. A safe-by-design approach to the development of gold nanoboxes as carriers for internalization into cancer cells. *Biomaterials*, 2014. **35**(9): 2543-2557.

Cui, C. Liu, J. Shen, D. Gao, J. Zhu, H-Y Chen. Gold Nanoparticle–Colloidal Carbon Nanosphere Hybrid Material: Preparation, Characterization, and Application for an Amplified Electrochemical Immunoassay. *Advanced Functional Materials*, 2008. **18**(15): 2197-2204.

J. Spadavecchia, R. Perumal, A.Barras, J. Lyskawa, P.Woisel, W. Laure, C-M Pradier, R. Boukherroub, S. Szunerits. Amplified plasmonic detection of DNA hybridization using doxorubicin-capped gold particles. *Analyst*, 2014. **139**(1): 157-164.

Oral insulin delivery and biodistribution of biopolymers-based nanoparticles

Marlene A. Lopes[1], Denise Aniceto[1], Raquel Seiça[1], Francisco Veiga[1], António J. Ribeiro[2]

[1]CNC - Center for Neuroscience and Cell Biology, Faculty of Pharmacy, University of Coimbra, 3000-548 Coimbra, Portugal
[2]I3S, Instituto de Investigação e Inovação em Saúde, Universidade do Porto, 4150-180 Porto, Portugal and Group Genetics of Cognitive Dysfunction, IBMC – Instituto de Biologia Molecular e Celular, Universidade do Porto

Abstract: Alginate-dextran sulfate based nanoparticles complexed with a chitosan-polyethylene glycol-albumin shell can be considered suitable carriers for oral insulin delivery. Nanoparticles were obtained by co-surfactant and ultrasonication assisted emulsification/internal gelation technology. This technology makes use of natural occurring polymers which are a suitable choice, due to their excellent biocompatibility, drug carrying ability, adjustable controlled-release property, lower cost, abundance in nature and easier application (Stops et al, 2008). Physicochemical characterization revealed them as suitable carriers for oral delivery of insulin. Nanoparticles with a mean diameter of 166±0.84nm were able to well-preserve their integrity in simulated gastric fluid. In simulated intestinal fluid, nanoparticles morphology changed and a sustained and controlled release of insulin was observed during 3h. Size variation of coated and uncoated nanoparticles across the simulated fluids were controlled over the time and pH increment, due to polymer pH dependent behavior. Insulin secondary structure during nanoparticles preparation was analysed. Biodistribution of ^{99m}Tc-albumin and ^{99m}Tc-albumin-nanoparticles was monitored during 24h after oral administration to mice. 99mTc-albumin-nanoparticles showed a different behavior compared to 99mTc-albumin, since the activity in the duodenum's and small intestine's wall was maintained for 60 min while the activity in the small intestine content was already residual. The interaction between albumin and chitosan, a positively charged biopolymer with mucoadhesive properties, allows the interaction of these nanoparticles with intestinal cells. After oral administration of insulin-loaded nanoparticles to diabetic Wistar rats, the glycemic reductions attained by both doses after 10h were -69 ($p<0.05$) and – 63% ($p<0.05$) with 50 and 100 IU/kg insulin-loaded nanoparticles, respectively. Compared with subcutaneous insulin, the oral insulin-loaded nanoparticles showed more sustained and long-term effect. After 10 h of oral administration of 50IU/Kg insulin-loaded nanoparticles, intraperitoneal glucose tolerance tests were compared between three animal models, diabetic Wistar (type 1 diabetic model), GK (type 2 diabetic model) and healthy Wistar rats. In both diabetic models, glycemia increased to a lesser extent in rats receiving the formulation and 1h30 after of the glucose challenge, a significantly faster decrease was noticed. After 3h, no statistical differences were obtained between GK groups, in contrast to the behavior of wistar diabetic rats. Although the pancreatic islets of GK rats are defective, this genetically modified model of type 2 diabetes have the islets partly damaged but could still secrete a little insulin and glucagon. (Li et al, 2013). Therefore, the exogenous insulin may cover-up the effect of insulin-loaded nanoparticles. Comparison of the response between normal Wistar and GK rats showed that GK rats have a slower metabolic decomposition rate of glucose. Our results demonstrate that these biopolymers-based nanoparticles may provide an efficient template for the oral delivery of insulin.
Keywords: biopolymers, insulin, oral delivery, nanoparticles, type 1 and type 2 diabetic models, radioactive labeling.

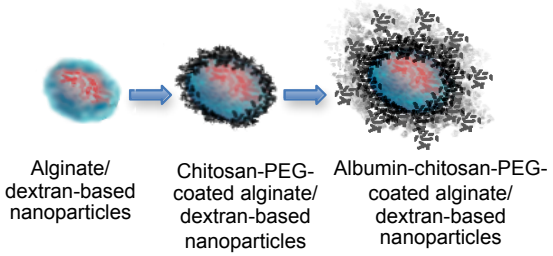

Figure 1. Nanoparticles coating process.

References:

Stops, F., Fell, J., Collett, J., Martini, L. (2008) Floating dosage forms to prolong gastro-retention—The characterisation of calcium alginate beads. *Int. J. Pharm.* 350(1–2):301-311.

Li, X., Qi, J., Xie, Y., Zhang, X., Hu, S., Xu, Y., Lu, Y., Wu, W. (2013) Nanoemulsions coated with alginate/chitosan as oral insulin delivery systems: preparation, characterization, and hypoglycemic effect in rats. *Int. J. Nanomedicine.* 8:23-32.

IONCs: a versatile tool for hyperthermia, imaging and controlled drug delivery

Maria Elena Materia, Pablo Guardia, Hamilton Kakwere, Ayyappan Sathya, Manuel Pernia, Simone Nitti, Giammarino Pugliese, Liberato Manna and Teresa Pellegrino

Istituto Italiano di Tecnologia, via Morego 30, 16163 Genova, Italy

Iron Oxide nanocubes (IONCs) are among the best iron-based nanoparticles for hyperthermia treatment and magnetic resonance imaging (MRI). Properly functionalized they are also important tools for transport and controlled release of drugs. Moreover it was demonstrated that the controlled aggregation of multiple highly magnetic interacting IONCs in a polymeric shell has a significant effect on the heating performance and on the efficiency as contrast agent of these nanoparticles.

The "magnetically mediated hyperthermia" (MMH) represents a novel therapeutic concept based on the generation of heat *via* an alternating magnetic field (AMF) exploiting magnetic nanoparticles (MNPs) as heating *foci*. The heating efficiency of a heat probe is evaluated by its specific absorption rate (SAR) value, which provides the power absorbed per unit mass of magnetic material (W/g) when exposed to an alternating magnetic field (AMF).

In this work we studied the SAR values of single IONCs and clusters of the latter named magnetic nanobeads (MNBs). These samples are made water-soluble by using recently novel methods developed by us. It was observed in particular a considerable SAR decrease when the IONCs are aggregated into MNBs. This trend was also confirmed by the SAR measurements performed in solvents with different viscosity. For the same samples were also performed the relaxivity measurements which showed very high values of r_2/r_1 for MNBs respect IONCs.

To fully exploit the outstanding heating ability of IONCs, these particles were functionalized with a thermo-responsive polymer (based on *N*-isopropylacrylamide). These nanohybrid structures were used as drug carrier for chemotherapy: Doxorubicin (DOXO) was loaded at room temperature and after encapsulation in the polymer, was released under the AMF using technical conditions biomedically safe for patients ($Hf < 5 \times 10^9$ $Am^{-1}s^{-1}$). The temperature increase generated by IONCs in the AMF induces the coil-globule transition of the polymer which in turns triggers the drug expulsion from the hybrid nanostructures (Figure 1).

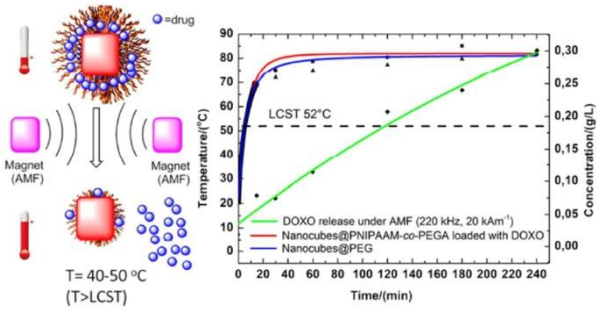

Figure 1: schematic representation of DOXO release from IONCs functionalized with a T-responsive polymer under AMF. The graph shows the amount of DOXO released over the time together with the temperature profiles for the IONCs with and without the thermo-responsive shell.

References

1) M. E. Materia et al., *Langmuicr*, **31**, 808.
2) H. Kakwere et al., Functionalization of Strongly Interacting Magnetic Nanocubes with (Thermo)responsive Coating and their Application in Hyperthermia and Heat-Triggered Drug Delivery, *ACS Appl. Mater. Interfaces*, Just Accepted Manuscript.
3) P. Guardia et al., *J. Mater. Chem. B*, **2**, 4426.
4) P. Guardia et al., *ACS Nano*, **6**, 3080.
5) R. Di Corato et al., *Macromol. Biosci.*, **9**, 952.
6) R. Di Corato et al., *ACS Nano*, **5**, 1109.

A Novel Wound Dressing Coated with Self-Assembling Peptide Nanofibrils as a Drug Carrier

Reem Alazragi and Amalia Aggeli
Centre for Molecular Nanoscience, School of Chemistry, University of Leeds, United Kingdom

Abstract: The delivery of therapeutic agents into wounds is a developing area. The release of a drug to wounds in a control manner is rearley reported. The uncontrolled release is a common limitation of drug releasing dressings. If the release rate is too high, the drug can be unloaded from the dressing before infection is arrested. Furthermore, a 'burst release' within the first few hours may lead to overdose cytotoxcity, which can give rise to delayed wound healing, or to the development of antibiotic resistance [1]. Inversely, if the release rate is too low, the drug delivery may be below the effective therapeutic dose that is required to be effective. Another limitation caused by uncontrolled drug release from wound dressings is that it leads to the need for frequent changes. When the dressing is removed, the newly formed epithelium can be damaged, so limiting dressing changes is usually considered to be beneficial [1, 2].

To overcome these limitations, attention has been paid to develop materials that provide potential for controlled drug delivery. Controlled drug delivery to wounds normally means the delivery of an active agent to the wound site in a sustained manner. The ideal bioactive dressing should release the drug at the optimum therapeutic concentration followed by a sustained constant delivery [2]. These criteria can limit the frequency of dressing changes. Under these circumstances patient compliance can be improved, especially in those suffering from chronic wounds, where the patient needs to undergo extended periods of treatment [3]. In light of such considerations, there is a need for a more conservative approach for smart wound-care materials that are more effective and more functional than traditional materials. Optimistically, the addition of pH-responsive self-assembling peptide nanofibrils (Figure 1) as a biofunctional component to medical fabrics could have the potential to combine the advantages of triggered release with slow kinetic release.

This project is an attempt to contribute to the development of smart medical textiles, in particular, to development of controlled drug-release textiles for wound care that can imediatly release the drug when triggered by the pH of bacteria. Here, for this purpose, cellulosic fabrics were coated with the fibril-encapsulated antibiotics (Figure 2) to develop a smart pH-stimulus responsivness dressing, which was then assessed for the ability to inhibit the growth of *staphylococcus epidermidis*. The results showed that the dressings were stimulated by the pH of bacteria and released the loaded drug. Hopefully, this dressing could by clinically applied on infected wounds to release the drug only when required and reduce the problem of bacterial resistance to antibiotics in wound care applications.

Keywords: self-assembling peptide, wound dressing, drug delivery.

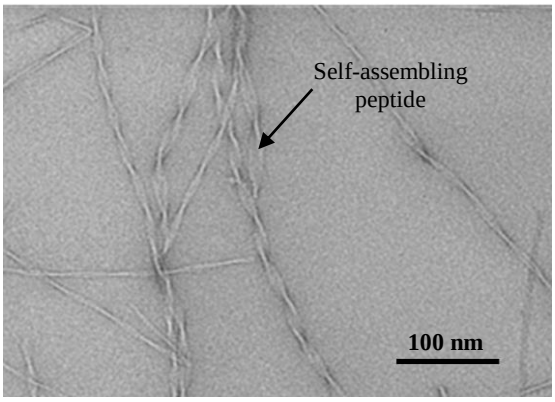

Figure 1: TEM image of self-assempling peptide fibrils.

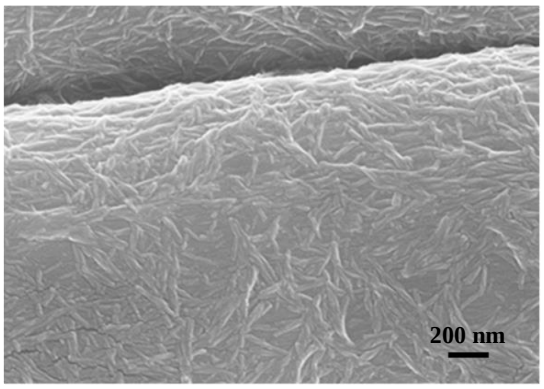

Figure 2: SEM image of a dressing coated with peptide fibrils containing vancomycin.

References:

1. Loke, W.K., et al., *Wound dressing with sustained anti-microbial capability.* Journal of Biomedical Materials Research, 2000. 53(1): p. 8-17.

2. Costache, M.C., et al., *Polymer–xerogel composites for controlled release wound dressings.* Biomaterials, 2010. 31(24): p. 6336-6343.

3. Boateng, J.S., et al., *Wound healing dressings and drug delivery systems: a review.* Journal of Pharmaceutical Sciences, 2008. 97(8): p. 2892-2923.

Core-cone Structured Monodispersed Mesoporous Silica Manoparticles with Ultra-large Cavity for Protein Delivery

Chun Xu
Australian Institute for Bioengineering and Nanotechnology, The University of Queensland, Brisbane, QLD 4072, Australia

Abstract: Mesoporous silica nanoparticles (MSNs) have attracted much attention as a new generation of drug delivery vehicles. Delivering therapeutic proteins into cells is an important challenge for many medical applications including cancer therapy, vaccination and regenerative medicine. Traditional MSNs usually have small pore sizes (<13 nm), which greatly hinders their encapsulation and intracellular delivery of therapeutic proteins. In this work a new type of monodispersed mesoporous silica nanoparticles with a core-cone structure (MSN-CC) has been synthesized. The large cone-shaped pores are formed by silica lamellae closely packed encircling a spherical core, showing a structure similar to the flower dahlia. MSN-CC has a large pore size of 45 nm and a high pore volume of 2.59 cm^3 g^{-1}, the highest pore volume of all MSN with radial structures. A supramolecular self-assembly mechanism is proposed to explain the formation of MSN-CC, and first time cone-like vesicles are reported in self-assembled objects. MSN-CC demonstrates a high loading capacity of large proteins and successfully delivers bioactive β-galactosidase (β-gal) into cells, showing their potential as efficient nanocarriers for the cellular delivery of proteins with large molecular weights. To our knowledge, our study is the first report on intracellular delivery of large functional proteins above 100 kDa using MSNs, providing a safer delivery tool for large proteins instead of previous transduction peptide based ones.

Keywords: Mesoporous silica nanoparticles, large radial pores, supramolecular selfprotein delivery

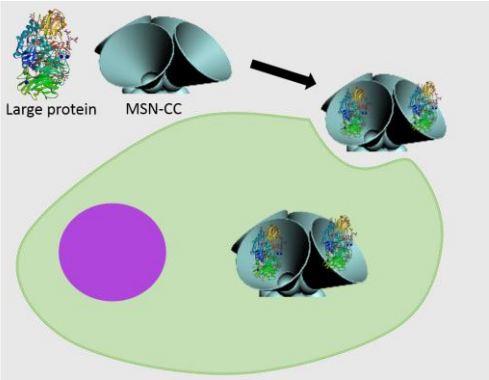

Figure 1: The process of delivery of large functional proteins into cells using MSN-CC.

References:

Xu, C., Yu, C.Z. (2015) Core-cone Structured Monodispersed Mesoporous Silica Manoparticles with Ultra-large Cavity for Protein Delivery, *Small.*, Under Review

Xu, C., Yu, C.Z. (2014), Rod-like mesoporous silica nanoparticles with rough surfaces for enhanced cellular delivery, *J. Mater. Chem. B*, 2, 253-256

Impact of the Polyethylenimine Conjugation Mode on the Cell Transfection Efficiency of Silica Nanovectors

X. Wang, S. Masse, G. Laurent, C. Hélary, T. Coradin
Sorbonne Universités, UPMC Univ Paris 06 and CNRS, UMR 7574, Chimie de la Matière Condensée de Paris, France

Abstract: Efficient gene delivery relies largely on the design of intracellular vectors (Guo *et al.*; 2011). Among the non-viral vectors, silica nanoparticles (SiNP) have attracted increasing attention due to tunable size/ mesoporisity and versitile surface chemistry (Mamaevaa *et al.*; 2013). The main strategy is to modify SiNP with amine groups to complex the negatively charged plasmid DNA. Nowadays, it's of special interest to modify SiNP surface with a cationic polymer, polyethylenimine (PEI). PEI alone is a very efficient transgene vector and the availability of various conjugation methods to SiNP facilitates the optimization of the vector design. Nevertheless, the impact of conjugation mode on cell transfection remains unknown and so far PEI modified SiNP, especially covalent bonded ones, targets mainly at the delivery of siRNA rather than plasmid DNA (Buchman *et al.*; 2013).

In our study, we utilized three approaches to conjugate PEI (25 kDa) to SiNP surface and evaluated the systems as delivery vectors for plasmid DNA. Previously, we have systematically studied the feasibility to graft PEI through direct physical adsorption (SiNP@PEI, Figure 1a) and excellent transfection efficiency could be maintained while cytoxicity of PEI was reduced (WANG *et al.*; 2015). Meanwhile, we proposed two other methods for comparation. On the one hand, we modified SiNP first with $-SO_3$ and then PEI was introduced by stronger electrostatic adsorption (Figure 1b, SiNP@SO_3@PEI). On the other hand, SiNP was grafted with -Cl and -Cl was then substituted by the amine group of PEI (SiNP@Cl@PEI, Figure 1c).

Successful modifications were first confirmed with zeta potential measurement and elemental anaylsis. PEI conformation at nano-interface was investigated further with XPS and solid-state NMR. The highest rigidity of PEI over particles was observed with SiNP@PEI, followed by SiNP@SO3@PEI and finally SiNP@Cl@PEI. In principle, lowest rigidity allowed the flexibility and therefore the highest DNA compaction capability. Surprisingly, the trend SiNP@PEI> SiNP@SO3@PEI>> SiNP@Cl@PEI was obtained in terms of transfection efficiency. It should be noted that the interactions between PEI and SiNP evolved in the opposite order, correlated with the difficulty of PEI release from the interface. Hence, this sharp contrast suggested the release of PEI from the particle plays a more important role in the intracellular gene delivery. Another important outcome of our studies was concerned with safety when applied as nanomedicine. It was found that at comparable doses, PEI alone showed detrimental effect while all the SiNP modified with PEI exhibited no cytotoxicity.

Keywords: silica nanoparticles, polyethylenimine, solid-state NMR, surface modification, gene delivery.

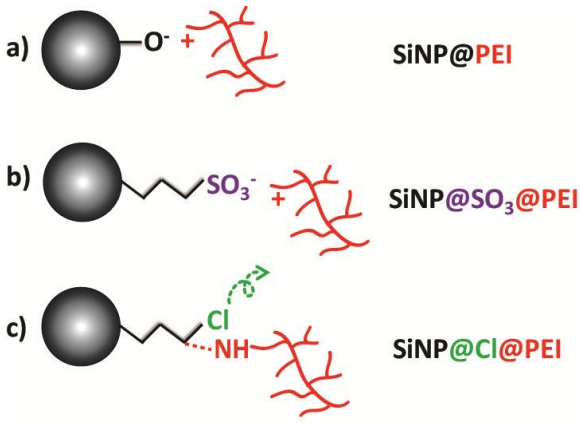

Figure 1: illustration of PEI conjugation mode to SiNP surface. a) adsorption with silanols; b) adsorption with sulfonate; c) covalent bonding by substitution of -Cl with amine of PEI.

References:

Guo, X., Huang, L. (2011) Recent Advances in Nonviral Vectors for Gene Delivery, *Acc. Chem. Res.*, 45, 971–979.

Mamaevaa, V., Sahlgrena, C., Lindén, M. (2013) Mesoporous silica nanoparticles in medicine—Recent advances, *Adv. Drug Deliv. Rev.*, 65, 689–702.

Buchman, YK., Lellouche Emmanuel.,Zigdon, S., Bechor, M.,Michaeli, S.,Lellouche, JP.(2013) Silica Nanoparticles and Polyethyleneimine (PEI)-Mediated Functionalization: A New Method of PEI Covalent Attachment for siRNA Delivery Applications, *Bioconjugate Chem.*, 24, 2076–2087.

WANG, X., Helary, C., Coradin, T. (2015) Local and Sustained Gene Delivery in Silica-Collagen Nanocomposites, *ACS Appl. Mater. Interfaces*, 7, 2503–2511.

PEI – Starch Nanoparticles for siRNA based Gene Silencing Therapy for Cancer

Berke Bilgenur Kandemir[1,3*], Bülent Özpolat[5], Gamze Torun Köse[3,4], Vasıf Hasırcı[1,2,3]
Middle East Technical University (METU), Departments of [1]Biotechnology and [2]Biological Sciences Ankara, Turkey
[3]BIOMATEN, METU, Center of Excellence in Biomaterials and Tissue Engineering, Ankara, Turkey
[4]Yeditepe University, Department of Genetics and Bioengineering, Istanbul, Turkey
[5]University of Texas, Department of Experimental Therapeutics, MD Anderson Cancer Center, Houston TX, USA

Abstract: Conventional cancer treatment techniques are not sufficiently efficient and they even are harmful for healthy tissues. Recent studies suggest that siRNA based gene silencing can be used as a highly effective targeted therapy (Ozpolat *et al.*; 2013). However, siRNA delivery into tumors and target tissues have proved to be difficult (Tekedereli et al., 2012). This study aimed to develop an siRNA delivery system to cancer cells using positively charged nanospheres constructed of PEI and S.

PEI-starch nanospheres were prepared at different ratios by water-in-oil microemulsion method. Genipin was used to crosslink PEI molecules. The PEI-starch nanospheres were characterized by measuring the zeta potential and the particle size, studying the topography with SEM, and measuring release rate of their content by spectrofluorometer. We also evaluated siRNA and nanaoparticle uptake and target downmodulation by confocal laser scanning microscopy (CLSM) and western blot analysis.

The mean diameter of PEI-starch incorporating siRNA was 84.6 nm. Zeta potential of PEI-starch nanospheres increased when the PEI /starch ratios were increased and was the highest (8.7 mV) at PEI:Starch, 9:1 (w/w) (Table 1).

Table 1: Surface potential of PEI: starch nanospheres and viability of MCF 7 cells treated with PEI – starch nanospheres constructed with PEI: starch (w/w) ratios of 1:9, 1:3, 1:1, 3:1 and 9:1.

PEI:starch (w:w)	Zeta potential (mV)	Cell viability (%)
1:9	-31	90.7
1:3	-26	86.6
1:1	-19	85.6
3:1	0	81.9
9:1	9	78.0

The nanospheres released 50 % of their siRNA content in the first 3 days and all of the content in a week. CLSM micrographs show the nanospheres and siRNA were taken up by MCF 7 breast cancer cells (Figure 1). Western blot analysis demonstrated that EF2-Kinase siRNA loaded nanospheres significantly inhibited EF2K protein expression (90-100%) (Figure 2).

Keywords: siRNA, drug delivery, nanoshere, polyethylenimine, starch, cancer therapy, nanomedicine

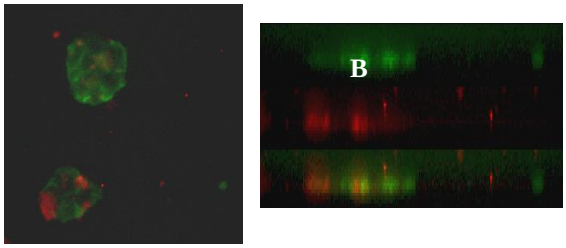

Figure 1: Confocal microscopy of MCF 7 cells treated with Alexa-555 labelled siRNA loaded PEI-starch nanospheres (A) fluorescence image of MCF 7 cells (green) treated with Alexa-555 labelled siRNA loaded PEI-starch nanospheres (red) (x 40), (B) Z-stack.

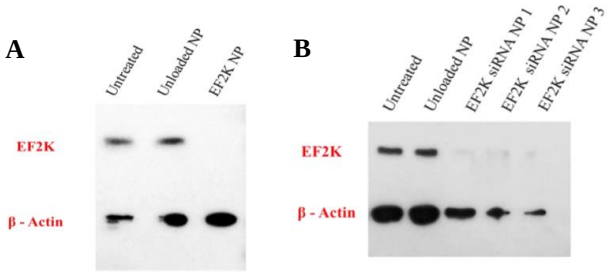

Figure 2: Western blot analysis of MCF 7 cells treated for 72 h (100 nM EF2K siRNA and 100 000 cells per well). (A) with EF2K siRNA loaded nanospheres (NP), (B) with various batches of EF2K siRNA loaded nanospheres (NP) (NP1, NP2, NP3).

In this study construction of a novel PEI-starch based siRNA carrier to initiate apoptosis in breast cancer cells was aimed. The PEI–starch nanospheres effectively penetrated into MCF 7 cells. Thus, we showed that the PEI-starch nanospheres are suitable in size, charge, release kinetics and as such they exhibit a potential to serve as an efficient vector for siRNA delivery to cancer cells.

References:

Ozpolat, B., Sood, A. K., & Lopez-Berestein, G. (2014), Liposomal siRNA nanocarriers for cancer therapy. *Adv. Drug Deliv. Rev.*, 66, 110-116.

Tekedereli, I., Alpay, S. N., Tavares, C. D., ... & Ozpolat, B. (2012), Targeted silencing of elongation factor 2 kinase suppresses growth and sensitizes tumors to doxorubicin in an orthotopic model of breast cancer. PloS one, 7(7), e41171.

Synthesis of l-PEI and 2MPA Coated Biocompatible Silver Sulfide QDs as Transfection Vectors

Didar Asik ,Fatma Demir and Havva Yagci Acar
Koc University, Graduate School of Materials Science and Engineering, Rumelifeneri Yolu, Sarıyer-34450, Istanbul, Turkey

Abstract: Gene therapy has become very popular approach to fight cancer. In recent years, efforts of improving non-viral gene delivery techniques and transfection vectors have been increased. Due to its high transfection efficiency, cationic polyethylene-imine (PEI) polymer is one of the most popular vectors, yet molecular weight and structure dependent toxicity of PEI is an important issue. High transfection efficiency along with high biocompatibility is desired for practical purposes. Therefore, usually molecular weight is kept at and below 25kDa and sometimes lineer PEI is preferred over branched one. Besides, tracking the delivery of genes and/or the outcome of the gene therapy with diagnostic tools is highly desired. Organic fluorescent dyes conjugated to the vectors or genes can be used for optical tracking however, organic dyes have a very short luminescence lifetime which is disadvantages in long experimental procedures. Quantum dots with resistance to photobleaching and long luminescence lifetime emerged as alternative fluorescent tags in biomedical research. In literature there are few reports on cadmium chalcogenide bound PEI as a transfection vectors however, Cd-chalcogenides are usually toxic and emit in the visible region which is far from being ideal for in vivo experiments.
Here, we will describe the development of new quantum dots which emit in the medical window (Near infrared: 700-900nm) which are composed of more cytocompatable lineer PEI and highly cytocompatible Ag_2S. Effect of PEI molecular weight and reaction parameters on the properties of quantum dots and their ability in gene trasfection will be discussed.

Keywords: Quantum Dots, NIR, Nanomedicine, Transfection Agent, PEI, Ag_2S, Theranostic, P53, Gene Transfection

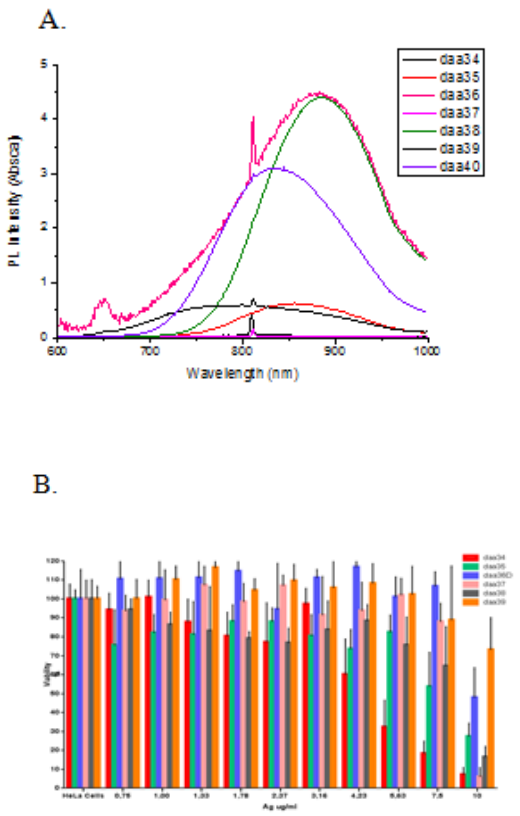

Figure 1. (A) PL intensity versus wavelength graph of quantum dots with different l-PEI and 2MPA ratios. (B) Dose dependent viability of HeLa cells determined by MTT.

References:

[1] I. Hocaoglu, M. N. Cizmeciyan, R. Erdem, C. Ozen, A. Kurt, A. Sennaroglu and H. Yagci Acar, Development of highly luminescent and cytocompatible near-IR-emitting aqueous Ag2S quantum dots, J. Mater. Chem, **2012**, 22, 14674.

[2] Yezhelyev, M.V.,Qi,L.,ORegan, R.M., Nie, S. And Gao, X, Proton-sponge coated quantum dots for siRNA delivery and intracellular imaging, Journal of American Chemical Society, **2008**, 130, 9006-12.

The Role of Triblock Amphiphilic Copolymers for DNA Translocation Through Lipid Bilayers

B. Rasolonjatovo,[1] C.Huin, [1*] B.Pitard,[2] J.Mathé,[1] V.Bennevault-Celton,[3] T.Le Gall,[4] T.Montier,[4] P.Lehn,[4] H.Chéradame,[1] P.Guégan,[3,5]

[1]LAMBE, UMR8587, UEVE-CNRS-CEA, Evry, France
[2]Institut du Thorax, INSERM UMR1087, CNRS 6291, Nantes, France
[3]CNRS, UMR8232, IPCM, Chimies des Polymères, Paris, France
[4]INSERM U613, Hôpital Morvan – CHU Brest – I3S, Brest, France
[5]Sorbonne Universités, UPMC, Univ Paris 6, UMR8232, IPCM, Chimie des Polymères, Paris, France

Abstract: Gene therapy consists in delivering DNA inside a cell to obtain a therapeutic effect. In the case of intramuscular injections, the most efficient synthetic vectors are neutral amphiphilic block copolymers, compared to naked DNA and cationic polymers (Chèvre *et al.*, 2011). Block chemical nature has an influence on the transfection efficiency and toxicity (Pomel *et al.*, 2008). Neutral amphiphilic block copolymers could induce transitory pores in lipid bilayers, pores allowing plasmid translocation, which could be a good indication for gene transfer mechanism with such copolymers (Huin *et al.*, 2011).

A family of ABA triblock copolymers (TBCP), having a hydrophobic poly(tetrahydrofuran) block and two hydrophilic poly(2-methyl-2-oxazoline) blocks, was synthesized using cationic ring opening polymerization. Experimental conditions allowed a good control of the structures. Critical aggregation concentration and characteristic parameters, evidencing macromolecular self-assembly, were determined. Studies of micelle formation (using DLS, ITC, Dosy NMR, Fluorescence) led us to draw a relationship between copolymer structure and physicochemical properties in solution, showing the formation of a core-corona structure (Rasolonjatovo *et al.*, 2014).

Interactions of copolymers with model lipid bilayers were evaluated by 'Black Lipid Membrane' experiments and the ability of plasmid (9kb) translocation was studied (Figure).

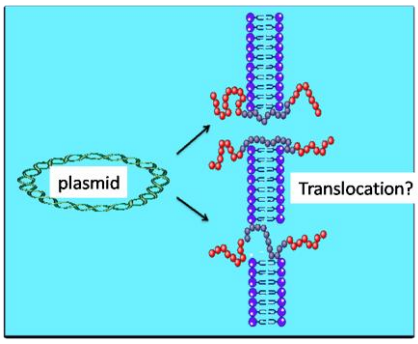

Figure : Plasmid Translocation assisted by a TBCP through lipid membrane.

TBCPs were finally used as vectors of pCMV-Luc, by using intramuscular injections in Swiss female mice.

Correlation between physicochemical properties, patch-clamp analyses and biological results was established. The TBCP structural parameters have a strong influence on the transfection efficiency, one of the most important for this kind of applications.

Keywords: amphiphilic block copolymers, gene therapy, plasmid translocation.

References:

Chèvre, R., Le Bihan, L., Beilvert, F., Chatin, B., Barteau, B., Mével, M., Lambert, O., Pitard, B. (2011) Amphiphilic block copolymers enhance the cellular uptake of DNA molecules through a facilitated plasma membrane transport, *Nucleic Acids Research*, 39, 1610-1622.

Pomel, C., Leborgne, C., Cheradame, H., Scherman, D., Kichler, A., Guégan, P. (2008) Synthesis and Evaluation of Amphiphilic Poly(tetrahydrofuran-*b*-ethylene oxide) Copolymers for DNA Delivery into Skeletal Muscle, *Pharmaceutical Research*, 25, 2963-2971.

Huin, C., Le Gall, T., Barteau, B., Pitard, B., Montier, T., Lehn, P., Chéradame, H., Guégan, P. (2011) Evidence of DNA transfer across a model membrane by a neutral amphiphilic block copolymer, *Journal of Gene Medicine*, 13, 538-548.

Rasolonjatovo, B., Gomez, J.P., Meme, W., Goncalves, C., Huin, C., Bennevault-Celton, V., Le Gall, T., Montier, T., Lehn, P., Cheradame, H., Midoux, P., Guegan, P. (2014) Poly (2-methyl-2-oxazoline)-b-poly(tetrahydrofuran)-b-poly(2-methyl-2-oxazoline) amphiphilic triblock copolymers: synthesis, physicochemical characterizations and hydrosolubilizing properties, *Biomacromolecules*, 16, 748-756.

Synthesis and Characterization of Folate-Targeted Poly(ethylene glycol) Coated Cationic Ag_2S QDs for Tumor Targeted Gene Delivery

F. Demir[1*], R. Khodadust[1], D. Asik[1], H. Yagci Acar[123]
[1]*Koc University, Graduate School of Materials Science and Engineering, Istanbul, Turkey*
[2]*Koc University, Department of Chemistry, Istanbul, Turkey*
[3]*KUYTAM, Koc University, Surface Science and Technology Center, Istanbul, Turkey*

Cationic quantum dots are promising nanomaterials in biological applications, especially in drug/gene delivery. However, most of the designed cationic quantum dots are cytotoxic (Li et al., 2008) and emit in the visible range (400–700 nm) where the penetration depth of the light into the tissue is very low and autofluorescence from tissue/cells appear. Ag_2S QDs that emit in the near-infrared region (NIR) overcome these problems and present highly biocompatible structures with the negligible toxicity (Hocaoglu *et al.*, 2014).

The most prominent cationic polymer used in gene delivery is polyethylenimine with high DNA condensation capacity and transfection efficiency (Yue *et. al.*, 2011). However, the polymer shows toxicity due to highly cationic character. PEGylation is a solution to reduce the toxicity by lowering the surface charge and interactions with blood and extracellular components (Zhang *et al.*, 2010). As a result of PEGylation, the blood circulation time extends and the biocompatibility increases but uptake decreases. Targeting ligands help by receptor-mediated endocytosis to enhance the uptake. Folic acid is one of the most used ligands for tumor therapy because of the over-expression of folate receptor in cancer cells.

In this study, NIR emitting cationic Ag_2S QDs coated with poleyethleneimine (PEI) and l-cystein were PEGylated to reduce the toxicity of PEI and targeted by folic acid (FA) to cancer cells. The QDs in different coating ratio of PEI and l-cystein were studied to develop highly stable, luminescent, biocompatible non-viral gene delivery systems. Nanoparticle composition is determined by ICP-OES, NMR and elemental analysis. DLS and zeta potential measurements showed an increase in the size of the QDs and decrease in the zeta potential of the cationic QDs after FA-PEGylation. Cytotoxicity analyses demonstrated the improvement in the cell viability of the QDs thanks to PEGylation and increase in the uptake with folate targeting. These QDs successfully condensed p53-GFP plasmids at and above N/P ratio of 5. Transfection efficiency and influence of particle properties on trasfection efficiency will be discussed.

Overall, folate-targeted poly(ethylene glycol) coated cationic Ag_2S QDs present a promising gene delivery system with optical detection opportunity in the NIR, biocompatibility and high transfection efficiency.

Keywords: Near IR Ag_2S quantum dots, PEGylation, folic acid, gene delivery.

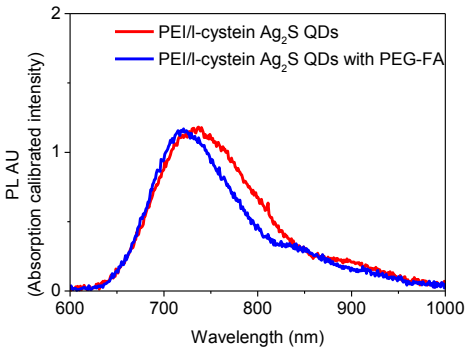

Figure 1: Photoluminescence spectra of the Ag_2S QD and FA-PEGylated Ag_2S QDs

References:

Li. H., Shih WH., Shih WY., Chen L., Tseng SJ., Tang SC. (2008) Transfection of aqueous CdS quantum dots using polyethylenimine, *Nanotechnology* 19, 475101.

Hocaoglu I., Demir F., Birer O., Kiraz A., Sevrin C., Grandfils C., H. Yagci Acar, Emission tunable, cyto/hemocompatible, near-IR-emitting Ag2S quantum dots by aqueous decomposition of DMSA, Nanoscale, 2014, 6, 11921.

Yue Y., Jin F., Deng R., Cai J., Dai Z., Lin MCM., Kung HF., Mattebjergc M., Andresen T., Wu C. (2011) Revisit complexation between DNA and polyethylenimine - Effect of length of free polycationic chains on gene transfection, *Journal of Controlled Release* 152,143–15.

Zhang C., Gao S., Jiang W., Lin S., Du F., Li Z., Huang W. (2010) Targeted minicircle DNA delivery using folate-poly(ethylene glycol)-polyethylenimine as non-viral carrier, *Biomaterials*, 31, 6075-6086.

A Systemic Approach For Manipulating Geometries Of Nano Gold And Nano Silver in Synthesis for Controlling Vector Borne Diseases

Soam Prakash, Advance and Env. Parasitology and Vector Control Biotechnology Laboratories, Department Of Zoology, Faculty Of Science, Dayalbagh Educational Institute, Dayalbagh, Agra 282 005, India

Abstract: The synthesis of metallic nanoparticles is an active area of academic and, more significantly, industrial applied research in nanotechnology. Currently nanoparticle research is an area of intense scientific interest in controlling diseases of global nature. Silver (Ag) and Gold (Au) nanoparticles (NPs) have been the focus of fungi and plant based syntheses for controlling vector o populations of mosquitoes which can be specifically of one species or more therefore could be targeted with each interfacing device explored geometrically. Silver and gold nanoparticles are nanoparticles of silver and gold. These particles are of between 1 nm and 100 nm in size. Silver and gold have been use in the wide variety of potential applications accordingly with their geometries. There is a crucial need to manipulate geometries to produce new insecticides. Synthesizing nanoparticles target specific need manipulating their geometries which we have experimented during synthesizing nanoparticles with a system science approach. The mosquitocidal activity of silver and gold nanoparticles using each fungi is a system. The system science applications in synthesis could be of great help as the precision in geometry of new particle can be predictable with dynamic model presented by us for target specific mosquitoes. (Soni and Prakash (2012a ,2012b,2014).

The holistic view precisely obtained during synthesis can be manipulated in creating equations by altering physical, chemical and biological system as shown in figures(1,2) parameters for each geometry required for the cause.

Keywords: Nano Gold, Nano Silver, Mosquito Control, System Science, Nano Geometries

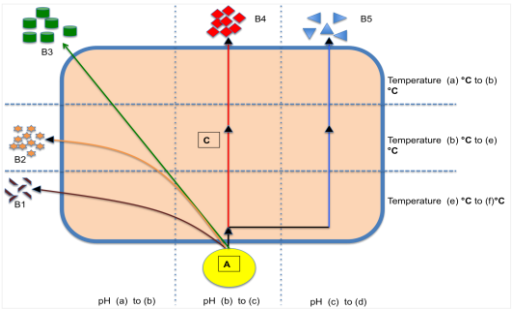

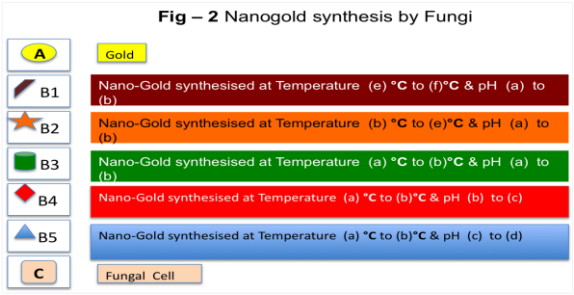

Fig1,2: illustrating diagrammatically the fundamental strategy to manipulate geometries on nanoparticles by changing their physical, chemical and biological systems

References:

Soni,N. and Prakash, S. (2012) Efficacy of fungus mediated silver and gold nanoparticles against *Aedes aegypti* larvae. *Parasitology Research*. Volume 110, Issue 1, pp 175-184.

Soni,N. and Prakash, S. (2012) Fungal-mediated nano silver: an effective adulticide against mosquito. *Parasitology Research*. Volume 111, Issue 5, pp 2091-2098.

Soni,N. and Prakash, S. 2014.Green Nanoparticles for Mosquito Control. *The Scientific World Journal.* http://dx.doi.org/10.1155/2014/496362

Influence of TiO_2 and Al_2O_3 Addition on Mechanical Properties of Dental Zirconia

Özlem AĞAÇ[1], Abdullah ÖZTÜRK[2], Jongee PARK[1]

[1]ATILIM University, Metallurgical and Materials Engineering Department, İncek Ankara 06836, Turkey

[2]Middle East Technical University, Metallurgical and Materials Engineering Department, Ankara 06531, Turkey

Abstract: Zirconia-based ceramics have generated considerable interests in the dental community as restorative dental materials due to their high mechanical and chemical properties (Kaya *et al.*, 2012). This study was to produce dental zirconia ceramics by adding titania and alumina as a dopant. Mechanical ball milling was introduced to add the additives into zirconia practically. The shaped samples were sintered at 1350°C-1550°C for 2 hrs. Bulk density and shrinkage were calculated to investigate the effect of additives. The mechanical property was determined using the method of Vickers indentationand fracture toughness after sintering. SEM was used for analysis of grain size and surface morphology. XRD was operated to examine the crystalline phases in the titania and alumina-added zirconia ceramics during heat treatment. Table 1 shows the hardness and fracture toughness densification behaviour of various zirconia ceramics that contain different amounts of TiO_2 and Al_2O_3 at different sintering temperatures. It is noted that the addition of TiO_2 has been effective in lowering the sintering temperature, even though the density increased with increasing sintering temperature (Park *et al.*, 2008). Beside, addition of Al_2O_3 decreased the density of zirconia with increasing sintering temperature (Matsui *et al.*, 2008). However, hardness and fracture toughness were increased with adding alumina. As a result, co-doping of TiO_2 and Al_2O_3 addition decreased the sintering temperature and enhanced the mechanical properties.

Keywords: zirconia dental ceramics, TiO_2, Al_2O_3, Vicker's hardness, fracture toughness

Table 1: Hardness & fracture toughness of zirconia with different amount of alumina and titania

Sample	**Hardness (H_V)**	**Fracture Toughness (K_{IC})**
Pure zirconia	1220±4	4.55±0.40
0.5 wt%TiO_2-ZrO_2	1331±22	4.74±0.30
1 wt% TiO_2-ZrO_2	1215±3	4.63±0.06
0.5 wt%TiO_2- 1 wt%Al_2O_3-ZrO_2	1346±0.14	5.32±0.2
0.5 wt%TiO_2- 2 wt%Al_2O_3-ZrO_2	1296±6	4.61±0.05

References:

Kaya, G., (2012) "Production and characterization of self-colored dental zirconia blocks", Ceramics International, 39, 511-517.

Park, J., Ozturk, A., (2008) "Effect of TiO2 addition on the crystallization and tribological properties of MgO–CaO–SiO2–P2O5–F glasses", Thermochimica Acta, 470, 60-66.

Matsui K, Yamakawa T, Uehara M, Enomoto N, Hojo J. Mechanism of alumina-enhanced sintering of fine zirconia powder: influence of alumina concentration on the initial stage sintering. J Am Ceram Soc 2008;91:1888–97.

Piezoresistive Strain Sensing Characteristics of Nano-carbon Composites

G. R. Choi,[1] H. K. Park,[1] H. Huh,[1] K. T. Lim, [2] B. K. Choi,[2] S. Y. Kim,[2] I. Kang[2*]
[1] Korea Institute of Industrial Technology, Chonan, Korea
[2]Pukyong National University, Busan, Korea

Abstract: In this study, the piezoresistive sensing properties of nano-carbon e.g. CNTs (Carbon Nanotubes) and xGnP (eXfoliated Graphite Nano Platelet), based composites are characterized for their applications of strain sensors. The nano-carbon composites show peculiar piezoresistive characteristics depending on their matrixes with respect to their strain variations.

In the case of hard matrix composites, they demonstrated quite linear bidirectional piezoresistive responses to strain and their piezoresistivity tend to increase to tension and to decrease to compression (Kang et al., 2006). The strain response of hard composites such as an epoxy presented fairly symmetrical and reversible behavior, and the gauge factors obtained were about ~200 within the range of 1,000 micro-strain. The xGnP composites revealed much higher strain sensitivity than CNTs composites (Kim *et al*., 2011). The static and dynamic voltage output responses of the composite sensors were also experimentally studied and were compared with those of a conventional foil strain gages. The voltage outputs by using signal processing systems were fairly stable and they showed fairy linear responses at both of loading and unloading cases with little hysteresis.

However, soft matrix based nano-carbon composites have not only non-symmetric responses but also demonstrated incrementally unidirectional piezoresistivity under both of tension and compression (Kang *et al*., 2011). The resistivity of the nano-carbon soft composites increased even compressive force condition due to the destruction of the existing conductivity of the filler (Jing *et al*., 2006). The voltage output was distorted under a quasi-dynamic test due to their unsymmetrical piezoresistive characteristics. The nano-carbon soft composite sensor showed quite tardy response to its settling time test under static deflections and that would be a hurdle for its real time applications. Furthermore, since the soft sensor did not have directional voltage output to tension and compression, it only could be utilized as a mono-directional force sensor such as a compressive touch sensor.

The strain sensor system made of nano-carbon composites can monitor structures continuously for electrical impedance and piezoresistive signals indicating structural deterioration and impact which may be sufficient to cause damage in real time. The composite sensors can be easily installed on composite structures using a spray-on technique, making the sensor low cost and practical. Strain or impact applied to the structure can be detected by the highly sensitive nano-carbon composite sensors. They induce change of piezoresistivity of the structure and that converts into voltage output consequently by means of simple signal processing system. The piezoresistive nano composite sensor is lightweight and easily applied to the structural surface, and there is no stress concentration, no piezoelectrics, no amplifier, and no storage of high frequency waveforms. Nano piezoresistive composite sensor is expected to be a cost effective and sensitive multi-functional sensor for composites and other damage monitoring applications in the field of engineering sensing..

Keywords: strain sensor, nano carbon, carbon nanotubes, exfoliated graphite nano-platelet, nano composite, smart material.

References:

Kang, I., Schulz, M., J., Kim, J., H., Shanov,V., Shi, D. (2006), A carbon nanotube strain sensor for structural health monitoring, *Smart Materials and Structures*, 15, 737-748.

Kim, Y. –J., Cha, J. Y., Ham, H., Huh, H., So, D. –S., Kang, I. (2011) "Preparation of piezoresistive nano smart hybrid material based on grapheme, *Current Applied Physics*, 11, S350-S352.

Kang, I., Khaleque, M. A., Yoo, Y., Yoon, P. J., Kim, S. –Y., Lim, T. K. (2011) Preparation and properties of ethylene propylene diene rubber/multi walled carbon nanotube composites for strain sensitive materials, *Composites: Part A*, 42, 623–630.

Jing, M. -J., Dang, Z. -M., Xu, H. -P. (2006) Significant temperature and pressure sensitivities of electrical properties in chemically modified multiwall carbon nanotube/methylvinyl silicone rubber nanocomposites, *Appl. Phys. Lett.*, 89, 182902.

Plasmonic nanoparticle interaction with cell for photoacoustic cancer imaging

Miya Ishihara[1,*], Takeshi Hirasawa[1], Ryota Sato[2], Toshiharu Teranishi[2]
[1]Department of Medical Engineering, National Defense Medical College, 3-2, Namiki, Tokorozawa, Japan
[2]Institute for Chemical Research, Kyoto University, Gokasho, Uji, Japan

Abstract: Molecular imaging promises to expand existing medical imaging techniques beyond the typical visualization of anatomical features to incorporate functional and pathological information based on contrast agents that include targeting capabilities.

Photoacoustic (PA), imaging a noninvasive molecular imaging modality based on optical excitation and ultrasonic detection has the potential for molecular imaging at high resolution and deep inside the tissue. PA imaging contrast agents using gold nanoparticles (Au NPs) plays a key role in the development of an imaging technology with molecular specificity and sensitivity because the primary advantages of Au NPs lie in their large absorption cross section with unique spectra due to the surface plasmon resonance effect and bioconjugation capability, which means that the gold nanoparticles can be specifically targeted to molecules and/or cells (Thakor *et al*., 2011).

The purpose of our study is to establish deeply penetrating PA molecular imaging technology. We performed a comprehensive PA measurement of various Au NPs to design exogenous imaging agents for enhancing the contrast. The PA signal amplitudes were sensitive to the size and shape of the gold nanoparticles. We also investigated the effects of surface charge of Au NPs on photoacoustic (PA) signal from cultured various cell (Figure 1, Ishihara *et al*., 2014). Our findings are crucial to the design and synthesis of Au NPs as PA imaging contrast agents with maximized diagnostic efficacy.

Keywords: Photoacoustic, Gold Nanoparticle, Polyhedron, Anion, Cation, Localized Surface Plasmon Resonance, cellular uptake, Ultrasound, Pulsed Laser, Tomography, P(VDF-TrFE) film

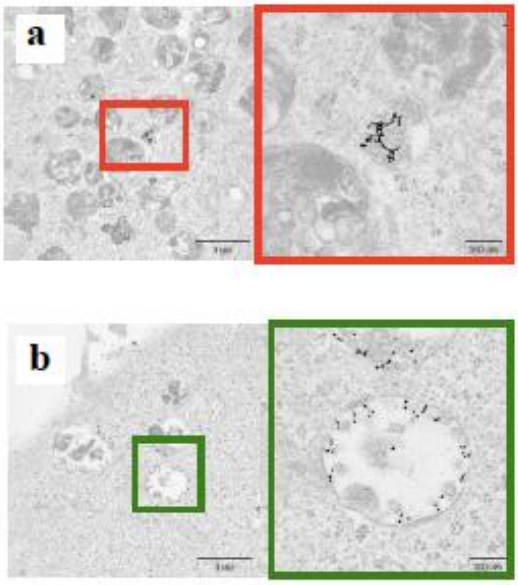

Figure 1: TEM images of different surface charges of Au NPs in cultured A549 cell (3 hours incubation). The cationic Au NPs do not aggregate in the cell (b), but on the other hand, the anionic Au NPs aggregate (a). The uptake of Au NPs by A549 cells (non-phagocytic cells) was highly dependent on the types of surface charge.

References:

Thakor, S., Jokerst, J., Zavaleta, C., Massoud, T. F., and Gambhir, S. S. (2011), Gold Nanoparticles: A Revival in Precious Metal Administration to Patients, *Nano Lett.*, 11(10), 4029-4036.

Ishihara, M., Hirasawa, T., Okawa, S., Sato, R., Urano, Y., and Teranishi, T. (2014), The effect of surface charge of plasmonic gold nanoparticles on photoacoustic signal, *Proc. of SPIE*, 8943, 89434D-89434D-6.

Acknowledgement: This study was partially supported by JST Collaborative Research Based on Industrial Demand (In vivo Molecular Imaging: Towards Biophotonics Innovations in Medicine).

Novel hybrid nanoparticles using upconversion luminescence for *in vivo* imaging

N. Francolon[1]*, F. Leccia[2], E. Jouberton[3], D. Boyer[1], I. Miladi[3], Delphine Felder-Flesch[4], Sylvie Begin-Colin[4],L. Morel[2], E. Miot-Noirault[3], J-M. Chezal[3], R.Mahiou[1]

[1]*Université Clermont Auvergne, Institut de Chimie de Clermont-Ferrand, UMR 6296 CNRS / UBP / ENSCCF - 63171 AUBIERE*
[2]*Université Clermont Auvergne, Génétique Reproduction et Développement, CNRS, UMR 6247, INSERM, U931 - 63000 CLERMONT-FD*
[3]*Université Clermont Auvergne, Imagerie Moléculaire et Thérapie Vectorisée, UMR 990, INSERM, UdA - 63000 CLERMONT-FD*
[4]*Université de Strasbourg, Institut de Physique et Chimie des Matériaux de Strasbourg, CNRS, UMR 7504, 67034 STRASBOURG*

Abstract: Currently, targeted fluorescent nanoparticles (NPs) have become a major interest in the field of nanomedecine. Especially, upconverting nanoparticles (UCNPs) have attracted much attention due to their peculiar properties, relevant for bioimaging applications in the infrared range. In this work, we developed new multifunctional UCNPs for *in vivo* imaging, particularly in the case of prostate cancer.

These materials permit the conversion of near infrared (NIR) radiations into photons of higher energy (NIR, visible and ultraviolet) via a multiphoton mechanism. In comparison with UV excitation, fluorescence imaging based on NIR light, which is only weakly absorbed by biological tissue, leads to deeper and non-invasive diagnosis. Among the lanthanide doped materials, $NaYF_4$ was reported as the most efficient lattice for UC process. This well-known host was synthetized via a thermolysis process using oleic acid and octadecene in order to obtain spherical and crystallized nanoparticles with a narrow size distribution.

Moreover the UCNPs are functionalized in order to make them biocompatible and decrease their toxicity. To this aim, we have used the ligand exchange method, with two types of molecules: PEG-phosphate and dendronized molecules. In fact these previous molecules are more and more developed for biomedical applications.

Then, the interaction of the water-soluble UCNPs with living cells was investigated. In particular, LNCaP prostate cancer cells were incubated with nanoparticles and have shown low toxicity.

Finally, some *in vivo* tests have been done on mice in order to shown the feasibility of our UCNPs for biological application. Figure 1 presents the *in vivo* whole body images of nude mice with injections of a solution at 1 mg/mL of $NaYF_4$@dendrons (50µL intramuscular –IM- and 20µL subcutaneous – SC). A significant UCL signal was observed for both injections and show the potential of these UCNPs.

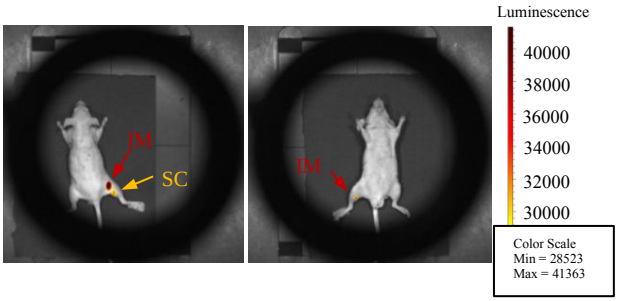

Figure 1 : In vivo imaging of NPs@dendrons injected in mice (power of the laser = 71mW/cm²)

Acknowledgment : The authors would like to thanks the *Région Auvergne* and the *Fonds Européen de Développement Régional* (R72-p2 : 2012-2015) for their financial support.

Efficient and Spatial-Selection Delivery of Quantum Dots in Live Cells by Gold Nanoparticle Medicated Photoporation

R. Xiong[1,2,*], J. Demeestera[1], S. C. De Smedta[1], K. Braeckmans[1,2]
[1]Laboratory of General Biochemistry and Physical Pharmacy, Ghent University, Ottergemsesteenweg 460, 9000 Ghent, Belgium;
[2]Centre for Nano- and Biophotonics, Ottergemsesteenweg 460, 9000 Ghent, Belgium;

Abstract: Quantum Dots (QDs) as fluorescent probes have attracted considerable interest in many biological and biomedical applications, especially cellular imaging. In comparison with conventional molecular dyes, QDs have several unique advantages such as broad absorption with narrow emission spectra, high resistance against photobleaching, and size-tunable fluorescent emission. To date, QDs have been successfully applied to label fixed and permeabilized cells, or to label membrane proteins in living cells. To extend their use for more general subcellular labeling of living cells, efficient cytosolic delivery into live cells is required, which remains a major challenge. Recently, gold nanoparticle (AuNP) medicated photoporation was shown to be an efficient, non-toxic approach to deliver macromolecules from tens of kDa to hundreds of kDa in live cells. By irradiating AuNPs attached the cell membrane with pulsed laser light of sufficient energy, 'explosive' water vapour nanobubbles (VNB) can be formed around these AuNPs. When the thermal energy of the AuNP is consumed, the VNB violently collapses and causes local damage to the cell membrane by high-pressure shock waves. Using this approach we demonstrated that large macromolecules, such as 500 kDa FITC-dextran, could be introduced into the cytoplasm with negligible cytotoxicity (Xiong *et al.* ; 2014). Considering that the size of PEGylated QDs is similar to the hydrodynamic radius of 500 kDa dextran, here we have evaluated laser-induced VNB mediated membrane poration can also efficiently deliver QDs in cells with low toxicity as shown in Figure 1. Additionally, we also show a spatial-selection delivery of QDs can be easily realized by this AuNP meditated photoporation with laser patterned scanning the cell sample (Figure 2).

Keywords: QDs, spatial-selection delivery, photoporation, vapor nanobubble, gold nanoparticle.

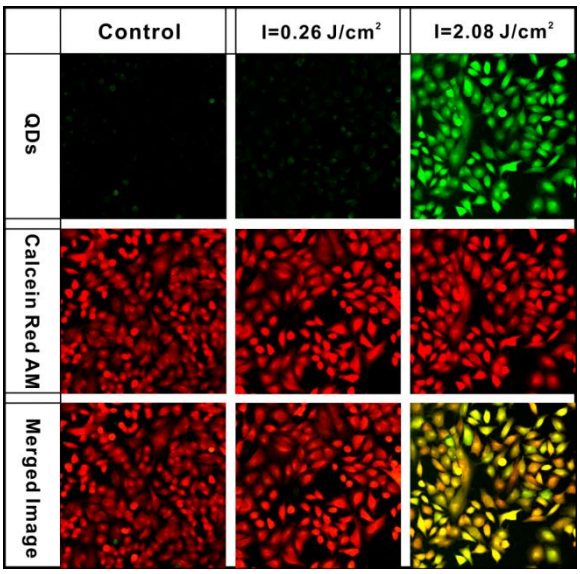

Figure 1: Confocal images showing the delivery of PEG-coated QDs in the green channel (first row) and the viability of HeLa cells labeled with calcein red AM in the red channel (second row). An overlay of green and red images is shown in the bottom row. The first of column is the negative control (cells treated with 2.08 J/cm^2 laser light but without AuNPs), the second and third column show the delivery efficiency of QDs as a function of laser fluence. The field of view is 410 µm by 410 µm.

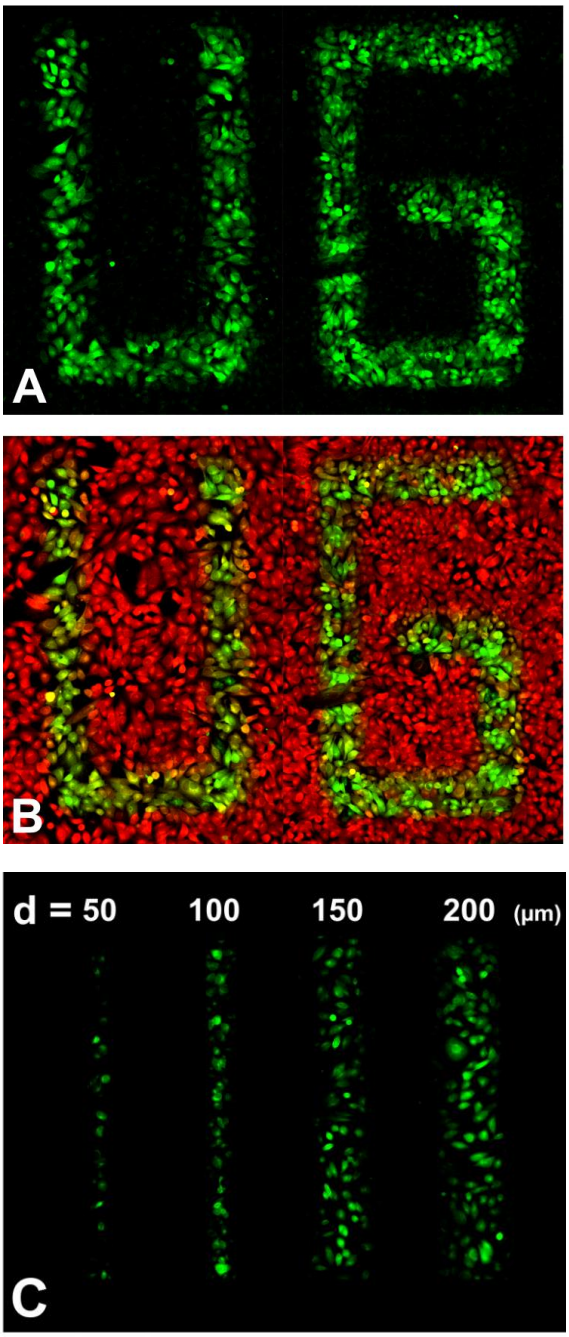

Figure 2: Spatial-selection delivery of QDs into live cells by VNBs inducing photoporation. A. Confocal image in green channel shows the QDs were selectively delivered into the cells in the patterned region by letters of 'U' and 'G' after VNBs inducing photoporation treatment with laser fluence of 2.08 J/cm^2. B. An image merged red channel of cell viable fluorescence of Calcein red AM with the channel of green fluorescence of QDs. C. Linearly patterned scanning the cell samples to estimate the delivery resolution of spatial selection by adjusted the laser beam size from 50 μm to 200 μm at a fixed laser fluence of 1.81 J/cm^2 The size of letters 'U' and 'G' in A and B is 800 μm by 400 μm.

Reference:

Xiong, R., Raemdonck, K., Peynshaert, K., et al., (2014), "Comparison of gold nanoparticle mediated photoporation: vapor nanobubbles outperform direct heating for delivering macromolecules in live cells," *ACS Nano*, 8(6), 6288-96

Nanoparticles functionalized with an antibody: toward an specific contrast agent of brain tumors by MRI

S. Richard[1], M. Boucher[2], A. Herbet[3], Y. Lalatonne[1], S. Mériaux[2], D. Boquet[3], L. Motte[1]
[1] Université Paris 13, Sorbonne Paris Cité, CSPBAT, UMR CNRS 7244,
74 Rue Marcel Cachin, 93017 Bobigny,France
[2] CEA, DSV, I[2]BM, NeuroSpin, Unité d'imagerie par IRM et de Spectroscopie (UNIRS),
Saclay, 91191 Gif-sur-Yvette, France
[3] CEA, DSV, iBiTec-S, SPI, Laboratoire d'Etude du Métabolisme des Médicaments (LEMM),
Saclay, 91191 Gif-sur-Yvette, France

Abstract: Endothelin receptors are clearly identified and related with initiation and progression of certain type of cancers[1]. Glioma, the most common primary brain tumor in humans, is associated with a deregulation of the endothelin axis, leading to an overexpression of endothelin B receptor (ETBR)[2,3]. Targeting glioma cells with the monoclonal antibody rendomab B1 (RB1) directed against ETBR[4], is a promising therapeutic strategy[5]. Antibodies are playing a central role as targeted therapeutics for oncological applications[6]. Concurrently, iron oxide nanoparticles (NPs) are promising tools for molecular imaging applications, including magnetic resonance imaging (MRI), exploiting their superparamagnetic behavior. This study aims to develop an experimental multimodal nanoplateform : iron oxide nanoparticles functionalized with a specific antibody and fluorescent probes for the diagnostic by MRI and the guided surgery.

In this project, iron oxide nanoparticles surface was directly coated with caffeic acid and functionalized with antibody. *In vitro* relaxometry measurements were performed to assess longitudinal r_1 and transverse r_2 relaxivities at 7 T. *In vivo* experiments were carried out on Swiss mice by acquiring T_2*-weighted images before and after intravenous injection of NPs and computing 3D angiograms to reveal vasculature enhancement.

We obtained the first imaging tracer based on iron oxide NPs functionalized with fluorescent dye-labelled RB1 antibody leading to a bi-modal contrast agent. This new tracer conserved the recognition properties for ETBR for both affinity and specificity and a fluorescent visualization was obtained with the functionalized NPs, as demonstrated by flow cytometry experiments. Additionnaly, the iron oxide nanoplatform exhibited highly efficient MRI contrasting properties to be detected in mouse brain when acquiring *in vivo* images at 7 T.

In conclusion, the main outcome of this work is a fully functional tracer targeting the membrane protein ETBR overexpressed in the glioma and playing a key role in the development of the tumors. This new generation of imaging tracer with a constraint nanometric size, as obtained here, leads the way to new promising therapeutic approaches to target glioma tumoral cells, and with a great potential to deeply enhance the detection threshold of small tumoral masses.

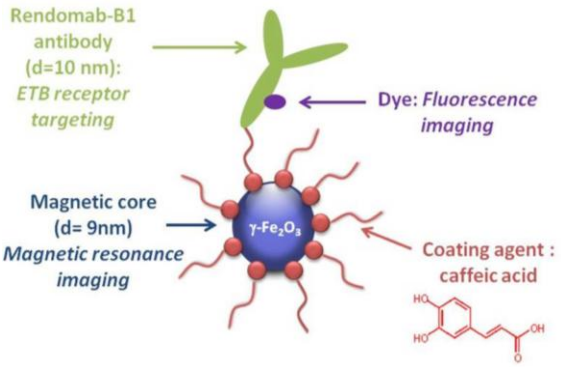

Figure 1: Multimodal Superparamagnetic nanoplatform functionnalized with antibody for dual imaging of brain tumors

References:

1. Bagnato A, Rosanò L. The endothelin axis in cancer. *Int J Biochem Cell Biol* 2008; **40**(8):1443-1451.
2. Paolillo M, Russo MA, Curti D, Lanni C, Schinelli S, et al. Endothelin B receptor antagonists block proliferation and induce apoptosis in glioma cells. *Pharmacol Res* 2010; **61**(4):306–315.
3. Montgomery J.P, Patterson PH, et al. Endothelin receptor B antagonists decrease glioma cell viability independently of their cognate receptor. *BMC Cancer* 2008; **8**:354-354.
4. Allard B, Wijkhuisen A, Borrull A, Deshayes F, Priam F, Lamourette P, et al. Generation and characterization of rendomab-B1, a monoclonal antibody displaying potent and specific antagonism of the human endothelin B receptor. *MAbs* 2013; **5**(1):56-69.
5. Maguire, J.J., Davenport, A.P. Endothelin@25 – new agonists, antagonists, inhibitors and emerging research frontiers: IUPHAR Review 12. *Br. J. Pharmacol*. 2014 in press doi:10.1111/bph.12874
6. Sliwkowski MX, Mellman I. Antibody therapeutics in cancer. *Science* 2013; **341**(6151):1192-1198.

Specificity and Sensitivity comparative study between phage PVP-S1 and monoclonal antibody as receptor in polydiacetylene vesicles for *Salmonella* colorimetric detection

T. V. de Oliveira[1,2*], N. de F. F. Soares[1], C. M. Carvalho[2,3], J. S. dos R. Coimbra[1], N. J. de Andrade[1], J. Azeredo[2,3], E. A. A. Medeiros[1], P. P. Freitas[2]

[1] University Federal of Viçosa, Department of food technology, Packaging laboratory, Viçosa, MG, Brazil.

[2] International Iberian Nanotechnology Laboratory, Braga, Portugal.

[3] Centre of Biological Engineering, University of Minho, Braga, Portugal.

Abstract: Polydiacetylene polymer (PDA) has been intensively studied because of its properties as colour change from blue to red and change from non-fluorescent to fluorescent form due to an external stimulus that lead to a reorientation of the PDA within the organized structure. External stimulus could be temperature, pH, solvent influence, bacteria presence, mechanical stresses and others (Oliveira *et al.*, 2012). Pires *et al.* (2010) support the hypothesis that such phenomena occurred due to conformational changes associated with the functional group rotation around the simple carbon-carbon bond present in PDA chains. When the backbones of PDA conjugated polymer chains are perturbed, the delocalized π-network induces changes in electronic absorption and emission properties (Huo *et al.*, 1999). For a particular colour change, it is possible to incorporate a compound in the polydiacetylene carboxyl groups that will work as a specific receptor for the bacteria detection. This technology can be used for the detection of pathogens and thus is important to avoid food contamination once the standard technology demands long time and people trained.

The selection of the receptor used in the PDA is the first critical step to develop a biosensor with improved selectivity, selectivity and stability. For this reason, the aim of this study was to make a comparative study between two recognition molecules: phage PVP-S1 (Santos et al., 2011) and a monoclonal antibody in the PDA sensor for the detection *of Salmonella*. Antibodies lack specificity, poor separation efficiency and sensitivity. Phages are extremely specific, withstand harsh environments, are economically and easily produced, show high stability during storage and thus present potential for bacterial detection. Overall the selection of the recognition molecule that show the best features is important to develop a simple and rapid sensor for the industry and consumer's life. The specificity of the sensor was proven by using *Staphylococus aures* and *Escherichia coli* as gram-positive and gram-negative controls, respectively.

Other controls as LB medium and with PDA were performed to ensure that the colour change did not occurred due to another external stimulus. Controls maintained the colour around blue (peaks in 640 nm) and upon *Salmonella* Enteretidis presence the colour changed to red (peaks in 540 nm) as verified by spectroscopic analysis. Colorimetric response was calculated as Charych *et al.* (1993) to quantify colour transition (Figure 1).

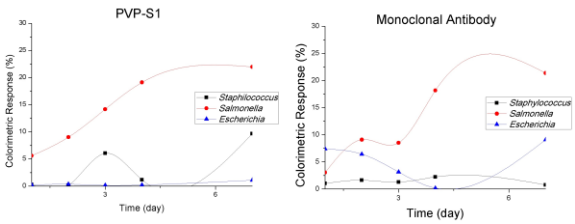

Figure 1: Colorimetric response obtained after the interaction of the different bacteria with with phage PVP-S1 (a) and antibody (b) as specific receptors in the PDA sensor

Monoclonal Antibody showed the highest colorimetric response and the PVP-S1 was more stable. Therefore both receptors improved the PDA sensor sensitivity and specificity and thus can be used as biorecognition molecules to the development of the PDA sensor.

Keywords: polydiacetylene vesicles, monoclonal antibody, *Salmonella* detection, phages, specificity, sensitivity.

References:

Oliveira, C. P. de; Soares, N. de F. F.; Fontes, E. A. F.; Oliveira, T. V. de; Maradini Filho, A. M. (2012). Behaviour of polydiacetylene vesicles under different conditions of temperature, pH and chemical components of Milk. Food Chem. 135, 1052-1056.

Huo, Q.; Wang, S.; Pissloup, A.; Verma, D.; Leblanc, R. M. (1999) Unusual chromatic properties observed from polymerized dipeptide diacetylenes. Chem. Com. 16, 1601-1602.

Pires, A. C. S.; Soares, N. de F. F.; Silva, L. H. M. da; Silva, M. C. H. da; Mageste, A. B.; Soares, R. F; Teixeira, A. V. N. C.; Andrade, N. J. de. (2010). Thermodynamic Study of Colorimetric Transitions in Polydiacetylene Vesicles Induced by the Solvent Effect. J. of Phys. Chem. 114, 13365-13371.

Charych, D. H.; Nagy, J. O.; Spevak, W. (1993) Direct colorimetric detection of a receptor-ligand interaction by a polymerized bilayer assembly. Scien. 261, 585-588.

Santos, S.; Kropinski, A.M.; Ceyssens, P.-J.; Ackermann, H.W.; Villegas, A.; Lavigne, R.; Carvalho, C.M.; Krylov,V.N.; Ferreira, E.C.; Azeredo, J. (2011). Genomic and proteomic characterization of the broad host range Salmonella phage PVP-SE1 - The creation of a new phage genus. Journal of Virology 85:21, 11265-11273

Nanoarchitectonics with Lipid and DNA Building Blocks: *In situ* Millisecond Time-Resolved SAXS Investigation

B. Angelov[1], A. Angelova[2,*], M. Drechsler[3], S. Lesieur[2]

[1]Institute of Macromolecular Chemistry, Academy of Sciences of the Czech Republic, Heyrovsky Sq. 2, CZ-16206 Prague, Czech Republic

[2]CNRS UMR8612 Institut Galien Paris-Sud, Univ Paris Sud 11, F-92296 Châtenay-Malabry, France

[3]Laboratory for Soft Matter Electron Microscopy, Bayreuth Institute of Macromolecular Research, University of Bayreuth, D-95440 Bayreuth, Germany

Abstract: Cubic lipid membranes are highly efficient for uptake of DNA building blocks (Angelov *et al*., 2013, Angelova *et al*., 2015). The kinetic pathway of self-association of neurotrophic plasmid DNA (pDNA) to cationic cubosomes was investigated by millisecond time-resolved small-angle X-ray scattering (SAXS) coupled to a rapid-mixing stopped flow device. Binding of pDNA to the nanochannel-type cationic lipid nanocarriers considerably modified the curvature of the lipid/water interfaces and led to the formation of onion-type lipoplex complexes. The ultrafast structural dynamics of the complexation and assembly of the lipid particles with pDNA building blocks was revealed thanks to the high brightness of available synchrotron X-ray source. Rapid mixing stopped-flow experiments, coupled to synchrotron SAXS on the subsecond timescale, produced a vast amount of experimental structural data. The purpose of this work is to present the key steps of the SAXS data treatment for the case of self-assembly and complexation of cationic lipid particles (vesicles or cubosomes) with plasmid DNA in the course of a rapid mixing stopped-flow process. This approach is significant for the structural analysis of rapidly forming soft-matter biomacromolecular delivery systems.

Keywords: soft nanoarchitectures, lipid bilayer building blocks, plasmid DNA, bicontinuous cubic mesoporous materials, self-assembled nanochannel networks, membrane curvature, time-resolved SAXS.

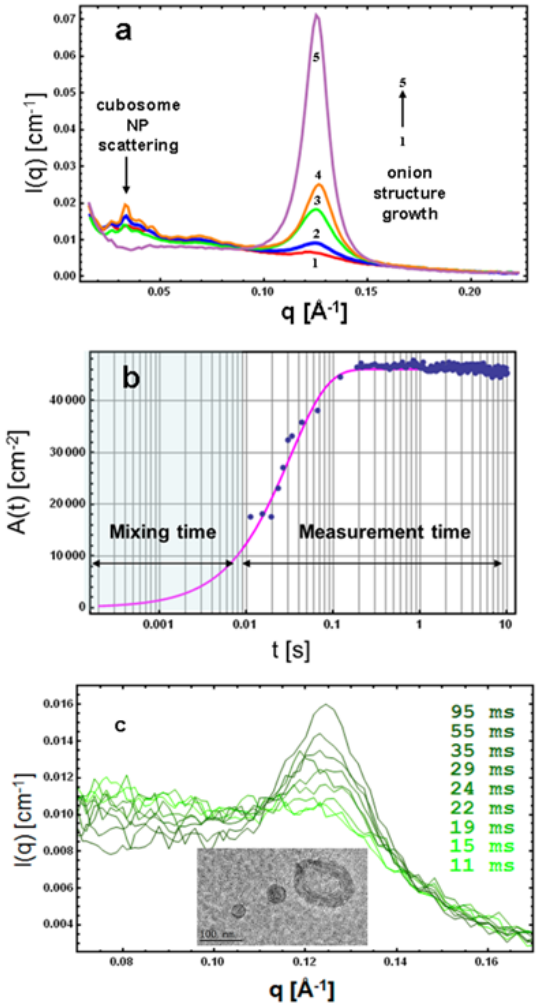

Figure 1: Plasmid DNA-driven transformation of nanochannel-type lipid carriers into tightly packed layered architectures involving compacted DNA macromolecules. (a) SAXS patterns showing that the curved lipid membranes in the cubosome nanoparticles are transformed, with the increase in the pDNA upload, into lower-curvature onion-membrane complexes encapsulating pDNA. (b) Kinetic dependence of the Bragg peaks intensity characterizing the pathway of the lipoplex formation. (c) Millisecond time-resolved SAXS patterns upon *in situ* monitoring of the lipoplex formation with a rapid-mixing stopped-flow device.

References:

Angelov, B., Angelova, A., Filippov, S. K., Narayanan, T., Drechsler, M., Štěpánek, P., Couvreur, P., Lesieur, S. (2013) DNA/fusogenic lipid nanocarrier assembly: Millisecond structural dynamics, *J. Phys. Chem. Lett*., 4, 1959−1964.

Angelova, A., Angelov, B., Mutafchieva, R., Lesieur, S. (2015) Biocompatible mesoporous and soft nanoarchitectures, *J. Inorg. Organomet. Polym.*, DOI: 10.1007/s10904-014-0143-8, In press.

A New Generation of Flower-Like Nanobiocatalyst for Superior Enzymatic Activity

Ismail Ocsoy 1, 2,*, Nalan Özdemir1, Burcu Somturk1
1Department of Chemistry, Faculty of Science, Erciyes University, Kayseri, 38039 Turkey
2Nanotechnology Research and Implementation Center (ERNAM), Erciyes University, Kayseri, 38039 Turkey

Abstract: Although several types of enzyme immobilization methods have been developed and used, enzyme activities were decreased or were not reached to satisfactory level yet compared to free enzymes. The activity enhancement has been remained unsolved problem till an encouraging discovery in synthesis of organic-inorganic flower shaped hybrid nanomaterial. Herein we report for the first time to the use of Fe^{2+} to form enzyme based hybrid flower shaped nano particles (HFNP) with superior catalytic activity and stability. In the project, the synthesis of HFNP was carried out by using horseradish peroxidase (HRP) as a model enzyme and Fe^{2+} metal ions as model ions. HRP, as an important enzyme, was selected for its unique properties such as wide catalytic activity, high sensitivity and common substrate specificity. HRP enzyme has been used in many areas as the removal of phenols from polluted waters, organic synthesis, biosensor design, and clinic and micro-analytic. Fe^{2+} metal ions was utilized for both reasons 1) they act as corner stones and main driving forces for the formation of HFNP and 2)it is known that even very low magnetic field has a positive effect on activity of HRP. Thus, we proved that the HFNP exhibited superior enzyme activity and stability due to several reasons such as high surface area of HFNP which does not result in significant mass-transfer limitations, cooperative effects due to nanoscale-entrapped HRP molecules, effective localized HRP concentration and unique shape effect. We demonstrated that the HFNP formed at +4°C in 10 mM PBS (pH 7.4) exhibited dramatically high catalytic activity towards guaiacol used as a model substrate. The HFNP only lost %2 of their initial activity within 30 days when the mixture of HFNP and substrate was stored at +4°C in 10 mM PBS (pH 6.8). In addition to that, we benefited from excellent activity performance of the HFNP, they were rationally and successfully used to oxidize dopamine molecule to colored quinone-type product

Keywords: Enzyme, hybrid nanoflower, activity measurement, metal ion and dopamine detectio

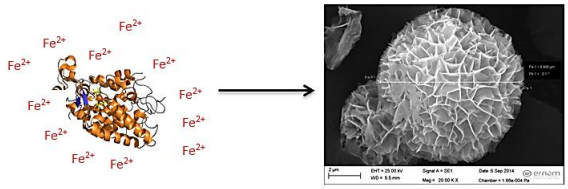

Figure 1: Figure illustrating the formation of organic-inorganic hybrid flower shape nano materials: Fe^{2+} ions incorporated horseradish peroxidase enzyme for the formation of nanoflower.

References:

Ocsoy, I., Gulbakan, B., Shukoor, M., Xiong, X., Chen, T., Powell, D. H., Tan, W. (2013) Aptamer-Conjugated Multifunctional Nanoflowers as a Platform for Targeting, Capture, and Detection in Laser Desorption Ionization Mass Spectrometry, ACS Nano. 7 417-427.

Ge, J., Lei, J., Zare, R. N. (2012) Protein–inorganic hybrid nanoflowers, Nature Nano. 7. 428–432

Somtürk, B., Kalın, R., Özdemir, N. (2014) Purification of peroxidase from red cabbage (Brassica oleracea var. capitata f. rubra) by affinity chromatography, App. Biochem. Biotechnol. 173. 1815–1828.

Porous nanoparticles entrapped pipette tips for sensitive detection of biomolecules

Chang Lei
Australian Institute for Bioengineering and Nanotechnology
The University of Queensland
Brisbane, QLD, Australia

Abstract: In recent years, nanomaterials with ordered pores have been widely used for biomolecules detection due to the properties of tuneable pore size, high surface area and easily surface modification. Particularly, the combinations of nanomaterial with some advanced techniques, such as mass spectrometer, ensure the accurate analysis of biomolecules.(Lei, Qian et al. 2013) However, the analysis of some low abundance biomolecules (e.g. insulin) in complex biological samples is still difficult. To solve the problem, a combo-pore approach utilizes materials with different pore sizes for sample pre-treatment has been developed for the sensitive detection of insulin. This advanced approach has been applied prior to mass spectrometer or enzyme linked immunosorbent assay (ELISA) to achieve better detection sensitivity in urine/serum.(Lei, Noonan et al. 2014, Qian, Zhou et al. 2014) Furthermore, a novel combo-pipette-tips (Figure) with different porous materials entrapped are developed as "smart" device for convenient pre-treatment. The application of nanoparticle entrapped pipette tips for sample pre-treatment has the advantages of simple operation and less sample loss. As both combo-pore approach and nanoparticle entrapped tips can be special designed for different targets, they are expected to hold great potential for application in the sensitive detection of various other biomolecules of commercial and clinical significance.

Keywords: nanomaterial, mesoporous, mass spectrometer, biomolecules, pipette tips, insulin, sensitive detection.

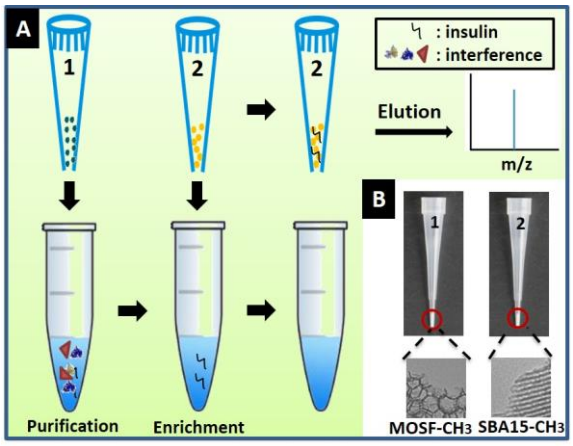

Figure Schematic illustration showing (A) the process of using combo-pipette-tips for insulin detection; (B) TEM images of fabricated tips with macroporous material MOSF-CH_3 (1) and mesoporous material SBA15-CH_3 (2).

References:

C. Lei., O. Noonan, S. Jambhrunkar, K. Qian, C. Xu, J. Zhang, A. Nouwens and C. Z. Yu (2014). "Sensitive Detection of Human Insulin Using a Designed Combined Pore Approach." *Small* **10**(12): 2413-2418.

C. Lei., K. Qian, O. Noonan, A. Nouwensa and C. Z. Yu (2013). "Applications of nanomaterials in mass spectrometry analysis." *Nanoscale* **5**(24): 12033-12042.

K. Qian., L. Zhou, J. Zhang, C. Lei and C. Yu (2014). "A combo-pore approach for the programmable extraction of peptides/proteins." *Nanoscale* **6**(10): 5121-5125.

Ultrasensitive magnetic particles/DNAzymes based biosensors for clinical applications

Stefano Persano[1,2,3], Giuseppe Vecchio[1], Paola Valentini[1], Pier Paolo Pompa[1]*.
[1] Istituto Italiano di Tecnologia, Center for Bio-Molecular Nanotechnologies@UniLe, Via Barsanti, 73010 Arnesano (Lecce), Italy.
[2] Università del Salento, Via Provinciale Monteroni, 73100 Lecce, Italy.
[3] Houston Methodist Research Institute, 6670 Bertner Avenue, Houston, 77030 Houston (TX), United States of America (USA)

Abstract: Traditional *in vitro* diagnostic is based on assays and procedures optimized for modern clinical laboratories, equipped with all the necessary instrumentation. However, these high-tech and costly tests are not suitable to address the current diagnostic challenges of preventive medicine, ultra-early diagnosis, and large-scale population screenings. To address these issues, innovative diagnostic tests need more simplified procedures, resulting in cheap, rapid, instrument-free analyses that can be performed also in non-specialized settings, at the point-of-care (POC). In this framework, we show here two hybrid strategies for the sensitive detection of Human Papilloma Virus (HPV) and RNases activity. HPV is a very important analytical target, due to its broad diffusion and clinically relevant association with cervical cancer. Generally, the main obstacle for developing simplified testing for nucleic acid targets is their rather low concentration in clinical samples that does not match the sensitivity of most common assays; usually, the target needs to be amplified by PCR (Polymerase Chain Reaction), which requires dedicated instrumentation. In this context, we developed a polymerase reaction free, low-cost and sensitive assay for the colorimetric detection of HPV, based on the use of a smart design exploiting magnetic microparticles, chimeric RNA/DNAzyme oligonucleotides, and double signal amplification (Fig. 1). This method allows obtaining a fast response with a detection limit of 10 pM, avoiding the amplification of the target via traditional PCR. On the other side, the detection of RNases activity has also great importance in a wide range of biomedical applications, including assessment of RNase contamination in molecular biology and screening of new antiviral drugs and RNase inhibitors. In this regard, we proposed a new versatile strategy that allows the detection of several classes of RNases with better sensitivity then existing assays. Our two-step approach consists of a DNA-RNA-DNA chimeric Hairpin Probe (cHP) conjugated to magnetic microparticles (MMP), a DNAzyme sequence and molecular beacons (see Fig. 2).
Our assays permit the detection of low amount of analyte by the use of an amplification step exploiting the catalytic activity of DNAzyme molecules. These characteristics, coupled with the small volume of samples needed by our approaches, make our assays suitable for future implementations, such as low cost Lab-On-a-Chip and high-throughput screening applications.

Keywords: HPV, DNAzymes, Magnetic microparticles, RNase, chimeric DNA-RNA.

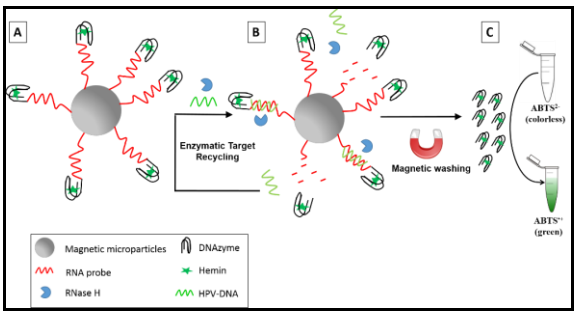

Figure 1: Schematic representation of the colorimetric detection platform based on RNase H-assisted target DNA recycling and generation of the colorimetric signal catalyzed by the peroxidase-mimicking DNAzyme. (A) DNAzyme-hemin complexes are immobilized onto magnetic microparticles (MMPs) via streptavidin-biotin interactions. (B) HPV DNA target recycling in the presence of RNase H. (C) DNAzyme-catalyzed oxidation of the ABTS substrate and generation of the colorimetric signal.

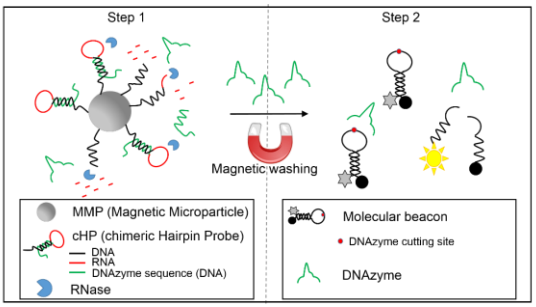

Figure 2. Schematic illustration of the two-step RNase assay. The DNA-RNA-DNA chimeric Hairpin Probe (cHP) is immobilized by biotin-streptavidin interaction onto Magnetic Microparticles (MMP) in order to obtain the MMP-cHPs complex. In the first step, the digestion of the RNA portion of cHPs by RNase allows the release of DNAzyme. After magnetic washing, the released DNAzyme is added to FAM/Dabcyl molecular beacon. In the second step, the catalytic activity of the DNAzyme on the molecular beacons generates fluorescence signal.

References:

- S. Persano, P. Valentini, J.H. Kim, and P.P. Pompa "Colorimetric detection of Human Papilloma Virus by double isothermal amplification" *Chem. Comm.* 49, 10605 (2013).
- S. Persano, G. Vecchio, and P.P. Pompa "A hybrid chimeric system for versatile and ultrasensitive RNase detection" (under review).

Immobilization of pyranose 2-oxidase onto functionalized electrospun regenerated cellulose ultrafine fibers: a novel heterogeneous catalyst

W. Panatdasirisuk,[1] T. Vongsetskul,[1,*] J. Sucharitakul,[2] P. Chaiyen,[3] P. Tangboriboonrat[1]
[1]Department of Chemistry, Faculty of Science, Mahidol University, Bangkok 10400 Thailand
[2]Department of Biochemistry, Faculty of Dentistry, Chulalongkorn University, Bangkok 10330 Thailand
[3]Department of Biochemistry and Center of Excellence in Protein Structure and Function, Faculty of Science, Mahidol University, Bangkok 10400 Thailand

Abstract: Pyranose 2-oxidase (P2O), catalyzing the oxidation of aldopyranoses and useful for sugar synthesis, was successfully immobilized onto electrospun regenerated cellulose (RC) ultrafine fibers with diamaters of 229 ± 42 nm. First, the electrospun cellulose acetate fibers were fabricated from 17% w/w CA (MW ~ 3 x 104 g/mol) with 5% w/w Tween 80 dissolved in mixed solvent of water (25% w/w) and acetic acid (75% w/w) at an applied voltage of 25 kV and a fiber collection distance of 10 cm. Then, the fibers were immersed into 0.5 M ethanolic potassium hydroxide solution to hydrolyze the CA fibers and obtain RC fibers, treated with glutaraldehyde to generate aldehyde groups on the fiber surface, and immersed in P2O buffer solution to immobilize it onto the RC fibers. Effects of the immobilization process on thermal stability and pH of P2O activity were investigated. Results indicated that P2O immobilized onto RC fibers tolerated the temperature changes and pH 2 better than the free P2O did, and the optimum pH for P2O and P2O-RC operation was 5.5 and 5, respectively. Therefore, P2O-immobilized RC fibers are potentially useful as a heterogeneous catalyst under the conditions in which free P2O could not endure.

Keywords: electrospinning; ultrafine fiber; enzyme immobilization; cellulose; pyranose 2-oxidase.

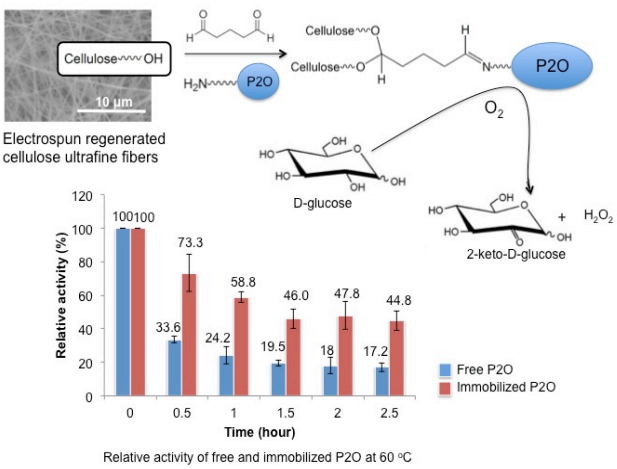

Figure 1: Pyranose 2-oxidases (P2O) were immobilized onto the electrospun regenerated cellulose ultrafine fibers (RC) and were used as catalyst in oxidation of D-glucose. P2O-RC shown better high temperature tolerance than that of P2O.

References:

Panatdasirisuk, W., Vongsetskul, T., Sucharitakul, J., Chaiyen, P., Tangboriboonrat, P. (2015), Functionalized electrospun regenerated cellulose fibers for immobilizing pyranose 2-oxidase, *React. Funct. Polym.,* 86, 47-51.

Srisook, T., Vongsetskul, T., Sucharitakul, J., Chaiyen, P., Tangboriboonrat, P. (2014), Immobilization of 3-hydroxybenzoate 6-hydroxylase onto functionalized electrospun polycaprolactone ultrafine fibers: A novel heterogeneous catalyst, *React. Funct. Polym.,* 82, 41–46.

Huang, X., Chen, P., Huang, F., Ou, Y., Chen, M., Xu, Z. (2011), Immobilization of Candida rugosa lipase on electrospun cellulose nanofiber membrane, *J. Mol. Cat. B: Enzymatic,* 70, 95-100.

Ultra-sensitive Silicon Nanowires for hormone detection

R. S. Forsyth, R. M. Bigham, M. A. Mohd Azmi[1], Z. Tehrani[1, 2], K. A. D. Walker[1, 2], and O. J. Guy[1, 2].
Centre for Nanohealth, College of Engineering, Swansea University, Singleton Park, Swansea, U.K.
Email: 652686@swansea.ac.uk

Abstract: From clinical diagnostics, explosive detection to biomarker detection, POC devices have many applications. Detecting biomarkers at low levels can lead to the detection of illness and disease earlier on, resulting in better prognosis. As more and more biomarkers are being discovered the need for the development of biosensors is becoming increasingly apparent. Salivary biosensors are particularly desirable as they exhibit many advantageous traits such as decreased sample preparation time whilst also limiting the need for more invasive procedures. The ability of semiconducting Silicon nanowires (SiNWs) to convey electrical signals along with their small, portable size and relatively low costs make them a desirable platform for the development of point-of-care (POC) biosensors. Here we demonstrate the fabrication process of SiNWs using a combination of electron beam lithography (EBL), ultraviolet (UV) lithography and Substrate Conformal Imprint Lithography (SCIL). The devices were patterned onto a 100 mm diameter silicon-on-insulator (SOI) wafer. This method is highly repeatable with a high-throughput patterning high quality nanostructures on a reduced timescale when compared to more traditional techniques of just EBL and UV lithography making the SCIL method more cost effective [1]. The SiNW devices made with this method were then functionalized to have amine groups attached using the electrochemical method of diazotization. Diazotization consists of the reductive grafting of the aryl salt diazonium to the sensor surface using cyclic voltammetry followed by the reduction of a nitro group to an amine group by chronoamperometry. As a result this presents an opportunity to attach of a bio-receptor of choice [2]. The devices were then biofunctionalized with an antibody against a hormone biomarker and a calibration was carried out for different hormone concentrations. The methods used for analyte detection were electrochemical impedance spectroscopy (EIS), cyclic voltammetry and simple I(V) measurement. The devices were compared to an ELISA to compare the limits of detection, both at the lowest concentration and at the concentration of saturation

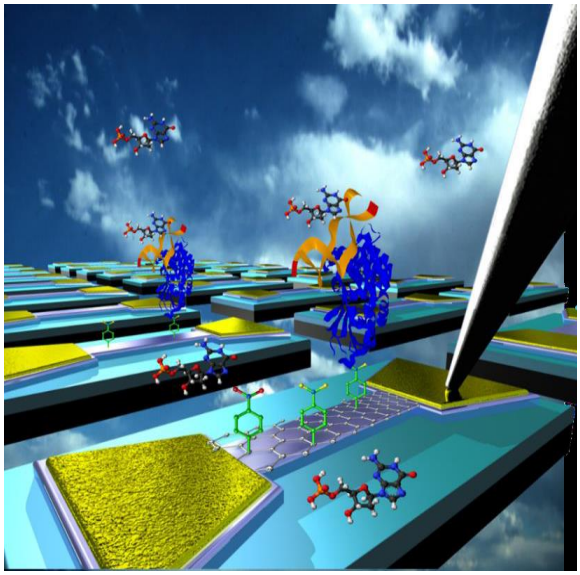

Figure 1: A schematic showing the functionalization of the SiNW surface using the diazotization method (reprinted from Mohd Azmi MA).

References:

1. Mohd Azmi MA, Tehrani Z, Lewis RP, Walker KAD, Jones DR, Daniels DR, et al. Highly sensitive covalently functionalised integrated silicon nanowire biosensor devices for detection of cancer risk biomarker. Biosensors & bioelectronics. 2014;52:216-24.

2. Guy OJ, Burwell G, Tehrani Z, Castaing A, Walker KA, Doak SH. Graphene nano-biosensors for detection of cancer risk. Heterosic & Wasmpe 2011. 2012;711:246-52.

Blocking Viral DNA Replication by Employing a Resonance Frequency Generated by Ag4O4 — A Real World Solution.

Presented by: Leigh J. Mack, MD, PhD
CIMTESES Foundation, Curacao

Abstract: Ag4O4 is a tetrahedral nanocrystalline silver particle that has been found to have some very specific attributes in inhibiting DNA polymerase and reverse transcriptase in several strains of viruses. It is believed that the virus to cell signalling prior to cell receptor contact is hindered. This signalling is disrupted by the outer ring electrons of Ag4O4 creating a small magnetic/charged field that disrupts the viruses from being able to make direct contact with receptor on the cell membrane or the phospholipid layer . The multiple valency property of the Ag4O4 particle is short multiple electrons in the outermost ring. This condition creates a gaining and losing of electrons at a rate that has been found to create a small magnetic field. This field can thus disrupt viral replication efficacy without damaging the surrounding cells of the body. The presentation shall include multiple studies with solid evidence of the efficacy of this particle against viruses along with information and studies of the safety level of this technology.

Keywords: Ag4O4, silver oxide, silver crystalline nano particle, frequencies for viral disruption, viruses, nanomedicine in practice.

Figure A: Figure illustrates the Ag4o4 tetrahedral structure and how it is a unique silver ion. Figure B illustrates the size and electron rings of the Ag4O4 nanoparticle. Figures are courtesy of American Biotech Labs, Inc.

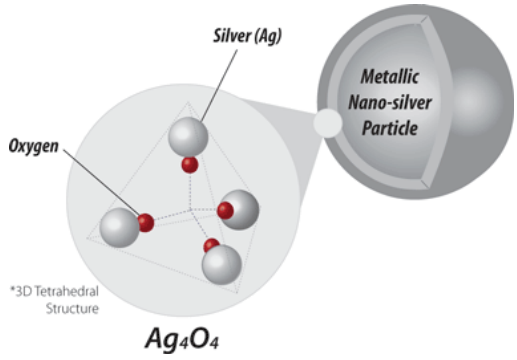

Figure A

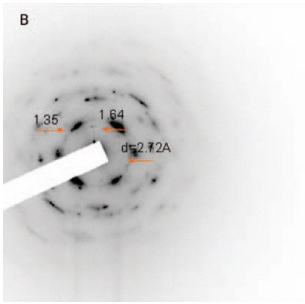

Figure B

References:

Mack, L. J. (2013) Nanomedicine - New approaches in neutralizing viruses at the cellular level, *J Stem Cell Res Ther* 2013, 3:5

Gonzalez, E. R. (2013) Formulary Clinical Review 23 PPM Silver Hydrogel Wound Dressing Gel 84:04.16 Misc. Local Anti-Infectives, Marshall University School Of Medicine.

Synthsis and cytocompatability of functionalized multi-walled carbon nanotubes derivatives

Ahmed A. Haroun
National Research Center, Chemical Industries Research Division, 12622 Dokki, Cairo, Egypt

Abstract: Innovative functionalized multi-walled carbon nanotubes (MWCNTs) are emerging tool in the nanobiotechnology applications. However, thier toxic effects on environment and health have become an issue of strong concern. In the present study, we address the impact of functionalized MWCNTs on different cell lines such as: normal melanocytes (HFB4), liver carcinoma (HEPG2) and breast carcinoma (MCF7). Moreover, the prepared nanomaterials were characterized using different analytical tools; Fourier transform infrared spectroscopy (FTIR), X-ray diffraction patterns (XRD), differantial scanning calorimetry (DSC), scanning and transmission electron microscopes (SEM and TEM). The results showed that most of the functionalized MWCNTs exhibited low cytotoxic effects in comparison with the unfunctionalized ones.

Keywords: nanobiotechnology, multi-walled carbon nanotubes, cytotoxicity, cell growth, cell adhesion, grafting copolymerization.

Acknowledgment: This work was a part from the project which financially supported by National Research Center, Cairo, Egypt.

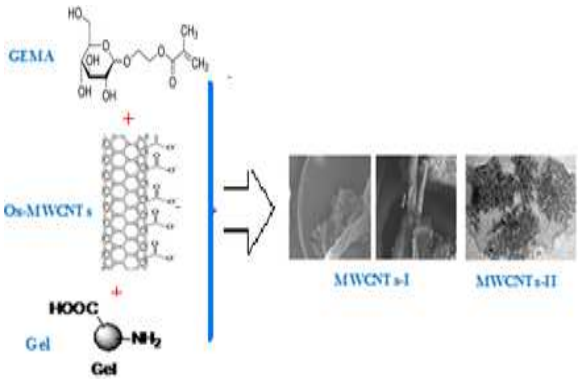

Figure 1: illustrating schematic representation of the prepared functionalized multi-walled carbon nanotubes using (Gel) gelatin and 2-glycosyloxyethyl methacrylate (GEMA).

References:

Haroun, A.A., Taie, H.A. (2014), Characterization and *in vitro* cytotoxicity study of functionalized carbon nanotubes using ß-cyclodextrin, *Macromol Symposia* 337, 25-33 .

Haroun A.A., Abo-Zeid, M.A., Youssef, A.M., Gamal-Eldeen, A.M. (2013), *In vitro* biological study of gelatin/PLG nanocomposite using MCF-7 breast cancer, *J. Biomed Mater Res A.*, 101A**,** 1388-1396 .

Yuan S., Xiong, G., Roguin, A., Choong, C.(2012), Immobilization of gelatin onto poly(glycidyl methacrylate)-grafted polycaprolactone substrates for improves for Improved cell-material interactions, *Biointerphases* 7, 30.

Marshall, M.W., Popa-Nita, S., Shapter, J.G. (2006), Measurement of functionalized carbon nanotubes carboxylic acid groups using a simple chemical process, *Carbon* 44, 1137.

Skehan, P., Storeng, R.et al. (1990), New colorimetric cytotoxicity assay for anti-cancer drug screening, *J. Natl. Cancer Inst.* 82, 1107.

Development of high sensitive devices using optical tweezers and diamond nanocrystals

J. R. Maze[1,*], N. Figueroa[1], R. Gonzalez[1], N. Casanova[1],V. Waselowski[1], F. Sazunic[1], A. Chandía[2], F. Morales[3], L. Martinez[1], C. Wilson[4], A. Álvarez[2], M. Kogan[3]
[1]Institute of Physics, Pontificia Universidad Catolica de Chile, Santiago, Chile
[2]Faculty of Biological Sciences, Pontificia Universidad Catolica de Chile, Santiago, Chile
[3]Faculty of Chemistry and Pharmaceutical Sciences, University of Chile, Santiago, Chile
[4]Department of Biochemistry and Molecular Biology, University of Chile, Santiago, Chile

Abstract: The development of high sensitive detectors at the nanoscale is of crucial importance for understanding the dynamics of individual biological specimens such as proteins or analytes and the subsequent implementation of protocols in molecular diagnoses and early disease detection. Here we report recent progress in studying the mechanical properties of DNA aptamers related with the red tide using optical tweezers. We have constructed a macromolecule consisting of a lambda DNA sleeve – DNA aptamer – lambda DNA sleeve. By attaching functionalized dielectric microspheres to both ends of this macromolecule we study its mechanical properties using a multiple-trap home-built optical tweezers. For generating multiple traps we used a two-acousto optical deflector in x-y configuration able to switch from trap to trap in less than a microsecond. Each dielectric particle is trapped by intermittently by switching the trap on each particle creating a trapping potential on average. The force applied to the macromolecule is measured by a quadrant photodiode. In addition, we report the development of a device based on diamond nanocrystals able to read the concentration of proteins/analytes or reading the properties of a fluid. We use the optical response to external perturbations, such as magnetic and electric fields, of nitrogen-vacancy color centers in diamond nanocrystals (Maze *et al.*, 2011) to monitor in real time the concentration of analytes and fluid properties. We functionalized the surface of nanocrystals with ad-hoc ligands such as peptide CLPFFD to enhance the affinity to specific analytes such as toxic aggregates of A-beta protein. The effective change of surface charge at the surface of nanocrystals changes the properties of color centers such as their fluorescent spectra and spin coherence that we monitor using a home-built confocal microscope and microwave spectroscopic techniques such as Ramsey and echo spectrocopy.

Acknowledgements: we acknowledge support from CONICYT Associative Investigation Program (PIA) grant No ACT1108 – Nanobiotec.

Keywords: aptamers, optical tweezers, diamond nanocrystals, color centers, ligand/analyte interaction.

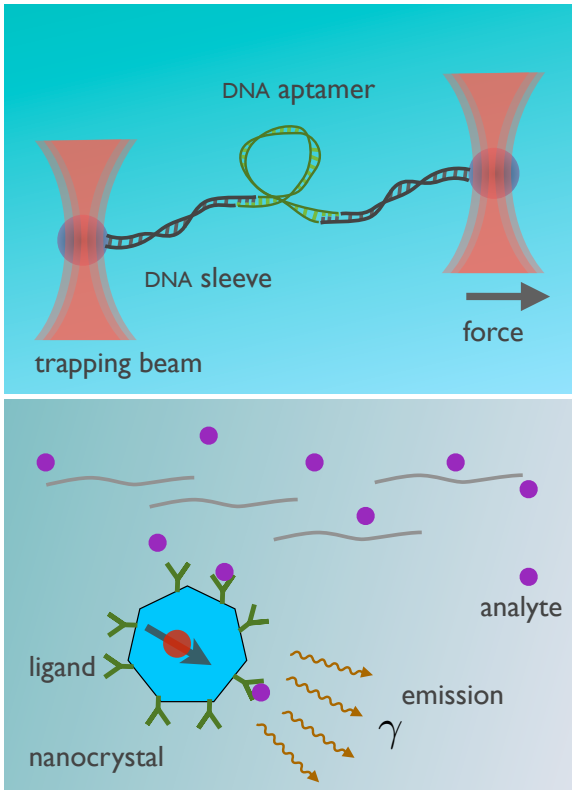

Figure 1. Top: illustration of the optical tweezers configuration to study DNA aptamers. A particular termination of DNA sleeve has been used to attach a DNA-aptamer at both ends. Each DNA sleeves is attached to dielectric microspheres trapped by a multiple trap optical tweezers. Bottom: illustration of the device using surface functionalized diamond nanocrystals. By observing the emission of color centers in the nanocrystal we infer the concentration of analyte in the fluid.

References:

Maze, J. R., Gali, A., Togan, E., Chu, Y., Trifonov, A., Kaxiras, E., and Lukin, M. D. (2011), Properties of nitrogen-vacancy centers in diamond: the group theoretic approach, *New J. Phys.* **13**, 025025.

Maze, J. R. et al. (2008), Nanoscale magnetic sensing with an individual electronic spin in diamond, *Nature* **455**, 644-647.

Versatile and easy to fabricate advanced surfaces to enhance the performance of DNA microarray detection

M.J. Bañuls,[1,*] D. González-Lucas,[1] R. Puchades,[1] A. Maquieira[1]
[1] IDM, Department of Chemistry, Universitat Politècnica de València, Valencia, Spain

Abstract: Nature shows us the capability of micro/nanostructured surfaces to become into water-repellant surfaces, a phenomena known as *lotus effect*, because it is observed in lotus leaves (Dawood et al. 2011). Advances in nanotechnology, including micro/nanoelectromechanical systems (MEMS/NEMS) have stimulated the development of new materials directed at artificially replicating such biomimetic surfaces for applications such as self cleaning, antifogging surfaces, humidity control for electronics devices, etc (Celia et al. 2013). But, most of the described methods are costly, and require specific equipments, or harsh conditions, being difficult to use them on many fields, specially those related to the biological field.

Regarding DNA detection, the microarraying of nucleic acids (NA) on solid supports has become an area of fundamental interest (Sassolas, Leca-Bouvier, and Blum 2008). Microarrays are an alternative to homogeneous assays because they allow easy continuous monitoring and miniaturization. Thus, they have been used in clinical diagnosis and environmental monitoring, among many other applications.

However, enhance the performance of microarray technologies in issues such as sensitivity, and specificity, remains still a challenge that can be hardly solved using conventional surface chemistries.

In this work, we hypothesised that to consider the material, the surface, the probe attachment and target recognition in an holistic manner; and combine it with superhydrophobicity/superhydrophilicity surface modulation, can drive to the design of advanced microarrays with improved performance. For that, we functionalised glass slides with a micro/nanoporous polymer employing a modification of the procedure described recently by Levkin (Feng et al. 2014). Then, the polymer was modified by organosilane chemistry, and thiolated NA probes were covalently attached to the surface by thiol-ene click chemistry, to create superhydrophilic domains. The rest of the surface was derivatized to reach superhydrophobicity. The microarray created in that way was evaluated by hybridization assays with the fluorescence labelled anti-probe, and compared to other conventional microarray surfaces. Our results show that the holistic consideration increases up to 5fold the signal observed after the hybridisation, compared to standard microarrays. These high performance microarrays could have potential application in fields where high sensititvity is required, such as microRNA detection.

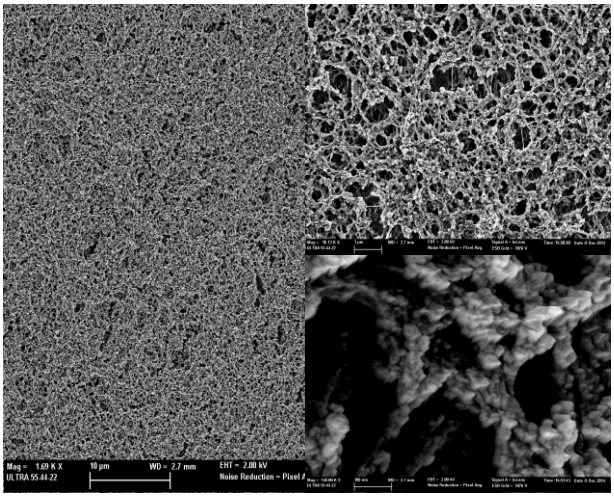

Keywords: micro/nanoporous surfaces, nucleic acid detection, microarray, thiol-ene click chemistry, holistic surfaces.

Figure 1: FESEM images at different magnifications of the micro/nanoporous polymer employed to develop the high performance microarray.

References:

M. K. Dawood et al., "Mimicking Both Petal and Lotus Effects on a Single Silicon Substrate by Tuning the Wettability of Nanostructured Surfaces," *Langmuir* 27, no. 7 (2011): 4126–33.

Elena Celia et al., "Recent Advances in Designing Superhydrophobic Surfaces," *Journal of Colloid and Interface Science* 402 (2013): 1–18.

Audrey Sassolas, Béatrice D Leca-Bouvier, and Loïc J Blum, "DNA Biosensors and Microarrays.," *Chemical Reviews* 108, no. 1 (January 2008): 109–39.

Wenqian Feng et al., "Surface Patterning via Thiol-Yne Click Chemistry: An Extremely Fast and Versatile Approach to Superhydrophilic-Superhydrophobic Micropatterns," *Advanced Materials Interfaces* 1, no. 7 (October 15, 2014).

DNA detection using Si-nanosandwich

A. Chernev[1], N. Bagraev[2], L. Klyachkin[2], A. Emelyanov[1], M. Dubina[1]
[1] St. Petersburg Academic University – Nanotechnology Research and Education Centre RAS, 8/3 Khlopin str., St. Petersburg 194021, Russia
[2] Ioffe Physical-Technical Institute of the Russian Academy of Sciences, 26 Polytechnicheskaya str., St. Petersburg 194021, Russia

Real-time amplification and detection of nucleic acid has given rise to the development of life science research and molecular diagnostics. These methods became a basis of the techniques that are applied for express detection and quantification of small amounts of nucleic acid and have a wide array of applications. However these techniques for real-time detection of nucleic acid require precision optics as well as fluorescently labelled sequence-specific probes or fluorescent dyes for DNA labelling. Therefore this is a huge disadvantage of such techniques due to the indirect oligonucleotides signal collection. Several attempts have been made to resolve this problem.

Recently, a semiconductor-based nucleic acid sequencer that uses the pH-sensing capability of ion sensitive field effect transistors (ISFET) has been demonstrated[1]. Another device that is able to amplify and simultaneously detect DNA using embedded heaters, temperature sensors and ISFET sensor arrays appears to be also very effective[2]. The most important result of the works mentioned was to provide the amplification and the detection simultaneously. Nevertheless, despite the development of an ISFET technology[3], there are still challenges that cannot be met with it. Since the principle of an ISFET-based sensor is the pH sensing mechanism that is not target-specific, this leads to the most crucial disadvantage of it.

Here we present a new method of oligonucleotides detection by the excitation of their self-resonant modes that correspond to the unique combination of the nucleotide sequence and the whole molecular shape.

Therefore the method suggested to detect the oligonucleotides is based on the interaction of Silicon nanosandwich with nucleic acids deposited on its surface. This Silicon nanosandwich represents the ultra-narrow p-type Silicon quantum well, confined by the delta barriers heavily doped with Boron on the n-Si (100) wafer. The edge channels of this QW have been shown to be effective source of THz emission[4], [5]. In order to enhance the selective THz line emission, the corresponding system micro cavities is inserted in the plane of QW. Such devices allow the creation of the THz spectra that are close to oligonucleotides self-resonant modes. Thus, the self-resonant modes excitation of oligonucleotides deposited in the QW plane becomes possible, with provided by feedback giving rise to the changes in the conductance of edge channels.

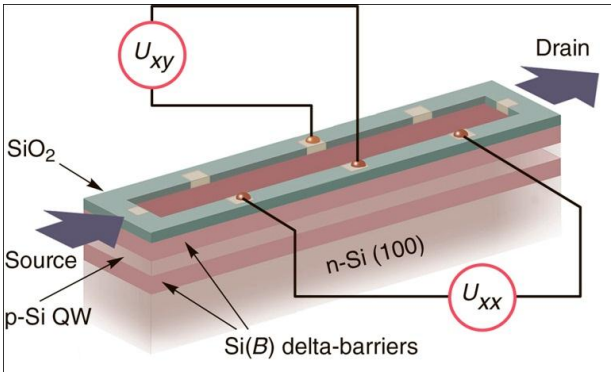

Figure 1: Silicon nanosandwich that represents the ultra-narrow silicon quantum well of the p-type Si confined by the delta-barriers heavily doped with boron on the n-type Si (100) wafer.

Keywords: DNA detection with semiconductor device, THz pumping, silicon nanosandwich, short oligonucleotides detection.

References:

Jonathan M. Rothberg et al., (2011) An integrated semiconductor device enabling non-optical genome sequencing, Nature, Vol. 475.

Toumazou C. *et al.* (2013) Simultaneous DNA amplification and detection using a pH-sensing semiconductor system, *Nat. Methods* 10, 641–646.

I Lundstrom, M S Shlvaraman, C S Svenson and L Lundkvlst, (1975) Hydrogen-sensltlve MOS field effect transistor, Appl Phys Lett 26, 55 – 57

N.T. Bagraev, L.E. Klyachkin, A.A. Kudryavtsev, A.M. Malyarenko, V.V. Romanov, (2010) Superconductor Properties for Silicon Nanostructures. In “Superconductor”, edited by A. Luiz, SCIYO, chap.4, p.p. 69-92.

N.T. Bagraev, L.E. Klyachkin, A.M. Malyarenko, B.A. Novikov (2007) Infrared and theraherz nanoelectronic devices for biology and medicine // Innovations Vol. 12 (110), C. 99-104.

DNA Sensing at femtomolar level using microfluidic electro-chemical cell: advantages of carbon-based transducers

B. Zribi,[1,2,*] H. Korri-Youssoufi,[2] A. Ouerghi,[1] A. Cavanna,[1] A. Madouri,[1] A-M Haghiri-Gosnet[1]
[1]Laboratoire de Photonique et de Nanostructures, LPN UPR20, CNRS, route de Nozay, 91460 Marcoussis, France
[2]ICMMO, UMR-CNRS 8182, Bât 420, University Paris-Sud, 91405 Orsay, France

Abstract: The development of extremely sensitive, highly selective, simple, robust and yet inexpensive biosensing platforms is essential for a wide range of applications, including clinical diagnostics, environmental monitoring and food safety testing. Since accurate diagnostics need specific detection of very small amounts of DNA, there is a need to develop simple label-free DNA hybridization platforms without extensive sample pretreatments able to detect very low concentration below the femtomolar.
Microfluidics for the manipulation of small volumes of biological fluid is a tool of choice that allows multiplex analyses in independent micro-channels. Electrochemical detection appears as a gold start method for biosensors development since it gives direct sensitive measurement in real sample and is fully compatible with handheld systems (Miodek *et al*, 2013). Pairs of electrodes can be simply integrated into microchannels using conventional lithography processes (Faure *et al*, 2014; Méance *et al*, 2014). These electrochemical fluidic devices can thus be connected to handheld electronic readers giving access to portability and facility for their application in point of care system in diagnostic.
We report a microfluidic-multiplexed platform that integrates several electrochemical cells with a reduced volume at one hundred nanoliter scale capable of achieving ultra-sensitive direct electrochemical detection of DNA. Our approach is based on the localized immobilization of DNA on carbon nanotubes in each microfluidic chamber by the electrochemical patterning method. Introduction of redox marker such as ferrocene between the biological receptor and the MWCNTs transducer allows to measure the charge transfer through current of redox signal. The hybridization reaction of immobilized single strand sequence from Hepatitis C virus and their complementary target (HCV virus) is used as biological model. We demonstrate that this hybridization reaction in the confined space of the fluidic microchamber improves the sensitivity of the signal. Electrochemical DNA sensing in such microfluidic device allows direct detection at 0.1 femtomolar level. Compare to a bulk electrochemical cell featuring an identical biosensor and displaying a limit of detection of 1 picomolar, it corresponds to a decrease with four orders of magnitude. Comparison of NTCs with other promising carbon-based transducer materials, such as epitaxial graphene multilayers and reported CVD graphene bilayers will be reported. We envision that this microfluidic approach will find useful future applications in the field of biosensing for practical devices for biology, medicine and environment.

Keywords: DNA, direct electrochemical sensing, microfluidic plateform, detection limit, carbon nanotubes, ferrocene, biomedical applications.

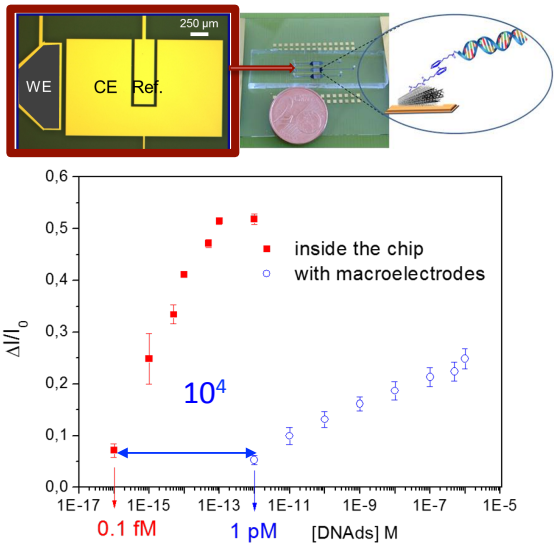

Figure 1: Top view of the fluidic chip with 3 independent microchannels and the electrochemical response as function of DNA concentration.

References:

Miodek, A; Castillo, G.; Hianik, T.; Korri-Youssoufi H. (2013) Electrochemical Aptasensor of Human Cellular Prion Based on Multiwalled Carbon Nanotubes Modified with Dendrimers: A Platform for Connecting Redox Markers and Aptamers, *Anal. Chem.*, 85, 7704−7712

Faure, M.; Pallandre, A.; Chebil, S.; Le Potier, I.; Taverna, M.; Tribollet, B.; Deslouis, C.; Haghiri-Gosnet, A-M.; Gamby, J.; (2014) Improved electrochemical detection of a transthyretin synthetic peptide in the nanomolar range with a two-electrodes system integrated in a glass/PDMS microchip, *Lab Chip* ,14, 2800-2805

Méance, S.; Gamby, J.; Faure, M.; Kou, Q.; Haghiri-Gosnet, A-M. (2014), Electrochemiluminescence on-a-chip: towards a hand-held electrically powered optofluidic source, *Talanta*, 129, 150-154

Selection of peptide motifs for the detection of small molecules in biotechnological applications

C. Di Natale[1,2], C. Cosenza[1], P.L. Scognamiglio[1], E.Battista[1], F. Causa[1,2,3] and P.A.Netti[1,2,3]

[1]Center for Advanced Biomaterials for Healthcare@CRIB, Istituto Italiano di Tecnologia (IIT), Largo Barsanti e Matteucci 53, 80125 Naples, Italy
[2]Department of Chemical and Materials Engineering and Industrial Production, University of Naples 'Federico II', Naples, Italy.
[3]Interdisciplinary Research Centre on Biomaterials (CRIB), University "Federico II", Piazzale Tecchio 80, 80125 Naples, Italy

Abstract: Mycotoxins are fluorescent low-molecular-weight natural products produced as secondary metabolites by fungi in milk and dried fruits.These metabolites are chemical stable molecules that cause disease and death in human beings (Bennet *et al*.,2003). Control strategies are therefore necessary for any food where such toxins could be presented . Current analytical determination includes immuno- and bio-luminescent assays, HPLC (fluorescence detection), TLC, gas and liquid chromatography coupled to mass spectroscopy (Rai *et al*., 2012). However all of them present high costs and skilled quality control operators.

Our idea is to develop a peptide-based biosensor for fluorescence detection in a sensitive, specific and unsophisticated manner. To this aim a integrated approach has been developed to select specific peptide motif to capture aflatoxins. On one side it has been conducted through computation modeling using a Cdocker alghoritm to determine the Binding energy of all possible peptide combinations against Aflatoxin, using as building blocks eight different amino-acids chosen by considering their different chemical properties. On the other, from combinatorial peptide libraries obtained with the same building blocks best Aflatoxin binders were selected by SPR (Surface Plasmon Resonance). In figure 1A in according to docking and SPR analysis, an example of best binder sequence of Aflatoxin M1 is reported.

Peptides sequences selected by proposed approach can be easly integrated in microparticles or covalently attached on microfabricated surfaces, opening the rout towards a direct detection of aflatoxins in small volume both in liquid and solid environments.

An example of selected peptide conjugated on Polystirene-PEG beads for the fluorescence detection of Aflatoxin M1is reported in figure 1C.

Proposed approach is also applicable to other small molecules or contaminat whose sensitive detection is indispensable for food, biochemical or medical applications.

Keywords: Mycotoxins, Peptide Library, Molecular Docking, Polymeric microparticles, Material Functionalization.

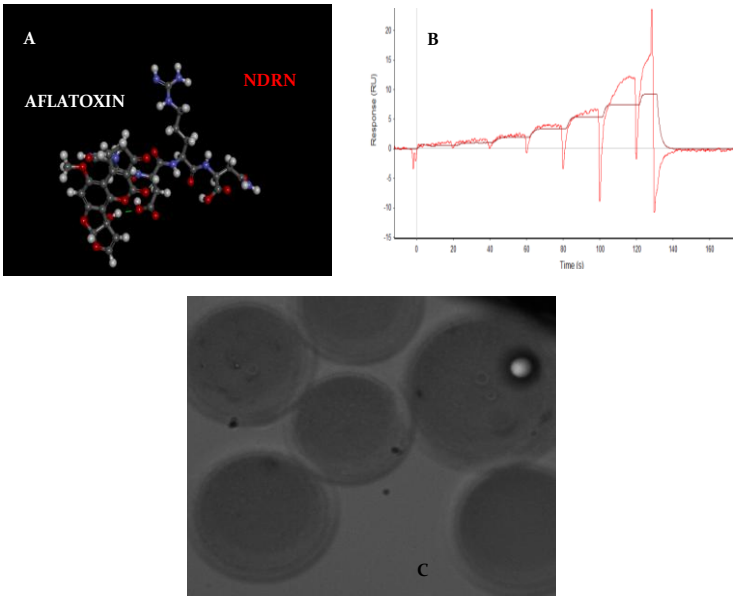

Figure.1:Docking (A) and SPR (B) results of the best Aflatoxin M1 binding peptide sequence. (C) Example of selected peptide conjugated on Polystirene-PEG beads for the fluorescence detection of Aflatoxin M1.

References:

Bennet J.W. and Klich M. (2003) Mycotoxins, *Clinical Microbiology Reviews*.

Rai M.K., Bonde S.K., Ingle A.P. and Gade A.K. (2012) Mycotoxin: rapid detection, differentiation and safety, *Journal of Pharmaceutical Education and Research*.

Wu, G.; Robertson, D. H.; Brooks, C. L. III and Vieth, M. (2003) Detailed Analysis of Grid-Based Molecular Docking: A Case Study of CDOCKER - A CHARMm-Based MD Docking Algorithm, *Journal of Computational Chemistry*.

Covalent functionalization of SWNT with Ciprofloxacin for enhancing its antibacterial activity

M. Assali,[1*] F. Abdallah,[1] R. Khayyat,[2] A.N. Zaid[1]
[1]Department of pharmacy, Faculty of Medicine & Health sciences, An Najah N. University, Nablus, Palestine.
[2]Department of biomedical sciences, Faculty of Medicine & Health sciences, An Najah N. University, Nablus, Palestine.
Email: m.d.assali@najah.edu

Abstract: Despite the modern medicinal chemistry in designing new therapeutic agents by using different new innovative techniques in molecular modeling and combinatorial chemistry, beside to their expensive cost, infectious diseases continue to be one of the greatest health challenges worldwide (Cohen, M. L., 2000). The main disadvantages for conventional antibiotics are the development of multiple drug resistance and adverse side effects. Recent advancement in nanoscience and nanotechnology has expanded our ability to design and construct nanomaterials with targeting, therapeutic, and diagnostic functions (Cheon, J., et al. 2008; Huang, W. C., et al. 2008). Among nanotechnology-derived materials, carbon nanotubes (CNTs) have stimulated a great interest for biomedical applications because of their unique mechanical, electrical, thermal and spectroscopic properties (Liu, Z.; et al. 2009). Nevertheless, advances in these directions have been hampered by the insolubility of CNTs in most solvents, and most importantly in water where they exist as ropes and large bundles. To overcome these problems we have recently development various approximations for the water solubilzation of SWCNTs (Assali, M. et al.; 2009, 2010).

So, here we aim to develop a new nano-antibiotic based on carbon nanotubes by functionalizing them covalently with Ciprofloxacin antibiotic and proposing that the large surface area of CNT and/or this new nan-prodrug will prevent the bacteria to throw them out once they penetrate the membrane, figure 1.

In the present communication, the following points will be discussed: (i) the modular synthetic strategies developed for the synthesis of the nanoconjugate, (ii) the characterization of the formed nanoantibiotic by various analytical techniques like AFM, UV-Vis, FTIR, TGA, and (iii) the ability of the prepared nanosystems to specifically attack different types of bacteria.

Keywords: nanoantibiotics, carbon nanotubes, ciprofloxacin, bacterial infection.

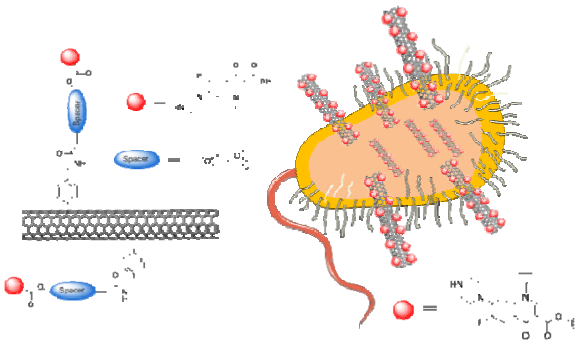

Figure 1: Figure illustrating the covalent functionalization of SWCNT with ciprofloxacin antibiotic (left), the right figure demonstrates the entrance of SWNT-cipro inside the bacteria.

References:

Cohen, M. L. (2000) *Nature*, 406, 762–767.
Cheon, J.; Lee, J. H. (2008) *Acc. Chem. Res.*, 41, 1630–1640.
Huang, W. C.; Tsa, P. J.; Che, Y. C. (2007) *Nanomedicine*, 2, 777–787.
Liu, Z.; Tabakman, S.; Welsher, K.; Dai, H. (2009) *Nano Res.*, 2, 85−120.
Assali, M.; Pernia Leal, M.; Fernandez, I.; Baati, R.; Mioskowski, C.; Khiar. N. (2009) *Soft Matter*, 5, 948.
Assali, M.; Pernia Leal, M.; Fernandez, I.; Baati, R.; Khiar. N. (2010) *Nano Res.*, 3, 764-778.

High-aspect ratio nanostructures for cellular applications

N. Buch-Månson,[1] S. Bonde,[1] K.R. Rostgaard,[1] J. Bolinsson,[2] J. Nygård,[2] K.L. Martinez[1,*]
[1] Nano-science Center and Department of Chemistry, Univ. Copenhagen, Denmark
[2] Nano-science Center and Center for Quantum Devices, Niels Bohr Institute, Univ. Copenhagen, Denmark

Abstract: The endeavour of exploiting arrays of vertical one-dimensional nanostructures for cellular applications is experiencing a pronounced surge of activity (Bonde *et al.* 2014). The interest is rooted in the intrinsic properties of high-aspect-ratio nanostructures.
With a height comparable to a mammalian cell, and a diameter 100-1000 times smaller, arrays of nanostructures can be interfaced in various ways with cells and are thereby suitable for various applications spanning from transfection of cells to monitoring of intracellular signals. Each of these applications requires a particular interface of nanostructures with living cells, which can be achieved by tuning the nanotopography of the surface (diameter, length and density).
In this communication, we will present a theoretical model of cell settling of arrays of nanostructures allowing the rational design of a suitable nanotopography for the application foreseen (Buch Månson *et al.* submitted). After validating the model experimentally, we will present a study behaviour on arrays of nanostructures and evaluate the effect of the nanotopography on their adhesion, migration and proliferation (Berthing *et al.* 2011, Berthing *et al.* 2012, Bonde *et al.* 2013). The study was performed using ordered arrays of vertical InAs nanowires and the throughput of the systematic cellular studies was facilitated by the design of multidensity nanowire arrays exhibiting 6 different types of nanotopography on a singe chip. We demonstrated that arrays of InAs nanowires provide a cell-promoting surface, which affects both cell division and focal adhesion up-regulation. Furthermore, a systematic variation in NW spacing affects both the detailed cell morphology and adhesion properties.

Keywords: nanowire, nanostructure, nanopillars, nanotopography, live cell biosensing.

A

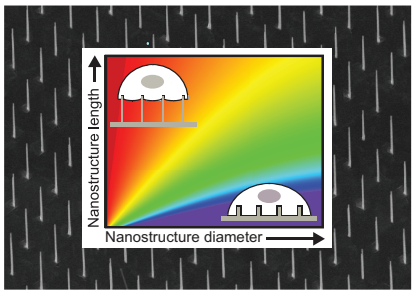

B

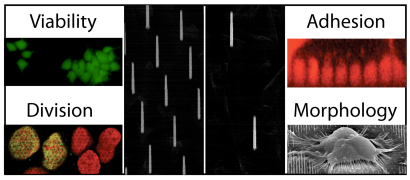

Figure illustrating the influence of nanostructure topography on cell settling (A), and cell behavior on various nanotopgraphies (B).

References:

Berthing, T., Bonde, S., Utko, P., Sørensen, C.B., Nygård, J., Martinez, K.L. (2011) Intact mammalian cell function on semi-conductor nanowire arrays: new perspectives for cell-based biosensing, *Small,* 7(5), 640-647

Berthing, T., Bonde, S., Rostgaard, K.R., Madsen, M. H., Sørensen, C.B., Nygård, J., Martinez, K.L. (2012) Cell membrane conformation at vertical nanowire array interface revealed by fluorescence imaging, *Nanotechnology,* 23, 415102

Bonde, S., Berthing, T., Madsen, M. H., Andersen, T. K., Buch Månson, N., Guo, L., Li, X., Badique, F., Anselme, K., Nygård, J., Martinez, K.L. (2013) Tuning InAs nanowire density for HEK293 cell viability, adhesion and morphology – perspectives for nanowire-based biosensors, *ACS applied Materials & Interfaces,* 5(21):10510-9

Bonde, S., Buch Månson, N., Rostgaard, K.R., Andersen, T. K., Berthing, T., Martinez, K.L. (2014) Exploring arrays of vertical one-dimensional nanostructures for cellular investigations, *Nanotechnology,* 25, 362001

Buch Månson, N., Bonde, S., Bolinsson, J., Berthing, T., Nygård, J., Martinez, K.L. (2014) Simple means to complicated ends: Towards a better prediction of cell settling on nanostructure arrays, *submitted*

A Development of Microstrip Patch Antenna with Graphene and Titanium Dioxide For Orthopaedic Implants

N. Fugto,[1,] S. Chaisiri,[2,] R. Kaewon,[3,] S. Sirivisoot,[1]
[1]Biological Engineering, Faculty of Engineering, King Mongkuiversity of Technology Thonburi, Thung Kru, Bangkok, Thailand
[2]Automotion Engineering, Department of Instrumentation and Electronic Engineering, Faculty of Engineering, King Monhkut's University of Technology North Bangkok, Bangsue, Bangkok, Thailand
[3]Department of Electrical, Faculty of Engineering and Industrial Technology, Silpakorn University, Sanamchan palace campus, Muang, Nakornprathom, Thailand

Abstract: An implantable antenna in biomedical devices is used as a wireless communication device to send and receive data signal between an implantable circuit inside the human body and an electronic receiver outside, as shown in Figure 1. However, implantable antenna design still has many problems including a large size of antenna, biotoxicity of antenna materials to the human tissue caused by metallic material, and the low efficiency of radiation of implantable antennas (Soontornpipit *et al*., 2004, 2011). This work is a mathematical method to solve these problems. We developed a new design of antenna using mathematical modeling with MATLAB programming. Specifically, in this study, graphene is used as a patch antenna since it has an excellent biocompatibility and flexibility to modify its electrical properties (Fatikow *et al*., 2012). Titanium, widely used for orthopaedic implants, is used as a dielectric substrate to reduce the antenna size. An EMCoS Antenna VLab software is used to simulate our new design antenna in two environments: inside and outside the human body in order to test the efficiency of antenna radiation. The results of this study suggest that our designed antenna has small size and light weight which can reduce the burden of patient when wearing. The effect of graphene on implantable antenna includes good electromagnetical properties such as return loss or power radiation, moreover, its notching can also improve radiation efficiency of the overall implantable antenna.

Keywords: Biomedical devices, biomedical application, orthopaedic implant, graphene, antenna.

Figure 1: A diagram of implantable antenna used in orthopaedic implant. The antenna is a receiving and transmitting wireless device communicating with the antenna outside the humam body. The efficiency of antenna is varied with its material, size, and shape.

References:

Fatikow, S., V. Eichhorn, et al. (2012). "Nanomaterials Enter the Silicon-Based CMOS Era: Nanorobotic Technologies for Nanoelectronic Devices". Nanotechnology Magazine, *IEEE*, **6**, 14-18.

Soontornpipit, P. "Development of Microstrip Antenna for Multiband and Broadband Applications" (preparing manuscipt).

Soontornpipit, P., C. M. Furse, et al. (2004). "Design of implantable microstrip antenna for communication with medical implants". Microwave Theory and Techniques, *IEEE Transactions*, **52**, 1944-1951.

Nanoscale Modification of Natural Cell-derived Matrices for Tissue Engineering Applications

M.P. Hwang[1], R. Subbiah[2], K. Park[1,2]
[1]Korea Institute of Science and Technology, Center for Biomaterials, Seoul, Republic of Korea
[2]University of Science and Technology, Biomedical Engineering Department, Daejeon, Republic of Korea

Abstract: Interest in the interaction between cells and their surrounding environment continues to grow, underscored by a wide spectrum of studies demonstrating substrate-dependent cellular behavior. Given that the extracellular matrix (ECM) plays a structural role in addition to one of biophysical transduction, understanding its effect on cells is essential. In particular, many groups have shed light on the effect of substrate stiffness on cell differentiation. However, non-biological materials such as polyacrylamide or PDMS are often used in such studies, and as a result, examining the effect of topography and chemistry of natural ECM on cellular behavior is difficult. From this perspective, natural cell-derived matrices – ECM obtained via removal of overlying cells – is an extremely attractive option recently emerging. Herein, we synthesize natural preosteoblast-derived matrices (PDM) and crosslink them with genipin to varying degrees to induce structural changes of the ECM fibers at the nano- and micro-level. An increase in crosslinking density results in a transition of secondary structure from α-helix to β-sheet, and then to random coil structure, as determined via circular dichorism spectroscopy (Figure 1A). Qualitative analysis of TEM images corroborate these observations (Figure 1B). Given the increase in crosslinking density, changes to the PDM stiffness accompany the structural modifications, as determined via AFM. Finally, we examine the effect of using PDM on preosteoblast behavior and report that increasing crosslinking of PDM results in smaller cells with larger aspect ratios (Figure 2A). Furthermore, preosteoblasts were shown to undergo osteogenic differentiation more effectively with increasing crosslinking density of PDM (Figure 2B). This study highlights the advantages of using natural cell-derived matrices over conventional substrates, and we propose that secondary structural changes to an underlying substrate in conjunction with changes in stiffness affect cellular behavior. We envision the expansion of such information for more efficient applications in tissue engineering.

Keywords: natural cell-derived matrices, ECM, osteogenesis, decellularization, tissue engineering

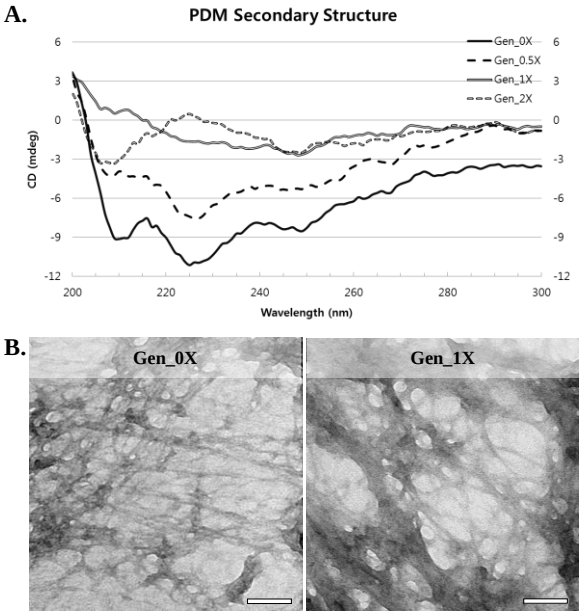

Figure 1. A. CD readings indicate changes to secondary structure of PDM. B. TEM (scale: 100nm)

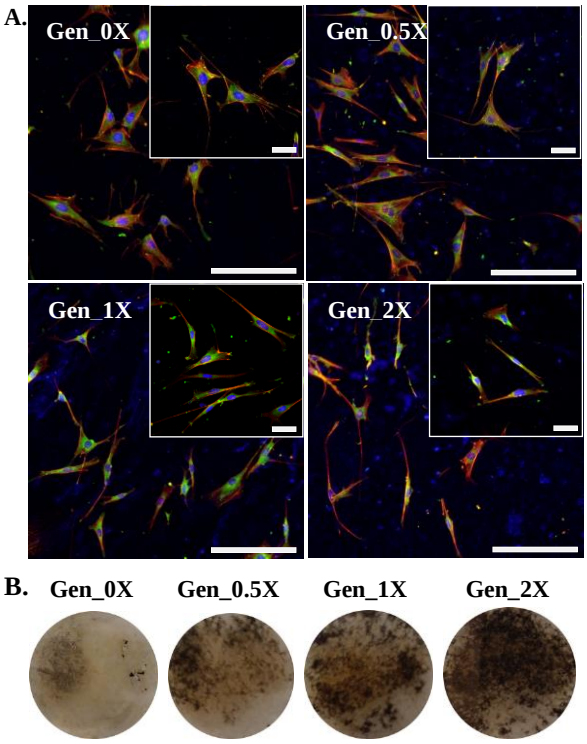

Figure 2. A) Immunofluorescence (R: f-actin; G: vinculin, B: dapi) (scale: 200μm; inset: 50μm). B) Ca^{2+} deposition is examined via Von Kossa staining.

Modular Assembly Gadolinium-Coated Nanoliposomes Enabling Detection of Ischemic Vasculature

C. Smith,[1] S. Zimmerman,[2] Sanjay Misra,[3] H. Kong[4]
[1]Department of Chemical & Biomolecular Engineering, University of Illinois at Urbana-Champaign, Urbana, USA
[2]Department of Chemistry, University of Illinois at Urbana-Champaign, Urbana, USA
[3]Department of Radiology, Mayo Clinic, Rochester, USA
[3]Department of Bioengineering, University of Illinois at Urbana-Champaign, Urbana, USA

Abstract: Nanoparticle formulations incorporate multiple components, including both diagnostic and therapeutic functionalities, within a single construct. Direct encapsulation of such units, however, can lead to unfavorable interactions between encapsulated materials, as well as reduced performance of the nanoparticle. While surface functionalization serves as a method of spatial organization, subsequent reaction and purification steps can be detrimental to the formulation. To this end, we synthesized a chitosan modified with hydrophobic, octadecyl chains and gadolinium-chelating diethylenetriaminepentaacetic acid, named as a polymeric fastener. In this way, the chitosan fastener was able to link gadolinium, an MRI contrast agent, to the surface of liposomes by self-assembly. Due to the localization of gadolinium on the liposome surface, we were able to achieve enhanced relaxivity compared to gadolinium loaded within the liposome. The resulting gadolinium-coated liposome enabled us to successfully detect and image vascular defects in an ischemic hindlimb and kidney using MRI.

In addition, we improved the stability of the liposome-fastener complex in physiological fluid by cross-linking lipids of the liposome using $DC_{8,9}PC$ lipids, which contained the photo cross-linkable diyne moiety. This approach not only stabilized the liposome, but also enhanced its association with the functional fastener. Interestingly, cross-linking the lipids after attachment of the fastener, rather than prior, was critical in enhancing the initial association with the fastener, as well as stabilizing it in serum. Ultimately, the strategy proved effective in enhancing MRI contrast nearly two-fold per liposome dose after one hour of serum exposure. Taken together, we believe that both polymeric fastener and lipid cross-linking will be broadly useful in spatially organizing functional cues in nanoparticles and further extending their lifetimes.

Keywords: polymer fastener, MRI, vasculature, gadolinium, liposome, self-assembly

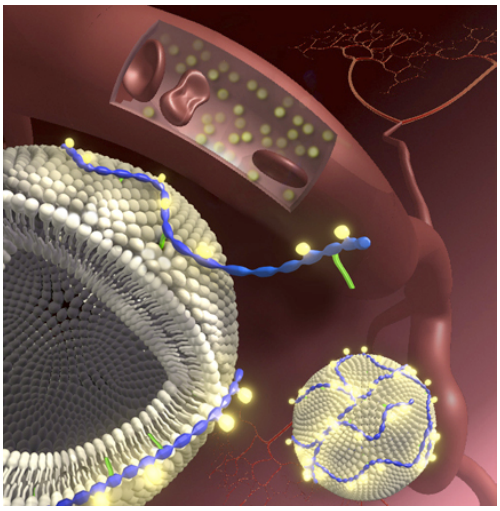

Figure 1: Figure illustrating the gadolinium-coated liposome that accumulate in ischemic vasculature and highlight the area in an MR image

References:

C. Smith, A. Shkumatov, S. Withers, J. Glockner, S. Misra, E. Roy, C-H, Wong, S. Zimmerman, & Kong, H.J. (2013) A Polymeric Fastener can Easily Functionalize Liposome Surfaces with Gadolinium for Enhanced Magnetic Resonance Imaging *ACS Nano* 7:9599-9610.

C. Smith & Kong, H.J. (2014), Cross-Linkable Liposomes Stabilize a Magnetic Resonance Contrast-Enhancing Polymeric Fastener. *Langmuir* 30:3697-3704.

Pluronic F127 coated superparamagnetic nanoparticles for Human Umbilical Vein Endothelial Cell tracking via magnetic resonance imaging

Bárbara Argibay,[1] Ramón Iglesias,[1] María Pérez-Mato,[1] Tomás Sobrino,[1] Andrés Beiras,[2] José Rivas,[3,4] Uwe Himmelreich,[5] José Castillo,[1] Francisco Campos.[1]
[1]Department of Neurology, Clinical Neurosciences Research Laboratory, Health Research Institute of Santiago de Compostela (IDIS), University Clinical Hospital Hospital, Santiago de Compostela, Spain.
[2]Department of Morphological Sciences, University of Santiago de Compostela, Santiago de Compostela, Spain.
[3]INL - International Iberian Nanotechnology Laboratory, Braga, Portugal.
[4]Department of Applied Physics, Technological Research Institute, Nanotechnolgy and Magnetism Lab—NANOMAG, University of Santiago de Compostela, Spain.
[5]Department of Imaging and Pathology, Biomedical MRI/Mosaic, KU Leuven, Leuven, Belgium.

Abstract: Cell based therapies have emerged as a alternative approaches to conventional pharmacological treatments due to their multipotential action mechanisms. Integration in the host, immunomodulation processes or growth factors secretion are the possible ways of action, however fundamental questions related to cell type, characterization and dosage, therapeutic timing versus toxicity or the relationship between biodistribution, fate and outcome must be elucidated.[1-4]

In order to monitor *in vivo* administered cells and its relationship with the underlying mechanisms of stem cell therapy, superparamagnetic nanoparticles (MNPs) as magnetic resonance imaging (MRI) contrast agent are the perfect candidate for it. Thus, MNPs labeled cells can be tracked *in vivo* via MRI without harmful effects, providing real-time information about their biodistribution but the pathologic condition of the organ as well.[5,6]

In this study, we have synthesized Pluronic F127-coated superparamagnetic nanoparticles (P-MNPs) and we have validated their use for cell tracking. For such purpose, we have studied the influence of different concentrations of P-MNPs (35µg/mL and 15µg/mL) and incubation times (24h and 6h) in vitro in Human Umbilical Vein Endothelial Cells (HUVECs) culture, by studying cellular proliferation after labeling, the viability of labeled and non-labeled cells, Prussian Blue assessment of labeling (Fig.1A,B), transmission electron microscopy (TEM) of labeled cells to demonstrate the full internalization of the MNPs (Fig.1C), the quantification of internalized iron depending on the concentration and incubation time, and MRI signal of HUVEC cells after P-MNPs labeling. This deep *in vitro* characterization will elucidate the best conditions for HUVEC tagging with P-MNPs for further *in vivo* experiments.

Keywords: Stem cell therapy, superparamagnetic nanoparticles, Human Umbilical Vein Endothelial Cells, cell labeling, cell tracking, magnetic resonance imaging, contrast agents.

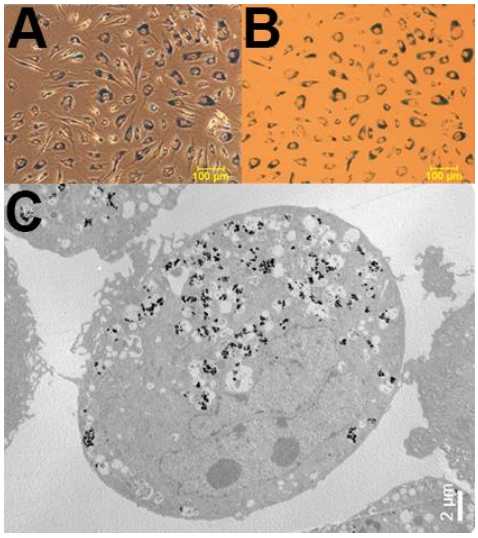

Figure 1: (A) P-MNPs labeled HUVEC cells in phase constrast optical microscopy after Prussian Blue Staining, (B) in bright field optical microscopy after Prussian Blue Staining, (C) TEM micrograph of labeled cells.

References:

1. Haraguchi Y, Shimizu T, Yamato M, Okano T (2012) Concise review: cell therapy and tissue engineering for cardiovascular disease. Stem Cells Transl Med 1: 136-141. 2. Yavagal DR, Lin B, Raval AP, Garza PS, Dong C, et al. (2014) Efficacy and dose-dependent safety of intra-arterial delivery of mesenchymal stem cells in a rodent stroke model. PLoS One 9: e93735.
3. Wu CC, Chen YC, Chang YC, Wang LW, Lin YC, et al. (2013) Human umbilical vein endothelial cells protect against hypoxic-ischemic damage in neonatal brain via stromal cell-derived factor 1/C-X-C chemokine receptor type 4. Stroke 44: 1402-1409.
4. Tang ZC, Liao WY, Tang AC, Tsai SJ, Hsieh PC (2011) The enhancement of endothelial cell therapy for angiogenesis in hindlimb ischemia using hyaluronan. Biomaterials 32: 75-86.
5. Jain TK, Morales MA, Sahoo SK, Leslie-Pelecky DL, Labhasetwar V (2005) Iron oxide nanoparticles for sustained delivery of anticancer agents. Mol Pharm 2: 194-205.
6. Jain TK, Foy SP, Erokwu B, Dimitrijevic S, Flask CA, et al. (2009) Magnetic resonance imaging of multifunctional pluronic stabilized iron-oxide nanoparticles in tumor-bearing mice. Biomaterials 30: 6748-6756.

Preparation, Biological Activity and Mechanism of Action of Ag and AgBr Nanoparticles

P. Suchomel,[1,2,*] L. Kvitek,[1,2] A. Panacek,[1,2] R. Prucek,[1,2] J. Hrbac,[2] R. Vecerova,[3] R. Zboril[1,2]
[1]Regional Centre of Advanced Technologies and Materials, Faculty of Science, Palacky University, Olomouc, Czech Republic
[2]Department of Physical Chemistry, Faculty of Science, Palacky University, Olomouc, Czech Republic
[3]Department of Microbiology, Faculty of Medicine and Dentistry, Palacky University, Olomouc, Czech Republic

Abstract: Silver nanoparticles (Ag NPs) and nanoparticles of insoluble silver compounds such as Ag_2O, AgOH or AgX (X = Cl, Br or I) became one of the most discussed branches of nanoscience in the several last decades. Ag NPs attract due to their unique physical, chemical, optical and biological properties great attention in the scientific research. Because of expected inability of bacteria to develop resistance against antibacterial action of silver based nanomaterials, nowadays, there are intensively studied their biological properties, namely antifungal, antiviral and particularly antibacterial activities together with their cytotoxicity. According to this, silver based nanomaterials find their use in medicine (catheters, implants, prostheses) (Rupp *et al.*; 2004, Stevens *et al.*; 2011), and are used to improve commercial products (textiles, deodorants) (Perelshtein *et al.*; 2013).

In this work, the preparation of silver bromide NPs, their reduction to the silver NPs and the diverse mechanism of antimicrobial activity of AgBr and Ag NPs against gram-positive and gram-negative bacteria and also against several strains of candida was explored. The AgBr nanoparticles (NPs) were prepared by simple precipitation of silver nitrate by potassium bromide in the presence of stabilizing polymers (PEG, PVP, PVA and HEC). It was found, that used polymers influence significantly the size of the prepared AgBr NPs dependently on the mode of interaction of polymer with Ag^+ ions. Small NPs (diameter of about 60-70 nm) were formed in the presence of the polymers with low interaction as are PEG and HEC, the polymers which interact with Ag^+ strongly produce nearly two times bigger NPs (120-130 nm). The prepared AgBr NPs were reduced to Ag NPs by using of $NaBH_4$. The sizes of the produced Ag NPs followed the same trends – the smallest NPs were produced in the presence of PEG and HEC polymers. Prepared AgBr and Ag NPs dispersions were tested for their biological activity. The obtained results of antimicrobial activity of AgBr and Ag NPs are discussed in terms of possible mechanism of the action of these NPs against tested microbial strains. The AgBr NPs are more effective against gram-negative bacteria and tested yeast strains while Ag NPs show the best antibacterial action against gram-positive bacteria strains.

References:

Perelshtein, I., Ruderman, Y., Perkas, N., Beddow, J., Singh, G., Vinatoru, M., Gedanken, A. (2013), The sonochemical coating of cotton withstands 65 washing cycles at hospital washing standards and retains its antibacterial properties, *Cellulose*, 20, 1215–1221.

Rupp, M. E., Fitzgerald, T., Marion, N., Helget, V., Puumala, S., Anderson, J. R., Fey, P. D. (2004), Efect of silver-coated urinary catheters: Efficacy, cost-effectiveness, and antimicrobial resistance, *Am. J. Infect. Control*, 32, 445–450.

Stevens, K. N. J., Croes, S., Boersma, R. S., Stobberingh, E. E., van der Marel, C., van der Veen, F. H., Koole, L. H. (2011), Hydrophilic surface coatings with embedded biocidal silver nanoparticles and sodium heparin for central venous catheters, *Biomaterials*, 32, 1264–1269.

Preparation of Novel Selenium Nanoparticles with Strong *In Vitro* and *In Vivo* Anti-cancer Efficacy Using Tiger Milk Mushroom

Ka-Hing Wong
Department of Applied Biology and Chemical Technology, The Hong Kong Polytechnic University, Hong Kong

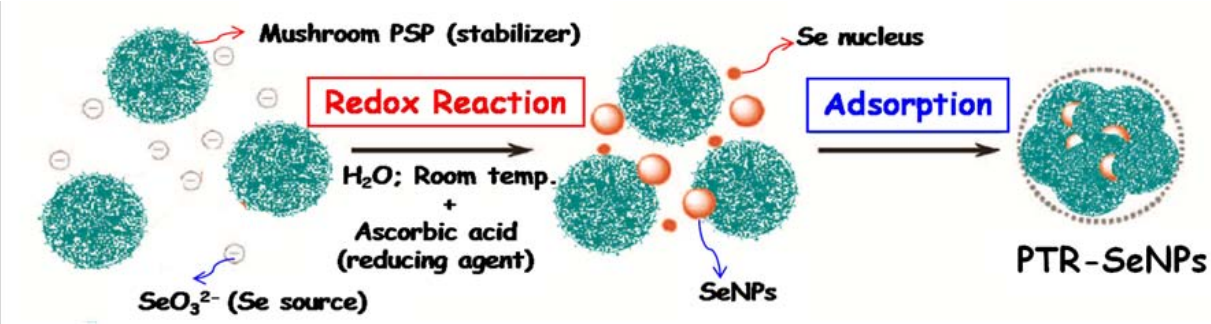

Figure 1: Schematic illustration of PTR-SeNPs preparation using PSP isolated from tiger milk mushroom

Abstract: Selenium is an essential trace minerals to human health. In the past decades, substantial amount of evidences have been acculmulated to support its role in cancer treatment. The anti-cancer efficacy and toxicity of selenium are highly dependent on its chemical form and dosage. Recently, selenium nanoparticles (SeNPs) have become the new research target, since they were found to possess remarkable anti-cancer efficacy and low toxicity.

By using a polysaccharide-protein complex (PSP) isolated from the tiger milk mushroom (*Pleurotus tuber-regium)*, our research team has successfully prepared novel SeNPs (PTR-SeNPs) under a simple redox system, in which sodium selenite and ascorbic acid were used as the Se source and reducing agent, respectively. In contrast to normal cells, the PTR-SeNPs were found to significantly inhibit the growth of human breast carcinoma MCF-7 cells (IC_{50} = 3.7μM) by apoptosis induction via activating a ROS-mediated mitochondrial pathway. Comparing with the IC_{50} value of native SeNPs (200μM) and PSP (400μg/mL), interestingly, the mushroom PSP surface decoration did not only stabilize the SeNPs, but also significantly enhance their cellular uptake and anti-proliferative effect on the MCF-7 cells. More importantly, our recent *in vivo* anti-tumor study demonstrated that PTR-SeNPs (ranged from 2.5 to 7.5 mg/kg) significantly inhibit the growth of MCF-7 xenografts (33.9-76.7%) transplanted in BALB/c nude mice in a dose-dependent manner after 16 days of intravenous injection.

It is the first study of its kind to prepare SeNPs with strong anti-cancer efficacy using mushroom PSP as the stabilizer. We anticipate that findings of this study could provide significant insights on developing the PTR-SeNPs into next generation anti-tumor agents. Our long term goal is to develop economical, safe and evidence-based anti-tumor agents for our community, hereby alleviating the now spiraling cost of cancer treatments in the public healthcare system.

Keywords: selenium nanoparticles, tiger milk mushroom, anti-cancer efficacy

References:

Wu, H., Zhu, H., Li, X., Liu, Z., Zheng, W., Chen, T., Yu, B., Wong, KH. (2013) Induction of apoptosis and cell cycle arrest in A549 human lung adenocarcinoma cells by surface encapping selenium nanoparticles: an effect enhanced by polysaccharides-protein complexes from *Polyporus rhinocerus*, *J. Agri.Food Chem.*, 61, 9859-9866.

Wu, H., Chen, T., Liu, W., Li, Y., Zheng, W., Man, C., Wong, MK., Wong, KH. (2012) Surface decoration of selenium nanoparticles by mushroom polysaccharide-protein complexes to achieve enhanced cellular uptake and anti-cancer activity. *J. Mater. Chem.*, 22, 9602-9610.

Wong, KH., Cheung, PCK. (2008) Sclerotium of culinary-medicinal King Tuber Oyster mushroom *Pleurotus tuberregium* (Fr.) Singer (Agaricomycetideae): its cultivation, biochemical composition and biopharmacological effects (review). *Int J Med Mushrooms*, 10, 303-313.

Conductive polypyrrole: a promising interface for attachment and proliferation of mammalian cells

Angel E. Fernández-Duke,[1] Blanca E. Millán-Chiu[1,2],
Concepción Arenas-Arrocena[3] & Luz M. López-Marín[1,*]

[1]Centro de Física Aplicada y Tecnología Avanzada, Universidad Nacional Autónoma de México, Campus Juriquilla, Querétaro, México, [2]Cátedra CONACyT, [3]University Escuela Nacional de Estudios Superiores, Universidad Nacional Autónoma de México, Unidad León, León, Guanajuato, México.

Abstract: Cell-based assays have emerged as low-cost, rapid and non-invasive alternatives for a great variety of biological analyses, encompassing areas from basic research to clinical and industrial applications. Development of high through-put cell-based assays depend on the availability of miniaturizable surfaces where cells could remain attached after repeated cycles of washing. At present, substrates for cellular growth in biosensors are mostly based on polydimethylsiloxane (PDMS), However, cell adhesion onto PDMS is insufficient, and high added value biomolecules, such as poly-lysine or fibronectin, must be used to increase cell attachment (Mehling and Tay; 2014). Polypyrrole, a conductive polymer, is known to be highly biocompatible, and has been evaluated for tissue regeneration purposes (Balint *et al* 2014). Due to the unique combination of properties in this material, including electric conductivity, flexibility, and low cost, its use as a biosensor support for cellular growth would be very valuable. In this work, polypyrrole was evaluated as an interface for supporting growth of various mammalian cells. Electrochemically synthesized polypyrrole films were incubated with different immortalized adherent cell lines, and analyzed by confocal microscopy, MTT cell proliferation assays and scanning electron microscopy. Our results showed that polypyrrole is a good support for cell attachment and proliferation of mammalian cells. Moreover, further assays showed that polypyrrole allowed the adherence and/or activation and proliferation of primary cultures from mouse spleen cells, thus indicating the usefulness of this material for a wide set of cell-based assays.

Keywords: semiconducting polymers, polypyrrole, cell adherence, cell proliferation, biomedical applications.

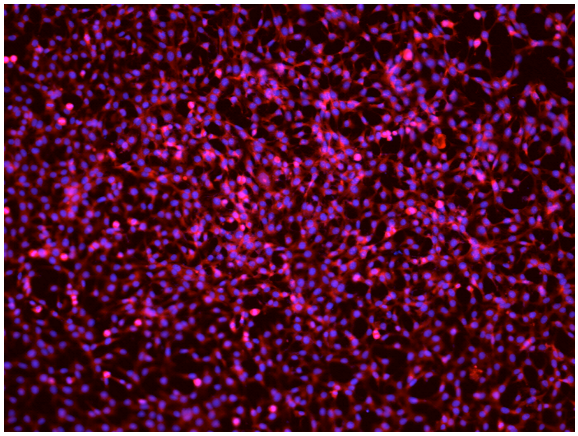

Figure 1: Fluorescence microscopy of the murine fibroblast line, NIH 3T3, after 72 hours of growth onto polypyrrole support. Cytoskeletal was stained with Cy3 coupled-anti-beta actin antibody (red). Staining with DAPI was used to visualize cell nuclei (blue).

References:

Mehling, M., Savas, T. (2014) Microfluidic cell culture, *Curr. Opin. Biotech.*, 25, 95-102.

Balint, R., Cassidy, N. J., Cartmell, S. H. (2014) Conductive polymers: Towards a smart biomaterial for tissue engineering. *Acta Biomater.*, 10, 2341-2353.

Acknowledgments:

This work was supported by CONACyT, Mexico, through Grant 214076. The authors thank Nydia Hernández, Martin García-Servín & Alicia del Real for excellent technical assistance.

An *In Vitro* Study of Osteoblast Behaviors on Graphene Oxide Electrodeposited on Anodized Titanium

P. Tanurat,[1*] S. Sirivisoot[1]

[1] Biological Engineering Program , Faculty of Engineering, King Mongkut's University of Technology Thonburi Bangkok, Thailand

Abstract: Titanium is one of the most popular light-weight metals used for orthopaedic implants. Because their physical property and excellent biocompatibility (Yamaguchi *et al*., 2001). In order to increase osseointegration, surface modification of titanium mimicking a nanoscale hierarchical structure was widely studied (Zhang *et al.*, 2013). Anodization is a method has been used to frabication titanium dioxide (TiO_2) nanotube arrays on titanium surface in order to increase osteointegration (Minagar *et al.*, 2012). Using graphene oxide (GO) coating on biomaterial surfaces is a great potential for long-term use of orthopaedic implants due to its biocompatibility and antibacterial property (Zhu *et al*., 2010). The aim of this study is to frabicate anodized titanium coated with graphene oxide (ATiGO) using anodization and electrodeposition of graphene oxide, respectively. Scanning electron microscopy (SEM) was used to investigate surface morphology (Figure 1). Their physiochemical properties were evaluated by energy-dispersive X-ray spectroscopy (EDX), X-ray diffractrometer (XRD), thermogravimetric analysis (TGA), and X-ray photoelectron spectroscopy (XPS). Furthermore, cell proliferation of mouse osteoblastic cell line (MC3T3-E1) was investigated using MTT assay. Enzyme linked immunosorbent assay (ELISA), calcium assays and osteocalcin immunofluorescence analyses were used to evaluate osteogenic differentiation of cells. The results from ATiGO, GO coated on titanium (TiGO), anodized titanium (ATi), and pure titanium (Ti) were compared and discussed. The results in the present study suggest that graphene oxide can promote osteoblast behaviors when compared with anodized titanium and pure titanium without GO coating.

Keywords: TiO_2 nanotubes, graphene oxide, orthopaedic application, anodization, electrodeposition

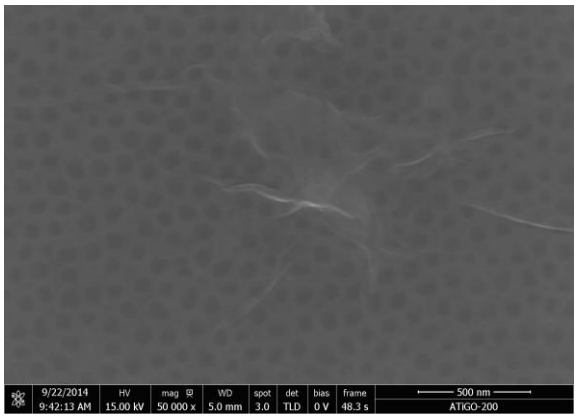

Figure 1: Top sectional scanning electron microscope image of 200 µg/ml of graphene oxide electrodeposited on anodized titanium (ATiGO200). A thin layer of reduced graphene oxide covers titanium dioxide nanotube array.

References:

Yamaguchi, K., Konishi, H., Hara, S., and Motomura, Y. (2001), Biocompatibility studies of titanium-based alloy pedicle screw and rod system: histological aspects, *Spine J.*, 1, 60-268.

Zhang, W.,Qingfeng H., Ling, X., Jinhua L., Yuqin, J., Guifang, L., Xuanyong, L. and Xinquan, J. (2013), Effects of a hybrid micro/ nanorod topography-modified titanium implant on adhesion and osteogenic differentiation in rat bone marrow mesenchymal stem cells, *Int. J. Nanomedicine.*, 8, 257-265.

Minagar, S., Chris, T.C., Berndt, J.W., Elena, I. and Cuie, W. (2012), A review of the application of anodization for the fabrication of nanotubes on metal implant surfaces, *Acta Biomaterials*, 8, 2875-2888.

Zhu, Y., Shanthi, M., Weiwei, C., Xuesong, L., Ji, W.S., Jeffrey, R. P., and Rodney, S. R. (2010), Graphene and Graphene Oxide: Synthesis, Properties,and Applications, *J. Adv. Material*., 12, 1–19.

STM Imaging of Yellow Fluorescent Protein under Ambient Condition

Hanis Mohd Yusoff,[1*] Izabela I. Rzeznicka,[2,3] Hirotaka Hoshi,[4] Shinji Kajimoto[2], Noriko Nishizawa Horimoto[2], Kazuhiro Sogawa[4] and Hiroshi Fukumura[2]

[1]School of Fundamental Science, Universiti Malaysia Terengganu, 21030 Kuala Terengganu, Terengganu, Malaysia.

[2]Department of Chemistry, Graduate School of Science, Tohoku University, Aramaki Aza-Aoba, Aoba-ku, Sendai 980-8578, Miyagi, Japan.

[3]Institute for International Education, Tohoku University, Katahira 2-Chome, Aoba-ku, Sendai 980-8577, Miyagi, Japan.

[4]Department of Biomolecular Science, Graduate School of Life Sciences, Tohoku University, Aramaki Aza-Aoba-ku, Sendai 980-8578, Japan.

Abstract: Fluorescent proteins have shown tremendous applications especially in localizing proteins of interest within cells. To our knowledge there are few scanning tunneling microscopy (STM) or scanning tunneling spectroscopy (STS) studies regarding fluorescent proteins. Several works related with fluorescence dynamics such as lifetime and anisotropy decay of fluorescent protein in solution have been reported (Suhling *et al*., 2002). Knowing the nature of adsorbed protein is interesting in the area such as biomaterials and pharmacology (Norde, 1986). In this study, a fluorescent protein (FP) has been chosen as a model to understand protein behaviour when adsorbed on a surface. Citrine from yellow fluorescent protein (YFP) variants has been chosen among other variants. Histidine tags are always used in the purification of protein and can as well be used as chemical handles on bare gold surfaces (Korpany *et al.*, 2012). STM was used to study protein's morphology on surfaces. Citrine was dried on hydrophilically and hydrophobically modified gold surfaces by drop cast protein solution on the freshly modified surfaces. The drop cast solution formed a "ring-like" pattern having a concentrated and visible rim. Citrine films were observed with an STM under ambient conditions. From STM images obtained, citrine molecules adsorbed more uniformly packed crystal-like protein layers on hydrophilic surface. While on hydrophobic surface, citrine molecules were more randomly adsorbed forming some aggregates on non homogenous layers. Furthermore, time-resolved anisotropy clearly has shown the tendency of fast and randomized layers on hydrophobic surface to compare with on hydrophilic surface.

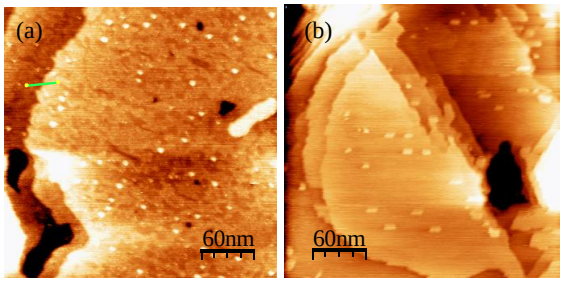

Figure 1: STM images of citrine film on hydrophilically modified surface (a) hydrophobically modified surface (b). Scanning condition I_t = 600 pA for hydrophilic surface, I_t = 800 pA for hydrophobic surface, V_{bias} = 0.2 V was used for both modified surfaces.

Keywords: fluorescent proteins, scanning tunneling microscopy, anisotropy decay

References:

Suhling, K., Davis, D., Phillips, D. (2002) The influence of solvent viscosity on the fluorescence decay and time-resolved anisotropy of green fluorescent protein, *J. Fluorescence.*, 12, 91-95.

Norde, W. (1986) Adsorption of proteins from solution at the solid–liquid interface, *Adv. Colloid Interface Sci.*, 25, 267-340.

Korpany, K. V., Langat, P., Kim, D. M., Edelman, N., Cooper, D. R., Nadeau, J., Blum, A. S. (2012), Conductance switching in the photoswitchable protein dronpa, *Journal of the American Chemical Society*, 134, 16119-16122.

Nano- and Microfabricated Hydrogels for Regenerative Engineering

Ali Khademhosseini, Ph.D, Professor
Department of Medicine, Brigham and Women's Hospital,
Harvard Medical School, Cambridge, MA
Harvard-MIT Division of Health Sciences and Technology, MIT, Cambridge, MA
Wyss Institute for Biologically Inspired Engineering, Harvard University, Boston, MA

Abstract:
Engineered materials that integrate advances in polymer chemistry, nanotechnology, and biological sciences have the potential to create powerful medical therapies. Our group aims to engineer tissue regenerative therapies using water-containing polymer networks, called hydrogels, that can regulate cell behavior. Specifically, we have developed photocrosslinkable hybrid hydrogels that combine natural biomolecules with nanoparticles to regulate the chemical, biological, mechanical and electrical properties of gels. These functional scaffolds induce the differentiation of stem cells to desired cell types and direct the formation of vascularized heart or bone tissues. Since tissue function is highly dependent on architecture, we have also used microfabrication methods, such as microfluidics, photolithography, bioprinting, and molding, to regulate the architecture of these materials. We have employed these strategies to generate miniaturized tissues. To create tissue complexity, we have also developed directed assembly techniques to compile small tissue modules into larger constructs. It is anticipated that such approaches will lead to the development of next-generation regenerative therapeutics and biomedical devices.

SEEC Microscopy : An innovative optical technique for the live and label-free study of a enzymatic reaction in liquid

A.Egea,[1] N.Médard,[2,*] M.Métivier,[2] C.Vieu,[1]
[1]LAAS-CNRS, 7 avenue du Colonel Roche, 31400 Toulouse, France
[2]Nanolane, Technopole Université, 10 rue Xavier Bichat, 72000 Le Mans, France

Abstract: Nowadays, label-free In-Vitro Diagnostic (IVD) is in higher demand due to the steric, electronic influence of labeled molecules on biological samples. However, in the absence of chemical amplification, it is a challenge for label-free biosensing to achieve the same degree of sensitivity as those exhibited by standard enzyme-linked immunosorbent assay (ELISA). In this sense, significant optical label-free biosensors are reported performing well: SPR, SPRi, QCM-D, OWLS… But even if these techniques show quite good sensitivity, none of them offer high-lateral resolution imaging and direct thickness measurements capacities.
Few years ago, was developed the SEEC (Surface Enhanced Ellipsometric Contrast) Microscopy, an innovative advanced optical technique based on ellipsometric and interference principles. This technique offers live and label-free topographic imaging of organic, inorganic and biological samples with a high precision and accuracy (down to 0.1nm). This technique has been successfully applied to the study of nanometric films and structures, biological layers, nano-objects…Compared to existing techniques, the SEEC microscopy offers a unique combination of acquisition mode capabilities : non-contact, label-free, live imaging, nanometric sensitivity, topographic analysis…
Recently, a SEEC study was performed to monitor a dynamic enzymatic reaction in real-time and in liquid. Biochemical reactions taking place on surface molecular patterns were not only tracked but also fully characterized thanks to the topography imaging capability of the technique. This study was performed on 5µm x 5µm patterns to illustrate the ability of the SEEC technique to perform ultra-high density multiplexing analyses.

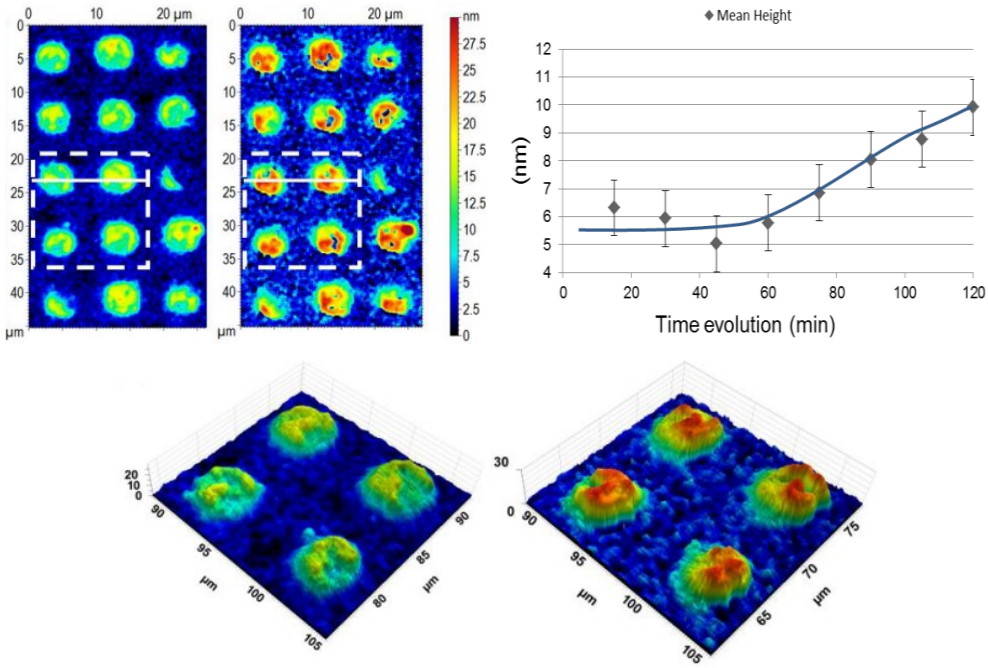

Figure 1: SEEC analysis of biochips hybridation (enzymatic reactions)
A.Topographic images (t_0 and t_0+120min) B. Biochip thickness vs. hybridation time C. 3D views

References:

Egea, A.M.C., Métivier, M., Croguennoc, P., Remaud-Simeon, M., Vieu, C. (2014), Real-Time Monitoring of Dextransucrase-Based Enzymatic Reaction Through Surface-Enhanced Ellipsometric Contrast (SEEC) Microscopy in Liquid Environment, *BioNanoSci., 4, 37-45*

Biocompatibility of nanovesicles derived from microbial cells: an assessment towards vaccine applications

Blanca E. Millán-Chiu[1,2,*], Angel O. Tinoco-Martínez[1],
Vicente D. Compeán-García[1] & Luz M. López-Marín[1]
[1]Centro de Física Aplicada y Tecnología Avanzada, Universidad Nacional Autónoma de México,
Campus Juriquilla, Querétaro, México, [2]Cátedra CONACyT

Abstract: Due to the emergence of immunosuppressive conditions worldwide, the development of acellular vaccines constitutes a major need. Nanotechnology provides a wide set of approaches for the development of cell-free vaccines, including antigen- or/and microbial gene-functionalized nanocarriers. A recent modality of acellular vaccines is the use of cell-free nanovesicles (André et al; 2004). In this work, we explored a method for the production of *Mycobacterium*-derived nanovesicles, performed their physical and chemical characterization, and assessed their biocompatibility and genotoxicity traits.

Ultracentrifugation and dialysis were explored as purification methods. Physical characterization of nanovesicles was performed through transmission electron microscopy and dynamic light scattering analyses. Chemical identification of nanovesicles was performed through thin-layer-chromatography analysis of lipids and sodium-dodecyl-sulfate polyacrylamide gel electrophoresis of proteins. For biocompatibility tests, we focused on the study of cytotoxic, genotoxic and hemolytic effects of microbial-derived vesicles on NIH-3T3 mouse fibroblast cells. Cell viability was tested using the 3-(4, 5-dimethlthiazol-2-yl) 2,5-diphenyl tetrazolium bromide (MTT) colorimetric assay. DNA lesions were evaluated using the single-cell gel alkaline electrophoresis (comet) assay and observed by fluorescence microscopy. Hemolytic effects were tested by the Neun-Dobrovolskaia method (2011).

Physico-chemical analysis of vesicles show that a large variety of microbial molecules may compose the obtained nanovesicles, thus suggesting that both innate and adaptive immune responses could be activated by this newly developed vaccine system.

Keywords: nanovesicles, nanosafety, vaccines, comet assay, biocompatibility tests.

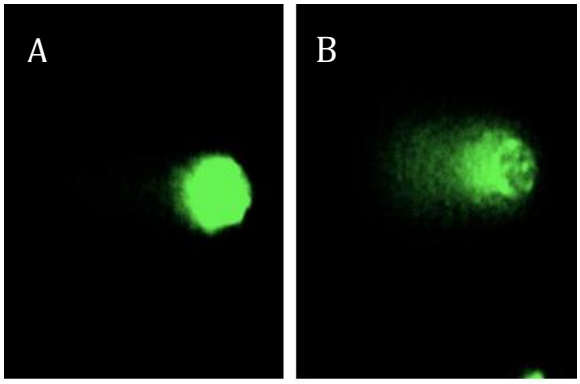

Figure 1: Single cell alkaline electrophoresis (comet assay) showing the nuclear material of a control cell (A), and the characteristic comet tail, which is attributed to alterations in the genetic material caused by exposure to various external mutagen agents (B).

References:

André, F., Chaput, N., Schartz, N. E. C. et al (2004), Exosomes as potent cell-free peptide-based vaccine. *J. Immunol.*, 172, 2126-2136.

Neun, B. W., Dobrovolskaia, M. A. (2011) Characterization of nanoparticles intended for drug delivery. *Methods Mol. Biol.* 697, 121-130.

Acknowledgments:

This work was supported by DGAPA, UNAM, Mexico, through Grant IT200615. The authors thank Nydia Hernández, Lourdes Palma & Francisco Fernández for excellent technical assistance.

$Fe_{3-\delta}O_4$ nanoparticles inhibit *Clostridium difficile* spore germination: an in vitro and in vivo study

Wei-Ting Lee,[1] Shang-Rung Wu,[2] Ya-Na Wu,[2] Yi-Hsuan Chen,[3] Chen-Sheng Yeh,[4] Pei-Jane Tsai,[1,3*] Dar-Bin Shieh[1,2*]

[1]Institute of Basic Medical Sciences, National Cheng Kung University, Tainan 70101, Taiwan

[2]Institute of Oral Medicine and Department of Stomatology, National Cheng Kung University Hospital, National Cheng Kung University, Tainan 70101, Taiwan

[3]Department of Medical Laboratory Science and Biotechnology, National Cheng Kung University, Tainan 70101, Taiwan

[4]Department of Chemistry, National Cheng-Kung University, Tainan 70101, Taiwan

Abstract: *Clostridium difficile* infection (CDI) has emerged to be an important cause of global healthcare-associated infection (Ananthakrishnan *et al*.; 2010). Resistance of CD spores to various preventive and therapeutic measures post a significant threat in CDI (Paredes-Sabja *et al*.; 2014). Nanomaterials have been explored for potential applications in anti-microbials with intrinsic advantages of low drug-resistance issue and high efficacy. We discovered the 22 nm octahedral $Fe_{3-\delta}O_4$ single crystal nanoparticles with a strong inhibitory effect to CD spore germination *in vitro* and *in vivo*. The nanocrytal presented excellent saturation magnetization (94 emu/g) close to the bulk due to the presence of alpha iron. Such particle showed a dose dependent inhibition of CD spores germination (62% growth inhibition at 50 μg/mL) for 20 minutes of exposure. At 500 μg/mL, the inhibition rate is close to that of sodium hypochloride. CDI animal model established in NF-κB-reporter mice using oral gavage with CD spores presented significant bowel inflammation in the MOCK compared to $Fe_{3-\delta}O_4$ nanoparticle treated group as revealed by In Vivo Imaging System. S-layer protein and a conserved hypothetical protein were released from CD spores after for 20 minutes of $Fe_{3-\delta}O_4$ nanoparticle exposure. Cryo-electron tomography clearly showed binding of the nanoparticles to CD spores' surface followed by disruption of the spores. Pro-inflammatory cytokines including IL-1β, TNF-α, and INF-γ and inflammatory cell infiltrations were significantly suppressed after nanoparticle treatment. These results provide nano-material based strategy for CDI control and potential therapeutic mechanisms that encourage further clinical translational development.

Keywords: Clostridium, spore, infection, nanoparticle, Cryo-electron microscope, in vivo test

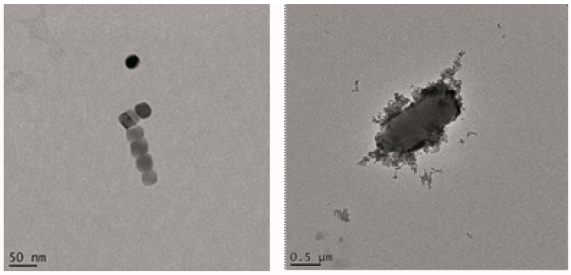

Figure 1: Transmission electron microscopy revealed the typical 22nm octahedral iron oxide nanoparticles (left). When treated with $Fe_{3-\delta}O_4$ nanoparticles, these particles attached to spore surfaces and compromise the integrity of the spaore (right).

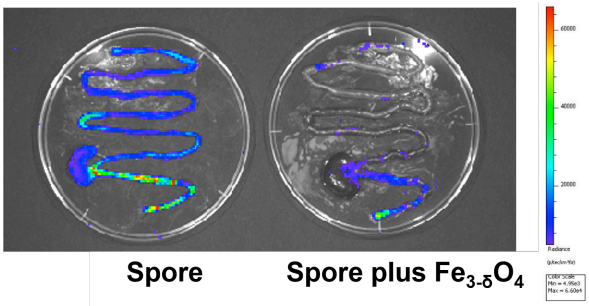

Figure 2: The spore-induced CDI presented extensive bowel inflammation in the NF-κB-reporter mice as revealed by IVIS (left). Such inflammation was significantly attenuated by oral administration of 500μg/mL $Fe_{3-\delta}O_4$ treatment (right).

References:

Ananthakrishnan AN. (2010), Clostridium difficile infection: epidemiology, risk factors and management, *Nat Rev Gastroenterol Hepatol*., 1, 17-26.

Paredes-Sabja D, Shen A, Sorg JA. (2014), Clostridium difficile spore biology: sporulation, germination, and spore structural proteins, *Trends Microbiol*., 7, 406-416

Identification of critical Monte Carlo simulation parameters in nanoparticles radiosensitization

P. Retif,[1,2,3] T. Bastogne,[1,3,4,5] M. Barberi-Heyob[1,3,5]
[1]Université de Lorraine, CRAN, UMR 7039, BP 70239, 54506 Vandoeuvre-lès-Nancy, France
[2] CHR Metz-Thionville, Hôpital de Mercy, Service de radiothérapie, Ars-Laquenexy, 57530, France
[3]CNRS, CRAN, UMR 7039, BP 70239, 54506 Vandoeuvre-lès-Nancy, France
[4]INRIA, BIGS, France
[5]CYBERnano, Telecom Nancy, 193 av. Paul Muller, 54506 Villers-lès-Nancy, FRANCE

Abstract: The use of nano-objects as radiosensitizers is rapidly increasing and has become a major subject of interest as a new strategy to fight cancer. This concept has already been proven *in vitro* and *in vivo* by a number of authors (Butterworth *et al.*, 2012) but only a few nanoparticles (NPs) are undergoing clinical trials. Even though a lot of preclinical studies are conducted to investigate the effects of nano-objects combined with X-rays on cells/tissues/tumor, there is still a serious lack of knowledge about their physical and chemical mechanisms.

A common way to investigate their properties is to use Monte-Carlo simulation methods with particle transport codes such as Geant4 (Agostinelli *et al.*, 2003). These simulations are time consuming, strongly code or model dependent and do not compare well between each other. It has already been noticed that the lack of standardization in preclinical studies of nano-radiosensitizers could partially explain the low number of translation to clinical applications (Retif *et al.*, 2015). That seems to become problematic in the field of NPs (Kodiha *et al.*, 2015).

In this study, a sensitivity analysis is performed to estimate the impact of eight simulation parameters on the variability of two numerical responses: the dose enhancement and the dose diffusion in seven spatial regions of interest shown in Figure 1. The physical modeling and Monte Carlo simulations are supported by the Geant4-GATE environment. The simulated nano-object is a single 100 nm gold nanoparticle. A Box and Behnken design of numerical experiments was carried out to estimate the statistical relevance of the simulations factors.

Finally three simulation parameters: the Auger effect, the medium type and the fluence level, have been identified as critical factors and therefore have to be chosen carefully and to be kept constant between interlaboratory comparisons of numerical simulations. Another factor: the cutoff energy may have a significant impact on the diffusion response. However, whatever the studied response, four simulation parameters have negligible effects: the working volume, the spatial resolution and cutoff, and the computer. Those results bring new contributions to improve the robustness of numerical simulations of nanoparticles activated by X-ray and proposes directions for standardization in this scientific area.

Keywords: nanoparticle, cancer, radiotherapy, modeling, simulation, design of experiments, statistics.

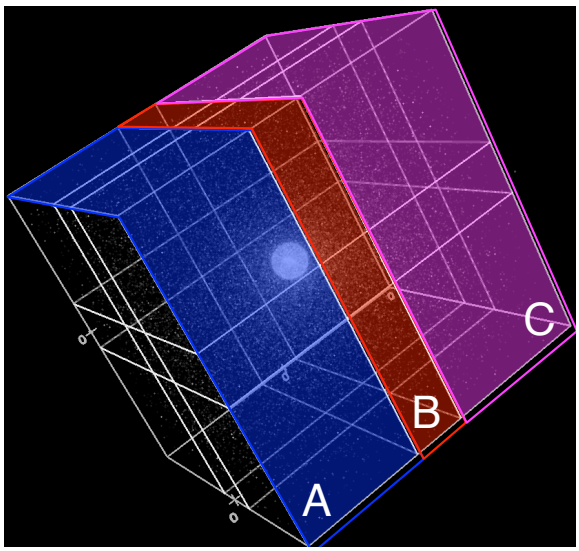

Figure 1: Cubic domain of simulation in which seven spatial regions of interest have been defined. Only the central region is composed of a single 100 nm gold nanoparticle.

References:

Butterworth K. T., McMahon S. J., Currell F. J., , Prise K. M. (2012) Physical basis and biological mechanisms of gold nanoparticle radiosensitization, *Nanoscale*, vol. 4, no. 16, pp. 4830–4838.

Agostinelli S., Allison J., Amako K. A., Apostolakis J., Araujo H., Arce P., Asai M., Axen D., Banerjee S., Barrand G. *et al*. (2003) Geant4 a simulation toolkit, *Nucl. Instrum. Meth. A*, vol. 506, no. 3, pp. 250–303.

Retif P., Pinel S., Toussaint M., Frochot C., Chouikrat R., Bastogne T., Barberi-Heyob M. (2015) Nanoparticles for radiation therapy enhancement : the key parameters, *Theranostics*, In Press.

Kodiha M., Wang Y. M., Hutter E., Maysinger D., and Stochaj U. (2015), Off to the organelles-killing cancer cells with targeted gold nanoparticles, *Theranostics*, vol. 5, no. 4, pp. 357–70.

The spread of multi-wall carbon nanotubes to the room air as a result of their mixing in the fume hood

E. Jankowska, T. Jankowski, W. Zatorski, P. Sobiech
Central Institute for Labour Protection - National Research Institute, Czerniakowska 16, 00-701 Warsaw, Poland

Abstract: Processes with possible emission of multi-wall carbon nanotubes (MWCNTs) should be carried-out in fume hood (LEV) or in full containment systems, which should interact with the general ventilation system of the room. Ensure proper interaction of ventilation systems in the room is essential to provide protection from exposure to particles of both workers, who work with nanomaterials, as well as other staff in those room.

The possibility of particles emission and their spread to the room air were determined by measurements of particles concentrations (using DiscMini's) before (background) and during processes of mixing of nanomaterial (MWCNTs 10-20nm from Cheap Tubes). Location of measuring points in the room are shown in Figure 1.

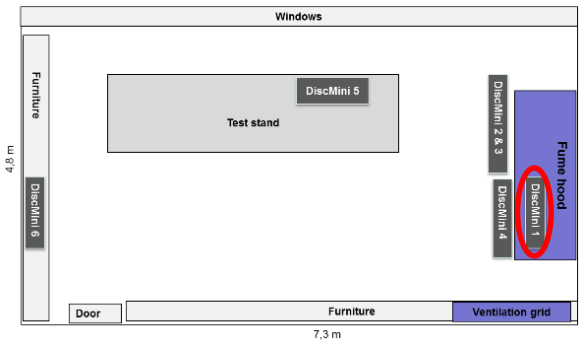

Figure 1. Location of measuring points in the room: place of MWCNTs emission during mixing.

Processes of mixing were carried-out inside LEV, in the room equiped with grid of general ventilation, for situations were LEV was switched-off (air supply to the room 137m^3/h, air exhaust 121m^3/h) and switched-on (air supply to the room 360m^3/h, air exhaust 969m^3/h).

Received results were the base for calculated ratio (P/B), showing of increase number concentrations as a result of mixing MWCNTs (P) compare to background (B). Criteria for determination of the likelihood of emission or the spread particles in the room air are following: P/B ≥ 2 - likely, P/B >1,05 to <2 - possibly/not excluded, P/B <1,05 - no likely (Brouwer *et al.;* 2013).

Keywords: ventilation, MWCNTs, emission, the spread of particles in the room air

Acknowledgements: This work presents the results of the projects: SCAFFOLD (GA 280535) and II.P.02 (CIOP-PIB).

It was found, that multi-wall carbon nanotubes (MWCNTs) emitted during processes of mixing the spread to the room air, even in the areas located far from place of mixing (more than 6m - DiscMini6) – Table 1. Switched-on LEV results of decreasing of emission of MWCNTs (Figure 2c) compare that when LEV was switched-off (Figure 2a). However for both situations (LEV switched-off/on) to the air were emitted MWCNTs (Figure 2b and 2d).

Table 1. Likelihood emission or the spread particles in the room air.

Fume hood	Possibility of MWCNTs emission during mixing (in fume hood – DiscMini1)	Possibility of the spread of MWCNTs, emitted during mixing, to the room air (in five points in the room)
Switched - off	P/B=10,2 (likely)	DiscMini's 2: P/B=12,8 (likely) 3: P/B=10,0 (likely) 4: P/B=6,2 (likely) 5: P/B=1,8 (possibly) 6: P/B=2,4 (likely)
Switched - on	P/B=2,0 (likely)	DiscMini's 2: P/B=1,2 (possibly) 3: P/B=1,2 (possibly) 4: P/B=1,3 (possibly) 5: P/B=1,2 (possibly) 6: P/B=1,1 (possibly)

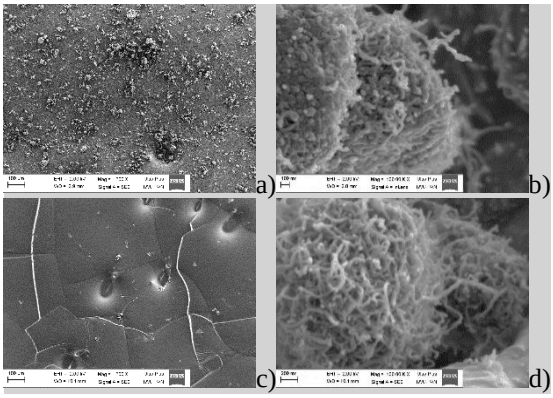

Figure 2. Electron microscopy (SEM) analysis: a), b) LEV switched-off; c), d) LEV switched-on.

References:

Brouwer D., van Duuren-Stuurman B., Berges M., Bard D., Jankowska E., Moehlmann C., Pelzer J., Mark D.: Workplace air measurements and likelihood of exposure to manufactured nano-objects, agglomerates, and aggregates. J Nanopart Res. 2013 15:2090.

The DaNa$^{2.0}$ Knowledge Base Nanomaterials – quality-approved and easy-to-understand information on current nanosafety research

C. Marquardt[1], H.F. Krug[2], D. Kuehnel[3], F. Paul[4], C. Steinbach[4], K. Nau[1]
[1]Karlsruhe Institute of Technology (KIT), Institute for Applied Computer Science, Hermann-von-Helmholtz-Platz 1, 76344 Eggenstein-Leopoldshafen, Germany
[2]Empa - Swiss Federal Laboratories for Materials Science and Technology, General Management - International Research Cooperation, Lerchenfeldstrasse 5, 9014 St. Gallen, Switzerland
[3]Helmholtz-Centre for Environmental Research (UFZ), Department Bioanalytical Ecotoxicology, Permoserstrasse 15, 04318 Leipzig, Germany
[4]DECHEMA e.V. Society for Chemical Engineering and Biotechnology, Theodor-Heuss-Allee 25, 60486 Frankfurt a. M., Germany
Email: clarissa.marquardt@kit.edu

Abstract: Nanotechnology will bring about fundamental changes of basic research as well as of many sectors of industry. It will also have a great impact on our daily life ranging from electronics to the health care system. However, consumers often miss reliable and easy-to-understand information on nanomaterials and nanotechnology and don't know where to get such information. Besides the great need to respond to basic questions such as *"Are there any risks for myself and the environment?"* there is a growing demand for tools to manage and assess the rapidly increasing number of publications related to nanosafety issues. Therefore the international DaNa2.0 expert team brings together its expertise and knowledge from different research areas dealing with all aspects of nanosafety research in order to create and provide a non-biased, quality-approved and up-to-date knowledge base for more transparency on www.nanopartikel.info. The DaNa$^{2.0}$ project publishes articles covering latest research results on nanomaterials with regard to their influence on humans and the environment in an easily comprehensible way. For this purpose, scientific publications, reports, project results and latest news on human and environmental toxicology are analysed using the *«Literature Criteria Checklist»*. This customised methodology developed by the DaNa expert team helps to discriminate between high- and low quality publications and thus facilitates the evaluation process of scientific publications. The mandatory and desirable assessment criteria were developed in accordance with common quality criteria acknowledged worldwide within the scientific community. Another unique feature of the DaNa knowledge base is the integrated application-based database that provides a unique link between nanomaterials in real applications (e.g. environmental remediation or medical products) and their potential impacts/ toxicological effect(s) that can be easily accessed by the interested visitor.

Additionally, DaNa$^{2.0}$ provides a list of FAQs, a link platform with contact data to other information portals and the opportunity to directly pose questions to our experts via E-mail. DaNa$^{2.0}$ is also present on Twitter, follow us @nano_info.

DaNa$^{2.0}$ is a German umbrella project funded by the German Federal Ministry of Education and Research

Keywords: knowledge base nanomaterials, literature criteria checklist, quality assessment of publications

References:

Kühnel D., Marquardt C., Nau K., Krug H.F., Mathes B., Steinbach C. (2014). Environmental impacts of nanomaterials: providing comprehensive information on exposure, transport and ecotoxicity - the project DaNa2.0. Environmental Sciences Europe, 26(1): 21.

Kimmig, D., C. Marquardt, K. Nau, A. Schmidt, M. Dickerhof (2014). Considerations about the implementation of a public knowledge base regarding nanotechnology. Computational Science & Discovery 7(1): 014001.

In vitro study of lung surfactant-nanoparticle interactions for evaluating nanotoxicity

*P. Lai[1], W. Daear[1], M. Anikovskiy[2], R. Loebenberg[3], E.J. Prenner[1]
[1]University of Calgary, Department of Biological Sciences, Calgary, Alberta, Canada
[2]University of Calgary, Department of Chemistry, Calgary Alberta, Canada
[3]University of Alberta, Faculty of Pharmacy and Pharmaceutical Sciences, Edmonton, Alberta, Canada

Abstract: The nanoparticles generated from industrial processes and those designed for use in medicine has increased our levels of exposure. Exposure to nanoparticles arises from either byproducts of industry or combustion as those seen from car exhausts. Although nanoparticles are continually being developed at an accelerated pace the understanding of the health impacts these nanomaterials have not been fully evaluated. The lungs are continually exposed to the environment and have evolved efficient mechanisms to remove particulate matter. The nanosized particles are less effectively removed in comparison to their micro sized counterparts. The impact of nanoparticles on the lungs has not been fully characterized. Drug delivery aims to use inhalable nanoparticles for treatment of pulmonary disease. The lungs offer several advantages including a large surface area for deposition of molecules and a thin alveolar epithelial layer to cross before entering systemic circulation. Combining these two features allows for a large dose of drugs and materials to be delivered that can be rapidly absorbed into the body. Pulmonary drug delivery shows great potential in the treatment of lung disease however it is unclear how these may impact respiratory function. Our research focuses on understanding the interaction between nanoparticles and lung surfactant models. Through this we can understand the nanotoxicity effects and be able to create safer inhalable drug carriers.

During inhalation particles can deposit on the surface of trachea, bronchiolar and alveolar regions of the lungs. For efficient delivery of therapeutics, nanoparticles will need to deposit within the alveoli where molecules are able to cross into the blood-stream. Before reaching the alveoli epithelial cells then the vasculature, the nanoparticles must first interact with the lung surfactant. Lung surfactant is a single molecule thick layer of lipids and proteins, it is responsible for lowering the surface tension in the alveoli required to maintain breathing. Disruption of surfactant results in impaired lung function and may lead to irreversible alveolar collapse.

Here we use lung surfactant as a model to evaluate the impact of nanoparticles on respiratory function. This in vitro method uses a Langmuir trough to measure the surface pressure-area isotherms of lung surfactant (Fig. 1). A high surface pressure corresponds to the ability of surfactant to be compressed to small areas while remaining stable. The end goal is to be able to screen different nanoparticles to determine their impact on surfactant function. This will allow for a first screen of airborne nanoparticles to determine their potential impact on lung surfactant function (Al-Hallak et al 2010).

The two nanoparticles used were gelatin and polyisobutylcyanoacrylate, both are being tested for inhalable drug delivery. Gelatin is a natural polymer derived from collagen that is nontoxic and biodegradable. Polyisobutylcyanoacrylate is a synthetic polymer and derivatives are already being used in the medical field. The lung surfactant model used is made up of the two most common lipid classes found in vivo, namely phosphatidylcholines and phosphatidylglycerols. This will allow us to vary the nature of the lipids used and to have tight control over lipid ratios and concentrations to determine if there are preferential interactions of nanoparticles with specific lipid depending on the headgroup, fatty acid tail saturation or the film packing as a function of composition. This is compared against a clinical surfactant to compare results. The information gained here will be used to help create a better mod-el for lung surfactant and aid in creating safer nanoparticles.

Keywords: inhalable therapy, nanoparticles, in vitro, surface pressure-area isotherms, lung surfactant.

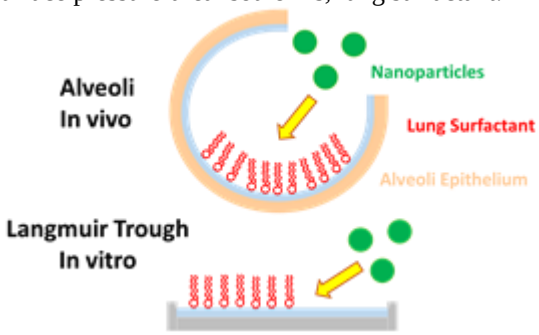

Figure 1: Schematic showing the in vitro aspect of the Langmuir trough and compared to the in vivo alveoli situation.

References:

Al-Hallak, K.M.H.D., Azarmi, S., Sun, C., Lai, P., Prenner, E.J., Roa, W.H., Löbenberg, R. (2010) Pulmonary toxicity of polysorbate-80-coated inhalable nanoparticles; In vitro and In vivo evaluation. AAPS J., 12(3),294-299

Effect of Gold Nanoparticle Shape of Cellular Uptake and Toxicity

Catherine Carnovale[1,2], Vipul Bansal[1], Ravi Shukla[1], Gary Bryant[2]

1. Ian Potter NanoBioSensing Facility, NanoBiotechnology Research Laboratory, School of Applied Sciences, RMIT University, GPO Box 2476, Melbourne VIC 3001, Australia
2. Centre for Molecular and Nanoscale Physics, School of Applied Sciences, RMIT University, GPO Box 2476, Melbourne VIC 3001, Australia

Abstract: The ability to adapt parameters during nanoparticle synthesis has led to the creation of a vast catalogue of gold nanoparticles (AuNPs) that differ in size, shape, surface charge, surface corona and chemical composition. AuNPs are continuing to attract research interest for biomedical applications, as they appear to be well tolerated in biological systems while providing opportunities for facile surface manipulations as well as exhibiting interesting optical properties (Shukla *et al*., 2005). Spherical AuNPs possess limited potential for surface plasmon resonance tuning, however altering the shape of AuNPs gives rise to interesting optical properties which can be suited to biological sensing, cellular imaging and cancer treatment.

While developments in the synthesis of AuNPs have been rapid in recent times, our understanding of their biological impact, in particular the effects of shape, size, chemical composition and surface corona, has struggled to keep pace. It is commonly thought that changes in shape could significantly influence the way that particles are recognised, processed and excreted by cells, however this effect has not been fully explored.

All inorganic nanoparticles, including gold, invoke the formation of a protein corona upon introduction to protein rich solutions such as biological media or blood. The biological response after a nanoparticle enters the blood stream is thought to be influenced by the protein species which bind to the nanoparticle, as well as protein orientation, binding strength and conformation (Alkilany *et al*., 2009). Despite the small number of studies in this area, it is generally agreed that shape affects the manner in which a protein can bind to the surface of a nanoparticle, with the introduction of such features as variable curvature, flat planes, sharp edges, corners, and pores. Such features may favour or hinder binding of individual proteins depending on their conformation, or cause them to undergo structural changes after binding.

In this paper we synthesise AuNPs with comparable surface functionalisation in various shapes (Figure 1) and explore the biological effects in two ways: first, using human serum albumin (HSA) - the most abundant protein in human blood - we explore the role of shape in protein corona formation; and second, we report on the effects of shape on uptake and toxicity in mammalian cells.

Keywords: Gold nanoparticles, toxicity, cellular uptake, protein corona, shape.

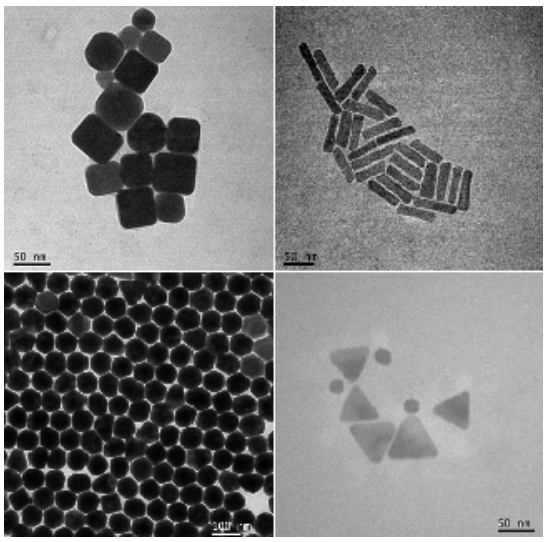

Figure 1: Scanning electron microscope image of various shaped gold nanoparticles as synthesized for biological experimentation.

References:

Shukla, R., Bansal, V., Chaudhary, M., Basu, A., Bhonde, R. R., & Sastry, M. (2005), Biocompatibility of Gold Nanoparticles and Their Endocytotic Fate Inside the Cellular Compartment: A Microscopic Overview. *Langmuir*, 21(23), 10644-10654.

Alkilany, A. M., Nagaria, P. K., Hexel, C. R., Shaw, T. J., Murphy, C. J., & Wyatt, M. D. (2009), Cellular uptake and cytotoxicity of gold nanorods: molecular origin of cytotoxicity and surface effects. *Small*, 5(6), 701-708.

Genotoxicity and Mutagenicity Screening of Engineered Nanomaterials:

G. Vecchio,[1,*] M. Fenech,[2] P.P. Pompa,[1] N. Voelcker[3]

[1]Istituto Italiano di Tecnologia, Center for Bio-Molecular Nanotechnologies@Unile, 73010 Arnesano (Lecce), Italy
[2]CSIRO Food and Nutritional Sciences, Adelaide, SA 5000, Australia
[3]Mawson Institute, University of South Australia, Mawson Lakes, SA 5095, Australia
[*]Giuseppe Vecchio, email giuseppe.vecchio@iit.it; giuseppevec@gmail.com

Abstract: The rapid growth of nanotechnology and concomitantly the increased rate of synthesis of engineered nanomaterials (ENMs) has led to an increasing and ubiquitous presence of ENMs in our environment. As a consequence, it is important to be able to characterise the nano-bio interactions between living organisms and ENMs. Furthermore, despite the great scientific effort and large economic investments for research projects in the field of nanotoxicology (34 projects dedicated to nanomaterial toxicology worth over €100 million within the European Seventh Framework -FP7- Programme), nanotoxicology studies have not yet provided any clear and unequivocal answers on the toxicity of nanomaterials (McCall, et al.; 2013). In addition, recent studies have revealed genotoxic and mutagenic risks associated with ENMs exacerbating this situation (Vecchio et al.; 2012), highlighting the urgent necessity to deeply examine and define the possible toxicological effects of ENMs and their physico-chemical characteristics. It should be noted that the combinatorial diversity of nanomaterials makes their rapid toxicological classification difficult without the application of high-throughput screening (HTS) approaches. In this context, we will show the mutagenic effects induced by AuNPs in Drosophila melanogaster and a new HTS platform based on the cytokinesis-block micronucle-us (CBMN) assay, that has been successfully applied in the evaluation of the cytotoxic and genotoxic effects induced by AgNPs and SiO2NPs, and the role of their physico-chemical properties such as composition, surface coating, size and surface charge (Vecchio et al.; 2014). In particular, our results demonstrate the catastrophic effects due to the mutagenic events induced by ENMs in the Drosophila offspring and the capability of our HTS platform to assess cyto- and genotoxicity induced by different ENMs in primary human lymphocytes. Finally, we will show the future strategy to evaluate these effects and to thoroughly analyse the molecular basis of nano/bio interactions by coupling the Drosophila genetic tools and the developed HTS platform.

Keywords: genotoxicity, mutagenicity, high-throughput screening.

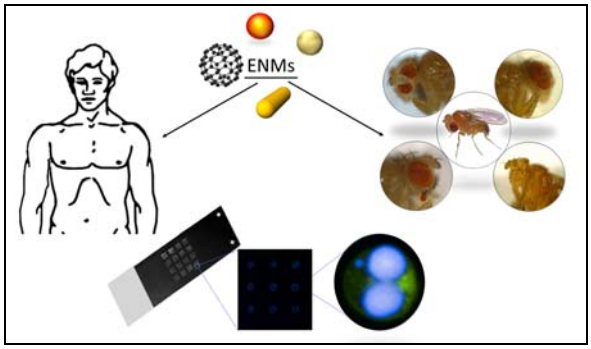

Figure 1: Schematic representation for ENMs genotoxicity and mutagenicity assessment by *in-vivo* and *in-vitro* approaches. Comparison between the ENMs induced genotoxicity evaluated in primary human lymphocytes (*in-vitro* approach) and in *Drosophila* haemocyte (*in-vivo* approach) using the new developed HTS platform. Assessment of the relationship between the mutagenic and genotoxic effects induced by nanomaterials in *Drosophila*.

References:

McCall, M. J., Coleman, V. A., Herrmann, J., Kirby, J. K., Gardner, I. R., Brent, P. J., Johnson, C. M. (2013) A tiered approach, *Nat. Nanotech.*, 8, 307–308

Vecchio, G., Galeone, A., Brunetti, V., Maiorano, G., Rizzello, L., Sabella, S., Cingolani, R., Pompa P.P. (2012) Mutagenic effects of gold nanoparticles induce aberrant phenotypes in Drosophila melanogaster, *Nanomedicine: NBM*, 8, 1-7

Vecchio, G., Fenech, M., Pompa, P. P., Voelcker N. H. (2014) Lab-on-a-Chip-Based High-Throughput Screening of the Genotoxicity of Engineered Nanomaterials, *SMALL*, 10, 2721–2734

Impact of ageing and protein remediation in the life-cycle of metal oxide nanoparticles in the organism

J. Volatron[1*] , F. Carn[1], M. Hemadi[2], Y. Javed[3], D. Alloyeau[3], F. Gazeau[1]
[1]Laboratoire Matière et Systèmes Complexes, 10 rue Alice Domon et Léonie Duquet, 75205 Paris cedex 13
[2]Laboratoire ITODYS, UMR 7086, Université Paris Diderot, 15 rue J.A. de Baïf, 75205 Paris cedex 13
[3]Laboratoire Matériaux et Phénomènes Quantiques, 10 rue Alice Domon et Léonie Duquet, 75205 Paris cedex 13

Abstract: The use of inorganic nanoparticles in the field of the nanomedecine is rapidly expanding allowing news treatments for various diseases. Thanks to their size, optical or magnetic properties and functionalization, metal oxide nanoparticles are widely used for their significant potential in theranostics. Although the potential toxicity of such nanomaterials are extensively studied, their long term fate, their degradation and the evolution of their properties in the organism are still poorly understood. Here we propose a multi-scale approach to study the life cycle of metal oxide nanoparticles in biological environments based on the evolution of their physical and morphological properties.

Our group have previously shown that iron oxide nanoparticles injected intravenously in mice underwent local intracellular degradation within lysosomes of macrophages in spleen and liver (L. Lartigue, ACS 2013) . The coexistence of iron rich ferritin protein in vicinity of degraded nanoparticles (Figure 1) suggests the implication of these iron storage protein in the remediation of iron released by nanoparticles. In this work, we aim to decipher the degradation mechanism of iron oxide, cobalt iron oxide and gold-iron oxide nanohybrids and their processing by endogenous proteins such as apoferritin.

We used an in vitro lysosome like medium to study the kinetic of degradation of the different nanomaterials depending on their composition and coating in presence and absence of apoferritin. The evolution of magnetic properties (currently used in medical applications like MRI or magnetically induced therapeutic hyperthermia) was studied by combining Nuclear Magnetic Resonance Dispersion (NMRD) and Electronic Paramagnetic Resonance (EPR). In parallel, the evolution of the morphology and the size of the nanoparticles were studied by using Dynamic Light Scattering (DLS) and Transmission Electronic Microscopy (TEM). Then we have investigated the transfer of iron and cobalt from nanoparticles to apoferritin by using UV-visible spectroscopy and TEM. This combination of methods highlights the mechanism of the nanoparticle degradation and the remediation and protein storage of metals from the nanoparticles.

Finally, to compare and understand the future of NPs in vivo, we have examined the evolution of the protein corona depending on the coating of the NPs, and the role of the protein corona involved in the degradation of NPs.

.

Keywords: Ageing and degradation of NPs, protein remediation, magnetic nanoparticles, Electroni Paramagnetic Resonnance, Nuclear Magnetic Resonnance Dispersion, UV-visible spectroscopy.

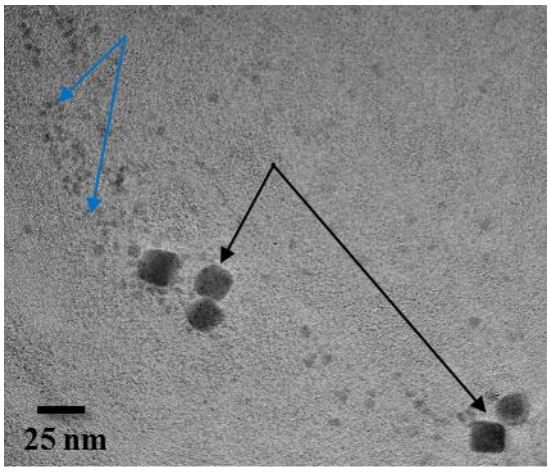

Figure 1: Figure illustrating intracellular degradation of PEG coated nanocubes (black arrows) in lysosomes after intravenous injection. Blue arrows show the coexistence of ferritin with degradated nanocubes.

References:

L. Lartigue, D. Alloyeau, J. Kolosnjaj-Tabi, Y. Javed, P. Guardia, A. Riedinger, C. Péchoux, T. Pellegrino, C. Wilhelm, F. Gazeau (2013) Biodegradation of Iron Oxide Nanocubes: High-Resolution In Situ Monitoring, *ACS Nano*, 7, 3939-3952

Size and morphology dependence of gold nanorods and gold nanospheres in the nanotoxicological process: *in vitro*, *in vivo* and membrane models studies

J. Cancino,[1,*] P.M.P. Lins,[1] V.S. Marangoni,[1] J.C.F. Besson,[2] M.E.C. Cancino,[2] M.R.M. Natali,[2] V. Zucolotto[1]
[1] University of São Paulo, Physics Institute of São Carlos, Nanomedicine and Nanotoxicology Group, São Paulo, Brazil. [2]Morphologic Science Department, State University of Maringá, Paraná, Brazil.

Abstract: The need for adequate toxicology testing of nanomaterial-based products should be addressed to help clarify which classes of nanomaterials or which behaviors/characteristics of such particles may indicate potential toxicity to human health or to the environment. However, conventional toxicology protocols for pharmaceutical validation are not adequate in terms of investigating nanoparticle toxicology because of the possible interactions between the nanomaterials and some of the utilized reagents. To understanding the real interaction or mechanisms involved in the nanoparticles/cell interface as nanotoxicity aspects, several techniques have been applying . Traditional biologic protocols, physical chemical and analytical methods have been updated and combined with *in vitro* and *in vitro* analysis for this purpose (Walczyk *et al*., 2010). But there is still the need to develop new methodologies to study the interactions between cell membrane and nanoparticles at the molecular level, especially because the uptake assessment is highly dependent of the membrane characteristics and nanoparticle charges, shape and size. Here, we report the influence of morphology and size of gold nanorods and gold nanospheres coated or not with human albumin serum using *in vivo*, *in vitro* and membrane models assays (Figure 1). The increase in the nanorods size as well as the protein corona decrease the uptake process according our *in vivo* and *in vitro* results, which was also confirmed by membrane model analysis, indicating that the size and morphology have high influence in the toxicology aspect. In addition, we introduce to the nanotoxicology community an alternative technique to understand the interactions of nanoparticles and membrane models composed by phospholipids, which may contribute to understand the interaction and possible mechanisms of adsorption and uptake process (Cancino *et al.,* 2013a,b). This study will also permit us to discuss the importance of combining techniques to better understand the nanotoxicity of nanomaterials and biological systems.

Keywords: nanotoxicology, nanorods, nanospheres, phospholipids, membrane model, in vitro, in vivo.

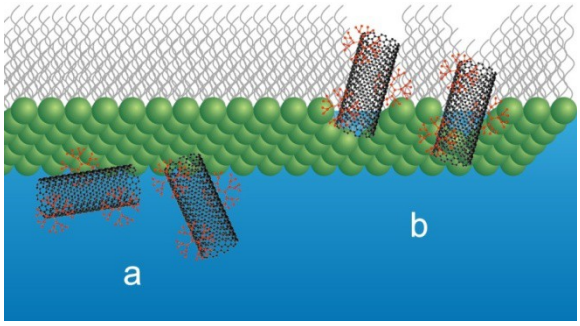

Figure 1: Illustration of a membrane composed by phospholipids which can be helpful to understand the interactions of nanomaterials and cell membranes.

References:

Walczyk, D., Bombelli, F.B., Monopoli, M.P., Lynch, I., Dawson, K.A. (2010) What the cell "sees" in bionanosciences. *JACS*, 132, 5761-5768.

Cancino, J., Nobre, T. M., Oliveira, Jr., O.N., Machado, S. A. S., Zucolotto, V. (2013a) A new strategy to investigate the toxicity of nanomaterials using Langmuir monolayers as membrane models. *Nanotoxicology*, 7, 61-70.

Cancino, J., Paino, I.M.M., Micocci, K.C., Selistre-de-Araujo, H. S., Zucolotto, V. (2013b) In vitro nanotoxicity of single-walled carbon nanotube-dendrimer nanocomplexes against murine myoblast cells. *Toxicology Letters*. 219, 18-25.

Nano MatEn 2015:
Nanotech for Energy & Environment

Effect of halide-mixing on the electronic transmission in organometallic perovskites

G. Berdiyorov[1,*], M. El-Amine Madjet[1], Fedwa El-Mellouhi[1], F. H. Alharbi[1], and S. Kais[1]
[1] Qatar Environment and Energy Research Institute, Qatar Foundation, P.O.Box 5825, Doha, Qatar

Abstract: Organic-inorganic hybrid perovskite materials, such as methylammonium lead iodide ($CH_3NH_3PbI_3$), have received a revival of interest in recent years as novel light harvesters with a solar conversion efficiency rapidly approaching 20% [1]. This high efficiency is mainly related to: i) proper band structure, which enable light absorption across most of the solar spectrum; ii) relatively long diffusion lengths; iii) relatively high mobility of charge carriers; and most importantly iv) less sensitivity to topological defects. Because of its tolerance for defects, lead halide perovskite solar cells can be fabricated using low-temperature solution methods that result in low manufacturing cost. In addition, structural, electronic and optical properties of $CH_3NH_3PbI_3$ can further be refined by chemical engineering, e.g., through mixing halogen atoms. In this respect, Cl and Br are expected to be the most efficient candidates capable of tuning the properties of the material. Despite the large number of experimental and computational studies, the role of halide-mixing remains poorly understood [2,3].

In this work we use density-functional theory in combination with the nonequilibrium Green's function formalism to study the effect of iodide/chloride and iodide/bromide mixing on the electronic transmission in lead based organometallic perovskite $CH_3NH_3PbI_3$, in its room temperature tetragonal phase. We found that the conductance of $CH_3NH_3PbI_3$ can be increased by almost an order of magnitude by partial halide-mixing (see Fig. 1). Largest conductance is observed for small concentration of bromide substitutions located at the equatorial sites. All the systems show similar response to applied voltage: the band gap increases and the transmission decreases with increasing voltage. Our findings are in good agreement with the recent experiment, where on the effect of chlorine substitutions on the structural, electrical and optical properties of $CH_3NH_3PbI_3$ was studied [2]. Full halide substitution has similar effect on the electronic transport properties of the lead-halide perovskites

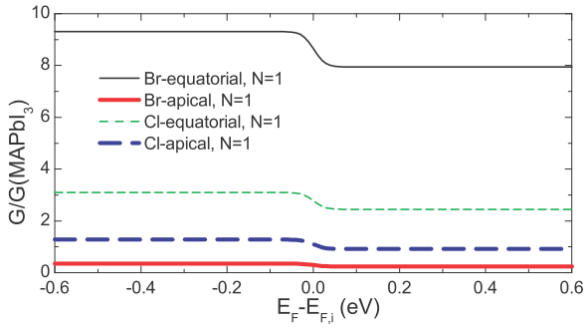

Figure 1: Conductance of $CH_3NH_3PbI_{3-x}Br_x$ (solid curves) and $CH_3NH_3PbI_{3-x}Cl_x$ (dashed curves) samples with a single halide substitution at the equatorial (thin curves) and apical (thicker curves) sites. The results are normalized to the conductance of $CH_3NH_3PbI_3$.

References:

[1] National Renewable Energy Laboratory, Best Research-Cell Efficiencies; www.nrel.gov/ncpv/ images/efficiency chart.jpg.
[2] S. Dharani et al., Nanoscale **6**, 13854 (2014).
[3] E. Edri et al., Nano Lett. **14**, 1000 (2014).

Nanoparticles-based Plasmonic Organic Photovoltaic Devices for Enhanced Performance and Stability

G. Kakavelakis[1], M. Krassas[1], M.M. Stylianakis[1], N. Vaenas[1], K. Savva,[1,2], E. Stratakis,[1,2], E. Kymakis[1,*]
[1] Center of Materials Technology and Photonics & Electrical Engineering Department, Technological Educational Institute (TEI) of Crete, Heraklion 71004 Crete, Greece, kymakis@staff.teicrete.gr
[2]Institute of Electronic Structure and Laser, Foundation for Research and Technology - Hellas, P.O. Box 1527, 711 10 Heraklion Crete, Greece

Abstract: Recent advances in polymer synthesis and device engineering of organic photovoltaic devices (OPVs) have led to power conversion efficiencies (PCEs) reaching 10% for single bulk heterojunction devices (Liu *et al.*, 2014). The utilization of randomly distributed nanoparticles (NPs) in almost every layer of the OPV device can significantly enhance both the device performance and stability. In particular, PCE can be enhanced by a) plasmonic near field enhancement absorption from small diameter NPs b) increased optical path length through scattering effects from large diameter NPs and c) enhanced morphology in the photoactive layer (Stratakis, Kymakis 2013). NPs of various sizes, shapes and configurations have been integrated into OPV device architecture in order to tune and enhance, in a wavelength-dependent manner, the optical absorption of the respective devices. As a result impressive improvements in the respective device efficiencies were achieved. In particular, enhancement of both the efficiency and stability of bulk heterojunction polymer-fullenene (P3HT:PCBM, P3HT:ICBA, PCDTBT:$PC_{70}BM$, PTB7:$PC_{70}BM$) devices is demonstrated by the addition of Au and Al, formed by ablation of metallic targets in liquids with pico- and femtosecond laser pulses, in either the active layer or in the interface between the buffer and the active layers (Kakavelakis *et al*. 2013,2014). A performance enhancement of 15% to 30% was observed in all polymer-fullerene systems. The highest enhancement of 30% was observed with Al NPs in P3HT:PCBM, while the highest efficiency of 9.1% was observed in the PTB7:$PC_{70}BM$. The PCE is postulated to be enhanced by exploiting increased absorption around the small diameter NPs integrated into the active layer as well as strong light scattering from the large diameter NPs and clusters, both effects stemming from the excitation of the LSP waves at the NP/photoactive layer interface. Moreover, the devices with Au and Al in the active layer die after ~65 hrs and ~150 hrs under continuous illumination respectively, compared with the pristine devices which die after ~30 hrs (Paci et al. 2013). Moreover, particular attention will be paid on the effect of NPs passivation and functionalization on the PCE. In this context, it was found that the highest PCE can be achieved with the incorporation of NPs in the photoactive layer, which the NPs metallic core is in direct contact with the active layer polymer component. On the other hand, the presence of a terminating coating in the NPs, leads to a reduction in the PCE due to enhanced recombination

Keywords: plasmonic organic photovoltaic, scattering, nanoparticles, laser ablation.

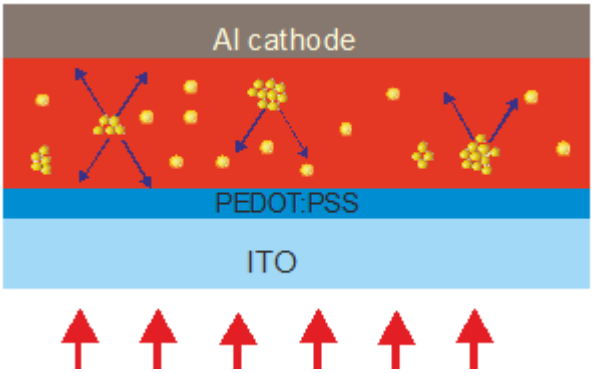

Figure 1: A schematic diagram of the OPV devices, showing distribution of NPs as individual and as clusters

References:

Liu, Y. Zhao J., Li Z., Mu C., Ma W., Hu H., Jiang K., Lin H., Ade H., Yan Y. (2011) Aggregation and morphology control enables multiple cases of high-efficiency polymer solar cells, Nature Communications, 5, 5293

Stratakis E., Kymakis E., (2013) Nanoparticles-based Plasmonic Organic Photovoltaic Devices, *Materials Today*, 16 (4), 133-146

Kakavelakis G., Stratakis E., Kymakis E., (2013) Aluminum nanoparticles for efficient and stable organic photovoltaics , *RSC Advances*, 3 (37), 16288-16291

Kakavelakis G., Stratakis E., Kymakis E., (2014) Synergetic Plasmonic Effect of Al and Au Nanoparticles for Efficiency Enhancement of Air Processed Organic Photovoltaic Devices, *Chemical Communications*, 50 (40), 5285 – 5287

Paci B., Bailo D., Albertini V., Wright J., Ferrero C., Spyropoulos G.D., Stratakis E.,Kymakis, E., (2013) Spatially-resolved in-situ Structural Study of Organic Electronic Devices with Nanoscale Resolution: the Plasmonic Photovoltaics Case Study, *Advanced Materials*, 25(34), 4760–4765

One-pot Fabrication of Nb-doped TiO_2 Photoanode for Dye-sensitized Solar Cells

Yu-Ting Huang[1], Ya-Huei Chang[1], Peng Zhai[1], Nga Yu Hau[1], Shien-Ping Feng [1,*]
[1]Department of Mechanical Engineering, The University of Hong Kong, Pokfulam Rd., Hong Kong

Abstract: Dye sensitized solar cells (DSSCs) have received great attention to use as a potential alternative for low-cost clean energy.(Zhang *et al.*, 2013) A typical DSSC comprises a dye-sensitized nanocrystalline TiO_2 film coating on a transparent conductive oxide (TCO) glass as photoanode, a liquid redox electrolyte containing an I^-/I^{3-} redox couple, and a platinum (Pt) catalyst as counter electrode (CE). (Oregan *et al.*, 1991) A facile one-pot synthesis of Nb^{5+}-doped TiO_2 nanoparticles (NPs) with low cost and high yield efficiency for photoelectrode of DSSCs is reported based sol-gel solution. The Nb^{5+}-doped TiO_2 NPs with Nb dopants of 0~5 mol% are prepared by directly mixing commercial TiO_2 slurry with a functionalized Nb_2O_5 gel following by heat treatment without using hydrothermal method. The functional Nb_2O_5 gel is obtained by UV treatment of a mixture of $NbCl_5$ powder precursor, ethanol and water as solvent with a certain ratio. The as-prepared NPs, which characterized by field emission scanning electron microscopy (FESEM), field emission transmission electron microscopy (FETEM), exhibit well-crystallized pure anatase TiO_2 phase with uniform particle distribution and average size of about 15~18 nm. The Raman and XPS results demonstrate that the Nb is well doped into the TiO_2 lattice and the substitution of Nb^{5+} on Ti^{4+} is formed using this cost-effective method. The incorporation of Nb^{5+} leads to a stronger and broader light absorption in visible light range (red shift) and a decrease of band gap with increasing Nb dopant content, which importantly enhances the efficiencies of light-harvesting and electron injection, and effectively suppresses the charge recombination. The best energy conversion efficiency of 8.45% is achieved based on 2.0 mol% Nb-doped TiO_2, which presents a significant improvement of 18.9% compared with the undoped TiO_2 cell. (Figure 1(a)) This method provides a simple and cost-effective mass-production route to synthesis n-type metallic ion doped TiO_2 nanoparticles as excellent photoanode materials.

Keywords: TiO_2 nanoparticles; One pot; Doping; Photovoltaic; Dye-sensitized solar cell.

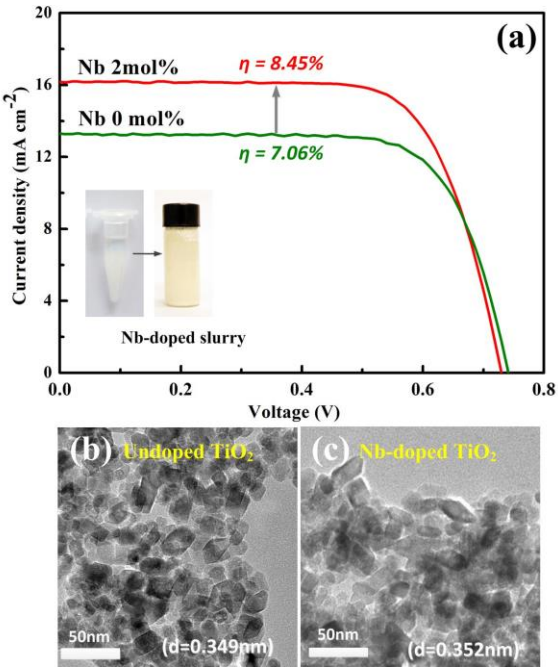

Figure 1. (a) Illustrating the photocurrent density-photovoltage (J-V) curves for DSSCs based on the undoped and 2.0 mol% Nb-doped TiO_2 NPs electrodes. (b)The TEM images of the undoped TiO_2 nanoparticles. (c) The TEM images of the 2mol% Nb-doped TiO_2 nanoparticles.

References:

Zhang S., Yang X., Numata Y., Han L. (2013), Highly efficient dye-sensitized solar cells: progress and future challenges, *Energy Environ. Sci.*, 6, 1443-64.

Oregan B., Gratzel M. (1991), A Low-Cost, High-Efficiency Solar-Cell Based on Dye-Sensitized Colloidal TiO_2 Films. *Nature*., 353, 737-740.

Highly stable carbon nanofluids for solar thermal collectors

Sara Mesgari*, Natasha Hjerrild, Robert A. Taylor
University of New South Wales, Sydney, NSW, Australia.

Abstract: Carbon nanofluids are engineered materials with controllable thermal and optical properties. For solar thermal collectors they are uniquely well-suited, due to their high spectral absorptivity over the entire solar range (Figure 1). Their application as solar thermal absorbers, however, has been impeded by difficulties in achieving stable nanofluid suspensions at elevated temperatures (Taylor *et al.*; 2013). Dispersing carbon nanotubes (CNTs) in the base fluid is challenging due to the strong inter-particle interaction arising from the high surface energy of CNTs as well as their hydrophobic nature. (Premkumar *et al.*; 2012) A number of chemical functionalization methods including oxidation using strong acids, polymer grafting and mild oxidation using potassium persulfate are available to achieve stable dispersions of CNTs in polar solvents, but polar solvents are limited to relatively low temperature (Zhang *et al.*; 2009, Singh *et al.*; 2009). Thus, high temperature stabilisation techniques for carbon nanofluids have not yet been identified. In this study, a comprehensive series of experiments were conducted to identify appropriate base fluids and functionalization methods to produce CNT nanofluid dispersions with high stability at elevated temperatures of up to 250 °C. Different forms of CNTs including, single-walled carbon nanotubes (SWCNTs), double-walled carbon nanotubes (DWCNTs) and multi-walled carbon nanotubes (MWCNTs) were chemically functionalized to obtain stable dispersions in water, Glycerol and Therminol (a synthetic (non-polar) oil). The stability of chemically functionalized carbon nanotube dispersions at different temperatures including 80, 150, 200 and 250 °C was investigated. The results of broadband UV-VIS-NIR spectroscopy showed no agglomeration in the mildly oxidised multi-walled nanotubes (MWCNTs) dispersed in Therminol when heated to 250 °C, highlighting this low-cost material as a potential candidate for use in the new generation of nanofluid-based solar thermal collectors. The nanofluids with high stability at temperatures as high as 250 °C developed in this study are expected to open a new class of highly stable nanofluids for use as solar thermal absorbers.

Keywords: solar thermal collectors, carbon nanotubes, nanofluids, thermal stability.

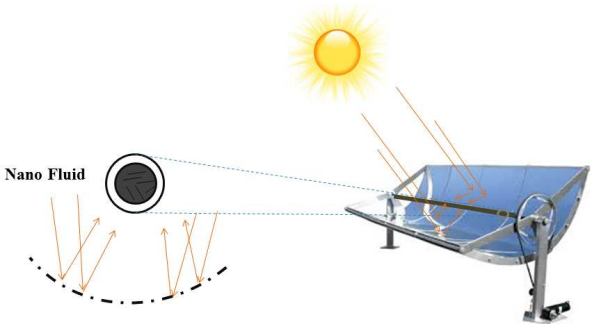

Figure 1: Structure of nanofluid based solar thermal collectors.

References:

Robert Taylor, Sylvain Coulombe, Todd Otanicar, Patrick Phelan, Andrey Gunawan, Wei Lv, Gary Rosengarten, Ravi Prasher, Himanshu Tyagi. (2013), Small particles, big impacts: A review of the diverse applications of nanofluids. *J. Appl. Phys.* 113, 011301.

Premkumar, T.; Mezzenga, R.; Geckeler, K. E. (2012), Carbon nanotubes in the liquid phase: Addressing the issue of dispersion. *Small*, 8 (9), 1299-1313.

Singh, P.; Campidelli, S.; Giordani, S.; Bonifazi, D.; Bianco, A.; Prato, M. (2009), Organic functionalisation and characterisation of single-walled carbon nanotubes. *Chem Soc Rev.* 38 (8), 2214-2230.

Zhang, L., Q.-Q. Ni, Natsuki. T. (2009). One-step preparation of water-soluble single-walled carbon nanotubes. Applied Surface Science 255(15): 7095-7099.

Perovskite Solar Cell Modules built on Vertical TiO_2 Nanorods with High Efficiency and Stability

Azhar Fakharuddin[1,2], Francesco Di Giacomo[2], Fabio Matteocci[2], Alessandro L. Palma[2], Irfan Ahmed,[1] Aldo Di Carlo[2], Thomas M. Brown[*2], and Rajan Jose[*1]

[1]Nanostructured Renewable Energy Materials Laboratory, Faculty of Industrial Sciences and Technology (FIST), Universiti Malaysia Pahang, 26300 Kuantan, Malaysia
[2]C.H.O.S.E. (Centre for Hybrid and Organic Solar Energy), Department of Electronic Engineering, University of Rome "Tor Vergata",via del Politecnico 1, Rome, 00133 Italy.

Abstract:

Organometallic halide perovskite solar cells (PSCs) has achieved a certified efficiency (PCE) of 20.1%, which is nearly seven times higher than the first report in 2009 (~3%). Typically, perovskite precursor ($CH_3NH_3PbX_3$, where X=I, Br, Cl) are deposited on a mesoporous or compact thin layer of metal oxide semiconductor (MOS) on a conducting glass substrate (FTO) to fabricate PSCs. Although TiO_2 nanoparticle films are the frequently employed electron transport layers (ETL) in these devices, alternative nanostructures such as nanowires and nanorods are also employed owing to their higher electron mobility. We have employed rutile nanorods (NRs) as ETL in PSCs and found that NRs scaffold is beneficial for long term durable performance. We compared the performance and the durability of two types of scaffolds, i.e., pristine and $TiCl_4$ treated NRs (Figure 1a), and observed that although the $TiCl_4$ treatment resulted in ~100% improved performance (PCE ~12.2%) compared to pristine NRs (PCE ~6.4%) the latter showed 10% improvement in performance after ~1300 h whereas the PCE of the former droped by ~60% of initial value (Figure 1b). We attribute the origin of durable photovoltaic performance in pristine NR based devices to their morphology and crystallinity. Although NRs based devices provide improved electronic transport and durable perovskite solar cells, as demonstrated in our study, the primary issue towards their up-scaling is the difficulty in their patterning. We have patterned NR based large area substrates via laser ablation without significantly damaging the conducting oxide layer. The solid state perovskite solar cells made of these patterned substrates resulted in PCE ~7.8% higher than a reference module of TiO_2 nanoparticles (~6.7%) owing to their improved charge collection. The results demonstrate the first report of high efficiency large area perovskite solar modules based on rutile nanorods.

Keywords: Solar cells, electron collection in perovskite solar cells, stability of perovskite solar cells, 1-dimensional nanomaterials for perovskite solar cells.

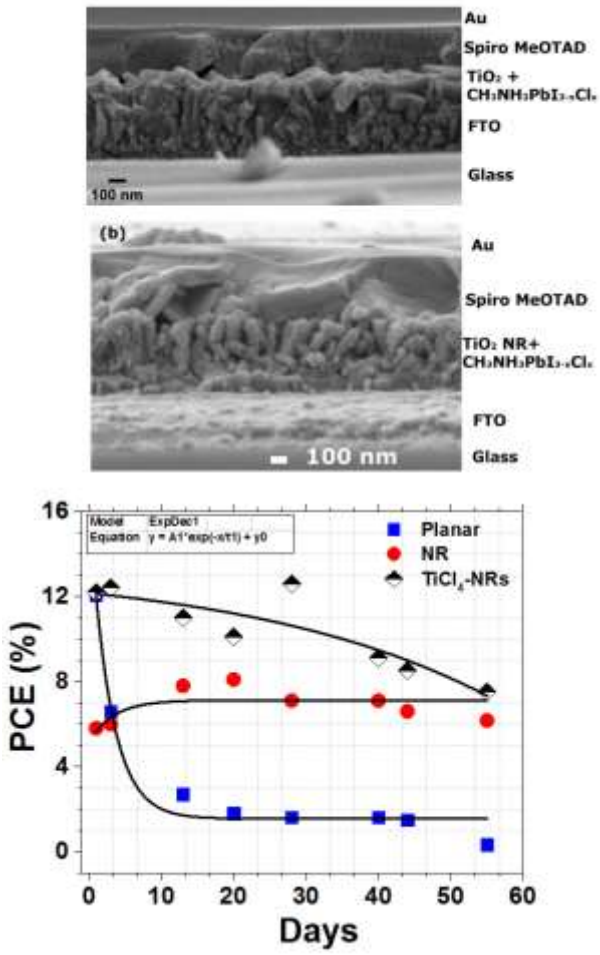

Figure 1: (a) External quantum efficiency (EQE) of nanorods (half-filled black circles) and TiO_2 based (black solid triangles) perovskite modules and (b) J-V curves of the same modules.

References:

G. Xing, N. Mathews, S. Sun, S.S. Lim, Y.M. Lam, M. Graẗzel, S. Mhaisalkar, T.C. Sum, Long-Range Balanced Electron and Hole-Transport Lengths in Organic-Inorganic $CH_3NH_3PbI_3$Science 342 (2013) 344-347.

Fakharuddin A., Di Giacomo F., Ahmed I., Wali Q., T.M. Brown, R. Jose. Role of morphology and crystallinity of electron transport layer on long term durable performance of perovskite solar cells (accepted), *J. Pow. Sources*, Jan 2015.

The Development of Alumina Nanofluids-based ferro/ferricyanide Electrolyte and their Applications on Thermogalvanic Cells

Chang Liu,[1] Shien-Ping Feng.[1,*]
[1]Department of Mechanical Engineering, The University of Hong Kong, Pokfulam Rd., Hong Kong.

Abstract: Considerable attentions have been devoted to using nanofluids for augmenting mass transport in colloidal systems. Due to the combined effect of local convection and percolation, nanofluids show a predominate enhancement on conductivity and diffusivity (Prasher *et al.*, 2012). Thus nanofluids are expected to develop critical conductivity of electrolyte for thermogalvanic cells because of aspiring response to convection. However, nanofluids in electrolyte are seldom studied due to intrinsic instability of nanofluids, especially, in electrolyte with high ionic strength. We report practicable processes to fabricate 10nm γ-alumina nanofluids-based ferro/ferricyanide electrolyte with enhancing electrical conductivity and feasible stability by introducing nanogrinding in conjunction with ultrasonic processing. Experimental study is performed to investigate limiting currents of ferro/ferricyanide redox couple in nanofluids based on rotating disk electrode (Figure 1). Diffusion coefficients are deduced from the function of limiting current with respect to angular velocity (Sara *et al.*, 2011). The diffusivity of alumina nanofluids-based electrolyte possesses an obvious enhancement with the increasing of angular velocity, showing a critical derivation from homogeneous pure ferro/ferricyanide electrolyte at high angular velocities. We postulate a new model to describe the diffusivity change of alumina nanofluids-based electrolyte under sheared flow on the basis of both aggregation kinetics and local convection. In addition, thermogalvanic device test is conducted to determined Seebeck coefficient of alumina nanofluids-based electrolyte at temperature differences (Hu *et al.*, 2010). Alumina nanofluids-based electrolyte is confined by relatively high viscosity, which counteracts to the thermal conductivity and therefore to capture favorable figure of merit, contributing to high energy conversion efficiency for thermogalvanic cells.

Keywords: alumina nanofluids, electrolyte, stability, electrical conductivity, thermal conductivity, diffusivity, rotating disk electrode, thermogalvanic cells, energy conversion efficiency.

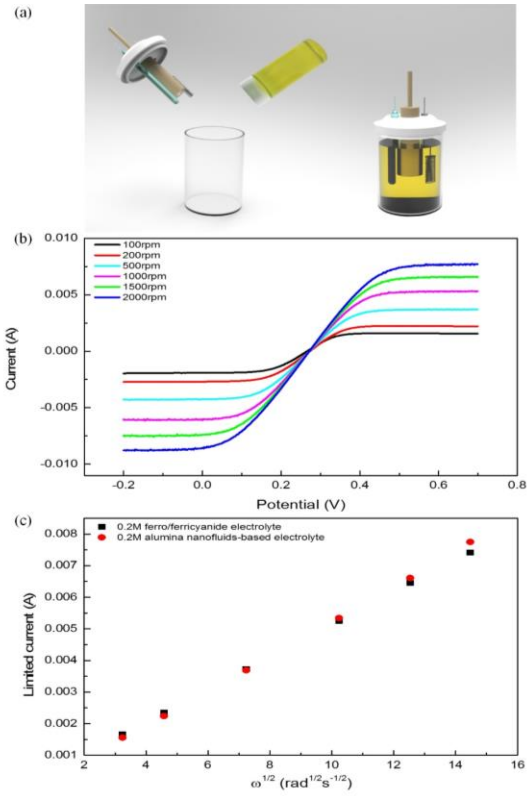

Figure 1: (a) Schematic diagram of the experimental setup for measuring diffusivity of alumina nanofluids-based electrolyte. (b) Voltammograms of ferro/ferricyanide redox couple in alumina nanofluids under various rotating velocities. (c) Limiting current of 0.2M ferro/ferricyanide electrolyte and 0.2M alumina nanofluids-based ferro/ferricyanide electrolyte as a function of rotating velocity. The slope gives the diffusion behaviors of electrolytes.

References:

Prasher, R., Phelan, P. E., & Bhattacharya, P. (2006). Effect of Aggregation Kinetics on the Thermal Conductivity of Nanoscale Colloidal Solutions (Nanofluid). *Nano Letters, 6*(7), 1529-1534.

Sara, O. N., İçer, F., Yapici, S., & Sahin, B. (2011). Effect of suspended CuO nanoparticles on mass transfer to a rotating disc electrode. *Experimental Thermal and Fluid Science, 35*(3), 558-564.

Hu, R., Cola, B. A., Haram, N., Barisci, J. N., Lee, S., Stoughton, S., Baughman, R. H. (2010). Harvesting Waste Thermal Energy Using a Carbon-Nanotube-Based Thermo-Electrochemical Cell. *Nano Letters, 10*(3), 838-846.

Soft, Compressible and Interdigitated 3D Energy Storage Devices Built by Layer-by-Layer Assembly Inside Aerogels

A. Marais,[1,*] G. Nyström,[1] E. Karabulut[1], L. Wågberg[1,2], Y.Cui[3], M. Hamedi[4]
[1] Fibre and Polymer Technology, KTH Royal Institute of Technology, Stockholm, Sweden
[2]Wallenberg Wood Science Center (WWSC), KTH Royal Institute of Technology, Stockholm, Sweden
[3]Stanford Univ McCullough Bldg, Stanford, California, USA
[4]Chemistry Chemical Biology, Harvard, Cambridge, Massachusetts, USA

Abstract: A controlled formation of fully three dimensional (3D) energy storage devices has been a challenge over the past decade. So far, the few examples of 3D devices rely on advanced processing techniques, limited by material compatibility as well as scalability.
In this study, we propose a new method for a detailed tailoring of interdigitated 3D supercapacitor and batteries inside open-cell and high surface area porous materials such as nanocellulose aerogels (Nyström *et al.*, submitted). The method, consisting of a sequential deposition of active materials via Layer-by-Layer self assembly (Decher, 1997), is rapid (each layer is assembled within seconds), precise (control over the layer thickness at the nanometer level) and versatile (can be used for a very wide range of substrates and materials) (Hamedi *et al.*, 2013).
3D supercapacitors based on carbon nanotubes electrodes were prepared using this method (Figure 1). In order to show the versatility of the method, hybrid batteries were also prepared, incorporating copper hexacyanoferrate nanoparticles (Wessels *et al.*, 2011) as the cathode redox active material.
Our results demonstrate that the self-assembly of interdigitated thin films inside aerogels is a rapid, precise, and scalable route for building high surface area 3D devices. Furthermore, the devices are soft, flexible and stable under extreme compressions (up to 75%).
The presented method and results pave the way for a new class of energy storage devices combining high performance, flexibility and compressibility.

Keywords: high surface area, interdigitated, 3D, electronics, battery, supercapacitor, flexible, compressible, Layer-by-Layer assembly

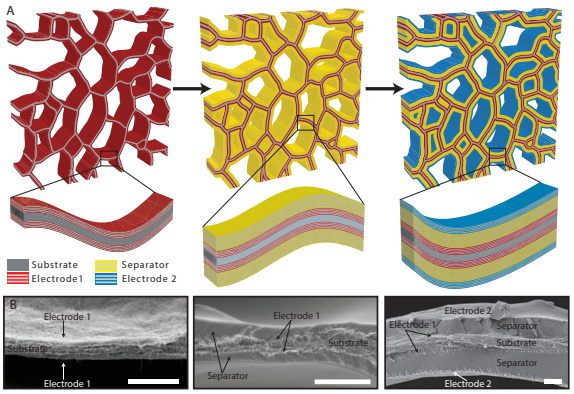

Figure 1: (A) schematic description of the step-by-step build-up of 3D interdigitated devices in the bulk of the aerogel using LbL self assembly, and (B) SEM images of cross sections of LbL-coated aerogels, taken at the corresponding steps of the build-up procedure (the scale bars are 2 µm).

References:

Nyström, G., Marais, A., Karabulut, E., Cui, Y., Wågberg, L., Hamedi, M. (Submitted), Self-assembled three-dimensional and compressible interdigitated thin film batteries and supercapacitors.

Hamedi, M., Karabulut, E., Marais, A., Herland, A., Nyström, G., Wågberg, L. (2013), Nanocellulose aerogels functionalized by rapid Layer-by-Layer assembly for high charge storage and beyond, *Angew. Chem., Int. Ed.,* 52, 12038-12042.

Decher, G. (1997) Fuzzy nanoassemblies: Toward layered polymeric multicomposites, *Science*, 277, 1232-1237.

Wessells, C. D., Huggins, R. A., Cui, Y. (2011), Copper hexacyanoferrate battery electrodes with long cycle life and high power. *Nat. Commun.*, 2, 550.

Numerial study of MAXI3 (X=Pb, Sn) perovskite based hetero-junction solar cells

M. Guo[1,2] G. Shao [1,3,*]

[1] Institute for Renewable Energy and Environmental Technologies, University of Bolton. Bolton BL3 5AB, UK

[2] Faculty of Materials Science and Engineering, Hubei University, Wuhan, 430062, P. R. China

[3] UK-China Centre for Multifunctional Nanomaterials, Zhengzhou University, Zhengzhou 450001, China

Abstract: The main driver for the development of new solar cells is to address the high cost problem of Si-based technologies. Recently, perovskite based solar cells have been developed, which quickly passed the efficiency threshold of most emerging thin-film devices and thus has triggered a new round of explosive activities in photovaltic research in using perovskite for solar energy harvest. The current focus for this class of solar cells is largely on further enhancement of efficiency and replacement of Pb. In this work, numerial simulation of MAXI3 (X=Pb, Sn) perovskite based hetero-junction solar cells were conducted using AMPS-1D, aiming to offer physical insight to guide materials selection and device engineering. MASnI3 is investigated as an alternative layer for Pb based optical absorber. Both two-layered (SnO_2/Perovskite) and three-layered (SnO_2/Pervoskite/p-type) architectures are studied, with perovskite being the major light-absorption material in both cases. The results show that the three-layered device is far more efficient than the two-layered, when the former is designed into a window/absorber/voltage-enhancer (WAV) construction, this being in excellent agreement with the outcome of our recent modelling work [1,2]. Cu_2O is shown to be the best candidate among three p-type materials (P3HT, Spiro-OMeTAD and Cu_2O). Comparing to $MAPbI_3$, the same efficiency can be achieved using a thinner layer of $MASnI_3$ as the absorber. With suitable distribution of charged carrier densities through out the three layers, optimal efficiency above 35% can be achived with a total thickness less than 1 um.

Keywords: perovskite solar cell, WAV structure, $MAXI_3$ (X = Pb,Sn), numerical simulation.

*E-mail: gs6@bolton.ac.uk

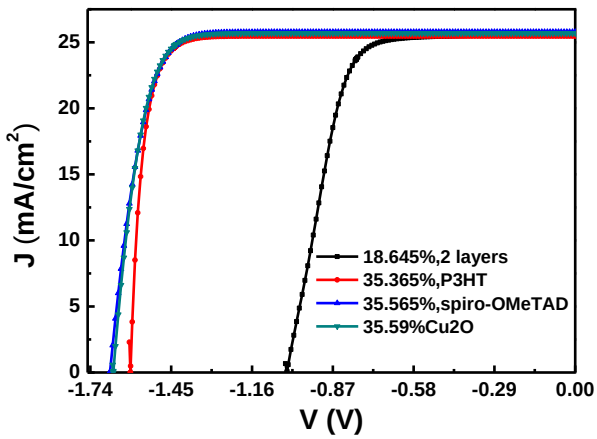

Figure 1: J-V curve using $MAPbI_3$ as absorber layer. Higher efficiency can be achieved by the three-layered design.

References:

[1] L. Zhu, G. Shao, J. Luo, Numerical study of metal oxide heterojunction solar cells. *Semicond Sci Tech* 2011; 26: 085026.

[2] L. Zhu, J. Luo, G. Shao, Milne W I. Numerical study of metal oxide Schottky type solar cells. *Sol Energ Mat Sol C* 2013; 111: 141

Stability of organic solar cells using composites materials of inorganic nanostructures and polymers for efficient organic photovoltaics: time-resolved structural/morphological studies

B. Paci [1,*], A. Generosi [1], M. Guaragno, V. Rossi Albertini [1], E. Stratakis[2,3], E. Kymakis[2]

1. Istituto di Struttura della Materia, Consiglio Nazionale Delle ricerche, ISM-CNR, Via Fosso del Cavaliere 100, 00133 Roma, Italy. * barbara.paci@ism.cnr.it
2 Center of Materials Technology and Photonics & Electrical Engineering Department, School of Applied Tecnology, Technological Educational Institute (TEI) of Crete, Heraklion, 71004, Crete, Greece.
3 Institute of Electronic Structure and Laser (IESL), Foundation for Research and Technology-Hellas (FORTH), & Dept. Of Materials Science and Technology, Univ. Of Crete, Heraklion, Crete, Greece

Abstract: Increasing research interest is devoted to bulk heterojunction (BHJ) organic photovoltaic (OPV) cells, showing low cost large-scale production, flexibility, light weight and low enviromental impact. Recently, it has become clear how the optical and transport properties of the organic active film in OPVs, are strongly connected to their structural, morphological and interfacial proprieties. Here, we discusss our recent results on devices incorporating metallic nanoparticles (NPs) in the photoactive layer, in order to take advantage of the ability of the metallic NPs to rise the BHJ optical absorption by the excitation of Localized Surface Plasmon Resonance. The photovoltaic, structural, morphological and interface properties and aging effects are evaluated by in-situ by time-resolved Energy Dispersive X-ray Reflectivity/Diffraction (EDXR/EDXD) techniques applied jointly with in-situ atomic force microscopy (AFM). The results of our unconventional approach, based on time-resolved EDXR/AFM cross-monitoring, showed the incorporation of metallic NPs allowed to control both the bulk and the interface morphological degradation pathways. In particular, time-resolved EDXR showed that doping the active film of the devices with Au NPs protects the metallic electrode buried interface against degradation (figure 1). This can be ascribed to a NP-mediated mitigation of the photo-oxidation effect at the cathode–active layer interface. As a result, aging experiments demonstrate that Nps doped devices show enhanced PV properties and durability.
These findings indicate novel strategies, employing plasmonic metal NPs, as a fundamental step for the development of more stable OPV architectures. Besides the impact of indicating novel approaches for the developing of more efficient and stable organic devices, this work demonstrate the great potential of the joint EDXR/AFM technique in the study of nanolayered structures.

Keywords: Bulk heterojunction organic photovoltaic devices, plasmoic effect, polymer inorganic nanoparticles nanocomposites, time-resolved joint EDXR/AFM characterization, stability enhancement.

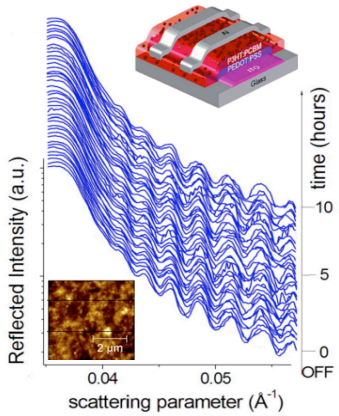

Figure 1: Time-resolved EDXR analysis of OPV device incorporating metal NPs, demonstrating a NPs mediated mitigation of the aging effects.

References:

B. Paci, A. Generosi, V. Rossi Albertini, G.Spyropoulos, E. Stratakis, E.; Kymakis, (2012) Enhancement of photo/thermal stability of organic bulk heterojunction photovoltaic devices via gold nanoparticles doping of the active layer. *Nanoscale*, **4** (23), 7452 – 7459.
B. Paci, A. Generosi, D. Bailo , V. Rossi Albertini, G.Spyropoulos, E. Stratakis, E.; Kymakis (2011) Enhanced Structural Stability and Performance Durability of Bulk Heterojunction Photovoltaic Devices Incorporating Metallic Nanoparticles. *Advanced Functional Materials,* **21**, 3578-3582.
B. Paci, D. Bailo, V. Rossi Albertini, J.Wright, C. Ferrero, G.D. Spyropoulos, E. Stratakis, E. Kymakis, (2013), Spatially-Resolved In-Situ Structural Study of Organic Electronic Devices with Nanoscale Resolution: The Plasmonic Photovoltaic Case Study, *Adv. Mater.*, **25**, 4760.

Understanding Lithium solvation in ionic liquids from first principles molecular dynamics simulations

Ali Kachmar, Marcelo Carignano
Qatar Environment and Energy Research Institute, Qatar Foundation, PO Box 5825, Doha, Qatar

Abstract: Ionic liquids are being considered as an alternative electrolyte for Li-ion batteries. The main reason behind this application is the non-flammability of many ionic liquids that will eliminate one of the major safety issues affecting this technology. In this particular case, we investigate the solvation of lithium (Li) in Ethylammonium Nitrate (EAN). The study relies on a combination of classical, and first principles molecular dynamics simulations using the Gromacs and CP2K software packages, respectively [1,2]. Starting with an existing force field we initially performed a classical simulation in order to obtain a molecular arrangement that was then used as the starting configuration for the first principles simulations. We found that the first principles results give a lower Li-Oxygen average coordination number when compared to recently reported classical simulations [3]. The issue of the discrepancy between classical and first principles predictions for the coordination has been already discussed in the literature for cations solvated in water [4,7]. In particular, our ab-initio simulations conclusively show that only three nitrate molecules solvate the lithium ion in a planar arrangement, namely, the Li ion is located on or very close to the plane defined by the three nitrogen atoms corresponding to nitrate molecules (Figure 1).

Keywords: Li-ion batteries, Ionic liquids, Lithium solvation, First Prinicples Molecular Dynamics simulations.

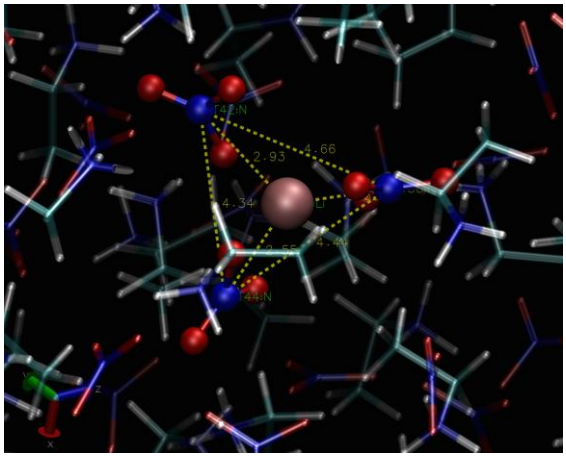

Figure 1: A snapshot illustrating the solvated Li^+ in EAN (Ethylammonuim Nitrate)

References:

[1] http://www.gromacs.org

[2] CP2K, http://www.cp2k.org/

[3] Méndez-Morales, Trinidad and Carrete, Jesús and Cabeza, Óscar and Russina, Olga and Triolo, Alessandro and Gallego, Luis J. and Varela, Luis M. J. Phys. Chem. B, 2014, 118, 761-770.

[4] Bakó, I. and Hutter, J. and Pálinkás, G. J. Chem. Phys, 2002, 117, 9838-9843.

[5] Bakó, I. and Hutter, J. and Pálinkás, G. J. Phys. Chem. A, 2006, 110, 2188-2194.

[6] Ikeda, T. and B, Mauro, T, Kiyoyuki J. Chem. Phys. 2007, 126, 034501-9.

[7] Ikeda, T. and B, Mauro J. Chem. Phy. 2012, 137, 041101-4.

Nanomaterials Impacts Across the Life Cycle: Case Study LCA on Organic Photovoltaic Solar Cells

M. Tsang,[1,2,] G. Sonnemann,[1,2] D. Bassani,[1,2] P. Garrigues[1,2]
1 University of Bordeaux, Institute of Molecular Sciences, France
2 CNRS (Le Centre National de la Recherche Scientifique), Institute of Molecular Sciences, France.

Abstract: This paper presents the work of an life-cycle assessment (LCA) case study involving organic photovoltaic (OPV) technology, particularly technology using the nanomaterial Phenyl-C61-Butyric-Acid-Methyl-Ester (PCBM), and the implications acrossthe life-cycle of using engineered nanomaterials in produc systems.

Although solar technology converts freely available solar into useful forms of energy such as electricity, potential environmental impacts result may from processing, production and disposal of these products and materials. The objective of this paper is to highlight the influence of nanomaterials in the life-cycle impacts of organic photovoltaic cells, particularly their potential impact on human health and ecotoxicity.

This work will present a cradle-to-grave LCA comparing OPV solar cells, including the use and end-of-life phases. Previous work of ours included the cradle-to-gate LCA, comparing the functional unit of 1Wp of electricity produced for OPV and conventional cells.

The results of that cradle-to-gate study demonstrate that from a life cycle perspective, organic solar cells perform better than conventional solar cells. The models and results assessed also show that further improvements can still be gained for OPV cells with material choices and fabrication methods of the solar cell.

The results of this previous assessment failed to incorporate the impacts (i.e. toxicity) from the nanomaterials themselves which are used in the active layer of the photovoltaic system. Potential emissions and exposure to nanomaterials could present themselves during manufacturing of the nanomaterials or production of the solar cell itself.

Our recent work is furthering the assessment of OPV cells, by evaluating impacts throughout the entire life-cycle of the product. The use phase and end-of-life considerations are being included by changing the functional unit to agree with various types of use phase scenarios such as solar panels used in throw away devices, medium-term devices, and standard long-term solar arrays and panels. Additionaly, various end-of-life considerations will be taken into account including landfilling, incineration and possibly recycling.

In this regard particular attention will be given to the environmental flows associated with the fullerenes across all life-cycle stages. The nanomaterial impacts including the percent contribution of total life-cycle impacts as well as the emissions, fate/transport, exposure and toxicity resulting from the fullerenes will be assessed. The latter will consist largely of a qualitative assessment, and also an overview of how these points of interest can be better integrated into life-cycle assessment impact methods.

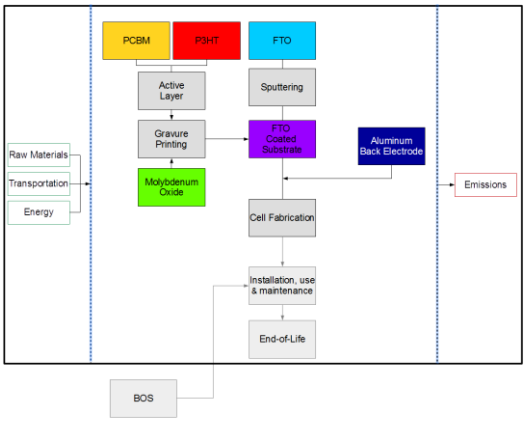

Fig. 1 System boundaries for the life-cycle assessment.

References:

[1] A. Roes, E. Alsema, K. Blok and M. Patel, "Ex-Ante Environmental and Economic Evaluation of Polymer PV," *Progress in Photovoltaics*, pp. 372-393, 2009.

[2] A. Anctil, C. W. Babbitt, R. P. Raffaelle and B. J. Landi, "Material and Energy Intensity of Fullerene Production," *Environmental Science and Technology*, pp. 2353-2359, 2012.

[3] B. C. Thompson and J. M. Frechet, "Polymer Fullerene Composite Solar Cells," *Angewandte Chemie International Edition*, vol. 47, no. 1, pp. 58-77, 2007.

[4] N. Espinosa, R. Garcia-Valverde, A. Urbina and F. Krebs, "A LCA of Polymer Solar Cell Modules Prepared Using Roll-to-Roll Methods Under Ambient Conditions," *Solar Energy Materials and Solar Cells*, pp. 1293-1302, 2011.

[5] J. Swantson, "Thiophene," in *Ulmann's Encyclopdeia of Industrial Chemistry*, B. Elvers, Ed., Weinheim , Wiley-VCH, 2007.

[6] G. G. Graf, "Tin, Tin Alloys, and Tin Compounds," in *Ulmann's Encyclopdeia of Industrial Chemistry*, B. Elvers, Ed., Weinheim, Wiley-VCH, 2007.

[7] F. Krebs, "Roll to Roll Fabrication of Monolithic Large Area Polymer Solar Cells Free from Indium Tin Oxide," *Solar Energy Materials and Solar Cells*, pp. 1636-1641, 2009.

[8] S. Aukkaravittayapun, N. Wongtida, T. Kasecwatin, S. Charojrochkul, K. Unnanon and P. Chindaudom, "Large Scale F-Doped SnO2 Coating on Glass by Spray Pyrolysis," *Thin Solid Films*, vol. 1, no. 1, pp. 117-120, 2006.

[9] R. Gacia-Valverde, J. Cherni and A. Urbina, "LCA of Organic Photovoltaic Technologies," *Progress in Photovoltaics*, pp. 535-558, 2010.

Sol-gel complex synthesis of biphasic anatase-brookite photocatalysts for hydrogen production

J. Drbohlavova,[1] V. Kasparek,[1] K. Castkova,[1] M. Kralova,[1] and J. Cihlar,[1]
[1]Central European Institute of Technology, Brno University of Technology, Brno, Czech Republic

Abstract: Research of efficient photocatalytic materials for hydrogen production still gain a lot of attraction. The current efforts to synthesize the biphasic titania photocatalytic nanoparticles are based on mixing of titanium precursor (usually titanium alkoxide) with a donor (e.g. lactic acid) in a ratio of 1:3 resulting predominantly in the formation of brookite phase instead of real biphasic structures (Cihlar *et al.*; 2015). Here we present a sophisticated and and reproduceable method to obtain the anatase-brookite crystals with a high reaction yield. This method requires only mild hydrothermal conditions such as normal pressure and temperature below 100 °C, and does not suffer from the formation of unfavourable single phase product. The aim of work was to study the optimal reactant concentration, titanium isopropoxide and lactic acid, to achive the highest photocatalytic activity in the production of hydrogen.
The synthesized titania biphasic nanoparticles were characterized by transmission electron miscopy, BET adsorption isotherm, X-ray diffraction spectroscopy and photoelectrochemical spectroscopy. The obtained TEM results (Figure 1) showed the crystallite size corresponds to 3–6 nm which is in a good correlation with results from XRD analysis. BET analysis revealed the active surface as high as 250 m^2/g. The photocatalytic activity in the hydrogen production was evaluated with respect to donor and titanium precursor ratio and different forms – either colloidal or deposited. As expected, we have found the photocatalytic activity of prepared biphasic photocatalysts in colloidal form is approximately 9 times higher in hydrogen production than spray-coated dense photocatalytic layers.

Keywords: titania nanoparticles, biphasic photocatalyst, anatase, brookite, sol-gel, chelate synthesis, hydrothermal synthesis, hydrogen production, photoelectrochemical spectroscopy.

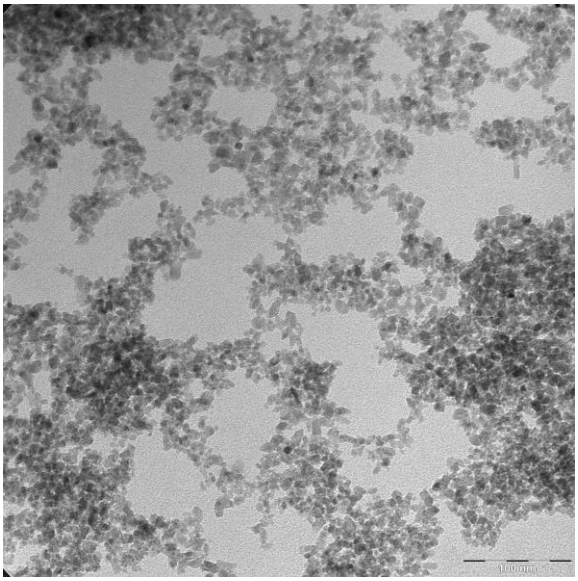

Figure 1: TEM image of biphasic anatase-brookite nanoparticles with the size of 3–6 nm (the bar corresponds to 100 nm).

References:

Cihlar, J., Kasparek, V., Kralova, M., Castkova, K. (2015), Biphasic anatase-brookite nanoparticles prepared by sol–gel complex synthesis and their photocatalytic activity in hydrogen production, *Int. J. of Hydrogen Energy*, 40 (7), 2950-2962.

Oxygen Electroreduction on Platinum Nanoparticles Deposited on D-glucose Derived Carbon

Masoud Taleb[1*], Irina Hussainova[2], Jaak Nerut[3], Thomas Thomberg[4], Tauno Tooming[5], Enn Lust[6]

[1] Department of Materials Engineering, Tallinn University of Technology, Estonia, masoud.taleb@ttu.ee
[2]Department of Materials Engineering, Tallinn University of Technology, Estonia, irina.hussainova@ttu.ee
[3] Institute of Physical Chemistry, University of Tartu, Estonia, Jaak.nerut@ut.ee
[4] Institute of Physical Chemistry, University of Tartu, Estonia, Thomas.thomberg@ut.ee
[5] Institute of Physical Chemistry, University of Tartu, Estonia, Tauno.tooming@ut.ee
[6] Institute of Physical Chemistry, University of Tartu, Estonia, enn.lust@ut.ee

Abstract: Proton Exchange Membrane Fuel cells (PEMFC) are counted as clean and very promising energy conversion devices. They are still expensive and their performance and durability are not very persuasive. One of the developing aspects is the structure of the carbon support, which can affect the overall performance and price. In this study, a new type of microporous-mesoporous carbon material synthesized from D-glucose and posttreated with CO_2 was used as the carbon support for Pt catalyst. This material, was prepared in the laboratory of the Institute of Chemistry, Tartu University and Pt nanoparticles were precipitated on this support via borohydride reduction method. Both unmodified and modified materials were characterized by physical techniques (XRD, Raman spectroscopy, N_2 adsorption/desorption method, HRSEM, SEM-EDS and HRTEM) and electrochemical techniques (cyclic voltammetry, rotating disk electrode method and electrochemical impedance spectroscopy). Raman spectroscopy technique confirmed the disordered amorphous structure of the synthesized carbon material. The presence of the Pt was attested by SEM-EDS and XRD. N_2 adsorption/desorption data showed the distribution of the pore sizes in materials and revealed the microporous-mesoporous structure of both materials. HRSEM and HRTEM presented a visual image of the C and Pt-HTC materials and confirmed the spherical shape and good dispersion of Pt nanoparticles. Cyclic voltammetry and impedance spectroscopy data, revealed considerably high capacitance for both unmodified and modified materials in 0.5 M H_2SO_4 solution. The ORR activity in 0.5 M H_2SO_4 solution investigated by cyclic voltammetry and rotating disc electrode method showed much higher activity for Pt-HTC compared to pure carbon material.

Keywords: PEM fuel cell cathode, oxygen electroreduction, Pt catalyst, D-glucose derived

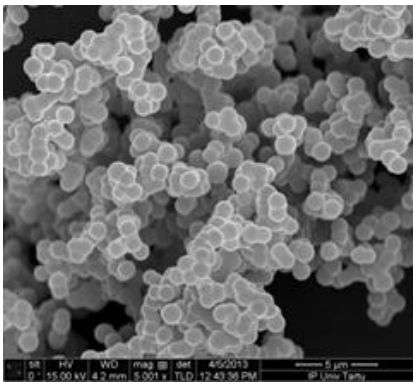

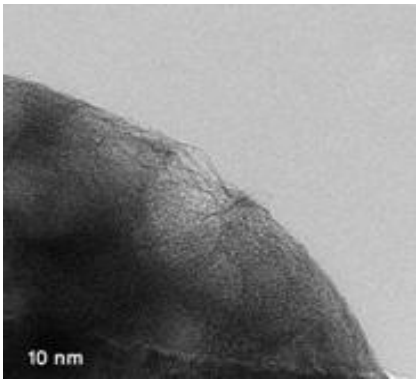

References:

S. Sepp, E. Härk, P. Valk, K. Vaarmets, J. Nerut, R. Jäger, E. Lust, Impact of the Pt catalyst on the oxygen electroreduction reaction kinetics on various carbon supports, J. Solid State Electrochem. 18 (2014) 1223-1229.

E. Härk, J. Nerut, K.Vaarmets, I. Tallo, H. Kurig, J. Eskusson, K. Kontturi, E. Lust, Electrochemical impedance characteristics and electroreduction of oxygen at tungsten carbide derived micro-mesoporous carbon electrodes, J. Electroanal. Chem. 689 (2013) 176-184.

E. Lust, E.Härk, J. Nerut, K. Vaarmets, Pt and Pt-Ru catalysts for polymer electrolyte fuel cells deposited onto carbide derived carbon supports, Electrochim. Acta 101 (2012) 130-141.

Fabrication of heterostructure between Tin oxides and TiO_2 nanobelts for application in photocatalysis and gas sensing

Hong Liu,[1,2,*] Guohui Chen[1]
[1]State Key Laboratory of Crystal Materials, Shandong University, Jinan, Shandong 250100, China
[2] Beijing Institute of Nanoenergy and Nanosystems, Chinese Academy of Science, Beijing 100864, China.

Abstract: Heterostructure properly designed between semiconductors has been proved efficient for the realization of new or improved properties (Hong Liu *et al.*; 2014). Due to its ultrahigh surface-to-volume ratios and diversified functional properties, one dimensional TiO_2 nanobelts are ideal backbones for the growth of other nanostructures. We report the synthesis of novel hierarchical scaly Sn_3O_4/TiO_2 nanobelts via a facile hydrothermal method, the Sn_3O_4 nanoflakes with a size range of 100-400 nm and thickness of 20-40 nm are perpendicularly grown along the c-axis direction on TiO_2 nanobelts, which are 50-200 nm in width, 20-40 nm in thickness and up to several micrometers in length, to form a heterostructure system. The matching band positions cause greater separation of photoexcited charge carriers, which should be responsible for the enhanced photocatalytic pollutant degradation and hydrogen evolution under either UV or visible light irradiation (Guohui Chen *et al.*; 2015). Further thermal oxidation of Sn_3O_4/TiO_2 at elevated temperature attains SnO_2/TiO_2 heterostructure. Experiments indicated its desirable gas sensitivity toward ethanol at operating temperature as low as 43℃ (Figure 1). To elucidate the possible mechanism, the oxidation process of Sn_3O_4 are examed and analyzed. The Sn_3O_4 experiences two processes of decomposition and oxidation, with metal Sn as intermediate phase, resulting in SnO_2 nanosheets and nanoparticles. We anticipate that the exposed high-energy facets of (4.75 -4.75 -9.594) SnO_2 that converted from triclinic phase Sn_3O_4 should play critical role in the low temperature gas sensing performance. This study provide a photocatalyst with broad spectrum absorption and a gas sensor with intrinsic low operating temperature.

Keywords: TiO_2 nanobelts, Sn_3O_4, SnO_2, heterostructure, photocatalytic activity, hydrogen evolution, thermal oxidation, gas sensing.

Figure 1: Figure illustrating the gas sensitivity towards ethanol and atomic structure for SnO_2 exposed facets in two types: (4.75 -4.75 -9.594) and (001).

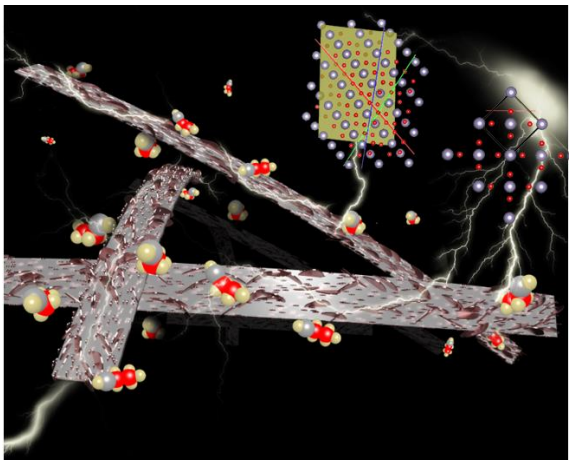

References:

Hong Liu, Jian Tian, Zhenhuan Zhao, Robert I. Boughton. (2014), Recent progress in design, synthesis, and applications of one-dimensional TiO_2 nanostructured surface heterostructures: a review, *Chem. Soc. Rev.*, 43, 6920-6937.

Guohui Chen, Shaozheng Ji, Jerome Claverie, Hong Liu. (2015), Synthesis of scaly Sn_3O_4/TiO_2 nanobelt heterostructures for enhanced UV-visible light photocatalytic activity, *Nanoscale*, 7, 3117-3125.

Efficient and Stable Photo electrochemical Water-oxidation Performance of ZnO NRs with Ultrathin Cobalt Layer

Nandanapalli Koteeswara Reddy,[1*] Sebastian Wahl,[1] Peter Bogdanoff,[2] Nicola Pinna[1]
[1]Institue of Chemistry, Humboldt University, Adlershof, 12489 Berlin, Germany
[2]Institute of Solar Fuels, Helmholtz-Zentrum Berlin für Materialien und Energie GmbH, Hahn-Meitner-Platz 1, D-14109 Berlin

Abstract: Efficient and stable electrochemical water oxidation (ECWO) performance was observed from ultrathin cobalt layer coated aligned zinc oxide (ZnO) nanorod structures. ZnO NRs have been developed on ZnO layer coated FTO substrates using low-temperature chemical bath deposition (Devika *et al.;* 2015). Structural, morphology and optical properties were studied. Prior to ECWO measurements, a thin cobalt layer was coated on ZnO NRs by electrochemical deposition, which plays a role as protective as well as catalyst layer (Figure 1a). The ECWO performance of the structures was studied in specially designed three electrode electrochemical cell using a platinum wire as counter electrode and Ag/AgCl KCl saturated electrode as reference electrode. The measurements were carried out in pH=10 electrolyte solution (borax with sodium hydroxide) (Bora *et al.;* 2014) under dark as well as front illumination (Xenon lamp with and without UV filter) conditions. The photocurrent density (J) versus potential curves of the cobalt coated ZnO NRs anodes are shown in Figure 1b. The dark response of as-grown ZnO NRs is very less, which is in the order of $\mu A/cm^2$. However, under UV light illumination, the structures exhibited very good photoresponse and also showed the current density in the order of mA/cm^2. The ratio between illumination and dark current density at a potential of 0.5 V is found to be 455. Further, very good photoelectrochemical stability in the duration of 30 minutes is noticed at the potential of 0.5 V.

Keywords: ZnO nanorods, ZnO/Co core/shell structures, photoelectrochemical studies, Energy harvesting applications.

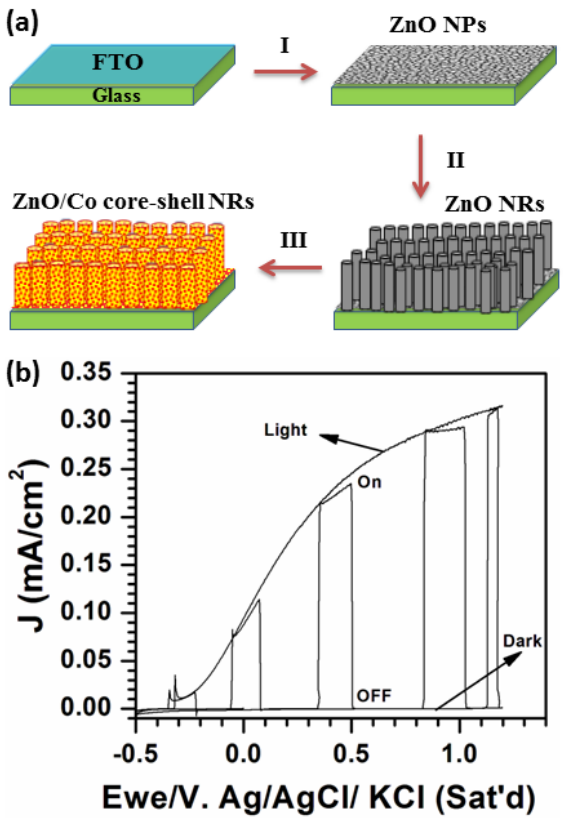

Figure : (a) Schematic diagram of growth of aligned ZnO NRs and (b) photochemical water oxidation response under dark and light (with and without chopping)

References:

Devika, M., Koteeswara Reddy, N., Tu, C. W. (2015) ZnO/ITO core/shell nanostructure electrodes for future prototype solar cell devices**,** *RSC Advances* 5**,** 2891.

Bora, D. K. and Braun, A. (2014) Solution processed transparent nano-particulate ZnO thin film electrode for photoelectrochemical water oxidation, *RSC Adv.* 4, 23562

New sensor for direct detection of pesticides in water by Raman spectroscopy coupled with enzymatic functionalized nanoparticles.

El Alami .A [1.2*], Lagarde.F [1], Mimouna.B [2] , Daniel.P [1]
1. Institute of Molecules and Materials UMR CNRS 6283 Le Mans;
2. Solid Physics Laboratory, Team polymers and nanomaterials, FSDM, Fez, Morocco;

Abstract: Pesticides are worldwidely used in agriculture and industries[*Ahlborg et al.*, 1961]. Some of them are highly toxic and may perturb some vital functions in organisms. In this framework it is very important to dispose of tools able to detect very fast and with very high sensitivity these kinds of compounds. In this work an acetylcholinesterase (ACHE) biosensor was developed in the goal of a direct detection of pesticides in water. Our method is based on Surface Enhanced Raman Scattering (SERS) phenomenon which corresponds to the increasing of a Raman signal when an analyte is at the vicinity of a metallic rough surface. Organophosphored and carbamate pesticides are known to block the activity of ACHE, an important enzyme implied in nervous system functioning[*George et al.*, 1961]. The activity of ACHE is a sensitive indicator of the presence of pesticides and its inhibition was already used for detection purpose. Here, once immobilized via an electrochemical process[*Kengne-Momo et al.*, 2010], the enzyme was placed at the contact of its substrate (acetylcholine(ATC)) and the enzymatic reaction (transformation of the substrate in choline and acetic acid) was monitored by Raman spectroscopy. By using dedicated gold nanoparticles(Au Nps), the Raman signal of the generated products was detected and enhanced giving a specific SERS spectrum, reference spectra of a "healthy" enzyme (fegure 1). In presence of pesticides, the enzyme is inhibited leading to the absence of enzymatic reaction and to a different Raman spectra (fegure 2). In this study, paraoxon and carbaryl were used as model pesticides and the first results showed that this biosensor gave highly sensitive and very fast responses. This biosensor can be used for a non-specific and on-line detection of enzyme inhibitors.

Keywords: Acétylcholinestérase, Raman SERS, Pesticides, Au nanoparticles.

.

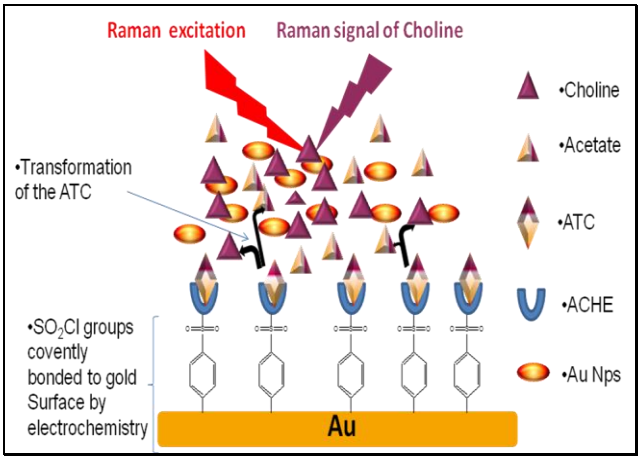

Figure 1: Activity of Acetylcholinesterase in the absence of pesticides.

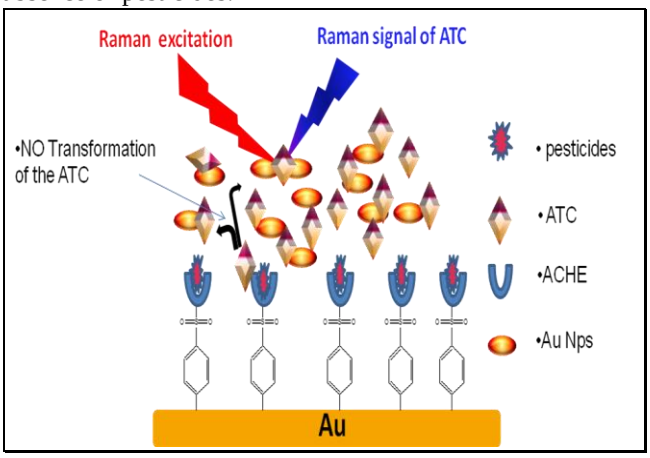

Figure2: Inhibition of the Activity of Acetylcholinesterase by the pesticides.

References:

Ahlborg, U., Akerblom, M., Almeida, W.. (1991), Public health impact of pesticides used in agricultur, Geneva:World Health Organisation. 128p.

George, L., Ellman, K., Courtney,D., ANDRES V., Robert, M.,(1 961), A new and rapid colorimetric determination of acetylcholinesterase activit, Biochemical harmacology .7:88-95.

Kengne-Momo, R. P., Jeyachandran, Y. L., Assaf, A. , Esnault, C., Daniel, P., Pilard, J. F. , Durand, M. J. ,Lagarde, F. Dongo, E., Thouand, G.(2010), A simple method of surface functionalisation for immuno-specific immobilisation of protein,; Anal Bioanal Chem 398:1249–1255.

Graphene Coating and Nanocrystalline Alloy Structure: Novel Approaches for Remarkable Corrosion Resistance

R.K. Singh Raman
Department of Mechanical and Aerospace Engineering
Department of Chemical Engineering
Monash University (Melbourne), Vic 3800, Australia

Abstract
This talk will present two novel approaches for mitigation of corrosion. The associated research has also involved considerable degree of surface analysis.

Ultra-thin Graphene Layer for Corrosion Resistance
Graphene research was awarded Nobel Prize in 2010 [1]. A monolayer or a few atomic layer thick graphene coatings on metals have been shown to improve their corrosion resistance by nearly orders of magnitude (Figure 1). Though there are very few studies reported on the topic of corrosion resistance due to graphene coating, there is still considerable variability in the degree of improvement. For example, improvement in aqueous corrosion resistance of copper due to graphene coating is reported to vary from insignificant to nearly 2 orders of magnitude [2-5], whereas the improvement for nickel can be in excess of an order of magnitude. This presentation will review the most recent research on graphene that has been claimed as 'the thinnest known corrosion-protecting coating', and potential application of such disruptive approach to corrosion resistance of steels.

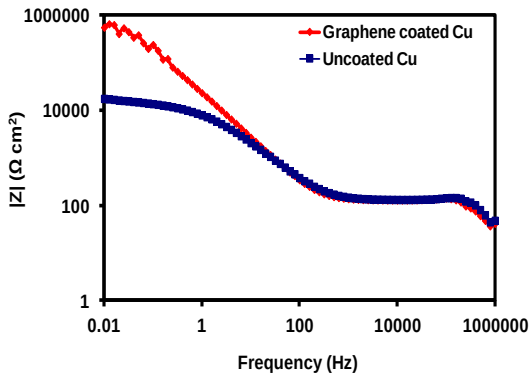

Fig. 1 Bode plots confirming the graphene coated Cu to have ~2 orders of magnitude superior corrosion resistance in sea water than the uncoated Cu [2] (Note, the magnitude of |Z| (on the y-axis) at the lowest frequencies represents corrosion resistance).

Nanocrystalline Structure for Oxidation Resistance
The second part will demonstrate remarkable resistance to oxidation as result of the nanocrystalline alloy structure. This will include an elaborate description of the author's own hypothesis that nanocrystalline structure can impart extraordinary oxidation resistance, and the validation of this hypothesis (as shown in the Figure 2). A thorough surface/subsurface characterization of oxidized alloys, using secondary ion mass spectrometry has provided a sound mechanistic understanding of the remarkable improvement in oxidation as result of nanocrystalline structure. The data to be presented will include the results establishing that a Fe-Cr nanocrystalline alloy with only 10wt% Cr can provide as much oxidation resistance as a Fe-20Cr alloy, suggesting possibility of Fe-Cr alloys with the necessary corrosion resistance at much lower Cr contents. As another exciting potential application of this work, the nanocrystalline powders of Fe-Cr alloys synthesized in this study could be used for developing corrosion resistance coating having considerably low Cr contents.
Keywords: protein folding, nanoporous sol-gel glasses, silica-based biomaterials, circular dichroism spectroscopy, surface hydration, crowding effects, micropatterning, biomedical applications.

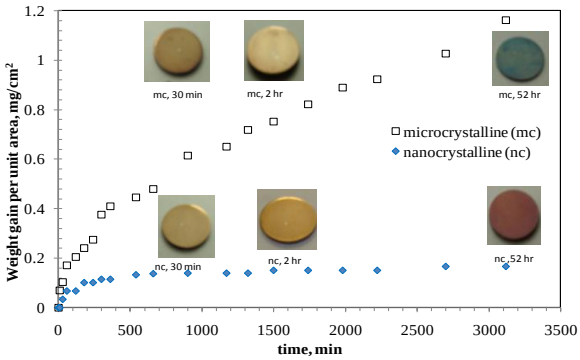

Fig 2: Oxidation kinetics of nanocrystalline (*nc*) and microcrystalline (*mc*) Fe-10Cr alloys oxidised at 300 °C for 3120 min [6].

References
1. A.K. Geim, K.S. Novoselov, The rise of graphene, Nat Mater, 6 (2007) 183-191.
2. R.K. Singh Raman, P. Chakraborty Banerjee, et al, Protecting copper from electrochemical degradation by graphene coating, Carbon, 50 (2012) 4040.
3. Chen, L. Brown, M. Levendorf, W. Cai, S.-Y. Ju, J. Edgeworth, X. Li, C.W. Magnuson, A. Velamakanni, R.D. Piner, J. Kang, J. Park, R.S. Ruoff, Oxidation Resistance of Graphene-Coated Cu and Cu/Ni Alloy, ACS Nano, 5 (2011) 1321.
4. N.T. Kirkland, T. Schiller, N. Medhekar, N. Birbilis, Exploring graphene as a corrosion protection barrier, Corrosion Science, 56 (2012) 1.
5. D. Prasai, J.C. Tuberquia, R.R. Harl, G.K. Jennings, K.I. Bolotin, Graphene: Corrosion-Inhibiting Coating, ACS Nano, 6 (2012) 1102-1108.
6. R.K. Singh Raman, R. K. Gupta, Carl C. Koch, Synthesis Challenges and Extraordinary Resistance to Environmental Degradation of Nanocrystalline vis-à-vis Microcrystalline Fe-Cr Alloys, *Philosophical Magazine*, 90 (2010) 3233.

Characterization and application of multicomponent nano-particles in the immobilization of heavy metals from water and liquid and solid minig tailings

L. Cumbal[1], C. Bastidas[1] and D. Delgado[1]
[1]Centro de Nanociencia y Nanotecnología, Universidad de las Fuerzas Armadas-ESPE, P.O. Box: 1715 231B, Sangolquí, Ecuador

Abstract: Iron based nanoparticles have been used in remediation of solvent chlorides, PBCs, pesticides and heady metals at laboratory level (Liu & Zhao, 2007; Xiong et al., 2009; Zhao et al., 2009; Kim et al., 2011). However there are no studies of applications of nanoparticles to simultaneously remove several heavy metals. In this study multicomponent nanoparticles (Fe/FeSNPs) were synthesized using sodium sulfate, ferric chloride and sodium borohydride. Nanoparticles as prepared were characterized and used to remove a group of heavy metals from water and liquid ans solid mining tailings. Dynamic light scattering, transmission electron microscopy, infrared spectrophotometry, X-ray diffraction, and X-ray photoelectron spectrometry were used to characterize nanoparticles. Average size of the spheres is 30 nm. FTIR spectrum of a sample of nanoparticles after removal of Cu^{2+} shows changes on peaks that imply the existence of residual hydroxyl groups on the surface of Fe/FeS nanoparticles. The latter mechanism may promote the formation of complex of Sur-OH-Cu^{2+} and Sur-O-Cu^{2+} during the adsorption of Cu^{2+}.. A XRD spectrum provides Fe peaks and amorphous content of FeS. In addition, XPS spectra give peaks of $Fe2p_{2/3}$ and $Fe2p_{1/2}$, they show a decrease of binding energy after contacting the Fe/FeSNPs with Cu^{2+} (Cumbal et at., 2014) and peaks of $Cu2p_{1/2}$ and $Cu2p_{3/2}$ show CuO formation.
Removal tests were performed contacting the multicomponent nanoparticles with acidic contaminated water and soils. For artificial water samples, heavy metals were removed in more than 95%. Kinetic tests conducted under aerobic environment, pH 3 and 18% (v/v) of nanoparticles demonstrate the best removal is accomplished after 4 hours of treatment and a pseudo-second order of reaction fits experimental data. Tests of isothermal adsorption showed a capacity (q) of approximately 140mg/g for 200mg/L Cu^{2+} as initial concentration. The nanoparticles were also used to remove heavy metals from mining liquid tailings. More than 90% was achieved after 8 hours of treatment. Whereas, in soil samples the immobilization of heavy metals was around 85%. Currently, we are performing lecheate tests to find out if the final product is chemically stable.

Keywords: Multicomponent nanoparticles, heavy metals, tailings, mining.

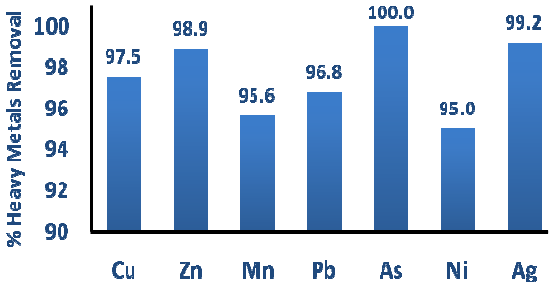

Figure 1: Removal of heavy metals using Fe/FeS nanoparticles from liquid tailings

References:

Xiong Z., Zhao D., Pan G. (2009). Rapid and controlled transformation of nitrate in water and brine by stabilized iron nanoparticles. *Journal of Nanoparticle Research*. 11(4): 807-819.

Zhao D., He F., Xu Y., Li R. (2009). *Patent Nº 7581902.* USA.

Kim E-J., Kim J-H., Azad A-M., Chang Y-S. (2011). Facile Synthesis and Characterization of Fe/FeS Nanoparticles for Environmental Applications. *Matter Interfaces*, 3: 1457–1462.

Cumbal L., Delgado D., Bastidas C. and Debut A. Multicomponent nanoparticles for remediation of heavy metals. 248th ACS Conference, August 10-14,2014.

Characterization of Nanosized Metallic Sulfide Catalysts Obtained by Thermal Decomposition of Nanoemulsions

Andres M. Quesada Perez[*1], Sara Omani[*1], Ali Katrib[*2] and Ali Bumajdad[*2]
[*1]: Kuwait Institute for Scientific Research, Petroleum Refining Center, Ahmadi, Kuwait.
*2: Kuwait University, Department of Chemistry, Kuwait.

Abstract: Many studies have shown that it is possible to prepare more active hydrotreating (HDT) catalysts using nanotechnology (Song, 2003; Escobar et al., 2005). Nanocatalysts have been developed to improve the catalytic processes in the conversion of heavy fractions (Khadziev et al., 2007; Lott and Lee, 2005). An ultra-dispersed catalyst of cobalt-molybdenum and nickel-molybdenum sulfide (CoMoS, NiMoS), and the method of preparation (Pereira et al., 2011) were evaluated for the hydrodesulfirization (HDS) of heavy fractions. The effects of the properties of the catalyst's precursors on the final catalysts particle size formation were studied, showing the effect of the aggregation process of the nanoparticles produced.

Despite many researchers and commercial companies having worked on the development of nanotechnologies for the conversion of heavy fractions, it has not yet been possible to establish a process based on nanotechnology in the refinery. Since light crude production is declining, the refinery will treat more heavy oil fractions in the coming years. Consequently, many opportunities are still open to develop process technologies based on nanotechnology that can be technically operational and economically feasible to treat heavy oil fractions.

This paper presents the characterization of the solids obtained by thermal decomposition of nanoemulsion under typical hydrotreating conditions. The products were characterized using ultra-violet spectroscopy (UV-VIS), X-ray photoelectron spectroscopy (XPS), transmission electron microscopy (TEM).

Nanosized metallic sulfide catalysts were obtained with a particle size below 100 nm. The figure 1 shows the TEM image of the solid obtained from the thermal decomposition of the emulsion containing molybdenum and sufur precursor. The image shows the presence MoS_2 slab with a particle size distribution below 100 nm (40 to 50 nm; 30 to 40 slabs/particle).

Keywords: Hydroterating, hydroconversion, nanosized metallic sulfide catalyst.

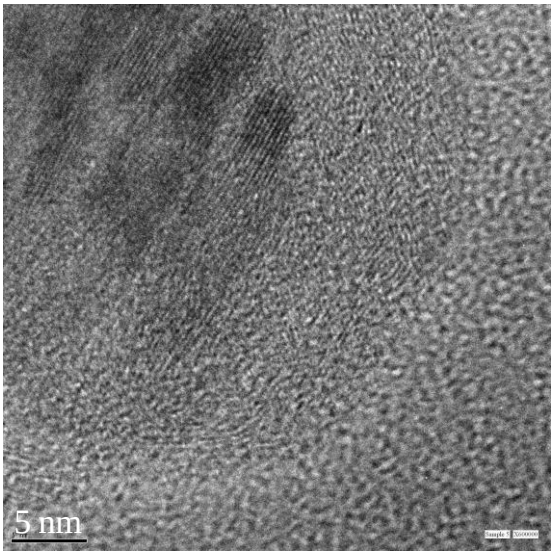

Figure 1: Transmisson electron microscopy of molybdenum sulfide

References:

Song, S. 2003. An overview of new approaches to deep desulfurization for ultra-clean gasoline, diesel fuel and jet fuel. *Catalysis Today* 86: 211-263.

Escobar, J.; J. Toledo; M. Cortés; M. Mosqueira; V. Pérez; G. Ferrat; F. López-Salinas; and E. Torres-García. 2005. Highly active sulfide CoMo catalyst on nano-structured TiO2. *Catalysis Today* 106: 222-226.

Khadziev, S.; H. Kadiev; V. Mezhidov; J. Zarkesh; R. Hashemi and S. Masoudian. 2007. Process for hydroconverting of a heavy hydrocarbonaceous feedstock. US Patent 2007/0045156 A1.

Lott, R. and L. Lee. 2005. Hydroprocessing method and system for upgrading heavy oil using a colloidal or molecular catalyst. US Patent No. 0241993 A1.

Pereira, P; V. Ali-Marcano; F. Lopez-Linares; and A. Vasquez. 2011. Ultradispersed catalyst composition and methods of preparation. US Patent No. 2011/0105307 A1

Surface Functionalization of TiO_2 Nanoparticle and its Application for Biodiesel Production from Locally Sourced Used Cooking Oil

J. Gardy[a,*], A. Hassanpour[a], X. Lai[a], M. Ahmed[b]
[a] Institute of Particle Science & Engineering (IPSE), School of Chemical and Process Engineering (SCAPE), University of Leeds, LS2 9JT Leeds, UK.
[b] Nanotechnology Integrated Bioengineering Centre, University of Ulster, Jordanstown, BT37 0QB Belfast, UK.
[*] Corresponding author. Tel.: +447516239311; Email address: pmjlia@leeds.ac.uk

Abstract: The biodiesel industry is an emerging alternative for managing the demands of transportation, industrial processes and residential consumption by being eco-friendly, biodegradable and readily available [1]. Around 90% of current biodiesel in industry is made by transesterification process of triglycerides with low molecular weight alcohols over homogenous acid or base catalysts. However, the biodiesel industry faces a few problems due to the high costs of biodiesel raw materials and biodiesel processing including separation, purification and neutralisation of by-products have been the main challenges for its commercial availability [2-4]. These problems can be addressed by using cheap feedstocks such as used cooking oil and replacing the conventional catalysts with catalysts highly tolerant to moisture and free fatty acids because free fatty acids and moisture contents in cheap raw materials have adverse on the activity of the catalysts.

The present work is focused on the preparation of a novel functionalised titanium dioxide nano-catalyst from titanium dioxide and suspended 1,3-propanesultone in toluene under reflux for 72 hours at agitation rate of 250 RPM and its tested for the simultaneously esterification and transesterification of locally sourced used cooking oil which contains high concentration of free fatty acids. The synthesised nano-catalyst has been characterised by several analytical techniques, such as FT-IR, XRD, SEM, TEM, XPS, TGA-FTIR, and N_2 adsorption-desorption isotherms.

The effect of catalyst loading, reaction temperature, time of transesterification, and methanol to oil ratio on the biodiesel yield was investigated. It was found that under certain process parameters a yield of 98.3% can be achieved using functionalised TiO_2 as a catalyst. Furthermore, it was found that the catalyst activity slightly dropped by 3.7% after three runs of transesterification of used cooking oil.

Keywords: Functionalised TiO_2 nanoparticle, Biodiesel, Used cooking oil, Solid acid catalyst

References:

1. Ma, F. and M.A. Hanna, *Biodiesel production: a review.* Bioresource Technology, **1999**. 70(1): p. 1-15.
2. Zhang, Y., M.A. Dubé, D.D. McLean, and M. Kates, *Biodiesel production from waste cooking oil: 2. Economic assessment and sensitivity analysis.* Bioresource Technology, **2003**. 90(3): p. 229-240.
3. Javidialesaadi, A. and S. Raeissi, *Biodiesel production from high free fatty acid-content oils: Experimental investigation of the pretreatment step.* APCBEE Procedia, **2013**. 5(0): p. 474-478.
4. Chai, M., Q. Tu, M. Lu, and Y.J. Yang, *Esterification pretreatment of free fatty acid in biodiesel production, from laboratory to industry.* Fuel Processing Technology, **2014**. 125: p. 106-113.

Photopolymerization of Water-Soluble Acrylic Monomers Induced by PbS and CdS Nanoparticles

Y. Yar,[1,*] E. Buz,[2] H. Yagci Acar,[1]
[1] Koc University, Graduate School of Materials Science and Engineering, Rumelifeneri Yolu, Sarıyer, 34450 Istanbul, Turkey
[3] Koc University, Department of Chemistry, Rumelifeneri Yolu, Sarıyer, 34450 Istanbul, Turkey

Abstract: Photo-induced radical polymerization is the most widely used technique because of its applicability to a wide range of monomers, solvents and simple experimental conditions. This process has gained interest and well known in industrial applications. These include coatings, inks, adhesives, varnishes, dyes and photolithography which can be performed without the need of solvents, at room temperature and the reactions are simply initiated by light (typically in the ultraviolet or visible region of the light spectrum). Previous studies have shown that semiconductors or suspensions of semiconductor particles can act as photo-initiators to start the polymerization.[1,2] Higher photo-efficiencies were observed when smaller colloidal particles were chosen as photo-initiators.[2] Recently, it was shown that nanocomposite hydrogels can be synthesized through the initiation of polymerization with the use of semiconductor nanoparticles (ZnO, TiO_2, Fe_2O_3, SnO_2, ZrO_2, CdSe, or CdTe) even under sunlight irradiation.[3] Much effort has devoted to free radical polymerization techniques mainly because of the presence of a wide range of photo-initiators. However, semiconductors have rarely been used as initiators to prepare polymers. These preliminary works can trigger striking advantages for both the classical photoinitiated polymerization systems and modern curing applications.

In our talk, we will discuss the use of PbS and CdS quantum dots as new photoinitiators. The coating on the surface of these semiconductor materials are important to induce a photopolymerization. In our study, we will try to elucidate the possible mechanism for the radical initiation. The effect of the solvent, wavelength of the light selected for the photopolymerization reactions will be discussed.

Keywords: semiconductor materilas, lead sulfide, cadmiumsulfide, quantum dot, photopolymerization

Figure 1: Gelation of the poly(ethyleneglycol) diacrylate induced by PbS quantum dots.

References:

[1] A.J. Hoffman, H. Yee, G. Mills, M.R. Hofmann, Polymerization of methyl methacrylate using q-sized ZnO colloids, *J. Phys. Chem. 1992*, 96, 5540.

[2] A.J. Hoffman, H. Yee, G. Mills, M.R. Hofmann, Q-sized CdS: Synthesized, characterization and efficiency of photoinitiation of polymerization of several vinylic monomers, *J. Phys. Chem. 1992*, 96, 5546.

[3] D. Zhang, J. Yang, S. Bao, Q. Wu, Q. Wang, Semiconductor nanoparticle-based hydrogels prepared via self-initiated polymerization under sunlight, even visible light, *Scientific Reports* 2013, 3, 1399.

Design and synthesis of copper chalcogenide nanostructures for energy conversion and storage

Xinqi Chen,[1,2] Chao Han,[1] Zhen Li,[1,*] Shixue Dou [1]
[1]University of Wollongong, Institute for Superconducting and Electronic Materials, Wollongong, Australia
[2]Central China Normal University, Institute of Nanoscience and Nanotechnology, Wuhan, China
Email: zhenl@uow.edu.au; Tel: +61-2-42215163; Fax: +61-2-42215731

Abstract: Copper chalcogenide nanostructures (i.e., one-dimensional nanowires and nanotubes) have been the focus of interest because of their unique properties and great potential in various applications. Here, we demonstrate our recent results in preparation and application of copper chalcogenide nanostructures. First, we prepared copper telluride nanocubes, nanoparticles and nanosheets through the high-temperature solvothermal approach, and then applied them as anodes of lithium-ion batteries (Han *et al.; J. Mater. Chem. A*, 2014). Second, we prepared copper selenide nanowires by the hydrothermal method, and showed their potential application in thermoelectrics (Chen *et al.*; *J. Colloid Interface Sci.*, 2015). These two fabrications are relied on high temperature. In our third report, we prepared $Cu_{2-x}E$ (E =S, Se) micro-/nano-tubes (NTs) with a hierarchical architecture by using copper nanowires (Cu NWs) and stable selenium and sulphur powder as precursors at room temperature, with the assistance of theoretical prediction (Chen *et al.*; *Chem. Eur. J.*, 2015). Interestingly, two-dimensional (2D) nanosheets could be prepared from Cu NWs by simply increasing amount of ligands (or using different ligands) during preparation. The resultant $Cu_{2-x}E$ (E = S, Se) NTs were used as counter electrodes (CEs) of quantum-dot-sensitized solar cells (QDSSCs) to achieve a conversion efficiency (η) of 5.02% and 6.25%, respectively, much higher than that of QDSSCs made with Au CE (η = 2.94%). Fourth, copper silver chalcogenide ternay nanoparticles were prepared at room temperature in a large-scale, which showed a temperature-dependent transition of metallic-n-p conductivity. These ternary nanoparticles can simutanely serve as building blocks of thermoelectric legs for conversion of heat into electricity (Han *et al.; J. Am. Chem. Soc.*, 2014). Our research provides several ways to prepare copper chalcogenide nanostructures for diverse applications.

Keywords: copper chalcogenide, nanostrctures, semiconductors, room-temperature synthesis, counter electrodes.

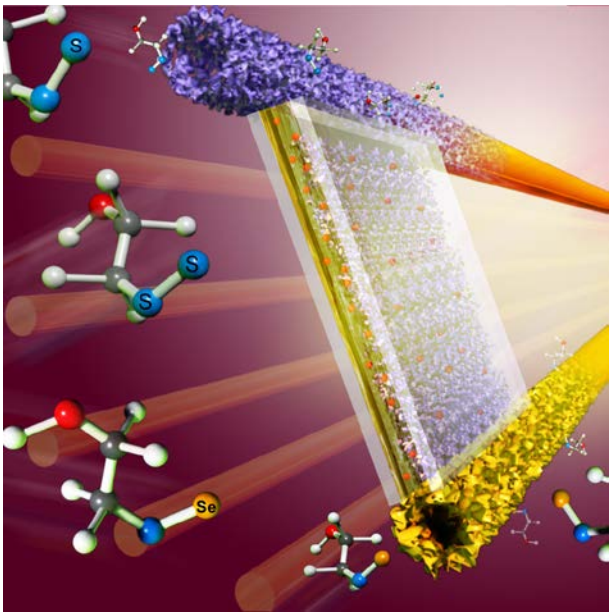

Figure 1: Abstract illustrating the mechanism of reaction from Cu NWs to $Cu_{2-x}E$ (E = S, Se) NTs in the presence of thiol ligands and $Cu_{2-x}E$ (E = S, Se) NTs serving as building blocks for high-performance CEs of QDSSCs.

References:

Han, C., Li, Z., Li, W. J., Chou, S. L., Dou, S. X. (2014) Controlled synthesis of copper telluride nanostructures for long-cycling anodes in lithium ion batteries, *J. Mater. Chem. A*, 2, 11683-11690.

Chen, X. Q., Li, Z., Bai, Y., Sun, Q., Wang, L. Z., Dou, S. X. (2015) Room-temperature synthesis of $Cu_{2-x}E$ (E=S, Se) nanotubes with hierarchical architeture as counter electrodes of quantum-dot-sensitized solar cells, *Chem. Eur. J.*, 21, 1055-1063.

Chen, X. Q., Li, Z., Yang, J. P., Sun, Q., Dou, S. X. (2015) Aqueous preparation of surfactant-free copper selenide nanowires, *J. Colloid Interface Sci.*, 442, 140-146.

Han, C., Sun, Q., Cheng, Z. X., Wang, J. L., Li, Z., Lu, G. Q., Dou, S. X. (2014) Ambient scalable synthesis of surfactant-free thermoelectric CuAgSe nanoparticles with reversible metallic-n-p conductivity Transition, *J. Am. Chem. Soc.*, 316, 17626-17633.

Reduced Carrier Recombination in PbS - $CuInS_2$ Quantum Dot Solar Cells

Zhenhua Sun,[1] Gary Sitbon,[1] Thomas Pons,[1] Artem A. Bakulin,[2] and Zhuoying Chen[1*]
[1]LPEM, UMR 8213, PSL Research University, ESPCI-ParisTech/CNRS/UPMC, 10 rue Vauquelin, F-75231 Paris Cedex 5, France
[2]FOM Institute AMOLF, Science Park 104, Amsterdam 1098 XG, The Netherlands
Email: Zhuoying.chen@espci.fr

Abstract: Colloidal nanocrystal quantum dots (QDs) offer exciting opportunities for solution-processed optoelectronic applications such as photovoltaics due to their size-tunable bandgap and the multiple excitation generation phenomenon, a mechanism by which the Shockley-Queisser limit can be potentially bypassed.[1,2] So far, metal oxide/QD bi-layer depleted heterojunction is among the most efficient QD solar cell architecture allowing a power conversion efficiency (PCE) as high as 8.92% on PbS QD solar cells.[3,4] One important issue hindering the progress of many third-generation solar cells is carrier recombination.[5] In metal oxide/QD heterojunction solar cells, carrier recombination happens not only at the donor-acceptor (TiO_2/QD) interface but also inside the QD layer which has a typical thickness of a few hundred nanometers. Photogenerated charges need to travel across the entire QD active layer to be collected. During this process carrier recombination leads to photocurrent loss and thus, to inefficient solar cells.[6]

Under this context, the possibility to separate electrons and holes in different areas of the active layer, for example by using a mixture of different QDs, can lead to a substantial suppression of the recombination rates. Towards this goal, in this work we propose an "bottom-up" approach based on the partial spatial segregation of charge carriers to boost photocurrent in QD solar cells. Here, Zn-doped $CuInS_2$ (Zn-CIS) QDs, *p*-type QDs of reduced toxicity compared to PbS, are incorporated into the PbS matrix of TiO_2/PbS QD heterojunction solar cells. In this binary QD blend Zn-CIS QDs provide recombination "shelters" where only holes but not electrons from PbS are allowed to enter. Different volume fractions of Zn-CIS QDs in the PbS QD matrix were examined: a 10% (v/v) addition of Zn-CIS QDs can lead to a ~30% increase in short circuit current density (Jsc), a ~20% increase in power conversion efficiency (PCE), and prolonged recombination time constants compared to solar cells built from PbS QDs only. In agreement with the charge transfer process identified through ultrafast pump/probe spectroscopy between these two QD components, transient photovoltage characteristics of single-component and binary QDs solar cells reveal longer carrier recombination time constants associated with the incorporation of Zn-CIS QDs. This work presents a straightforward, solution-processed method based on the incorporation of another QDs in the PbS QD matrix to control the carrier dynamics in colloidal QD materials and enhance solar cell performance.

Keywords: nanocrystal solar cells, quantum dot solar cells, charge separation, carrier recombination, PbS nanocrystals

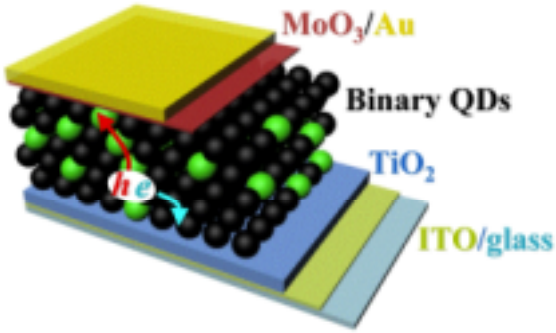

Figure 1: Figure illustrating the fundamental process redeucing carrier recombinations in the binary QD solar cells investigated in this study.

References:

[1] Ehrler, B.; Walker, B. J.; Bohm, M. L.; Wilson, M. W. B.; Vaynzof, Y.; Friend, R. H.; Greenham, N. C., In situ measurement of exciton energy in hybrid singlet-fission solar cells. *Nat Commun* **2012,** 3, 1019.

[2] Semonin, O. E.; Luther, J. M.; Choi, S.; Chen, H. Y.; Gao, J. B.; Nozik, A. J.; Beard, M. C., Peak External Photocurrent Quantum Efficiency Exceeding 100% via MEG in a Quantum Dot Solar Cell. *Science* **2011,** 334, 1530-1533.

[3] Chuang, C.-H. M.; Brown, P. R.; Bulovic, V.; Bawendi, M. G., Improved Performance and Stability in Quantum Dot Solar Cells through Band Alignment Engineering. *Nature Materials* **2014,** 13, 796-801.

[4] Yuan, M.; Voznyy, O.; Zhitomirsky, D.; Kanjanaboos, P.; Sargent, E. H., Synergistic Doping of Fullerene Electron Transport Layer and Colloidal Quantum Dot Solids Enhances Solar Cell Performance. *Advanced Materials* **2014**, DOI: 10.1002/adma.201404411.

[5] Docampo, P.; Guldin, S.; Leijtens, T.; Noel, N. K.; Steiner, U.; Snaith, H. J., Lessons Learned: From Dye-Sensitized Solar Cells to All-Solid-State Hybrid Devices. *Advanced Materials* **2014,** 26, 4013-4030.

[6] Li, L.; Yang, X. C.; Gao, J. J.; Tian, H. N.; Zhao, J. Z.; Hagfeldt, A.; Sun, L. C., Highly Efficient CdS Quantum Dot-Sensitized Solar Cells Based on a Modified Polysulfide Electrolyte. *Journal of the American Chemical Society* **2011,** 133, 8458-8460.

Session V: Other Nano Applications

Nanotechnology in Food Packaging Industry: Opportunities and Challenges

Vasco Teixeira
GRF-Functional Coatings Group, Physics Department, University of Minho
PT-4800-058 Guimaraes, Portugal
Tel: +351-253510465/00, Fax: +351-253510401, Email: vasco@fisica.uminho.pt

Abstract: Nanosciences and nanotechnologies are highly promising areas for research and industrial innovation, with a potential both to boost the competitiveness of many industries which will lead to new emerging and fast growing markets. It is predicted that nanotechnology production approaches will change about 25% of the food packaging business in the next decade, which means a yearly over $ 30 billion market. The major market trends include enhancing the performance of packaging materials, prolonging shelf life, antimicrobial packaging and interactive/sensorial packaging.

One of the main priorities in food packaging technology is to keep the original properties of the food. This goal is achieved by keeping all the nutrients in the original conditions, by ensure minimum interaction between environment and the packaged food and reducing microbial growth

In the field of nanoparticles and nanotechnology-based thin films, new approaches using nanoscale effects can be used to design, create or model nanocomposite systems with significantly optimized or enhanced properties of high interest to the food, health and biomedical industry. With the development of nanotechnology in various areas of materials science the potential use of novel surfaces and more reliable materials by employing nanomaterials and nanostructured thin films in food packaging, security pharmaceutical labels, novel polymeric containers for food contact, medical surface instruments, bio-implants, and even coated nanoparticles for bionanotechnology can be considered.

The use of plastic containers in the food and beverage market has dramatically increased because they are lightweight, unbreakable, convenient, resealable and they may be clear. PET bottles have gradually replaced glass bottles and metal cans as the most common packaging for liquid foods, such as carbonated soft drinks, tea, water, soy sauce and edible oil.In this field of new packaging technologies, nanostructured architectures coatings such as nanocomposite films are given the unique role of enhancing food impact over the consumer's health. For example, the unique properties of diamond like carbon (DLC) film, including its chemical inertness and impermeability, make it possible for new applications in food, beverage and medical market segments. The ability of using thin films and nanoparticles with transparent properties a more flexible and transparent packaging materials will provide the consumers with fresher and customized packs where the products can be observed as they are.

In this presentation it will be presented an overview of the nanotechnology approaches to produce nanostructured materials for food and health industry. Topics to be discussed include introduction to nanocoatings concepts (from functional nanocomposite and graded coatings to smart nanomaterial surfaces used in packaging and biomedical industry) produced by clean PVD technologies (Physical Vapour Deposition) and other deposition techniques. An overview of the current research, existing technological applications and future industrial materials and components will be highlighted. As example for future trends in nanotech-based food packaging will also include research and development on sensorial packaging which can monitor the food and transmit information on its quality. For instance, the ultimate pH of meat greatly affects its quality. Monitoring this parameter can give to consumers information regarding manner of transportation of animals from the farm to the abattoir; diet restrictions; mixing animals of different lots and pathological conditions. With embedded nanosensors in the packaging surface materials, consumers will be able to check the food quality inside or even to track the history of the pack. Electronics built on thin film substrates could be used in future sensory packaging applications (examples include nanoRFIDs).

Nanotechnology: Promises and challenges for future

Dr. Akbar S. Khan[1], [1]Senior Scientist and Program Director, CB Directorate, Defense Threat Reduction Agency, Fort Belvoir, Virginia, USA, Akbar.Khan@dtra.mil

Abstract: Nanotechnology is science, engineering, and technology conducted at the nanoscale, which is about 1 to 100 nanometers. All things, both living and non-living, are constructed of atoms. The nano-scale sparks so much interest because when a substance is artificially created, structured atom by atom, it can have different or enhanced properties compared with the same substance as it occurs naturally, which includes increased chemical reactivity, optical, magnetic, or electrical properties. Nanotechnologies aim to exploit these properties to create devices, systems, and structures with new characteristics and functions. For example, researchers hope to construct from the very 'bottom' (that is to say, atom by atom) a substance as strong as diamond, but more flexible and far less expensive. It would also be possible to manufacture a substance in the shape and size needed such as a thin string as strong as steel.

So far Nanotechnology is applied in various areas (1) applied design a water filtration system on the nano-scale that is so efficient, it only lets water molecules through it. (2) Is used to create filters and sensors to screen out toxins or adjust flavors, and packaging to sense when the food inside is spoiling and alert the customer. (3) The ability to assemble Nano-scale particles that could be targeted at certain parts of the body or certain viruses in the blood. (4) Economical solar cells to make solar power economical and diminish our dependency on coal, oil, nuclear fuel and fuel wood. (5) To clean up the environment. To clean up oil spills, imagine a scrubber built from tiny nanotubes that could manipulate the atoms in an oil spill to render it harmless.

Just like any new technology, there are varieties of health, environmental and safety risks to this technology from free rather fixed manufactured nanoparticles. In initial studies, manufactured nanoparticles have shown toxic properties. They can enter the human body in various ways, reach vital organs via the blood stream, and possibly damage tissue. Due to their small size, the properties of nanoparticles not only differ from bulk material of the same composition but also show different interaction patterns with the human body. These promises and challenges of Nanotechnology will be presented here.

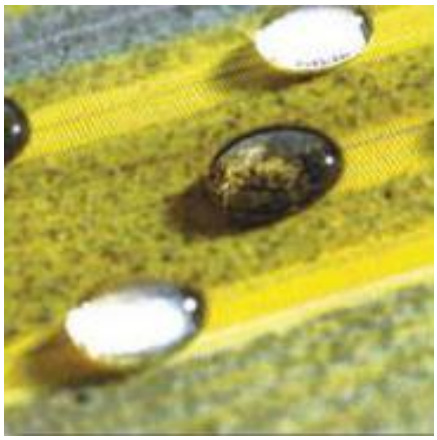

Figure 1: An illustration of water shield self-cleaning paint using Nano-particles

Keywords: Nanoparticles, Safety, risks, chemical reactivity, filtration system, applied design, nano-particle drug delivery.

References:

1. Satterfield, T., Kandlikar, M., Beaudrie, C. E. H., Conti, J., Herr Harthorn, B. (2009), 'Anticipating the perceived risk of nanotechnologies', *Nature Nanotechnology*, 4, 752-758.
2. Aitken, R., Borm, P., Donaldson, K., Ichihara, G., Loft, S., Marano, F., Maynard, A., Oberdörster, G., Stamm, H., Stonem V., Tran, L., Wallin, H. (2009), 'Nanoparticles – one word: A multiplicity of different hazards,' *Nanotoxicology*, 3, 263-264.

Antimicrobial properties of graphene oxide and reduced graphene oxide

M. A. Buccheri[2], S. Scalese[1,*], D. D'Angelo[1], F. Spanò[3], G. Compagnini[3], G. Rappazzo[4] and V. Privitera[2]
[1] CNR-IMM, Z.I. Strada VIII n.5, I-95121 Catania (Italy)-[2] CNR-IMM via S. Sofia n.64 I-95123 Catania (Italy)
[3] Dip. di Chimica, Università degli Studi di Catania, via S. Sofia 64, I-95123 Catania (Italy)
[4]Dip. di Scienze Biologiche, Geologiche e Ambientali –Università degli Studi di Catania (Italy)
*silvia.scalese@imm.cnr.it, phone: +39 095 5968235

Purification of water from contaminants toxic to humans is attracting an increasing interest due to the rise of environmental pollution and scarcity of the available water resources in large areas of the earth.

Carbon-based materials are suitable for both the filtration of microorganisms and the ability to adsorb heavy metals, provided that their surfaces are adequately functionalized [1]. In particular, graphene oxide (GO) was recently proposed for the removal of pollutants from water [2]. GO is composed of graphene flakes with carboxyl, hydroxyl and epoxy groups at the edges or the surfaces. Moreover, GO shows semiconducting properties and the energy gap can be tuned by a reduction of the oxygen functional groups. Recently, graphene and GO were tested as antimicrobial agent affecting the integrity of *E. coli* bacterial membrane [3]. Our work aims to elucidate the antimicrobial properties of the GO or rGO.

GO in water solution was prepared by the Hummer's method while rGO was obtained by laser irradiation of the initial GO solution. The solutions were characterized by IR and UV-visible spectroscopy as well as by scanning electron microscopy (SEM) (an example is shown in figure 1) and transmission electron microscopy (TEM).

Antimicrobial properties have been investigated using *Escherichia coli* ATCC25922 as a model organism. Survival rates of *E.coli* were evaluated by CFU count after 1h or 2h exposure to GO and rGO. In our experimental system, rGO seemed to be more effective than GO in reducing bacterial survival, with only 20% of the initial *E. coli* population being able to survive. These results were then confirmed by the WST-1 Assay, an assay able to investigate bacterial metabolism. Moreover, our analysis on the mechanism of action of GO and rGO indicated that their antimicrobial effect was mainly due to mechanical damage exerted towards the bacterial membrane. Furthermore, Fish Embryo Toxicity (FET) test showed that neither mortality nor sublethal effects were caused by the different solutions tested.

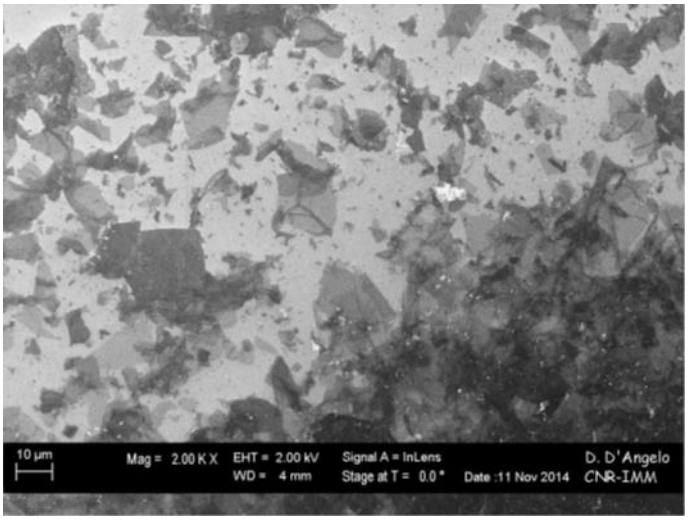

Fig.1. SEM image of GO reduced by 4h laser treatment.

[1] G. P. Rao, C. Lu, F. Su, *Separ. Purif. Technol. 58 (2007) 224*
[2] T.-F. Yeh, J. Cihlar, C.-Y- Chang, C. Chang and H. Teng, *Mater. Today 16 (2013) 78*
[3] S. Liu, T. H. Zeng, M. Hofmann, E. Burcombe, J. Wei, R. Jiang, J. Kong, Y. Chen, *ACS Nano 5 (2011) 6971*

Phosphonium Quat-Modified Nanoclays for In-Situ Polyester Nanocomposite Development: Optimisation of Modification for Particle Performance.

Benjamin J. Naden,[1*] Laura Pilon,[1]
[1]Pera Technology Ltd., Chemistry and Biotechnology, Pera Business Park, Nottingham Road, Melton Mowbray, Leicestershire, LE13 0PB, UK

Abstract: Bentonite clays are often used as a functional nano-additive to polymers for enhanced mechanical and physicochemical properties for a range of applications. To realise the nano effect of well dispersed discrete particles it is necessary to organically modify the particles to overcome the thermodynamic incompatibility of the inorganic clay with the polymer matrix. This paper describes the synthesis and characterisation of an organically-modified nanoclay for the development of a polymer composite that provides enhanced gas barrier properties to packaging film when print applied to the plastic film substrate. In-situ polymerisation of the polyester-nanoclay composite was selected for optimum clay nanoparticle dispersion due to the exfoliating effect of the growing polymer chains. In addition, this presents the opportunity to involve a reactive clay modifier that can participate in the chain propagation process, providing the clay particle with very strong linkage to the polymer matrix, potentially resulting in good stability and enhanced mechanical and barrier properties.

Quaternary ammonium surfactants are commonly used for surface modification, providing both compatibility with the matrix and separation of the particles by intercalation. Phosphonium salts offer a more thermally stable alternative to ammonium modifiers; a property that is particularly attractive considering the relatively high temperatures to which the particles are exposed to during polyester synthesis. Organoclays were synthesised by cation exchange modification of sodium montmorillonite (Na^+MMA) with (1-Tetradecyl)triphenylphosphonium bromide (TDTPPBr), (3-Carboxypropyl)triphenyl phosphonium bromide (CPTPPBr), and (1-Hexyl)triphenyl phosphonium bromide (HTPPBr). Particle intercalation was evaluated using standard techniques, including XRD and TEM for inter-gallery spacing of the modified nanoclays, and TGA for thermal stability. Also, a technique was developed to measure dispersibility of the modified particles in an appropriate solvent, using the Mie scattering model to relate light scattering and absorption energy to particle size, enabling the prediction of potential exfoliation in the polymer composite and/or coating formulation.

The shorter alkyl chain modifiers (CPTPPBr and HTPPBr) displayed limited affinity for the clay surface in the cation exchange process, resulting in low modifier to inorganic ratio and poor platelet separation and dispersion quality. By contrast, TDTPPBr showed high surface adsorption behaviour, resulting in good intercalation and dispersion quality. A relationship between organic modifier content and clay tactoid d-spacing was observed, with maximum d-spacing achieved well before maximum surfactant adsorption was reached. Particle dispersion evaluation revealed that there was also a relationship between modifier addition and dispersion quality, suggesting there is an optimum modifier to clay mass ratio that coincides with the onset of the d-spacing plateau, beyond which dispersion quality deteriorated. TDTPPBr-modified organoclay properties compared well with commercial grade ammonium-modified organoclays, with greater d-spacing observed and comparable dispersion quality. Phosphonium-modified clays exhibited enhanced stability up to typical polyester esterification reaction temperature (~250°C) compared to the commercial grades.

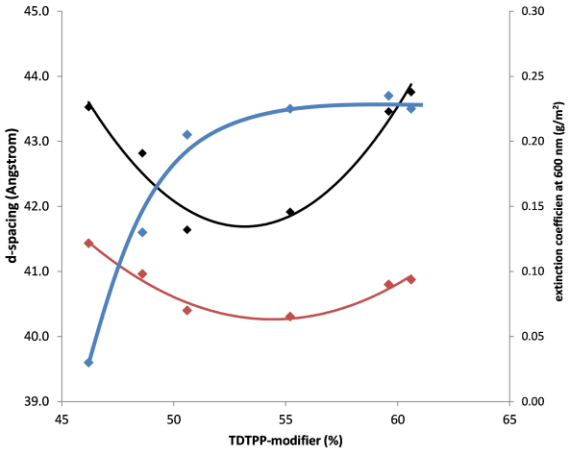

Figure 1: Correlation of organoclay d-spacing (blue diamonds) and particle dispersion spectral performance versus modified clay organic content. Clay particle extinction coefficients calculated from mass of inorganic component (black diamonds) and mass of total organoclay (red diamonds).

Keywords: organically-modified nanoclay, phosphonium salts, gas barrier, in-situ polymerization, thermal stability, tactoid d-spacing, platelet separation, extinction coefficient, Mie scattering, nanoparticle dispersion.

Efficient Design of Flexible and Low-cost Dual Band RFID inkjet printed antenna using silver nanoparticles ink

Ahmed M. Mansour[1,2], Bassant M. Hamza[1,2], Nader Shehata[1,3], Mohammed R. M. Rizk[1,2]
[1]Center of Smart Nanotechnology and Photonics (CSNP), SmartCI research center, Alexandria University, Alexandria, Egypt.
[2]Department of Electrical Engineering, Faculty of Engineering, Alexandria University, Alexandria, Egypt.
[3]Department of Engineering Mathematics and Physics, Faculty of Engineering, Alexandria University, Alexandria, Egypt.

Abstract: This work aims to fabricate light and flexible antennas, printing techniques are used such as screen and inkjet procedures. In this paper, a dual band RFID is fabricated using new, efficient and low cost printing technique based on commercial inkjet printer. A simple CPW Z-shaped antenna is fabricated on a low cost paper substrate with conductive silver nanoparticles (~100 nm size) ink which has been selected to implement the antenna shape and to improve the characteristics of the antenna depending on their higher surface to volume ratio, with thickness of the printed layer around 230 microns. The fabricated antenna has dual bands frequency for this shape;one at 780 MHz and the other at 1.4 GHz. The resistance of the antenna has been improved through annealing up to less than 1 ohm/cm^2.

Keywords: printed antenna, inkjet-printing, , silver nanoparticles ink.

I- Introduction

Radio Frequency Identification (RFID) is an important wireless technology that has wide variety of applications, such as mobile radio communication devices [1-3]. However the currently used fabrication techniques and materials are relatively costive and badly affect on the environment. In this paper, we use feasible and commercial method for printing on extremely low cost substrates for fabricating electronic circuits and RF structures using a normal inkjet printer with avoiding custom and expensive equipment. The used ink is silver Nano-particles inks ensure higher performance of inkjet-printing process. So, we would discuss the printing technique and the analysis of a simple printed antenna via silver nanoparticles ink.

II- Expermintal Work

A simple Z-shaped printed antennas is selected to be the printed antenna design due to its conformability and its higher gain [4]. The geometry of the antenna is shown in Fig.1. The ink is filled via silver nanoparticles ink into a special cartridge to be fitted with the printer. The morphology of the surface is imaged using JEOL SEM. The printed antenna has been analyzed using a network analyzer. The antenna is connected with a SMA connector using conductive tape with resistance equls to 2 Ω / cm.

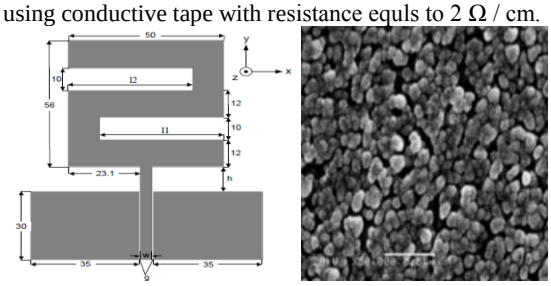

Figure 1: Figure illustrating Z-shaped CPW-fed printed antenna configuration (dimensions in mm) and SEM image of the morphology of the antenna's surface

I- Results & Discussions

Both printed antennas on a board and on a glossy paper are shown in Fig. 2. Fig.1 shows the SEM image the morphology of the antenna's surface which is printed on a glossy paper at room temperature. The SEM image shows smooth and uniform morphology. The mean diameter of the nanoparticles is found to be around 100 nm, and the mean thickness of the printed layer around 230 microns. Fig. 4 shows the network analyzer characterization of the printed antenna with a notch band close to 900 MHz.

Figure 2: Figure illustrating Z-shaped antenna on glossy paper and PCB.

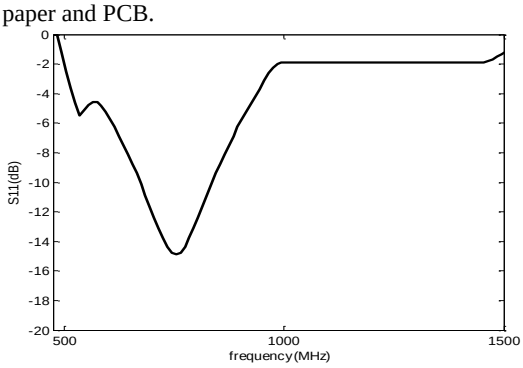

Figure 3: Network analyzer analysis of the printed antenna.

II- Conclusion

This paper present an efficient design for RFID inkjet printed antenna on a flexible, low-cost and enviromental friendly material a using silver nanoparticles ink producing a dual band frequencies that can be used in different RFID applications. Our future work is try to testing the effect of expose samples to temperature, printing multilayer and both at different temperature value and how could this affect the return loss, radiation pattern, antenna gain ... etc.

References

[1] Instant Inkjet Circuits: Lab-based Inkjet Printing to Support Rapid Prototyping of UbiComp Devices.UbiComp'13, September 8–12, 2013, Zurich, Switzerland. ACM 978-1-4503-1770-2/13/09.

[2] L.Yang, A.Rida, R.Vyas and M.M. Tentzeris, "RFID Tag and RF Structures on Paper Substrates using Inkjet-Printing Technology," IEEE Transactions on Microwave Theory and Techniques, vol. 55, no.12, part 2, pp. 2894-2901, Dec. 2007.

[3] K.P. Ray and Y. Ranga, "CPW-fed modified rectangular printed monopole antenna with slot," Microwave and Optoelectronics Conference, 2007 IMOC 2007 SBMO/IEEE MTT-S International, pp.79-81, Oct. 29 2007-Nov. 1 2007.

[4] Rod Waterhouse," Printed Antennas for Wireless Communications," ISBN: 978-0-470-51069-8, Oct. 2007.

0D based resistive switching mechanism

M. Paradinas[1], Z. Konstantinovic[1], S. Valencia[2], R. Abrudan[2], A. Pomar[1], F. Sandiumenge[1], Ll. Balcells[1], B. Martinez[1], C. Ocal[1]
[1]Institut de Ciéncia de Materials de Barcelona-CSIC, Campus UAB, 08193 Bellaterra, Spain
[2] Helmholtz-Zentrum-Berlin, Albert-Einstein-Str. 15, 12489 Berlin, Germany

Abstract: The ever increasing demand for massive information storage and high speed management of the information has boosted the search for new non-volatile memory devices in the last decade. Local transport properties (I-V characteristics) exploring NP/perovskite oxide interfaces is of crucial importance for both, the study of the resistive switching mechanism and the development of new resistive memories. In particular, the observation of resistive switching in 2D and 1D systems is promising for using low dimensional nanostructures in non-volatile data storage devices. Thus, for instance, hysteretic I-V curves in $La_{0.7}Sr_{0.3}MnO_3$ (LSMO) thin films (Moreno *et al.*, 2010, Peña *et al.*, 2014) or Zn oxide nanowires (Cheng *et al.*, 2013) can be used to identify the bipolar or unipolar nature of the observed switching process.

We present a further generation of nanoscale memresistors based on unipolar resistive switching behaviour, observed in self-assembly of magnetic nanoparticles (NPs). Local transport properties on iron-oxide/manganite nanostructures (Fe-NP/LSMO) are studied using conductive scanning force microcopy (CSFM). Iron-oxide nanoparticles were assembled on top of fully spin-polarized manganite thin films by RF sputtering (Konstantinovic *et al.*, 2013). Assembly of nanoparticles exhibits at room temperature a voltage-current hysteresis with four different states: initial, electroformed, IN and OFF (Figure 1). Such behaviour could be interpreted in terms of two simultaneous bipolar responses, associated to two existing interfaces (tip/NP and NP/manganite) and their corresponding Schotcky's barrier.

Keywords: MEM resistors, resistive switching mechanism, CSFM, iron-oxide nanoparticles, functional oxides

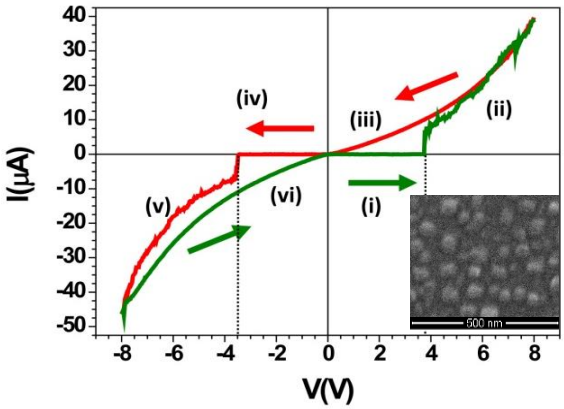

Figure 1: Figure illustrating typical I-V characteristics of Pt/Fe-NP/LSMO system presented in linear scales. The voltage sweep direction and current response is indicated by arrows and roman numbering.

References:

Cheng, B., Ouyang, Z., Chen, C., Xiao, Y., Lei, S. (2013), Individual Zn_2SnO_4-sheathed ZnO heterostructure nanowires for efficient resistive switching memory controlled by interface states. *Sci. Rep.*, *3*, 3249.

Konstantinovic, Z., Sandiumenge, F., Santiso, J., Balcells, Martinez, B. (2013), Self-assembled pit arrays as templates for the integration of Au nanocrystals in oxide surfaces, *Nanoscale*, *5*, 1001–1008.

Moreno, C.S., Munuera, C., Valencia, S., Kronast, F., Obradors, X., Ocal, C. (2010), Reversible Resistive Switching and Multilevel Recording in $La_{0.7}Sr_{0.3}MnO_3$ Thin Films for Low Cost Nonvolatile Memories, *Nanoletters*, *10*, 3828-3835.

Peña, L., Garzon, L., Galceran, R., Pomar, A., Bozzo, B., Konstantinovic, Z., Sandiumenge, F., Balcells, Ll., Ocal, C., Martinez, B. (2014), Macroscopic evidence of nanoscale resistive switching in $La_{0.7}Sr_{0.3}MnO_3$ micro-fabricated bridges, *J. of Phys.: Condens. Matter*, *26*, 395919.

Photocatalytic Silver/Silver Chloride Polymer Nanocomposites

E. W. Tate,[1*] J. H. Johnston,[1,2]
[1]Victoria University of Wellington, School of Chemical and Physical Sciences, Wellington, New Zealand
[2]MacDiarmid Institute for Advanced Materials and Nanotechnology, New Zealand

Abstract: The photochemical activity of silver chlorides is well known in black and white photography, in which a portion of the Ag^+ in the silver chloride crystals is photo-reduced to Ag^0 to provide the image. It has be shown that if the silver chloride crystals are of a nanosize then upon exposure to UV light, smaller nanosize domains of Ag^0 are produced on the surface of the silver chloride through the partial photoreduction of Ag^+ to Ag^0 (Wang *et al*., 2008, Choi *et al*., 2010). These Ag^0 nanodomains exhibit surface plasmon resonance effects. The resulting hybrid silver/silver chloride nanoparticles exhibit interesting photocatalytic properties and are considered to be members of a group of photocatalysts known as plasmonic photocatalysts (Choi *et al*., 2010, An *et al*., 2010). Here the photocatalytic mechanism and photostability of the nanoparticles is enhanced by the surface plasmon resonance of noble metal nanodomains on the surface of the silver chloride nanoparticles (Choi *et al*., 2010, An *et al*., 2010, Zhang *et al*., 2013).

In our recent work, novel silver/silver chloride composite materials were produced using the support materials of polyurethane paint dispersions and nylon 6,6 (Tate and Johnston, 2014). This was achieved through the development of a simple aqueous synthesis method, utilising the substrate to control the size and shape of the silver chloride nanoparticles and their stabilisation within the support material. These were then exposed to UV light to generate the silver nanodomains and hence form plasmonic silver/silver chloride photocatalysts. This successfully incorporated the plasmonic photocatalyst nanoparticles within the support material.

UV-Visible spectroscopy, XRD, SEM and EDS were used to characterise the silver/silver chloride nanoparticles and their distribution within the composites. The photocatalytic activity of silver/silver chloride composites was evaluated by the photodegradation of methylene blue, and were shown to be effective photocatalysts. Due to the inherent antimicrobial properties of the silver/silver chloride nanoparticles, the composite materials were also seen to display significant antimicrobial action against *E. Coli*. These novel composite materials have promising applications in water treatment, where the photocatalytic mechanism is effective in the reduction of organic contaminants, whilst the Ag^+ simultaneously imparts antimicrobial action. This has lead to the design and incorporation of these novel nanocomposites into a labscale reactor system for water treatment.

Keywords: Silver/Silver Chloride, Photocatalyst, Nanocomposite

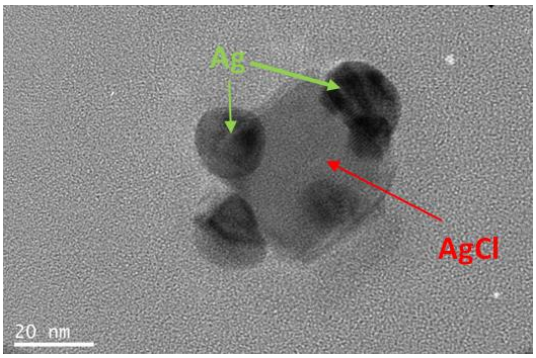

Figure 1: TEM image of Ag/AgCl plasmonic photocatalyst nanoparticle.

References:

Wang, P., Huang, B., Qin, X., Zhang, X., Dai, Y., Wei, J., Whangbo, M.-H. (2008) Ag@AgCl: a highly efficient and stable photocatalyst active under visible light. *Angew. Chem. Int. Ed. Engl.*, 47, 7931–7933.

Choi, M.; Shin, K.; Jang, J. (2010) Plasmonic photocatalytic system using silver chloride/silver nanostructures under visible light. *J. Colloid Interface Sci.*, 341, 83–87.

An, C.; Peng, S.; Sun, Y. (2010) Facile synthesis of sunlight-driven AgCl:Ag plasmonic nanophotocatalyst. *Adv. Mater.*, 22, 2570–2574.

Zhang, X.; Chen, Y. L.; Liu, R.-S.; Tsai, D. P. (2013) Plasmonic photocatalysis. *Rep. Prog. Phys.*, 76, DOI: 10.1088/0034–4885/76/4/046401.

Tate, E. W.; Johnston, J. H. (2014) Photocatalytic silver/silver chloride polymer nanocomposites. *Nanomater. Energy*, 3, 222–228.

Ammonia gas sensing properties of ZnO nanowires synthesized by thermal oxidation of Zn film

B. Behera and S. Chandra*
Centre for Applied Research in Electronics
Indian Institute of Technology Delhi, HauzKhas, New Delhi 110016, INDIA
*E-mail: sudhirchandra1950@gmail.com

Abstract: ZnO is a semiconducting metal oxide material having potential applications in sensors, optical and solar cell devices (*Wang.; 2004*). Gas sensing properties of various ZnO nanostructures such as nanowires, nanorods, nanobelts and nanotubes have been widely investigated for a variety of gases (*Mirabbaszadeh et al. ; 2012*). However, sensitivity, reduction in operating temperature, low cost and integration in MEMS processing are some of the issues which are still being addressed.

In this work, long, dense and uniformly distributed ZnO nanowires have been synthesized and studied as the sensing element for detection of ammonia gas. 130 nm thick Zn film was deposited on oxidized Si substrate by RF magnetron sputtering in Ar ambient at the rate of 4.5 nm/min. After that, film was thermally oxidized at 600 ^{o}C in moist environment for 1 hour. The structural phase of post-oxidized sample indicated that Zn film was completely oxidized to form ZnO. The SEM image showed that dense nanowires were formed. A sensor was fabricated incorporating ZnO nanowires and deposited Cr-Au IDE structure of 30 µm width/gap. The resistance between IDE pads was measured in air ambient and in presence of test gas (ammonia). Exposure to ammonia gas results in release of electrons and thus the resistance decreases as per folowing reaction (*Chang et al.; 2010*).

$$2NH_3 + 3O^{2-} \text{ (or } 3O^{-} \text{ (ads))} \rightarrow 3H_2O + N_2 + 3e^{-}$$

The sensor showed excellent sensitivity of about 17% for 5 ppm of ammonia gas at 200 ^{o}C operating temperature.

Keywords: Thermal oxidation, ZnO nanowires, Gas sensing, Ammonia.

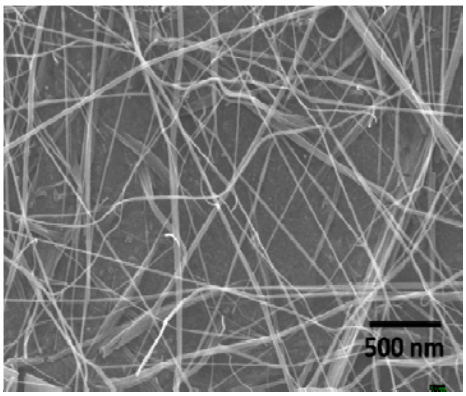

(a)

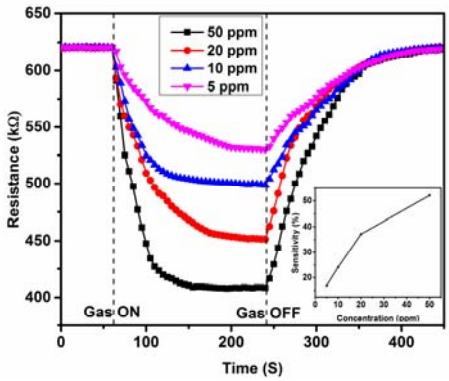

(b)

Figure: (a) SEM image of ZnO nanowires synthesized from 130 nm thick Zn film oxidized at 600 ^{o}C in moist environment (b) Change in resistance of ZnO nanowire upon exposure to 5-50 ppm of ammonia gas

References:

Wang Z L (2004) Zinc oxide nanostructures: growth, properties and applications *J. Phys. Condens. Matter,* 16, R829.

Mirabbaszadeh K and Mehrabian M, (2012) Synthesis and properties of ZnO nanorods as ethanol gas sensors, *Phys. Scr.,* 85, 035701.

Chang, Shoou Jinn, Wen Yin Weng, Cheng Liang Hsu, and Ting Jen Hsueh. (2010) High Sensitivity of a ZnO Nanowire-based Ammonia Gas Sensor with Pt Nano-particles., *Nano Communication Networks,* 1, 4: 283–88.

Long-term corrosion protection by a nano-composite thin PEA-TiO_2-HMDSO coating

L. Ejenstam,[1,2,*] M. Tuominen,[2] J. Pan,[1] A. Swerin,[1,2] P.M. Claesson [1,2]
[1]KTH Royal Institue of Technology, School of Chemical Science and Engineering, Department of Chemistry, Division of Surface and Corrosion Science, SE-10044 Stockholm, Sweden
[2]SP Technical Research Institute of Sweden – Chemistry, Materials and Surfaces, Box 5607, SE-11486 Stockholm, Sweden

Abstract: Lately there has been a tremendous interest in corrosion protection by different organic coating systems due to new regulations coming into place (Montemor, 2014). Here we present a thin nano-composite coating system showing very good corrosion protective properties for carbon steel during an exstended period of 100 days. As basecoat a 10 µm thick, UV-cured, polyester acrylate (PEA) coating (Sababi, 2013) was used. Then a middle layer of TiO_2 nanoparticles, ca. 1 µm thick, was deposited on the PEA basecoat by liquid flame spray (LFS) to enhance the surface roughness, following the procedure described by Teisala et al (2010). To lower the surface energy of the coating, a thin top coat layer of hexamethyldisiloxane (HMDSO), ca. 0.05 µm thick, was applied on the surface by plasma treatment. The nano-composite coatings were applied onto carbon steel substrates and then immersed in 3 wt% NaCl solution to evaluate the corrosion protection. The corrosion protective properties of the individual layers were also evaluated for comparision. Open circuit potential (OCP) and electrochemical impedance (EIS) measurements were performed regularly during the long exposure. The PEA basecoat alone show an impedance level of 10^5 Ωcm^2 for more than 80 days. The addition of the TiO_2 particle layer on top of the PEA did not significantly change the corrosion protective properties of the coating. However, the whole coating system consisting of all three layers (PEA-TiO_2-HMDSO), ca. 11 µm thick, exhibits a superhydrophobic surface and a remarkable improvement of the corrosion protective properties. The impedance of the nanocomposite coating remains over 10^8 Ωcm^2 for the long time of 100 days (figure 1). Interestingly, the photos of this surface (immersed in 3 wt% NaCl) show that corrosion started after 20 days, probably at a pin hole in the coating, but did not proceed during the prolonged exposure (inset in figure 1). The combined properties of each layer in this coating system result in an excellent corrosion protection of the underlying carbon steel substrate.

Keywords: corrosion protection, nanocomposite, organic coating, electrochemical impedance, contact angle, liquid flame spray.

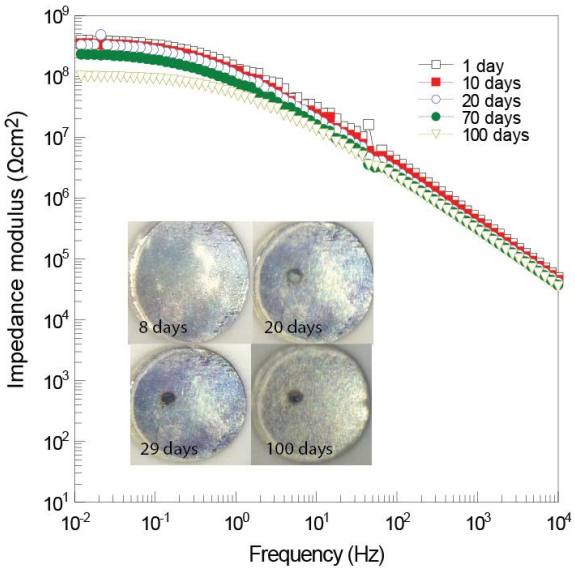

Figure 1: Bode plots of the electrochemical impedance spectra for the nano-composite coating immersed in 3 wt% NaCl solution, showing the good corrosion protective properties of the coating lasting for the very long period of 100 days. Also included are photos of the surface taken at different times of immersion, showing that corrosion started at a local defect, proceeded very slowly over time and did not cause the whole coating to fail.

References:

Montemor, M.F. (2014), Functional and smart coatings for corrosion protection: A review of recent advances. *Surface and Coatings Technology*, 258, 17-37.

Sababi, M. (2013), Nanocomposite coatings for corrosion protection. *Doctoral thesis in surface and corrosion science*, Stockholm, Sweden.

Teisala, H., et al. (2010), Development of superhydrophobic coating on paperboard surface using the Liquid Flame Spray. *Surface and Coatings Technology*, 205(2), 436-445.

Branched Polymer Nanoreactors for Catalysis by Design

V.O. Rodionov,* K.V. Bukhryakov, C. Mugemana
[1]KAUST Catalysis Center and Division of Physical Sciences and Engineering, King Abdullah University of Science and Technology, Thuwal, 23955-6900, Kingdom of Saudi Arabia

Abstract: Nature's enzymes are extremely efficient catalysts. Their remarkable properties result from precise preorganization of the local environment and functional groups around the catalytic sites and close participation of metal ions, prosthetic groups and cofactors (Fersht, 1999).
Chemist-designed, enzyme-inspired nanoscale catalysts have been the focus of intensive investigation, and a number of highly successful designs have been reported (Gao, 2012; Dwars *et al.,* 2005). Among the nanoscale catalyst supports, branched constructs such as dendrimers and star polymers are unique in that they can be designed to approximate some of the key features of natural biopolymers (Hecht and Fréchet, 2001). To date, the complexity of synthetic approaches to these well-defined branched macromolecules, especially those bearing reactive or catalytic moieties, has limited their use in catalysis. Striking examples of organocatalysis with globular macromolecules are more prevalent than examples of metal-complex catalysis, in part due to the difficulties involved in tethering of elusive transition metal ions to carbon-and-heteroatom based supports.
Here we shall present several examples of enzyme-inspired organotransition metal catalysts supported on branched macromolecules with nanoscale dimensions. The catalytic activities and properties of such systems are unattainable with small-molecule versions of the same catalytic moieties. The presentation will have a specific focus on Grubbs-type alkene metathesis catalysts for ring-opening polymerizations of monomers with low degrees of strain, and palladium-NHC cross-coupling catalysts not susceptible to aggregation.

Keywords: star polymers, catalysis, nanoreactors, alkene metathesis, cross-coupling reactions, N-heterocyclic carbenes, click chemistry, crowding effects, site isolation.

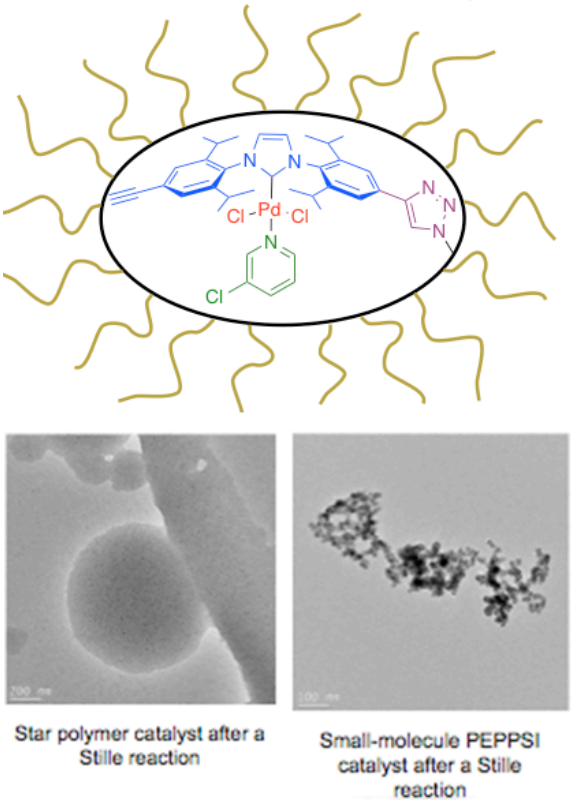

Figure 1: A star polymer nanoreactor for Pd-catalyzed cross-couplings. Unlike the corresponding small-molecule catalyst (PEPPSI), the polymer nanocatalyst demonstrates remarkable stability to aggregation.

References:

T. Dwars, E. Paetzold, G. Oehme, *Angew. Chem., Int. Ed.* **2005**, *44*, 7174-7199.

A. Fersht, *Structure and Mechanism in Protein Science: A Guide to Enzyme Catalysis and Protein Folding*, W. H. Freeman, New York, NY, **1999**.

H. Gao, *Macromol. Rapid Commun.* **2012**, *33*, 722-734.

S. Hecht, J. M. J. Fréchet, *Angew. Chem., Int. Ed.* **2001**, *40*, 74-91.

Novel Nanogold Coloured Wool Textiles, Aulana®, for Luxury Markets

J.H. Johnston,[1,2*] K.A. Lucas[2]
[1]School of Chemical and Physical Sciences, Victoria University of Wellington, Wellington, New Zealand
[2]Noble Bond Ltd, Wellington, New Zealand. *jim@noblebond.co.nz*

Abstract: Nanogold particles in different colours have been formed and bound to the keratin protein in wool fibres to produce an innovative, boutique colour range of nanogold-wool textiles, branded Aulana®, for high value international luxury markets.

Aulana® captures the exciting and unique opportunity whereby the prestige and high value of gold are linked directly to the high quality of New Zealand wool through the use of nanogold as novel stable colourfast colourants in the wool, for the international high quality fashion apparel, luxury textiles, carpet and rug markets (Johnston and Lucas 2013; www.aulana.co.nz) (Figure 1). This utilises the localised surface plasmon resonance properties of nanogold wherein the colour exhibited by the gold is dependent upon the size and shape of the nanogold particles and the dielectric constant of the surrounding material (Johnston and Lucas 2011, 2013; Liz-Marzán 2004, Kelly et.al. 2003). XPS measurements show the gold in the nanoparticles is chemically bound to the sulfur and nitrogen containing amino acids in the wool fibre proteins (Johnston and Lucas 2011). SEM images and associated X-ray elemental mapping show they reside predomiunately on the cuticle surfaces and edges. Spherical particles of gold about 10-20 nm are pink-purple in colour. Figure 2 (left) shows the relation between the gold nanoparticle size and the colour of the nanogold wool product. Precise control of the particle size enables the colour to be changed progressively through shades of pink, red, purple, blue-grey to grey (Figure 2 right). Nanogold colourants cannot fade or denature in sunlight and hence the nanogold coloured wool products exhibit excellent lightfastness.

The proprietary Aulana® technology and product suite have been developed from a laboratory scale using 0.1 g wool and progressed to pilot and commercial scale production now using kilogram quantities of wool in loose, combed top or yarn form (Figure 2 right) and fabric, as required. Precise control over the gold nanoparticle formation and chemical binding to the wool fibres to produce a uniform, durable nanogold-wool product is essential. Noble Bond Ltd, the owner of the Aulana® brand, is commercialising Aulana® products for use in luxury wool apparel, upholstery textiles, rugs and carpets. Aspects of the science, technology and the product development of these innovative nanogold wool products will be presented.

Keywords: nanogold, wool, textiles, Aulana, rug

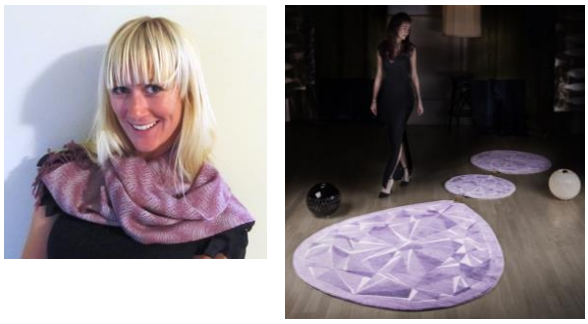

Figure 1: Nanogold Aulana® scarf (left) and Aulana® "Midas" rug (right).

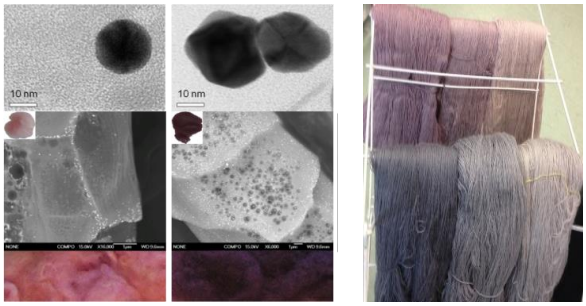

Figure 2: (left) TEM and SEM images of gold nanoparticles on the cuticle surfaces and edges for pink and purple nanogold coloured wool; (right) nanogold wool yarn in pink and grey colours.

References:

Johnston J.H., Lucas K.A. *(2011*) Nanogold synthesis in wool fibres: novel colourants, *Gold Bull.*, 44(2), 85-89.

Johnston, J.H., Lucas, K.L. (2013) Method for binding metal nanoparticles to substrates, *NZ Patent Application.*

Liz-Marzán, L. (2004) Nanomaterials: formation and colour, *Mater. Today*, 7, 26-31

Kelly K.L., Coronado E., Zhao L.L., Schatz G.C. (2003) The optical properties of metal nanoparticles: the influence of size, shape, and dielectric environment, *J. Phys. Chem. B* 107(3), 668–677.

Nanotechnology for more Efficient Sustainable Buildings

Ramy B. Fou'aad
Department of Architecture, Faculty of Engineering – Alexandria University, Alexandria - Egypt
ramybf@msn.com

Introduction: Construction is a massive global industry, with a very high environmental footprint. Many key players in the construction industry are pushing towards a more sustainable future, adopting new materials and new techniques.
Green building professionals want to apply sustainable development in the design, construction and operation of buildings. They struggle to minimize the use of non-renewable resources like petroleum, natural gas and coal, and reduce waste and pollutants. Energy conservation is highly important to green building as it both saves resources and minimize waste and pollutants.

"*It is not as though nanotechnology will be an option; it is going to be essential for coming up with sustainable technologies.*" advises Paul Anastas, director of the American Chemical Society-Green Chemistry Institute.

Globally, nanotechnologies are expected to reduce carbon foot print in three key areas: transportation, insulation in residential and commercial buildings, and generation of renewable photovoltaic energy. It is needless to mention that the last two of these three areas are centered in the building industry, pointing that building will in fact lead the green nano revolution.

Case Study: Focusing on energy efficiency, proceeded a study contains three examples (detached single family house) represents conventional architecture, sustainable architecture and nano-enhanced sustainable architecture, the study illustrated how the convergence between sustainable architecture and nanotechnology using today's *on-shelf* certain nanomaterials products would make better, healthier, and energy efficient architecture.

The study reviews the convergence between sustainable architecture and nanotechnology via diagnostic approach in the theoretical level of analysis, using comparison of three examples of architecture, following the scientific methods, by a number of tools collected from multiple scientifically trusted resources, to guarantee the best theoretical results.

The results of this case study are rough results, but it is the nearest thing to the right.
More in-depth real life research would reveal more precise results.

Tools to form and analyze the results and show indications that helps in understanding the case study:
• Common factors of sustainability measuring systems LEED and BREEAM.
• Solar Irradiance Calculator.
• Energy Load Estimation Calculator.
• Carbon calculator.
• EPC (Energy Performance Certificate).
• Home energy check.

	LEED	BREEAM	Common
Site	•	•	•
Management		•	
Health	•	•	•
Energy	•	•	•
Water	•	•	•
Materials	•	•	•
Transportation	•	•	•
Waste	•	•	•
pollution		•	
Innovation	•		
Awareness	•		

Table1: Illustrates comparison of key areas of rating of two of most important rating tools of sustainability: LEED and BREEAM, where the dot illustrates fulfilment of the key area. It shows clearly the common factors between two methods, (Site – Health – Energy – Water – Materials – Transportation – Waste) seven key areas are the most important factors which must be fulfilled by a building in order to be GREEN certified.

This study is fulfilled by 2 steps:

1)Applying 7 key areas common in sustainable building measuring tools:
(Site - Materials - Water - Energy - Waste - Transportation - Health)

- ✓ Waste – Transportation – Health:

Those keys will not be concluded in the comparison and will be considered fulfilled as it is mostly affected by inhabitants' behavior (Waste – Transportation) or irrelevant to the research (Health).
•Transportation: Using less private transportation in favor of public transportation, bicycling or walking.
•Waste: Fallowing waste reduction guide lines (reduce – reuse – recycle).
•Health: Using Nanomaterials regarding indoor environmental quality (air/water purification).

✓ Site - Materials - Water - Energy

Core of comparison, will be fulfilled based on three levels:

•Heat gain/loss (Site – Materials).

•Energy consumption (Water - Energy).

•Using renewable energy sources to produce energy needed.

2)Analyzing consumption efficiency:

1. Environmental efficiency.

Measuring carbon foot print of energy used in every case.

2. Energy efficiency.

Rating how effectively energy that is needed around the property is used.

3. Economic efficiency.

Economic efficiency is measured by money, the balance between revenues and costs, this will be via 3 steps:

•Cost of energy for every case according to Egyptian electricity selling prices.

•How much economic beneficial is using sustainable technology and nanomaterial.

•How much economic using solar energy instead of governmental electricity grid.

Conclusion:

Home Energy Check		
Conventional House	Sustainable House	Nano Sustainable House
		

Table 2:Conventional house is way **in**efficient compared to sustainable and nano-sustainable houses, comes last with **F** rating is prove for very high running cost in terms of energy, that assures the great beneficiary of sustainable technology used.

Enhancing sustainable technology with nanomaterials, resulted in better efficiency, and thus better rating (A instead of B)

After using sustainable technologies and nanomaterials in residential sector (detached single family house):

1-Reduction in energy cost 90%, which covers cost of installed technology.

2-Very environmental beneficial, reducing carbon emissions by 95%, saving more than 900 trees.

3-Using nanomaterials proved to raise EPC from B to A.

4-Clean and healthy indoor environmental quality due to nanomaterials used.

5-Energy efficiency house equals higher property value.

6-It is sure that enhanced house costs more to build, choosing to go green means higher cost and higher value as well. While choosing a conventional house that costs less to build, you will have a higher energy bill each month.

7-Well insulated building needs only a smaller, thus cheaper heating and cooling system, the heating and cooling system may only be needed as an occasional supplement. Savings on the initial and running cost of a heating and cooling system surely will offset much of additional cost for converting house into sustainability.

8-If the green house is supported by solar PV system, this would significantly reduce electricity bill, and in some countries applying FiT , the house turns to be source of income.

9-Using Nano-based materials in green house was a significant effect in two areas of three, first in reducing energy loads used by the house, and second in generating energy needed by the house.

References:

Elvin, George. *Nanotechnology for Green Building.* s.l. : Green Technology Forum, 2007.

U.S. Green Building Council. LEED. [Online] 2014. http://www.usgbc.org/leed

breeam.org. BREEM. [Online] 2014. http://www.breeam.org

Solar Electricity Handbook. Solar Irradiance. [Online] 2013. http://solarelectricityhandbook.com/solar-irradiance.html

Sinai Solar. Sinai Solar. [Online] 2013. http://www.sinaisolarenergy.com

Climate FriendlyTM. carbon footprint calculator. [Online] 2011. http://www.climatefriendly.com/personal/calculators/electricity

energy saving trust. Home Energy Check. *energy saving trust.* [Online] 2014. http://www.energysavingtrust.org.uk/Insulation/Home-Energy-Check

Dynamic and Static Fluid Loss Characteristics and Rheological Properties of Nano-Based Drilling Fluids

Z. Vryzas,[1*] O. Mahmoud,[2] H. Nasr-El-Din [2], V. C. Kelessidis [1]
[1]Texas A&M University at Qatar, Department of Petroleum Engineering, Doha, Qatar
[2]Texas A&M University, Department of Petroleum Engineering, College Station, U.S.A.

Abstract: Nanotechnology has already contributed significantly to technological advances in energy industry and has the potential to revolutionalize drilling industry. Nanomaterials are considered to be the one of the best candidates for smart fluids formation which can improve the performance of conventional drilling fluids. The demand for more efficient drilling technologies necessitates development of innovative drilling fluids. Drilling deeper, longer and more challenging wells in harsh HPHT (High-Pressure and High-Temperature) environments has been made possible by improvements in drilling technologies, including more efficient and effective drilling fluids. The key challenge in developing such drilling fluids is to maintain the stability of key fluid properties such as rheology and fluid loss particularly at higher temperatures and pressures. Formulation of novel water-based fluids under the optimal concentrations, increase the efficiency of drilling operations for the maximum recovery of new and matured HPHT reservoirs. The aim is for oil industry to apply improved drilling fluid recipes, so as to achieve more efficient drilling process with a simultaneous reduction in the environmental footprint. Nanoparticles can play significant role in the development of such smart drilling fluids because due to their small size it is anticipated that they will provide unique filtration properties.

This work focuses on the lab techniques for assessing and analyzing advanced water-based drilling fluids containing iron oxide and silica nanoparticles. These nanofluids are used to reduce fluid loss in water-based drilling fluid containing bentonite. Their performance is assessed utilizing both API HPHT/LPLT (American Petroleum Institute, Low-Pressure and Low-Temperature) filter press as well as a dynamic HPHT filter press with agitation. Comparison between static and dynamic conditions depicts the behavior of the fluids in different environments under elevated pressures and temperatures. Scanning Electron Microscope (SEM) pictures were used to analyze the nanoparticle size range. Analysis by SEM of the filter cake produced reveals their good performance by giving deep insights for their microstructure, the interfacial phenomena and the interaction between bentonite particles and the nanoparticles. Zeta potential measurements using Phase Analysis Light Scattering (PALS) method were used to assess the stability of the developed suspensions. The changes in the rheological properties of the nanofluids were measured at HTHP conditions using a standard Fann type viscometer, vane cup rheometer and concentric cylinder rheometer and showed good rheological behavior.

The examined nanoparticles have the potential not only to significantly reduce the fluid losses but also to maintain the rheological properties of the fluid. Their relatively low concentration in the drilling system provides a base for more efficient, environmental friendly and safer drilling practices. Their unique characteristics are expected to play a vital role in solving many technical challenges encountered during oil and gas drilling operations.

Keywords: nanoparticles, nano-fluids, drilling fluid, rheology, fluid loss, HPHT drilling

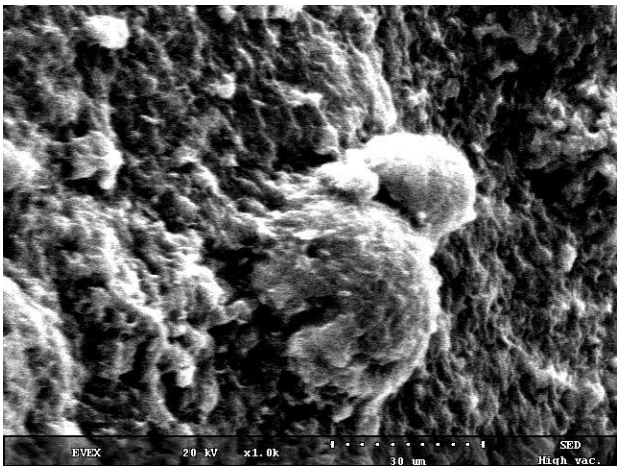

Figure 1: SEM image (30 µm magnification) for the surface of filter cake formed with the addition of 0.5 wt.% iron oxide nanoparticles.

Surface-Bound Ligands Modulate Chemoselectivity and Activity of a Bimetallic Nanoparticle Catalyst

V.O. Rodionov,* K.B. Vu,* K.V. Bukhryakov
KAUST Catalysis Center and Division of Physical Sciences and Engineering, King Abdullah University of Science and Technology, Thuwal, 23955-6900, Kingdom of Saudi Arabia

Abstract: Transition metal nanoparticles (NPs) and nanoclusters are a privileged class of metal colloids (Rocoux *et al.,* 2002). Their high surface areas, and the strong correspondence between particle sizes/shapes and surface chemistries make these species uniquely suited for applications in catalysis (Bell, 2003; Astruc *et al.,* 2005). Small, catalytically active NPs are also some of the more unstable colloids due to their tendency to aggregate. To address this problem, NP catalysts are typically arrayed on solid supports, which may also act as synergistic co-catalysts.
NPs and metal clusters can also be stabilized and solubilized with the aid of surface adsorbates, which range from simple surfactants and amphiphilic copolymers to strongly binding/soft ligands, such as thiols. Naturally, the adsorbate-stabilized NPs lose some or all of their catalytic competency (Naranyan *et al.,* 2005; Niu and Li, 2013). The metal surface accessibility is limited compared to "naked" NPs, and the catalytic sites are easily poisoned by thiols and amines.
We describe an approach to dispersible, catalytically-active, adsorbate-stabilized NPs. Our design is based on bimetallic NPs comprised of metals that feature significantly different affinities towards a specific class of adsorbates. Thus, with judicious choice of metal composition and surface ligand chemistry, the particle aggregation could be prevented, while the catalytic activity of the unprotected "islands" of the non-adsorbing metal could be preserved (Figure 1). This approach was applied to a bimetallic (PtFe) NP catalyst stabilized by carboxylate surface ligands that bind preferentially to one of the metals (Fe). NPs stabilized by fluorous ligands were found to be remarkably competent in catalyzing the hydrogenation of cinnamaldehyde, while NPs stabilized by hydrocarbon ligands were significantly less active. The chain length of the fluorous ligands and the composition of the surface monolayer played a key role in determining the chemoselectivity of the FePt NP catalysts.

Keywords: nanoparticles, catalysis, selective hydrogenation, cinnamaldehyde, ligand effects, fluorous chemistry, nanocatalysis.

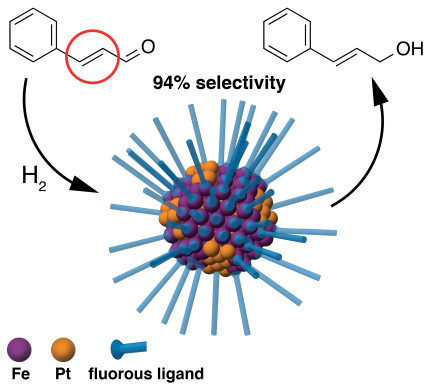

Figure 1: Catalysis with selectively-protected bimetallic FePt NPs. With judiciously chosen fluorous ligand, remarkable activity and selectivity of catalysis were achieved.

References:

Astruc, D.; Lu, F.; Aranzaes, J. R. *Angew. Chem., Int. Ed.* **2005**, *44*, 7852-7872.

Bell, A. T. *Science* **2003**, *299*, 1688-1691.

Narayanan, R.; El-Sayed, M. A. *J. Phys. Chem. B* **2005**, *109*, 12663-12676.

Niu, Z.; Li, Y. *Chem. Mater.* **2013**, *26*, 72-83.

Roucoux, A.; Schulz, J.; Patin, H. *Chem. Rev.* **2002**, *102*, 3757-3778.

Effects of Nanotechnology Materials on Architectural Design – Applications, Possibilities and Future Trends

N.K.Parthenopoulou[1,3], M.Malindretos[2,3]

[1]Architect Engineer, M.B.A. University of Macedonia, MSc in Construction Management A.U.Th., PhD Candidate in Architectural Design and Architectural Technology
[2]Professor of Architectural Design and Architectural Technology
[3]5th Department of School of Architecture, Faculty of Engineering, Aristotle University of Thessaloniki, University Campus, Postal Code 541 24, Thessaloniki

Abstract: Materials have been affecting architectural design since the beginning of human civilization and architectural expression. In the 20th century *Le Corbusier* quoted that a "house is a machine for living in". Now, the 21rst century leads towards a new correlation: "a house can be a living machine, a living organism". The use of advanced technology has provided a wide range of possibilities in the implementation of architectural design. Nanotechnology in construction materials enables high performance in terms of energy, light, security and intelligence (Leydecker, 2008), and furthermore provides new, innovative and revolutionary materials that can alter the design and performance of buildings. This has led to the launch of the Nanoarchitecture, where nanotechnology integration concerns not only the use of nanomaterials and manipulation techniques but also the reconsideration of forms and design methods – ultra high performance buildings (dynamic, interactive) (Johansen, 2002). In this sense, external surfaces can react and adapt to the environment, featuring the qualities of self-assembly, self-healing and self-repair. Nanomaterials are proven to be effective at aiding structures that suffer climatic strain both in performance and economy over time (Parthenopoulou, Angelides, 2010) and in enhancing existing structures. Throughout a research in existing and potential applications of nanotechnology and smart materials in architecture, this study demonstrates the level of influence of nanomaterials on architectural design and attempts at setting the basis for proposing an innovative system of outer "skin".

Keywords: nanomaterials, nanoarchitecture, construction applications

Figure 1. Architectural nanotechnology projects: NanoVentSkin (left) is a surface system that consists of nanoturbines that filter the air and produce energy and Carbon Tower (right) is made entirely out of carbon nanofibers.

References:

Addington, D., & Schodek, D. (2004). Smart Materials and Technologies: for the Architecture and Design Professions. Boston: Architectural Press.

Ashby, M. F., Ferreira, P. J., & Schodek, D. L. (2009). Nanomaterials, Nanotechnologies and Design. USA: Butterworth-Heinemann (Elsevier).

Johansen, J. (2002). NanoArchitecture: A New Species of Architecture. New York: Princeton Architectural Press.

Leydecker, S. (2008). Nano Materials. Berlin: Birkhauser Verlag AG.

Parthenopoulou, N., Angelides, D. (2010) Construction Materials Protecting Structures that Suffer Cilmatic Strain. Thessaloniki, AUTh.

Synthesis, Characterization and Catalytic Performance of Supported Nickel Nanoparticles in Methane Steam Reforming

M.J. Al-Marri, S. Ali,* M. M. Khader
Gas Processing Center, College of Engineering, Qatar University, Doha, P. O. Box 2713, Qatar

Abstract: Steam reforming of methane from natural gas provides the main source of hydrogen for most of petrochemical and petroleum refining applications. The efficiency of the reforming process depends upon an effective catalyst and thus this work aimed to produce a highly active nickel based nano-catalysts for methane reforming which is resistant to deactivation. Two nickel based catalysts namely nickel supported on 10wt%silica/alumina (Ni/SA) and nickel nanoparticles dispersed over 10wt%silica/alumina (Ni.NPs/SA) were synthesized and their catalytic activities for the steam reforming of methane were investigated. Ni/SA was prepared using deposition precipitation method while for the synthesis of Ni.NPs/SA nanoparticles were synthesized as a first step and dispersed over the surface of the substrate. Catalysts were characterized using various analytic techniques such as transmission electron microscopy (TEM), nano-scanning electron microscopy (NSEM), X-ray photoelectron spectroscopy (XPS), nitrogen physisorption, temperature programmed reduction (TPR) and temperature programmed oxidation (TPO). Methane steam reforming was carried out in quartz fixed bed reactor (in temperature range between 600-900^{0}C and at atmospheric pressure) connected online to a mass spectrum.

Among the catalyst tested, Ni nanoparticles supported on 10wt%$SiO_2.Al_2O_3$ exhibited better catalytic performances in methane steam reforming than that of Ni/SA. In all temperature studied Ni.NPs/SA catalyst exhibited high methane conversions (100% methane consumption was achieved at operating temperature of 750^{0}C), high selectivities to H_2 and excellent thermal stability. Even under the sever conditions of S/C = 1, at an operating reaction temperature of 750^{0}C (for a period of 60 hours), it showed stability, higher methane conversions, better selectivities to H_2 and excellent resistance to coke deposition as compared to that of Ni/SA catalyst.

Keywords: steam reforming, Ni nanoparticles, coke deposition.

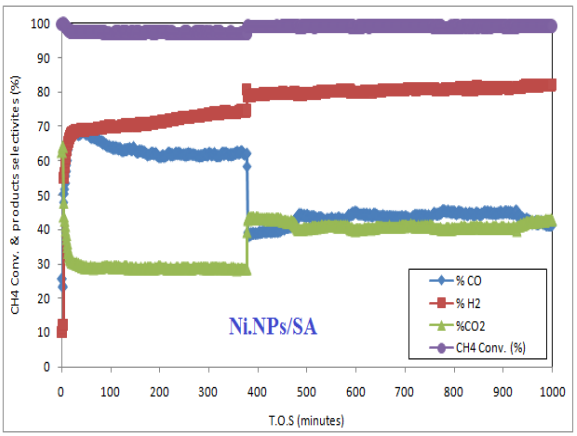

Figure 1: Figure illustrating the performance and products distribution in time on stream over Nickel Nanoparticles in methane steam reforming at 800^{0}C.

Allied Events

nano tech 2016
International Nanotechnology Exhibition & Conference

7th BANGALORE INDIA NANO
Research • Industry • Academia

With the support of

Media Partners

www.setcor.org
www.nanotechfrance.com

Posters Session I - A
Advanced NanoMaterials

One-step preparation of amylose and β-carotene nanoparticle inclusion microbeads using amylosucrase from *Deinococcus geothermalis*

Carlos Andres Letona,* Min-Cheol Lim, and Young-Rok Kim
Institute of Life Sciences and Resources & Department of Food Science and Biotechnology, College of Life Sciences, Kyung Hee University, Yongin, Republic of Korea

Abstract: The purpose of this study was to create an one-step inclusion complex of β-carotene nanoparticle (β-cNP) using amylose as a host molecule based on enzymatic polymerization using amylosucrase from *Deinococcus geothermalis* (DgAS). β-cNPs were prepared by rotary evaporation methods using tetrahydrofuran (THF, miscible in water) to dissolve the β-carotene and lecithin as emulsifier. After complete evaporation of THF, well dispersed nanoparticles of β-carotene (β-cNP) with size of 50 nm in water were obtatined. Our previous study demonstrated the possible capicatiy of DgAS to produce amylose nanocomposite microbeads which containing hydrophobic guest molecule such as carbon nanotube (Min-Cheol et al.; 2011). In this study we used the β-carotene as a candidate guest molecule, a hydrophobic chemical which is susceptible to photodegradation, chemical oxidation and thermal degradiation, those properties make it difficult to use as an ingredient in functional products and thus reduce its bioavailability (C. Boon et al.; 2010). However, to overcome this issue, we added β-cNPs into the DgAS enzyme reaction solution to entrap this guest molecule into the amylose microbeads during the synthesis of amylose chains. Because the β-carotene was present as nanoparticle we could increase the dissolution rate in aqueous phase and provide a more stable interaction with synthezised amylose chains. The morphology of produced amylose microbeads and amylose-β-cNP inclusion microbeads were analyzed by FE-SEM, DSC, XRD and Raman spectroscopy were performed to confirm the inclusion complex of β-cNP into the amylose microbeads. The encapsulation yield test shows a 94% β-carotene were encapsulated in the amylose microbeads. We expect this study helps to enhance the properties of β-carotene and further uses in functional foods or as a food delivery system.

Keywords: Amylose, β-carotene, nano particles, inclusion complex, food delivery.

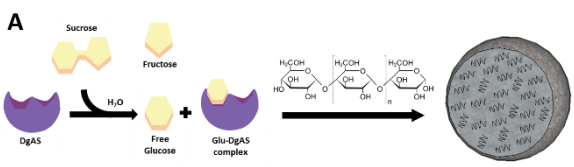

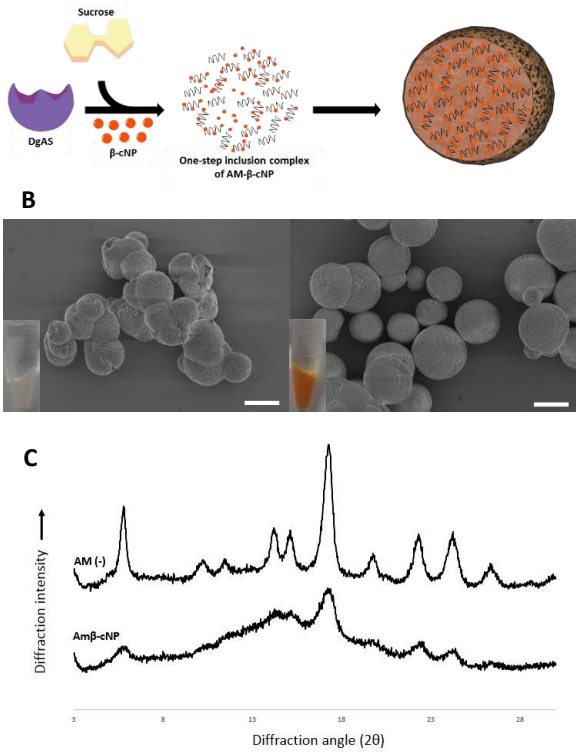

Figure 1: **(A)** Schematic drawings show the enzymat-ic synthesis of amylose microbead and amylose and β-cNP inclusion microbead. **(B)** FE-SEM images of amylose beads without β-cNP and amylose beads with β-cNP (Scale bar is 3 μm). **(C)** XRD analysis showing the lost of amylose crystallinity by the complexation with β-cNP.

References:

Min-Cheol L., Dong-Ho S., Ji-Hoon J., Cheon-Seok P., Young-Rok K. (2014) Enzymatic synthesis of amylose nanocomposite microbeads using amylosucrase from *Deinococcus geothermalis*, *RSC Adv., 4, 26421*.

C. Boon, D. McClements, J. Weiss (2010) Factors Influencing the Chemical Stability of Carotenoids in Foods, *Critical Reviews in Food Science and Nutrition, 50:515-532.*

Acknowledgments:

This work was supported by the Korea Research Foundation Grant (NRF-2013R1A1A2061841).

Encapsulation of water molecules in cyclic peptide nanotube

P. Tiangtrong,[1] N. Thamwattana,[2] D. Baowan[1]
[1]Department of Mathematics, Faculty of Science, Mahidol University, Rama VI Rd., Bangkok 10400 Thailand
[2]School of Mathematics and Applied Statistics, University of Wollongong, Wollongong, NSW 2522, Austraria

Abstract: Cyclic peptide nanotubes, form by the self-assembly process of the cyclic peptides, have attracted interest from many areas of science. The manipulation of the functional side chains and the number of amino acids on the cyclic peptides will change the ease of synthesis and ability to control the properties of inner and outer surfaces (Scanlon *et al*.; 2008). Cyclic peptide nanotubes can be used as artificial transmembrane channels for transporting ion, bio molecules and waters into cells. In this research, we study the interaction of a water molecule in a cyclo[(-D-Ala-L-Ala)$_4$-] peptide nanotube by using the Lennard-Jones potential and a continuum approach. Mathematical modelling and elementary mechanic are utilized to determine an exact formula of the interaction energy between the water molecule and the peptide nanotube. We assume that there are a sphere of two hydrogen atoms uniformly distributed over the surface of water moleclue and a single oxygen atom located at its centre, and each cyclic peptide subunit has an inner and an outer cylindrical surfaces. The result shows that the water molecule can be encapsulated into the cyclic peptide nanotube, and the acceptance behaviour does not depend on the number of cyclic peptide subunits. Moreover, we study the offset behaviour of the water molecule when it is inside the nanotube as shown in Fig.1. The water molecule prefers to be off-axis and closer to the inner surface of the cyclic peptide nanotube. We also consider the interaction between two water molecules inside the nanotube. Our study supports the arrangement of water molecule in 1-2-1-2 file (Song *et al*.; 2013, Liu *et al*.; 2010, Engels *et al*.; 1995) inside the cyclic peptide nanotube. This research is a theoretical study to understand the water molecules behaviour inside the cyclic peptide nanotube.

Keywords: cyclic peptide nanotube, water molecules, artificial transmembrane channels, interaction energy, offset positions, Lennard-Jones potential.

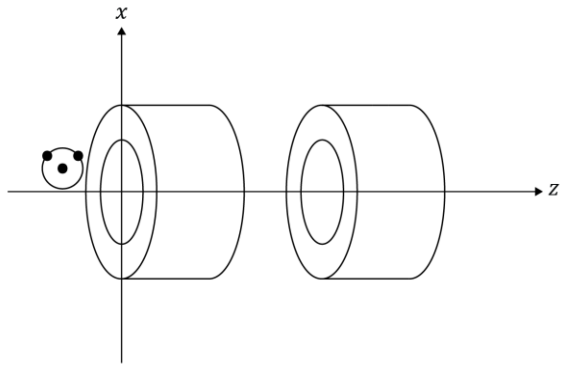

Figure 1: Schematic model for the interaction between an offset water molecule and a cyclic peptide nanotube comprising two cyclic peptide subunits.

References:

Scanlon, S., Aggeli, A. (2008), Self-assembling peptide nanotubes, *Nano Today*, 3(3-4), 22-30.

Song, X., Fan, J., Liu, D., Li, H., Li, R. (2013), Molecular dynamics study of Na^+ transportation in a cyclic peptide nanotube and its influences on water behaviors in the tube, *J. Mol. Model*, 19(10), 4271-4282.

Liu, J., Fan, J., Tang, M., Zhou, W. (2010), Molecular dynamics simulation for the structure of the water chain in a transmembrane peptide nanotube, *J. Phys. Chem. A*, 114, 2376-2383.

Engels, M., Bashford, D., Ghadiri, M.R. (1995), Structure and dynamics of self-assembling peptide nanotubes and the channel-mediated water organization and self-diffusion. A molecular dynamics study, *J. Am. Chem. Soc.*, 117(36), 9151-9158.

PDMS Surface Property Study and Sol-gel Modification Methods for the Immobilization of Unstable Enzyme

Hongyan Bi[1,*], Ana Carolina Fernandes[2], Filipe Cardoso[2,], Marina Brito[1], Susana Isabel Pinheiro Cardoso[2], Paulo Freitas[1]

[1] International Iberian Nanotechnology Laboratory (INL), Braga, Portugal
[2] INESC Microsistemas e Nanotecnologias (INESC MN), Lisbon, Portugal

* Correspondence should be addressed to Dr. Hongyan Bi
Tel: + 351 253 140 112; Fax: +351 253 140 119
E-mail: hongyan.bi@inl.int

Abstract: Microfluidic devices have shown great promises in biomedical and diagnostic applications, tissue engineering, environmental monitoring, food safety, and so on.[1] PDMS based microfluidic devices have been widely used in bioanalytical studies. One of the major applications of the microfluidic chips is to work as an enzymatic reactor for *in-vitro* metabolism studies. We report here the activity maintenance of unstable enzymes immobilized in PDMS microfluidic channels with different strategies, including the sol-gel encapsulation of enzymes, physisorptive adsorption of enzymes to the inner surface of PDMS channels with and without xerogel deposition. From fluorescence characterization, the adsorption of proteins to the unmodified PDMS microchannel showed the largest amount of immobilized proteins in 1 hour, but few proteins could still be maintained on the surface after overnight incubation of the protein solution in such a channel. The sol-gel encapsulation and adsorption on xerogel filled microchannel methods could also form protein modified PDMS microchannel. Ascorbate oxidase, an unstable enzyme, was immobilized by the three protocols in PDMS microchips to form enzymatic reactors. Their activities were evaluated based on their catalysis ability to the oxidation of ascorbic acid. It was found that the enzymatic reactor formed by adsorption of enzyme on the xerogel coated PDMS microchannel showed the strongest enzymatic activity, although the protein adsorption amount should be lower in the case comparing with those of the other two protocols. This protocol holds advantages of i) highly maintaining the enzyme activity because of the short time for enzyme immobilization, and ii) taking advantage of xerogel filled microchannel in reducing diffusional effects of enzymatic reaction in microchannel. This study can provide an easy method to build a PDMS microfluidic channel based bio-device for unstable enzyme catalyzed drug reaction.

Keywords: sol-gel encapsulation, PDMS microfluidic chip, ascorbic acid; kinetics; utilization factor, biosensor

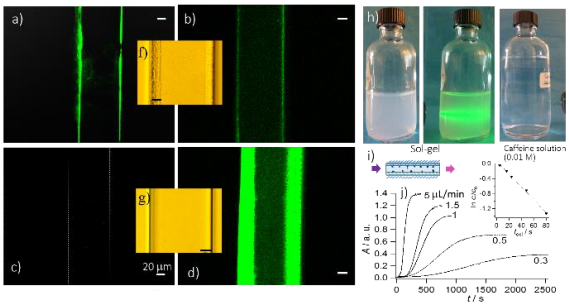

Figure 1: Confocal fluorescence microscopic images of proteins under different deposition methods on PDMS microfluidic channels by (a) sol-gel encapsulation; (b) absorption on xerogel deposited channel; 1 hour (c) and overnight (d) loading on untreated channel. (f) and (g) are the microscopic picture of channel with and without deposition of xerogel. (h) Pictures of synthesized sol-gel suspension compared with aqueous solution. (i) Scheme of microfluidic channel for activity investigation of enzymes by UV/vis absorbance change of substrate. (j) Representative UV/vis absorbance change when controlling the drug substrate through microfluidic channel at different rate. Inlet of (j) is the semi-logarithm plot of the corresponding concentration change of ascorbic acid as a function of the reaction time between them.

References:

1 D. Eicher and C. A. Merten, "Microfluidic devices for diagnostic applications," Expert Rev. Mol. Diagn. **11** (5), 505-519 (2011).

New Methods for Creating Nanocomposites Based on Carbon Nanotubes and Graphene Nanoplatelets

E.A. Burakova, A.V. Gerasimova, A.V. Melezhyk, A.G. Tkachev
Department "Technology and Methods of Nanoproducts Manufacturing", Tambov State Technical University, Tambov, Russian Federation

Abstract: Carbon nanoparticles (nanotubes, graphene) are widely used as units for building various nanocomposite materials. Commonly, these nanocomposites contain nanotubes and/or graphene and some functional components - for example, nanosized particles (metals, metal oxides, metal sulfides, sulfur), layers (polyaniline, polypyrrole), biological molecules, etc. The common problems in the synthesis of such materials are as follows:
1) obtaining solutions of well-dispersed nanoparticles or their precursors with sufficient concentration;
2) bringing the components into contact to assemble the desired structure;
3) separating the product from solution with saving the designed structure.
Different experimental procedures have been developed to perform those tasks. One of the most flexible approaches used for the synthesis of graphene-based nanocomposites implies the using of water-soluble graphene oxide as graphene precursor and its combination with different functional components; the graphene oxide is then reduced to graphene layers, which trap the particles of a functional component. If desired, the latter can be chemically attached to the graphene layers. Depending on synthesis conditions, the final product can be obtained in the form of a gel or coagulated precipitate. Such an approach is very flexible, but it is confined to using graphene oxide because of specific properties of this compound (high solubility in water, easy reducibility to graphene). It is interesting to develop a similar method of obtaining nanocomposites applicable for different carbon nanoparticles. It should be noted that the solubility of carbon nanotubes (CNTs) and graphene nanoplatelets (GNPs) in aqueous solutions of common surfactants is very low (order of 0.001-0.05 g/L) which impedes the mass synthesis of nanocomposites. To overcome this problem, we have developed a new method based on the modification of CNTs and GNPs with phenolformaldehyde resin (PFR). It was revealed that the water-soluble PFR reacts with the CNTs or GNPs containing surface oxygen groups. Presumably, the PFR is attached to the surface of the oxidized CNTs and GNPs via reactive methylol groups. The solubility of the so modified carbon nanomaterials in water is very high and reaches 10 g/L and more (Figure 1). The solutions are stable and do not precipitate during centrifuging. The presence of oxygen groups on the surface of the CNTs or GNP is essential. The non-oxidized CNTs or GNPs are only slightly solubilized by the PFR. The second issue, valuable for creating nanocomposites, is that these solutions are stable only at alkaline pH (9-11). Presumably, the ionization of phenol groups in alkaline media prevents aggregation of carbon nanoparticles due to electrostatic repulsion. When the pH is lowered to neutral or acidic, coagulation occurs. Depending on synthesis conditions, the coagulation results in the formation of a precipitate or gel. Some analogy with a classical sol-gel transition in inorganic systems can be drawn. When some nanosized functional component were introduced into the original alkaline solution of PFR-modified carbon nanoparticles, this component appeared to be trapped in the coagulated product. Besides simple trapping of the nanoparticles, different chemical reactions can take place due to high reactivity of methylol groups. These may be the reactions with excess phenolformaldehyde resin, or with precursors of different inorganic nanosized particles. Moreover, complex nanocomposites like CNT/GNP/(functional component) can be easily obtained. Using the approach herein described, we have prepared the following nanocomposites:
a) CNT/PFR, b) GNP/PFR, c) CNT/TiO_2, d) GNP/TiO_2, e) CNT/GNP, f) CNT/epoxy, g) GNP/epoxy, and h) GNP/porous carbon.

The work was performed within the framework of the Federal Target Program "Research and Development in Priority Areas of the Scientific and Technological Complex of Russia for 2014-2020" (State Contract of July 22, 2014 No. 14.577.21.0091; Unique Identifier for Applied Scientific Researches: RFMEFI57714X0091).

Keywords: carbon nanotubes, graphene nanoplatelets, phenolformaldehyde resin, nanocomposites, sol-gel.

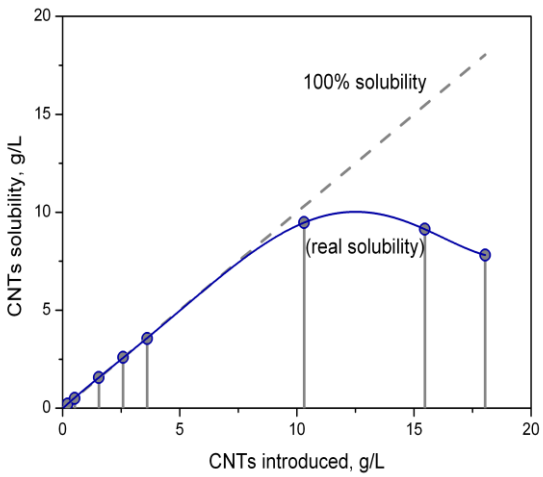

Figure 1: Solubility of the CNTs Taunit-M (external diameter 8-15 nm), modified with phenolformaldehyde resin, in water. The dash line corresponds (theoretically) to the complete dissolution of the original CNTs.

Preparation of Polybutadiene-Silica Nanoparticles via Differential Microemulsion Polymerization and their Hydrogenated Nanoparticles by Diimide Reduction

T. Tancharernrat,[1*] G. L. Rempel,[2] P. Prasassarakich[1]
[1]Chulalongkorn University, Faculty of Science, Department of Chemical Technology, Bangkok, 10330, Thailand
[2]University of Waterloo, Department of Chemical Engineering, Ontario, N2L3G1, Canada

Abstract: Nanocomposite materials (polymer/silica) have increasing potential for future applications due to the advantageous properties of the polymer species such as elasticity, processibility with silica particles providing high thermal stability and reinforcement (Kongsinlark *et al.*; 2012, Tancharernrat *et al.*; 2014). Polybutadiene (PB)-silica nanoparticles with core-shell morphology were successfully synthesized via differential microemulsion polymerization using potassium persulfate (KPS) as an initiator and sodium dodecyl sulfate (SDS) as a surfactant. The effects of silica loading and surfactant concentration on monomer conversion, particle size, grafting efficiency and silica encapsulation efficiency were investigated. A high monomer conversion (81.5%), grafting efficiency (78.5%) and small particle size (27 nm) with narrow size distribution was obtained at optimum reaction conditions with low surfactant concentration, 5 wt.% based on monomer. However, the C=C of PB are sensitive to oxygen, ozone and heat resulting in rubber degradation and the reduction of mechanical and thermal properties (Kongsinlark *et al.*; 2013, Piya-areetham *et al.*; 2013). Thus, the PB-silica latex could be hydrogenated by diimide reduction in the presence of hydrazine and hydrogen peroxide providing the hydrogenated polybutadiene (HPB)-silica. The HPB-silica was characterized by ^{1}H nuclear magnetic resonance spectroscopy. The highest hydrogenation degree of 98.6% was achieved at a ratio of hydrazine to hydrogen peroxide of 0.75:1. A proposed formation mechanism for the formation of PB-silica and HPB-silica core-shell nanoparticles is illustrated in Scheme 1. A new nanocomposite of PB-silica and HPB-silica could be used as a nanofiller in natural rubber (NR). Especially, NR/HPB-silica composites had improved mechanical and thermal properties, and exhibited good resistance toward ozone exposure.

Keywords: emulsion polymerization, diimide hydrogenation, nano-structures, particle-reinforcement, mechanical properties, thermal properties.

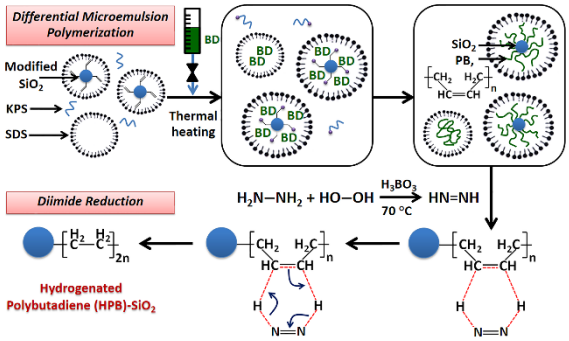

Scheme 1: Schematic of a proposed formation mechanism for the formation of PB-silica and HPB-silica core-shell nanoparticles.

References:

Kongsinlark, A., Rempel, G.L., Prasassarakich, P. (2012), Synthesis of monodispersed polyisoprene–silica nanoparticles via differential microemulsion polymerization and mechanical properties of polyisoprene nanocomposite, *Chem. Eng. J.* 193-194, 215–226.

Kongsinlark, A., Rempel, G.L., Prasassarakich, P. (2013), Hydrogenated polyisoprene-silica nanoparticles and their applications for nanocomposites with enhanced mechanical properties and thermal stability, *J. Nanopart. Res.* 15, 1612-1617.

Piya-areetham, P., Prasassarakich, P., Rempel, G.L. (2013), Aqueous-phase hydrogenation of nanosized polyisoprene emulsion using rhodium catalysts, *Eur. Polym. J.* 49, 2584–2595.

Tancharernrat, T., Rempel, G.L., Prasassarakich, P. (2014), Preparation of styrene butadiene copolymer-silica nanocomposites via differential microemulsion polymerization and NR/SBR-SiO_2 membranes for pervaporation of water-ethanol mixtures, *Chem. Eng. J.* 258, 290–300.

Construction Copper-Based (I) Superstructures via Recrystallization

Y. Shang[1,2], L. Guo[1], G. Y. Shang[2]
[1] School of Chemistry and Environment, Beihang University, Beijing 100191, P. R. China
[2] School of Physics, Beihang University, Beijing 100191, P. R. China

Abstract:
Assembling inorganic NPs into 3D superstructures with defined morphologies is of particular interest (Wang *et al.*, 2012). It may form the basis of a new engineering strategy instead of mechanical assembly of individual parts by using simple and elegant manufacturing methods (Kowalczyk *et al.*, 2012; Auyeung, E. *et al.*, 2014). We explore a novel strategy for the construction of 3D Cu_2O superstructures with defined morphologies employing Cu_2O mesoporous spheres (Shang *et al.*, 2012) with the diameter of ~ 300 nm as the building blocks. The concept of "recrystallization-induced self-assembly" (RISA) is successfully achieved in this work (Shang *et al.*, 2014). The key of this unique strategy is governed by a balance between the hydrolysis and recrystallization rate of inorganic CuCl intermediates through precisely adjusting the experimental parameters. The geometry of the products can be tuned as cubes or tetrahedrons, which is proved to be dependent on the growth behavior of CuCl (Figure 1a). The overall strategy in this work could extend the application of recrystallization in guiding the construction of assemblies (Figure 1b, c), such as (CuBr, CuI), and offers a unique clue for assembling larger particles into complicated 3D superstructures.

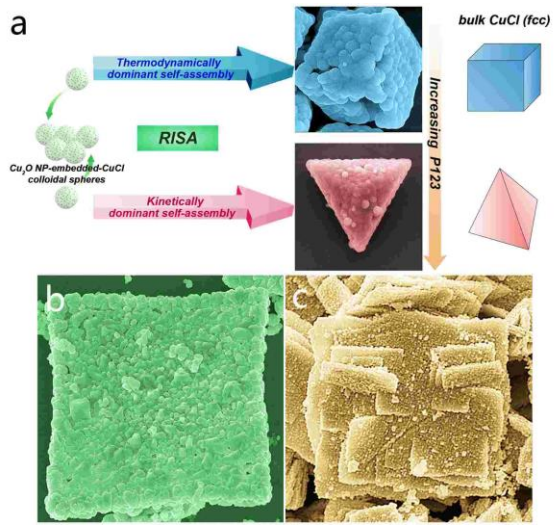

Figure 1: (a) Correlation between the geometry of the Cu_2O superstructures and their self-assembly kinetics; (b) SEM image of CuBr superstructure; (c) SEM image of CuI superstructure.

References:

Wang, T.;. Zhuang, J. Q.; Lynch, J.; Chen, O.; Wang, Z. L.; Wang, X. R.; LaMontagne, D.; Wu, H. M.; Wang, Z. W.; Cao, Y. C. (2012), Self-Assembled Colloidal Superparticles from Nanorods, *Science*, 338, 358-363.

Kowalczyk, B.; Bishop. K. J. M.; Lagzi, I.; Wang, D. W.; Wei Y. H., Han, S. B.; Grzybowski, B. A. (2012), Charged Nanoparticles as Supramolecular Surfactants for Controlling the Growth and Stability of Microcrystals, *Nat. Mater.*, 11, 227-232.

Auyeung, E.; Li, T. I.; Senesi, A. J.; Schmucker, A. L.; Pals, B. C.; de la Cruz, M. O.; Mirkin, C. A. (2014), DNA-Mediated Nanoparticle Crystallization into Wulff Polyhedra, *Nature*, 505, 73-77.

Shang, Y.; Zhang, D. F.; Guo, L. (2012), CuCl-Intermediated Construction of Short-Range-Ordered Cu_2O Mesoporous Spheres with Excellent Adsorption Performance, *J. Mater. Chem.*, 22, 856-861.

Shang, Y.; Shao, Y. M.; Zhang, D. F.; Guo, L. (2014), Recrystallization-Induced Self-Assembly for the Growth of Cu_2O Superstructures, *Angew. Chem. Int. Ed.*, 53, 11514-11518.

Bio-reduction of Graphene Oxide by Natural Products

E. ÖZTÜRK[1,2], S. ŞİMŞEK[1], B. ÖZBEK[1]
[1]Yildiz Technical University, Chemical Engineering Department, Istanbul,Turkey
[1]Yildiz Technical University, Central Science and Technology Application and Research Center, Istanbul,Turkey

Abstract: In recent years, graphene which is one of the carbon nanomaterials has generated a great deal of interest especially in material science owing to its unique properties such as high surface area, excellent thermal conductivity, high optical transparency and exceptional mechanical strength (Edwards *et al*., 2013). Graphene has a hexagonal arranged structure of bonded sp^2 carbon atoms, promises a wide range of areas from electronics to biomedical applications (Agharkar *et al.*, 2014).

Graphene has been produced by different methods like micromechanical cleavage, electrochemical exfoliation, epitaxial growth on silicon carbide, chemical vapor decomposition and chemical reduction of graphene oxide (Edwards *et al*., 2013; Whitener *et al.*, 2014). Chemical reduction of graphene oxide is the most common method which includes exfoliation of graphite to graphene oxide and reduction of graphene oxide to graphene by reducing agents like hydrazine and its derivatives. Although this method provides cost effective and bulk production, the toxic nature of reducing agents restricting its applications in bio-related sciences. To overcome this disadvantage, scientists have turned their faces to green chemistry. Based on the studies in which the biomolecules, microorganisms and plant extracts were used as reducing agents for the synthesis of metal particles, the possibility of usage natural-based molecules for the reduction of graphene oxide has been investigated (Agharkar *et al.*, 2014; Thakur *et al.*, 2014; Iravani, 2011). Besides the non-toxic structure of these natural compounds, utilization of them as reducing agents, provide cheaper synthesis reactions due to cheap raw material and low-cost isolation processes.

In the present study, to exploit the superior features of the reactions which are performed by green chemicals and to increase the usage chance of graphene derivatives in bio-related applications, the graphene oxide was synthesized by Hummer's method. Then, the aqeous extracts of plants (rose hip, melissa, salvia, lavandula, laurel and yarrow) were used for reduction process. The reduction performance of plant extracts were examined and characterized by using Ultraviolet-Visible Spectroscopy, Fourier Transform-Infrared Spectroscopy, Scanning Electron Microscope and Thermogravimetric Analysis. After characterization process, the optimum samples were determined. Thus, the potential uses of the optimum samples to generate biologically safe and biocompatible composites are aimed for the further studies.

Keywords: graphene oxide, bio-reduction, green reduction, natural product, characterization

References:

Edwards, R.S. and Coleman, K.S. (2013), Graphene synthesis: relationship to applications, *Nanoscale*, 5, 38-51.

Agharkar M., Kohrekar S., Hidouri S. and Azeez M. M. (2014), Trends in green reduction of graphene oxides, issues and challenges: A review, *Materials Research Bulletin*, 59, 323-328.

Whitener Jr. K. E. and Sheehan P. E.(2014), Graphene synthesis, *Diamond & Related Materials*, 46, 25-34.

Thakur S. and Karak N. (2012), Green reduction of graphene oxide by aqeous phytoextracts, *Carbon*, 50, 5331-5339.

Iravani, S. (2011), Green synthesis of metal nanoparticles using plants, *Green Chemistry*, 13, 2638-2650.

Simple Synthesis of Magnetic Nanoparticles for same shape and size without Size separation

H. Y. NOH[1], Y. J. EOM[1], Mohamed Abbas[1,2] and C.G. KIM[1,*]
[1] Daegu Gyungbuk Institute of Science and Technology, Department of Emerging Material Science, Daegu, South Korea
[2]National Research Centre, Ceramics Department, 12311Cairo, Egypt

Abstract : Much progress for synthesis of nanoparticle process for shape and size control has been made over the twenty years. Among many material for nanoparticle, magnetic nanoparticles based on iron have been studied by many researcher because it is particularly applicable to bio and medical fields for tracking target cells (Panklhurst. Q. A, . J. Phys. D: Appl. Phys. 2003, 36, R167-R181). Studies for magnetic property in accordance with shape and size of nanoparticle is necessary for using bio-medical application (Colombo. M et al, Chem. Soc. Rev 2012, 41, 4306-4334). Therefore, we study easy synthesis of magnetic nanoparticle for shape control and analysis the magnetic properties depend on same shape of particles and different component materials on similar size. We study to compare two magnetic nanoparticles (Fe_3O_4, $CoFe_2O_4$) using thermal decomposition method (Park. J et al., Angew. Chem. Int. Ed. 2007, 46, 4630-4660). For this study, we control experimental conditions which are just one surfactant concentrations and experimental time for making easy synthesis. And we obtain same shape (cube, hexagon) and same size (50~60 nm) of Fe_3O_4 and $CoFe_2O_4$ nanoparticles respectively. Like this way to make nanoparticle, We measured X-ray diffraction (XRD) and Electron Diffraction Pattern (EDP) for identifying crystalline planes of making nanoparticles. By measuring Electron Diffraction Spectroscopy (EDS) we acscertain existence of each materials. And we get high resolution images of each nanoparticles using Field Emission Transmission Electron Microscope (FE-TEM) (Figure 1). Finally, for measuring magnetic property, We use Superconducting Quantum Interface Device (SQUID). In the result, We observe making same shape of nanpaticle about different materials by same condition and changing each nanoparticle shape by temperature and surfactant concentrations. And we obtained saturation magnetization value at 4 K exhibited that Fe_3O_4 is 120 emu/g and $CoFe_2O_4$ is 53 emu/g. This study will discuss more simple synthesis process for controlling shape and size using thermal decomposition and suggest more effective shape and size of magnetic nanoparticle on bio-medical applications.

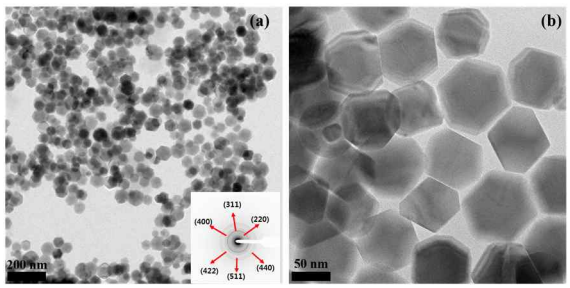

Figure 1 : High resolution FE-TEM and EDP images (a) Hexagon shape of Fe_3O_4 magnetic nanoparticle and its crystalline plane (b) High resolution image of hexagon shape of Fe_3O_4 magnetic nanoparticle.

Keywords: Magnetic nanoparticle, Thermal decomposistion, Superconducting Quantum Interface Device (SQUID), Shape control, Fe_3O_4, $CoFe_2O_4$, Simple synthesis, shape control

References:

Colombo. M et al., Biological Applications of Magnetic Nanoparticles. Chem. Soc. Rev 2012, 41, 4306-4334.

Park. J. et al., Synthesis of Monodisperse Spherical Nanocrystals. Angew. Chem. Int. Ed. 2007, 46, 4630-4660.

Pankhurst. Q. A., Applications of magnetic nanoparticles in biomedicine. J. Phys. D: Appl. Phys. 2003, 36, R167-R181.

Acid hydrolysis to improve the production of Bacterial Cellulose Nanocrystals

P. Paximada[1], E.A. Dimitrakopoulou[1], C. Fasseas[2], I. Mandala[1]
[1]Agricultural University of Athens, Department of Food Science and Human Nutrition, 75 Iera Odos, 11855, Votanikos, Athens, Greece
[2]Laboratory of Electron Microscopy, Dept. Crop Science, Agricultural University of Athens, Greece

Abstract: A research area that has been receiving much attention recently is the modification of cellulose for the development of nanocrystals. Cellulose is the most abundant natural polysaccharide, being the major structural component of plants. Recently, bacterial cellulose (BC) has received attention and has been used in many areas, thanks to its distinctive advantages. BC provides material with limited contaminants present and specifically without any hemicelluloses or various by-products which generally surround cellulose molecules. With this advantage, it is possible to hydrolyze BC with milder conditions and, thus, avoid the use of strong acids.
This work aims at examining the various factors that affect cellulose nanocrystals (BCNCs) extraction from bacterial cellulose (BC). Specifically, the effect of hydrolysis time, temperature and the kind of acid on the properties of the obtained nanocrystals were studied. In order to evaluate the effects of hydrolysis on BC, morphology, rheology, phase separation and particles size were investigated.
The morphology of BCNCs, examined by TEM, showed a decrease in the nanocrystals' length when increasing hydrolysis time, as expected. What is more, characteristic features of BCNCs were their large aspect ratios and flat, ribbon like cross sections. As far as the G' and G'' are concerned, they were dependent on the hydrolysis time and the kind of the acid used. The rheology profiles of all the samples were shear thinning. The present nanoscale cellulose fibrils open several challenging options for applications in many industries.

Keywords: Bacterial cellulose, nanocrystals, hydrolysis

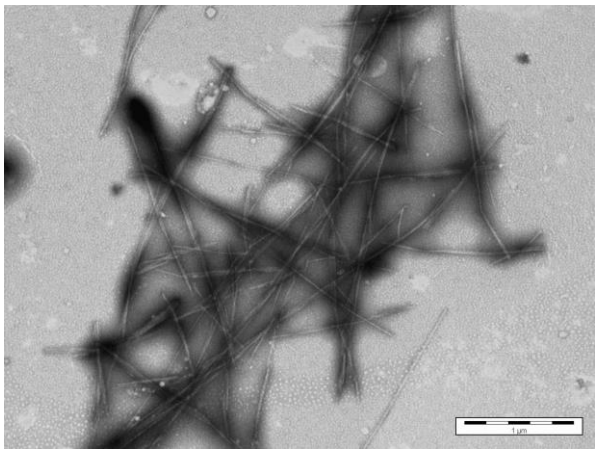

Figure 1: Bacterial cellulose nanocrystals after 72 hour hydrolysis.

Acknowledgements: This work is part of the "Nonastru" project (11ΣΥΝ-2-718), implemented within the National Strategic Reference Framework (NSRF) 2007-2013 and co-financed by National (Greek Ministry - General Secretariat of Research and Technology) and Community Funds (E.U.-European Social Fund)

High Pressure Laminates containing Fluorinated Polyhedral Oligomeric Silsesquioxanes

S. Magina,[1*] D. Evtuguin,[1] I. Portugal,[1] J. Ferra, [2] P. Cruz, [3]
[1]CICECO – Aveiro Institute of Materials, Department of Chemistry, University of Aveiro, Aveiro, Portugal
[2]EuroResinas – Indústrias Químicas SA, Sines, Portugal
[3]SONAE Indústria de Revestimentos (SIR), Maia, Portugal

Abstract: High Pressure Laminates (HPLs) are considered the most versatile and ubiquitous decorative materials used by the furnishing and building industries to produce furniture, countertops, flooring and wall panelling surfaces. They exhibit high durability and special surface properties including chemical, heat, stain and wear resistance. HPLs consist of an assembly of resin-saturated layers of kraft-paper, topped by a single decorative paper layer and in some cases a finishing protective overlay (Figure 1), cured by heat and high-pressure treatments.

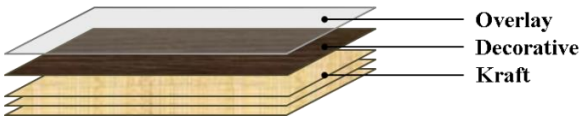

Figure 1. Scheme of a typical assembly of an HPL.

The development of hydrophobic surfaces is achieved by reducing the surface free energy (e.g. by incorporating/grafting a low surface energy material such as a fluorinated compounds) and/or by increasing the surface roughness for instance using compounds such as Polyhedral Oligomeric Silsesquioxanes (POSS). Both strategies can be combined using a fluorinated POSS such as Fluorohexyl-POSS (FH-POSS).
FH-POSS (1H,1H,2H,2H-nonafluorohexyl)$_8$Si$_8$O$_{12}$, was synthesized through the simple, single-step, base-catalyzed condensation of 1H,1H,2H,2H-nonafluorohexyltriethoxysilane in alcoholic media (Tuteja *et al*., 2007; Mabry *et al*., 2008). The fine white powder obtained was characterized by Differential Scanning Calorimetry (DSC), Scanning Electron Microscopy (SEM) and Powder X-Ray Diffraction (XRD).
FH-POSS particles were incorporated (0.25%, 0.50%, 0.75% and 1.0% w/w) into melamine-formadehyde (MF) resin formulations. Decorative and overlay papers were impregnated with the FH-POSS-MF resin formulations in order to provide multiple functionalities to the ensuing HPLs, namely abrasion resistance (due to the robust polyhedric Si-O cages of POSS) and dirt-repellence (particularly, due to the rich fluor-based alkyl chain that lowers the surface free energy of the ensuing HPLs' surfaces).
The HPLs produced using the standard paper (STD) and the FH-POSS-based decorative and overlay papers were tested by proven industrial procedures (EN 438-2:2005). Contact angle (CA) measurements were carried out using three probe liquids (water, formamide and diiodomethane) to assess wettability of the FH-POSS-HPLs and to determine the optimal amount of FH-POSS to use.
FH-POSS-HPLs presented higher CA comparing to the STD-HPL hence higher hydrophobicity, especially when using at least 0.50% of FH-POSS in the MF resin formulation. Higher loads (0.75% and 1.0% of FH-POSS particles in the MF resin) provided better results however the ensuing HPLs have an undesirable wittish appearance. CA measurements made over a two-month period showed that FH-POSS-HPLs became more hydrophobic, suggesting an improvement in dirt-repellence properties that occurs during resin curing.
Additionally, an increase of the abrasion resistance of FH-POSS-HPLs comparing with the STD-HPL was observed, being proportional to the FH-POSS content.

Keywords: high pressure laminates, fluorinated POSS, contact angle, surface free energy, abrasion resistance.

References:
Tuteja, A., Choi, W., Ma, M., Mabry, J. M., Mazzella, S. A., Rutledge, G. C., McKinley, G. H., Cohen, R. E. (2007), Designing Superoleophobic Surfaces, *Science*, 318, 1618-1622.

Mabry, J. M.; Vij, A.; Iacono, S. T.; Viers, B. D. (2008); Fluorinated Polyhedral Oligomeric Silsesquioxanes (F-POSS), *Angew. Chem. Int. Ed*., 47, 4137 –4140.

Acknowledgements: This work was developed in CICECO–Aveiro Institute of Materials and is funded by ERDF Funds through Operational Competitiveness Programme – COMPETE in the frame of the project 2GLAM – FCOMP-01-0124-FEDER-23006. Sandra Magina thanks Margarida Nogueira (from SIR) for experimental support during paper impregnation and HPL production.

Green Synthesis of Gold Nanoparticles by Using *Peltophorum pterocarpum* Flower Extracts

M. Balamurugan,[1] S. Kaushik,[2] S. Saravanan[1]*
[1]Centre for Photonics and Nanotechnology, Sona College of Technology, Salem – 636 005, Tamilnadu, INDIA
[2]The Indian Public School, Senapathipalayam, Erode- 638112, Tamilnadu, INDIA

Abstract: Nanotechnology emerges from the physical, chemical, biological and engineering sciences where novel techniques are being developed to probe and manipulate single atoms and molecules. Among the noble metal nanoparticles, gold has enormous potential applications in various fields (Daniel *et al*., 2004). Currently, we are in the need to develop safe, reliable, clean and eco-friendly methods for the preparation of nanoparticles. The biosynthesis of metal nanoparticles, as an emerging highlight of the intersection of nanotechnology has received increasing attention due to a growing need to develop rapid, clean, non-toxic, simple and environmentally friendly synthetic technologies. The use of plants parts in similar synthesis methodologies is a stimulating prospect that is currently under enormous investigation, having significant potential utilization (Mollick *et. al*., 2014). In this present study, gold nanoparticles (Au NPs) were synthesized by using aqueous chloroauric acid as gold precursor and *Peltophorum pterocarpum* (PP) flower extract both as reducing and capping agent in water solvent.

Keywords: gold nanoparticles, green synthesis.

A 20 mL of PP flower extract was slowly dripped into 1 mM of aqueous chloroauric acid to synthesize the Au NPs at room temperature as well as elevated temperature. After adding the flower extract a visible colour changes were observed as the yellow color solution turn to pale pink, it indicates the formation of Au NPs. The colour changes in the precursor solution is a preliminary identification for formation of metal nanoparticles.

The obtained samples were characterized by using various technique including UV-Visible Spectrophotometer (UV-Vis) and Transmission Electron Microscopy (TEM). Figure 1 shows the UV-Vis spectrum (350-800 nm) of Au NPs before and after mixing the flower extrat. The spectra illustrate the reduction of gold ions and formation nanoparticles. After adding the PP flower extract into gold precursor, the intensity of UV-Vis absorbance increased with time duration, it indicated the formation of Au NPs. The spectrum shows sharp absorption maximum (λ_{max}) around ≈557 nm and confirmed the presence of Au NPs. This peak appeared due to the excitation of electrons in the conduction band of Au NPs induced by the electromagnetic field (Mollick *et. al*., 2014).

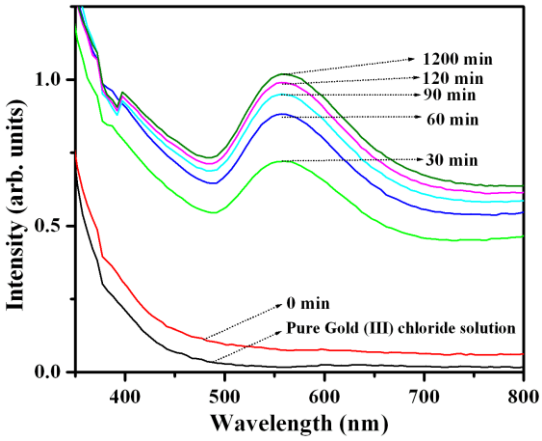

Figure. 1. UV-Vis. spectrum of gold nanoparticles prepared at room temperature.

Figure 2 shows the TEM image of gold nanoparticles prepared at room temperature. The image shows the nanostructure and morphology of Au NPs with good dispersion and the size of the NPs varied from 10-30 nm.

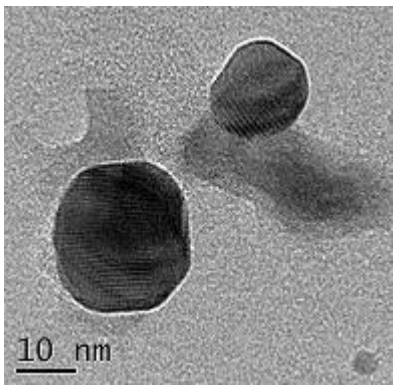

Figure. 2. TEM image of gold nanoparticles prepared at room temperature.

References:

Daniel, M.C., Astruc. D. (2004) Gold Nanoparticles: Assembly, Supramolecular Chemistry, Quantum-Size-Related Properties, and Applications toward Biology, Catalysis, and Nanotechnology, *Chem. Rev.* 104, 293-346.

Mollick, M.M.R., Bhowmick, B., Mondal, D., Maity, D., Rana, D., Dash, S.K., Chattopadhyay, S., Roy, S., Sarkar, J., Acharya, K., Chakrabortye, M., Chattopadhyay, D. (2014) Anticancer (in vitro) and antimicrobial effect of gold nanoparticles synthesized using *Abelmoschus esculentus* (L.) pulp extract via a green route, *RSC Adv.*, 4, 37838–37848.

STABILIZATION METAL NANOPARTICLES BY CROWN COMPOUNDS WITH AMINE AND HYDROXYL GROUPS IN MACROCYCLIC RING AND STUDING THEIR PROPERTIES.

A.L.Shabanov[1], Z.O.Gakhramanova[1], L.Z.Vezirova[1], A.M.Maharramov[2], M.A.Ramazanov[2], U.A.Hasanova[2], F.V.Hajiyeva[2]

[1]*Azerbaijan State Oil Academy, Department*

[2]*Baku State University, Department Chemical Physics of Nanomaterials, Nanoresearch Laboratory, Zahid Khalilov Str. 23, Baku, Azerbaijan*

nanomaterials@bsu.az , mamed_r50@mail.ru

Abstract. In this work presented the results of researches on stabilization of metal nanoparticles by crown compounds with amine and hydroxyl groups in macrocyclic ring and studying their properties.

Synthesis and studies of functional substituted crown ethers is a matter of great scientific and practical interest. These macroheterocyclic compounds can reveal biological activity due to unique structural peculiarities. Nitrogen containing crown ethers are attractive research objects because its possible application in boundary with organic chemistry fields.

Introduction of amine and hydroxyl groups in macrocyclic ring of crown ethers influences on supramolecular properties of synthesized compounds. The results of carried researches show that the presence of two amine and one hydroxyl groups in macrocyclic ring leads to self-assembling of crown compounds in such a way that it becomes able to include the metal and metal oxides nanoparticles in its cavity. The synthesized crown ether was used as stabilizer of Fe_3O_4, Fe^0, Ag^0 nanopatrticles. It is assumed that the presence of these functional groups in macrocyclic ring allow crown ether molecule to pass from two-dimensional structure (2D) to three-dimensional structure. So, it is supposed to be the existing multi-central non-valence interactions between crown ethers molecules and metal nanoparticles that lead to formation of supramolecular assembly.

Structure of prepared compounds have been analysed by elemental analysis, IR, NMR and mass-spectroscopy methods of analysis. Prepared nanostructures crown@Fe_3O_4, crown@Fe^0, crown@Ag^0 have been studied by scanning electron SEM, atomic force microscopy AFM, X-ray diffraction methods of analysis. On the basis of carried out analytical researches were found the size of metal and metal oxides nanoparticles that stabilised by macrocycle is in 6-17 nm interval. The quantity of loading of nanoparticles was determined on the basis of Lambert-Buger-Ber law as well as atom absorption spectroscopy method of analysis. It was found that the results of both analysis methods are correlated very well.

Key words: crown-compounds, supramolecular chemistry, diazacrown ethers, hydroxyl containing crown ether, metal nanoparticles.

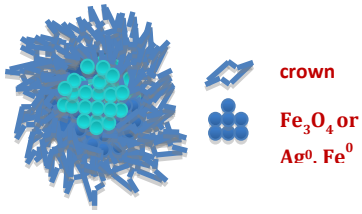

Nanoparticle model CROWN@Fe_3O_4 and CROWN@Fe^0

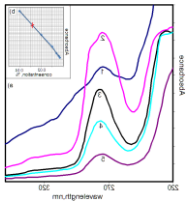

UV spectra of CROWN@Fe_3O_4

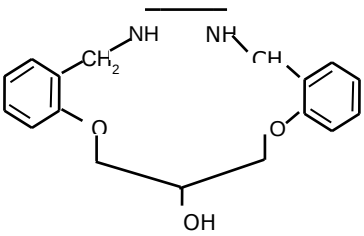

References:

1. Jean-Marie Lehn **Supramolecular Chemistry:Concepts and Perspectives** :19 MAY 2006 ISBN: 9783527293124 ISBN: 9783527607433

2. Shabanov A.L. Synthesis and perspectives of functional substituted crown ethers // Rus. Chem. J. (J. Of Rus.. Chem. Soc. D.I. Mendeleyev). 1991. T 36. № 4. C. 456 - 467.

3. Etwood J.V., Etwood J.L. Supramolecular Chemistry. M.: «Academkniga» 2007. P. 480

Novel Fractal Metamaterial subwavelength structure for sensors application

Y Trabelsi[1], H Alkorre[2], J Stiens[3], M Kanzari[4] and R Vouncks[5]

[1] *Univesity of Tunis ELManar, National Engineering School of Tunisia (ENIT), Tunisia*
2,3,5 Vrije Universiteit Brussel, Belgium, Pleinlaan 2 ,1050 Brussel.

Abstract:

The fractal metamaterial configurations , operating at the millimeter-wave scale are studied , in terms of design, fabrication, and characterization.
We report our work conducted on the design, simulation and -fabrication of microwave sensors based on a fractal split-ring resonator (FSRR) structure operating at 140 GHz. Furthermore, we attainted a wide and of high transmittance left-handed band, as was established by transmission measurements and corresponding simulations.
We observed both numerically and experimentally at around 140 GHz a tapered frequency band for which the fractal SRR metamaterial was High resonant frequency and had a negative permittivity and permeability. The effect of different geometrical restrictions and the order of the fractal curve on the performances are investigated.
We analyzed the transmission band with respect to fractal order of two configuration connected and disconnected metals form witch composed the considered metamaterials slab at the normal incident propagation direction.

Keywords :
metamaterial; sensing ; Thin-film sensor; Split Ring resonators, Fractal SRR .

References :

H. Tao, N. I. Landy, C. M. Bingham, X. Zhang, R. D. Averitt, and W. J. Padilla, "A metamaterial absorber for the terahertz regime: design, fabrication and characterization," Opt. Express 16, 7181 ,2008.

J. F. O'Hara, R. Singh, I. Brener, E. Smirnova, J. Han, A. J. Taylor, and W. Zhang, "Thin-film sensing with planar terahertz metamaterials: sensitivity and limitations," *Opt. Express 16, 1786,2008.*

C. Debus and P. Haring Bolivar, "Frequency selective surfaces for high sensitivity terahertz sensing," *Appl.Phys. Lett. 91, 184102 ,2007.*

A. K. Azad, J. Dai, and W. Zhang, "Transmission properties of terahertz pulses through subwavelength double split-ring resonators", *Optics Letters, Vol. 31, No. 5, pp. 634-636, 2006.*
T. Koschny and M. Kafesaki. , " Effective Medium Theory of Left- Handed Materials". *Physical Review Letters, Vol. 93, No. 10, pp. 1-4, 2004.*

Combined Mechanical Disordering – Reactive Synthesis, Possible Method of Bulk Nanocrystalline Intermetallics Obtaining

R.L. Orban[1], A. Lawley[2], M. Orban[1]
[1]Technical University of Cluj-Napoca, Romania
[2]Drexel University, Philadelphia, USA

Abstract: The vast potential of intermetallics applications in the modern technique, arising from their known very attractive properties, became obvious [1].Their elaboration is based on reaction synthesis from components, e.g. in ExoMelt process [2]. However, even if, after casting in ingots, at elevated temperatures they exhibit a certain ductility, allowing processing by hot working. e.g. to obtain billets, tubes, sheets and even forgings, their further machining into final products is nearly impossible due to the high brightness and low fracture toughness at ambient temperature, drastically limiting their applications [1]. These are determined, as it is known, by their low symmetry of crystal structure (e.g. with only three slip systems in NiAl [1], which prohibits the operation of at least five independent slip systems required for plastic flow [3].

A promising way to overcome these drawbacks of intermetallics is their obtaining in a nanocrystalline state. The most facile way for this purpose seems to be Mechanical Alloying applied to the reactive component mixture (MA), continued after the compound synthesis (the crossing point of curves a and b in Fig. 1), with Mechanical Disordering (MD)[4]. But this leads to their obtaining as fine nanocrystalline powder. Several methods have been proposed to obtain bulk nanocrystalline materials from this powder (e.g. spark plasma sintering, double sintering etc.), without of their consecration [5].

In this paper is proposed a new possible method of bulk nanocrystalline intermetallics obtaining, in two stages: i) controlled MA, applied to the stoichiometric elemental powdered component mixture – determining their strong cold working and energetic state increasing - conducted only up to the

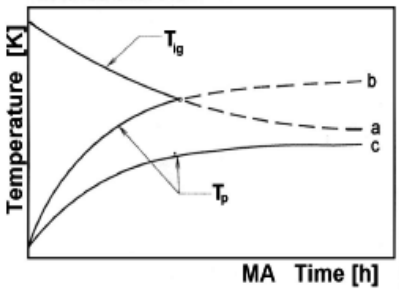

Fig. 1.

particle crystal structure disordering and its transformation into a nanocrystalline one, without to be reached the ignition temperature, T_{ig}, of compound synthesis reaction (before a-b crossing point, Fig. 1); ii) Compound reactive synthesis from the as obtained nanocrystalline powder mixture, combined with its consolidation. It is expected that, due to the high enenergetic state of nanocrystalline powder and intimate mixture of components, both synthesis and consolidation (e.g. under an appropriate pressure) are possible in solid state, by diffusion [6], at a low enough temperature to preserve the nanocrystalline structure in the obtained bulk material.

The method has been successfully applied to the obtaining of bulk nanocrystalline NiAl (Fig. 2).

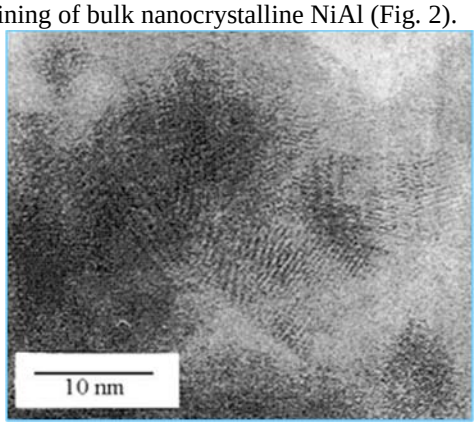

Fig. 2.

Its conducting conditions will be extensively presented in the proposed paper.

Keywords: Intermetllics, Mechanical Alloying, Reactive synthesis, Bulk nanocrystalline NiAl.

Fig. 1. Variation of the Ignition Temperature of Synthesis Reaction and of Particle one, vs. MA time.
Fig. 2. HRTEM image of the obtained bulk NiAl.

References:

[1] Sauthoff, G. Definition of Intermetallics & General Considerations. In *Intermetallics*, John Wiley & Sons, 2008, p. 1-13.
[2] Deevi, S.C.; Sikk, V.K., Exo-Melt^{TM} process for melting and casting intermetallics. In *Intermetallics*, Vol. 5 , Iss. 1, 1997, p. 17–27.
[3] Reed-Hill, R.E. Dislocation & Plastic Deform. In *Physical Metallurgy Principles*, 2008, p. 119-157.
[4] Orban, R.L. New Research Directions in Powder Metallurgy. In *Romanian Reports in Physics*, Vol. 56, No. 3, 2004, p. 557-570.
[5] German R.M. *Powder Metallurgy and Particulate Materials Processing: The Processes, Materials, Products, Properties and Applications.*. MPIF, Princeton, New Jersey, USA, 2005.
[6] Ferro, R.; Saccone, A. Direct synthesis of intermetallic phases/Solid-state synthjesis. In *Intermetallic Chemistry*, Elsevier, 2008, p. 566-572.

Effect of blending ratio of polymer layer on structural properties of polymer-coated mesoporous silica nanoparticles

Ş. Ünal, B. Özbek
Yildiz Technical University, Department of Chemical Engineering,
Davutpasa Campus, 34210, Esenler/Istanbul, Turkey;
tel. +90 212 383 4761, fax: +90 212 383 4725;
e-mail: suunal@yildiz.edu.tr.

Abstract: Mesoporous silica nanoparticles (MSNs) have great potential as nanocarrier for biomolecules because of its biocompatibility, low toxicity, large surface area, high porosity, modifiable pore diameter, and adjustable surface properties[1]. Chitosan (CS) is non-toxic, user-friendly, abundant and widely-used inexpensive polysaccharide. The amino and hydroxyl groups of chitosan provide great potential as adsorbent of protein and heavy metal ion, as catalytic matrix for enzyme immobilization and as carrier for drug loading processes[2]. Chitosan has a highly hydrophilic and a swelling structure in aqueous media which causes to lose its mechanical strength because of its high water content[3].

Blending PAA and CS provides increased mechanical strength and pH stability via eliminating the structural disadvantage of chitosan[4]. Linear polymers (such poly(acrylic acid) (PAA) chain were grafted onto the surface of MSNs) show pH-dependent behaviour which can provide increased enzyme reuse and also the usage as biosensor[5].

In the present study, chitosan/poly(acrylic acid) shell was coated on mesoporous silica nanoparticle cores through polymerization. First, MSNs were successfully prepared via sol-gel method1. Subsequently, acrylic acid (AA) monomers were polymerized on the MSNs. The effect of the ratio between the amounts of CS and AA to the physicochemical properties of particles was investigated through necessary characterization methods.

Keywords: Silica nanoparticle; chitosan; polymer; poly(acrylic acid); coatings

References:

1. Peng et al. (2013), “A pH-responsive nano-carrier with mesoporous silica nanoparticles cores and poly(acrylic acid) shell-layers: Fabrication, characterization and properties for controlled release of salidroside” International Journal of Pharmaceutics 446: 153–159.

2. Zhao H., Xu J., Lan W., Wang T., Luo G., (2013), “The Microfluidic production of porous chitosan/silica hybrid microspheres and its Cu(II) adsorption performance”, Chemical Engineering Journal 229: 82–89.

3. Lei Z., Bi S., (2007), “The silica-coated chitosan particle from a layer-by-layer approach for pectinase immobilization “, Enzyme and Microbial Technology 40: 1442-1447.

4. Dai J., Yan H., Yang H., Cheng R. J. Dai et al., (2010), “Simple method for preparation of chitosan/poly(acrylic acid) blending hydrogel beads and adsorption of copper(II) from aqueous solutions”, Chemical Engineering Journal 165: 240–249.

5. Tang H., Guoa J., Sun Y., Chang B., Ren Q, Yang W., (2011), “Facile synthesis of pH sensitive polymer-coated mesoporous silica nanoparticles and their application in drug delivery”, International Journal of Pharmaceutics 421, 388–396.

Targetting and Applications of Magnetic Nanoparticles

P. Taparia,[1,*] S. Jindal,[2]
[1]Department of Metallurgy and Material Sciences, Indian Institute of Technology, Roorkee, India
[2] Department of Biotechnology, Indian Institute of Technology, Roorkee, India

Abstract: Recent advances in targeting and application of "intelligent" Magnetic Nanoparticles (MNPs), which have led to widespread experimentation due to their multi-modal capabilities, have been reviewed. Particularly, application of MNPs is highly promising for the treatment of fatal diseases such as Cancer. Dual usage of MNPs to perform drug delivery and optical imaging has been studied in vivo and in vitro. Further, the role of MNPs in Positron Emission Tomography (PET) and Magnetic Hyperthermia will be discussed in detail. Therapeutic potential of 'intelligent' MNPs having a suitable recognition layer and a therapeutic load, is high; but their development is challenging. Polymer, Protein and Silane based recognition layers are being examined to solve this problem. Moreover, these core/shell structures of MNPs have the advantages of good dispersion, high stability against oxidation, favorable specificity and appreciable amount of drug that can be loaded to the shell after coating. Also, recent literature has shown that reliance solely on the Enhanced Permeability and Retention (EPR) effect is insufficient for nanoparticles to penetrate the tumor intersitium, as a result, the use of active and intelligent targeting agents has become increasingly important. Here we also review some of the drawbacks associated with the use of MNPs for drug delivery.

Keywords: Positron Emission Tomography, Magnetic Hyperthermia, Recognition Layers, shell coating, Enhanced Permeability and Retention, targeting agents, drug delivery, biomedical applications.

References:

Chomoucka, J., Drbohlavova, J., Huska, D., Adam, V., Kizek, R., Hubalek, J. (2010) Magnetic nanoparticles and targeted drug delivering, *Pharmacological Research*, *62*, 144-149.

Spencer, D. S., Puranik, A. S., Peppas, N. A. (2015) Intelligent nanoparticles for advanced drug delivery in cancer treatment, *Current Opinion in Chemical Engineering*, 7, 84-92.

$In_xGa_{1-x}N$/GaN QDs by coaxial growth on non-polar n-GaN NW

Ji Hyeon Park, Jae Kwan Sim, Dae Young Um, Taek Soo Jang, Da som Lee and Cheul Ro Lee*
Semiconductor Materials Process Laboratory, School of Advanced Materials Engineering, Engineering College, Research Center for Advanced Materials Development (RCAMD), Chonbuk National University, Baekje-daero 567, Jeonju 561-756, Republic of Korea

Abstract: Nanowires based devices are among those techniques and have drawn much attention in the last few years for improving device performances.
In This abstract demonstrates for the merits of an immediate InAlGaN capping layer over self-assembled $In_xGa_{1-x}N$/GaN GaN quantum dots (QDs) coaxially grown on the m-plane and r-plane of n-GaN nanowires on Si (111) substrate using metal organic chemical vapor deposition. For comparative analysis, we prepared $In_xGa_{1-x}N$/GaN QD samples both with and without quaternary capping. Figure 1 shows the UHR-SEM image of the proposed structure with $In_xGa_{1-x}N$ QDs on a single n-GaN NW when quaternary capping was applied over dots in the active region. InAlGaN capping layer acted as a strain-driven phase separation alloy. Inhomogeneous surface strain over the dots helped this quaternary alloy in forming an indium concentration gradient over $In_xGa_{1-x}N$ QDs and thus, indium out-diffusion from the dots was reduced. Quaternary alloy capped samples exhibited vertically stacked, highly dense, pyramidal $In_xGa_{1-x}N$/GaN QDs of improved carrier confinement grown as the active region on n-GaN NWs. In contrast, the nonexistence of InAlGaN capping over InGaN/GaN QDs caused deformation of the dots due to In-Ga inter-diffusion between the dots and the GaN barrier layer. Figure 2 shows the temperature dependent PL study was carried out for the sample composed of quaternary alloy capped $In_xGa_{1-x}N$ QDs on n-GaN NWs. This coaxially fabricated $In_xGa_{1-x}N$/GaN QDs on defect free n-GaN nanowires have various excellent characteristics and can be widely applicable to new optoelectronics semiconductor devices.

Key Words: InGaN quantum dots, GaN nanowire, InAlGaN capping, inhomogeneous strain, metal organic chemical vapor deposition, blue light emitting diodes

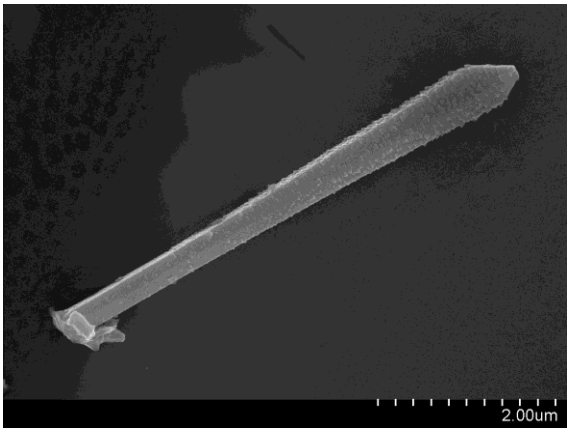

Figure 1: Ultra-high resolution SEM (UHR-SEM) image of a single n-GaN NW composed of InAlGaN capped two layered active $In_xGa_{1-x}N$ QDs inside.

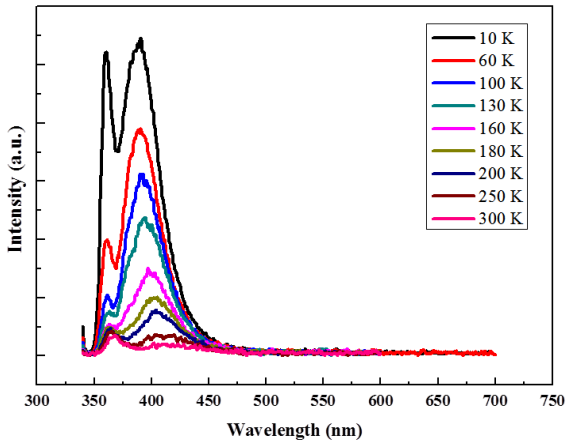

Figure 2: Temperature dependent PL study was carried out for the sample composed of quaternary alloy capped $In_xGa_{1-x}N$ QDs on n-GaN NWs.

References:

A. M. Morales, C. M. Lieber, (1998) *Science*, **279**, 208-211.
Z. Zhong, F. Qian, D. Wang, C. M. Lieber (2003) *Nano Lett*, **3**, 343-346.
O. L. Muskens, S. L. Diedenhofen, M. H. M. van Weert, M. T. Borgström, E. P. A. M. Bakkers, J. G. Rivas,(2008) *Adv. Funct. Mater*, **18**, 1039-1046.

The Effect Of Assembly Conditions and Nanoparticle Conditions on Size, Morphology and Polydispersity Of Magnetic Nanoparticle Clusters

Sarah M. Martyn,[1] Dr. Dermot F. Brougham[1]
[1]School of Chemical Sciences, Dublin City University, Glasnevin, Dublin 9, Ireland

Abstract: Colloidally stable superparamagnetic iron oxide nanoparticles (SPIONs) are well known to be excellent contrast agents in MRI applications[1,2]. Larger particles are preferable; however the effectiveness of SPIONs as contrast agents is limited by their size, as above a threshold of ~20 nm, ferromagnetic properties emerge, causing irreversible aggregation which can lead to the formation of blockages in the vasculature of patients.

One potential alternative is the formation of controlled aggregates of the SPIONs into polymer stabilized assemblies (NPCs)[3]. These assemblies retain the superparamagnetic properties of the individual particles while increasing the effectiveness of the system as a contrast medium. In this study the effect of NP shape and size, polymer type and other assembly conditions, on the formation of NPCs was investigated. NPC properties were analyzed by transmission electron microscopy (TEM), dynamic light scattering (DLS), hyperthermia and field cycling nuclear magnetic relaxation spectroscopy (FFC-NMR). These analyses combined have allowed us to determine the effect of cluster size and morphology on the magnetic properties of the NPCs generated.

On preparation of colloidally stable NPCs signal surpression was observed in sample relaxivity, a shift in the frequency at which maximum relaxivity was also observed, consistent with the presence of larger particles. It should be noted that these observations were more profound in the case of faceted nanoparticles. The ratio of R_2/R_1 at 60 MHz was also found to increase dramatically on the formation of clusters indicating that NPCs are potentially useful as T_2 weighted MRI Contrast agents.

Keywords: Nanoparticles, Iron Oxide Nanoparticle Assemblies, size-control, Nuclear Resonance Dispersion Relaxometry, superparamagnetism, MRI, contrast agents, biomedical applications.

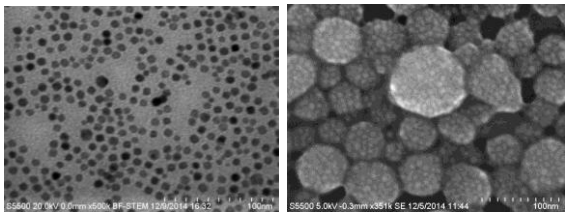

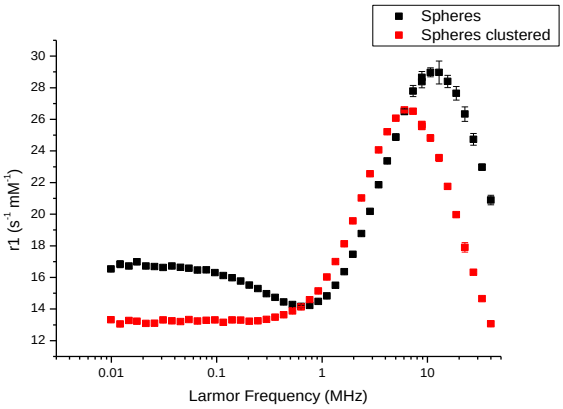

Figure 1: Iron Oxide nanoparticles (top-left) and Nanoparticle Clusters prepared by polymer mediated assembly (top-right), (below) Nuclear Magnetic Relaxation Dispersion Curve demonstrating a shift in magnetic response as a result of the clustering experiment

References:

1 Pankhurst, Q.A. , Connolly, J., Jones, S.K., Dobson, J.. (2003). Applications of magnetic nanoparticles in biomedicine. *Journal of Physics D: Applied Physics*. 36 (13), R167-R181.

2 Babes, L. 'Synthesis Of Iron Oxide Nanoparticles Used As MRI Contrast Agents: A Parametric Study'. *Journal of Colloid and Interface Science* 212.2 (1999): 474-482. Web. 20 Apr. 2015.

3 Stolarczyk, J.K., Ghosh, S., Brougham, D.F.. (2009). Controlled growth of nanoparticle clusters through competitive stabilizer desorption. *Angewandte Chemie International Edition*. 48 (1), 175-178.

Polyurethane/GO Nanocomposites and Vapor Barrier properties

Eunsung Yoo,[1,2,*] Kwangbo Shim,[1,2] Hoon Huh[1]
[1]Korea institute of industrial technology, Cheonan, Korea
[2] Hanyang University, Seoul, Korea

Abstract:

Polyurethane(PU) has been used in various applications such as fibers, coatings, adhesives and biomimetic materials. Despite of good deformability, low stiffness and tensile strength can limit its use in structural applications, especially for PU with low hard block content. Water vapor and gas permeability can be another drawback. The weak mechanical and gas barrier properties can be reinforced by the elastomeric matrix with rigid, impermeable nanofillers.

The graphene with two dimensional structure(2D) has a unique elctron mobilty (> 20,00 cm2/Vs), very high thermal conductivty (480-530 W/mk) and excelnt mechanical properties (Young's moduls : ~1 TPa, Ultimate strength :~130GPa). It has ben considerd as a promising functional filler. Adding highly exfoliated carbon layers can significantly change a mechanical and electrical properties of polymers at extremely small loading. Unlike carbon nanotubes that can provide similar mechanical and electrical benefits, these impermeable two-dimensional sheets can reduce gas permeability of host membranes

In this study, we focused on preparation, morphology, and properties of PU/GO nanocomposites. Solvent blending was also used to prepare GO and isocyanate treated GO composites. We observed mechanical, and water vapor barrier properties of PU by addition GO.

Keywords: polyurethane, water vapor barrier, PU/graphene nanocomposites, isocyanate treated GO .

References:

Woods, G. The ICI Polyurethanes Book; Wiley: New York, 1990.

Lamda, N. M. K.; Woodhouse, K. A.; Cooper, S. L. Polyurethanesin Biomedical Applications; CRC Press: Boca Raton, FL, 1998.

Liff, S. M.; Kumar, N.; McKinley, G. H. Nat. Mater. 2007, 6,76–83.

Koerner, H.; Price, G.; Pearce, N. A.; Alexander, M.; Vaia, R. A. Nat. Mater. 2004, 3, 115–120.

Osman, M. A.; Mittal, V.; Morbidelli, M.; Suter, U. W. Macro-olecules 2003, 36, 9851–9858

Lee, C.; Wei, X.; Kysar, J. W.; Hone, J. Science 2008, 321, 385–388.

Novoselov, K. S.; Geim, A. K.; Morozov, S. V.; Jiang, D.; Zhang, Y.; Dubonos, S. V.; Grigorieva, I. V.; Firsov, A. A. Science 2004, 306, 666–669.

Stankovich, S.; Dikin, D. A.; Dommett, G. H. B.; Kohlhaas, K. M.;Zimney, E. J.; Stach, E. A.; Piner, R. D.; Nguyen, S. T.; Ruoff, R. S. Nature 2006, 442, 282–286.

Ramanathan, T.; Abdala, A. A.; Stankovich, S.; Dikin, D. A.; Herrera-Alonso, M.; Piner, R. D.; Adamson, D. H.; Schniepp, H. C.; Chen, X.; Ruoff, R. S.; Nguyen, S. T.; Aksay, I. A.; Prud'- Homme, R. K.; Brinson, L. C. Nat. Nanotechnol. 2008, 3, 327–331.

Kim, H.; Macosko, C. W. Macromolecules 2008, 41, 3317–3327.

Kim, H.; Macosko, C. W. Polymer 2009, 50, 3797–3809.

Fabrication of Electrospun Polyvinyl Alcohol / Polysaccharide Composite Nanofibers and their Prebiotic and Antibacterial Activities

Walaa Wahbi,[1,2] Rania Siam, [1,3] Wael Mamdouh[1,2]*
[1]Yousef Jameel Science and Technology Research Center (YJSTRC), School of Sciences and Engineering (SSE), The American University in Cairo (AUC), AUC Avenue, P.O. Box 74, New Cairo 11835, Egypt.
[2]Department of Chemistry, School of Sciences and Engineering (SSE), The American University in Cairo (AUC), AUC Avenue, P.O. Box 74, New Cairo 11835, Egypt.
[3]Department of Biology and Biotechnology Graduate Program, School of Sciences and Engineering (SSE), The American University in Cairo (AUC), AUC Avenue, P.O. Box 74, New Cairo 11835, Egypt

Abstract: In an attempt to develop novel natural nanofibers with enhanced prebiotic and antimicrobial activities, polymer composites and nanomaterials play a vital role and exhibit superior properties. Among the different types of nanomaterials, nanofibers have attracted a lot of attention in various fields due to their large surface area per unit mass and advanced mechanical performance. Nanofibers are potential candidates to be used in many fields such as drug delivery systems, nano-sensors, filtration media, and medical applications, etc (Ramakrishna *et al*; 2006). Electrospinning technique was used and the experimental parameters were optimized to fabricate uniform electrospun polysaccharide composite nanofibers (CNFs) to be tested for their prebiotic and antimicrobial activities. The aqueous solution of polysaccharides could not be directly electrospun into nanofibers. Therefore, electrospinning was aided by mixing polysaccharides with polyvinyl alcohol (PVA)(Wang *et al*; 2011).We report the influence of different parameters (concentration, applied voltage and solution flow rate) on the composite nanofibers fabrication. The most uniform nanofibers were obtained were tested for their prebiotic activity with *Lactobacillus sp.* and antibacterial activity with *E. coli* and *S. aureus* bacteria. The fabricated composite nanofibers showed enhanced prebiotic and antibacterial activity compared to the original solutions. These results open new avenues for fabricating prebiotic and antibacterial products from natural materials with superior biomedical activities.

Keywords: electrospinning, nanofibers, prebiotic, polysaccharides, natural materials.

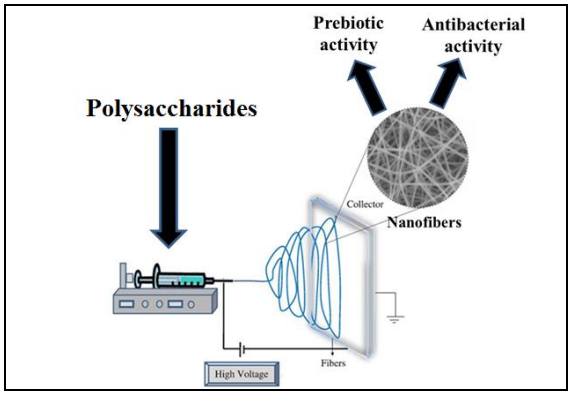

Figure 1: Figure illustrating the study and representing the results: Fabrication of natural composite nanofibers from using polysaccharides and investigating their prebiotic and antibacterial activities.

References:

Ramakrishna, S.; Fujihara, K.; Teo, W.; Yong, T.; Ma, Z.; and Ramaseshan, R(2006). Electrospun nanofibers: solving global issues, *Mater. today* , *9*, 40–50.

Wang, H.; Wang, W.; Jiang, S.; Zhai, L.; Jiang. Q., (2011), Poly(vinyl alcohol)/Oxidized Starch Fibres via Electrospinning Technique: Fabrication and Characterization, *Iran. Polym. J.*, *20*, 551–558.

Zanin, M. H. A.; Cerize, N. N. P.; A. M. de Oliveira(2011). Production of Nanofibers by Electrospinning Technology: Overview and Application in Cosmetics. *Nanocosmetics and Nanomedicines*; pp. 311–332.

Efficiency improvement in Dye Sensidized Solar Cells by Plasmonic effect of green synthesized Silver Nanoparticles

S.Saravanan,[1]* R.Kato,[2] M.Balamurugan,[1] S.Kaushik,[3] T.Soga[2]
[1]Centre for Photonics and Nanotechnology, Sona College of Technology, Salem – 636005, Tamilnadu, INDIA
[2] Department of Frontier Materials, Nagoya Institute of Technology, Nagoya 466-8555, JAPAN
[3]The Indian Public School, Senapathipalayam, Erode- 638112, Tamilnadu, INDIA

Abstract: Eco-friendly green synthesis with plant extracts plays a very important role in nanotechnology, without any harmful chemicals. In this report, the synthesis of uniform silver nanoparticles (Ag NPs) was developed by treating silver ions with *Peltophorum pterocarpum* (PP) extract at room temperature and elevated temperatures. The X-ray diffraction analysis confirmed that the synthesized Ag NPs are single crystallines. Ag NPs, with an approximate size of 15–30 nm were observed in the transmission electron microscopy (TEM) image. A plasmonic effect of silver nanoparticles (Ag NPs) in dye-sensitized solar cells (DSSCs) is studied.

Introduction: Synthesis of NPs is presently an important area of research, searching for an eco-friendly manner and green materials for current science. The biological method has emerged as a green alternative, for it is environment-friendly, cost-effective, and easily scaled-up. In the last few years a concept of surface plasmon resonance has been introduced to the DSSC employing noble metals of Ag (Ishikawa *et.al*., 2004) or Au.

Keywords: silver nanoparticles, green synthesis, plasmonic effect, dye sensidized solar cell.

Synthesis of Silver Nanoparticles (Ag NPs): Fresh 3 grams of PP flowers were washed and immersed in 300 mL boiling distilled water for 30 minutes. The cooled filtrate obtained was stored at 4°C for further use. The 100 mL of 0.01 M $AgNO_3$ aqueous solution was reacted with 20 mL drops of the obtained extract solutions in a flask with stirring for 30 minutes and then continued stirring for 1hour.

Characterization of Ag NPs: Phase formation of the synthesized NPs was characterized by X-ray diffraction. Four main characteristic diffraction peaks for Ag were observed at 2θ=38.1, 44.3, 64.7, 77.7, which correspond to the (111), (200), (220), and (311). Figure 1 (a) and (b) depicts the TEM and SAED pictures of Ag NPs respectively. As shown in the figure the morphology of the AgNP was spherical with an average size of 15-30 nm.

DSSC preparation: The TiO_2 (P-25) layers without/with Ag NPs (1, 2 and 3 wt%) have been immersed in an ethanol solution of a Ruthenium complex based dye for 18hrs. DSSCs were fabricated by attaching a Pt glass counter electrode to photoanode, by inserting polymer film (50 μm) between two electrodes, and injecting the iodide based electrolyte into the space between two electrodes.

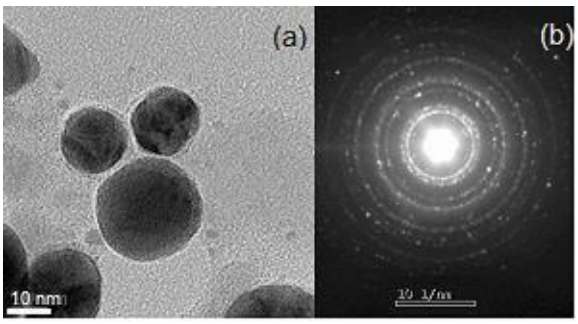

Figure 1. (a) TEM and (b) SAED picture of green synthesized silver Nanoparticles.

Results and Discussions: Short-circuit current density (Jsc) and conversion efficiency are shown in Figure 2 for non doped and 1, 2 and 3 wt% of Ag NPs doped DSSCs. As shown in the figure the efficiency has decreased for 1 wt% and for 2 wt% of Ag doped the efficencey increased from 2.83% to 3.62% (nearly 28% when compared to the non doped sample). Also the Jsc has increased for 2, 3 wt% of Ag doped sample. The FF is also increased nearly 7% for 2 wt% compared to the non doped sample.

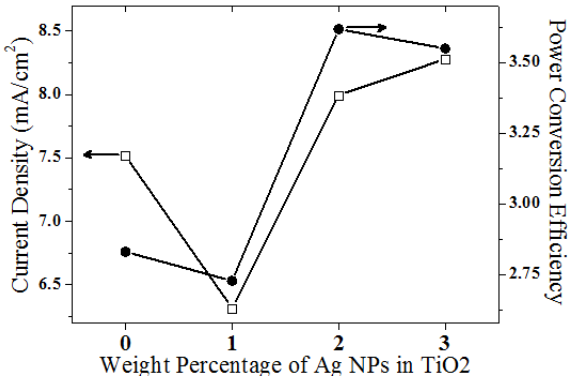

Figure 2. The short circuit curren density and power conversion efficiency against the Ag doping.

Conclusions: In this study, we developed a simple, green, and efficient route to synthesize Ag NPs by treating silver ions with PP flower. DSSCs were fabricated with different doping of green synthesized Ag NPs in TiO_2. The 2 wt% of Ag doping in TiO_2 increased the efficiency around 28%.

Reference:

Ishikawa, K. Wen, C.-J. Yamada, K. and Okubo, T. (2004), The photocurrent of dye-sensitized solar cells enhanced by the surface plasmon resonance, *Journal of Chemical Engineering of Japan*, 37, 645–649.

Obtention of Spirulina nanoparticles by mechanical milling

Neri-Torres, E.E.[1*], Chanona-Pérez, J.J.[1], Cárdenas-Pérez, S.[1], Marín-Bustamante, M.Q.[1], Cásarez-Santiago, R.G.[1], Calderón-Benavides, H.[2], Chamorro-Cevallos, G.[1], Suárez-Najera E.[1]
[1]Escuela Nacional de Ciencias Biológicas-Instituto Politécnico Nacional, Prolongación de Carpio y Plan de Ayala s/n, Col. Santo Tomas C.P. 11340 México, D.F.
[2]Escuela Superior de Física y Matemáticas-Instituto Politécnico Nacional. Av. Instituto Politécnico Nacional Edificio 9, Unidad Profesional Adolfo López Mateos, Zacatenco, C.P. 07738, México, D. F.

Abstract: Nanotechnology has taken great importance in the food industry for create different functional and nutraceutical foodstuffs, since the nanoscale material construction cause changes on the bioactive potential of biological due the material becomes thousand times more small that the original. The target is to reach particles with nanometer sizes for improve the functional and nutraceutical potential of the proteins, amino acids, essential fatty acids, minerals, sulfolipids, glycolipids and phycobiliprteins contained in Spirulina (Belay, 2008).
The raw material was aspersion-dried powder of *Arthrospira maxima* (Spirulina), which had an initial size of 6±5 µm. A Spex mill was used according to reported by Lu & Lay (1998) in a kinetic experimental design which was applied to obtain the nanoparticles. The work was performed in four times (1, 2, 3 and 4 hours), due to the Spirulina may be considered how a soft material. After the milling, the powder was collected and stored in controlled environment. Atomic force microscopy (AFM, Multimode V, Bruker, USA) was used to measure the particle size by image analysis (Figure 1A)take into account the ISO 13322 (p=0.1 and geometric standard deviation "GSC" of 1.15) . The results showed that two hours of milling was the optimal condition for obtain a 75% of Spirulina nanoparticles below of 100 nm and an average size of 91±3.5 nm. In the case of milling times of 3h and 4h the increase of particle size could be due to a heating of samples caused by an agglomeration phenomena into the powders. The characteristic mean size was also calculated with images obtained with scanning electron microscopy (SEM, JSM-7800F, Jeol, USA) and the number mean size was calculated how is described in the standard ISO 13322 (p=0.05 and GSC of 1.15). To determine the measurement was performed an image analysis with imageJ (1.48v). The results obtained by means of SEM were agreeing with the particle size distribution obtained by AFM (Figure 1B). On the other hand, the transmission electron microscopy (TEM, JEM-2100, Jeol, US) was used to corroborate the size particle in the time of 2 hours of milling reached the nanoscale. In the Figure 1C there are some alignment patterns that could be due to a linear arrangement of polymeric structure of the carbohydrates contained in the Spirulina. An important parameter of the powders material is the repose angle; the results showed that the repose angle was increased in relation to decrease of particle size. The values of repose angle at 1h and 2h of milling were showed significant difference with the reference and the milling samples at 3h and 4h also have significant difference with the reference.
The smallest values of particle size have concordance with the greatest values of repose angle due to that the samples were very cohesive. In the case of crystallinity index values, these decreased when the milling time was increased.
Then with these findings we proceeded to carry out a proof of X-rays spectroscopy (DRX, Rigaku miniflex 600, US). To obtain the crystallinity index was applied the method of Segal. Those data also observed a tendency to decrease of crystallinity index, however, it is not evident a large change because is possible that the material into the mill present molecular rearrangement by the contaier's friction force.
In conclusion was possible to obtain nanoparticles with a mean particle size of 91±3.5 with only two hours of milling. Thus the Spex mill is simple technology to obtain nanoparticles due that it requires short times of milling and low consume of energy. It was possible to observe relationships between the particles size, crystallinity index and repose angle.
Keywords: Spirulina, nanoparticles, electron microscopy

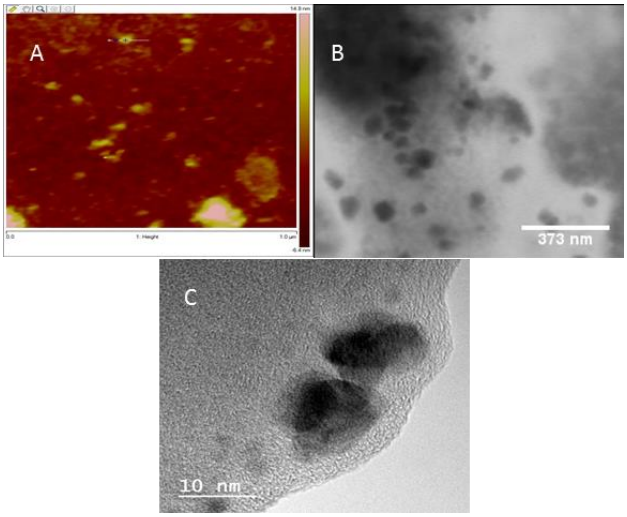

Figure 1. Evidence of each microscopy technique used for the characterization of nanoparticles of Arthrospira maxima. A) AFM, B) SEM y C) TEM.

References:

Belay, A. Spirulina (*Arthrospira)*: Production and quality assurance. In: Spirulina in human nutrition and health. 2008. Ed. Gershwin, M.E., Belay, A. Taylor and Francis. USA. Pp 1-26.
Lü, L., Lai, M. O. 1998. Mechanical alloying. Kluber academic publishers. Massachusetts, USA.

The influence of removal of stabiliser on the selective oxidation of cycloalkenes using supported gold nano-particles

Hamed Alshammari[a], Peter J. Miedziak[b] and Graham J. Hutchings[b]
[a]Chemistry Department, Faculty of Science, Ha'il University, P. Box 2440, 81451 Ha'il, Saudi Arabia
[b]Cardiff Catalysis Institute, Cardiff University, Park Place, Cardiff, UK CF10 3AT

Abstract: The oxidation of cyclic alkenes such cyclohexene and cyclooctene has been carried out under green solvent-free conditions using ambient air as the oxidant gas with a carbon-supported gold catalyst. We show that oxidation of cyclic alkenes under solvent free conditions can be oxidised in the absence of radical initiators when the cyclic alkenes are free of stabilisers. We show that radical initiators are only required for this reaction when the cyclic alkene contains a stabilizer molecule, such as 6-bis(t-butyl)-4-methylphenol (BHT) or 3-octadecyl-(3,5-di-t-butyl-4-hydroxyphenyl)-propanoate (irganox 1076). We show that either removing the stabilizer chemically or sourcing the cyclo-alkane without the stabilizer the oxidation, both with and without radical initiator, is identical as showing in figure 1 and 2. This indicates that the only function of the radical initiator is to counteract the stabilizer.

Keywords: oxidation of alkene, nanopartical, initiator.

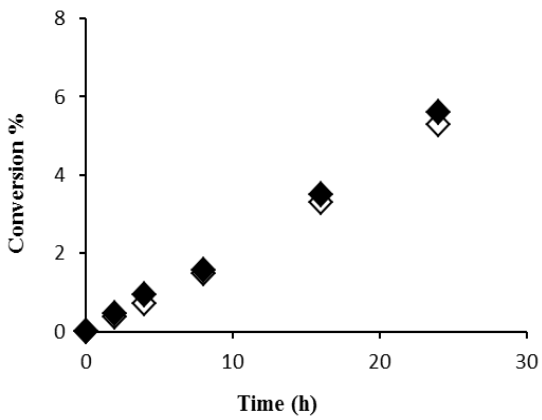

Figure 1: Effect of reaction time for the conversion of cis-cyclooctene containing stabilizer with TBHP (solid diamonds) and cis-cyclooctene after removal of stabilizer without TBHP (open diamonds). Reaction conditions: 5 ml of *cis*-cyclooctene, 0.06g Au/G, glass reactor, TBHP (0.032×10^{-3} mol), 80 ºC and atmospheric pressure.

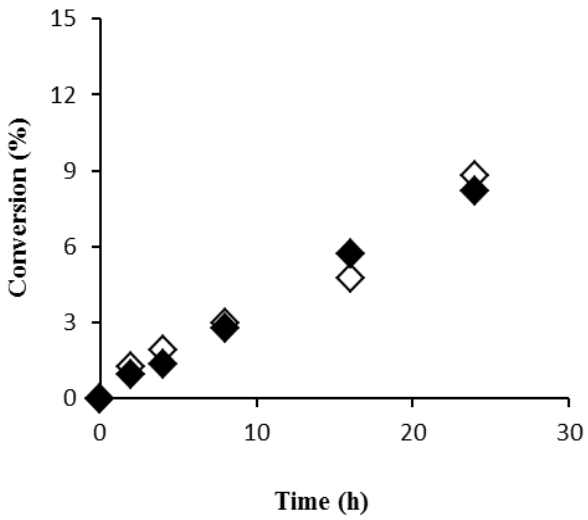

Figure 2: Effect of reaction time for the conversion of cyclohexene containing stabilizer with TBHP (solid diamonds) and cyclohexene inhibitor-free without TBHP (open diamonds). Reaction conditions: 5 ml of cyclohexene, 0.06g Au/G, glass reactor, TBHP (0.032×10^{-3} mol), 60ºC and atmospheric pressure.

References:

M.D. Hughes, Y.-J. Xu, P. Jenkins, P. McMorn, P. Landon, D.I. Enache, A.F. Carley, G.A. Attard, G.J. Hutchings, F. King, E.H. Stitt, P. Johnston, K. Griffin, C.J. Kiely, Nature, 437 (2005) 1132-1135.

S. Bawaked, N.F. Dummer, N. Dimitratos, D. Bethell, Q. He, C.J. Kiely, G.J. Hutchings, Green Chemistry, 11 (2009) 1037-1044.

Posters Session I – B
Nanomaterials Characterization / Properties and Tools

Study of chairlity by High Resolution Optical Microscope of Si-CNT Prepared by Plasma Sputtering without catalyst

Bassam M. Mustafa, Anwar M. Ezzat and Mohammad M. Uonis
Department of Physics, College of Science, Mosul University, Mosul, Iraq

Abstract: Fabrication of Si-CNT (silicon- carbon nano tube) junction is done by plasma sputtering of Carbon from graphite rods in Argon gas atmosphere, without catalysts for thicknesses 10 – 82 nanometer . Study of images of the specimen by Scanning electron microscope shows that the carbon layer is in the form carbon nanotubes with diameters about 30 nanometer The Raman, x-ray and the energy dispersive x-ray (EDXR) spectra shows peaks characteristics of the carbon nanotubes . More careful study of the carbon layer surface by high resolution optical microscope is done using both transmission and reflection methods , then images are amplified more by computer software .The transmission images for carbon layer on the glass substrate shows two dimensional nanotubes structures . Images taken by reflection of white light from the carbon layer on Si-C junction, shows clearly zigzag nanotubes chairlity The I-V measurements using gold electrodes shows semiconducting behavior ensuring the zigzag chairlity .

Keywords: Carbon nanotubes, Plasma sputtering, Si-C junction, chairlity.

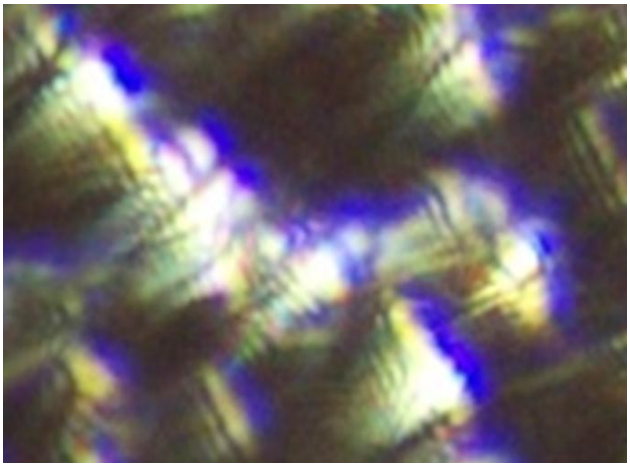

Figure 1: show the images for carbon nano layers deposited on silicon wafer taken by high resolusion light microscope with a digital camera after magnification by 850% by computer software.

References:

Uonis, M. , Mustafa, B. and Ezzat, A. (2014) The Role of Sputtering Current on the Optical and Electrical Properties of Si-C Junction. World Journal of Nano Science and Engineering, 4,90-96.
doi: 10.4236/wjnse.2014.42012.

Uonis, M. , Mustafa, B. and Ezzat, A. (2014) The Effect of Carbon Rod—Specimens Distance on the Structural and Electrical Properties of Carbon Nanotube. World Journal of Nano Science and Engineering, 4,105-110. doi:10.4236/wjnse.2014.43014.

Gas-Generating Theranostic Nanoparticles for Ultrasound Imaging and Photodynamic Therapy

D. J. Park,[1] K. H. Min,[1] S. C. Lee[2,*]
[1]Department of Life and Nanopharmaceutical Science, College of Pharmacy, Kyung Hee University, Seoul, Republic of Korea
[2]Department of Maxillofacial Biomedical Engineering, School of Dentistry, Kyung Hee University, Seoul, Republic of Korea

Abstract: Recently, theranostic nanoparticles, which integrate imaging and therapeutic functionalities, have played a central role in the improvement of tumor treatment. In this work, we develop a gas-generating calcium carbonate ($CaCO_3$) mineralized nanoparticle ($CaCO_3$-MNPs) that can generate carbon dioxide (CO_2) bubbles and trigger the release of photosensitizers in response to tumoral acidic pH for ultrasound (US) imaging and simultaneous therapy of tumors. To visualize CO_2 generation, in vitro contrast-enhanced ultrasound imaging and quantitative analysis of CO_2 amounts were investigated at various pH values. In vitro phototoxicity and singlet oxygen generation experiments were carried out in order to verify photodynamic effect of the photosensitizer from the nanoparticles. This work suggests that $CaCO_3$ mineralized photosensitizer-encapsulated nanoparticles can serve as theranostic nanoparticles for US imaging-guided photodynamic therapy.

Keywords: calcium carbonate, photosensitizer, mineralization, ultrasound imaging, theranostics, photodynamic therapy

As llustrated in Figure 1, we prepared Ce6-loaded mineralized nanoparticles by poly(ethylene glycol)-b-poly(L-aspartic acid) (PEG-PAsp)-mediated $CaCO_3$ mineralization in the presence of calcium cations, carbonate anions, and a negatively charged photosensitizer, chlorin e6 (Ce6). TEM images indicated that the nanoparticles had a spherical shape and a mean diameter of 300 nm. To visualize CO_2 generation from dissolved $CaCO_3$ in tumoral acidic pH, in vitro contrast-enhanced ultrasound image and quantitative analysis of CO_2 amounts were investigated at various pH. In vitro experiments showed that the $CaCO_3$-MNPs generated strong echogenic signals at tumoral pH (6.4) due to CO_2 bubble generation, whereas, at pH 7.4, there was no noticeable US contrast signals (Figure 2). In vitro phototoxicity and singlet oxygen generation experiments were carried out in order to verify photodynamic effect of Ce6 from mineralized nanoparticles. The $CaCO_3$-MNPs effectively released Ce6 at pH 6.4, and expressed the effective photodynamic therapeutic activity for MCF-7 breast cancer cells.

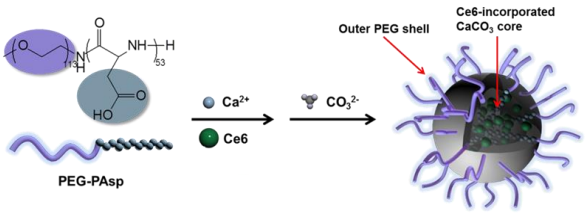

Figure 1. Fabrication of Ce6-loaded $CaCO_3$ mineralized nanoparticles through PEG-PAsp-mediated mineralization.

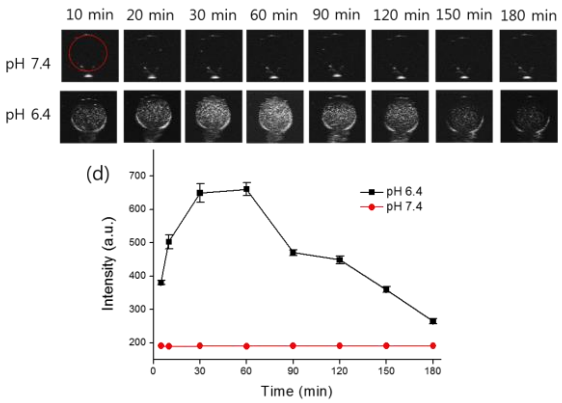

Figure 2. pH-Dependent in vitro US imaging profiles as a function of time.

References:

Rim, H. P., Min, K. H., Lee, H. J., Jeong, S. Y., Lee, S. C. (2011) pH-Tunable calcium phosphate covered mesoporous silica nanocontainers for intracellular controlled release of guest drugs, *Angew. Chem. Int. Ed.*, 50, 8853-8857.

Min, K. H., Lee, H. J., Kim, K., Kwon, I. C., Jeong, S. Y., Lee, S. C. (2012), The tumor accumulation and therapeutic efficacy of doxorubicin carried in calcium phosphate-reinforced polymer nanoparticles, *Biomaterials*, 33, 5788-5797.

Min, K. H., Min. H. S., Lee, H. J., Park, D. J., Yhee, J. Y., Kim, K., Kwon. I. C., Jeong, S. Y., Silvestre, O. F., Chen, J., Hwang, Y.-S., Kim, E.-C., Lee, S. C. pH-Controlled Gas-Generating Mineralized Nanoparticles: A Theranostic Agent for Ultrasound Imaging and Therapy of Cancers, *ACS Nano*, In Press.

The application of ultrasonic spectroscopy to the study of the gelation and chain relaxation properties of dually crosslinked hydrogels

K. Khouzami*, C. Branca, C. Crupi, S. Rifici, G. Ruello, U. Wanderlingh, G. D'Angelo
Dipartimento di Fisica e Scienze della Terra, Università di Messina, Viale S. D'Alcontres 31 98166 Messina

Abstract: One strategy to create chemical and physical cross-links simultaneously is to introduce into the chemical network hydrogen bonding with clay nanofillers. Understanding the gelation process and relaxation mechanisms of these systems is crucially important for predicting hydrogel performances in terms of degree of swelling and viscoelastic properties.

In this study, ultrasonic spectroscopy has been used to investigate the gelation kinetics and chain-relaxation properties of glutaraldehyde-cross-linked chitosan and chitosan- montmorillonite nanocomposite hydrogels.

Low intensity ultrasound was applied to the investigated systems. By measuring the amplitude of the wave in the pulse, the ultrasonic velocity and attenuation at frequencies between 5 and 25 MHz and at room temperature were determined simultaneously as a function of the time.

In all the investigated samples, we observed that the kinetics of gelation consist of two stages; a pre-gelation, indicated by fast increase in the ultrasound velocity and attenuation, and a gelation, that is revealed by inflection in the ultrasound velocity and attenuation trends.

The increase of the ultrasound attenuation is due to the viscous losses, while the increases in the ultrasonic velocity reflects the increase in the longitudinal modulus of the sample due to the contribution of the gel network.

The effects of the cross-linker and clay concentration on the hydrogel acoustic behavior have been also analysed and correlated with the elastic response of the systems.

The results demonstrate the reliability of ultrasonic spectroscopy in describing in details the network formation processes. If used in parallel with other tecniques, such as rheology and light scattering, it should help us to better understand the viscoelastic processes associated with the physical or chemical gelation and the crosslinking in hydrogel systems.

Keywords:
biomaterials, nanoporous hydrogels, polysaccharide, crosslinking, viscoelasticity, ultrasonic spectroscopy.

New challenges in TiO_2 nanoparticle characterisation and separation by Flow Field Fractionation

J. Omar, A. Boix, C. von Holst

European Commission, Joint Research Centre, Institute for Reference Materials and Measurements (EC-JRC-IRMM), Retieseweg 111, 2440 Geel, Belgium

Titanium dioxide is a widely used additive which can appear in a broad variety of final products such as paint pigments, toothpastes, sunscreens, coffee creamers, food colorants, etc. due to its different properties. The European Commission's Joint Research Centre (JRC) established a repository with Representative Test Materials (RTMs) consisting of different types of particulate nanomaterials, from which three titanium dioxide materials were chosen for this study: NM 101, NM 102 and NM 104. All the materials presented a different particle size (mean particle size 38, 132 and 67 nm respectively), the first two RTMs are known as anatase mineral and the last RTM as rutile.

The aim of this study was to develop a separation and characterisation method for each of the chosen RTMs by means of Field Flow Fractionation (FFF) system. In a first approach, the most suitable dispersant and eluent were chosen for each of the RTMs among them water, sodium pyrophosphate, Novachem and BSA. Next, the FFF system was optimized for each material employing experimental design: the tip flow, cross flow, detector flow and focusing time were studied. Concerning the sample preparation, the use of Focused Ultrasound Systems is becoming more and more necessary, however, the impact of the ultrasounds (time and amplitude) in the RTM was also studied by means of Experimental Design.

Diamagnetism of Superparamagnetic Ni Nanoparticles Incapsulated in Carbon Shells

A. Manukyan,[1*] A. Mirzakhanyan,[1] H. Gyulasaryan,[1] M. Farle,[2] E. Sharoyan[1]
[1]Institute for Physical Research, NAS of Armenia, Laboratory of Solid State Physics, Ashtarak-2, Armenia
[2] Universität Duisburg-Essen, Fakultät für Physik and Center for Nanointegration, Duisburg, Germany

Abstract: Using the method of solid-phase pyrolysis of solid solutions of nickel phthalocyanine – metal-free phthalocyanine, $\{(NiPc)_x(H_2Pc)_{1-x},\ 0<x<1\}$, we prepared single-domain ferromagnetic and superparamagnetic Ni nanoparticles coated by graphite-like shells, i.e. Ni@C nanocomposites. A considerable diamagnetism was observed in case of ultrafine Ni nanoparticles when their mean size, d_m, was less than 17 nm.

The dependence is shown in Figure 1 of the total and diamagnetic parts of the magnetization of Ni@C nanocomposites upon external magnetic field at 300K. The values of the concentration, c, of Ni in carbon were equal to 0; 0.5; 0.75; and 2.5 at % and the values of diamagnetic susceptibility were -1×10^{-6}; -3×10^{-5}; -2×10^{-5}; and -6×10^{-6} emu/(g·Oe) correspondingly. The diamagnetism in Ni-containing samples is substantially higher as compared to that of the carbon matrix $\chi^{dia}(c=0.5) = 30\chi^{dia}(c=0)$. Unfortunately, it is not possible to compare the diamagnetism of Ni@C nanocomposites with that of bulk Ni samples since no data exists about diamagnetism of bulk Ni. Evdently, the ferromagnetic magnetization in bulk Ni is so strong that it makes it impossible to observe the diamagnetic magnetization. The observation of diamagnetism in ferromagnetic metals becomes possible in case of small nanoparticles in superparamagnetic state. The paramagnetism of these nanoparticles is very low at high temperatures (100–300 K) due to $M_{para} \sim 1/T$. On the other hand our results reveal the drastic increase of diamagnetism in small metal nanoparticles. We considered possible mechanisms that can give rise to considerable diamagnetism in Ni@C nanocomposites. The "giant" diamagnetism in non-ferromagnetic nanoparticles was earlier observed in single-crystalline Au nanorods (van Rhee *et al*.; 2013).

This work was supported by the grant of Volkswagen Stiftung project A108857.

Keywords: diamagnetism in Ni nanoparticles, nickel-carbon nanocompisites, solid-phase pyrolysis, superparamagnetism.

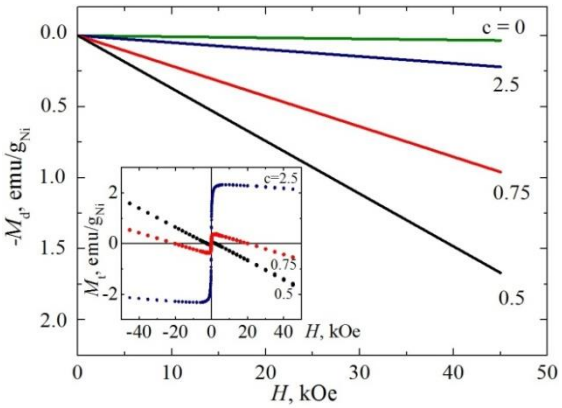

Figure 1: The dependences of the total and diamagnetic parts of the magnetization of Ni@C nanocomposites upon external magnetic field at 300 K.

References:

van Rhee, P.G., Zijlstra, P., Verhagen, T.G.A., Aarts, J., Katsnelson, M.I., Maan, J.C., Orrit, M., Christianen, P.C.M. (2013) Giant Magnetic Susceptibility of Gold Nanorods Detected by Magnetic Alignment, *Phys. Rev. Lett.*, 111, 127202.

Beryllium oxide nanowires and their optical properties for dosimetric applications

E. Pajuste*, G. Kizane, J. Prikulis, D. Erts
Institute of Chemical Physics, University of Latvia, 4 blvd. Kronvalda, Riga, LV-1586, Latvia
Phone: +371 67033883, Fax +371 67033883, E-mail: elina.pajuste@lu.lv

Abstract: Beryllium oxide is a material with a wide range of applications owing to its unusual combination of optical, thermal, dielectric and mechanical properties. Due to its high sensitivity and near tissue-equivalence beryllium oxide is used also as a OSL (optically stimulated luminescence) dosimeter[1]. It has been observed that luminescent (thermal and optical) dosimetric response of nano-phosphorus has an increased dose range with good linearity over its microcrystalline counterparts[2]. In nanostructured form dosimetric materials have a considerably higher measured dose upper limit[3]. This characteristic is of marked interest in several dosimeter applications for e.g. radiation therapy of cancer, where extremely high doses are delivered to the tumour volume, and border protection where exposure to unknown source is potentially possible. Therefore it can be expected that nanostructured beryllium oxide would have better dosimetric performance over the microcrystalline one.

Beryllium nanowires with a diameter in range from 10 – 100 nm and length of 50 μm were obtained by a high temperature oxidation process of beryllium in the atmosphere of low oxygen content. The optical properties of the nanowires were compared to that of microstructured beryllium oxide powder. Emission spectra was measured for both BeO nanowires and powder by optical stimulation with different excitation wavelengths. A significant change of photoluminiscence spectra were observed in beryllium oxide nanowires if stimulated by the ultraviolet and green excitition. Preliminary irradiation experiments with the accelerated electrons have been performed (Figure 2) and dosimetric response assessed.

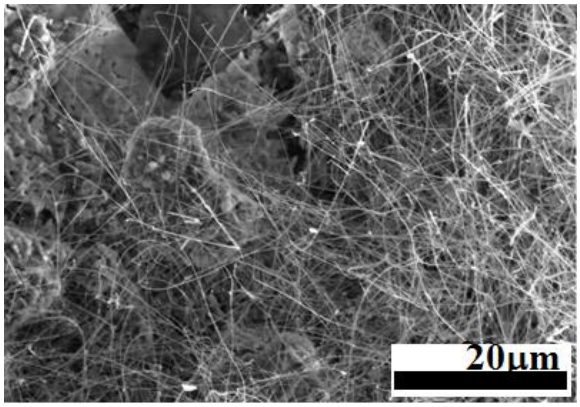

Figure 1: Beryllium oxide nanowires

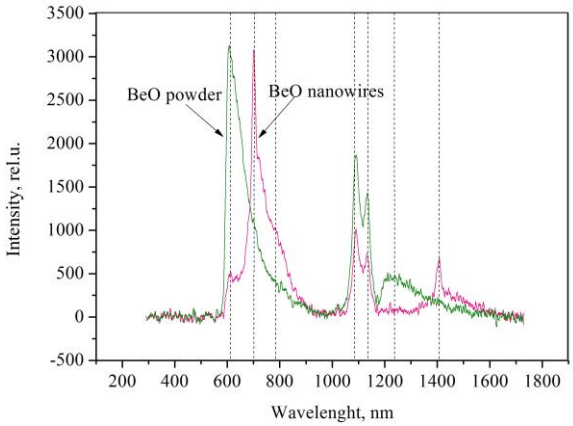

Figure 2: Photoluminiscence induced by green light excitation of BeO microcrystalline powder and nanowires after 500 Gy dose irradiation with 5 MeV accelerated electrons

This work was done within ESF project 2013/0028/1DP/1.1.1.2.0/13/APIA/VIAA/054.

References:

1. Jahn, A., M. Sommer, W. Ullrich, M. Wickert and J. Henniger (2013) The BeOmax system – Dosimetry using OSL of BeO for several applications. *Radiation Measurements*, **56**,. 324-327.
2. Kortov, V.S. (2010) Nanophosphors and outlooks for their use in ionizing radiation detection. *Radiation Measurements*,. **45**(3–6),512-515.
3. Erfani Haghiri, M., E. Saion, N. Soltani and W. SAffiey wan Abdullah (2014), Thermoluminescence Properties of Nanostructured Calcium Borate as a Sensitive Radiation Dosimeter for High Radiation Doses *Advanced Materials Research*, **832**, 189 -194.

Computer microscopy of biological liquid dry patterns for medical diagnostics and modeling of their properties by dissipative dynamics methods

P. Lebedev-Stepanov ,[1,2,*] M. Buzoverya,[3] I. Shishpor[3], K. Vlasov[2]
[1]Photochemistry Center RAS, Moscow, Russia
[2]National Research Nuclear University MEPhI, Moscow, Russia
[3] Sarov State Physics Technical Institute, Sarov, Russia

Abstract:

A number of papers devoted to heat and mass transfer into colloidal solution evaporating drops on a flat substrate have been published over the last years, mainly due to the importance of this problem for fundamental and applied sciences and technologies.
Report demonstrates some capabilities of the hardware-software complex *Morfo* in the field of solving the diagnostics problems of the human body in normal state, and when pathology states are being developed (Fig.1) [1,2]. The complex's application has allowed obtaining of interesting results not only in biomedical applications, but also acquisition of interesting data on the processes of facies structure formation**.**
Also we are elaborating the useful software complex to predictive modeling of setup, spreading, evaporation of liquid droplet of inkjet size, as well as self-assembly of solvated monodisperse nanoparticles from the drop during evaporation (Fig. 2), [3]. The most difficult case for modeling is a drop of biological liquid (such as blood serum, tear, saliva et al.) which consists of many different components of solution and forms the complex dry pattern onto substrate as a final stage of solvent evaporation process.
The modern computer methods are not yet able to model such a system in details. This study includes consideration of perspectives of further development of DPD methods to describing the formation of the dry pattern (Fig.3) which gives the new opportunities for interpretation of this process and pattern diagnostics optimization.

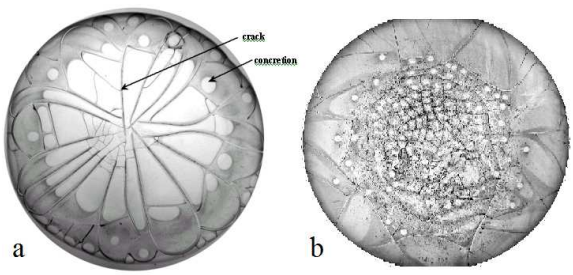

Figure 1: Blood serum facies: a – norm; b – pathology.

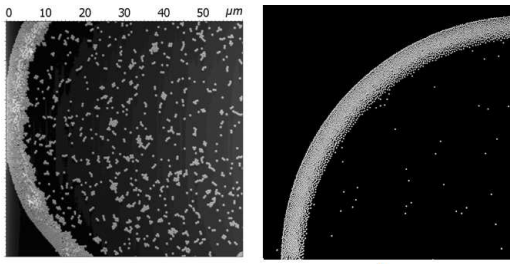

a b

Figire 2: a - ASM image of inkjet droplet pattern which consists of monodisperse colloidal particles. b –DPD numerically modeling pattern. The calculation visualization was performed via VMD 1.8.

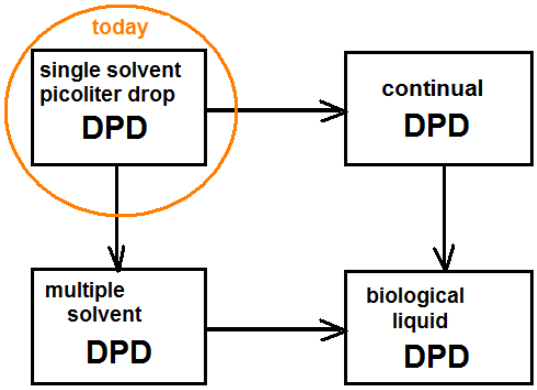

Figure 3: Running status and perspectives in modelling by dissipative particle dynamics (DPD)

Keywords: microstructural bio-liquids' analysis, quantitative microscopy, cracks, concretions, hardware-software complex, biomedical applications, dissipative particle dynamics (DPD), self-assembly, computer modeling, nanoparticles.

References:

1. Shabalin, V., Shatokhina, S. (2001), The human being bio-liquids' morphology, Moscow, Khrizostom. 304 P.
2. Buzoverya, M, Shishpor, I., Potekhina, Yu., Shcherbak, Yu. (2012), The bio-liquids' microstructural analysis, *Journal of Technical Physics*, 82, 7, 123-128.
3. Lebedev-Stepanov, P., Vlasov K. (2013), Simulation of self-assembly in an evaporating droplet of colloidal solution by dissipative particle dynamics, *Colloids and Surfaces A: Physicochem. Eng. Aspects*, 432, 132–138.

Theoretical studies on electronic and magnetic properties of a two-dimensional Mn-Pc and Mn-TCNB monolayers

M. MABROUK[1,2*], R. HAYN[1]
[1]Aix-Marseille Université, CNRS, IM2NP-UMR 7334, 13397 Marseille Cedex 20, France
[2]Laboratory for Advanced Materials and Interfaces, Faculty of Sciences of Monastir, Avenue of the Environment, 5019 Monastir, Tunisia

Abstract: The electronic and magnetic properties of a two-dimensional manganese phthalocyanine Mn-Pc monolayer and the metal-ligand network Mn-TCNB (Figure 1) are investigated by first principal calculations based on density functional theory with the inclusion of the Hubbard like-Coulomb term.
We show that both structures have a metallic behavior with a total magnetic moment of about 3 μ_B (Koudia *et al.*, 2014). We notice that a partial screening is present in the Mn-TCNB monolayer where a local moment S=5/2 at the Mn centers is reduced by unpaired electrons at the ligands. Such a picture explains the recent XMCD measurements of Mn-TCNB (Giovanelli *et al.*, 2014). Our results present theoretical insight of new metal-organic networks being important for future molecular spintronics.

Keywords: Manganese phthalocyanine, TCNB, half-metal, molecular spinctronics, Density function theory.

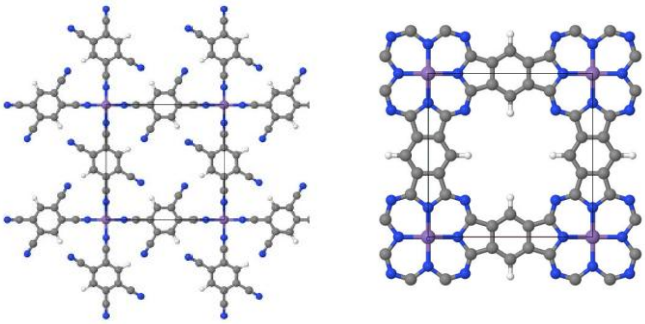

Figure 1: Structure of the 2D Mn-TCNB and Mn-Pc networks respectively. The Mn, N, C, and H atoms are highlighted in violet, blue, gray, and white, respectively. The square represent the unit cell.

References:

Giovanelli, L., Savoyant, A., Abel, M., Maccherozzi, F., Ksari, Y., Koudia, M., Hayn, R., Choueikani, F., Otero, E., Ohresser, P., Themlin, J.-M., Dhesi, S. S., Clair, S. (2014), Magnetic Coupling and Single-Ion Anisotropy in Surface-Supported Mn-Based Metal–Organic Networks, *J. Phys. Chem. C*, 118, 11738-11744.

Koudia, M., Abel, M. (2014), Step-by-step on-surface synthesis: from manganese phthalocyanines to their polymeric form, *Chem. Commun.*, 50, 8565-8567.

Band Structure of ABA-Trilayer Graphene Superlattice under the Application of Periodic Kronig-Penney Type of Potential

Salah Uddin,[1] K. S. Chan,[2*]
[1, 2*]Department of Physics and Materials Science, City University of Hong Kong

Abstract: After the discovery of graphene, theoretical physicists have been investigating methods to modify the electrical properties of massless Dirac quasiparticles. This work presents the development of a new numerical method to investigate the effect of one-dimensional periodic potential on the low energy band structure of ABA-trilayer graphene superlattice. This method can also be generalized to study multilayer graphene too. We use the Fourier transformation approach to convert the low energy continuum Hamiltonian of ABA-trilayer graphene near the Dirac point in one valley to a general ABA-trilayer graphene superlattice Hamiltonian. The electric potential is also converted to a periodic superlattice potential by applying the Fourier series. The superlattice Hamiltonian along with superlattice potential is then solved numerically and got the results which are discussed below.

We consider to different cases. (1) First we assume that all the three layers have the same potential. By increasing the barrier height of the superlattice potential and keeping the barrier and well width of the potential equal, extra Dirac points having the same electron-hole crossing energy as that of the original Dirac point are generated in the energy spectrum. These extra Dirac points emerge both from the original Dirac points as well as from the valleys developed in the energy spectrum. The symmetry of the conduction and valence band broken down by making the barrier and well width unequal. The position of the original Dirac point oscillate with periodic potential while the extra Dirac points shifted upward or downward depending on the barrier and well width. The number of extra Dirac points produce by increasing the barrier height (potential) when all the three layers have the same potential are shown in figure 1. (2) If we consider each layer has a different potential then extra Dirac points always emerges from the valleys in the spectrum. Each time two extra Dirac point emerge from each single valley so four Dirac points are generated at a particular potential. These extra Dirac points are not stable; two out of four Dirac points disappear from the spectrum by increasing the barrier height of each layer. This merging and emerging of additional Dirac points is completely different from the equal potential case. The results of different potential for each layer are similar to one discuss in (Uddin *et al.*; 2014) for ABC-trilayer graphene superlattice.

Keywords: band structure of ABA-trilayer graphene superlattice, electrical properties, superlattice potential.

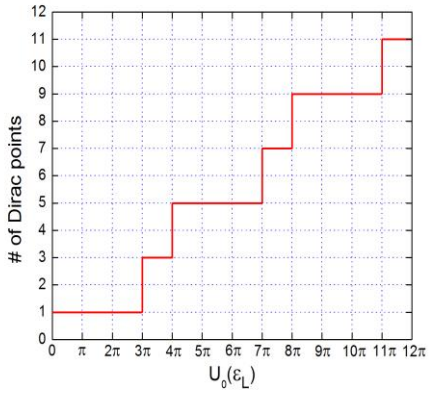

Fig. 1: Number of Dirac points (not including spin and valley degeneracies) in ABA-trilayer graphene superlattice versus barrier height.

REFERENCES

Uddin S., Chan K. S. (2014), Band structure of ABC-trilayer graphene superlattice, J. Appl. Phys. 116, 203704.

Fabrication of transparent AZO/ZnO/ITO ReRAM devices and their switching characteristics depending on the deposition temperature of ZnO active layer

K. Y. Kim,[1] C. H. Cho,[2] H. J. Kim,[2] E. L. Shim[3], and Y. J. Choi,[1]
[1] Sejong University, Department of Nanotechnology & Advanced Materials Engineering, Seoul, Republic of Korea
[2] Myongji University, Department of Physics, Gyeonggi, Republic of Korea
[3] Halla University, School of Mechanical & Automotive Engineering, Gangwon-do, Republic of Korea

Abstract: In this research, we reported the dependence of the resistive switching characteristics of transparent resistive random access memory (ReRAM) devices with AZO/ZnO/ITO structures on the deposition temperature of the ZnO active layer. During the formation of the ZnO thin film layer in the ReRAM devices, we studied the structural changes due to changes in the substrate temperature. In general, structural changes of active layers are closely related to the resistive switching characteristics of the ReRAM device. Based on the structural changes of ZnO thin film with the substrate temperature, we compared the resistive switching characteristics of the corresponding ReRAM devices. When the deposition temperature is increased, we confirmed the ZnO thin film changed properties: grain size and thin film property. In addition, the resistive switching characteristics declined. As a result, the ReRAM device with a ZnO film deposited at room temperature showed the best characteristics: forming at the lowest voltage (below 3 V), set and reset occurring between –1 V and 1 V, more than 300 cycles of endurance, and more than 10,000 s retention time.

Keywords: Resistive random access memory (ReRAM), ZnO, thin films, temperature dependence.

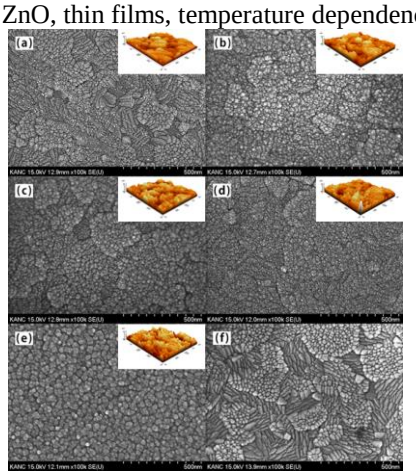

Fig. 1. (a) The SEM data of ITO thin film. The SEM data of ZnO thin film for different substrate temperatures: (b) room temperature, (c) 150℃, (d) 300℃, and (e) 450℃. (f) The ITO thin film with respect to the annealing temperature at 450℃. Insets are corresponding AFM images.

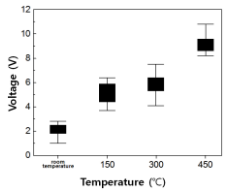

Fig. 2. Forming voltage of the ReRAM device with ITO/ZnO/AZO structure with respect to the substrate temperature.

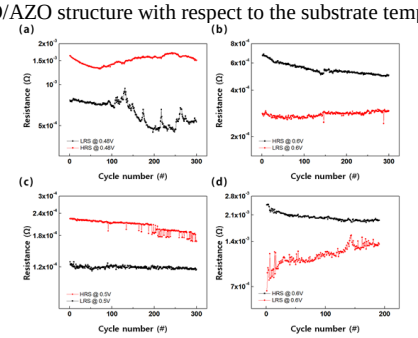

Fig. 3. Endurance of ITO/ZnO/AZO ReRAM device for different substrate temperatures: (a) room temperature, (b) 150℃, (c) 300℃, and (d) 450℃.

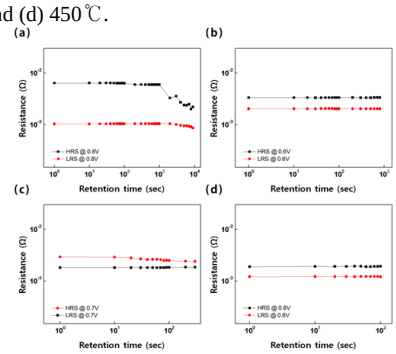

Fig. 4. Retention of the ITO/ZnO/AZO ReRAM device for different substrate temperatures: (a) room temperature, (b) 150℃, (c) 300℃, and (d) 450℃.

References:

Akinaga, H., Shima, H. (2010), Resistive Random Access Memory (ReRAM) Based on Metal Oxides, *Proceedings of the IEEE.*, 98, 2237-2251.

Xu, N., Liu, L., Sun, X., Liu, X., Han, D., Wang, Y., Han, R., Kang, J., Yu, B. (2008), Characteristics and mechanism of conduction/set process in Ti N/Zn O/Pt resistance switching random-access memories, *J. Appl. Phys.*, 92, 232112.

Singh, S., Srinivasa, R, S., Major, S, S., (2007) Effect of substrate temperature on the structure and optical properties of ZnO thin films deposited by reactive rf magnetron sputtering, *Thin Solid Films.*, 515, 8718-8722.

Physico-chemical properties of Fe-doped alumino-silicate nanotubes

E. Bahadori,[1] E. Shafia,[1] S. Esposito,[2] M. Armandi,[1] B. Bonelli,[1*]

[1] Department of Applied Science and Technology, Politecnico di Torino, Torino, Italy

[2] Department of Civil and Mechanical Engineering, Università degli Studi di Cassino, Cassino (FR), Italy

Abstract: Imogolite (IMO) is a an alumino-silicate occurring as single-walled nanotubes (NTs) with chemical formula $(OH)_3Al_2O_3SiOH$, having an outer surface made by Al-O-Al and Al(OH)Al groups and an inner surface lined by silanols (SiOH). IMO is diamagnetic and behaves as an insulator, but doping with small amount of iron could lead to new magnetic and conductive properties. Moreover, the presence of Fe sites at the outer surface of NTs, due to Fe replacing Al, could lead to interesting catalytic properties. In a previous work [1], we have investigated the synthesis of Fe-doped IMO by either direct synthesis or impregnation in basic medium so as to achieve precipitation of Fe-oxo, hydroxides. Unfortunately, the direct synthesis method proved to be very difficult, due to the presence of Fe-precursor in the synthesis medium, finally lowering the reaction yield, therefore the ionic exchange method would allow iron-doping in a simpler way.

In this work, Fe-doped NTs with an iron content of 1.4 wt. % were obtained by post-synthesis ion exchange of Imogolite ($(OH)_3Al_{2-x}Fe_xO_3SiOH$ with x = 0.05, Fex-IMO) and Methyl-Imogolite, an IMO analogous material in which inner SiOHs are replaced by $SiCH_3$ groups ($(OH)_3Al_{2-x}Fe_xO_3SiCH_3$ with x = 0.05, Fe_X-Me-IMO). Samples properties were investigated by X-ray Diffraction (XRD); N_2 sorption isotherms at 77 K and Diffuse Reflectance (DR) UV-Vis spectroscopy. The results were compared with previous research on a set of Fex-IMO samples obtained by direct synthesis and post-synthesis impregnation [1].

Evidence is given of the isomorphic substitution of Fe for Al in both Fex-IMO and Fex-Me-IMO samples, in that:

i) according to UV-vis spectroscopy, both Fe-containing samples exhibit UV bands , which can be attributed to ligand-to-metal (O–Fe) charge-transfer transitions of isolated Fe(III) ions in octahedral environment and to a small amount of FexOy nanoclusters [2];

ii) XRD patterns allow calculation of lattice parameter (*a*) values indicating that ionic exchange allows the isomorphic substitution of Al^{3+} by Fe^{3+} without alteration of the lattice parameter.

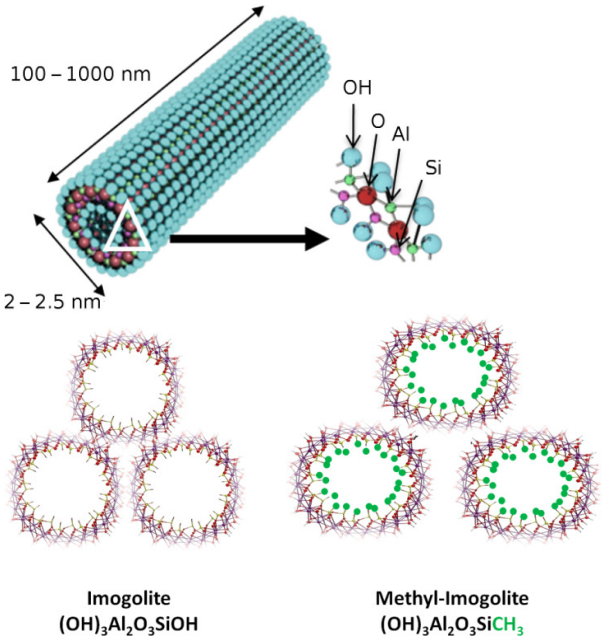

Figure 1: Section of Imogolite and Methyl-Imogolite nanotubes, in which ferric ions can replace Al^{3+}sites [3] , [4].

The ionic exchange therefore is a promising method to allow doping IMO NTs not only with iron, but also with other trivalent cations that could repace external Al, without altering the synthesis medium.

Keywords: Imogolite; nanotubes; isomorphic substitution; Fe-doping; Ion exchanging; adsorption; Direct synthesis.

References:

[1] Shafia, E., PhD thesis., Politecnico di torino.

[2] Wang, Y., Zhang, Q, H., Shishido, T., Takehira, K.,. (2002)., J. Catal., 209, 186-196.

[3] Garrone, E., Ugliengo, P., (1991)., Langmuir., 7, 1409-1412.

[4] Zanzottera, C., Armandi, M., Esposito, S., Bonelli, B., (2012)., J. Phys. Chem., 116, 20417−20425.

*Corresponding author: Prof. Barbara Bonelli
E-mail: barbara.bonelli@polito.it
Tel: +39-3392803713

Nanostructured Polymer Matrix Composites for High Performace Engineering Applications

T. Turcsán,[1,*] L. Mészáros,[1,2]
[1]Budapest University of Technology and Economics, Department of Polymer Engineering, Muegyetem rkp. 3., H-1111 Budapest, Hungary
[2]MTA–BME Research Group for Composite Science and Technology, Muegyetem rkp. 3., H-1111 Budapest, Hungary
*corresponding author, e-mail: turcsan@pt.bme.hu

Abstract: The researchers and developers intend to obtaine favourable mechanical and thermal properties on the field of polymer composites. The thermoset matrix polymer composites have great mechanical properties and relatively good thermal resistance compared to the thermoplastic ones, but they have not as good toughness as the thermoplastic polymer ones, ductile metals and alloys. The high performance polymer composites usually give rigid reactions to the quckly forthcoming and cyclic loads. Rigidity could be caused by the pronouncedly rapid crack propagation and fracture velocity inside of the composite. This is the reason why it is important to improve their toughness without decrease the great mechanical properties (Karger-Kocsis, 2005).

Usually the matrix of the polymer composite is responsible for the toughness of the complete material. Improvement in the toughness of the thermoset resins can be reached by several ways. One of them is creating nanostructure in the material by modificate its morphology. There are several ways to do this modification. On one hand it is possible by giving nanosized additives, nanoparticles to the resin on the other hand there is an opportunity to interblend different type of resins. During the crosslinking process of different mixed resins the compound can be divided to at least two segements by phase separation processes. Because of this phase separation in case of optimal conditions it is possible that nanostructured hybrid resin come into being with co-continuous conformation. In this nanostructured material, there are lots of entanglements of the molecule chains of the componenst by the way they have lots of secondary bounds between them. Additional flexibility and toughness of the matrix material can be reached by this mechanical bounding of named secondary bounds and entanglements. By reason of the mentioned phenomena the crack propagation of the hybrid resin is hampered because of lots of bounds and molecule chain intertanglementsin the material (Turcsán et al, 2014).

Using the mentioned phase separated hybrid resin as matrix material of fibre reinforced composite (Fig 1) it could result improved damping properties by the way enhanced toughness (Mészáros et al, 2014). In case of several fibre reinforcements there is a chance to set their surface threatment that this sizing to result better connenction to one component of the hybrid resin. If the better connected resin to the fibre is less rigid than the other one, it could work in couples with the reinforcement and other resin by the way effect another positive modification for damping properties and toughness.

Another possibly way to modificate the morphological structure of the composite is giving nanoparticles and phase separated nanostructured resin, too.

The main aim of our research work is to create nanostructured high performance fibre reinforced polymer composites for mechanical applications and investigate their morphological and mechanical properties bring into focus the toughness by the way to improve the durability of them.

Keywords: nanostructure, polymer composites, phase separated nanostructure, high performace composites, mechanical applications.

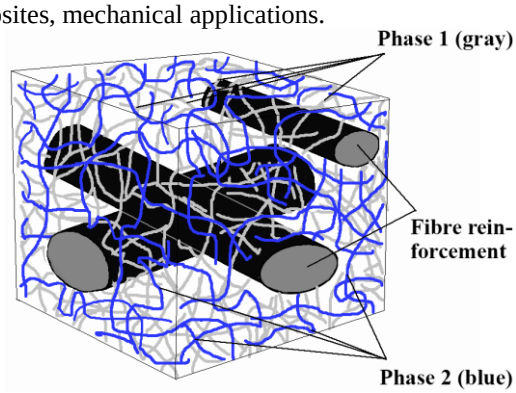

Figure 1: Theoretical structure of the co-continuous nanostructured multiphase system of a hybrid resin matrix fibre reinforced polymer composite

References:

Karger-Kocsis J. (2005) Simultaneous interpenetrating network structured vinylester/epoxy hybrids and their use in composites, in 'Micro- and Nanostructured Multiphase Polymer Blend Systems: Phase Morphology and Interfaces' CRC Press, Boca Raton.

Mészáros L., Turcsán T.(2014), Developemnt and mechanical properties of EP/VE hybrid composite systems, Periodica Plytechnica, Mechanical Engineering, 58, 127-133.

Turcsán T., Mészáros L (2014), Development of high-performance polymer composite with toughened matrix, The Fiber Society Spring 2014 Conference, May 21-23, 2014, Liberec, pp 69-70.

Fatigue properties of basalt fiber and carbon nanotube reinforced hybridcomposites

J. Szakács,[1,*] L. Mészáros [1,2]
[1]Budapest University of Technology and Economics, Department of Polymer Engineering, Muegyetem rkp. 3., H-1111 Budapest, Hungary
[2]MTA–BME Research Group for Composite Science and Technology, Muegyetem rkp. 3., H-1111 Budapest, Hungary
*corresponding author, e-mail: szakacs@pt.bme.hu

Abstract:
More and more researchers think that using an additional third phase might be an effective way to increase the mechanical performance of the polymer composite or endow it with new properties. This third phase can be another matrix component (thermoplastic or thermoset polymer) or reinforcing material. In the first case the main goal is often to create a co-continuous phase system and this way the energy consumption during the fracture process could be increased (Turcsán *et al.*, 2014). In the second case where two different reinforcing materials are used usually the aim is to increase the strength and the stiffness of the material. Beside microfibers as secondary reinforcing materials nanoparticles are also widely used like nanoclays, carbon nanotubes and graphene (Figure 1.).
Carbon based nanoparticles like carbon nanotubes and graphene have unique electrical, thermal and mechanical properties. Moreover graphene has the greatest tensile strength and modulus among the known materials (Lee *et al*, 2008). Nanoparticles have another great property what is the extremely high aspect ratio. The use of this filler can increase the mechanical attribute of the material.
In one of our previous study (Mészáros *et al*, 2013) positive effect of the nanoparticles on the polymers elasticity has been presented. A special cyclic test was carried out where the load was increased in every cycle. It was showed that the graphene and carbon nanotube efficiently decreased the residual deformation of hybrid composites in every load level that resulted in higher rate of elastic recovery compared to matrix material. That mean this material can be used at higher load level with less residual deformation. This statement may mean that this materials have higher life cycle in case of long time loading (creep and fatuigue)

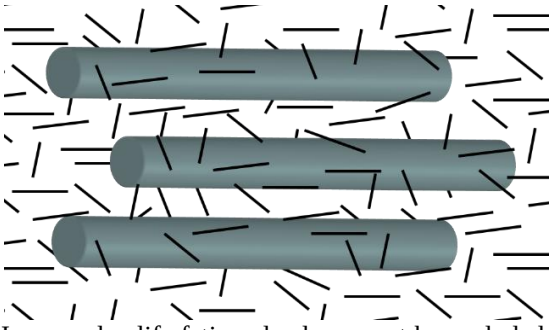

In everyday life fatigue loads can not be excluded in the case of structural polymer composite components. The positive effect of fibre reinforcement on the fatigue properties are well known and deeply investigated. Today, the researchers pay more attention to the fatigue crack propagation and the failure analysis.
The fatigue properties of hybrid reinforced composites is less investigated, however there are some studies that displays the positive effects of the hybridization. Grimmer *et al* (2010) investigated fatigue life of carbon nanotube and glass fibre reinforced epoxy matrix hybrid composites. The presence of relatively low amount of carbon nanotube reduced the cyclic delamination and crack propagation in the material significantly. This effect was more significant at lower levels of cyclic stress.
In this study hybrid composites were produced with carbon nanotube and basalt fibre reinforcement. The goal was to enhance the dispersion of the nanoparticles therefore achieve better quasi-static mechanical and fatigue performance.

Keywords: nanoparticles, carbon nanotube, polyamide, fatigue, hybrid composite

Figure 1: Figure illustrating the base concept of hybrid composites in case of well dispersed nanoparticles (cylinders as fibers and black lines as particles)

References:

Turcsán, T., Mészáros, L. (2014), Development and mechanical properties of carbon fibre reinforced EP/VE hybrid composite systems, *Periodica Polytechnica*, 58, 127-133.

Lee C., Wei X., Kysar J. W., Hone J. (2008), Mesurement of the elastic properties and intrinsic strength of monolayer Graphene, *Science*, 321, 385-388.

Mészáros, L., Szakács, J. (2013), Elastic recovery at graphene reinforced PA 6 nanocomposites. *5th International Nanocon Conference*, Brno, Czech Republic, pp. 1-5. Paper nr. 1955

Grimmer, C. S., Dharan, C. K. H. (2010), Enhancement of delamination fatigue resistance in carbon nanotube reinforced, *Composites Science and Technology*, 70, 901-908.

The influence of redistribution ions in subphase at the properties langmuir monolayer

Chumakov A. S.[1], Ermakov A. V.[1], Kim V. P.[2], Gorbachev I. A.[1], Glukhovskoy E. G.[1]
[1]Departament of nano- and biomedicine technology, Saratov State University named for N.G. Chernyshevsky, Russia
[2]Department of Physics, Moscov State University named for M.V. Lomonosov, Russia

Abstract: Currently, the Langmuir-Blodgett method allows to form monomolecular layers (ML) at the gas-liquid interface and receive a unique layered structure in which each monomolecular layer can have its own chemical composition, crystal structure and orientation of the molecules. Films and Langmuir ML can serve for nanotemplate arranged nanowire arrays, nanotubes or nanoparticles.

The formation of a monolayer and its structure depend on many factors. One of the least studied factors is the influence of the electric field. In this regard, the purpose of this study is to investigate the influence of the direction and magnitude of the electric field on the properties of ML, formed on the surface of water and aqueous solutions of $NiCl_2$.

Our experiments realized for the following cases: in the absence of electric fields, at the different directions of the electric field vector (upwards or downwards), in case of deionized water and $NiCl_2$ aqueous solutions. For these studies we designed the specific electrode system for an existing LB trough and redesigned barriers. The barriers were made in the form of hydrophobic fibers of dielectric material (or wires in the braided PTFE) disposed on the liquid subphase surface. These wires were stretched over a frame, and freely-moving above the upper electrode.

The experiments have revealed: the electric field exerts a significant influence on the formation of monolayers, in particular, during liquid phase formation. The second part of the isotherm (corresponding liquid phase) isotherms were significantly stretched, if subphase of deionized water was used. The increase was about 25% when a voltage to the electrodes was applied. This extension depends not so much on the direction of the vector field, but on the fact that the field is applied. We explain the liquid phase extension by the fact of the charge increasing (and change pH) of the surface region just under the ML. The ions H^+ or OH^- are integrated in the head groups of molecules that leads to the "loosening" of the latter.

If a $NiCl_2$ solution is used as a subphase, then we have the opposite effect. The formation of the liquid phase occurs later under the influence of the field. It is possible that some of the ions OH^- react with Ni^{2+} ions (when a positive potential to the upper electrode is appled) and prevents the salt formation reaction (NiArh), which loosens a monolayer without field. In other polarity tightened ions Cl^-, which do not react with the monolayer because the lower part is charged very negatively, and Ni^{+2} ions move downward, that is blocking the salt formation.
To confirm this assumption we created a new device, which allows us to make a preliminary separation of ions in the water before the experiment, and make a difference in the pH about four units without adding any buffers. This is achieved by using the water-containing vessel, that was divided in 2 parts by a semipermeable membrane (dialysis film) that eliminates the possibility of mechanical agitation of water, but cannot interfere with the free movement of ions. Thus, when we create a difference of potential between the different parts of the vessel, the ions are able to be separated and we obtain virtually pure (from chemical point of view) water, but its acidity will differ from the neutral pH value. Isotherms obtained on the preformed water have more clearly showed effect discovered previously, i.e. the increase of the area of conventional surfactant molecules at the part of liquid phase. This indicates that the separation of ions is a key factor that change the structure of the monolayer when electric field is applied.

Keywords: Langmuir-Blodgett method, monolayers, electric field, pH, isotherms.

The work is supported by grant № 14-12-00275 of Russian Science Foundation and Saratov State University.

References:

Glukhovskoy E.G. (RU), Brezesinski Gerald B. (DE), Gorbachev I.A. (RU), Kim V.P. (RU), Gur'yanov V.A. (RU) Device for the formation of monolayers by the Langmuir-Blodgett method in an electric field // Pat. RU 111297 IPC G01N 13/02. The Patentholder - Saratov State University named after N.G.Chernyshevsky. Published on: 10.12.2011. *Bul. № 34*

Chumakov A., Ermakov A., Kim V., Gorbachev I., Glukhovskoy E. Langmuir monolayers in the electric field // Symposium: Optics & Biophotonics. Saratov Fall Meeting 2013 (SFM'13). 25–28 Sept. 2013. Workshop: Low-dimensional structures III (Oral Report). URL: http://sfm.eventry.org/report/724

Control possibility of separation surfactant from nanoparticles solution by Langmuir method

K.I. Kosolapova [1], A.J.K. Al-Alwani [1], E.G. Glukhovskoy [1,2]
[1]Faculty of Nano- and Biomedical Technologies, Saratov State University, Russia
[2] Department of Educational and Research Institute of Nanostructures and Biosystems, Saratov State University , Russia

Abstract: Nanoparticles rectify it's very difficult due to small size (2-5nm). As well it's difficult due to a small selection of suitable solvents, irreversible adsorption with other materials, aggregation. Aggregation nanoparticles lead to a change in the size of the system elements. Change in the size of the system to make difficult selection of membrane with pore to a certain size.

In this work presented the results of studied that show the possibility of purification by membrane filtration solutions nanoparticles in chloroform/toluene and control possibility of separation undesirable molecules from nanoparticles solution by Langmuir method.

As you know for realization of Langmuir method for studying of monolayer on the water surfaces with very small concentration of solutions of nanoparticles. Typical concentrations are between 10^{-3} and 10^{-4} M.

By the experiment can be realized «inverse-problem» method: the determination of the solution concentration on the base knowledge parameters from compression isotherms.

Present results of experimental use one of the low-cost materials for the membrane. It was used for separation of organic molecules of the stabilizer (oleic acid) from initial solution nanoparticles.

Purification of nanoparticles, stabilized oleic acid, was carried out with using a specially assembled unit for 168 hours. Isotherm compression of the external solution were removing for observation and diffusion control during this time.

The solution of colloidal quantum dots stabilized oleic acid in chloroform to about 10^{-6} M concentration of 500 µl was placed in a dialysis bag which was immersed in the box with chloroform. The internal volume of the solution in the package was 500 µl , the volume of the external solution in a bank – 50 ml.

As a vessel for carry through a membrane filter was taken jar reagent plastic screw cap 100 ml.

Control and monitoring the diffusion of the surfactant through the membrane was done by measuring the surface pressure (isothermal compression) of the external solution. To measure the surface pressure setting used KSV Nima LB Trough KN2002.

Compression isotherms were recorded every 24 hours. For cleanliness before each measurement surface degreasing bath and purified with chloroform. As subphase used deionized water with a resistivity of 18 MOhm × cm. On the surface of the water each time make the same amount of material from the outer volume (of the solution in a glass container) – 500 µl. (Fig.1)

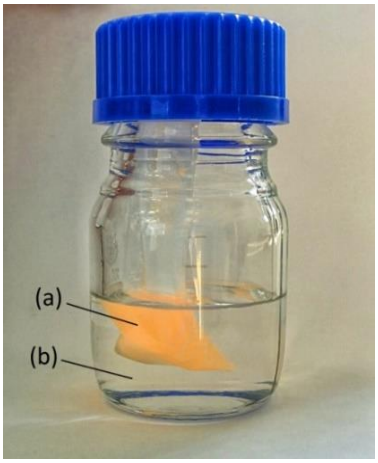

Fig.1. The process of separation: nanoparticles membrane solution bag (a), chloroform (b).

To investigate the changes in the number of surfactant in the external volume of the solution used Langmuir-Blodgett technique. In the process of compression isotherms were taken the outside solution during the membrane filtration of the solution of nanoparticles.

It is noticeable that the increases of maximum surface pressure with increasing filtration time. Obviously the Reducing of length of gas phase of external solution is due to increase the number of unbound molecules in the external volume of the solution. This growth is due to the process of diffusion of unbound molecules of oleic acid through polyethylene membrane.

Keywords: separation, purification, nanoparticles, pressure isotherms, Langmuir monolayer, Langmuir–Blodgett technique.

The work is supported by grant № 14-12-00275 of Russian Science Foundation and Saratov State University.

Analyzing size dependence of thermal conductivity of suspended graphene with Null-Point Scanning Thermal Microscopy

Gwangseok Hwang,[1,2] Ohmyoung Kwon,[1,*]
[1]School of Mechanical engineering, Korea University, Seoul, Republic of Korea
[2]TSP Nanoscopy, Seoul, Republic of Korea

Abstract: The characteristic length of graphene devices is approaching or even getting shorter than the mean free path of phonon. Thus, the size effect on the thermal conductivity of graphene should be seriously considered in the development of graphene-based nano-devices. However, current techniques used to measure the thermal conductivity of graphene, such as Raman spectroscopy and the thermal bridge method, are not suitable for observing such a size effect at the sub-micron scale. In this study, we rigorously re-derived the principal equation of null point scanning thermal microscopy (NP SThM) in terms of measuring the thermal properties to explain how this technique, which has already been proven to resolve the major problems of conventional SThM and be able to quantitatively measure the temperature profile (Hwang *et al.*, 2014; Yoon *et al.*, 2014), can be effectively utilized for quantitatively measuring the local thermal resistance with a nanoscale spatial resolution. Using NP SThM, we measured the relative change in the thermal conductivity of suspended chemical vapor deposition (CVD)-grown graphene disks with radii of 50–3680 nm and estimated the absolute value of the thermal conductivity of these disks in a diffusive regime (Figure 1, 2). We performed a theoretical analysis to demonstrate that the relative changes and absolute values of the thermal conductivity of the graphene disks were consistent. As demonstrated in this study, NP SThM will be very useful for the quantitative thermal characterization of not only CVD-grown graphene but various other nano-materials and -devices.

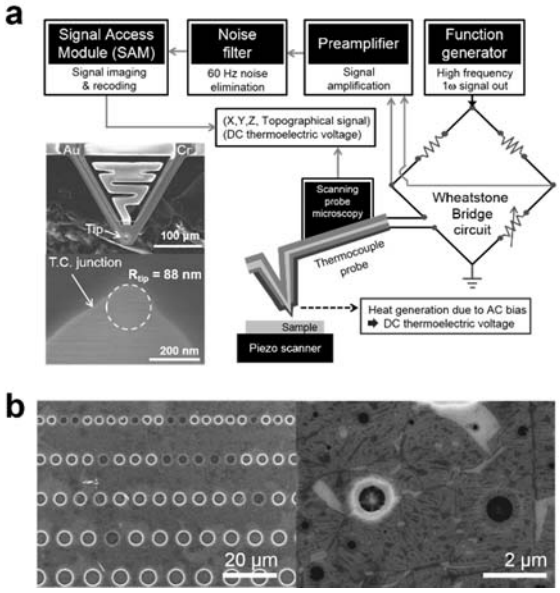

Figure 1: (a) Schematic diagram of experimental setup for NP SThM and SEM images of thermocouple SThM probes. (b) SEM images of micro- and nano-scale suspended CVD-grown graphene disks.

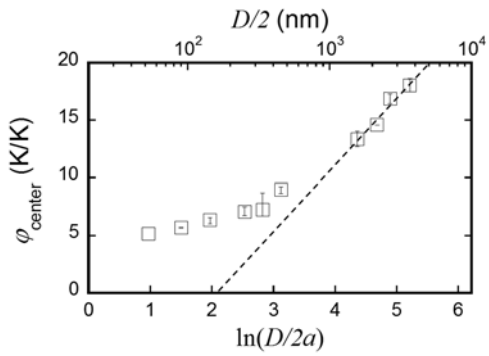

Figure 2: Value of φ at center of disk (φ_{center}) measured by NP SThM as function of ln ($D/2a$) for ten suspended graphene disks with radii of 50–3680 nm. Because $\varphi_{center} = (R_s + R_c)/R_p$ and R_p and R_c remain constant during the scanning, a change in φ_{center} means a change in R_s.

Keywords: graphene, thermal conductivity, null point scanning thermal microscopy (NP SThM), ballistic heat transport, diffusive transport, size effect, SThM probe, nanoscale thermal measurement.

Acknowledgments:
This work was supported by the Basic Science Research Program (NRF-2013R1A1A2012138) and Nano-material Technology Development Program (Green Nano Technology Development Program) (No. 2011-0030146) through the National Research Foundation of Korea (NRF) funded by the Ministry of Education, Science and Technology.

References:

Hwang, G., Chung, J., Kwon, O. (2014) Enabling low-noise null-point scanning thermal microscopy by the optimization of scanning thermal microscope probe through a rigorous theory of quantitative measurement, *Rev. Sci. Instrum.*, 85, 114901.

Yoon, K., Hwang, G., Chung, J., Kim, H., Kwon, O., Kihm, K. D., Lee, J. S. (2014) Measuring the thermal conductivity of residue-free suspended graphene bridge using null point scanning thermal microscopy, *Carbon*, 76, 77-83.

Three-Arm Star Block-Copolymers: Enzyme-Inspired Catalysts for Oxidation of Alcohols in Water

C. Mugemana, B.-T. Chen, K. V. Bukhryakov and V. Rodionov*[1]
[1]KAUST Catalysis Center and Division of Physical Sciences and Engineering,
King Abdullah University of Science and Technology, Thuwal, 23955-6900,
Kingdom of Saudi Arabia
*Email: valentin.rodionov@kaust.edu.sa

Abstract: The oxidation of alcohols to aldehydes has become the most challenging class of oxidation reaction in organic chemical synthesis since the large-scale applications are limited by safety issues associated with the combination of O_2 and organic solvents. The Cu/TEMPO (2,2,6,6-tetramethyl-1-piperidine-N-oxyl) system has emerged as one of the most attractive catalysts for selective aerobic oxidation of primary alcohols. (Stahl et al., 2011) The established protocols for Cu/TEMPO catalyzed alcohol oxidation strongly favor organic solvents, especially acetonitrile. We aimed to design an enzyme-inspired functional macromolecular architecture that could enable the transfer of this catalytic system to pure water. Such a transfer could enable large-scale applications of Cu/TEMPO, while circumventing the usual safety concerns associated with combining oxygen and organic solvents

The use of dendrimers (Astruc et al, 2001) and hyperbanched polymers (Fréchet et al, 2005) has been a successful strategy for improving catalyst dispersion properties and creating optimal local solvent environment. In this study, we present a pathway to enzyme-inspired catalytic materials based on star block-copolymers with limited branching. (Rodionov et al, 2014) These polymers incorporate hydrophilic, superhydrophobic, and polydentate metal-binding characteristics. (Figure 1) Starting with a tripodal, TBTA – inspired NMP initiator, a library of flurous amphiphilic star block copolymers was synthesized. These polymers assembled into well-defined nanostructures in water, and their mode of assembly could be controlled by changing the composition of the polymer. The prepared micelles were used for enzyme-inspired catalysis of alcohol oxidation.

Keywords: star polymers, enzyme-inspired catalyst, micelles, vesicles, homogenous catalysis, alcohol oxidation, block coppolymer self-assembly.

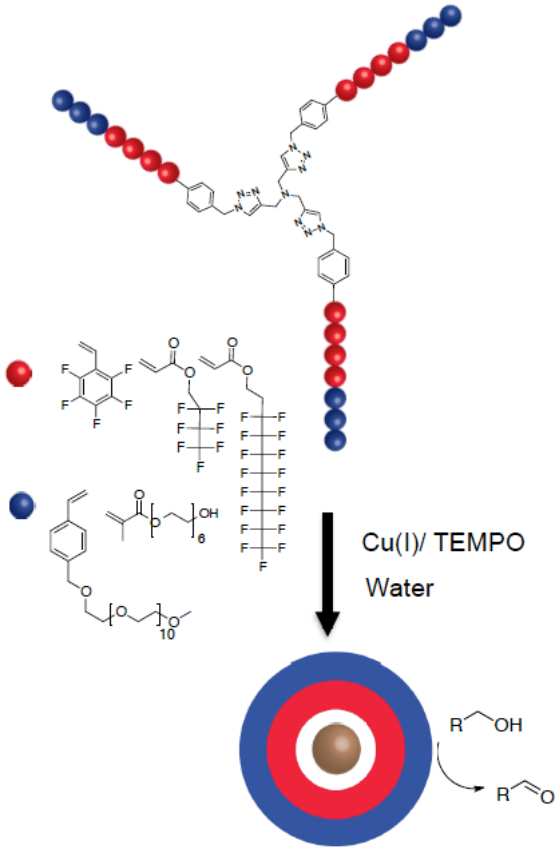

Figure 1: Representative scheme of three-arm block copolymers, their self-assembly in water and catalytic aerobic alcohol oxidation.

References:

Hoover, J.M., Stahl, S.S., (2011) Highly Practical Copper(I)/TEMPO Catalyst System for Chemoselective Aerobic Oxidation of Primary Alcohols *J. Am. Chem. Soc.* 133, 16901-16910.

Astruc, D., Chardac, F. (2001), Dendritic catalysts and dendrimers in catalysis, *Chem. Rev*, 101, 2991-3024

Helms, B., Guillaudeu, S.J., Xie, Y., Mcmurdo, M. Hawker, C.J., Fréchet, J.M.J. (2005), One-pot reaction cascade using star polymers with core-confined catalyst, *Angew. Chem. Int. Ed.*, 44, 6384-6387.

Mugemana, C., Batian, C.-T., Bukhriakov, K.V. Rodionov, V. (2014) Star Block-Copolymers: Enzyme-Inspired Catalysts for Oxidation of Alcohols in Water, *Chem. Commun.* 50, 7862-7865.

Hydrophobic Material with Polymeric Shell

G. Sugurbekova, A.Seralin, G.Demeuova, M.Baisariyev
Nazarbayev University, National Laboratory Astana, Astana city, Kazakhstan

Abstract:
Development of new materials and modification of surface, physical and chemical properties of nanostructured objects can greatly expand the range of possibilities for high technology and brings to the new level their application in various industries.

This study aims to obtain hydrophobic materials for multipurpose applications, including moisture-saving technologies in agriculture and construction.

We have proposed technology of producing superhydrophobic materials based on polymer, sand and fertilizer, which allows to regulate hydrophobic properties of materials by directional formation and surface modification. Superhydrophobic materials produced using this cheap and environmentally friendly technology exhibit high thermal stability and good performance. Use of complex mineral fertilizers of prolonged action also promotes the formation of superhydrophobic structured material.

Surfaces of superhydrophobic powder have complicated relief. Air bubbles can stabilize on the rough surface of the material, as a result forming a stable "air bag" condition in the cavities of the relief. When tested with water for water resistance, fluid was observed to partially flow over the gas phase than solid surface. At the liquid-gas interface, friction is very limited, which leads to a sudden increase of sliding capacity of such surfaces.

Studies were conducted to determine the wetting contact angle using a goniometer to determine the degree of hydrophobicity. Several types of superhydrophobic powders were obtained with contact angles of about 157 ° (Figure 1). Scanning electron microscopy (SEM) images depicting microstructure of the surface of materials showed that the composite materials consist of microparticles with core-shell structure.

The composition of the structures was studied using FTIR-spectral analysis method. IR spectra (Figure 2) of initial, intermediate and final products shows an acute, intense peak at 1258 cm^{-1}, indicating the presence of valence vibrations of $\vartheta_{(Si\text{-}CH3)}$. Relatively low peak at 2355 cm^{-1} refers to the fluctuations of hydrocarbon group CH_2, whereas bands at 2960 cm^{-1} refers to the fluctuations of CH_3. In the region from 787 to 790 cm^{-1} there is a very intense band with a shoulder at 668 cm^{-1}, which is also an indication of Si-C bonding. In the area of 1040 cm^{-1} Si-O-Si bridging is identified, followed by Si-O at 1010 cm^{-1}.
Keywords: Hydrophobic powder, hydrophobization, core-shell structure

Figure 1: Water droplet at the surface of hydrophobic material with a contact angle of 157°.

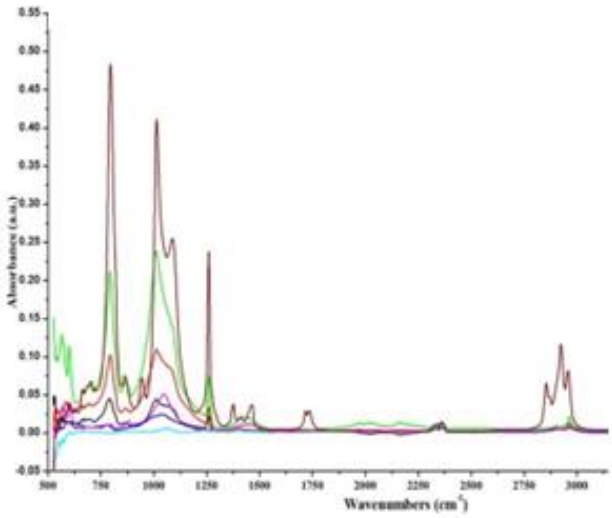

Figure 2: IR spectra of initial, intermediate and final products

Acknowledgement

This project was funded by Office of commercialization of PI “Nazarbayev University Research and Innovation System” based on Nazarbayev University.

New Performances of Fluorescent Photosensitive Glass Ceramics for Petabyte Optical Disk 3D Written by Direct Laser Interaction

S. I. Jinga,[1,*]E. Pavel[2]
[1*]Faculty of Applied Chemistry and Materials Science, "Politehnica" University of Bucharest, 011061 Bucharest, Romania
[2]Storex Technologies, 020892 Bucharest, Romania

Abstract: We report novel results for 3D recording of an optical disk with ultra-high density by changing glass matrix compositions and equilibrium between silver nanocrystals and fluorescent nanostructures. In the same time we try to find out which are the best ways to minimize the distances between fluorescent structures in 3D architectures of optical disks and to increase fluorescence intensity of 5nm cylindrical structure in order to achieve good performances in reading process of 3 D optical disk.
Our previous results [1-3] demonstrate the possibility to exceed the diffraction limit in glass- ceramics using a laser radiation with low energy.
Also, we demonstrate the performance of glass – ceramics which is able to storage up to density greater than 6 PB/disk [4].

Keywords: fluorescent photosensitive glass-ceramics, 3D direct laser writing, optical disk, data storage.

References:

1. Pavel E, Mihailecu M, Nicolae V B, Jinga S, Andronescu E, Rotiu E, et al. Holographic testing of fluorescent photosensitive glass-ceramics. Opt Commun 2011;284:930–3.

2. Pavel E, Jinga S, Andronescu E, Vasile B S ,Rotiu E ,Ionescu L, et al. 5nm structures produced by direct laser writing. Nanotechnology 2011; 22:025301.

3. Pavel E, Jinga S, Andronescu E, Vasile B S, Kada G, Tosa N,et al. 2nm quantum optical lithography. Opt Commun 2013; 291:259–63.

4. Pavel E, Jinga SI, Vasile BS, Dinescu A, Marinescu V, Trusca R, et al. Quantum optical lithographyfrom 1nm resolution to patterntransfer on silicon wafer. Opt LaserTechnol, 2014; 60:80–4

Pavel E, Jinga SI, Vasile BS, Dinescu A, Tosa N, Trusca R, 3D direct laser writing of Petabyte Optical Disk, Opt LaserTechnol, 2015; 71, 45-49

Iron Nanoparticles-Doped Water Treatment Residues for Arsenic Removal from Industrail Wastewater

P. Sarntanayoot, A. Imyim*
Department of Chemistry, Faculty of Science, Chulalongkorn University, Bangkok 10330, Thailand

Abstract: Arsenic (As) has been used in various industrial fields including agriculture, electronics, and metallurgy. Industrail wastewater can be contaminated by high levei of arsenic. Therefore, methods for the removal of arsenic from contaminated wastewater are critical and necessary. Adsorption is a commonly employed method for arsenic removal from aquous media. Various types of adsorbent have been developed. Arsenic is mostly found in inorganic forms which are trivalent (arsenite or As(III)) and pentavalent (arsenate or As(V)). Most of th adsorbents are effective only for As(V) removal. As(III) has to be oxdised using oxidizing agents such as chlorine dioxide, hypochlorite, potassium permanganate and monochloramine (Sorlini and Gialdini, 2012) to As(V) before its removal by adsorption. Zero-valent iron nanoparticles were also employed for simultaneous oxidation and reduction of As(III) to promote its removal efficiency (Du *et al*., 2013, Ramos *et al*., 2009, Yan *et al*., 2012). Low cost adsorbents such as water treatment residues (WTR) showed arsenic removal potential towards As(III) and As(V) due to alum and ferric hydroxide composition in the WTR (Kim *et al*. 2012). However, the removal efficiency of As(III) was still low. Thus in this research, the WTR is doped by iron nanoparticles and used for the removal of arsenic. The amount of iron was varied in the range of 2-10 %(w/w). The maximum As(III) adsorption capacities were 9.4, 11.8, 13.2,13.5, 15.1, 24.2 mg/g for 2, 4, 5, 6, 8, and 10 %(w/w) of loading iron. While the maximum As(III) adsorption capacity of bare WTR was 2.3 mg/g. The result reveals that iron nanoparticles plays an important role in the enhancement of adsorption capacity of As(III). In addition, the maximum As(V) adsorption capacity was 32.0 mg/g for 10 %(w/w) of loading iron. The pictures of adsorbents as well as SEM image were shown in Figure 1. The prepared materials shows a promising applicability for arsenic removal form high arsenic-contaminated industrail wastewaters.

Keywords: iron nanoparticles, water treatment residues, arsenite, oxidation-adsorption, removal, wastewater.

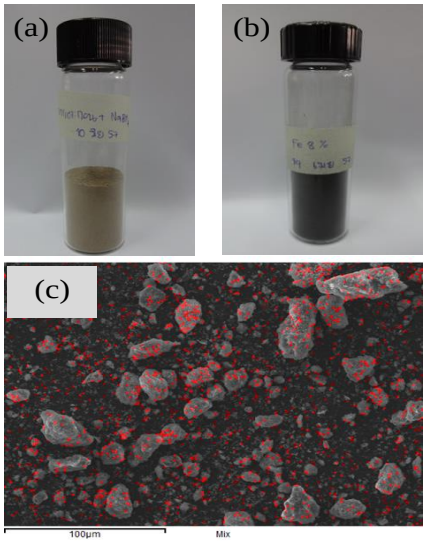

Figure 1: Photographs of (a) water treatment residues, (b) iron nanoparticles-doped water treatment residues, and (c) SEM image with EDX mapping of Fe (red spots).

References:

Du, Q., Zhang, S., Pan, B., Lv, L., Zhang, W., Zhang, Q. (2013) Bifunctional resin-ZVI composites for effective removal of arsenite through simultaneous adsorption and oxidation, *Water Res.*, 47, 6064-6074.

Kim, Y.S., Kim, D.H., Yang, J.S., Baek, K. (2012) Adsorption characteristics of As(III) and As(V) on alum sludge from water purification facilities, *Sep. Sci. Technol.*, 47(14-15), 2211-2217.

Ramos, M.A.V., Yan, W., Li, X., Koel, B.E. (2009) Simultaneous oxidation and reduction of arsenic by zero-valent iron nanoparticles: Understanding the significance of core-shell structure, *J. Phys. Chem. C.*, 113, 14591-14594.

Sorlini, S., Gialdini, F. (2012) Conventional oxidation treatments for the removal of arsenic with chlorine dioxide, hypochlorite, potassium permanganate and monochloramine, *Water Res.*, 44, 5653-5659.

Yan, W., Lien, H.L., Koel, B.E., Zhang, W.X. (2012) Critical review iron nanoparticles for environmental clean-up: Recent developments and future outlook, *Environ. Sci.: Processes Impacts.*, 15, 63-77.

Transfer and biotransformation of gold and silver nanoparticles through aquatic food chain

Xingchen Zhao, Qunfang Zhou, Guibin Jiang
State Key Laboratory of Environmental Chemistry and Ecotoxicology, Research Center for Eco-Environmental Sciences,Chinese Academy of Sciences, Beijing 100085, PR China

Abstract: Considerable attention has been paid recently to nanomaterials not only because of their application possibilities but the potential toxicities to humans and ecosystems. As an emerging environmental pollutant with unknown eco-environmental risks, nanomaterials should not relax our vigilance. Some nanomaterials process similar properties as persistent toxic substances (PTSs) such as less biodegradable and lipophilic. Pollutants like mercury, dichlorodiphenyltrichloroethane, hexachlorocyclohexane have taught us enough lessons how they display destructive forces to the environment (Chikuni *et al.*, 1997; Qiu *et al.*, 2005; Phillips *et al.*, 2005). The risk of nanoparticles entering these environments, as well as the effects on human health from people having contact with the nanoparticles, needs to be carefully assessed and investigated. Among all the food chains, fish-crustacean is one of the pillars of the global aquatic ecosystem. Besides, fish is an economically important species that have long been consumed by humans. Trophic accumulations of nanomaterials from the preys to fish give rise to the possibility that they may transfer finally to humans. In this study, we investigated the trophic transfer of noble metal nanoparticles from fairy shrimp (*Eubranchipus vernalis*) to Japanese medaka (*Oryzias latipes*). Four kinds of nanoparticles, hexadecyltrimethylammonium bromide (CTAB) coated silver nanospheres (CSNSs), CTAB coated gold nanospheres (CGNSs), CTAB coated gold nanorods (CGNRs), and poly(sodium-p-styrenesulfonate) coated gold nanorods (PGNRs) were employed to study the effects of shape, surface coating and core in the trophic transfer. Our findings hold the promise to highlight the potential for trophic transfer as an ecological impact of nanomaterials.

Keywords: silver nanoparticle, gold nanoparticle, uptake and depuration, bioaccumulation, biomagnification, biotransformation, food chain.

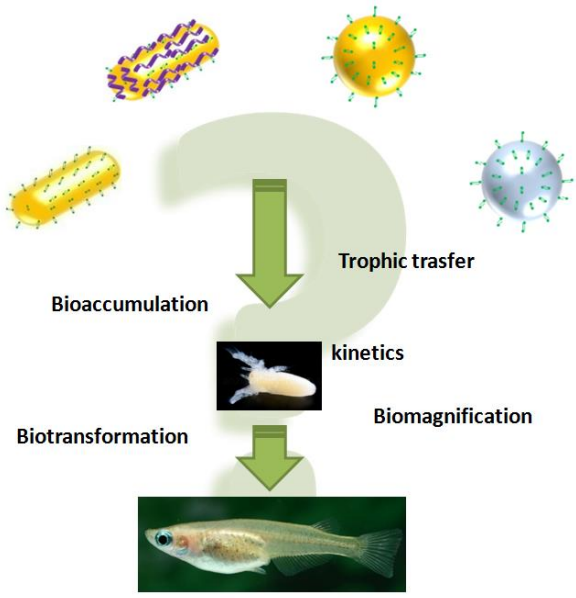

Figure 1: Figure illustrating the questions that we are tempting to solve experimentally: For the four kinds of materials, which one is likely to biomagnify? Which are the target organs for higher trophic level animals and what are the resulting effects for these organs after accumulation? Will nanoparticles transform chemically and physically as they travel up through food chains?

References:

Chikuni, O., Nhachi, C.F., Nyazema, N.Z., Polder, A., Nafstad, I., Skaare J.U. (1997) Assessment of environmental pollution by PCBs, DDT and its metabolites using human milk of mothers in Zimbabwe, *Sci. Total Environ.*, 1-2, 183-190.

Qiu, X., Zhu, T., Yao, B., Hu, J., Hu, S. (2005), Contribution of dicofol to the current DDT pollution in China, *Environ. Sci. Technol..*, 12, 4385-4390.

Phillips T.M., Seech A.G., Lee H., Trevors J.T. (2005), Biodegradation of hexachlorocyclohexane (HCH) by microorganisms, *Biodegradation*, 4, 363-392.

Nanotechnology in Food Packaging Industry: Opportunities and Challenges

Vasco Teixeira
GRF-Functional Coatings Group, Physics Department, University of Minho
PT-4800-058 Guimaraes, Portugal
Tel: +351-253510465/00, Fax: +351-253510401, Email: vasco@fisica.uminho.pt

Abstract: Nanosciences and nanotechnologies are highly promising areas for research and industrial innovation, with a potential both to boost the competitiveness of many industries which will lead to new emerging and fast growing markets. It is predicted that nanotechnology production approaches will change about 25% of the food packaging business in the next decade, which means a yearly over $ 30 billion market. The major market trends include enhancing the performance of packaging materials, prolonging shelf life, antimicrobial packaging and interactive/sensorial packaging.

One of the main priorities in food packaging technology is to keep the original properties of the food. This goal is achieved by keeping all the nutrients in the original conditions, by ensure minimum interaction between environment and the packaged food and reducing microbial growth

In the field of nanoparticles and nanotechnology-based thin films, new approaches using nanoscale effects can be used to design, create or model nanocomposite systems with significantly optimized or enhanced properties of high interest to the food, health and biomedical industry. With the development of nanotechnology in various areas of materials science the potential use of novel surfaces and more reliable materials by employing nanomaterials and nanostructured thin films in food packaging, security pharmaceutical labels, novel polymeric containers for food contact, medical surface instruments, bio-implants, and even coated nanoparticles for bionanotechnology can be considered.

The use of plastic containers in the food and beverage market has dramatically increased because they are lightweight, unbreakable, convenient, resealable and they may be clear. PET bottles have gradually replaced glass bottles and metal cans as the most common packaging for liquid foods, such as carbonated soft drinks, tea, water, soy sauce and edible oil.In this field of new packaging technologies, nanostructured architectures coatings such as nanocomposite films are given the unique role of enhancing food impact over the consumer's health. For example, the unique properties of diamond like carbon (DLC) film, including its chemical inertness and impermeability, make it possible for new applications in food, beverage and medical market segments. The ability of using thin films and nanoparticles with transparent properties a more flexible and transparent packaging materials will provide the consumers with fresher and customized packs where the products can be observed as they are.

In this presentation it will be presented an overview of the nanotechnology approaches to produce nanostructured materials for food and health industry. Topics to be discussed include introduction to nanocoatings concepts (from functional nanocomposite and graded coatings to smart nanomaterial surfaces used in packaging and biomedical industry) produced by clean PVD technologies (Physical Vapour Deposition) and other deposition techniques. An overview of the current research, existing technological applications and future industrial materials and components will be highlighted. As example for future trends in nanotech-based food packaging will also include research and development on sensorial packaging which can monitor the food and transmit information on its quality. For instance, the ultimate pH of meat greatly affects its quality. Monitoring this parameter can give to consumers information regarding manner of transportation of animals from the farm to the abattoir; diet restrictions; mixing animals of different lots and pathological conditions. With embedded nanosensors in the packaging surface materials, consumers will be able to check the food quality inside or even to track the history of the pack. Electronics built on thin film substrates could be used in future sensory packaging applications (examples include nanoRFIDs).

Inkjet printed polymer functionalized CNT gas sensor with enhanced sensing properties

A. S. Alshammari[1,2], M. R. Alenezi[2,3], K. T. Lai[2] and S. R. P. Silva[2]
[1]Department of Physics, College of Science, University of Hail, P.O. Box 2440, Hail, Saudi Arabia
[2]Advanced Technology Institute, Faculty of Engineering and Physical Sciences, University of Surrey, Guildford, GU2 7XH, UK
[3]College of Technological Studies, PAAET, P.O. Box 42325 Shuwaikh, Kuwait

Abstract: Gas sensing devices receive a considerable interest and can be found in wide range of domestic and industrial applications[1,2]. Here we report on fully printed carbon nanotubes gas sensors on flexible substrate with improved ethanol sensing characteristics. The sensors were fabricated via two simple steps: printing of the electrodes and the sensor active layer. The nanotubes were functionalised with carboxylic acid, surfactant and PEDOT:PSS and their sensing performance is investigated. The performance analysis shows significant enhancement in the sensitivity of the sensor with polymer wrapped nanotubes in comparison with other functionalisation methods with enhancement factor greater than 2.5. Moreover, a remarkable improvement in the response and recovery time of the sensor after polymer functionalisation is noticed. The combination of inkjet printing technique and polymer functionalised nanotubes could pave the way towards flexible, solution processable, low cost and high performance gas sensors.

Keywords: carbon nanotubes, polymer functionalization, inkjet printing, gas sensor.

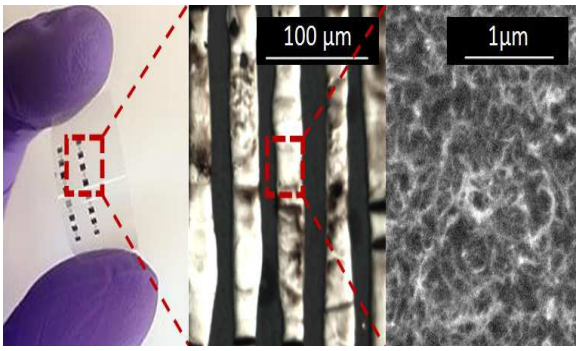

Figure 1: Figure shows a photograph of the printed gas sensor (left), optical microscope image of the printed silver interdigitated electrodes (middle) and SEM image of the printed carbon nanotubes (right).

References:

[1] Liu, C.-K., J.-M. Wu, and H.C. Shih, Sensors and Actuators B-Chemical, **150(2)** (2010) p. 641-648.

[2] M.F. Mabrook, C. Pearson, A.S. Jombert, D.A. Zeze, M.C. Petty, Carbon, **47(3) (**2009) p. 752-757.

Nanoindentation and image characterization of apple tissue and isolated cells (*Malus domestica*) by means of atomic force microscope

Cárdenas-Pérez, S.[1], Chanona-Pérez, J.[1], Neri-Torres, E.E., Marín-Bustamante, M.Q.[1], Cásarez-Santiago, R.G. [1] Méndez-Méndez, J.V.[2], Calderón-Domínguez, G.[1], Suárez-Najera E.[1]

[1]Escuela Nacional de Ciencias Biológicas-Instituto Politécnico Nacional. Prolongación de Carpio y Plan de Ayala s/n México D.F., C.P.11340. [2]Centro de Nanociencias y Micro y Nanotecnologías- Instituto Politécnico Nacional. Luis Enrique Erro s/n, Zacatenco, México

Abstract: The climacteric fruits undergo many morphometric changes during its storage and processing. Therefore, a method to evaluate the cell elastic properties is needed to explain the behavior of fruits during handling and food processing after harvesting at a micro and nanoscale. For this purpose, in this work it is proposed to indent tissue and isolated cells of apple (Golden delicious) using an atomic force microscope (AFM, Bruker, Bioscope Catalyst ScanAsyst, USA) with an indenter probe (NP-10/Sanasyst, Bruker, USA) was proved in order to obtain the corresponding force curves and Young's modulus (YM). The YM is an important parameter of stiffness already reported in literature as an important mechanical property of biologic samples (Milani et al. 2011). The benefit of the AFM is that it has the possibility to combine nano-mechanical properties with topography imaging, which could be very useful for the study of structure-related mechanical properties of fruits at the sub-cellular scale. The isolation of fruit cells in the apple was developed by a simple isolation technique (McAtee et al. 2009) and the tissue was obtained by using a bi-shave which allows to obtain thin slices of apple. Once the cells were isolated and thin tissue were also obtained, the respectively structure was observed in a light microscope for its morphological characterization (Nikon Eclipse Ni , Japan) which is adapted with a digital sight system (Nikon, DS-L3, Japan) this allows the capture of cell images in RGB color. These were analyzed with the software ImageJ v. 1.47 (National Institutes Health, Bethesda, MD, USA) and the shape of cells was characterized (diameter and circularity). The nanoindentation was carried out with the AFM in tissue cells as well as in isolated cells and it was obtained its respective force curves by using the Nanoscope analysis v1.4 software (Bruker, USA) from which the YM was determined by fitting each curve with Hertz model. In Figure 1a and 1b it is shown a the corresponding height image with a regular matrix (8 x 8 points) of nanoindentation points in apple tissue and isolated cell respectively, from which it is obtained the individual force curves as shown in Figure 1c. The force curve is formed by an initial curve (approaching curve) and a second curve (retraction curve) from which it is adjusted the Hertz model in order to obtain YM. The characterization of the isolated cells in 250 total samples showed a slighter difference in cell diameter with 210 ± 27 μm and circularity of 0.68 against cells in tissue with a diameter of 201.91 ± 42 μm and a circularity of 0.53. Otherwise, the YM was obtained in 10 different areas of 5 μm from tissue and isolated cell and a total of 640 curves were obtained. The YM average obtained was 0.740 ± 0.59 MPa for nanoindentation in tissue and 0.274 ± 0.16 MPa in isolated cells, these values correspond to some YM already obtained in other studies (Zdunek and Kurenda 2013). In overall, these studies are particularly useful in fruits because they could help us to explain the mechanical behavior that exists at nanometric level as well as the key of the mechanical changes that occur during post-harvest.

Keywords: nanoindentation, AFM, young´s modulus

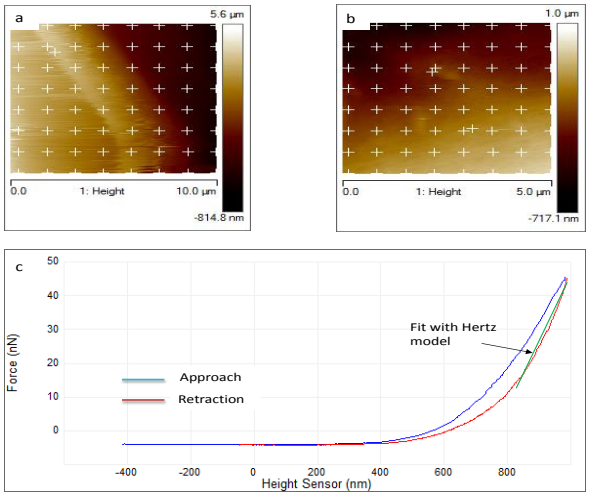

Figure 1 a and b. Illustrates the typical matrix of nanoindentation points from which it is generated the force curves in apple tissue and isolated cell respectively. c. Typical force curve obtained from the NanoScope Analysis software and fitted with Hertz model.

References:

Milani, P., Gholamirad, M., Traas, J., Arnéodo, A., Boudaoud, A., Argoul, F., Hamant, O. (2011). In vivo analysis of local wall stiffness at the shoot apical meristem in Arabidopsis using atomic force microscopy. Plant J 67: 1116–1123.

McAtee, P. A., Hallett, I. H., Johnston J.W., and Robert J. S. (2009). A rapid method of fruit cell isolation for cell size and shape measurements. Plant Methods. 5:5 46-48.

Zdunek, A., Kurenda, A. (2013). Probing plant cell mechanical properties with the atomic force microscope. InsideFood Symposium, 9-12 April 2013, Leuven, Belgium.

The role of the glycocalyx in cellular interactions between lung carcinoma cells and the endothelium

Katarzyna Malek-Zietek, Marta Targosz-Korecka, and Marek Szymonski
Center for Nanometer-Scale Science and Advanced Materials, NANOSAM, Faculty of Physics, Astronomy, and Applied Computer Science, Jagiellonian University, Krakow, Poland

Abstract:

A detailed understanding of the tumor extravasation mechanism is crucial for designing any therapeutic treatment against circulating tumor cells (CTCs) in the bloodstream. The endothelial glycocalyx (eGC) is an intravascular sugar-rich compartment that facilitates gliding of cells in the vascular network, particularly the CTCs. For several pathophysiological states of endothelial cells (ECs), such as inflammatory processes, eGC collapses, gradually shrinks and drops its negative charge. Under such conditions permeability of CTCs trough endothelium is higher and creation of metastases is much more likely. Adhesive interactions between cancer cells and the endothelium strongly depend on the structure of the glycocalyx. Therefore, we characterized the eGC of Primary Pulmonary Artery Endothelial Cells (PHAEC) and the glycocalyx layer of lung carcinoma cells (A549) cultured on fibronectin-rich surface. Nanoindentation spectroscopy with a spherical AFM probe was used to determine the eGC thickness and eGC stiffness before (reference) and after treatment of cells with heparinase I, heparin. Later, the adhesive interactions between lung cancer cells and ECs have been studied. A novel approach was employed to attach the living interactions were validated for living cells containing either a native, or enzymatically digested glycocalyx. Multiparameter analysis of the measured force-distance curves demonstrated that reduction of the glycocalyx layer by heparinise I caused stronger adhesive interactions between A549 cells and PHAEC. Adding to the measurement system heparin instead of heparinase I caused renewal of the glycocalyx and decrease of adhesive interactions between cells. Therefore, we conclude that the structure of the eGC strongly affects the adhesion process between CTCs and the endothelium.

Keywords: glycocalyx, endothelial cells, cancer cells, metastasis, nanoindentation spectroscopy, AFM-based single cell force spectroscopy.

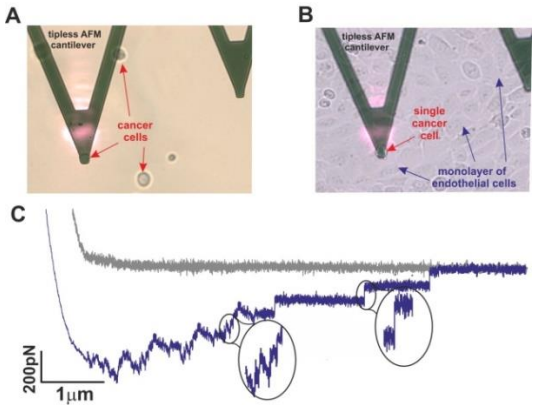

Figure 1: Methodology of single-cell force spectroscopy. **A)** Attaching a living cancer cell to the tip-less AFM cantilever. **B)** Monitoring adhesive interactions between cancer cell and ECs. **C)** Example of the force-distance curve.

Changes of the endothelium nano-mechanics in response to the vascular dysfunction – ex vivo studies for murine model of diabetes

Magdalena Jaglarz[1], Katarzyna Malek-Zietek [1],Marta Targosz-Korecka[1] ,
Stefan Chlopicki[2] and Marek Szymonski[1]
[1]Center for Nanometer-scale Science and Advanced Materials, Department of Physics of Nanostructures and Nanotechnology, Institute of Physics, Jagiellonian University, Prof. Stanislawa Lojasiewicza 11, 30-348 Krakow, Poland
[2] Jagiellonian Centre for Experimental Therapeutics (JCET), Bobrzynskiego 14, 30-348 Krakow, Poland

Abstract:
Endothelium plays an essential role in regulating blood pressure and vascular homeostasis.
The main purpose of the presented study was to relate the observations performed *in vitro* to classical *ex vivo* and *in vivo* models of endothelial dysfunction. Characterization of the endothelial nano-mechanics was performed for the non-fixed aorta in a murine model of hypertension induced by N-nitro-L-arginine methyl ester (L-NAME) as well as in diabetes model (db/db mice).
We have conducted analysis of changes in the morphology and elasticity of the first (from the lumen side) layer (endothelium + basal lamina) of the mouse aorta in healthy and pathological tissues. Elastic properties (stiffness) of the inner tissue surface were characterized using nanoindentation spectroscopy with a colloidal AFM tip, for various areas of the aortic wall.
Both models used in our studies are associated with the development of endothelium dysfunction, which affects the ability to contraction/diastole of the entire vessel. Additionally, biochemical analysis was used in order to determine NO production wich is correlated to nano-mechanical properieties.
Based on AFM nanoindentation model, the stiffnes parameters were determined for various stages of the diabetes development.The nanoindentation measurements revealed changes in stiffnes prameter of the first layer prior to NO release.The qualitative analysis of the tissue elasticity indicates that the above-mentioned diseases induce nanomechanical changes in the first layer of the aorta.

Keywords: Atomic Force Microscopy, Hyperglycemia, hypertension , vascular dysfunction.

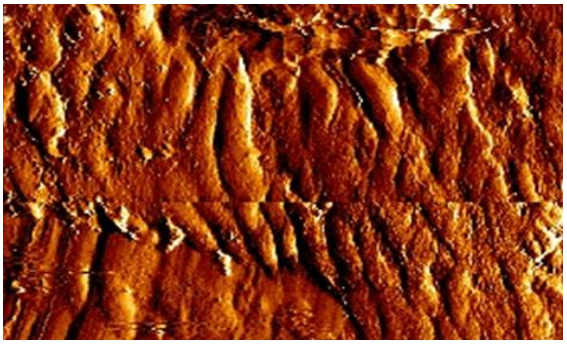

Figure 1: The morphology of the endothelial inner wall surface of the mouse aorta - control sample.

Posters Session II – A
Nanotech in Life Sciences and Medicine

Assessment of protein aggregates in the presence of nanoscale vaccine adjuvants.

M.J.W. Johnston, G.E. Frahm.

Biologics and Genetic Therapies Directorate, Health Canada, Ottawa, Canada

Abstract: The presence of sub-visible particles in therapeutic protein products has increasingly become a field of concern for the pharmaceutical industry and regulatory agencies [1,2]. Aggregates in the size range of 0.1-10 μm have been implicated in adverse reactions and/or reduction in efficacy of therapeutic products [1–5]. Micro flow imaging techniques have been developed for quantifying and characterizing sub-visible aggregates in the range of 2 to 80 microns [15(6)]. As valuable as these techniques are, the presence of opaque excipients or drug carrier systems (such as liposomes) for therapeutic proteins or vaccine adjuvants (such as lipid emulsions or cationic liposomes) may complicate their use. Presented here are studies to determine the capability of micro flow imaging to characterize and quantify particle standards (polystyrene (PS) microspheres, glass microspheres) or intentionally aggregated proteins when formulated with commercially available nanoscale adjuvants such as squalene based emulsions (approx. 200nm) or cationic liposomes (approx. 100nm). We report that micro flow imaging with a FlowCAM instrument can accurately count and size particle standards up to 50% emulsion or 100mM lipid concentration with 100nm liposomes. However we note that as supplied, squalene based emulsions contained 10-40 μm aggregates that present similar optical properties to PS and glass particle standards making calibration in this size range very difficult (Figure 1A). These aggregates may have implications for the assessment of therapeutic samples. Filtering the emulsion with a 0.22 μm membrane removed the aggregates and easily allows for assessment of standards in this size range. We also report on the ability of the instrument to characterize aggregates of model proteins (Figure 1B) for both squalene and liposome based nanoscale adjuvants.

Keywords: Vaccines, nano adjuvants, liposomes, emulsion

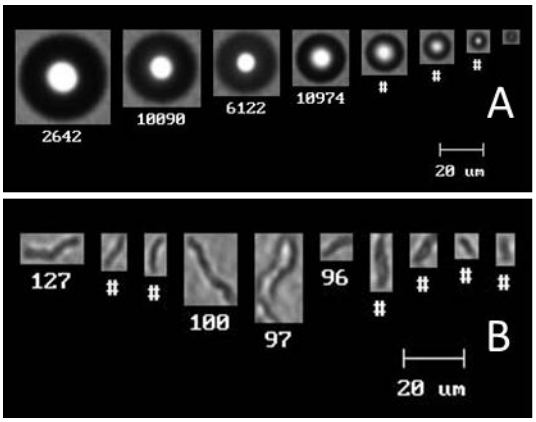

Figure 1. A: Aggregates found in unfiltered squalene based adjuvant showing similar morphology to polystyrene standards. B: Aggregates of BSA identified in the presence of liposome nanoscale adjuvants.

References:

1. Ripple DC, Dimitrova MN (2012) Protein particles: what we know and what we do not know. J Pharm Sci 101: 3568-3579.

2. Carpenter JF et al. (2009) Overlooking subvisible particles in therapeutic protein products: gaps that may compromise product quality. J Pharm Sci 98: 1201-1205.

3. Wang W. et al. (2012) Immunogenicity of protein aggregates--concerns and realities. Int J Pharm 431: 1-11.

4. Ratanji KD, Derrick JP, Dearman RJ, Kimber I (2013) Immunogenicity of therapeutic proteins: Influence of aggregation. J Immunotoxicol .

5. Carpenter J. et al. (2010) Meeting report on protein particles and immunogenicity of therapeutic proteins: filling in the gaps in risk evaluation and mitigation. Biologicals 38: 602-611.

6. Sharma DK, Oma P, Pollo MJ, Sukumar M (2010) Quantification and characterization of subvisible proteinaceous particles in opalescent mAb formulations using micro-flow imaging. J Pharm Sci 99: 2628-2642.

Kiteplatin Delivery by Hydroxyapatite Nanocrystals for the Treatment of Cancer.

Nicola Margiotta,[1,*] Marco Lelli,[2] Valentina Gandin,[3] Cristina Marzano,[3] Selene Merli,[2] Salvatore Savino,[1] Norberto Roveri,[2] James D. Hoeschele,[4] Giovanni Natile.[1]

[1]*Dipartimento di Chimica, Università degli Studi di Bari Aldo Moro. Via E. Orabona 4, 70125 Bari (Italy);*
[2]*Dipartimento di Chimica "G. Ciamician", Alma Mater Studiorum Università di Bologna, Bologna (Italy);*
[3]*Università di Padova, Dipartimento di Scienze del Farmaco, Via F. Marzolo 5, 35131 Padova (Italy);*
[4]*Department of Chemistry, Eastern Michigan University, Ypsilanti, Michigan 48197 (USA).*

Abstract: We have recently investigated the use of nanocrystalline hydroxypatite (HA) as bone-specific platinum-drug delivery device for the treatment of bone tumors by local implantation at the site of an osteosarcoma.[1-3] The inorganic composite materials can act both as bone substitute and as platinum drug releasing agent, with the score of inhibiting locally the tumour re-growth and of reducing the systemic toxicity typical of cisplatin (*cis*-$[PtCl_2(NH_3)_2]$) and other platinum-based antitumor drugs.

In the search for new Pt(II) derivatives endowed with broader spectrum of activity and inferior toxicity with respect to clinical approved antitumor Platinum drugs, we have recently highlighted that the oxaliplatin analog $[PtCl_2$(*cis*-1,4-DACH)] (kiteplatin; DACH = diaminocyclohexane) possessed a unique anticancer potential, being effective against several solid cancers. Furthermore, this derivative was able to circumvent both cisplatin and oxaliplatin resistance.[4]

We present in this work our attempts to load injectable HA nanocrystals with kiteplatin and its derivative [Pt(CBDCA)(*cis*-1,4-DACH)] (CBDCA = cyclobutanedicarboxylate) to be delivered at the site of solid cancers or of the skeletal metastases caused by many tumors.

The adsortption and desorption profiles have been determined by measuring, by ICP-MS, the concentration of Pt complexes remaining in the physiological-like buffers as a function of time.

The HAs used in this study form nanostructured aggregates of micrometric dimensions. However, the state of aggregation changes completely after the interaction with the platinum drug. The influence of pH on the release of the Pt-drugs from the composites has also been investigated.

The cytotoxic activity of the apatite-released Pt complexes has been tested against a panel of human carcinoma cell lines and in a human cancer cell line suitably selected for resistance to oxaliplatin or cisplatin. Cytotoxicity profiles of the apatite-released kiteplatin derivatives are discussed and compared with those obtained with the reference Pt chemotherapeutic drugs.

Keywords: platinum-based antitumor drugs, kiteplatin, injectable nanocrystals, hydroxyapatite, in vitro cytotoxicity, colorectal cancer.

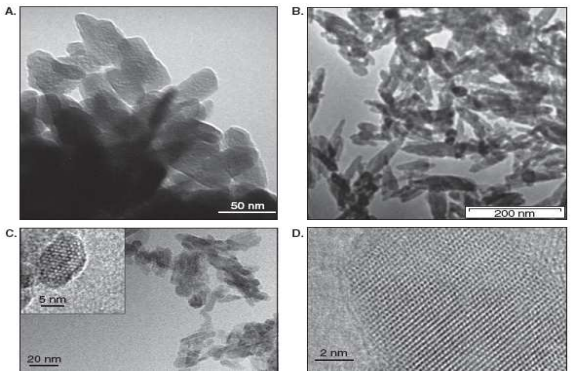

Figure 1: TEM high resolution images of hydroxyapatite nanocrystals loaded with the antitumor Pt-based drug kiteplatin. The controlled release of the platinum drug from the composite material could allow the obtainment of a cytotoxic effect against cancer cells.

References:

[1] M. Iafisco, N. Margiotta. *J. Inorg. Biochem.* **2012**, *117*, 237-247.
[2] M. Iafisco, B. Palazzo, *et al. J. Mater. Chem.* **2009**, *19*, 8385–8392.
[3] M. Iafisco, B. Palazzo, G.. Martra, N. Margiotta, S. Piccinonna, G. Natile, V. Gandin, C. Marzano, N. Roveri. *Nanoscale* **2012**, *4*, 206-217.
[4] N. Margiotta, C. Marzano, V. Gandin, D. Osella, M. Ravera, E. Gabano, J.A. Platts, E. Petruzzella, J.D. Hoeschele, G. Natile. *J. Med. Chem.* **2012**, *55*. 7182-7192.

Acknowledgments: the authors thank the University of Bari, the Italian "Ministero dell'Università e della Ricerca" (FIRB Accordi di Programma RBAP114AMK_009 – Rete Integrata per la Nano Medicina, RINAME), and the Inter-University Consortium for Research on the Chemistry of Metal Ions in Biological Systems (C.I.R.C.M.S.B., Bari, Italy) for support.

Self Micro-Emulsifying Drug Delivery Systems (SMEDDS) of Clove Oil for Fish Anesthesia

K. Janngeon,[1,*] S. Pikulkaew,[2] W. Chaisri[2], S. Okonogi[1,3]

[1]Chiang Mai University, Nanoscience and Nanotechnology Programme, The Graduate School, Chiang Mai, Thailand
[2]Chiang Mai University, Department of Food Animal Clinic, Faculty of Veterinary Medicine, Chiang Mai, Thailand
[3]Chiang Mai University, Department of Pharmaceutical Sciences, Faculty of Pharmacy, Chiang Mai, Thailand

Abstract: Self micro-emulsifying drug delivery systems (SMEDDS) are specialized form of delivery systems which form fine oil-in-water (O/W) microemulsions when exposed to aqueous media under conditions of gentle agitation or digestive motility that would be encountered in the GI tract (Attama and Nkemnele, 2005). Clove oil has been used as fish anesthetic agent but its lipid nature leads to a problem of aqueous miscibility (Cho and Heath, 2000). In this study, SMEDDS have been developed to enhance the aqueous solubility of clove oil. The formulations of the selected clove oil loaded SMEDDS (C-SMEDDS) were optimized by solubility assay, compatibility tests, and pseudo-ternary phase diagrams analysis. The pseudo-ternary phase diagrams were constructed using water titration method (Chen *et al*., 2004). Suitable formulations of C-SMEDDS were selected from the pseudo-ternary phase diagrams; Tween20 was used as a surfactant and ethanol or isopropanol was used as a co-surfactant (Figure 1). The formulations were further characterized by electrical conductivity, viscosity, particle size and morphology of the dispersed phase of the microemulsion. Selected C-SMEDDS were O/W microemulsion after mixing with water with the spherical internal droplet size of 11.1-43.6 nm and size distribution of 0.2-0.3 nm. The C-SMEDDS composed of 2:1 ratio of surfactant to co-surfactant showed high electrical conductivity of 17.8-26.6 µS/cm and low viscosity of 0.02-0.04 Pas. The C-SMEDDS stored at different conditions for 90 days demonstrated high physical stability at 4°C and room temperature. No phase separation was found in all temperature of storage but the color change from pale yellow to intense yellow was found in those kept at 45°C. The *in vivo* anesthetic activity of the selected C-SMEDDS, using clove oil ethanolic solution as a control was investigated in two fish species; *Cyprinus carpiokoi* and *Oreochromis niloticus*. It was found that the C-SMEDDS significantly caused shorter anesthetic induction time than the control solution in both kinds of fish. However, the anesthetic recovery time was depended on the type of the fish. *O. niloticus* received the C-SMEDDS showed shorter time of recovery than those received the control, in contrast with *C. carpiokoi* that showed longer recovery time than the control group.

Keywords: SMEDDS, clove oil, fish anesthesia, Tween20, ethanol, isopropanol

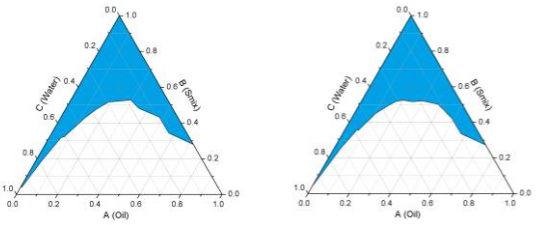

Tween20: ethanol Tween20: isopropanol

Figure 1: Pseudoternary phase diagrams of clove oil, Tween20, ethanol or isopropanol as co-surfactant and water. The ratio of surfactant and co-surfactant was 2:1.

References:

Attama A.A., Nkemnele, M.O. (2005), *In vitro* evaluation of drug release from self micro-emulsifying drug delivery systems using a biodegradable homolipid from *Capra hircus*, *Int. J. Pharm*., 304, 4-10.

Chen, H., Chang, X., Weng, T., Zhao, X., Gao, Z., Yang, Y., Xu, H., Yang. X. (2004), A study of microemulsion systems for transdermal delivery of triptolide. *J. Control. Release.*, 98, 427-436.

Cho, G.K., Heath, D.D. (2000), Comparison of tricaine methanesulphonate (MS222) and clove oil anaesthesia effects on the physiology of juvenile chinook salmon *Oncorhynchus tshawytscha* (Walbaum), *Aquac. Res*,. 31, 537-546.

Development and characerization of bovine serum albumin nanoparticles of amphotericin B

D. B. Ludwig,[1*] L. S. Pedroso,[1,2] N. M. Khalil,[1] R. M. Mainardes[1]
[1]State University of Midwest, UNICENTRO, Laboratory of Pharmaceutical Nanotechnology, Guarapuava, Brazil
[2]Guairacá College, Department of Pharmacy, Guarapuava, Brazil

Abstract: Amphotericin B (AmB), an antibiotic of polyene class, is naturally produced by *Streptomyces nodosus* (Gold *et al*.; 1956). This antifungal is the main choice for the treatment of sistemic fungal diseases, highlighting infections caused by *Cryptococcus neoformans* (Davey *et al*.; 1998). The most important problem for to use AmB is the toxicity. This antibiotic can cause many problems like nephrotoxicity, cardiotoxicity, hepatotoxicity, haematotoxicity and neutropenia (Annaloro *et al*.; 2009). The pharmaceutical nanotechnology is a good choice to reduce the problems with the toxicity of AmB because the nanoparticles can control the delivery of this polyene and can increase the pharmacokinetics properties for many kind of compounds (Mainardes *et al*.; 2010). The aim of this work is to develop and to characterize the AmB nanoparticles to treat meningitis caused by *C. neoformans*. The chosen method to obtain the nanoparticles was the coacervation method using bovine serum albumin. After the nanoparticle size and the polydispersity index were measured and the stability in freezer for seven weeks was tested. The obtained results were a good nanoparticle size with mean of 197,8 ± 28,7 nm and the polydispersity index with mean of 0,235 ± 0,085. The stability test was performed in freezer and the results was promising because the nanoparticle size mantained nearby 200 nm (Figure 1) and the polydispersity index was around 0,285 ± 0,021 during the seven weeks. It is possible to deduce with this study is that the bovine serum albumin nanoparticles with AmB are stable in freezing conditions and this can help the continuation of the study of this kind of nanoparticle to develop a new carrier for AmB to treat meningitis caused by *C. neoformans*.

Keywords: Amphotericin B, Antifungal Activity, Bovine Serum Albumin Nanoparticles, Toxicity.

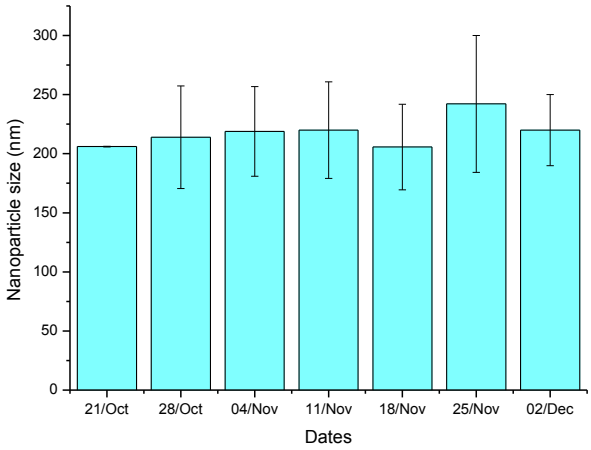

Figure 1: The nanopaticle size of bovine serum albumin nanoparticles of AmB after stability test in freezer during sevem weeks.

References:

Annaloro, C., Olivares, C., Usardi, P., Onida, F., Della Volpe, A., et al. (2009). Retrospective evaluation of amphotericin B deoxycholate toxicity in a single centre series of haematopoietic stem cell transplantation recipients. *J. Antimicrob. Chemother*. 63: 625–626.

Davey, K. G.; Holmes, A. D.; Johnson, E. M.; Szekely, A.; Warnock, D. W. (1998) Comparative evaluation of FUNGITEST and broth microdilution methods for antifungal drug susceptibility testing of *Candida* species and *Cryptococcus neoformans*. *J. Clin. Microbiol.*, 36, 926-930.

Gold, N.; Stout, H. A.; Pagano, J. F.; Donovick, R. (1956). Amphotericin A and B, antifungal antibiotics produced by a streptomycete. I. In vivo studies. *Antibiot. Annu.*, 1955-1956, 579-586.

Mainardes, R. M.; Khalil, N. M.; Gremião, M. P. D. (2010). Intranasal delivery of zidovudine by 12 PLA and PLA-PEG blend nanoparticles. *Int. J. Pharm.*, 16, 266-271.

Curcumin-loaded Bovine Serum Albumine Nanoparticles: Development and evaluation of stability and antioxidant activity.

L. E. A. Camargo,[1,2,*] R. M. Mainardes,[2] N. M. Khalil[2]
[1]Guairacá College, Department of Pharmacy, Guarapuava, Paraná, Brazil
[2]State University of Midwest, Laboratory of Pharmaceutical Nanotecnology, Guarapuava, Paraná, Brazil

Abstract: The polyphenol curcumin widely used as a spice, present several biological activities such antioxidantt, antitumoral, antiinflamtory, antifungal (Goel et al.; 2008). Curcumin present low bioavailability due its poor water solubility, instability in physiological to basic pH and the sensitive to the light (Khalil et al.; 2013). The use of nanostructured system as curcumin carriers has been described to improve its bioavailability and water solubility (Kim et al.; 2011), and the Bovine Serum Albumine (BSA) presents technical features to its became an excellent material for nanoparticles obtaining (Kratz; 2008). The curcumin-loaded BSA nanoparticles were obtained by the desolvation method. The mean size obtained was 149.63 ± 7.86 nm, the particle-size distribution presented a bimodal profile, with a polidispesity index of 0.16 ± 0.02. The curcumin entrapped efficiency was measured by HPLC and it was 45.09 ± 10.76%. The zeta potencial, -31.98 ± 2.74 mV presented, characterizes the nanoparticles solution stability, that was maintened without size and polidispersity index changes over room (21°C) and refrigerate (5°C) temperatures during 45 days, the stability wasn't manteined in freeze (-5°C) temperature. Curcumin scavenger activity was tested on $ABTS^{\bullet+}$ at physiological pH for 48h. The free curcumin, at 10 and 20 µg/mL, in T0 presented 27.27 ± 1.45 % and 37.81 ± 2 % of $ABTS^{\bullet+}$ inhibition respectively, and posteriorly occurred a significant decrease in its activity. After 4h, free curcumin had no presented scavenger activity on $ABTS^{\bullet+}$.The curcumin-loaded BSA nanoparticles, at 10 and 20 µg/mL, in T0 presented 55.08 ±1.696 % and 59.05 ±1.4163 % of $ABTS^{\bullet+}$ inhibition respectively, and posteriorly the scavenger activity on $ABTS^{\bullet+}$ was maintained, with few oscilation over 48 h. The curcumin fluorescence was also maitened in curcumin nanoparticulated. This study will permit us to evaluate the improve of the curcumin water solubility and its consequently bioavailability.

Keywords: curcumin, bovine serum albumine, nanoparticles, desolvation method, scavenger activity, bioavailability, water solubility, stability assay.

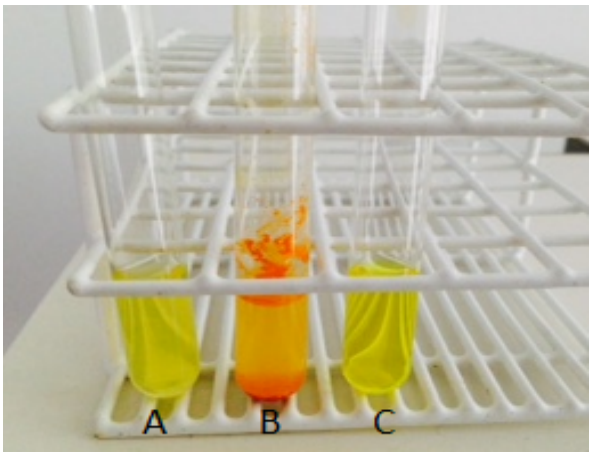

Figure 1: Curcumin-loaded Bovine Serum Albumine nanoparticles solution 50mg/mL in PBS pH 7.4 (A), free Curcumin solution 50mg/mL in PBS pH 7,4 pH solution (B) and Curcumin solution 50mg/mL dissolved inethanol (C).

References:

Goel, A., Kunnumakkara, A. B., Aggarwal, B. B. (2008), Curcumin as "Curecumin": From kitchen to clinic. *Bioch. Pharmac.,* 75, 787-809.

Khalil, N.M., Nascimento, T. C. F., Casa, D. M., Dalmolin, L. F., Mattos, A. C., Hoss, I., Romano, M. A., Mainardes, R. M. (2013), Pharmacokinetics of curcumin-loaded PLGA and PLGA–PEG blend nanoparticles after oral administration in rats. *Col. Surf.* 101, 353-360.

Kim, T. H., Jiang, H. H., Youn, Y. S., Park, C. W., Tak, K. K., Lee, S., Kim, H., Jon, S., Chen, X., Lee K. C. (2011). Preparation and characterization of water-soluble albumin-bound curcumin nanoparticles with improved antitumor activity. *Intern. J. Pharm.* 403, 285-291.

Kratz, F. A. (2008). Clinical update of using albumin as a drug vehicle — A commentary. *J. Control. Release*. 190, 331-336.

Silver Sub-nanometric Quantum Clusters as Potential Therapeutic Agents in Fight against Cancer

José M. Blanco[a], Javier Calvo[d], Enrique Carbó Argibay[a], Erea Borrajo Alonso[c], Fernando Domínguez[c], M. Arturo López Quintela[b], and José Rivas[a,b]

[a]International Iberian Nanotechnology Laboratory, 4715-330 Braga-Portugal
[b]Laboratorio de Magnetismo y Nanotecnología, Instituto de Investigaciones Tecnológicas, Universidad de Santiago de Compostela, E-15782, Santiago de Compostela, Spain
[c]Instituto de Investigación Sanitaria de Santiago de Compostela (IDIS), 15706 Santiago de Compostela, Spain
[d]Nanogap, 15895 Milladoiro, A Coruña, Spain

Abstract

One of the most important factor in the design of treatments against cancer is the degree of penetration of the drugs into the tumors to be treated. This parameter affects directly the effectiveness of antitumor drugs, decreasing or completely nullifying their antitumor activity. For this reason, it is necessary to find alternatives for drugs transport or develop new antitumor drugs with greater degree of penetration into the tumors. Atomic quantum clusters (AQCs) exhibit very interesting physical and chemical properties that make them particularly attractive for this purpose. This kind of clusters can become very small, even below 10 atoms, and with thicknesses under 0.5nm due to their planar structure. Their small size, comparable to Fermi wavelength of the electron (~0.52 nm for silver), places AQCs in the scale range where quantum confinement effects govern the material properties. Because of this, AQCs behave like molecules and do not exhibit charges in their structure. Their low molecular weight and the aforementioned absence of charge, increase the diffusivity of these sub-nanometric structures in biological tissues. In addition, AQCs below 10 atoms, have planar structures which make them especially interesting to interact with DNA. In order to evaluate the biological activity of AQCs against cancer, an easy and versatile method for synthesizing these type of particles has been developed, on the basis of a previous electrochemical method for the synthesis of nanoparticles[i]. Additionally, the first preclinical tests to evaluate the effectiveness of small silver AQCs have been carried out on isolated tumor cells.

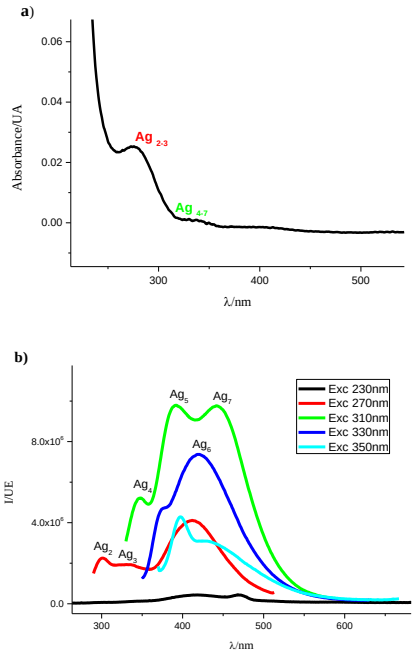

Fig 1. Characterization by Absorption and Fluorescence spectrophotometer of a sample of silver AQCs. **a)** UV-Vis absorption spectrum, **b)** Emission spectrum exciting between 230 and 350nm.

Acknowledgement: this work is supported by POCTEP (Operational Programme for Cross-border Cooperation Spain-Portugal), co-financed by the ERDF (European Regional Development Fund) under grant InveNNta Project.

.

[i] *J. Am. Chem. Soc.*, **1994**, *116* (16), pp 7401–7402

Development of the nanoconjugate for liver fluke targeting

A.G.Pershina,[1,5] A.M.Demin,[2] V.V.Ivanov, [1] O.B. Shevelev, [3] M.A. Uimin,[4] K.V. Nevskaya,[1] N.N. Shegoleva,[4] A.S. Minin,[4] A.E. Sazonov, [1] V.P. Krasnov, [2] L.M. Ogorodova[1]

[1]Siberian State Medical University, Tomsk, Russia
[2]Postovsky Institute of Organic Synthesis UB RAS, Yekaterinburg, Russia
[3]Cytology and Genetics SB RAS, Novosibirsk, Russia
[4]Institute of Metal Physics UB RAS, Ykaterinburg, Russia
[5]Tomsk Polytechnic University, Tomsk, Russia

Abstract: Nowadays, there are no biomedical tools for liver fluke direct imaging and targeting. The research aimed at the development, preparation and characterization of nanoconjugate based on superparamagnetic iron oxide (Fe_3O_4) nanoparticles (MNP), modified by silane derivatives and functionalized due to covalent bond formation with a pH-sensitive peptide (pHLIP) designed to detect the local acidosis zone formed around the fluke in vivo in opisthorchiasis infected liver.

The MNP with average diameter less than 20 nm were obtained by co-precipitation from the solutions of Fe^{3+} and Fe^{2+} salts. The surface of MNP were modified using (3-aminopropyl)trimethoxysilane (APTMS) and MNP with amino groups on the surface (MNP-APS-NH2) were received. The APTMS quantity was calculated according to element analysis data that was reached 0.60±0.06 mmol/g (PE 2400, II, Perkin Elmer). Then, pHLIP was bound on the MNP-APS-NH2 surface using hetero-functional cross-linker 6-Maleimidohexanoic acid *N*-hydroxysuccinimide ester (EMCS). The obtained nanoconjugate structure was proved by TEM (Philips CM30) and FTIR spectroscopy (Nicolet 6700, Thermo). According to TEM data there were no essential changes in the nanoparticles morphology after surface fictionalization: the average diameter and phase composition have not changed after processing. In FTIR spectra of obtained nanoconjugate the characteristic adsorption bands of Fe_3O_4 nanoparticles at 546 cm^{-1} (Fe-O) and pHLIP at 1638 (amide I) and at 1531 (amide II) as well as at 1445, 1402 cm^{-1} (amide III) were indicated. The stable water suspension of MNP modified by APTMS was obtained; the received nanoconjugate in suspension has average hydrodynamic diameter equal 155 nm (PdI 0.09) and z-potential – -22 mV (Zetasizer Nano ZS, Malvern Instruments Ltd.). The MRI contrast properties of nanoconjugate were tested in vitro and in vivo (Bruker, Biospec 117/16 USR), based on received data, the relaxivity coefficients r1 and r2 were calculated. The low cytotoxicity of nanoconjugate was proved using MTT-assay.

Keywords: nanoconjugate, superparamagnetic iron oxide nanoparticles, (3-aminopropyl)trimethoxysilane, MRI, liver fluke, cytotoxicity.

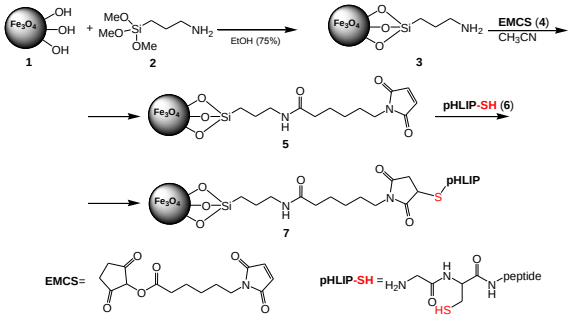

Figure 1: Figure illustrating the general sheme of nanoconjugate synthesis

This work is supported by RSF grant № 14-15-00247

A Peptide-Based Drug Design to Overcome Major Challenges on Cancer Treatments

A. Sanchez., A.D. Tinoco., L. Parham

University of Puerto Rico, Laboratory of Bioinorganic Chemistry, Rio Piedras, San Juan, Puerto Rico

Abstract: Cancer diagnosis is increasing at exponential rates. Patients and physicians are in need of novel and promising therapies to overcome the fatal disease. A promising option is a peptide-based drug design that would work by tricking the cell and interfering with the body's metabolic pathways. An example of these metabolic pathways that have awakened the researchers' attention is the SP/NK1R pathway. SP (Substance P), is a neuropeptide with multiples contributions in body regulation as: psychological stress, pain, inflammatory response, anti-apoptotic effects, and cell proliferation among others. Substance P receptor (NK1-R) is known to be overexpress in several cancer cell lines, and is involved in anti-apoptotic response (Muñoz and Coveñas, 2014).

This investigation is center in developing promising peptide-based drugs that can selectively attack cancer cells by two different ways: 1) blocking metabolic pathways that are known to promote cell proliferation and anti-apoptosis behavior, and 2) by interfering with the cancer cell's iron dependence mechanism. Cancer cells have a higher need of iron, therefore removing iron from them has been tested to slower tumor growth, and is a promising anti-tumor technique (Buss *et al*., 2003). The herein purposed lethal weapon is a peptide-based drug that can selectively get to the malignant cells and work as a drug by interfering with the cell's metabolic pathway, plus depleting the iron from the cells; to obtain an optimum result of cell death. A library of peptide-based drugs will be synthesized, tested, and characterized in order to target different types of malignancies by interfering with different metabolic pathways (Figure 1). Our preliminary efforts are center in the synthesis of a complex containing Ti(IV)-HBED-$SP_{homologus\ peptide}$. HBED has a good affinity for titanium (IV), but an even greater affinity for iron (III); which can function as the iron depleting agent by releasing Ti (IV) and up taking the Fe (III) (Parks *et al*., 2014). NK1R are over expressed in some cancer cell lines as for example pancreatic cancer cells. A drug that functions as a NK1 antagonist (to prevent proliferation of malignant cells, and trigger apoptosis), and that also has the ability of releasing titanium (IV) and uptake iron (III) from the cancer cells would be a powerful and promising treatment.

Keywords: peptide-based drug design, substance p, neurokinin 1 receptor (NK1R), cancer treatments, metabolic pathway, apoptosis, iron cell balance.

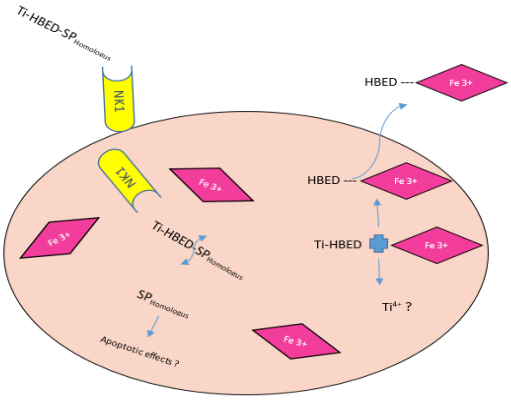

Figure 1. Peptide-based drug design. The complex enters the cell by the overexpressed receptor, and deliver the drug into the cell where the peptide stops cell proliferation and trigger apoptosis; while the HBED or other's high iron affinity molecules take iron out of the cell.

References:

Muñoz, M., Coveñas, R. (2014) Involvement of substance P and the NK-1 receptor in pancreatic cancer, *World J Gastroenterol*., 20(9**)**, 2321-2334

Buss, J. L., Torti, F. M., & Torti, S. V. (2003) The role of iron chelation in cancer therapy. *Curr. Med. Chem*., 10, 1021-1034.

Parks, T.B., Cruz, Y.M., Tinoco, A.D. (2014) Applying the Fe (III) binding property of a chemical transferrin mimetic to Ti(IV) anticancer drug design. *Inorg Chem*., 53(3), 1743-1749.

Superparamagnetic Iron Oxide Nanoparticles for Stem Cell Tracking by Magnetic Resonance Imaging

Noelia Guldris[1,3], Bárbara Argibay[2], Yury V. Kolen'ko[1], Enrique Carbó-Argibay[1], Ramón Iglesias[2], Francisco Campos[2], Laura M. Salonen[1], Manuel Bañobre-López[1], José Castillo[2], José Rivas[1,3]
[1]INL - International Iberian Nanotechnology Laboratory, Braga, Portugal
[2]Department of Neurology, Clinical Neurosciences Research Laboratory, Health Research Institute of Santiago de Compostela (IDIS), University Clinical Hospital, Santiago de Compostela, Spain
[3]Department of Applied Physics, Technological Research Institute, Nanotechnology and Magnetism Lab — NANOMAG, University of Santiago de Compostela, Spain

Abstract: Stroke is the second leading cause of death worldwide and the major cause of disability in Europe. This disease origins from a reduced blood supply into a region of the brain. The repercussions for the patient vary depending on the extent of the stroke and its location, but most patients suffer from body dysfunctions, such as disabilities in movement, speech, thought processes, and memory. In less severe cases, the healthy areas of the brain are able to assume the functions of the damaged ones. However, the major issue is the inability of the body to replace dead cells and therefore stem cell treatment may boost the repair systems within the brain.

Nowadays, mesenchymal stem cells (MSCs) are one of the most commonly used types of stem cells in clinical trials on stroke. They can be easily obtained and grown from bone marrow of the patient. The beneficial effect of MSCs is not related with producing new brain cells but rather, as suggested in some studies, with the release of substances from the injected MSCs that reduce inflammation and stimulate self-repair. More research is necessary to fully understand all the processes involved before safe therapies can be developed.

One of the main questions to be addressed is how and where the MSCs migrate within the body once they are injected. Cell tracking is used to visualize the cells when they are inside a living organism, and thus there is a need of labeling the cells. Therefore, cell-contrast agents and imaging technique chosen should accomplish several requirements: *e.g.* noninvasiveness, biocompatibility, and no alteration of stem cells properties should be necessary.

Hence, our approach relies on the use of Magnetic resonance imaging (MRI) as a highly convenient method due to its widespread availability in hospitals, as well as its remarkable characteristics like high spatial resolution, rapid acquisition and the absence of exposure to ionizing radiation. However, the sensitivity of MRI is still lower than other imaging techniques, *e.g.* fluorescence or bioluminescence. Therefore, the development of highly efficient contrast agents is crucial in order to enhance the soft tissue contrast (Fig. 1).

Here, we report on the use of superparamagnetic iron oxide nanoparticles (SPIONs) as MRI probes for stem cell tracking. Data will be shown regarding SPION magnetic properties, MSC uptake, cytotoxicity, and MRI visualization of the labeled MSCs.

Keywords: biomedical applications, cell tracking, contrast agent, MRI, MSC, SPION, stem cells, stroke.

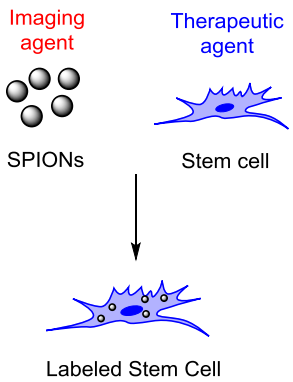

Figure 1: The basic concept of stem cell tracking using SPION labels.

Acknowledgement: This work is funded by POCTEP (Operational Programme for Cross-border Cooperation Spain-Portugal) and co-financed by the ERDF (European Regional Development Fund) under a grant for the InveNNta Project.

Phenylethyl Resorcinol in Nioesomes for Cosmetic formulation

J. Buruschat, and T. Amnuaikit*
Department of Pharmaceutical Technology, Faculty of Pharmaceutical Sciences,
Prince of SongklaUniversity, Songkhla, THAILAND.

Abstract: Niosomes are one of drug delivery system which made from non-ionic surfactant and have ability to entrap both hydrophilic and lipophilic drug. Cosmetic industry used niosomes to prevent antioxidant ingredient from oxidation and enhance penetration of poor permeable ingredient (Mahale *et al*., 2012). Property of non-ionic surfactant is also mild to skin. Phenylethyl Resorcinol was entrapped by niosomes using Brij™72 as non-ionic surfactant, it exhibited good physical appearance and the particle size was 0.97 to 2.44 µm. At surfactant: cholesterol ratio is 80:1, which had higher entrapment efficiency was 98.65±0.001%. The value of zeta potential of niosomes was -10.61 to -16.87 mV. Cholesterol content, HLB value of surfactant have effect to characteriztion of niosomes such as particle size, entrapment efficiency, zeta potential (Essa, 2010). Hydrophilic-lipophilic balance is also effect to formation of niosomes vesicle (Kamboj *et al*., 2014). Therefore, niosomes was used to encapsulate phenylethyl resorcinol for used in cosmetic formulation.

Keywords: Niosomes, non-ionic surfactant, phenylethyl resorcinol, Brij™72, drug delivery, entrapment efficiency, zeta potential, particle size.

References:

Essa E. A. (2010). Effect of formulation and processing variables on the particle size of sorbitan monopalmitate niosomes, *Asian J. Pharm.*, 4(*4*), 227-233.

Kamboj, S., Saini, V. and Bala, S. (2014). Formulation and characterization of drug loaded nonionic surfactant vesicles (Niosomes) for oral bioaviability enhancement,. *The science world Journal*, 2014, 1-8.

Mahale, N. B., Thakkar, P. D., Mali, R. G., Walunj, D. R., & Chaudhari, S. R. (2012). Niosomes: Novel sustained release nonionic stable vesicular systems — An overview. *Adv. Colloid Interface Sci*., *183–184*, 46-54.

Nanostructured lipid carriers containing amazon natural lipids for the encapsulation of benzophenone-3

Paula A. Lima,[1,*] Nelson Durán,[1]
[1]Institute of Chemistry, Biological Chemistry Laboratory, State University of Campinas (UNICAMP), Campinas - SP, Brazil

Abstract: Exposure to ultraviolet (UV) radiation is the main cause of various skin problems, including sunburn, photo-aging and skin cancer. Sunscreens are widely used to protect skin against the deleterious effects of UV radiation. 2-hydroxy-4-methoxybenzophenone, commonly known as benzophenone-3 (BP-3) or oxybenzone, is a strong UV absorber and one of the most important sunscreen agents, and has been available for over 40 years. BP-3 can penetrate skin and its absorption has been associated to endocrine disruption (Kim and Choi, 2014) and other problems. Nanostructured lipid carriers (NLCs) are promising systems which can provide, among other advantages, enhanced drug stability, controlled drug release and targeting and high drug loading (Chen *et al*, 2014). In this study, we aim to produce NLCs which may avoid penetration of BP-3 in skin, using natural lipids from amazon plants. We produced NLCs from the natural lipids cupuassu (*Theobroma grandiflorum*) butter, buriti (*Mauritia flexuosa*) oil and lanolin, containing the sunscreen BP-3via hot high pressure homogenization. Dynamic light scattering was used to determine average particle size, polydispersity index and zeta potential of the suspensions. BP-3 entrapment efficiency was estimated using UV absorption. The average size of the particles was around 170 nm, with polydispersity index of less than 0.2, which indicates a narrow size distribution. Zeta potential varied between -30 and -25 mV, indicating good stability. BP-3 entrapment efficiency was higher than 85%. Figure 1 shows the evolution of average particle size and zeta potential of the formulation containing BP-3 during 2 months. No significant changes were observed, which indicates good stability. The results show that the NLCs produced are promising carriers for the sunscreen BP-3. The evaluation of skin penetrability showed very low concentration at the startum corneum level. Low cytotoxicity of NLCs was found. The sun protection factor (SPF) of formulations containing BP-3 NLCs will be discussed.

Keywords: benzophenone-3, nanostructured lipid carriers, cupuassu butter, buriti oil.

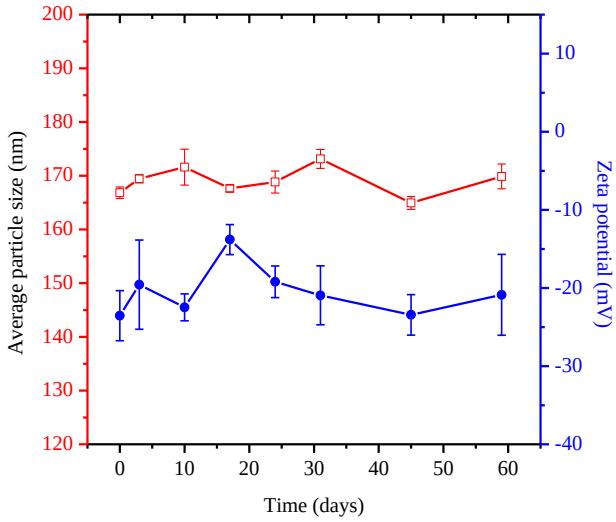

Figure 1: Evolution of average particle size and zeta potential of the formulation containing 10 % of benzophenone-3.

Acknowledgements: Support from FAPESP, CNPq, CAPES, INOMAT (MCTI/CNPq), NanoBioss (MCTI) and Brazilian Network on Nanotoxicology (MCTI/CNPq) are acknowledged.

References:

Kim, S., Choi, K. (2014), Occurrences, toxicities, and ecological risks of benzophenone-3, a common component of organic sunscreen products: A mini-review. *Environ. Int.*, 70 143–157.

Chen, Y., Yang, X., Zhao, L., Almásy, L., Garamus, V. M., Willumeit, R., Zou, A. (2014), Preparation and characterization of a nanostructured lipid carrier fora poorly soluble drug, *Colloids and Surfaces A: Physicochem. Eng. Aspects*, 455, 36–43.

Effect of phospholipid and ethanol concentrations on physical property of phenylethyl resorcinol loaded ethosome

T. Limsuwan, P. Boonme, T. Amnuaikit*
Department of Pharmaceutical Technology, Faculty of Pharmaceutical Sciences,
Prince of Songkla University, Songkhla, THAILAND

Abstract: Phenylethyl resorcinol (4-(1-phenylethyl) 1, 3-benzenediol) is a synthetically produced from resorcinol which inhibits the conversion of tyrosinase to L-3, 4-dihydroxyphenylalanine (L-DOPA). It is a newly skin-lightening agent. The aim of this research was to develop ethosome containing phenylethyl resorcinol to enhance water solubility and stability, and decrease skin irritation. In addition, the effect of phospholipid and ethanol on the physical appearance was investigated to obtain their suitable concentrations in the ethosome for application as a topical delivery system. The ethosome was prepared by thin-film hydration method and composed of 5%w/v phenylethyl resorcinol, 0.5%w/v cholesterol (CHOL), 3-6%w/v phospholipid (L-α-phosphatidylcholine from soybean; SPC), 10-50%v/v absolute ethanol and water up to 100%v/v. The results show that formulations containing 3-6%w/v SPC and 20-50%v/v ethanol had good physical appearance with yellow colloidal. This phenomenon may be due to a synergistic effect between ethanol and water as a co-solvent system with lipid vesicles of phospholipids, which can increase the solubility of phenylethyl resorcinol in the formulations. However, increasing the ethanol concentration up to 60% v/v resulted in precipitation in ethosome. Besides, after 1 week the formulations containing 50%v/v ethanol had precipitate too which indicate instability in these formulations. These could be explained by the effects of high ethanol concentrations on disruption of lipid vesicle which lead to decreasing drug entrapment efficiency and increasing precipitation of ethosome formulations. Therefore, these results clearly demonstrated that the suitable ethanol concentration in preparation of the phenylethyl resorcinol ethosome was between 20-40%v/v ethanol when combing with 3-6%w/v SPC and 0.5%w/v CHOL.

Keywords:phenylethyl resorcinol, ethosome, ethanol, vesicular drug delivery system

References:

Bendas, E.R., Tadros, M.I. (2007) Enhanced transdermal delivery of salbutamol sulfate via ethosomes. *AAPS PharmSciTech*, 8(4), E1-E8.

Linder, J. (2014) Topical Melasma Treatments, *Pigmentary Disorders*, 1, 115.

Touitou, E., Dayan, N., Bergelson, L., Godin, B., Eliaz, M. (2000) Ethosomes*:* Novelvesicular carriers for delivery, *J. Control Release*, 65(3), 403-418.

Clove Oil Loaded Nanoemulsions for Fish Anesthesia

S. Okonogi,[1,2,*] K. Janngeon,[2] W. Chaisri,[3] S. Pikulkaew,[3]

[1]Chiang Mai University, Nanoscience and Nanotechnology Programme, The Graduate School, Chiang Mai, Thailand
[2]Chiang Mai University, Department of Pharmaceutical Sciences, Faculty of Pharmacy, Chiang Mai, Thailand
[3]Chiang Mai University, Department of Food Animal Clinic, Faculty of Veterinary Medicine, Chiang Mai, Thailand

Abstract: Fish anesthesia is a biological state in fish induced by an external agent to ease handling and reduce fish stress. Clove oil is composed mainly of eugenol which can be used as natural fish anesthetic agent without any chemical hazard to the user and environment (King *et al.*, 2005). Due to the water insoluble property of clove oil, some organic solvents such as ethanol has to be used before mixing in fresh water. However, behavioral anesthesia of fish exposed to clove oil solution has been hyperactivity because of these organic solvents (Songkaew *et al.*, 2007). Nanoemulsions are emulsions with droplet size in the nanometric diameter range of approximately 20–200 nm. Nanoemulsions appear transparent or translucent, low viscosity, low surfactant, high kinetic stability against creaming or sedimentation (Solans *et al.*, 2005). Delivery of clove oil by nanoemulsions, therefore, could reduce the problem of using organic solvent. The purpose of this study was to develop nanoemulsions of clove oil. The effects of clove oil and surfactant on the emulsion characteristics and anesthetic activity in fish were investigated. The obtained emulsion properties were evaluated in terms of droplet size, size distribution, and zeta potential. The suitable formulations of clove oil loaded nanoemulsions (CLN) were selected to investigate for anesthetic induction time and anesthetic recovery time of koi carp (*Cyprinus carpiokoi)* and goldfish (*Carassius auratus)*. The clove oil in ethanol solution was used as a positive control. The results showed that CLN formulations composed of 10% clove oil with 5% Tween20 and 20% clove oil with 5-15% Tween20 yielded the stable nanoemulsions with rapidly dispersed into fine droplets having a mean size of 128.9-188.1 nm with the narrow size distribution of 0.2-0.3 nm and zeta-potential in the range of –25 to –30 mV. It was found that the fish anesthetic activity of CLN was dose dependent. Both kinds of fish that received CLN showed shorter anesthetic induction time than those received the control. However, the anesthetic recovery time was varied, depended on dose and type of fish.

Keywords: nanoemulsion, clove oil, fish anesthesia, induction time, recovery time, *Cyprinus carpiokoi*, *Carassius auratus*

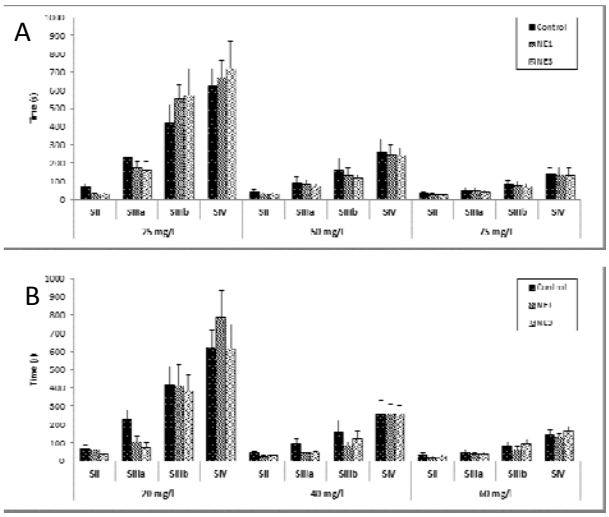

Figure 1: Induction time of anesthetic stage of koi carp (A) and goldfish (B) anaesthetized by clove oil loaded nanoemulsions with different concentrations of clove oil.

References:

King, W., Hooper, B., Hillsgrove, S., Benton, C., Berlinsky, D.L. (2005), The use of clove oil, metomidate, tricaine methanesulphonate and 2-phenoxyethanol for inducing anaesthesia and their effect on the cortisol stress response in black sea bass (*Centropristis striata* L.), *Aquac. Res.*, 36, 1442-1449.

Shah, R.B., Zidan, A.S., Funck, T., Tawakkul, M.A., Nguyenpho, A., Khan, M.A. (2007), Quality by design: characterization of self-nano-emulsified drug delivery systems (SNEDDs) using ultrasonic resonator technology, *Int. J. Pharm.*, 341, 189–194.

Songkaew, A., Chokboonmongkol C, Khattiya R, Wongsathein D, Mengumpun K, Pikulkaew S. (2007), Induction time and behavior of anesthesia and recovery in Mekong giant catfish (*Pangasianodon gigas*) after anesthetized with clove oil and tricaine methanesulfonate (MS-222), *TVMA J.*, 58, 12-21.

Optimization of *in vitro* conditions to treat cancer with magnetic hyperthermia

V. Vilas-Boas [a, b], B. Espiña [b], Y. Kolen'ko [b], M. Bañobre-Lopez [b], V. Martins [b] and F. Carvalho [a]

[a] REQUIMTE, Laboratório de Toxicologia, Departamento de Ciências Biológicas, Faculdade de Farmácia, Universidade do Porto, Rua de Jorge Viterbo Ferreira, 228, 4050-313 Porto, Portugal.

[b] International Iberian Nanotechnology Laboratory (INL). Avenida Mestre José Veiga 4715-330 Braga, Portugal

Abstract: According to the latest reports from the World Health Organization, cancer is one of the leading causes of death worldwide having killed nearly 8.2 million people in 2012 (1). Therefore finding new ways to cure cancer or prolong life is a great challenge for scientists. In this sense, magnetic hyperthermia (MHT) has emerged as an experimental anti-cancer strategy that maybe used either alone or as a sensitizing strategy. The aim of this study is to evaluate the ability of magnetic nanoparticles to kill tumour cells with MHT.

Superparamagnetic iron-oxide nanoparticles coated with poly-acrylic acid, having an average core diameter around 18nm and a surface charge of 97±3mV, were used as heat generators when submitted to an external magnetic field (EMF). Different combinations of amplitude and frequency of field were tested in order to obtain heating curves reaching deadly temperatures (between 41-46ºC), using low, well-tolerable, magnetite concentrations (0.5 g/L). MHT assays were performed with U87MG cells, an *in vitro* model of glioblastoma multiforme, the most aggressive type of primary brain tumours, in the presence of the above-described MNPs. When applying 869kHz+225*Oe* until the sample reached 46ºC, no significant difference was observed in cell viability, as estimated using the PrestoBlue metabolic rate assay. Nevertheless, decreasing the intensity of the applied EMF (499kHz+275*Oe* or 688kHz+250*Oe* until 44 or 46ºC were reached), therefore prolonging the exposure time to deadly temperatures, leads to a significant decrease in cell viability (of more than 50%). This fact was confirmed microscopically by double staining the cells with Annexin-V and Propidium Iodide, cell death indicators of apoptosis and necrosis pathways, respectively.

The results suggest that prolonging the time of exposure to temperatures above 41ºC for at least 30 minutes may turn MHT more efficient as a strategy to treat cancer.

Keywords: superparamagnetic iron-oxide nanoparticles; magnetic hyperthermia; cancer treatment; cell viability

References: (1) World Cancer Report 2014, Edited by Bernard W. Stewart and Christopher P. Wild

Acknowledgments: V. Vilas-Boas acknowledges Fundação para a Ciência e Tecnologia (FCT) for her PhD Grant SFRH/BD/82556/2011.

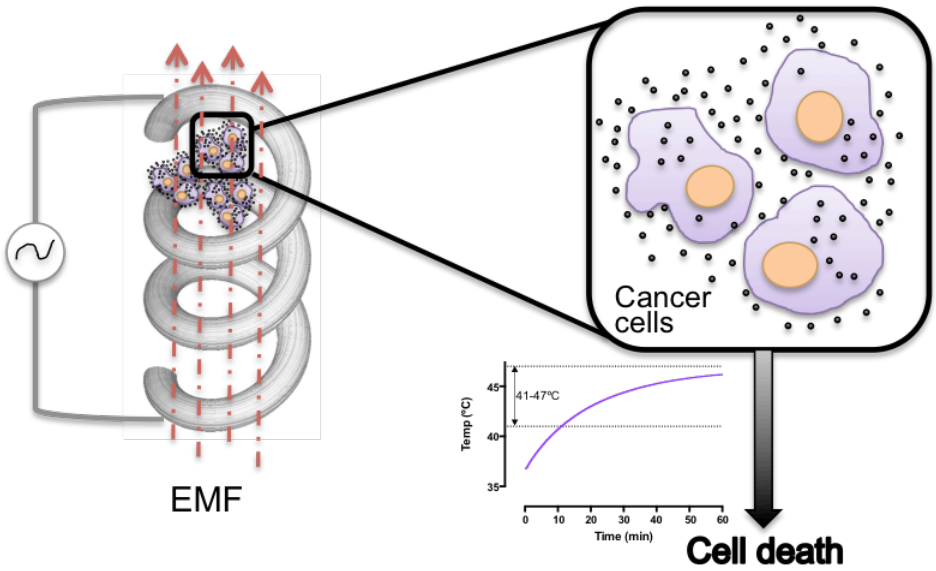

Figure 1: Schematic representation of the experimental design – cancer cells are incubated with the MNPs and then submitted to an external magnetic field that makes them vibrate, generating heat. If the temperatures reached are high enough and sustained for a certain period, significant cell death is observed.

Effective VEGF Binding to Au Nanocrystals with {111} Facets

Jeong Hun Kim[1,2,3], Dong Hyun Jo[1,2], Jong Wook Hong[4], Sang Woo Han[4], and Jin Hyoung Kim[1]

[1]Fight against Angiogenesis-Related Blindness (FARB) Laboratory, Seoul National University Hospital, Seoul, Republic of Korea
[2]Department of Biomedical Sciences, College of Medicine, Seoul National University, Seoul, Republic of Korea
[3]Department of Ophthalmology, College of Medicine, Seoul National University, Seoul, Republic of Korea
[4]Department of Chemistry and KI for the NanoCentury, KAIST, Daejeon, Republic of Korea, Republic of Korea

Abstract: Nanocrystals with well-defined shapes and crystallographic facets can provide novel opportunities to improve efficacy of nanoparticle-based biomedical applications. (Kim *et al*, 2011; Jo *et al*, 2012, 2014) This study demonstrates binding of vascular endothelial growth factor (VEGF), a main factor of pathological angiogenesis, to single-crystalline Au nanocrystals with {111} facets. Icosahedral and octahedral Au nanocrystals effectively scavenge VEGF molecules in culture media as their spherical counterparts with similar diameter. Furthermore, they suppress *in vitro* VEGF-induced activation of VEGF receptor and significantly inhibit *in vivo* VEGF-mediated retinal permeability. These results suggest that Au nanocrystals other than nanospheres provide a useful platform for detection and scavenging of VEGF for various human diseases with VEGF-driven pathological angiogenesis, including cancer, age-related macular degeneration, and diabetic complications. (Figure 1)

Keywords: Au nanocrystals, {111} facets, vascular endothelial growth factor, nanoparticle-protein interaction

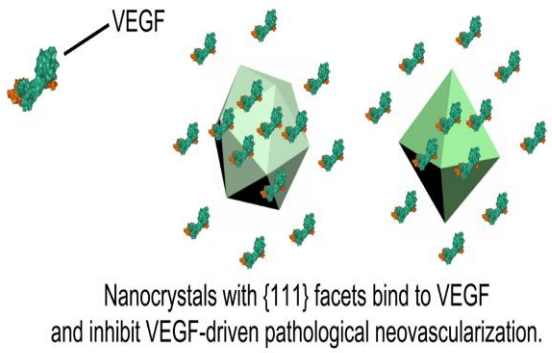

Figure 1: Gold nanospheres are known to bind to VEGF and suppress VEGF-mediated angiogenesis. In this study, Jo et al. reported gold nanocrystals with well-defined crystallographic {111} facets also exhibited anti-angiogenic effects. These results suggest that gold nanocrystals with (111) facets provide a useful platform for nanoparticle-based treatment of VEGF-driven pathological neovascularization in various human diseases including age-related macular degeneration, cancer, and diabetic retinopathy, beyond their current optical and catalytic applications.

References:

Kim, J.H., Kim, M.H., Jo, D.H., Yu, Y.S., Lee, T.G., Kim, J.H. (2011) The inhibition of retinal neovascularization by gold nanoparticles via suppression of VEGFR-2 activation. *Biomaterials*, 32, 1865-1871.

Jo, D.H., Kim, J.H., Yu, Y.S., Lee, T.G., Kim, J.H. (2012) Antiangiogenic effect of silicate nanoparticle on retinal neovascularization induced by vascular endothelial growth factor. *Nanomedicine*, 8, 784-791.

Jo, D.H., Kim, J.H., Son, J.G., Song, N.W., Kim, Y.I., Yu, Y.S., Lee, T.G., Kim, J.H. (2014) Anti-angiogenic effect of bare titanium dioxide nanoparticles on pathologic neovascularization without unbearable toxicity. *Nanomedicine*, 10, 1109-1117.

Toxicological Aspects of Graphene Oxide on Gill Cells of Adult Zebrafish (*Danio rerio*)

J. P. Souza[1], I. M. M. Paino[1], F. Santos[1], P. F. M. Nogueira[1], V. Zucolloto[1]
Nanomedicine and Nanotoxicology Group, Physics Institute of São Carlos (IFSC), University of São Paulo (USP), Brazil

Abstract: Graphene exhibits unique physical and chemical properties, which have motivated a wide range of applications. However, the use of graphene could result in its accumulation in aquatic environment where the risks for organisms are still unknown. In this study, zebrafish were exposed to graphene oxide for assessment of toxic effects on gill cells. Adult zebrafish (*Danio rerio*), including males and females (6 - 7 month old; body weight 0.31 ± 0.09g; body size 3.34 ± 0.31cm) were exposed to 0; 2 or 20 mg L^{-1} of graphene oxide during 24 h. Exposure were performed in glass containers under conditions of continuous aeration, 12:12 light:dark photoperiod, 24 ± 2°C of temperature, 60% of dissolved oxygen, without feeding, including four replicates per treatment, and one fish per replicate (OECD 1992). After exposure, fish were collected, anesthetized, and gill tissues from each group were harvested and treated with 4% of dispase solution for 15 min at room temperature (Ji *et al.,* 2011). As revealed by flow cytometric analysis (BD FACSCalibur Flow Cytometer equipped with 488 nm laser), there was a significant increase in the number of cell in early apoptotic phase (PI negative, FITC annexin-V positive), and by late apoptotic or already dead cells (FITC annexin-V and PI positive), compared to the control (Figure 1). Graphene oxide nanoparticles are small enough to pass through the secondary lamellae of the gills and achieve the gill surface layers. The gill epithelium is similar to the basic features of epithelial design of other vertebrate animals (e.g., lung). Our findings are important, since they may raise concerns of risks to other animals (Handy *et al.,* 2008) and human beings.

Keywords: nanotoxicity, nanoparticles, fish, aquatic environments, risk assessment, graphene oxide, cell viability.

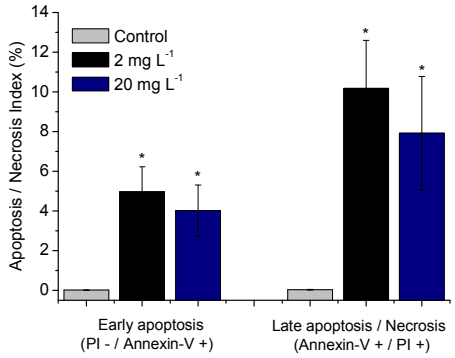

Figure 1: Percentage of number of gill cells of adult zebrafish in early apoptosis phase, late apoptosis or necrosis, relative to the total population after 24 h of exposure to zero, 2 and 20 mg L^{-1} of graphene oxide. * Means significant difference ($p < 0.05$ Tukey test) compared to the control.

References:

Ji, W., Liang, H., Zhou, W., Zhang, X. (2013) Apoptotic responses of zebrafish (*Danio rerio*) after exposure with microcystin-LR under different ambient temperatures, *J. Appl. Toxicol.,* 33, 799-806.

Handy, R. D., Henry, T. B., Scown T. M., Johnston, B. D., Tyler, C. R. (2008) Manufactured nanoparticles: their uptake and effects on fish - a mechanistic analysis, *Ecotoxicol.,* 17, 396-409.

Organization for Economic Cooperation and Development (OECD). *Guideline for Testing of Chemicals: Fish, Acute Toxicity Test*. OECD Nº 203, 1992.

Effect of Particle Size on Oral Absorption, Tissue Distribution, and Excretion of Food Grade Titanium Dioxide and Silica Nano-particles

Mi-rae Jo,[1] Soo-Jin Choi[1]
[1] Seoul Women's University, Department of Food Science and Technology, 621 Hwarangro, Nowon-gu, Seoul 139-774, South Korea

Abstract: Nanoparticles have been widely applied to many industries. Silica has been used as an anticaking agent in powdered mixes, seasonings, and coffee whiteners (Villota *et al.*; 1986) and titanium dioxide has been applied to enhance the white color of certain foods, such as dairy products and candies (Weir *et al.*; 2012). However, the question as to whether nanoparticles have potential toxic effects on human health remains to be answered. Moreover, little information is actually available about biokinetic behaviors of nanoparticles. In this study, biokinetics of titanium dioxide and silica nanoparticles was evaluated after single oral administration to rats, as compared with bulk sized materials. Effects of the presence of food ingredients on oral absorption were also evaluated. Quantitative analysis of titanium and silicon was performed with inductively coupled plasma-atomic emission spectroscopy (ICP-AES) and lithium metaborate fusion, followed by molybdenum blue method, respectively. The results showed that oral absorption of titanium dioxide was not significantly different between nano and bulk-sizes. However, rapid absorption rate and high abosorption efficiency of silica nanoparticles was found as compared with bulk-sized silica. No significant effect of particle size on tissue distribution and excretion was found in all the cases. On the other hand, oral absorption was highly affected by the presence of food ingredients. These findings will provide basic information to precit potential toxicity of nanoparticles as well as new insight on toxicity evaluation of nanoparticles applied to foods.

Keywords: titanium dioxide, silica, pharmacokinetics, interaction.

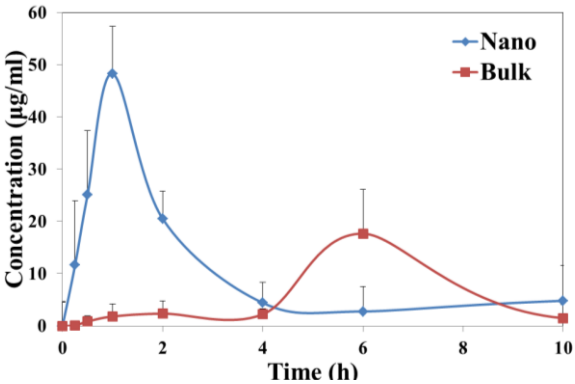

Figure 1: Oral absorption of food grade nanoparticles in rats after single dose administration.

References:

Weir, A., Westerhoff, P., Fabricius, L., Hristovski, K., & von Goetz, N. (2012) Titanium dioxide nanoparticles in food and personal care products, *Environ. Sci. Technol.*, 46, 2242-2250.

Villota, R., Hawkes, J. G., & Cochrane, H. (1986) Food applications and the toxicological and nutritional implications of amorphous silicon dioxide, *Crit. Rev. Food Sci. Nutr.*, *23*, 289-321.

Anti-angiogenic Effect of Gold and Silica Nanoparticles on Choroidal Neo-vascularization: Size Matters, Core does not

Jin Hyoung Kim[1], Dong Hyun Jo[1,2], Yuanze Piao[3], Tae Geol Lee[4], and Jeong Hun Kim[1,2,5]

[1]Fight against Angiogenesis-Related Blindness (FARB) Laboratory, Seoul National University Hospital, Seoul, Republic of Korea
[2]Department of Biomedical Sciences, College of Medicine, Seoul National University, Seoul, Republic of Korea
[3]Graduate School of Convergence Science and Technology, Seoul National University, Seoul, Republic of Korea
[4]Center for Nano-Bio Convergence, World Class Laboratory, Korea Research Institute of Standards and Science, Daejeon, Republic of Korea
[5]Department of Ophthalmology, College of Medicine, Seoul National University, Seoul, Republic of Korea

Abstract: Nanoparticles can be involved in biological activity such as apoptosis, angiogenesis, and oxidative stress by themselves. In particular, inorganic nanoparticles such as gold and silica nanoparticles are known to inhibit vascular endothelial growth factor (VEGF)-mediated pathologic angiogenesis. (Kim *et al*, 2011; Jo *et al*, 2012) In this study, we show that anti-angiogenic effect of inorganic nanospheres is determined by their own sizes. We demonstrate that 20 nm size gold and silica nanospheres suppress VEGF-induced activation of VEGF receptor-2, *in vitro* angiogenesis process, and *in vivo* pathologic angiogenesis more efficiently than their 100 nm size counterparts. Our results suggest that size determines inhibitory activity of gold and silica nanospheres to VEGF-mediated angiogenesis. (Figure 1)

Keywords: nanospheres, anti-angiogenesis effects, inorganic nanoparticles, vascular endothelial growth factor, pathologic angiogenesis

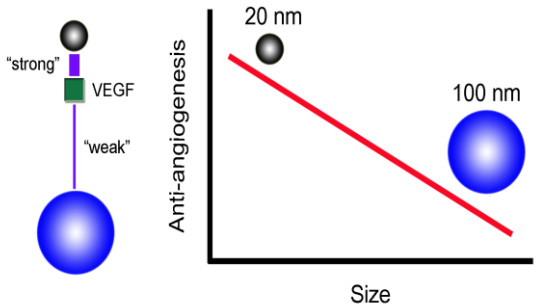

Figure 1: Figur 1 illustrates that the size determines inhibitory activity of monodisperse nanospheres to VEGF-mediated angiogenesis regardless of whether they were composed of gold or silica. 20 nm size nanospheres inhibit VEGF-induced angiogenesis more efficiently than their 100 nm size counterparts. We believe that material-independent, but size-dependent anti-angiogenic effect of inorganic nanospheres on pathologic angiogenesis will give insights to researchers who struggle to find out ways to utilize nanoparticles as therapeutic materials.

References:

Kim, J.H., Kim, M.H., Jo, D.H., Yu, Y.S., Lee, T.G., Kim, J.H. (2011) The inhibition of retinal neovascularization by gold nanoparticles via suppression of VEGFR-2 activation. *Biomaterials*, 32, 1865-1871.

Jo, D.H., Kim, J.H., Yu, Y.S., Lee, T.G., Kim, J.H. (2012) Antiangiogenic effect of silicate nanoparticle on retinal neovascularization induced by vascular endothelial growth factor. *Nanomedicine*, 8, 784-791.

Synthesis and surface modification of Fe_3O_4@SiO_2@Au NPs as theranostic agents for Nanomedicine applications.

I. Monaco,[1] N. T. Hong,[2] E. Locatelli,[1] M. Comes Franchini[1]
[1] Department of Industrial Chemistry "*Toso Montanari*", University of Bologna, Bologna, Italy
[2] Institute of Physics, Vietnam Academy of Science and Technology (VAST), Hanoi, Vietnam

Abstract: In the last decades, metallic nanomaterials represent a promising agent in cancer treatment such as hyperthermia therapy. In this study metallic nanoparticles consisting of multiple shells of iron oxide, silica and gold were synthetized (Fe_3O_4@SiO_2@Au). In this way we obtained a complex nanostructure that simultaneously possess magnetic proprieties of Fe (Lu *et al.* 2007) and optical properties of Au (Gao *et al.* 2009) to develop a novel theranostic system for the traetments of cancer deseases. The resulting nanoparticles have been completely characterized by different techniques such as UV-Vis, DLS and TEM.

Stability of nanoparticles is a crucial requirement for almost any application especially in the nanomedicine field. Native metals nanoparticles, are generally very sensitive to external environment and subjected to agglomeration if not in presence of stabilizing agents. Therefore, it is necessary to develop efficient strategies to improve the chemical stability of this nanosystem. The most straight forward method seems to be protection by an organic layer, which shields the surface of the particles from the environment.

In the case of metallic nanoparticles, organic ligands can be chemically anchored or physically adsorbed on nanoparticles' surface to form a single or double layer, which creates repulsive (mainly as steric repulsion) forces to balance the magnetic and the van der Waals attractive forces acting on the nanoparticles. The obtained Fe_3O_4@SiO_2@Au NPs were coated with an organic ligand by exchange ligand reaction to study their stability and final properties. The organic ligand selected for this purpose presents a thiol as functional group in order to maximize interaction with the gold surface (**Figure 1**). The resulted coated nanoparticles are now suitable for entrapment into biocompatible polymeric matrix to form a targetable water soluble nanocarrier for nanomedicine applications. As polymer the well-known polylactic-co-glycolic-co-polyethylene glycol (PLGA-PEG) was selected due to the Food and Drug Administration (FDA) approval in biomedical formulation and for its ability to create micelles (PMs) with a lipophilic core, which can host our lipophylic particles (Locatelli *et al.* 2015). With oil-in-water technique Fe_3O_4@SiO_2@Au@PMs were obtained. These polymeric micelles were then purified and characterized by different techniques to verify both stability and maintainance of the magnetic and optical proprieties from native metallic nanoparticles. In conclution the final nanosystems underwent biological studies aimed at the exploitation of both magnetic and optical properties, thus confirming the possibility to use this multishell system as theranostic agent.

Keywords: nanoparticles, iron, gold, silica, surface chemistry, micelles, theranostic agent.

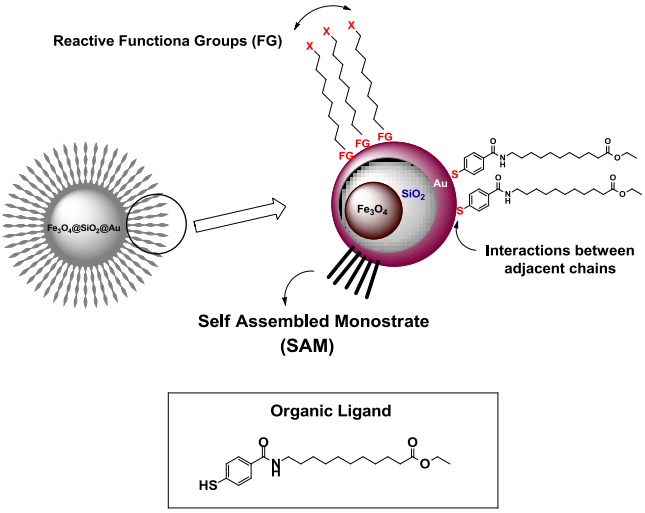

Figure 1: Self Assembled Monostrate (SAM) formation on NPs surface.

References:

Lu, H., Salabas, E. L., Schüth, F. (2007) Magnetic Nanoparticles: Synthesis, Protection, Functionalization, and Application, *Angew. Chem. Int. Ed.*, 46, 1222-1244.

Gao, J., Gu, H., Xu, B. (2009) Multifunctional Magnetic Nanoparticles: Design, Synthesis, and Biomedical Applications, *Acc. of Chem. Res.* 42, 1097-1107.

Locatelli, E., Monaco, I., Comes Franchini, M. (2015) Surface Modifications of Gold Nanorods (GNRs) for Applications in Nanomedicine. *RSC Adv.* DOI: 10.1039/C4RA16473C

Acknowledgements

This work has been supported with the funding of the *Ministero degli Affari Esteri e della Cooperazione Internazionale (MAECI)*. Project: *Progetto Bilaterale di "Grande Rilevanza" Italia-Vietnam*. Title: "Synthesis of hybrid magnetic nanocarriers for drug delivery in nanomedicine. Imaging and therapy against brain tumors".

Farnesina
Ministero degli Affari Esteri

Interactions of Zinc Oxide Nanoparticles with Dispersants: Cytotoxicity, Uptake, and Pharmacokinetics

S. J. Choi
University of Seoul Women's University, Department of Food Science and Technology, Laboratory of Nanofood & Toxicology, Seoul, Republic of Korea

Abstract: Zinc oxide (ZnO) nanoparticles have been extensively applied to various commercial products, such as catalyst, electronics, medical diagnosis, cosmetics, sunscreens, and food additives due to their catalytic, semi-conducting, magnetic, antimicrobial, and UV protection properties as well as their thermal conductivity (Fan *et al*., 2005). Along with growing concern about potential toxicity of ZnO nanoparticles, many researches have been recently focused on their toxicological effects in cultured cell lines as in animal models (Paek *et al*., 2013). For toxicity evaluation, nanoparticles should be well dispersed in aquous solution where some dispersants are indispensably added for better stability. However, dispersants used for biological evaluation can also affect cellular response, uptake behaviors, and toxicity of nanoparticles (Haniu *et al*., 2011). In the present study, the effects of ZnO nanoparticles prepared in different dispersing agents, such as citrate, carboxymethyl cellulose, and cell culture medium or distilled water were investigated in terms of cytotoxicity, cellular uptake, pharmacokinetics, and tissue distribution. We also compared biological behaviors of ZnO nanoparticles with those of zinc ions. The results demonstrated ZnO nanoparticles prepared under different conditions had almost the same particle size, morphology, and solubility, but their zeta potential was highly affected by the presence of dispersants. In terms of cellular response, ZnO dispersed in citrate exhibited the highest toxicity (Figure 1) and enhanced cellular uptake, although dispersants did not influence on energy-dependent uptake mechanism of ZnO. Pharmacokinetic study also showed that oral absorption efficiency differed from dispersants used, but significantly different tissue distribution was not found. These findings suggest that more careful caution is necessary for choice of appropriate disperants to evaluate biological responses of nanoparticles.

Keywords: ZnO nanoparticles, dispersant, cytotoxicity, cellular uptake, pharmacokinetics, tissue distribution.

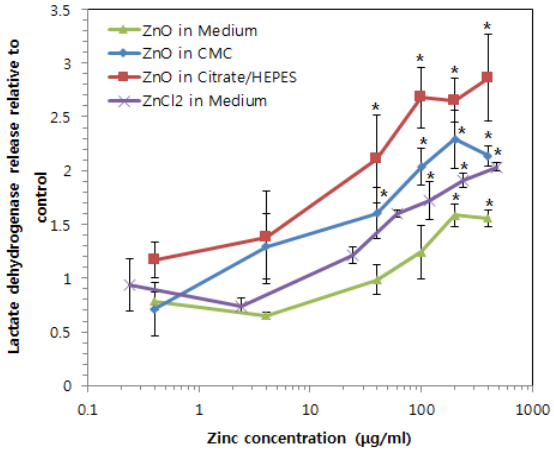

Figure 1: Cytotoxicity of ZnO nanoparticles prepared in different dispersants or cell culture medium in lung epithelial A549 cells after 24 h exposure.

References:

Fan, Z., Lu, J.G. (2005), Zinc oxide nanostructure: synthesis and properties, *J. Nanosci. Nanotechnol*., 5, 1561-1573

Paek, H.J., Lee, Y.J., Chung, H.E., Yoo, N.H., Lee, J.A., Kim, M.K., Lee, J.K., Jeong, J., Choi, S.J. (2013), Modulation of the pharmacokinetics of zinc oxide nanoparticles and their fates in vivo, *Nanoscale*, 5, 11416-11427

Haniu, H., Saito, N., Matsuda, Y., Kim, Y.A., Park, K.C., Tsukahara, T., Usui, Y., Aoki, K., Shimizu, M., Ogihara, N., Hara, K., Takanashi, S., Okamoto, M., Ishigaki, N., Nakamura, K., Kato, H. (2011), Effect of dispersant of multi-walled carbon nanotubes on cellular uptake and biological responses, *Int. J. Nanomed*., 6, 3295-3307

Transdermal resveratrol nanoethosomes; Preparation, Optimization; *In-vitro*, and *In-vivo* evaluation

H. Aldawsari1,[1] K. Hosny[1,2]

[1]Department of Pharmaceutics and Industrial Pharmacy, Faculty of pharmacy, King Abdulaziz University, Jeddah, Saudi Arabia
[2]Department of Pharmaceutics and Industrial Pharmacy, Faculty of Pharmacy, Beni Suef University, Beni Suef, Egypt

Abstract: Resveratrol is a prominent substance in currently pharmaceutical research. It is a naturally occurring non-flavanoid phenolic compound produced by some spermatophytes, notably grapes. It has been reported to possess antioxidant, neuroprotective, antiphotoaging and antiviral activities, and it also seems to play a role in the prevention and reduction of pathological processes such as inflammation. Resveratrol has been demonstrated to show benefits against skin disorders (Zhang *et al.*, 2007). However, trans-resveratrol has poor oral bioavailability, mainly because it is extensively metabolized in the body. The bioavailability of orally administered resveratrol is insufficient to permit high enough drug concentrations for systemic therapy (Hung *et al.*, 2008). The aim of the present study is to prepare, optimize, and evaluate resveratrol as transdermal nanoethosomal formulation, in order to enhance its bioavailability. Several factors as drug to phospholipid molar ratio, phospholipid to ethanol ratio, hydration medium pH, hydration time, and the temperature of hydration were investigated to study their effect on the particle size and entrapment efficiency (EE%) of resveratrol within nanoethosomes. The optimized formula was subjected to *in vitro* release, *Ex-vivo* permeation, and *in vivo* pharmacokinetic studies. The results indicated that optimum nanoethosomal formula was successfully formed with particle size 53 nm and entrapment efficiency 86%, also the bioavailability increased by more than 6-folds after transdermal application of optimized nanoethosolmal formula in comparison with commercially available product. From the above results it can be concluded that nanoethosomal formulation represents an efficacious carrier for transdermal delivery of Resveratrol.

Keywords: Resveratrol, nanoethosomes, *in vitro, ex vivo* and *in vivo* characterization, optimization of transdermal permeation.

References:

Zhang, G., Flach§, C., and Mendelsohn, R. (2007) Tracking the Dephosphorylation of Resveratrol Triphosphate in Skin by Confocal Raman Microscopy, *J Control Release*, 123(2): 141–147.

HUNG, C-F., LIN, Y-K., HUANG, Z-R., and FANG, J-Y. (2008) Delivery of Resveratrol, a Red Wine Polyphenol, from Solutions and Hydrogels via the Skin, *Biol. Pharm. Bull*, 31(5): 955—962.

Incorporation and release of gemcitabine prodrug in mesoporous silica nanoparticles

G. Berlier,[1] A. Malfanti,[2] I. Miletto,[1] E. Bottinelli,[1] D. Zonari,[2] G. Blandino,[2] B. Stella,[2] S. Arpicco[2]

[1]University of Torino, Dipartimento di Chimica and NIS (Nanostructured Interfaces and Surfaces) Centre, Torino, Italy
[2]University of Torino, Dipartimento di Scienza e Tecnologia del Farmaco, Torino, Italy

Abstract: In recent decades, mesoporous silica nanoparticles (MSNs) have been subjected of intense research (Mamaeva *et al.*; 2013). Compared to traditional organic nanocarriers (such as liposomes or other colloidal systems) these vehicles exhibit unique properties of inorganic nanomaterials, such as thermal and chemical stability and ease of chemical modification of surface silanol groups. MSNs show very interesting properties for the application in the development of drug delivery devices, such as stable mesoporous structure, high specific surface area (600-1000 m^2/g), large pore volume (0.6-1 cm^3/g), regular and tunable mesopore diameters (1.6–30 nm) and pore channel systems homogeneously organized in hexagonal mesostructures. Moreover, many types of MSNs have been shown to be nontoxic in many biological systems if they are prepared with certain optimized structural features and are applied in right dosage (Vivero-Escoto *et al.*; 2010).
Based on these considerations, the aim of this work was to explore the ability of different MSNs to be employed as a convenient vehicle for the delivery of antitumoral drugs. In particular, MSNs characterized by different surface functionalizations were studied as vehicles for the delivery of the antitumoral drug gemcitabine (GEM) and of its lipophilic prodrug to improve drug metabolic stability and *in vitro* and *in vivo* cytotoxic activity.
For this purpose, MSNs as such or with grafted aminopropyl and carboxyethyl groups were prepared and characterized. MSNs were produced by a sol-gel procedure in presence of the surfactant cetyltrimethylammonium bromide (CTAB) as structure directing agent and functionalized by post-synthesis grafting as previously reported (Sapino *et al.*; 2015). The obtained materials exhibited quasi-spherical particle morphology with an average particle size of ca. 100 ± 23 nm and regular and ordered cylindrical channels with hexagonal symmetry. Representative high resolution transmission electron microscopy (HRTEM) images of the samples are reported in Figure 1.

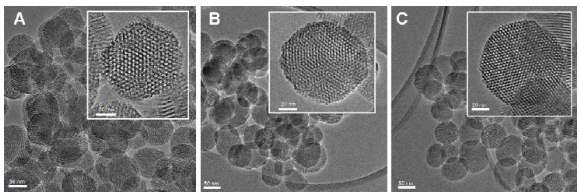

Figure 1: HRTEM images of A) MSNs; B) Carboxy-MSNs and C) Amino-MSNs.

The presence of the functional groups on the surface of Amino-MSNs and Carboxy-MSNs was confirmed by thermogravimetric analysis (TGA) and FTIR measurements.
Then, GEM loading capacity of different MSNs in relation with the nature of the functional group exposed was determined by HPLC. We observed that in our experimental conditions GEM was not loaded in any MSNs whatever tested ratios and incubation time. Thus, we decided to encapsulate a gemcitabine lipophilic prodrug, the 4-(*N*)-lauroylgemcitabine (C12GEM), whose calculated log P value is 4.84, higher than that of the parent drug (-1.4) (Stella *et al.*; 2007). C12GEM was efficiently loaded in the MSNs. Moreover, the results showed that the drug loading efficiency increased in the case of functionalized MSNs, in the order Carboxy- > Amino- > MSNs. This indicates that the insertion of functional groups on the MSN surface lead to an increase in the loading capacity, probably in relation to hydrophobic and hydrogen bonding interactions that stabilize the drug-MSNs complexes.
Similarly, the presence of functional groups on MSN surface influenced the drug release profile. *In vitro* C12GEM release experiments from drug-loaded MSNs were carried out by soaking samples in PBS buffer at 37 °C. As reported in Figure 2, all samples showed a very gradual and slow release, which is influenced by the presence of surface functional groups. In particular, the release rate of the MSNs was the fastest one, followed by Amino-MSNs and by Carboxy-MSNs that was the lowest. This indicates that the diffusion of the prodrug from the three samples to the buffer solution depends on the functionalization with a trend inverse to that found in the drug loading experiments. Carboxy-MSNs showed the

highest drug loading (23 µg/mg) and the lowest release in percentage, suggesting a relatively high interaction between C12GEM and the functional groups.

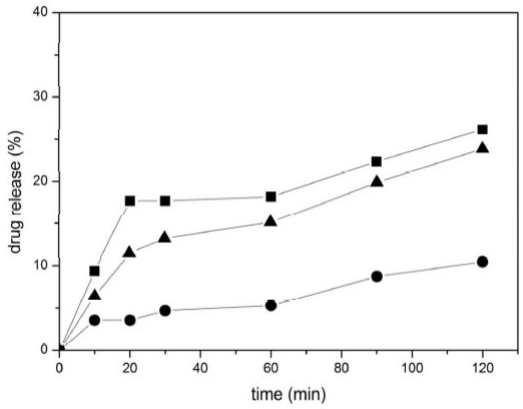

Figure 2: *In vitro* release profiles of MSN-C12GEM (■), Amino-MSN-C12GEM (▲) and Carboxy-MSN-C12GEM (●) in PBS medium at 37 °C. All experiments were done in triplicate. SD: ±10%.

Finally, the cytotoxicity of the different preparations was evaluated on MDA-MB-231 (human breast adenocarcinoma) and A2780 (human ovarian carcinoma) cells at different times (24, 48 and 72 h). Data showed that C12GEM-loaded MSNs were less cytotoxic than the free drug with an activity that increased with the incubating time indicating that all these systems are able to release the drug slowly and in a controlled manner.

Altogether the results demonstrate that these MSNs could be an interesting system for the delivery and extended release of anticancer drugs. In particular, our results highlight a dependence of the loading ability of MSNs on molecular properties of the drug, in particular the lipophilic character and steric hindrance, and on the MSN surface characteristics.

Keywords: nanoparticles, drug delivery systems, cancer chemotherapy, prodrugs, silica-based biomaterials, physicochemical properties, surface chemistry.

References:

Mamaeva, V., Sahlgren, C., Lindèn, M. (2013) Mesoporous silica nanoparticles in medicine - Recent advances, *Adv. Drug Deliv. Rev.,* 65, 689-702.

Sapino, S., Ugazio, E., Gastaldi, L., Miletto, I., Berlier, G., Zonari, D., Oliaro-Bosso, S. (2015) Mesoporous silica as topical nanocarriers for quercetin: characterization and in vitro studies, *Eur. J. Pharm. Biopharm.,* 89, 116-125.

Stella, B., Arpicco, S., Rocco, F., Marsaud, V., Renoir, J.M., Cattel, L., Couvreur, P. (2007) Encapsulation of gemcitabine lipophilic derivatives into polycyanoacrylate nanospheres and nanocapsules, *Int. J. Pharm.*, 344, 71-77.

Vivero-Escoto, J.L., Slowing, I.I., Trewyn, B.G., Lin, V.S.Y. (2010) Mesoporous silica nanoparticles for intracellular controlled drug delivery, *Small*, 6, 1952-1967.

Visual Analysis of Water permeability in Aquaporin Z incorporated Giant Unilarmellar Vesicles

Jun-Hee Lee,[1,*] Hyunil Ryu,[2] Tae-Joon Jeon,[2] Young-Rok Kim[1]
[1] Institute of Life Sciences and Resources & Department of Food Science and Biotechnology, College of Life Sciences, Kyung Hee University, Yongin, South Korea
[2]Depatment of Biological Engineering, Inha University, Incheon, South Korea

Abstract: Water permeability of aquaporin Z was investigated using Giant Unilamellar Vesicles (GUV). Because aquaporin Z has a selective permeability for water molecule in and out of the cell in biological system, It can be applied to design biological separation system. However, like other transmembrane protein, manipulation and application of aquaporin Z has many problems associated with expression, purification and integration of the protein into the membrane system. To solve these problems, we developed variable methods. Aquaporin Z was fused with Green fluorescence Protein (GFP) to visualize aquaporin Z in system. Hydrophobic nature of Aquaporin Z is another hurdle for purifying the protein in native form. Detergents are commonly used additives to facilitate the purification of transmembrane protein (Simons *et al.*; 1975). In this study, we purified GFP-fused aquaporin Z using triton X-100 as surfactant and observed green fluorescence of fused protein to track the location of aquaporin Z in the system. To the study of water permeability, GFP-fused aquaporin Z was needed to be reconstitute into the membrane platform. According to the report (Philippe *et al*.; 2004), membrane protein can be reconstituted into GUV using sequencial step. GUV reconstituted GFP-fused aquapotin Z was formed by electroformation method and those vesicles had green fluorescence (Figure 1). When outside solution of aquaporin Z-containing GUV was replaced to hypertonic salt, the volume of vesicle was changed as time-dependent. Reduced volume ratio after 20 minute was less ~50% compare with that of initial time, it agree with the report (Sheereen *et al*.; 2013). In this study, we established manipulation method of aquaporin Z that include visualization, purification, and reconstitution. Also water permeability of aquaporin Z was verified. This study will help to understanding of aquaporin Z character and apply to design of noble water purification system

Keywords: aquaporin Z, transmembrane protein, water permeability, green fluorescence protein, giant unilarmellar vesicle, electroformation, water purification system

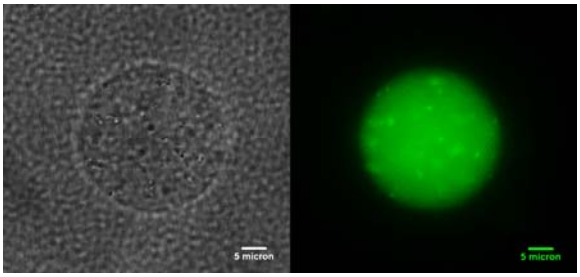

Figure 1: Figure illustrating the microscopy images of GUV reconstituted GFP-fused aquaporin Z. Left image was transmission image . Right image was fluorescence image. All images were same vesicle. Successfully, GFP fused aquaporin Z was incorporated into the GUV by electroformation method.

References:

Helenius, A., Simons, K. (1975) Solubilization of membranes by detergents, *Biochim. Biophys. Acta.*, 415, 29-79

Philippe, G., Jacques, P., Guillaume, L., Pierre, F., Jean-louis, R., Patricia, B. (2004), A new method for reconstitution of membrane proteins into giant unilamellar vesicles, *Biophys. J.*, 87, 419-429.

You jung, K., Harrison, S. W., Sheereen. M. (2013), A simple and versatile method for the formation of arrays of giant vesicles with controlled size and composition, *Adv. Mater.*, 25, 6834-3838.

Acknowledgments:

This work was supported by Pioneer Research Center Program (NRF-2012-0009575) both funded by the korean government

THE PRODUCTION AND THE CHARACTERIZATION OF SPIO NANOPARTICLES FOR MEDIATED TRANSFECTION OF PLASMID DNA

Zdenka Fohlerová[1], David Kovář[2], Jaromír Hubálek[1]
[1] CEITEC BUT, Technická 10, Brno ,[2] CEITEC MU, Kamenice 5, Brno, Czech Republic

Abstract: Transfection of eukaryotic cells is one of a key technology in cell biology being used in fundamental and applied research. To achieve a high transfection efficiency, reproducibility and low-toxicity on targeted cells when DNA plasmids is transfected, is highly desired. Several approaches using various nanoparticles (NPs) have been already evaluated but the comparison with standard chemical methods such as polyethylenimine (PEI) is still poor. In our work, we produce small monodispersed superparamagnetic nanoparticles (SPIO) as the suitable candidate for the assisted transfection of DNA expression plasmids. The synthesis of nanoparticles by co-precipitation method is presented and optimized in time, size, temperature and rate of base addition of core formation. The nanoparticles were stabilized with chitosan under physiological pH. DNA plasmids are expected to be integrated into the polymer coat, making the DNA-SPIO complex ready for the transfection via applied magnetic force and subsequently taken up by cells via endocytosis. Here, the DNA-SPIO complex is introduced in HEK cells to analyse the cellular toxicity and the effect on cell proliferation. The uptake of DNA plasmid was also evaluated by fluorescence microscopy to estimate the transfection efficiency by comparing fluorescently positive cells to the total quantity of cells and to see that no evident negative effect on cells is induced. The SPIO-mediated transfection will be compared with commercially available magnetic nanoparticles and PEI transfection agent.

Keywords: magnetic nanoparticles, plasmid DNA, polyethylenimine, transfection

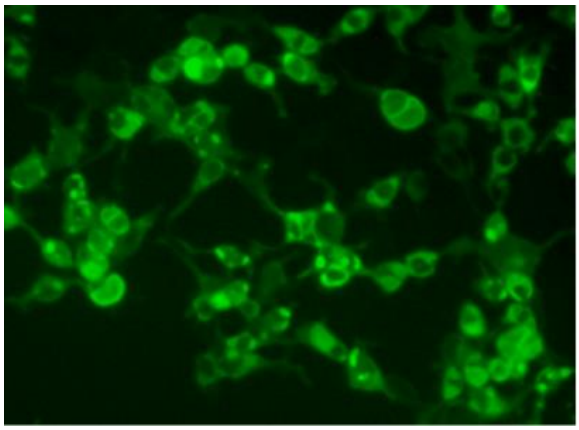

Figure 1: Figure illustrating the transfection of HEK293 cells with ChR-2 plasmid using magnetic nanoparticles.

References:

Durán M. et al., (2011), Comparison of nanoparticle-mediated transfection methods for DNA expression plasmids: efficiency and cytotoxicity, *Journal of Nanobiotechnology*, 9, 47

Mahdavi M. et al., (2013), Synthesis, Surface Modification and Characterisation of Biocompatible Magnetic Iron Oxide Nanoparticles for Biomedical Applications, *Molecules 18*(7), 7533-7548

Bertram J., (2006), MATra - Magnet Assisted Transfection: Combining Nanotechnology and Magnetic Forces to Improve Intracellular Delivery of Nucleic Acids, *Current Pharmaceutical Biotechnology* 7, 277–285.

Gold nanoparticle-based Immunoprecipitation (IP) sensor for Detection of Shiga toxin (Stx) from pathogenic *Escherichia coli*

Ki-Baek Jeong, Jun-Hee Lee, Min-Cheol Lim, and Young-Rok Kim
Institute of Life Sciences and Resources & Department of Food Science and Biotechnology, College of Life Sciences, Kyung Hee University, Yongin, Republic of Korea

Abstract: Ensuring food safety is critical in food industry. For decades, detection of toxins relevant to foodborne diseases have been widely performed in order to secure food safety. Shiga toxins (Stx) produced by *Escherichia coli* O157:H7 are one of the most virulence factors related to foodborne illness causing life-threatening conditions including kidney failure, neurological complications. Herein, we designed a method for rapid detection of foodborne virulence factors that can be applied to the field diagnosis. We developed gold nanoparticles (GNP) functionalized with specific antibodies (Ab) against Stx. GNP-Ab binds to Stx and creates GNP-Ab-Stx complexes through the specific antigen-antibody interactions. The complexes can bind to other GNP-Ab complexes via antigen–antibody bridging (Min-Cheol et al.; 2011). The antigen mediated complexes and free GNP-Ab are clearly distinguished by Radial chromatography (RC) because mobility of the complexes was affected by the formation of network structure in silica gel plate. When a drop of sample solution was placed onto the surface of silica gel plate, free GNP-Abs were spreading out from the drop site along with the solution. In the presence of target toxin, GNP-Ab forms complexes and their mobility decreases compared to free GNP-Ab. Therefore the sample with target toxin forms a small spot in the droplet site whereas the sample without target toxin forms a larger red circle derived from the unbound free GNP-Abs. The differences in mobility of the GNP-Ab in the absence or presence of target toxin is determined by radial chromatography. From the results, we could detect the existence of target toxins with naked eyes by checking the color distribution. Furthermore, we could apply this system to quantify the target toxin in test sample based on the color gradients of GNP. This method has advantages not only in detection time, cost efficiency but also in portability which is suitable for field diagnosis. This novel method has potential for ensuring food safety in field without conventional lab equipments.

Keywords: Gold nanoparticle, immunoprecipitation sensor, Shiga toxin, Radial chromatography, silica-gel plate, field diagnosis, color gradient.

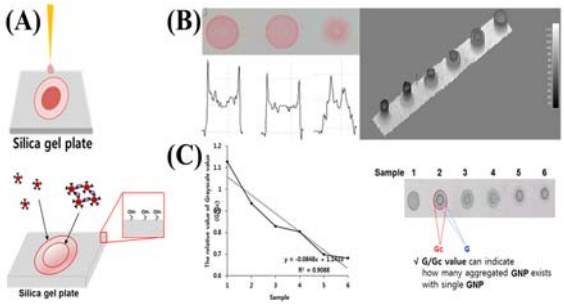

Figure 1: Whole scheme of the detection device based on immunoprecipitation. (A) Separation of GNP-Ab-Stx complexes and free GNP-Ab by radial chromatography (RC) on silica gel plate through capillary action. (B) RC results were analyzed by Image J software with line profiling and 3D image structuring. (C) Grayscale value of inner ring and outer ring (control) was used to calculate G/Gc value. G/Gc value shows the ratio of aggregated BNP-Ab-Stx complexes and unbound free GNP-Ab.

References:

Min-Cheol L., Yeo-Jae S., Tae-Joon J., Hae-Yeong K., Youn-Rok K.(2011) Microbead-assisted PDA sensor for the detection of genetically modified organisms, *Anal. Bioanal. Chem.*, 400:777-785

Saetbyeol P., Giyoung K., Jihea M. (2012) Improvement of Lateral Flow Assay for the rapid detection of *Salmonella*, *Food Eng. Prog.*, 16, 4, 333-339

Acknowledgement
This research was supported by a grant (S2176081) Small and Medium Business Administration in 2014.

Development of intelligent Drug Delivery Systems based on thermoresponsive gold nanoparticles

A. Cortijo Martín[1,2], B. van Mele[2], G. Bruylants[1]
[1]Engineering of Molecular NanoSystems, Ecole polytechnique de Bruxelles, Université libre de Bruxelles (Belgium), [2]Physical Chemistry and Polymer Science, Faculty of Engineering, Vrije Universiteit Brussel (Belgium)

Abstract: Thermoresponsive polymers have attracted much attention over the last decades because of their numerous potential applications in the biomedical field, for example as Drug Delivery Systems (DDS). These polymers exhibit a drastic influence of T on their conformation in solution: for example, Lower Critical Solution Temperature (LCST) polymers shift from a expended hydrophilic coil conformation at low temperatures (below their LCST) to a hydrophobic globular conformation at higher temperature (above their LCST).[1]

Our aim is to develop a thermocontrolled DDS (see Figure 1) by coupling a thermoresponsive polymer to gold nanoparticles (AuNP). AuNPs present a Localised Surface Plasmon Resonance (LSPR) band in the visible range and, by irradiating the AuNP at this band, it should be possible to induce the phase transition in the polymer.[2]

PNIPAM is a LCST polymer which displays good properties for the development of such kind of hybrid system.[1] PNIPAM of different sizes were synthesized with a thiol end-group and characterized by GPC, MTDSC and NMR. AuNP were synthesized following the Turkevich method and characterized by UV-Vis, DLS, TEM and SEM.

The different polymers were grafted on the particles, leading to AuNP-PNIPAM hybrids. The organic content of these hybrids was determined by TGA and their thermal behavior was studied in details by UV-Vis spectroscopy and DLS. The results show an important influence of the polymer size and of the ionic strength on the thermal behavior of the AuNP-PNIPAM hybrid systems.

With the aim to improve the control of the thermal behavior of the polymer, different strategies, such as the co-grafting of a hydrophilic polymer, were envisaged.

Keywords: gold nanoparticles, thermoresponsive polymer, PNIPAM, LSPR, Drug Delivery Systems

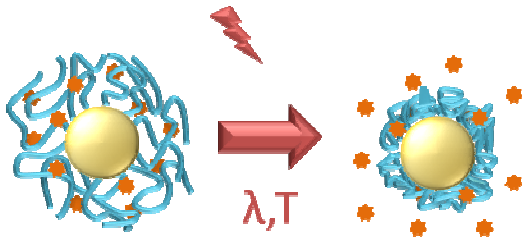

Figure 1: Controlled thermoresponsive drug delivery system.

References:

[1] K. Durme, G. Assche, B. Mele, *Macromolecules*, **2004**, 37(25) :9596-9605

[2]C. Said-Mohamed, J. Niskanen, D.Lairez, H.Tenhu , P. Maioli, N. Del Fatti, F. Vallée, Lay-Theng Lee, *J. Phys. Chem. C*, **2012,** *116* (23), pp 12660–12669

Development of a Mdm2 specific colorimetric biosensing platform using gold nanoparticles

M. Retout,[1] K. Bartik[1], Th. Doneux,[2] G. Bruylants[1]
[1] Engineering of Molecular Nanosystems, Ecole polytechnique de Bruxelles, Université Libre de Bruxelles, Belgium
[2]Analatycal Chemistry and Interfacial Chemistry, Faculté des Sciences, Université Libre de Bruxelles, Belgium

Abstract: Functionalized gold nanoparticles (GNPs) have attracted much attention during the past decade due to their potential applications in the biomedical field. GNPs present interesting optical properties such as their Localized Surface Plasmon Resonance (LSPR) which make them good candidate for the development of sensors (Taylor *et al.; 2012*). Our aim is to exploit the LSPR band of GNPs to develop a platform to detect the oncoprotein Mdm2.

Mdm2 plays a critical role in human cells as it is the main negative regulator of the tumor suppressor protein p53. This latter protein is deeply involved in the cellular response to the stress that can lead to the apparition of cancerous cells (Vousden *et al.;* 2002). In a number of human cancers, overexpression of the Mdm2 protein has been observed (Momand *et al.;* 1998) and its detection could be used in cancer diagnosis. Its regulation could furthermore lead to new therapies.

The platform is made of two sets of GNPs, each functionlized with a different peptidic aptamer, that can bind the targeted protein simultanously. In the presence of Mdm2 the GNPs aggregate with the protein playing the role of linking agent. The GNPs aggregation is an unambigous signal with the color of the solution changing from red to purple.

GNPs were synthesized and characterized (by TEM, DLS, UV-Vis) and then functionalized with peptide aptamers containing sequences identified in proteins known to interact naturally with Mdm2. A protocol was developed for the grafting of the aptamers on the GNPs surface and for the quantification of the grafting level. In the presence of Mdm2, but not of a control protein (BSA), GNPs aggregated and a significant change in the LSPR band was observed (Figure 1).

Keywords: protein detection, Gold nanoparticles, UV-vis spectroscopy, Biosensor, Peptidic aptamer, TEM, biomedical applications, Emission spectroscopy, Gold nanoparticles aggreagtion, LSPR

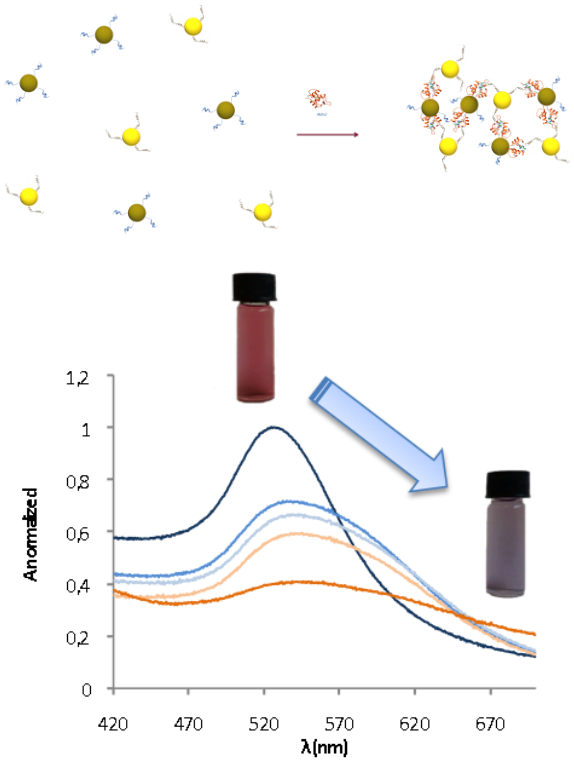

Figure 1: Aggregation of the two sets of gold nanoparticles in presence of the targeted protein (Mdm2)

References:

Vousden, K. H., Lu, X., (2002), Live or let die : the cell's response to p53, *Nat. Rev. Cancer*, 2:594-604

Momand, J., Jung, D., Wilczynski, S., Niland, J., (1998), The Mdm2 gene amplification database, *Nucleic Acids Res.*, pp. 3453–9

Taylor, R., Esteban, R., Mhajan, S., Coulston, R., Scherman, O., Aizpurua, J., Baumberg, J. (2012), Simple Composite Dipole Model for the Optical Modes of Strongly-Coupled Plasmonic Nanoparticles Aggregates *J. Phys. Chem*. C 116 25044

Enhanced Antibacterial Activity of Antibiotics in Combination with Silver Nanoparticles against Animal Bacteria

M. Smekalova,[1,*] V. Aragon,[2] A. Panacek,[1] L. Kvitek,[1] R. Zboril[1]
[1]Regional Centre of Advanced Technologies and Materials, Department of Physical Chemistry, Faculty of Science, Palacky University in Olomouc, Slechtitelu 11, 783 71 Olomouc, Czech Republic.
[2]Centre de Recerca en Sanitat Animal (CReSA), UAB-IRTA, Campus de la Universitat Autònoma de Barcelona, 08193 Bellaterra, Barcelona, Spain and Institut de Recerca i Tecnologia Agroalimentàries (IRTA), Barcelona, Spain

Abstract: Antibiotics are excessively used to treat and prevent animal infectious diseases which results in development and dissemination of bacterial resistance to antibiotics (Schwarz *et al*., 2001). Due to the decrease of antibiotics efficiency another ways of infection control has gained importance. Silver nanoparticles (AgNPs) are well-known for their strong antibacterial activity (Panacek *et al*., 2006) and they can also help to enhance the antibacterial effect of antibiotic therapy in humans (Hwang *et al*., 2012). Therefore, we studied combined therapy of AgNPs and antibiotics against veterinary bacteria. For this purpose, antibiotics with different modes of action were used. AgNPs 28 nm or 8 nm in size were synthesized through the reduction of complex cation $[Ag(NH_3)_2]^+$ by D-maltose or sodium borohydride, respectively. The comparison of minimal inhibitory concentration of AgNPs and antibiotics alone and in combination of each other was realized on the base of standard methods used in practice for evaluation of synergistic interaction of antibiotics with adjuvants (microdilution checkerboard method). The results showed that AgNPs possess synergistic, additive and indifferent activities against bacteria. No antagonistic interaction was observed. Moreover, we observed in some cases that antibiotic resistant bacteria become sensitive when antibiotic is combined with AgNPs. Our results point out to possibility of utilization of AgNPs in combination with antibiotics for treatment diseases caused by antibiotic resistant bacteria.

Keywords: silver nanoparticles, antibiotic resistant bacteria, synergy, microdilution checkerboard method.

References:

Schwarz, S., Kehrenberg, C., walsh, T.R. (2001), Use of antimicrobial agents in veterinary medicine and food animal production. *Int. J. Antimicrob. Agents*, 17, 431-7.

Panacek, A., Kvitek, L., Prucek, R., Kolar, M., Vecerova, R., Pizurova, N., Sharma, V.K., Nevecna, T., Zboril, R. (2006), Silver colloid nanoparticles: synthesis, characterization, and their antibacterial activity. *J. Phys. Chem. B*, 110, 16248–16253.

Hwang, I., Hwang, J.H., Choi, H., Kim, K.-J., Lee, D.G. (2012), Synergistic effects between silver nanoparticles and antibiotics and the mechanisms involved. *J. Med. Microbiol.*, 61, 1719–26.

The mechanisms for the radiosensitizing effects in high linear energy transfer radiation on colon cancer cells

Eun Ho Kim[1*], Youn Kyoung Jeong[2], Ilsung Cho[1], Seung Hoon You[1], Sung Ho Cho[1], Won-Gyun Jung[1,]
[1]Division of Heavy Ion Clinical Research, Korea Institute of Radiological and Medical Sciences, Seoul 139-706, South Korea; [2]Research Center for Radiotherapy, Korea Institute of Radiological and Medical Sciences, Seoul 139-706, South Korea

Abstract: The purpose of this study was to investigate the efficacy of Gold Nanoparticle as a radiosensitizer for use in combination therapy for colon cancer cells. Two human colon cancer cell lines (HCT116, HT29) were treated with GNP alone or with radiation followed by GNP. In vitro tests were evaluated by clonogenic survival assay, FACS analysis, western blotting, immunofluorescence, and comet assay. GNP significantly enhanced radiation efficacy under high and low Linear Energy Transfer (LET) radiation conditions *in vitro.* GNP, in combination with radiation, increased G2/M arrest and increased the cell population in the sub-G1 phase and the ROS level, ultimately increasing cellular apoptosis. GNP inhibits the repair of DNA damage caused by radiation and synergistically suppressed cell migration and invasion. The radiosensitizing effects of GNP are much higher in neutron (high LET)-irradiated cell lines than in γ (low LET)-irradiated cell lines. GNP synergistically enhances the radiosensitivity of colon cancer cells, suggesting it may have clinical utility in combination cancer treatment with high LET radiation.

Keywords: GNP, high LET radiation, radiosensitivity, colon cancer cells, DNA damage

Advantages and Obstacles of Using Microfluidic Based Immunoassay for the Detection of Cancer Biomarkers from Biofluids

R. Khnouf[1], D. Karasneh[1], A. Elbetieha[2], & B. Albiss [3]
[1]Department of Biomedical Engineering, Jordan University of Science and Technology, Irbid, Jordan
[2]Department of Applied Biological Sciences, Jordan University of Science and Technology, Irbid, Jordan
[3]Department of Applied Physics, Jordan University of Science and Technology, Irbid, Jordan

Abstract: Microfluidic devices also known as lab-on-chip devices have been a prime candidate for replacing popular biomarker detection techniques such as Enzyme-Linked- Immunoassays (ELISA) for advantages they provide such as reduced reagent and sample consumption, reduced time required, and reduced cost (Ng et al., 2010). In addition, microfluidic devices provide the potential of incorporating more than one process on the same device, one of which is filtration of biofluids such as blood before analyte detection (Sollier et al., 2009). In this work we present the design optimization process of a lab-on-chip device for the detection of Alfafetoprotein (a liver cancer biomarker) from blood (Figure 1). We report the effect of a variety of designs and parameters on the the filtration of red blood cells from blood samples before the detection of AFP using chip based immunoassay. Furthermore, we report differences in using different polymer substrates for the fabrication of such devices including polydimethylsiloxane (PDMS) and polymethylmethacrylate (PMMA) and study the material's effect on phenomena such as non-specific binding, blood clotting, and autofluorescence. We also study the device's ability to detect multiple proteins simultaneously. This study also considers the effect of detecting protein from a water sample versus detecting it from a whole blood sample in order to enable better implementing such technologies in the field.

Keywords: microfluidics, biomarker detection, Alfafetoprotein, immunoassay, biofluids, microfabrication, surface treatments, microchannels, fluorescence microscopy, blood filtration, polymethylmethacrylate, polydimethylsiloxane

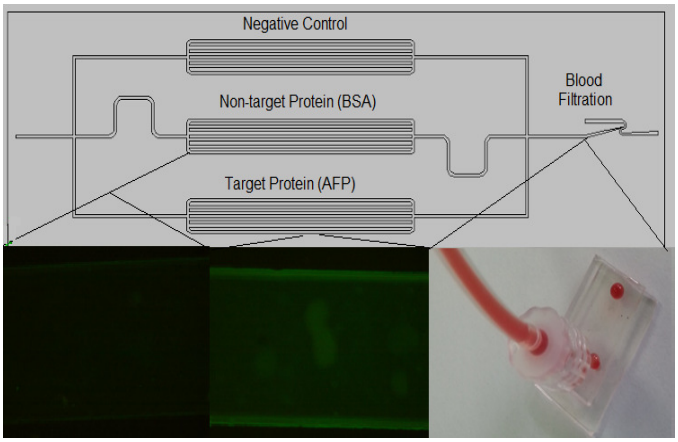

Figure 1: Microfluidic device design, where the device has a blood filtration region on the right and three detection zones to the left. The detection zones can be functionalized with antibodies of biomarkers of interest but in the above case the three regions two of the regions are functionalized with the target analyte antibody (anti-AFP), and the third region is not functionalized with anu antibodies as a negative control. Fluorescently tagged bovine serum albumin (BSA) was pumpued through the middle section – indicated on the figure, while fluorescently tagged AFP was pumped through the bottom section to ascertain the test's specificity.

References:

Ng, A.H.C., Uddayasankar, U., and Wheeler, A.R. (2010). Immunoassays in microfluidic systems. Anal. Bioanal. Chem. *397*, 991–1007.

Sollier, E., Rostaing, H., Pouteau, P., Fouillet, Y., and Achard, J.-L. (2009). Passive microfluidic devices for plasma extraction from whole human blood. Sens. Actuators B Chem. *141*, 617–624.

Efficient Encapsulation of Carboplatin Anticancer Molecule into Boron Nitride Nanotube : a Promising Drug Nanovector

M. El Khalifi,[1] E. Duverger [2], T. Gharbi[1], H. Boulhadour[1] and F. Picaud[1]
[1]Laboratoire de Nanomédecine, Imagerie et Thérapeutique, Université Franche-Comté (UFR Sciences et Techniques), Centre Hospitalier Universitaire de Besançon, 16 route de Gray, 25030 Besançon, France
[2]U Institut FEMTO-ST, 32 Avenue de l'Observatoire, 25044 Besançon, France

Abstract: Chemotherapy is frequently used to treat cancer patients. However, serious adverse effects are observed when drugs are systemically administered since they exhibit poor specificity in reaching tumor tissues(Yang et *al*., 2011). More, the efficacy of many potent and promising drug molecules is limited by their low water solubility, by the increased drug resistance and highly cytotoxic side effects (Samori, et *al*., 2010). To circumvent such important drawbacks, an efficient way of systemic transportation needs to be developed. Many of the pharmacological properties of conventional drugs can be improved through the use of nanocarriers(Allen TM et *al*., 2004). Anticancer drug transport is now become a central research since it would allow to localize the drug release near the tumor cell, avoiding secondary medical effect. We report a theoretical study based on molecular dynamics simulations to demonstrate that encapsulation of anticancer carboplatin molecule (CPT) is favored in boron nitride nanotube (BNNT). The ability of BNNT to vectorize CPT is improved since several drug molecules can be adsorbed inside the nanotube. Our simulations demonstrate that CPTs molecules are spontanously attracted to BNNT nanotube and are stable once encapsulated, forming cluster inside the nanotube. The storage capacity of BNNT is thus very large due to high confinement effects and hydrophobic interactions, favoring its filling with drug molecules until completion. Our calculations show in particular that we can fill the capsule by three drug molecules, opening the way to a very efficient drug transportation. To demonstrate it, the interaction of the filled nanovector with a membrane cell will be depicted in details. In particular, we will show that the CPT release is only effective when the BNNT penetrates the cell (Figure 1).

Keywords: boron nitride nanotube, therapeutic agents, cell membrane, all-atom molecular dynamic.

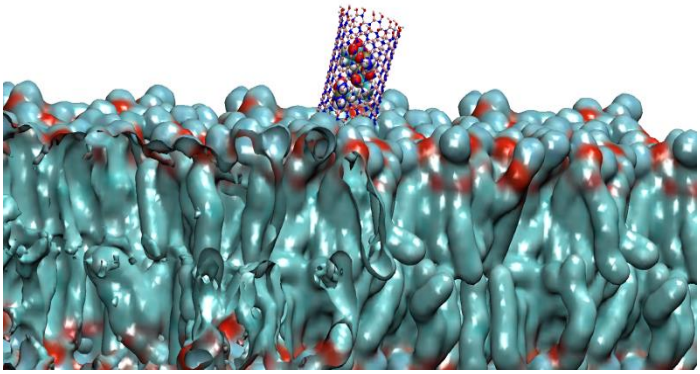

Figure 1: Completion of BNNT nanotube with CPTs drug.

References:

Samori, C., H. Ali-Boucetta, et al. (2010). "Enhanced anticancer activity of multi-walled carbon nanotube-methotrexate conjugates using cleavable linkers." *Chemical Communications* **46**(9): 1494-1496.

TM, Allen. and Cullis. PR (2004). "- Drug delivery systems: entering the mainstream." *Science* **303**(5665): 1818-22.

Yang, X., H. Hong, et al. (2011). "cRGD-functionalized, DOX-conjugated, and ^{64}Cu-labeled superparamagnetic iron oxide nanoparticles for targeted anticancer drug delivery and PET/MR imaging." *Biomaterials* **32**(17): 4151-4160.

Atomistic binding energy and Coarse grained simulation studies to understand the structure and drug release activity of Vancomycin loaded Lipid Polymer Nanoparticles (LPNs)

Suresh B Vepuri, Nasreen Seedat, Rahul Kalhapure, Chunderika Mocktar, Mahmoud Soliman and Thirumala Govender*
Discipline of Pharmaceutical Sciences, University of KwaZulu-Natal, Durban, South Africa

Abstract: Drug delivery is the most desired application of nanotechnology in medical and health sciences because of their advantages in target delivery, enhancement of bioavailability and potency. Our laboratory has been developing various antibacterial nano systems to combat drug resistance (*Kalhapure et al 2015*). The stability of nanoparticles is strictly governed by the free energy produced during nanoscale organization of molecules whilst the activity/drug release is influenced by the intermolecular forces at atomistic level. We performed a mesoscale simulation study and atomistic binding energy calculations to assess the stability and drug release pattern of the vancomycin (VAM) loaded lipid-polymer nanoparticles (LPNs) that were developed in our laboratory (*Seedat et.al. 2015)* The LPNs were composed of Eudragit RS100 (EUD) as the core and tripalmitin (GTP) as encapsulated lipid. Chitosan (CHT), Alginate (ALG) and Oleic acid (OA) were used as auxiliary agents to improve the encapsulation efficiency (EE). The coarse grained methodology of mesoscale simulation was successfully adopted for the above systems and the results suggested that the partially charged bead type polymeric core containing the charged and nonpolar bead type antibiotic is stabilized by the surface packing of nonpolar bead type tripalmitin. Optimized meso structures of all the LPNs were stable at their composition and the difference in free energy of nanoparticle formation among the LPNs clearly demonstrated their stability and ease of degradation. To identify the intermolecular forces governing the drug release mechanism of LPNs, binding free energy studies were performed on various complexes of the drug-polymer-lipid systems. The binding affinity data suggested that the encapsulation efficiency of EUD was increased due to supramolecular linking of the helper polymers by hydrogen bonding. In the presence of OA the drug was encapsulated preferably inside the fatty acid network. The high free binding energy for the OA system (ΔGbind = -3.48 Kcal/mol) compared to ALG (ΔGbind = -3.23 Kcal/mol) and native EUD systems (ΔGbind = -3.09 Kcal/mol) gave more stability for the complex and released the drug at a slower rate. Comparison of binding affinities among the helper polymer complexes revealed that CHT binding mode was relatively tighter than ALG due to higher number of electrostatic bonds in tetra and pentamolecular complexes (Figure 1). Though the ALG facilitated the EE as similar to CHT, the lower free energy of binding for the ALG system at high molecular level allowed the components to dissociate faster than CHT and hence the drug was released much faster than that of CHT and OA system. No major difference in drug release rate was observed among ALG and the native EUD system as the helper polymer was not tightly entangled with the EUD. Together with atomistic and mesosclae simulations this study was successful in assessing the stability of LPNs and explaining the performance of LPNs with respect to their experimental EE and DR.

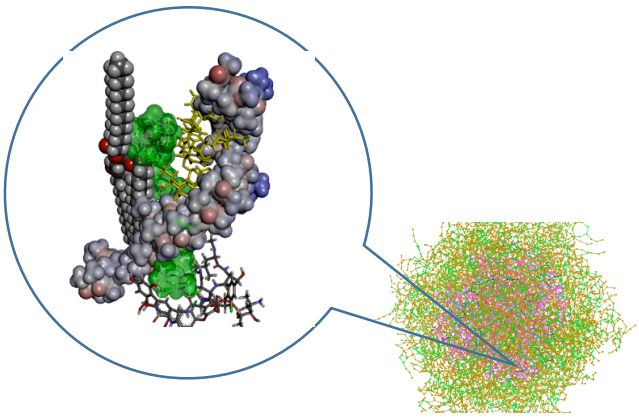

Keywords: lipid polymer nanoparticle, mesostructure, free energy of binding, intermolecular forces, encapsulation efficiency (EE), drug release (DR), stability, supramolecule.

Figure 1: Figure illustrating the stable mesostructure of LPN produced by coarse grained simulation and the atomistic level intermolecular interactions of the supramolecular complex (EUD-CHT-VAM) of the nanoparticle.

References:

Kalhapure, R.S, Mocktar, C., Sikwal, D.R., Sonawane, S.J., Kathiravan, M.K., Skelton, A., Govender, T. (2014), Ion pairing with linoleic acid simultaneously enhances encapsulation efficiency and antibacterial activity of vancomycin in solid lipid nanoparticles, *Colloids Suf., B*, 117, 303-311.

Seedat, N., Kalhapure, R., Mocktar, C., Govender, T. (2015), Enhancing vancomycin delivery via lipid-polymer hybrid nanoparticles, *1st European Conference on Pharmaceutics*, 13-14 April 2015, Reims, France.

Reliability, Availability, Maintainability and Safety Analysis for the Development of a Nano-material Plant

E. Davarpanah [1], M. Bodaghi [2]
[1.] Politecnico di Torino, Department of Energy (DENERG), Turin, Italy
[2.] Engineering Design and Advanced Manufacturing, MIT Portugal Program,
Faculty of Engineering, University of Porto, Porto, Portugal

Abstract: Emerging technologies could potentially cause some side effects with negative impact on environment, health, safety and sustainability. These impacts can destabilize the business strategies of the companies, which adopt technological innovations. Policies such as Reliability, Availability, Maintainability and Safety Analysis (RAMS) can reduce the previously mentioned risks and improve the competitiveness of those companies, which adopt this methodology in order to create safe and socially acceptable products (A.R. Köhler, C. Som., 2014). Availability and maintainability are important concepts in the early phase of plant construction in order to ensure the achievement of strategically business plan. Therefore, a series of design and operative decisions have to be taken to optimize the plant objectives (E. Godoy et al., 2015). For instance, applying RAMS analysis to a plant producing nano-sized materials for lubricants/oil products proves to be fundamental for design and management evaluation of the system performance. One relevant important issue is to address the detailed study of the failures, which are more probable to occur inside this type of nano plant. Common type of failures, namely system faults, emergency/interruptions and unmanaged accidents which happen due to technical breakdowns. Thus, improving the system reliability is a key chain for developing a productive system in a cost-effective manner. (M.C. Eti et al., 2007). In this paper, the advantages of applying the aforementioned methodology to a nano-material plant are explained. The case study is a real plant producing WS_2 powder from WO_3 in a batch process. The production process is based on the conversion of tungsten oxide into tungsten disulfide within specially designed chemical reactor. The approach reveals the plant design deficiencies, which could compromise the system functionality leading to production loss, human safety issues and environment negative consequences. The results show the most critical subsystems: reactor, hot pre-filter, H_2S and H_2 farms. Nevertheless, optimal logistic solutions for the procurement/supply of the maintenance/spare parts are evaluated in order to improve the system reliability and integrity.

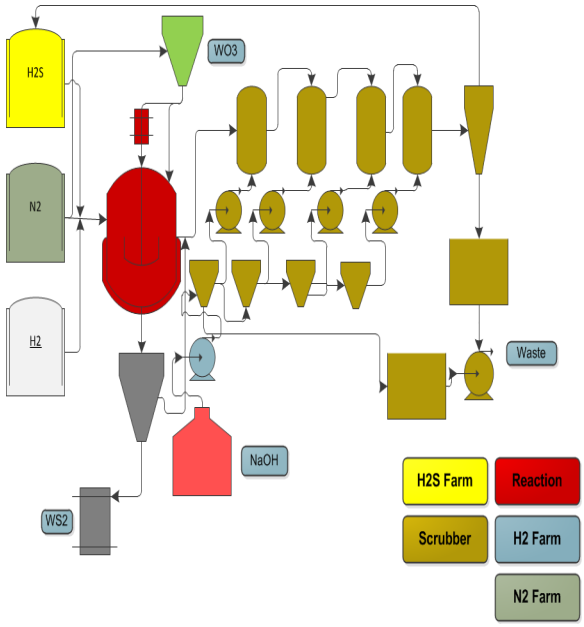

Keywords: RAMS analysis, system reliability, nano-material plant, maintenance/spare part logistics, operative strategies.

Fig 1: Figure demonstrates briefly the main sectors and connections of the used nano-material plant as a case study.

References:

Eti, M.C., Ogaji, S.O.T., Probert, S.D., (2007), Integrating reliability, availability, maintainability and supportability with risk analysis for improved operation of the Afam thermal power-station, *Int.J. Applied Energy*, 84, 202–221.

Kohler, A., Som, C., (2014), Risk preventative innovation strategies for emerging technologies the case of nano-textiles and smart textiles, *Int. J. Technovation*, 34, 420-430.

Goddy, E., Benz, S.J., Scenna, N. J., (2015), An optimization model for evaluating the economic impact of availability and maintenance notions during the synthesis and design of a powder plant, *Int. J. Computers and Chemical Engineering*, 75, 135–154.

Development of Liposomal Nanocarriers for Near-Infrared Dye: Preparation and Physico-Chemical Characterization

S. Koudelka,[1,2,*] J. Masek, [2] R. Mikulik, [1] J. Turanek[2]
[1]International Clinical Research Center, St. Anne´s University Hospital Brno, Czech Republic
[2] Veterinary Research Institute, Department of Pharmacology and Immunotherapy, Brno, Czech Republic

Abstract

Indocyanine green (ICG) is the only near-infrared (NIR) fluorescence dye approved by FDA for clinical applications. Fluorescence emission at 820 nm predetermines ICG to be eligible contrast agent for *in vivo* imaging with minimal interference from blood and tissue auto-fluorescence (450-600 nm). In aqueous environment, rapid degradation of ICG results in significant decrease of absorption and emission. Non-covalent association with human albumin, hydrophobic polymers or lipid vesicles (liposomes) stabilizes ICG, enhances emission intensity and shifts absorption peak to higher wavelengths. The versatility of liposomes to cargo either hydrophobic or hydrophilic entities in combination with tunable size and surface modification have been proven clinically useful. We have previously developed liposomal formulations of anticancer hydrophobic drugs and hydrophilic contrast agents for CT (Koudelka *et al*., 2010, 2014).

Now we report the preparation and physico-chemical characterization of liposomal ICG. ICG formulated either as cationic or as long-circulating liposomes (lipid/dye molar ratio, 200/1) was prepared by freeze-thaw extrusion followed by purification. Dynamic light scattering showed liposome mean size of 90-100 nm and polydispersity about 0.08. ICG entrapment efficacy of 50 and 41% was found for cationic and long-circulating liposomes, respectively. Association of ICG within the liposome bilayers resulted in shift of absorption peak from 776 to 804 nm (Figure 1). During 3 days at 4 and 37 °C, any decrease of ICG absorption peak was not observed for cationic liposomes while low and significant decrease was found for long-circulating liposome ICG and free ICG, respectively. The decrease rates were faster at 37° C. Lyophilization (lipid/sucrose molar ratio, 1:5) was used to stabilize ICG liposomes during storage. Upon lyophilizate rehydration, neither loss of entrapped ICG nor changes in original size was found for both types of liposomes. We have prepared stable cationic and long-circulating liposome ICG formulations. These developed ICG formulations represent suitable contrast agents for use in NIR fluorescence imaging *in vivo*.

Keywords: drug delivery, indocyanine green, liposomes, nanodelivery systems, nanotechnology, near-infrared (NIR) dyes, NIR fluorescence imaging, stability.

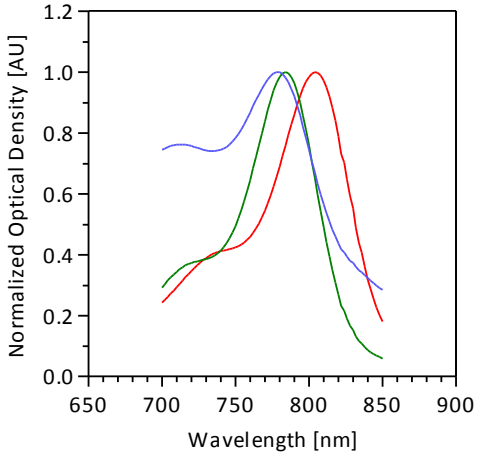

Figure 1: Normalized absorption spectra of different ICG formulations. Blue line represents ICG solubilized in 0.9% natrium chloride solution with peak at 776 nm. The shift of absorption peak to higher wavelength of 784 and 804 nm was observed for ICG solubilized in methanol (green line) and liposomal ICG (red line), respectively.

References

Koudelka, S., Turanek-Knotigova, P., Masek, J., Korvasova, Z., Skrabalova, M., Plockova, J., Bartheldyova, E., Turanek, J. (2010) Liposomes with high encapsulation capacity for paclitaxel: Preparation, characterization and in vivo anticancer effect, *J. Pharm. Sci.*, 99, 2434-2443.

Koudelka, S., Jelinkova, V., Turanek, J., Mikulik, R. (2014) Liposomal nanodelivery systems for iodine-based CT contrast agent, *Int. J. Stroke*, 9 (Suppl. 3), 181.

Acknowledgement

This work was supported by the following grants: GAP503/12/G147, MZE0002716202, CZ.1.05/1.1.00/02.0123 and CZ.1.07/2.3.00/30.0043.

Improved Antimicrobial Activity of Electrospun Graphene-Chitosan/Gelatin Nanofibrous-Based Nanocomposite Scaffolds

Isra H. Ali,[1,2] Amgad Ouf,[3] Mehmet Berat Taskin,[4] Jie Song,[4] Mingdong Dong,[4] Menglin Chen,[4] Rania Siam,[1,3,] Wael Mamdouh,[1,2*]

[1] Yousef Jameel Science and Technology Research Center (YJSTRC), School of Sciences and Engineering (SSE), The American University in Cairo (AUC), AUC Avenue, P.O. Box 74, New Cairo 11835, Egypt.

[2] Department of Chemistry, School of Sciences and Engineering (SSE), The American University in Cairo (AUC), AUC Avenue, P.O. Box 74, New Cairo 11835, Egypt.

[3] Department of Biology and Biotechnology Graduate Program, School of Sciences and Engineering (SSE), The American University in Cairo (AUC), AUC Avenue, P.O. Box 74, New Cairo 11835, Egypt.

[4] Interdisciplinary NanoScience Center (iNANO), Aarhus University, Gustav Wieds Vej 14, 8000 Aarhus, Denmark.

Abstract: Chitosan has attracted a lot of attention in the past few years particularly in biomedical and antimicrobial applications. Due to its noticeable antibacterial, biocompatibility, biodegradability, and swelling capcity, a number of wound dressings and antibacterial scaffolds have been developed by chitosan alone or in combination with other polymers, and/or nanofillers. A particular promising example for biomedical enginnering and antimicrobial applications is the chitosan/gelatin-based composite. Electrostatic interaction occuring between the positively charged chitosan surface and the negatively charged surface of gelatin molecules blocks the chitosan interaction with various negative moieties on the cellular membranes, and thus, leading to enhancement of cellular migration and proliferation on the material surface. Gelatin was reported to increase the material's hydrophilicity and consequently cell adhesion and spreading (Mao et al.). Electrospinning proved to be one of the most convenient techniques for fabricating nano/microfibrous mats that are highly porous interconnected nanocomposites through manipulating electrospinning parameters (Huang et al.). In this work, the preparation, characterization and antimicrobial evaluation of chitosan/gelatin bulk film, their corresponding electrospun nanofibrous nanocomposites, and chitosan/gelatin nanofibers reinforced with different amounts of graphene nanosheets will be presented. Spectroscopic and morphologicaol characterizations were carried out by using Fourier Transform Infrared (FT-IR) spectroscopy, Raman spectroscopy, transmission elcetron microscope (TEM), and Scanning electron microscopy (SEM) (the later is shown in Figure 1). Antimicrobial studies of the fabricated composites and nanocomposites against *Staphylococcus aureus* and *Escherichia coli* will also be presented. A reported drawback of gelatin is its bacterial growth enhancement effect. However, our results reveal that presence of chitosan in the the bulk film composite significantly masked the gelatin's bacterial growth enhancement effect, and the overall composites showed bacterial growth inhibition around 60 %. The antimicrobial activity of chitosan/gelatin electrospun nanofibers was enhanced by more 10% when compared to the corresponding casted film, which was attributed to increasing the aspect ratio of the produced electrospun nanofibers exposed to the bacteria compared to the bulk film. Finally, chitosan/gelatin/graphene nanosheets nanofibers showed enhanced antimicrobial activity of the produced nanofibers that exceeded 80% with both strains. These developed antibacterial scaffolds represent promising candidates that could be tailored and used for different biomedical and environmental applications such as wound dressing, skin regeneration, antibacterial coating, antibacterial food packaging, medical textiles, etc.

Keywords: chitosan, gelatin, electrospinning, nanocomposites, nanofibers, graphene nanosheets, antimicrobial, *Staphylococcus aureus*, *Escherichia coli*, biomedical, environmental applications.

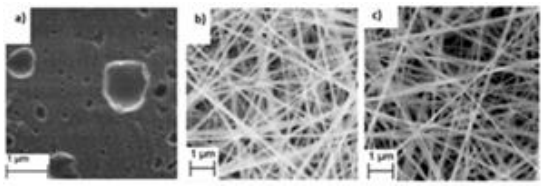

Figure 1: SEM images of : a.Chitosan/Gelatin casted film, b. Chitosan/Gelatin nanofibers, c. Chitosan/Gelatin nanofibers reinforced with graphene nanosheets.

References

Huang, Z., et al. (2003) A Review on Polymer Nanofibers by Electrospinning and Their Applications in Nanocomposites, *Comp. Sci and Tech.*, 63 (15), 2223-2253.

Mao, J., et al. (2004) A Preliminary Study on Chitosan and Gelatin Polyelectrolyte Complex Cytocompatibility by Cell Cycle and Apoptosis Analysis, *Biomater.*, 25 (18), 3973-3981.

Honey Chitosan Nanofibers Loaded With Natural Antimicrobials for Wound Dressing Applications

Wessam A Sarhan and Hassan M.E Azzazy
Novel Diagnostics & Therapeutics Research Group, Department of Chemistry, School of Sciences & Engineering, The American University in Cairo,New Cairo 11835, Egypt

Electrospun nanofibers have emerged as a promising candidate for wound dressing applications. Electrospun nanofibers show increased and controlled porosity allowing for enhanced exudate management. Moreover, nanofibers mimic the extracellular matrix of the skin thus enhance cell proliferation and migration and show increased surface to volume ratio allowing efficient loading of different hydrophilic and hydrophobic materials (Zahedi, et al., 2010).

Recently, we have managed to electrospin polyvinyl alcohol (PVA), chitosan and high honey concentration (40%) nanofibers using biocompatible solvents (1% acetic acid) (Sarhan & Azazzy., 2015). Such concentration that was previously reported unspinnable (Maleki, et al., 2013). High honey concentration, chitosan nanofibers represent an attractive candidate for advanced wound dressing due to their wound healing and antibacterial abilities. Thus, through the present work the Honey/Chitosan/PVA nanofibers (30%: 3.5%:7%) were loaded with two plant extracts to enhance their wound healing and antibacterial properties.

The first extract was obtained from a traditional plant well known for its enhanced antibacterial property. Whereas, the second extract was obtained from a wild herb that was collected from the mountains of Sinai.
The Honey/chitosan/PVA nanofibers loaded with the two extracts were characterized using Scanning electron microscope (SEM), Fourier Transform Infrared (FT-IR) spectroscopy, X-ray (XRD) diffractometer & differential scanning calorimetry (DSC). Moreover, the fibres were tested for their swelling abilities, porosity, antibacterial activity, cytotoxicity and wound healing ability. Remarkably, the inclusion of the plant extracts resulted in complete killing of *Staphylococcus aureus* and *Escherichia coli* and in increasing the swelling ability and porosity of the nanofibers to 500% & 97.7% respectively. Moreover, animal study revealed that the plant extract loaded Honey/Chitosan/PVA nanofibers showed improved wound healing of a full excisional 5mm wound in 15 days compared to 18 days for the control. No cytotoxicity was recorded for the developed nanofibers on cultured fibroblasts. In conclusion, novel, antimicrobial, biocompatible naturally based nanofibrous wound dressing was developed with enhanced antibacterial and wound healing ability.

Key words: Honey, Chitosan, Electrospinning, Plant extracts, Antimicrobial, Wound dressing.

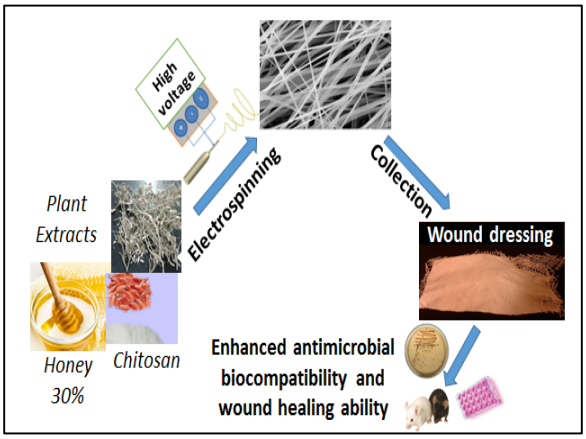

Figure 1: Illustrative diagram of the research and the main results. Honey, chitosan & plant extracts were electrospun with polyvinyl alcohol into nanofibers that were collected as prototype wound dressing. Experimental testing showed enhanced antimicrobial, biocompatibility and wound healing ability.

References:

Zahedi, et al., (2010). A review on wound dressings with an emphasis on electrospun nanofibrous polymeric bandages. Polymers for Advanced Technologies, 21(2), 77-95.

Maleki, et al., (2013). A novel honey-based nanofibrous scaffold for wound dressing application. Journal of Applied Polymer Science,127(5), 4086–4092.

Sarhan WA & Azazzy HME., (2015). High concentration honey chitosan electrospun nanofibers:Biocompatibility and antibacterial effects. Carbohydrate polymer, In press.

Doxorubicin loaded, pH-sensitive biodegradable naonogels and their bio-evaluation

P. Kumar[1], N. Yadav[2], A. Chhikara[1]* and M. Chopra[2]*
[1]Department of Chemistry, Dyal Singh College, University of Delhi, Lodhi Road, New Delhi-110003, India
[2]Dr. B. R. Ambedkar Center for Biomedical Research, University of Delhi, New Delhi-110007, India
Presenting author email: parveenkmr19@gmail.com; Corresponding author email: arunachhikara@gmail.com, mchopradu@gmail.com

Abstract: The pH-sensitive delivery system has been widely used in cancer therapy. The pH in tumors is lower than the normal tissues due to high rate of glycolysis in cancer cells. Therefore, pH-sensitive delivery systems can play important role for controlling delivery of drug in cancerous diseases. In biological systems, glutathione (GSH, a tripeptide) having a pendant sulfhydryl (−SH) groups as a cellular reducing agent is found at different concentrations in extracellular (2-20μM) and intracellular (2-10 mM) compartments in living cells. This large difference in the redox potential between extracellular and intracellular compartments as well as the further increased concentration of GSH in cancer cells promotes the disulfidethiol degradation platform in the development of glutathione responsive degradable polymeric nanocarriers for drug delivery system (Pan YJ et ai., 2012). We herein present the pH and Glutathione responsive biodegradable nanogels for the delivery of doxorubicin (Figure 1). Nanogel synthesis was carried out by AGET ATRP via cyclohexane-water inverse miniemulsion which was insoluble in various solvents including THF and water (Oh et al., 2006). Morphology and Size distribution characterization of the nanogels was carried out by TEM and DLS respectively, which were found to be almost spherical and their mean diameter was in the nanometre range. Doxorubicin was loaded into the nanogels by physical encapsulation method. Loading efficiency and loading level of doxorubicin was determined by UV spectroscopy and was found to be 28.73 % and 8.52 % respectively for 10 weight percent of the drug.

Keywords: biodegradable, nanogels, biomedical application, drug delivery, doxorubicin, glutathione

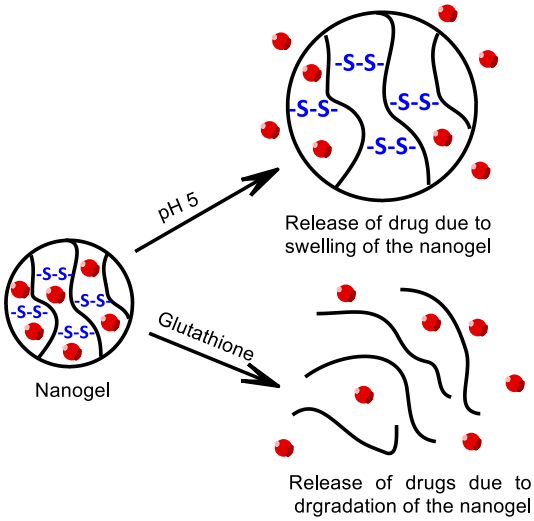

Figure 1: Figure illustrating the release of doxorubicin due to degradation and swelling of nanogels.

Fourier Transform Infrared (FTIR) spectra of doxorubicin, blank nanogels, and dox-nanogels were recorded. The Doxorubicin release study was performed at physiological (7.4) pH and acidic (5) pH. At pH 7.4, higher doxorubicin release was achieved as compare to release at pH 5. In-vitro cytotoxicity assay was performed by MTT assay on U87 cell-lines.

References:

Pan, YJ., Chen, YY., Wang, DR., Wei, C., Guo, J., Lu, DR., Chu, CC., Wang, CC., (2012), Redox/pH dual stimuli-responsive biodegradable nanohydrogels with varying responses to dithiothreitol and glutathione for controlled drug release. *Biomaterials.*, 33, 6570-6579.

Oh, JK., Tang, C., Gao., H, Tsarevsky, NV., Matyjaszewski, K., (2006), Inverse Miniemulsion ATRP: A New Method for Synthesis and Functionalization of Well-Defined Water-Soluble/Cross-Linked Polymeric Particles. *J. Am. Chem. Soc.*, 128, 5578-5584.

Increasing the efficiency of anticancer therapies using mono-dispersed chitosan nanoparticles

Mas Jaffri Masarudin[1*], Suzi M. Cutts[2], Don R. Phillips[2], and Paul J. Pigram[3]

[1]Department of Cell and Molecular Biology, Faculty of Biotechnology and Biomolecular Sciences, Universiti Putra Malaysia, Malaysia, [2]Department of Chemistry, School of Science, Technology and Engineering, La Trobe University, Australia, [3]Department of Physics, School of Science, Technology and Engineering, La Trobe University, Australia.

*Email: masjaffri@upm.edu.my

Abstract: This study describes the synthesis of hydrophobically-modified chitosan nanoparticles utilized for the enhanced delivery of radiolabelled [^{14}C]-doxorubicin. Factors influencing doxorubicin encapsulation were investigated, including drug concentration, TPP reactivity, as well as ionic interactions between various molecules during formation of CNP-[^{14}C]-doxorubicin involved in encapsulation efficiency. Time-dependent accumulation of released doxorubicin in individual cells treated with CNP-[^{14}C]-doxorubicin and drug release kinetics from the synthesized nanoparticles were also explored. CNP samples were synthesized through ionic gelation routes with sodium tripolyphosphate. A hydrophobic anchor was then linked to the chitosan polymer, by conjugation with palmitic acid via NHS-amine bridges. Estimation of drug loading and release were done, while time-dependent cell toxicity and accumulation studies were performed using Fluorescent-Activated Cell Sorting (FACS) analysis. Encapsulation efficiency of [^{14}C]-dox into hydrophobically modified CNP increased by up to 2-fold, potentiated through interactions of the amphiphilic drug with the palmitic chains of hydrophobically-modified CNP. This led to a retention of [^{14}C]-doxorubicin by a further 6 h (50% release, pH 7) compared to normal CNP, which demonstrated the potential of using hydrophobically-modified chitosan nanoparticles as a controlled release vector for doxorubicin, an advantageous characteristic for long term drug administration. Nanoparticle-mediated delivery of [^{14}C]-doxorubicin also led to an increase in toxicity at low doses of administration. The efficacy of the drug increased a further 2.4 fold using pCNP-[^{14}C]-doxorubicin. A hydrophobically-modified CNP system for the encapsulation of doxorubicin was develop, with the ability to prolong administration of the drug and increase its efficacy at lower doses.

Keywords: chitosan nanoparticles, doxorubicin, nanobiotechnology, nanomedicine, nanoparticles, drug delivery, biomedical applications.

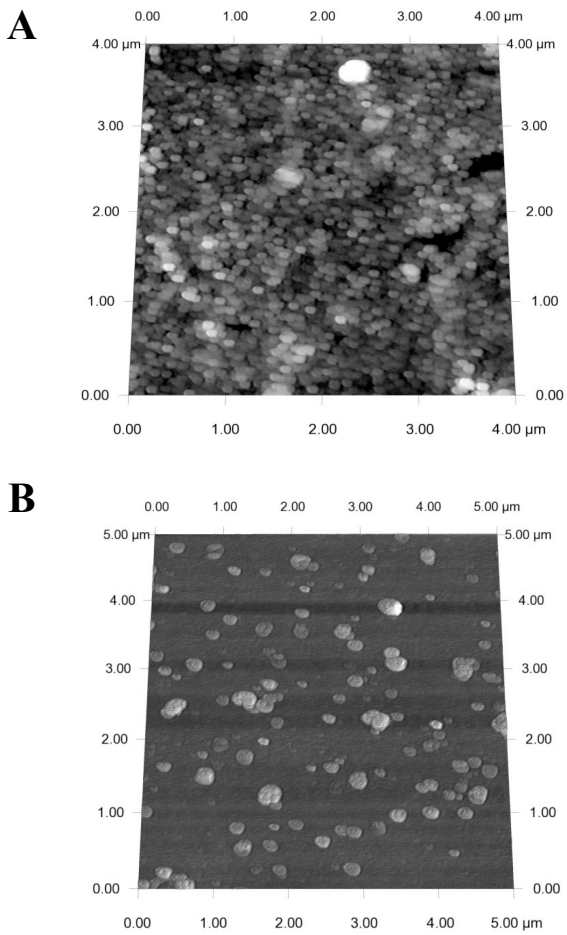

Figure 1: Figure illustrating morphological differences of (A) hydrophobically modified CNP, and (B) hydrophobically modified CNP loaded with [^{14}C]-doxorubicin, analyzed using Atomic Force Microscopy.

siRNA and miRNA-based SNAs to target canonical and non-canonical Bcl-2 signaling in glioblastomas

Northwestern University Center of Cancer Nanotechnology Excellence (NU-CCNE)

[1]Alexandra Chalastanis, [1]Fotini M. Kouri, [1]Samuel A. Jensen, [1]Lisa A. Hurley, [1,2]Timothy Sita, [2,3]Emily S. Day, [2,3]Caroline H. Ko, [2,3]Weston L. Daniel, [2,3]David A. Giljohann, [2,4]Alexander W Scott, [1]Yongfei Wu, [1]Andrea Calvert, [5]Markus A. Queisser, [6]Youjia Hua, [2,3]Timothy J. Merkel, [1]Chian-Yu Peng, [1]Carissa Ritner, [2,3]Liangliang Hao, [7]Hailei Zhang, [5]Jacob I Sznajder, [7]Lynda Chin, [2,3]Andrea J. Luthi, [2,3]Pinal C. Patel, [2,3]Joshua I. Cutler, [3]Matthew w. Rotz, [3,8,9]Thomas J. Meade, [10]John A. Kessler, [6]Marcus E. Peter, [2,3]Chad A. Mirkin, and [1]Alexander H. Stegh

[1]Ken and Ruth Davee Department of Neurology, The Northwestern Brain Tumor Institute, The Robert H. Lurie Comprehensive Cancer Center, [2]International Institute for Nanotechnology, [3]Department of Chemistry, [4]Department of Biomedical Engineering, [5]Division of Pulmonary and Critical Care Medicine, [6]Division of Hematology/Oncology, [7]The Broad Institute of Harvard and MIT, Department of Medical Oncology, Dana-Farber Cancer Institute, [8]Department of Molecular Biosciences, [9]Department of Neurobiology, [10]Department of Neurology, Northwestern University.

Despite decades of basic and clinical research, survival of patients diagnosed with glioblastoma multiforme (GBM), the most prevalent and aggressive form of malignant gliomas, has not changed significantly. A plethora of 'undruggable' genetic events that drive tumor progression together with the lack of drug delivery systems to overcome blood-brain and blood-tumor barriers conspired to make GBM an incurable disease.

We have sought to address these challenges by (a) identifying genetic mechanisms that act as roadblocks preventing therapies to induce tumor regression, and (b) by targeting these roadblocks using Spherical Nucleic Acids (SNAs). These are polyvalent gold nanoparticle loaded with small RNA interference (RNAi) molecules to silence aberrant gene expression.

We identified Bcl2L12 and Bcl-xL as oncogenes enabling tumor progression and micro-RNA-182 as a potent tumor suppressor. Bcl2L12, Bcl-xL and microRNA-182 are important cancer genes and therapeutic targets that regulate therapy susceptibility and tumor progression. Manipulating their expression made tumor cells vulnerable to anti-glioma therapies. Thus, we designed SNAs to silence Bcl2L12 and Bcl-xL expression, and to reconstitute GBM tumors with microRNA-182. We preclinically validated these SNAs *in vitro* in glioma cell lines and glioma-initiating cells (GICs) as well as in GBM mouse models in vivo.

RNAi has the potential to silence the expression of cancer genes, but has never entered the clinic due to the fact that conventional RNAi cannot silence gene expression persistently, has significant cytotoxic side effects, and cannot cross the blood brain barrier. On the contrary, SNAs were able to cross the blood-tumor barrier following intravenous administration, and disseminated throughout glioma tissue while reducing GBM burden without any toxicity. They silenced Bcl2L12 and Bcl-xL gene expression, and enabled expression of microRNA-182.

SNA treatment sensitized glioma cells toward several anti-glioma therapies, and when tested in GBM mouse models, SNAs slowed down tumor progression and increased survival of glioma-bearing mice.

Taken together, these results reveal that SNAs represent a promising therapeutic approach to overcome therapy resistance in GBM and, more broadly, SNA administration may represent a universal strategy to target aberrantly expressed cancer genes.

Nanosensors and nanomaterials for biomedicine

N.Casanova-M.[1]*, B. Céspedes[1], M Cisternas[1], N. Figueroa[1], R Gonzáles[1], A. Chandia[2], C. Contreras[3], R Segura[3], Pablo Conejeros[3], Francisco Morales [4], Marcelo Kogan[4], C.A.M. Wilson[4], M.Favre[1], H. Bhuyan[1], A.R Alvarez[2], S.A.Hevia[1], JR Maze[1].

[1] Instituto de Física, Pontificia Universidad Católica de Chile, Casilla 306, 6904411 Santiago, Chile.

[2] Facultad de Biología, Pontificia Universidad Católica de Chile, Casilla 193, C.P, 8331150 Santiago, Chile.

[3] Depto. de Química y Bioquímica, Universidad de Valparaíso, Av. Gran Bretaña 1111, Valparaíso, Chile.

[4]Facultad de Cs. Químicas y Farmacéuticas, Universidad de Chile Santos Dumont 964, Santiago, Chile.

Abstract: Nanotechnology presents a transverse and multidisciplinary approach that enveloves all scientific disciplines. This technology allows the creation of materials and devices with unique properties that find applications in various fields such as: electronics, the development of polymers, materials science, ceramics, biomedicine science, etc. Many problems of biological and medical interest arise from specimens in the range of the nanometers. In these nanoscale level problems, nanotechnology rises as the main path to achieving results. In particular project, we are carrying out multidisciplinary work in which we produce new materials and high-sensitivity sensors intended for use in biomedicine. We are considering the use of biosensors based on defects in solids and nanoporous membranes. I will show the advances obtained in nanoporous alumina films capable of detecting the peptide Aβ associated to Alzheimer's disease. Also the progress in the implementation of optical tweezers to know the mechanical properties of molecules related to red tide toxicity. Finally ,Iwill show the progress that has been achieved in the creation of biocompatible materials through plasma discharge.

Keywords: nanosensors, nanomaterials, biomedicine, alumina, peptide Aβ, nanodiamonds, NVC, red tide plasma discharge.

References:

Taylor, J. M. et al. High-sensitivity diamond magnetometer with nanoscale resolution. Nature Physics 4, 810–816 (2008)

Hall, L. T. et al. Monitoring ion-channel function in real time through quantum decoherence. Proceedings of the National Academy of Sciences of the United States of America 107, 18777–82 (2010). 1. Pan, S. & Rothberg

L. J. Interferometric Sensing of Biomolecular Binding Using Nanoporous Aluminum Oxide Templates. Nano Letters 3, 811–814 (2003).

Rossi, J. O., Ueda, M. & Barroso, J. J. Pulsed Power Modulators for Surface Treatment by Plasma Immersion Ion Implantation. Brazilian Journal of Physics 34, 1565–1571 (2004).

Modal parameter identification of perforated microplates from output data only

J. Lardiès
Institut FEMTO-ST, DMA, Rue de l'Epitaphe, 2500 Besançon, France

Abstract:

The design of micro electromechanical systems includes oscillating elements and components which are often perforated microplates supported by elastic suspension as shown in Figure 1. The main purpose of perforations is to reduce the damping and spring forces acting in the MEMS due to the fluid flow inside and around the micro structure. The study of the damping caused by surrounding fluid and by the dissipations in the material is very important to predict the dynamic response of the microsystem and to estimate some important parameters such as the quality factor, the switching time and the release time. G. De Pasquale and T. Veijola used numerical strategies for the estimation of the damping force acting on a perforate movable MEMS (De Pasquale *et al* 2008). Results from the 2D Perforated Profile Reynolds method and the simplied 2D ANSYS method are compared in the case of uniform perforation and perpendicular motion of the fluid. It was shown that ANSYS results contained a systematic error at small perforations and were not usable for large perforations. Very small damping forces are obtained by ANSYS and a correction equation for ANSYS was proposed.

In this paper, the model used to study the microplate behavior is constituted by the following parameters : the plate mass concentrated in the central plate, the damping coefficient and the stiffness coefficient which are constituted of fluidic and non fluidic components. Our purpose is to identify the modal parameters of the microplate : the eigenfrequency, the damping ratio and the stiffness from the displacement response only of the microstructure given in Figure 2. The dynamic measurements are conducted in the time domain by means of a laser vibrometer, details are given in the communication. With our approach, called subspace method (J. Lardiès *et al* 2011), it is not necessary to use the excitation force, only output measurements in the time domain are used.

The fundamental problem in modal parameter identification by the subspace method is the determination of the state space matrix (or transition matrix) which characterizes the dynamics of the system. In the communication we present a comparison of two subspace methods to estimate the transition matrix and the modal parameters of the perforated microplate. The first method uses properties of the shifted block controllability matrix and the second method uses properties of shifted columns of the block Hankel matrix. The procedures presented in the paper can identify closely eigenfrequencies that cannot be identified by the traditional Fourier transform. Numerical examples and an experimental example of a perforated microplate are presented. Figure 3 shows in red the identified displacement response of the perforated microplate, using a subspace method presented in the communication.

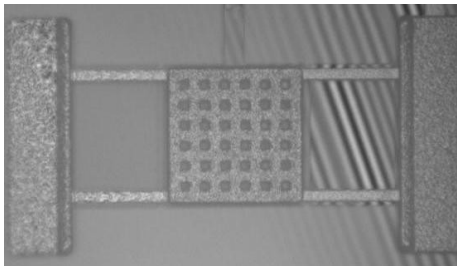

Figure 1. Optical image of the perforated microplate with four lateral elastic suspensions

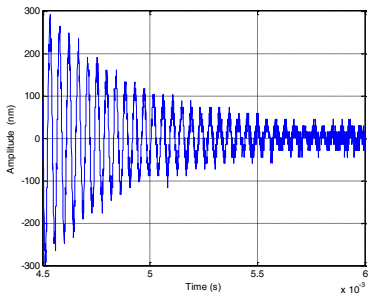

Figure 2. Displacement response of the perforated microplate

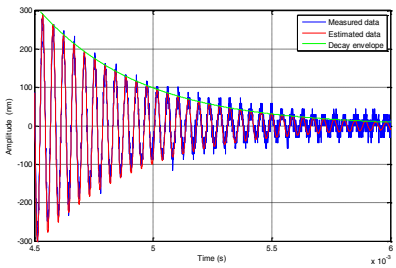

Figure 3. Comparison between the measured (in blue) and the reconstituted (in red) displacement response of the perforated microplate

Keywords: MEMS, microplate, oscillating system, dynamic response, time domain, modal parameters, subspace methods,experimental identification.

References:

De Pasquale G. and Veijola T. (2008) Comparative numerical study of FEM methods solving gas damping in perforated MEMS devices, *Microfluid Nanofluid* 5, 517-528

Lardiès J and Ta Minh-Ngi (2011) Modal parameter identification of stay cables from output-only measurements, *Mechanical Systems and Signal Processing, 25,* 133-150.

The Effect of 2-step Plasma Treatment for Single-walled Carbon Nanotube on Electrochemical Sensors

Joon Hyub Kim[1], Ki Beom Kim[1], Chan Won Park[2], Nam Ki Min[1*]
[1]Department of Control and Instrumentation Engineering, Korea University, Chungnam 339-700, Republic of Korea
[2]Department of Electrical Electronic Engineering, Kangwon National University, Chuncheon 200-701, Republic of Korea

Abstract: Carbon nanotubes (CNTs) have been widely used as active electrodes for electrochemical sensors because of their unique electrical, chemical, and mechanical properties such as high electrocatalytic activity (Wang *et al.*, 2002), large surface area (Cahill *et al.*, 1996), and the ability to alleviate surface fouling (Wang *et al.*, 2002). These properties lead to high chemical stability, effective electron transfer, high sensitivity, low detection limits, and an enhanced signal-to-noise ratio. However, the sensor applications by using CNT is limited owing to chemically inactive surface of the CNTs. Several investigators demonstrated that the sensitivity of CNT-based chemical sensors can be significantly improved by introducing defect sites along the sidewall of the CNTs when exposed to oxygen-based plasma. However, plasma-treated CNTs were found to try to revert to their original surface states over time, and to lead to relatively low sensitivity and weak interfacial bonding between biomolecules and CNTs because CNT had too little functional group by 1-step plasma treatment. In this study, we introduce the advantages and experimental procedure of 2-step plasma treatment on single-walled nanotube (SWCNT) films, and show results of increased immobilization efficiency of $CD4^+$ T cells for biosensor.

The integrated three-electrode system that consisted of a modified CNT working electrode (WE), an Ag/AgCl reference electrode, and a Pt counter electrode was fabricated by RF sputter, plasma-enhanced chemical vapor deposition and reactive-ion etching. After SWCNT modifying on WE by spray-coating method, SWCNT functionalization was performed by first O_2 plasma treatment to generate carboxyl groups and clean the SWCNT film. SWCNT film was stored at room temperature to recover the damaged SWCNT, and than was functionalized by second O_2 plasma treatment. $CD4^+$ T cells was immobilized on the 2-step plasma treated SWCNT film.

We measured the analytical performance characteristics of the 1- and 2-step O_2 plasma treated SWCNT electrodes-immobilized with anti-CD4 antibody by squre wave voltammetry (SWV). These peak currents were 0.0763 μA and 0.3263 μA, respectively, demonstrating that the 2-step treated electrode had an approximately 4.28 times larger current flow than the one-step treated electrode. Since the sensor signal can be greatly affected by the quantity and stability of immobilized biomolecules on the surface of the electrode, the high level current associated with the two-step O_2 plasma-treated electrode indicates a larger amount of functional groups and immobilized anti-CD4 mAbs.

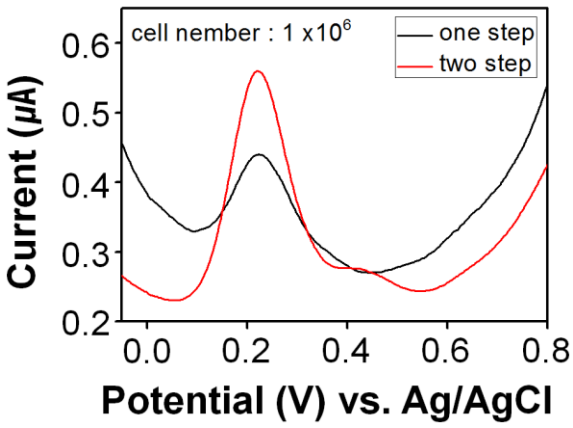

Figure 1: Comparison of sensitivity between 1- and 2-step O_2 plasma-treated SWCNT immunosensor : SWV of peak currents for 1- and 2-step O_2 plasma treated SWCNT electrodes following capture of $CD4^+$ T cells among 1 $\times 10^6$ splenocytes.

Keywords: SWCNT, electrochemical sensor, CD4+ T Cells, plasma treatment.

References:

Wang, Z., Liu, J., Liang, Q., Wang, Y., Luo, G. (2002), Carbon nanotube-modified electrodes for the simultaneous determination of dopamine and ascorbic acid, *Analyst*, 127, 653-658.

Cahill, P.A., Rohlfing, C.M. (1996), Theoretical studies of derivatized buckyballs and buckytubes, *Tetrahedron*, 52, 5247-5256.

Wang, J., Li, M., Shi, Z., Li, N., Gu, Z. (2002), Direct electrochemistry of cytochrome c at a glassy carbon electrode modified with single-wall carbon nanotubes, *Anal. Chem.*, 74, 1993-1997.

Theoretical predictions of luminescence due to cyclosiloxanes in nanostructured Silicon Rich Oxide films employing the Global Reactions Model.

N.D. Espinosa-Torres[*,1], J.A. Luna-López[1], J.F.J. Flores-Gracia[1], A.D. Hernández de la Luz[1], J. Martínez-Juárez[1] and G. Flores-Carrrasco[1].
[1]IC-CIDS Benemérita Universidad Autónoma de Puebla, C.U., Edif. 103 C-D, Col. San Manuel, C.P. 72570 Puebla, Pue., México.

Abstract:

Silicon Rich Oxide (SRO) thin films have been studied extensively and are very interesting due to their opto-electronic properties, particularly those related with luminescence. In general, lumi-nescent properties can provide significant information regarding the crystalline structure of a ma-terial and, in the case of SRO thin films, electro-luminescence properties are particularly im-portant since these films can be used to fabricate luminescent devices .
Recently we developed a theoretical model to describe a set of chemical reactions that can poten-tially occur during the process of obtaining silicon rich oxide (SRO) films, an outside stoichiome-try material, regardless of the technique used to grow such films. Particularly, chemical reactions that occur during the process of growing of SRO films by LPCVD technique were highlighted in the model presented. We suggest and evaluate either some types of molecules or resulting nanostructures and we predict theoretically, by applying the density functional theory, the con-tribution that they may have to the phenomenon of luminescence which is measured in SRO films. Also, we have calculated the opto-electronic properties of SRO films. The suggested mod-el provides enough information required to propose cyclosiloxanes structures. It is also possible to determine the molecular cyclosiloxanes structures which are modified due to the effect of heat treatment. We evaluated the annealed structures also. The motivation of this work is to apply a new model, which we had called the Global Reactions Model (GRM), for the theoretical study of the optical and electronics properties of Silicon Rich Oxides (SRO) structures regardless of the technique used to fabricate such structures.

Keywords:

GRM, luminescence, Silicon Rich-Oxide, Cyclosiloxanes, LPCVD, DFT..

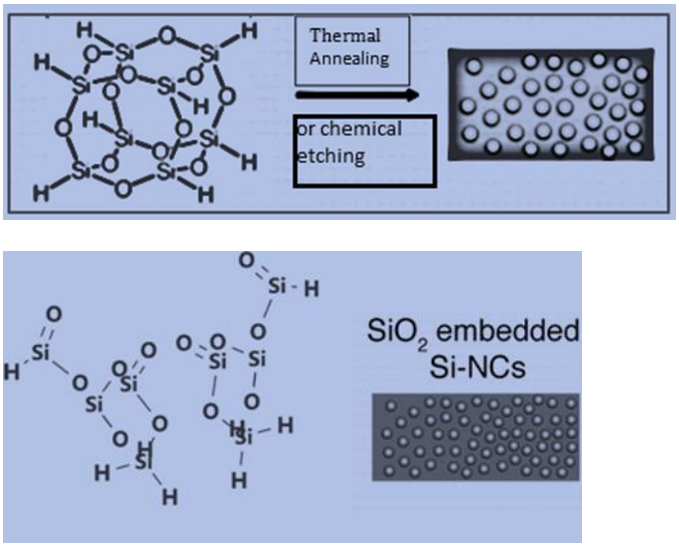

Figure 1:
Siloxane derivatives for n=4. Cage structure of hydrogen silsesquioxane (HSiO1.5)2n (top), and with two branched network structures 2(HSiO1.5)n (bottom).

References:

P. Mutti G. Ghislotti, S. Bertoni, L. Bonoldi, G. F. Cerofolini, L. Meda, E. Grilli and M. Guzzi: Room-temperature visible luminescence from silicon nanocrystals in silicon implanted SiO layers. Appl. Phys. Lett.1995, 6(7): 851–853.
http://ieeexplore.ieee.org/stamp/stamp.jsp?tp=&arnumber=1397891

Eric J. Henderson, Joel A. Kelly and Jonathan G. C. Veinot. (2009) Influence of HSiO1.5 Sol−Gel Polymer Structure and Composition on the Size and Luminescent Properties of Silicon Nanocrystals Chem. Mater., 21 (22), pp 5426–5434
http://pubs.acs.org/doi/pdf/10.1021/cm902028q Publication Date (Web): October 22, 2009 Copy-right © 2009 American Chemical Society.

Sensing Low Magnetic Field by Using Planar Hall Effect Sensor

Incheol Song[1], SiHong Aiden Lee[1], SungJoon Kim[1], CheolGi Kim[1*]
[1] Department of Emerging Materials Science Daegu Gyungbuk Institute of Science and Technology (DGIST)
Daegu, Techno-joongang-daero 333, South Korea

Abstract: The sensors can detect low magnetic field. The detection of picoTesla of magnetic field at room temperature has been used in many places where required the low magnetic field detection. However, it is hard to miniaturize systems now-a-day such as nano and pico-satelites or IC compass in mobile devices etc.

Therefore, many magnetoresistive (MR) sensors have been developed to decrease the detective field. (for example as tunneling magnetoresistive (TMR), spin-valve, giant magnetoresistive (GMR), and anisotropy magnetoresistive (AMR)) The detective field of these sensors has been stated around 100 pT at the frequency range from hundred Hz to few hundred kHz. However the AMR has more advantages in detection at lower frequency and it can detect 100 pT at around 10 Hz.

Among MR sensors, the voltage noise of PHE-AMR sensor is lower several order of magnitude compared to others such as TMR sensor or GMR and AMR sensor, because of its off-diagonal geometry.

However, the dectection of the magnetic field by MR sensor is difficult. In order to resolve this problem, we develop a highest sensitivity MR sensor based on the thin film with low magnetic noise. (i) We use the NiFe/Cu/IrMn trilayer structure; NiFe structure (the sensing layer) is amorphous state to minimize its structural noise. (ii) The sensor geometry is designed as a high sensitivity configuration – multi-ring, in which the current and voltage electrodes of the sensor is arranged in the way that the bridge has smallest off-set voltage to minimize the thermal noise. The limitation of the detective field is interpolating from drift voltage as a function of temperature from a set of the sensors where the length of one arm is changed.

Keywords: PHR sensor, Bio-sensor, Magnetic bead, Hall effect, DC sputter, FE-TEM, Helmholtz magnetic measure system.

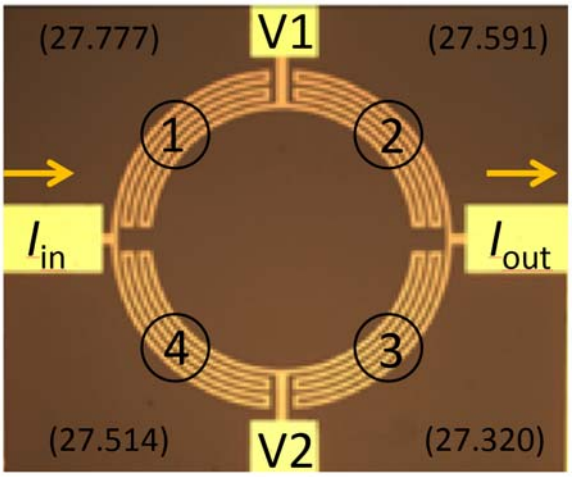

Figure 1: Ring sensor with information of thickness at the middle of the four arms, and the selection of current and voltage electrodes to minimize the voltage off-set

Active plasmonics: Growing Gold Nanoparticles on a Flexible Substrate to enable simple mechanical control of their Plasmonic Coupling

Ugo Cataldi[1,2], Roberto Caputo[1], Y. Kurylyak[1], Gérard Klein[2], Mahshid Chekini[2], Cesare Umeton[1] and Thomas Bürgi[2]

[1] LICRYL (Liquid Crystals Laboratory, IPCF-CNR), and Center of Excellence CEMIF.CAL and Department of Physics University of Calabria, 87036 Arcavacata di Rende (CS), Italy

[2]Dèpartement de Chimie Physique, Universitè de Genève, Quai Ernest-Ansermet 30, 1211 Gèneve, Switzerland

Abstract: A simple method is presented to control and trigger the coupling between plasmonic particles using both a growing process of gold nanoparticles (GNPs) and a mechanical strain applied to the elastomeric template where these GNPs are anchored. The large scale samples are prepared by first depositing and then further growing gold nanoparticles on a flexible PDMS tape. The growing processes of nanoparticles not only increase the sizes but change also the shape of nanostructures. Upon stretching the tape the particles move further apart in the direction of the stretching and closer together in the direction perpendicular to it. The synergy between the controlled growth of GNPs and the mechanical strain, leads to a drastic shift of the plasmon band and a color change of the sample. Furthermore, the stretching by only a few percent of the amorphous and initially isotropic sample results in a strong polarization-dependent plasmon shift. At smaller gap sizes between neighboring particles, induced by stretching the PDMS tape, the plasmon shift strongly deviates from the behaviour expected considering the plasmon ruler equation. This shows that multipolar coupling effects significantly contribute to the observed shift. Overall, these results indicate that a macroscopic mechanical strain allows one to control the coupling and therefore the electromagnetic field at the nanoscale..

Keywords: Gold nanoparticles, dipolar and multipolar coupling, PDMS, gold nanoparticles seed growth.

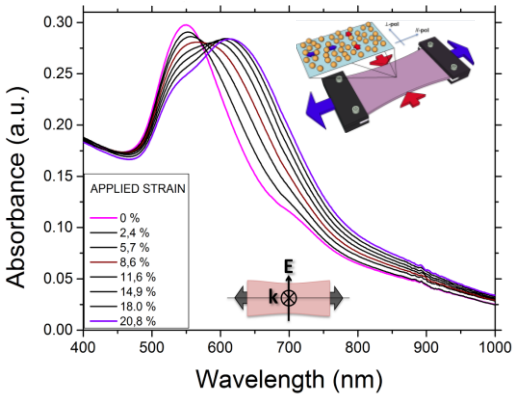

Fig. 1: In the figure is shown the development of plasmonic coupling with the increasing of mechanical strain of sample.

References:

Ugo Cataldi, Roberto Caputo, Yuriy Kurylyak, Gérard Klein, Mahshid Chekini, Cesare Umeton and Thomas Bürgi (2014) , "Growing Gold Nanoparticles on a Flexible Substrate to enable simple mechanical control of their Plasmonic Coupling", *J. Mater. Chem. C*, **2014**,2, 7927-7933

P. K. Jain, W. Y. Huang and M. A. El-Sayed (2007), "On the Universal Scaling Behaviour of the distance Decay of Plasmon Coupling in Metal Nanoparticles Pairs: A Plasmon Ruler Equation" *Nano Lett.*, 2007, **7**, 2080

Kenneth R. Brown and Michael J. Natan (1998), "Hydroxylamine Seeding of Colloidal Au Nanoparticles in solution and on Surfaces", *Langmuir* 1998**,** *14,* 726-728

PU-RGO composites and its properties for thermal conductive adhesive

Sukhoon Choi[1,2] , Sungjin Park[2], Hoon Huh[1,*]
[1]Korean Institute of Industrial Technology(KITECH), Cheonan, Korea
[2]Inha University, Incheon, Korea

Abstract: With the rapid development of electronic technology, the electronic components has been being gradually changed from isolated to highly integrated and modularized, which causes high heat flux for the electronic devices, and a great amount of heat is produced during the running. The stability of the electronic devices will be depressed by 10% as their temperature rises by every 2℃. So, the heat cumulation of electronic components will directly decrease the stability or shorten the life time of the electronic products. Meanwhile, it leads to some serious consequences. Therefore spreading the heat of the electronic devices effectively is very important.

Polyurethane(PU) has been known as a polymeric material that has high mechanical strength and has been widely used as adhesive, film, and etc.. But it has poor thermal or electrical conductivity.

Graphene is a monolayer of sp^2 hybridized carbon atoms arranged ib a two-dimensional honeycomb structure. It has great properties, for example, resistivity ($10^{-6}\Omega\cdot cm$), thermal conductivity(4.84~5.30 $x10^3$W/mK) and mechanical properties(tensile strength : 130GPa and Young`s modulus : 1TPa).

Recently, Graphene has been further used to fabricate polymer nanocomposites with integrated performance. Cai *et al*. reported a simple method to fabricate fully exfoliated graphene oxides in an organic solvents. With this method in hand, the barrier for well-dispersion of the graphene sheets in polymeric matrix can be easily removed.

Functional groups attached to the graphene oxides(GO) could provide active sites to form chemical bonds, acting as an ideal interface between the graphene and appropriate polymers. Polyurethane(PU) is such a polymer, as it can form chemical bonds with GO by reaction between the isocyanate groups at the end of the PU chains and hydroxyl groups on the graphene oxide.

In this work, we syntheszed several types of reduced ene Oxide(RGO) composite and checked several properties. Structure, morporlogy, thermal properties, and adhesion strength. Schem 1 shows reaction mechanism. Isocyanate reacts GO and urethane reaction

Keywords: Thermal conductivity adhesive, PU composite, Graphene oxide.

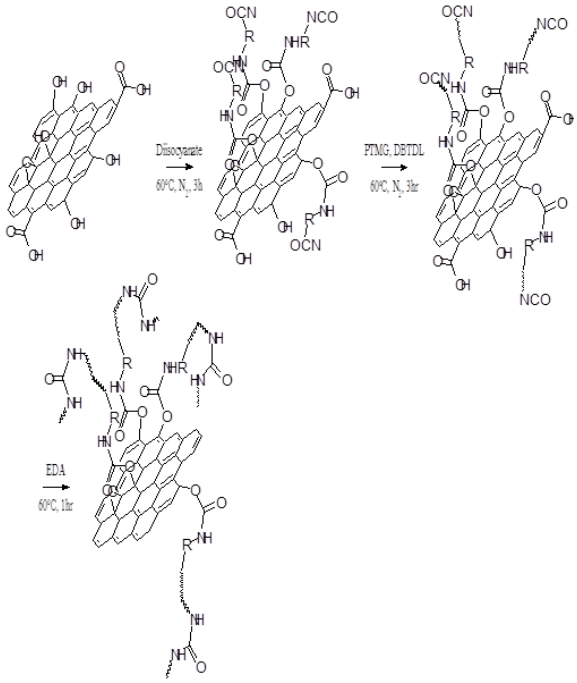

schem 1: Graphene oxide react with isocyanate and polyol react with unreated isocyanate function. Ethylene diamine(EDA) play role chain extender and reduct agent.

References:

H Lee, HM Jeong - Polym Polym Compos, 2010
Y.-X. Fu et al. / International Journal of Thermal Sciences 86 (2014) 276-283
Y. Li et al. / Materials and Design 47 (2013) 850–856
J. Mater. Chem., 2011, 21, 4222–4227

Posters Session II – C
Nano MatEn 2015 - Nanotech for Energy and Environment

Leaching of Nano-SiO_2 from Municipal Solid Waste

E.T. Sakallıoglu,[1] M. Bakırdoven,[1] I. Temizel,[1] C.S.Uyguner- Demirel,[1] B. Demirel,[1] N.K. Copty,[1] T.T. Onay,[1] T. Karanfil,[2]

[1]Bogazici University, Institute of Environmental Sciences, Bebek 34342 Istanbul, Turkey

[2]Clemson University, Department of Environmental Engineering and Earth Sciences, Anderson SC, USA

Abstract: The commercial use of nanomaterials has significantly increased in recent years. However, there is still limited information about the potential impacts of nanomaterials on the environment within the integrated solid waste management systems (Boldrin *et al.*, 2014). Nano SiO_2 is used in numerous commercial applications ranging from paint, coating, fire resistant glassware, electronics, pharmaceuticals and UV protection (Marcoux *et al.*, 2013). The widespread synthesis and uses of SiO_2 mean that large volumes of this nanomaterial will ultimately end up in landfills (Keller *et al.*, 2013). The main objective of this experimental work is to evaluate the leaching potential and behavior of nano SiO_2 within the municipal solid waste-leachate matrix. Therefore, batch experiments were conducted using fresh solid waste samples obtained from a real municipal solid waste (MSW) landfill located close to Istanbul, Turkey. The waste samples were spiked with different concentrations of SiO_2 in batch reactors. During the experiments, two different pH values were considered, namely basic 8-9 and acidic 5-6. The effect of ionic strength on the leaching characteristics of SiO_2 was also evaluated. Leachate samples were regularly collected over a three-day period and analyzed for pH, conductivity, particle size distribution and total Si concentration. A kinetic model was also developed to evaluate the deposition and detachment of SiO_2 onto the solid surface.

Keywords: Landfill, leaching, municipal solid waste, nanomaterial, SiO_2

References:

Boldrin, A., Hansen, S.F., Baun, A., Hartmann, N.I.B., Astrup, T.F. (2014) Environmental exposure assessment framework for nanoparticles in solid waste, *J. Nanopart. Res.*, 16, 2394.

Keller, A.A., McFerran, S., Lazareva, A., Suh, S. (2013) Global life cycle releases of engineered nanomaterials, *J. Nanopart. Res.*, 15, 1692.

Marcoux, M.A., Matias. M., Olivier, F., Keck, G. (2013) Review and prospect of emerging contaminants in waste –key issues and challenges linked to their presence in waste treatment schemes: general aspects and focus on nanoparticles, *Waste Manage.*, 33, 2147-2156.

The Role of Al_2O_3 and SiO_2 Nanoparticles on the Cycleability of Li-Air Batteries with TEGDME-PEO/$LiPF_6$ Electrolytes

A.Akbulut Uludağ[1], M. Tokur[2], H. Algul[2], T. Cetinkaya[2], M. Uysal[2], H. Akbulut[2]

[1] : Sakarya University, Dept. of Environmental Engineering, Esentepe Campus, 54187, Sakarya, Turkey

[2]: Sakarya University, Metallurgical & Materials Engineering Dept., Esentepe Campus, 54187, Sakarya, Turkey

Abstract: Rechargeable lithium-air (Li-air) batteries have the potential to provide gravimetric energy three to five times greater than that of conventional Li-ion batteries. Identifying the appropriate electrolyte is one prerequisite for the application of Li-air batteries[1]. In this work, an ether based electrolyte containing TEGDME/$LiPF_6$ was optimized, which possessed low viscosity and high ionic conductivity, under dry argon atmosphere in a glove box. In order to prevent air breathing cathode clogging by lithium oxide and provide stability of Li metal anode, an extensive work was carried out to provide most functional polymeric additives and Poly(ethylene oxide) (PEO) was found one of the most effective polymers as recently stated by different a work[2]. Two different inorganic fillers were chosen to add into the electrolyte to prevent conductivity decrease and provide stability of the air cell. Nano Al_2O_3 and SiO_2 were incorporated into TEGDME-PEO/$LiPF_6$ composite homogenously. Both PEO and nano ceramic powders were thought to promote the dissolution of lithium peroxide precipitates formed in course of discharge process and protect the anode against to the corrosion. Graphene/α-MnO_2 nanocomposite air breathing structure was used as cathode. In the carbon cathode materials, Graphene nanosheets (GNS) have been reported as ideal cathode materials for Li-O_2 batteries because of their unique morphology and structure that provide both diffusion channels for O_2 and active sites for cathode reactions. On the other hand, α-MnO_2 catalysts is helpful to increase the reversibility of the lithium-oxygen interactions due to hollandite type crystal structure of MnO_2 consists 2x2 tunnels. A lithium disk was used as anode while glass fiber was used as the separator in ECC-Air test cell. The cells were cyclically tested using 0.1 mA/cm^2 current density over a voltage range of 2.15-4.25 V. Electrochemical impedance spectroscopy (EIS) measurements was applied to investigate the effect of the polymeric and inorganic additives on the resistivity of the electrolyte. Results revealed that nanocomposite electrolyte structures provided not only good discharge capacity but also excellent stability of the Li-air cells. As can be seen in Fig.1, excellent cycleability was obtained by using the nanocomposite electrolytes with both organic (PEO) and inorganic (Al_2O_3, SiO_2) additions. Up to After the electrochemical cycling test, the cycles no significant capacity fade was detected and the ongoing studies show the air cell will show excellent stability with increasing cycle number. Morphologies of the cathodes were analyzed using scanning electron microscopy, X-ray diffraction analysis, and Raman spectroscopy to determine the occurrence of reaction products.

Keywords: Li-air battery, cycle life, stability, TEGDME, Al_2O_3 and SiO_2 additives, nanocomposite electrolyte, PEO,

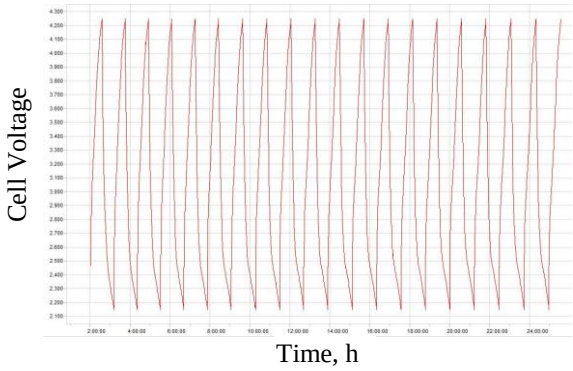

Fig. 1. Time-voltage behavior of TEGDME-PEO /$LiPF_6$/1 wt. % Al2O3 nanocomposite electrolyte.

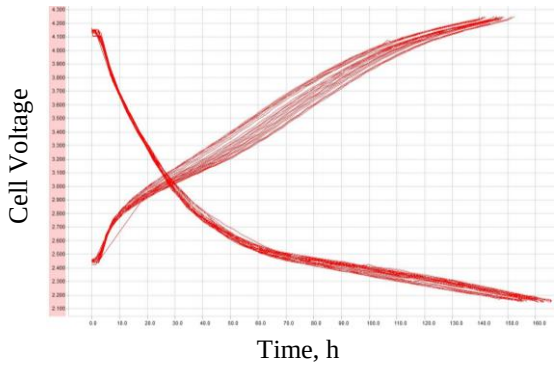

Fig. 1. Capacity-voltage behavior of TEGDME-PEO /$LiPF_6$/1 wt. % Al2O3 nanocomposite electrolyte

References:

1. G. Girishkumar, B. McCloskey , A. C. Luntz , S. Swanson and W. Wilcke, Lithium−Air Battery: Promise and Challenges, J. Phys. Chem. Lett., 2010, 1 (14), pp 2193–2203

2. Chibueze V. Amanchukwu, Jonathon R. Harding, Yang Shao-Horn, and Paula T. Hammond, Understanding the chemical stability of polymers for lithium-air batteries, Chem. Mater., Just Accepted Manuscript, DOI: 10.1021/cm5040003, 2014.

Transparent Hydrophobic Nanolayers on ETFESiOx Substrates for Solar Cells Encapsulation

G. Rossi,* P. Scarfato, L. Incarnato
Department of Industrial Engineering, University of Salerno, Fisciano (SA), ITALY

Abstract: Polymer materials are recently emerging as an interesting alternative to glass as encapsualnt and coating materials for preserving solar cells from the atmospheric degradation agents, due to their flexibility, affordable cost and transparency. However, they present the disadvantage of low barrier properties. Hydrophobic and more in general liquid barrier properties may significantly improve the protection guaranteed by the encapsulant materials, addressing issues like corrosion effects and loss of electrical performance and also adding self-cleaning properties to the surface thanks to the roll-off effect consequent to the hydrophobic behavior. Although several methods are reported in literature (Ling. Et al., 2009, Karunakaran et al., 2011) for obtaining hydrophobicity on substrates applicable to the solar cells sector, these methods are likely to be expensive and difficult to be implemented at industrial level because they are complex multi-step processes, including high temperature steps. In a previous work (Rossi et al., 2014) we developed a single step method to synthetise at room temperature a transparent hydrophobic self-assembled monolayer (SAM) chemisorbed on Polyethylene terephthalate (PET-SiOx) substrate, a standard coating for PV cells. In the present study, this method was applied on the bilayer Ethylene tetrafluoroethylene – Silicon Oxide (ETFE-SiOx), usually employed as frontsheet for solar cells, experimenting also a new precursor molecule. The SAM deposition was performed in anhydrous toluene using 1% concentration of two different precursor molecules: 1H,1H,2H,2H-per-fluorodecyltrichlorosilane (CFAS) and 1H,1H,2H,2H perfluorodecyltriethoxysilane. (EFAS). FTIR (Fourier Transform Infrared Spectroscopy) measurements carried out on the uncoated and nanocoated samples confirmed the successful deposition of the SAM Nanolayer on ETFESiOx substrate. The hydrophobic properties characterization of the nanocoated samples indicated that the surface substrate was changed from hydrophilic to hydrophobic for all the nanocoated systems. The oleophobic properties were also significantly enhanced by the SAM deposition, particularly for the CFAS nanocoated system that was modified from oleophilic to oleophobic (oil CA: 92°). Furthermore, the optical properties assessment revealed that only a slight transparency decrease occurred for CFAS nanocoated sample, while no substantial reduction of transmittance was detected for the EFAS nanocoated system.

Concluding, the adopted SAM procedure can represent an effective route for obtaining nanocoated polymer materials with enhanced barrier properties at sustainable costs, suitable to extend the lifetime of encapsulated solar cells.

Keywords: Hydrophobic Coatings, Oleophobic Coatings, Self-Assembly of Monolayers, FluoroAlkylsilanes, Solar Cells, Ethylene tetrafluoroethylene – Silicon Oxide.

Figure 1: H_2O and oil Average static contact angle on the SiOx side for samples: ETFE-SiOx uncoated and nanocoated with SAM of CFAS and EFAS.

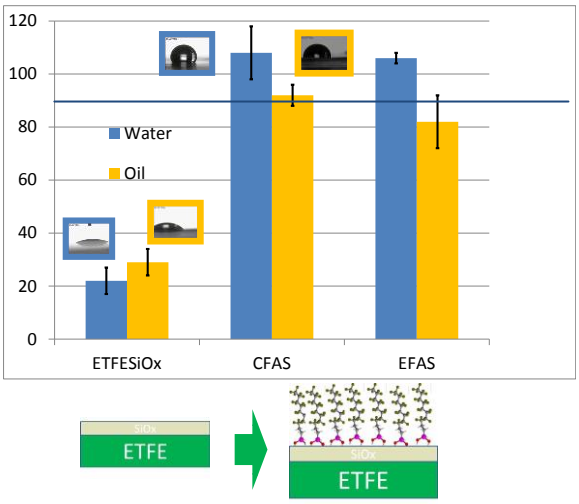

References:

Ling, X.Y., Phang, I. Y., Vancso, G.J., Huskens, J., Reinhoudt, D.N. (2009) Stable and Transparent Superhydrophobic Nanoparticle Films, *Langmuir*, 25, 3260–3263.

Karunakaran, R.G., Lu, C., Zhang Z., Yang, S. (2011), Transparent Superhydrophobic Surfaces from the Coassembly of Nanoparticles (≤100 nm), *Langmuir*, 27, 4594–4602.

Rossi, G., Altavilla, C., Scarfato, P., Ciambelli, P., Incarnato L. (2014), Deposition of transparent and flexible nanolayer barrier on standard coating materials for photovoltaic devices, *Surf. Coat. Technol.*, 239, 200-105.

Photovoltaic Response of Non-Toxic $CuInS_2$ Quantum Dot based Conducting Polymer Composite Films

I. Singh,[1,2,*] J. Singh,[2] A. Kumari,[2] P.K. Rao,[2] P.K. Bhatnagar[2]
[1]University of Delhi, Department of Electronics, SGTB Khalsa College, Delhi, India
[2]University of Delhi South Campus, Department of Electronic Science, New Delhi, India

Abstract: I-III-VI ternary compound non-toxic quantum dots (QDs) have recently attracted the scientific community because of their attractive electrical and optical properties (Allen *et al.*; 2008). $CuInS_2$ (CIS) is the most extensively studied form among various I-III-VI ternary compositions. It is environment friendly, has a small direct band gap of 1.5 eV (which is nearly the optimum band gap for a single junction photovoltaic device), high absorption coefficient ($>10^5$ cm^{-1}), high photoconductivity and possesses long term electronic stability (Lewerenz *et al.*; 2004). The Bohr exciton radius for CIS QDs is ~4 nm hence nanopaticles having size less than ~ 8 nm can show quantum confinement effects (Czekelius *et al.*; 1999). In the present work, we have studied the optical and electrical properties of poly(3-hexylthiophene) (P3HT) and CIS QDs based composite films. It is found that the absorption spectrum of the polymer film becomes broader by the incorporation of CIS QDs. The photoluminescence of the P3HT in the composite is also found to be quenched indicating an efficient charge transfer from polymer to the QDs. The electrical characterization of the P3HT:CIS composite film showed an improvement in the current density by more than an order of magnitude as compared with that of P3HT only device.

Keywords: conducting polymer, non toxic quantum dots, photovoltaic applications, thin films.

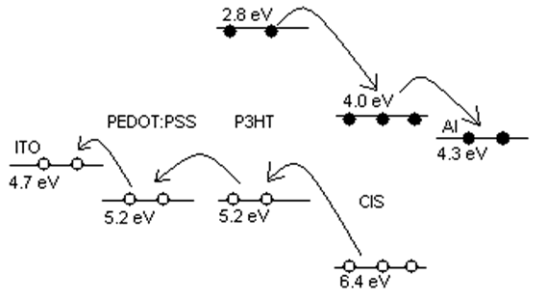

Figure 1: Energy band diagram of conducting polymer (P3HT): CIS QD composite structure

References:

Allen, P.M., Bawendi, M.G. (2008) Ternary I-III-VI quantum dots luminescent in the red to infrared, *J. Am. Chem. Soc.*,130, 9240-9241.

Lewerenz, H.J. (2004) Development of Copper Indium disulfide into a solar material, *Sol. Energy Mater. Sol. Cells*, 83, 395-407.

Czekelius, C., Hilgendorff, M., Spanhel, L., Bodja, I., Lerch, M., Miller, G., Bloeck, U., Su, D.S., Giersig, M. (1999) A simple colloidal route to nanocrystalline ZnO/$CuInS_2$ bilayers, *Adv. Mater.*, 11, 643-646.

Benefits of a compact TiO_2 layer for the elaboration of transparent TiO_2 nanotubes array on conducting glass

A. Krumpmann, A. Decroly

Department of Materials Science, Faculty of Engineering, University of Mons, Mons, Belgium

Abstract: Titania nanotubes obtained by the anodization method have received much attention due to numerous possible fields of application including sensors, photocatalysis or photovoltaics. Anodization is classically performed on Ti foils but for photovoltaic applications, the TiO_2 nanotube array layer has to be elaborated on a transparent substrate such as transparent conducting oxide (TCO) coated glass. Therefore a metallic Ti layer is sputtered on TCO and then anodized to be converted to a transparent TiO_2 nanotube array (TNA) layer (figure 1). We describe the impact of introducing an additional compact TiO_2 layer under the metallic Ti layer during the sputtering deposition and compare morphological and optical properties of titania nanotubes films made with and without this intermediate compact layer. These results show considerable improvements in the TNA layer macroscopic homogeneity when a compact layer is used. They are attributed to the limitation of an undesirable reaction of oxygen evolution that takes place preferentially at the TCO-electrolyte interface during anodization, causing a destructuration of the TNA layer. Thus, using a TiO_2 compact layer allows a better control of the anodization process and the transparency of the TNA layer in the visible range is also increased. Furthermore, for solar cell applications, the compact layer can act as a blocking layer which is a common way to reduce charge recombination.

Keywords: Titanium dioxide, thin films, nanotubes, 1-D nanostructures, anodization, solar cell applications.

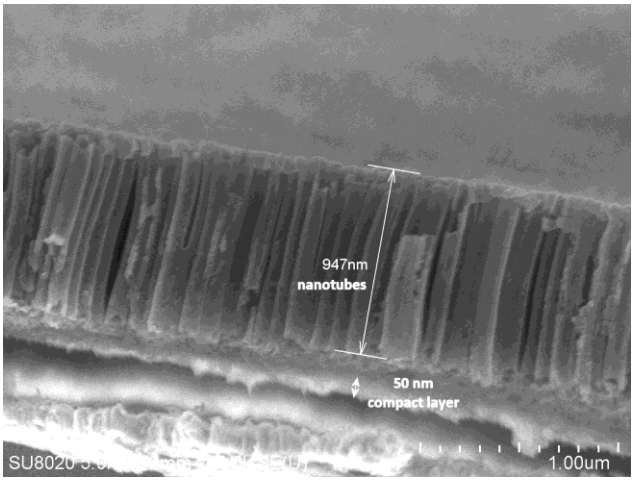

Figure 1: Scanning electron microscopy image of a 1 µm thick TiO_2 nanotube array film on TCO glass with an intermediate compact TiO_2 layer of approximately 50 nm.

Study of $LiFePO_4$ thin films as Li-ion battery cathode by in-situ electrochemical atomic force microscopy in aqueous electrolyte

J. X. Wu, G. Y. Shang*
School of Physics, Beihang University, Beijing 100191, P. R. China

Abstract:
Lithium-ion (Li-ion) batteries have been widely used as power sources for portable and mobile applications (Armand *et al.*, 2008). In order to prolong battery life, it is important to study the mechanisms that make battery capacity reduce with aging. Published results have show that morphological changes occur in aged cathodes. In this study, in-situ electrochemical atomic force microscopy (EC-AFM) that is combined atomic force microscopy with electrochemical methods was used to investigate morphological changes of $LiFePO_4$ thin film electrodes during charge and discharge processes in real time under aqueous environment (Demirocak *et al.*, 2014; Ramdon *et al.*, 2014). $LiFePO_4$ thin films were prepared by depositing them on Au/Si substrate using radio frequency magnetron sputtering deposition method. The films were firstly characterized by X-ray diffraction, and results showed that them were composed of $LiFePO_4$ phase with olivine structure. The SEM and AFM results show that the average size of particle was ~100 nm. The electrochemical performance of the film electrodes in Li_2SO_4 aqueous electrolyte was investigated by cyclic voltammetry. The lithium ion diffusion coefficient of the film electrode was estimated to be 2.31×10^{-7} cm^2s^{-1}, which is larger than that of $LiFePO_4$ powder of 5.53×10^{-8}. The decrease and increase in the size of the $LiFePO_4$ particles during charge and discharge were directly observed by EC-AFM, and relevant mechanism is discussed.

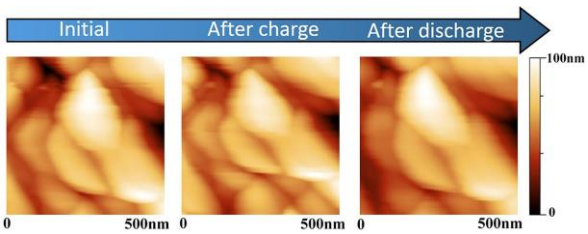

Figure 1: EC-AFM images show that the changes in the size of the $LiFePO_4$ film electrode during charge and discharge in the aqueous electrolyte.

References:
Armand, M.; Tarascon, J-M. (2008), Building better batteries, *Nature*, 451, 652-657.

Demirocak, D. E.; Bhushan, B. (2014), In situ atomic force microscopy analysis of morphology and particle size changes in Lithium Iron Phosphate cathode during discharge, *J. Colloid Interface Sci.*, 423, 151-157.

Ramdon, S.; Bhushan, B.; Nagpure, S. C. (2014), In situ electrochemical studies of lithium-ion battery cathodes using atomic force microscopy. *J. Power Sources*, 249, 373-384.

Textured fabrication of CdS/CdTe thin film PV cell with back contacts

Murugaiya Sridar Ilango[1,2], Sheela K Ramasesha[1,*]
[1]Indian Institute of Science, Divecha Centre for Climate Change, Bangalore, Karnataka, India
[2]Department of Physics, Jain University, Bangalore, Karnataka, India
*sheela@caos.iisc.ernet.in

Abstract: The basic function of a Solar cell is to absorb sunlight and convert light energy into electricity. The energy obtained is carbon free renewable source of energy without any moving part. The principle of solar cell came into lights when the great scientists Chapin, Pearson, and Fuller prepared a photovoltaic effect using poly-Si in 1954. Since silicon semiconductor technology was so widely studied, for more than 40 years solar cells were fabricated using silicon crystals. As a replacement for silicon, materials which can be used are amorphous silicon, CdTe, Cu (In, Ga) Se2, InP, CdSe and GaAs. Thin film solar cells are considered to be large area diodes, to increase the absorption of light and reduce the cost of fabrication. Electron-hole pairs are generated by the absorbed photons, the electric energy is formed when the excited carrier is swept across the potential field. The voltage generated during the separation of opposite charge helps in driving the current through external electric circuit. In a CdS/CdTe based solar cell the potential field or the depletion layer is formed at the interface of the CdS and CdTe layers. In this paper CdS is the window layer which has a wide band gap of 2.45 eV which allows most of the light to the absorber layer CdTe with a band gap of 1.45 eV. Photons from the sunlight are absorbed only when the energy is higher than the band gap of the absorber layer. Thin film Solar cells have a record efficiency of 19.6%, and commercially available CdTe PV panels of 12% (Green, et al., 2013). The loss due to reflection has limited all types of solar cells to a great extent. Hence, one method of trapping the light for more absorption is through nano-texturing of junction area. In commercial thin-film CdTe solar panels 4% of its energy is already reflected in the glass-air interface of the modules (Kaminski, et al., 2014). Nanostructuring of silicon has produced extensive research in solar cell application because of its low reflectance and enhanced light trapping technique (Oelhafen, et al., 2005). Along with the texturing of junction area, the concept of back contact is taken into account (Figure 1). As the front contact in a solar cell transmits only 50% of the solar radiation (Fan, et al., 2009), back contact research started after the publication of R.J Schwartz in 1975 as a substitute for cells which has front and rear contacts. The metal grids with narrow, closely packed metal lines can reduce series resistance (Dean, et al., 1975) but increases blockage of sunlight (by reflecting). As the front and rear contacts are placed at the rear surface, increases the packaging density of the panel and also gives raise to performance gain (Kerschaver, et al., 2006). So the performance of back contact solar cell is to be tested along with the increased junction area by texturing the interface surface.

Keywords: textured solar cell, back contact, CdS/CdTe, nanowall design, thin flim PV.

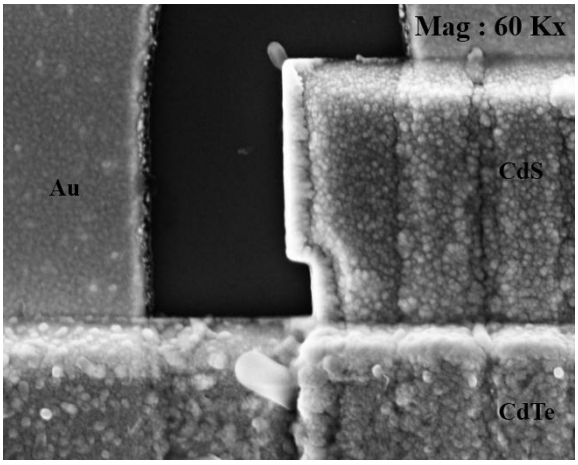

Figure 1: SEM image of Nano wall structure (Surface morphology)

References:

Dean R. H., Napoli L. S. and Liu S. G. (1975) Silicon solar cells for highly concentrated sunlight, *RCA Review*, 36, 324-335.

Fan Zhiyong [et al.] (2009)Three dimensional nanopillar array photovoltaics on low cost and flexible substrates, *nature materials*, 8, 648-653.

Green Martin A. [et al.] (2013) Solar cell efficiency tables (version 42), *Progress in Photovoltaics: Research and Applications*, 21, 827-837.

Kaminski P. M., Lisco F. and Walls J. M. Multilayer (2014) Broadband Antireflective Coatings for More Efficient Thin Film CdTe Solar Cells, IEEE Journal of Photovoltaics, 4, 452-456.

Kerschaver Emmanuel Van and Beaucarne Guy (2006)Back-contact Solar Cells: A Review, *Progress in Photovoltaics: Research and Applications*, 14,107-123.

Oelhafen P. and Schuler A. (2005) Nanostructured materials for solar energy conversion, *Solar Energy*, 79,110-121.

Nonradiative Electron and Hole Relaxation Dynamics in Organometallic Halide Perovskites

M.E. Madjet,[1] F. El-Mellouhi,[1,], G. Berdiyorov[1], S. Ashhab[1] A. Akimov[2] and S. Kais[1]
[1]Qatar Environment & Energy Research Institute, Qatar Foundation, PO Box 5825, Doha, Qatar
[2]Department of Chemistry, University of Southern California, Los Angeles, CA 90089

Abstract: Hybrid organic-inorganic perovskites, such as methylammonium (MA) lead iodide ($CH_3NH_3PbI_3$ or $MAPbI_3$), are promising new absorber materials for solar energy applications that have attracted significant interest in the last few years. Solar conversion efficiencies of more than 19% have been reported for these materials [1]. This high efficiency is mainly due the long diffusion lengths of charge carriers, low sensitivity to defects and high mobility of charge carriers. However, many fundamental processes related to the photophysics of these materials remain not fully understood.
The excitation of electrons from the valence band to conduction band results in the formation of hot electrons and holes, both of which lose most of their energy by cooling down to the band edges. Extracting hot carriers before they thermalize towards the recombination would lead to higher efficiency. Consequently, simulating the relaxation dynamics of photoexcited charge carriers is of great importance for further optimization of photovoltaic devices.
In order to understand in more detail the process of charge carrier dynamics in peroveskite materials, a theoretical description based on time-domain methods is required to enable shedding light on recent experimental finding on electron and hole relaxation dynamics [2] and also to guide future experimental investigations. A mixed quantum-classical approach based on trajectory surface hopping is used to describe the dynamics of hot charge carriers. In this approach, the electrons are described quantum mechanically by solving the Schroedinger equation and the nuclear degrees of freedom are propagated by independent classical trajectories, which are computed by solving the classical Newton's equations.

In this contribution, we address the non-radiative relaxation process of electrons and holes in organometallic perovskite $CH_3NH_3PbI_3$ when electrons are promoted to the conduction band from the valence-band. We perform nonadiabatic molecular dynamics simulations using the combination of the PYthon eXtension for Ab Initio Dynamics [3] package for quantum dynamics simulations interfaced with the Quantum Espresso electronic structure code. Our aim is to get a fundamental understanding of the intra-band relaxation process of hot electrons (holes) to the minimum (maximum) of the conduction (valence) band and how these processes are affected by perovskite composition and structure. Results on the perovskite materials $CH_3NH_3PbI_3$, $CH_3NH_3PbBr_3$, $CH_3NH_3PbCl_3$, $CH_3NH_3PbI_{3-x}Br_x$ and $CH_3NH_3PbI_{3-x}Cl_x$ will be presented.
The electron relaxation time values obtained from our simulation for $CH_3NH_3PbI_3$ are in good agreement with the experimental data reported in Ref. [2]. We also found that halogen-mixing $CH_3NH_3PbI_{3-x}Cl_x$ results in slowing down the electron and hole relaxation process, suggesting a longer life time in Cl-doped systems.

Keywords: Photovoltaic, perovskite, electron/hole transport, nonradiative carriers relaxation, nonadiabatic dynamics, surface hopping.

References:

[1] National Renewable Energy Laboratory, Best Research-Cell Efficiencies; www.nrel.gov/ncpv/images/efficiency chart.jpg

[2] Hung-Yu Hsu et al, Angew.Chem. Int. Ed. **53**, 1 (2014).

[3] A.V. Akimov and O.V. Prezhdo, J. Chem. Theory Comput. **9**, 4959 (2013).

C-Nanotube Based Infrared Thermo-Voltaic Cells and Detectors

T.Hosseini, N.Yavarishad and N. Kouklin
Dept. of Electrical Engineering, Univ. of Wisconsin-Milwaukee,P.O. Box 413
Milwaukee, WI, 53201, USA

Abstract: Sun radiation remains a key renewable energy source, with ~40% of its energy falling into the infrared part of the EM spectrum. This low grade energy, while available is thinly stretched over a relatively broad spectral window of ~ 0.7-3 μm. For a p-n junction based photovoltaic (PV) solar cell, a maximum voltage is limited by $V_{oc} \cong E_g/e$, where *e* stands for the unit charge. For ideal cells, the conversion efficiency is to scale linearly with E_g given by $\chi(\lambda) \sim \frac{1}{\lambda} \sim E_g$.[1] As the fabrication and deployment costs are to be on par with those of existing PV systems, IR-PV cells that inherit conventional design are to demonstrate at least order of magnitude lower efficiency-to-cost ratio. While several concepts were offered to harvest IR-sun radiation including antenna arrays and quantum dots, with their spectrally-broad absorption spectrum and the fabrication cost that has fallen precipitously, single-walled carbon nanotubes can pave a way to the development of indirect-type, cost-efficient photo-thermo-voltaic (PTV) cells.

Herein, we engineer and test two-terminal carbon nanotube photocells for the purpose of infrared photo-thermo-electric energy conversion and sensing. The photo-voltage and nonzero conversion efficiency were found to appear only for off-center illumination which can be explained within photo-generated heat flow model and not the contact effects. [2] Under incident optical powers of ca. 450 mW, the equivalent short-circuit current, $I_{SC,}$ and open-circuit voltage, $V_{OC,}$ stood at ca. 0.2 uA and ca. 0.5 mV, respectively. The cell prototypes yielded ~ 30 nW of electrical power that typically followed non-monotonic dependence on the incident light power given by $P_{\text{out max}} \sim P_{in}^{\beta}$, where $\beta = 1.08$. As the PTV cell can also utilized as IR-photosensor, its transient response was probed by carrying out off/on photocurrent tests at varied temperatures: 123, 253 & 300 ^{0}K. The photo-current, I_{ph} decayed with time as single exponential $I_{ph} \sim 1 - e^{-t/\tau}$ and the characteristic decay constant,τ was found to change linearly with I^{-1}_{dark} confirming that the transient respose is controlled by device circuitry and not heating/cooling processes. The concept might enable engineering and implementation of the carbon nanotube based PVT devices for application in heat recycling and self-powered infrared detectors.

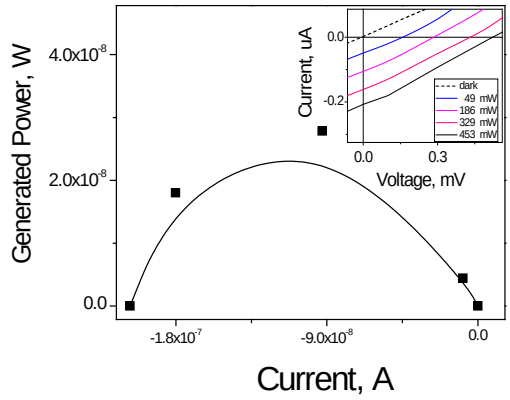

Keywords: infared, carbon, nanotubes, photovoltaic, sensors, cell.

Figure 1: Showing power vs. current characteristic of the PTV cell obtained at RT and incident power of ~ 450 mW. The inset shows I-Vs for different

References:

[1] S.M.Sze, "Semiconductor Devices", J.Willey and Sons, 2nd edition (2002)

[2] T. Hosseini, M. Omari. and N. Kouklin, Electr. Dev. Letters, 34 , 7 , 924-926 (2013)

Natural Biodefensive Nanoparticles for Pest Control in Soy Culture

A.L. Santos,[1*] V. Zucolotto,[1,2] B.T.R. Rhein,[1] I. Pezzopane,[1] G.Rosa[1]
[1]Nanomed Inc., São Carlos, Brazil
[2]University of São Paulo, Laboratory of Nanomedicine and Nanotoxicity, São Carlos, Brazil

Abstract: Nanomed Inc. has been developing a new methods for natural compounds controlled delivery system. A polymeric nanoparticle obtained via solvent evaporation is a new approach to delivery a natural and reactive compound to improve the treatment in soy culture, the most important culture in Brazil. This is a bioactivity essential oil against insects and other pests, flavoring agent used in cosmetic and food products however it was previously reported to have a skin- sensitizing ability and to cause allergic reactions (ATSUMI; FUJISAWA; TONOSAKI, 2005; MURRAY B. ISMAN, 2006). In spite of huge bioactivity, its reactivity and volatility reduce the action time. So, a controlled delivery system was developed, changing the surface area which may influence its toxicity. The nanoparticles cytotoxicity was evaluated in L929 fibroblasts, against a negative control and literature.
The enhancement of the natural active by encapsulation was able to protect it from oxidative degradation, and improve their fungicidal activity (GARG; SINGH, 2011).
We observe that these nanoparticles showed a similar behavior even in different delivery system (polymer). However with the concentration increase, there is the decrease of toxicity, with the higher viability in fibroblasts. Based on the different concetrations studies, it is possible to conclude that the cytotocity is not dose dependent. However, one notice the increase in the cellular apoptosis as the nanoparticle size decreases. So, the nanotoxicity is directly linked to the size of nanoparticle, and not related to the essential oil concentration.

Keywords: biodefensive, polymeric nanoparticles, natural-based material, cytotoxity, pest control, soy culture, agribusiness applications.

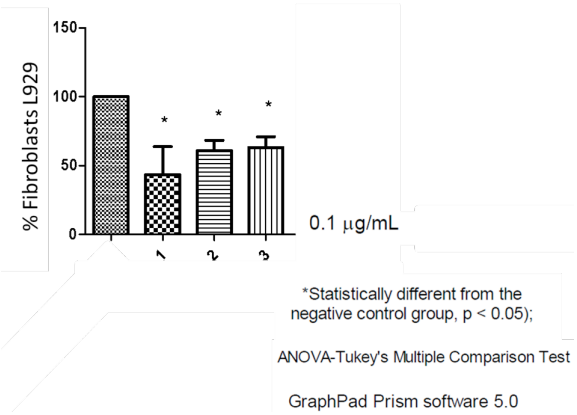

Figure 1: Figure of natural compound nanoparticles cytotoxicity in a different controlled delivery system, at 0.1 ppm concentrations. Samples: 1- PLA-natural compound 0.5%; 2- PCL- natural compound 1%; 3- PLA- natural compound 1%.

References:

ATSUMI, T.; FUJISAWA, S.; TONOSAKI, K. A comparative study of the antioxidant/prooxidant activities of eugenol and isoeugenol with various concentrations and oxidation conditions. **Toxicology in vitro**, v. 19, n. 8, p. 1025–33, dez. 2005.

GARG, A; SINGH, S. Enhancement in antifungal activity of eugenol in immunosuppressed rats through lipid nanocarriers. **Colloids and surfaces. B, Biointerfaces**, v. 87, n. 2, p. 280–8, 15 out. 2011.

MURRAY B. ISMAN, C. M. M. Pesticides based on plant essential oils: from traditional practice to commercialization. In: CARPINELLA, R. AND (Ed.). . **Naturally Occurring Bioactive Compounds**. [s.l.] Elsevier, 2006. p. 29–44.

Sol-Gel Production and Electrochemical Characterization of Free-Standing Metal Oxide/MWCNT Nanocomposite Anodes for Li-Ion Batteries

H. Köse, Ş. Karaal, A. O. Aydın, H. Akbulut
Sakarya University, 54187, Sakarya, Turkey

Abstract: Lithium ion batteries (LIBs) are one of the most promising candidates for electrochemical energy conversion and storage devices, in the scientific and industrial fields, with one of the best energy densities (Wang *et al.;* 2006). Zinc and tin dioxide based materials are being used as active anode materials for rechargeable lithium batteries, because the theoretical capacity of ZnO (978 $mAhg^{-1}$) and SnO_2 (1491 $mAhg^{-1}$) has been estimated to be superior to that of graphite (372 $mAhg^{-1}$) (Guler *et al.;* 2014, Ning *et al.;* 2008). High capacity anodes such as zinc and tin based usually suffer severe capacity fading, because of the quick aggregation of metal particles and the huge volume expansion during Li^+ insertion/extraction cycles (Huang *et al.*; 2011). To prevent the pulverization of the anodes and electrical detachment of active materials, MWCNT buckypaper substrates are considered as a buffer material during the battery applications (Guler *et al.;* 2014). In this work, ZnO/MWCNT and SnO_2/MWCNT buckypaper nanocomposite films were prepared as free-standing anode materials by sol–gel spin coating. Structural properties and electrochemical performances of metal oxides/MWCNT nanocomposite anodes were investigated and compared. As can be seen from Figure 1, it was aimed to accommodate the stresses arisen from the volume increase during charging process by using highly porous MWCNT network that coated with a thin layer of the metal oxides (MO). The structural properties of free-standing buckypaper composite film anodes were characterized by FEG-SEM (Field Emission Gun - Scanning Electron microscopy), TEM (Transmission Electron Microscopy), EDS (Energy Dispersive X-ray Spectroscopy) and XRD (X-ray Diffraction) tehcniques. Electrochemical performance tests, CV (Cyclic Voltammetry) and EIS (Electrochemical Impedance Spectroscopy) analyses of free-standing anodes of CR2016 type Li-ion batteries were also performed. The cells were charged and discharged at 25 °C between fixed voltage limits (2.5 V to 0.2 V).

Keywords: Li-ion battery applications, metal oxide/MWCNT nanocomposite anodes, sol-gel synthesis, spin coating method, structural and electrochemical characterization.

Figure 1: The illustration of the production of free-standing Metal Oxide/MWCNT anodes.

References:

Guler, M.O., Cetinkaya, T., Tocoglu, U., Akbulut, H. (2014), Electrochemical performance of MWCNT reinforced ZnO anodes for Li-ion batteries, *Microelectronic Eng.*, 118, 54–60.

Huang, X.H., Xia, X.H., Yuan, Y.F., Zhou, F. (2011), Porous ZnO nanosheets grown on copper substrates as anodes for lithium ion batteries, *Electrochim. Acta*, 56, 4960-4965.

Ning, Y., Jianhua, W., Yuzhong, G., Xiaolong, Z. (2008), SnO_2 Nanofibers Prepared by Sol-Gel Template Method , *Rare Metal Mater. Eng.*, 37, 694-696.

Wang, Y., Su, F., Lee, J.Y., Zhao, X.S. (2006), Crystalline Carbon Hollow Spheres, Crystalline Carbon−SnO_2 Hollow Spheres, and Crystalline SnO_2 Hollow Spheres: Synthesis and Performance in Reversible Li-Ion Storage, *Chem. Mater.*, 18, 1347-1353.

The Effect of Different Solvent Combination of $LiBF_4$ Electrolyte on Free-Standing SnO_2/MWCNT Nanocomposite Anode Capacity for Li-ion Batteries

Ş. Karaal, H. Köse, A. O. Aydın, H. Akbulut
Sakarya University, 54187, Sakarya, Turkey

Abstract: Owing to their high energy density, lithium-ion batteries are widely used in portable electronics (Xiang *et al.;* 2009). With a wide optical band gap (3.6 eV) tin dioxide is an n-type semiconductor material. For rechargeable lithium batteries, tin and tin oxide based materials are being used as active anode materials (Kose *et al.;* 2013). However, during Li^+ insertion/extraction cycles, anodes of such high capacity usually suffer severe capacity fading resulting from both the huge volume change and the quick aggregation of tin particles (Zhang *et al.;* 2009). MWCNT buckypaper substrates are considered as a buffer material during the battery applications in order to prevent the pulverization of the anodes and electrical detachment of active materials (Kose *et al.;* 2013). For commercial Li-ion cells, the typical non-aqueous electrolyte is a solution of $LiPF_6$ in linear and cyclic carbonates such as dimethyl carbonate and ethylene carbonate, respectively (Kerr *et al.;* 2003). Compared with $LiPF_6$, $LiBF_4$ has some advantages such as better thermal stability and lower sensitivity toward environmental moisture and its solution provides lower charge-transfer resistance, especially at low temperatures (Zhang *et al.;* 2006).In this work, free-standing SnO_2/MWCNT nanocomposite was used as anode, metallic Li as cathode and 1 molal $LiBF_4$ solution as electrolyte. It was aimed to determine the optimum ratio of Ethylene Carbonate (EC):Dimethyl Carbonate (DMC) solvents in 1 molal $LiBF_4$ electrolyte solutions for high capacity SnO_2/MWCNT buckypaper anode. Different EC : DMC (2:1, 1:1 and 1:2) solvent combinations were prepared in a glove box. For these electrolyte solutions, conductivity tests were applied. Structural properties and electrochemical performances of SnO_2/MWCNT nanocomposite anodes prepared by sol–gel spin coating method (Figure 1) were investigated. The structural properties of free-standing buckypaper composite anode was characterized by SEM (Scanning Electron microscopy), TEM (Transmission Electron Microscopy) EDS (Energy Dispersive X-ray Spectroscopy) and XRD (X-ray Diffraction) tehcniques. Electrochemical performance tests, CV (Cyclic Voltammetry) and EIS (Electrochemical Impedance Spectroscopy) analyses of free-standing anodes of CR2016 type Li-ion batteries were also performed. The cells were charged and discharged at 25 °C between fixed voltage limits (2.5 V to 0.2 V).

Keywords: Li-ion battery applications, $LiBF_4$ electrolyte, ethylene carbonate, dimethyl carbonate, SnO_2/MWCNT nanocomposite anodes, sol-gel synthesis, spin coating method, structural and electrochemical characterization.

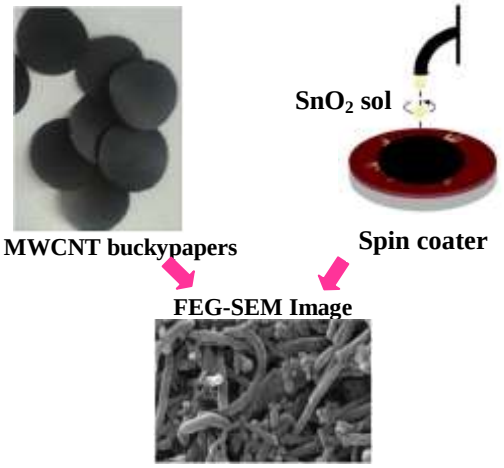

Figure 1: The representation of the production of free-standing SnO_2/MWCNT anodes.

References:

Kose, H., Aydin, A.O., Akbulut, H., (2013), Sol–gel preparation and electrochemical characterization of SnO_2/MWCNTs anode materials for Li-ion batteries, Applied Surface Science, 275, 160-167.

Sloop, S.E., Kerr, J.B., Kinoshita, K., (2003), The role of Li-ion battery electrolyte reactivity in performance decline and self-discharge, Journal of Power Sources, 119–121, 330-337.

Xiang, H.F., Wang, H., Chen, C.H., Ge, X.W., Guo, S., Sun, J.H., Hu, W.Q., (2009), Thermal stability of $LiPF_6$-based electrolyte and effect of contact with various delithiated cathodes of Li-ion batteries, Journal of Power Sources, 191, 575–581.

Zhang, H.-X., Feng, C., Zhai, Y.-C., Jiang, K.-L., Li, Q.-Q., Fan, S.-S., (2009), Cross-Stacked Carbon Nanotube Sheets Uniformly Loaded with SnO_2 Nanoparticles: A Novel Binder-Free and High-Capacity Anode Material for Lithium-Ion Batteries, Adv. Mater., 21, 2299-2304.

Zhang, S.S., Xu, K., Jow, T.R., (2006), Enhanced performance of Li-ion cell with $LiBF_4$-PC based electrolyte by addition of small amount of LiBOB, Journal of Power Sources, 156, 629-633.

Photocatalytic Activities of ZnO and ZnO/ZnS Synthesized by Microwave-Hydrothermal Method

N. Güy,[1*] Şeref Durmuş[1], M. Özacar,[1]
[1]Sakarya University, Department of Chemistry, Sakarya, Turkey

Abstract: Because of the diffussing of toxic and coloured wastewater into water sources, dyes have a bad effect on the nature of water like inhibitting sunlight penetration and reducing photosynthetic reaction. (Hu *et al*.; 2011). The techniques which are used for the treatment of dye waste effluents are usuallyare usually inefficient, non-destructive and costly. (Jia *et al*.; 2013). Heterogeneous semiconductor photocatalysts such as ZnO have an important role for the removal of dye pollutants from water. ZnO semiconductor has a wide bandgap energy of 3.37 eV and a relatively large exciton binding Energy (60 meV), thus can absorb only UV light with the wavelength equal to or less than 385 nm. But solar spectra contain only approximately 3%–5% UV light; therefore, the great mass of solar photons is useless for ZnO photocatalyst, which greatly limits its environmental applications (Ma *et al*.; 2011). The photocatalytic performance of ZnO can be improved by modification due to inhibit recombination of photogenerated electron-hole pairs. The band gap of ZnS (3.68 eV) is larger than that of ZnO, experimental results have demonstrated that the combination of these two wide bandgap semiconductors could yield a novel composite with the photo excitation threshold energy lower than those of the individual components (Ma *et al*.; 2013). In the present study, ZnO/ZnS nano photocatalysts were synthesized by microwave-hydrothermal method using different precursors as Sulfur source. The prepared photocatalysts were characterized by X-ray diffraction (XRD), field emission scanning electron microscopy (FESEM) and UV–visible (UV–vis). The photocatalytic activities samples and undoped ZnO have been studied for the degradation of dye, and have also been compared with together.
.

Keywords: Synthesis, photocatalyst, ZnO/ZnS, degradation

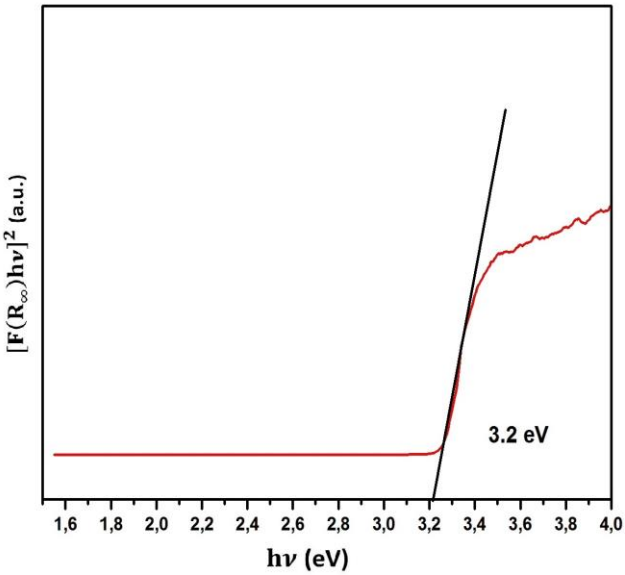

Figure 1: Kubelka-Munk transformed reflectance spectra of ZnO/ZnS

References:

Hu, Y., Qian, H., Liu, Y., Du, G., Zhang, F., Wang, L., Hu, X.(2011), A microwave-assisted rapid route to synthesize ZnO/ZnS core–Shell nanostructures via controllable surface sulfidation of ZnO nanorods, *CrystEngComm.*, 13, 3438-3443.

Jia, W., Jia, B., Qu, F., Wu, X., (2013), Towards a highly efficient simulated sunlight driven photocatalyst: a case of heterostructured ZnO/ZnS hybrid structure, *Dalton Trans*., 42, 14178-14187.

Ma, H., Han, J., Fu, Y., Song, Y., Yu, C., Dong, X., (2011), Synthesis of visible light responsive ZnO–ZnS/C photocatalyst by simple carbothermal reduction, *Applied Catalysis B: Environmental* 102, 417–423.

Ma, H., Cheng, X., Ma, C., Dong, X., Zhang, X., Xue, M., Zhang, X., Fu, Y., (2013), Synthesis, Characterization, and Photocatalytic Activity of N-Doped ZnO/ZnS Composites**,** *International Journal of Photoenergy*, 2013, 8 pages.

Polystyrene Micro/Nanofibers and its Application in the Removal of Crude Oil Spills

M. Alazab Alnaqbi[1,*], Afra Al Blooshi[1], Yaser. Greish[1], and Mahmoud Mohsin[2]
[1]Department of Chemistry, United Arab Emirates University, Al Ain, United Arab Emirates
[2]Department of Chemistry, University of Sharjah, Sharjah, United Arab Emirates

Abstract: Water pollution by crude oil has major environmental impact worldwide (M. Al-Azab *et al*. 2005). The great concern of the global community on the unfavorable and longstanding effects of spilt oil on ecosystems, created a vital need to develop materials for effective oil spill clean-ups (Xia, Y. Q *et al*. 2010). This work aimed to study the effectiveness and applications of PS polymer in clean-up of crude oil from oil spills.

Molecular weights of the fibrous polystyrene precursors, were in the range of 100,000 – 350,000 Dalton. Fibers were used for the removal of crude oil spills in seawater. Due to the hydrophobic nature of both the fibers and the crude oil, the later was instantly absorbed onto the fibers achieving a maximum sorption capacity of 220 g of crude oil per each gram of fiber.

Nano/Microfibers of polystyrene was prepared by electrospinning technique (Haitao Zhu *et al*. 2011). Fibers with a size range of 500 nm- 8 μm in diameter and below 100 m^2/g in surface area were prepared after a thorough optimization of the electrospinning process. Fibers prepared were tested for their oil absorption efficiency as a function of absorbent weight, time of absorption, and initial concentration of the polymer solution prior its conversion to fibers. Results showed an initial sorption capacity of a range of 60-200 g/g with microfibers prepared from 20% PS solution.

The surface area of the produced fibers varied based on fiber size distribution, which depends on variations in the electrospinning parameters. Hence, optimizations of the process were studied to achieve consistency in the fiber size distribution, and the surface area of the fibers as well. Results showed the importance of the high surface area and interconnectivity of the porosities within the PS microfibrous sorbent for the removal of the oil, making the microfibrous PS sorbents an excellent candidate for crude oil spill cleanup.

Keywords: nanofibers, polystyrene, crude oil, electrospinning

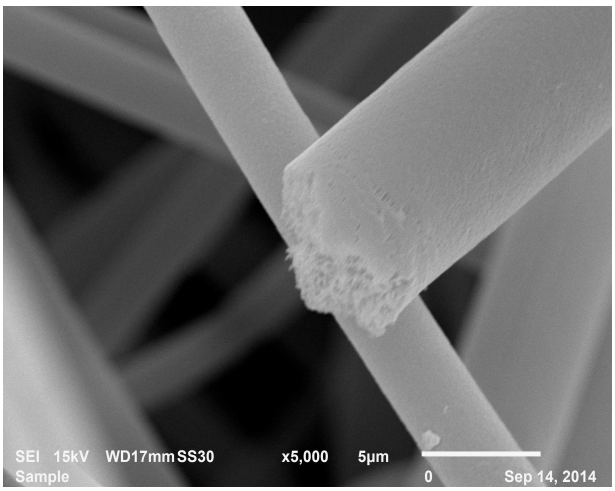

Figure 1: SEM image for electrospun PS fibers with mesoporosity and different size distribution. Polystyrene was dissolved in the proper solvent forming solutions of 20, 30, and 40 wt%. Electrospinning process conditions were optimized at a voltage of 20 kV, a feeding rate of 10 ml/hr, and a distance of 15 cm. Due to the high viscosity of the crude oil, their flow within the fibrous sorbent during the process of removal will be limited and requires macroporosity for a more efficient sorption and impregnation within the fibrous sorbent. The produced microfibers contained macroporosity by virtue of the interlocking between the fibers within the electrospun fibrous mesh.

References:

M. Al-Azab, E. El-Shorbagy and S. Al-Ghais (2005). Proceedings of the International Conference on "Oil Pollution and it Environmental Impact in the Arabian Gulf Region". Elsevier, ISBN: 978-0-444-52060-9.

Xia, Y. Q.; Boufadel, M. C. (2010) Lessons from the Exxon Valdez oil spill disaster in Alaska. *Disaster Adv*, 3 (4), 270−273

Haitao Zhu, Shanshan Qiu, Wei Jiang, Daxiong Wu, and Canying Zhang (2011), Evaluation of Electrospun Polyvinyl Chloride/Polystyrene Fibers As Sorbent Materials for Oil Spill Cleanup, *Environ. Sci. Technol*, 45, 4527–4531

Effects of biopolymer nano coils on sand dune stabilization and dust controlling

M. Aghaei Moghadam[1]*, K. Zangeneh[2]

[1] Biopolynet Inc, Fredericton, NB, Canada

[2] Biopolynet Inc, Fredericton, NB, Canada

*Email: mostafa@biopolynet.com

Abstract

Despite the large history and popularity of sand/dune stabilization in exploratory research, a unique method with large-scale applications has yet to be realized. The main impediments reside in the methods of the stabilizations currently in use, at the moment (a) no specific technology is available, (b) a particular stabilizer is necessary for each specific condition, (c) most products just stabilize the surface of sand dunes and (d) most applications require a long time to be fixed in large quantities in a predetermined and controllable fashion. Designing biopolymeric networks with controlled size and desirable properties is the best way to fix sand dune and dust. Thus we hereby describe a novel view and simple method to stabilize sand/dunes by designing a novel aqueous biopolymer coils system to spray on the sand/dune surface in order to make a network with sand/dune agents by penetration of aqueous biopolymer into the sand dune.

Carboxymethyl-nanocellulose:a versatile raw-material in coating industry

A. Reis,[1,*] R. Duarte,[1] J. Tedim,[2] A. Caetano,[2] A.P. Mendes de Sousa,[3] J. Ataíde,[3] D. Evtuguin[1]
[1]CICECO-Aveiro Institute of Materials, Department of Chemistry, University of Aveiro, 3810-193 Portugal
[2]CICECO-Aveiro Institute of Materials, Department of Materials and Ceramic Engineering, University of Aveiro, 3810-193 Portugal
[3]RAIZ, grupo PORTUCEL/SOPORCEL, 3801-501 Eixo, Portugal

Abstract: Cellulose is the most abundant polysaccharide and widespread biopolymer in nature. For this reason, cellulose and its derivatives are very attractive for the manufacture of sustainable biobased materials. Unlike cellulose, functionalized cellulose with carboxymethyl groups (CMC) is water soluble exhibiting a multitude of applications as gelling agent in food industry, as paint thickeners in coating industry and film packaging in food and paper industry (Klemm et al., 2005). Aside from its mechanical and water retention properties, the biocompatibility exhibited makes CMC a promising option as a support of biomolecules with chemical and biological activity for the development of biosensors and wound dressings (Carlsson et al., 2014). However, commercially available CMC powders have high degrees of substitution (DS) ranging between 0.5-1.2 and a high density of anionic charged groups by the presence of surface carboxylic groups. The high surface negative charge has a deleterious impact on the stability of the incorporated biomolecules (Carlsson et al., 2014) and even affecting the release behavior of incorporated drug (Valo et al., 2013).

In this study, we have synthetized CMC with various degrees of substitution (DS) using environment-friendly aqueous conditions. The functionalized CMC pulp with DS<0.2 was submitted to ultrahomogenization resulting in high quality carboxymethyl nanocellulose (NC) suspensions (over 90% of nanofibrils) through a energy-efficient process(energy reduction of >60% compared to unmodified NC). The carboxymethyl-NC films prepared by solvent casting exhibited improved optical and morphological properties whilst retaining the mechanical properties in the temperature range (-50 to 200°C) studied. Preliminary results obtained by electrochemical impedance spectroscopy (EIS) using functionalized nanocellulose in solution and as additives to protective coatings have shown improved anti-corrosion performance in coated substrates. The increased hydrophobicity and zeta potential of prepared CMC suspensions reveal great potential for industrial coating and will be further explored on the adsorption of molecules for biomedicine applications.

Keywords: carboxymethyl cellulose, transparent films, corrosion inhibitors, biomedical applications.

References:

Klemm, D., Heublein, B., Fink, H.P., Bohn, A. (2005) Cellulose: fascinating biopolymer and sustainable raw material, *Angew. Chem. Int.*, 44, 3358-3393.

Valo, H., Arola, S., Laaksonen, P., Torkkeli, M., Peltonen, L., Linder, M.B., Serimaa, R., Kuga, S., Hirvonen, J., Laaksonen, T. (2013), Drug release from nanoparticles embedded in four different nanofibrilar cellulose aerogels, *Eur. J. Pharm Sci.*, 50, 69-77.

Carlsson, D.O., Hua, K., Forsgren, J., Mihranyan, A. (2014), Aspirin degradation in surface-charged TEMPO-oxidized mesoporous crystalline nanocellulose. *Int. J. Pharma*. 461, 74-81.

Acknowledgements
This work was developed in CICECO-Aveiro Institute of Materials and is funded by ERDF Funds through Operational Competitiveness Programme – COMPETE in the frame of the project NMC– QREN 34169.

Graphene Reinforced Concrete

M.F. Craciun, D. Dimov

University of Exeter, Exeter, Devon, United Kingdom

Abstract:
This work presents the revolutionary idea of bridging the international research on nanoscience with traditional construction material concrete. The aim of the project is to introduce graphene - an one atom thick layer of graphite with two-dimensional properties, within the chemical matrix of cement. The stand-out mechanical properties of graphene such as very high ultimate tensile strength and retaining initial size after strain make it suitable for applications in the construction industry. There are two main liquid exfoliation methods of producing surfactant-stabilized graphene dispersions in aqueous environment [2],[3]. The first one uses sonication energy principles for breaking down layers of graphite and the addition of surfactant (Sodium Cholate) preserves all of their properties in water [3]. The second uses high-shear exfoliation machine which uses laws of turbulent forces to achieve even better quaility flakes with more consistent rate of dispersion [2]. The resultant solution from 48h of sonication is mixed with Ordinary Portland Cement (OPC), sand and aggregate to prepare standard 10x10x10cm concrete cubes for testing compressive strength. The results show that the addition of only 2.1mg/ml of graphene flakes increase the compressive strength by 9.8% when compared to cubes mixed with normal tap water, after 28days of curing time. The outcomes of the experiments prove the hypothesis that wonder nanomaterial alter the hydration crystals of the cementitious paste and the enhanced hydration reaction in the curing period of the concrete leads to many improvements [1]. The graphene reinforced concrete can revolutionize the construction industry and change the face of future infrastructure by introducing a very environmental friendly product.

Keywords: graphene, concrete, liquid exfoliation, cement, hydration reaction, compressive strength

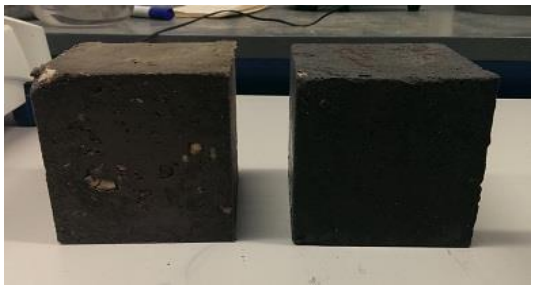

Figure 1: Two cubes above show the comparison between normal (tap water) concrete on the left and graphene reinforced one on the right. The addition of nanomaterials enhances the main chemical reaction during the hardening of concrete and this leads to increased compressive strength of the construction material.

References:

[1] A. Sedaghat, M. K.Ram, A. Zayed, R. Kamal, N. Shanahan, "Investigation of Physical Properties of Graphene-Cement Composite for Structural Applications," *Open Journal of Composite Materials*, 2014, 4, 12-21

[2] K. P. Paton, "Scalable production of large quantities of defect-free few-layer graphene by shear exfoliation in liquids*", Nature Materials*, April 2014, 10.1038/NMAT3944

[3] M. Lotya, P. J. King, U. Khan, S. De, J. N. Coleman, "High-Concentration, Surfactant-Stabilized Graphene Dispersions", *ACSNano*, 2010, Vol.4, No.6, 3155-3162

Quantum Dot Sensitized Solar Cells with Cuprous Sulfide Counter Electrode

Nuno Marques Ferreira, César Bernardo, Isabel Moura, Paulo J. G. Coutinho, Anabela G. Rolo, Mikhail Vasilevskiy, M. Pastor, F. Fernandes, V. Teixeira, J.O.Carneiro, Anura Samantilleke*
Centro de Física, Universidade do Minho, Campus de Gualtar, 4710-057, Braga, Portugal

Abstract: Although, solution processing is a promising route for the realization of low-cost, large-area devices with short energy payback time and high specific power, low-temperature fabrication conditions and good atmospheric stability while maintaining a high efficiency remains a major technical challenge. However, the recent report of a certified efficiency of 8.55% for a ZnO/PbS Quantum dot (QD) solar cell (SC) achieved by engineering the band alignment of the QD layers through the use of different ligand treatments promises the possibility of newapproaches towards the goal of high-performance air-stable solar cells compatible with simple solution processes (Chuang et al, 2014). CdSe QDs with an absorption onset in the red or near infrared are equally promising (Kamat, 2008). In this work, QDSCs based on a mesoporous structure of TiO2 and a polysulfide redox electrolyte, were prepared by adsorption of colloidal CdSe QD absorbers onto the photoanode, with and without linkers. CdSe/ZnS QDs were synthesized within aqueous pools of reverse micelles, based on standard wet chemistry methods, while alkylphosphine oxide (TOPO) functionalized CdSe QDs were prepared by reactions of organo-metallic precursors at high temperature. A chlorine surface treatment performed on TiO2 prior to sensitisation improved QD adsorption on the photoanode. An electrochemically deposited Cu2S/conducting glass (CTO), which has a higher tolerance to polysulfide electrolyte, was used as the counter electrode. The Cu2S film, composed of interconnected nanoflakes, showed good catalytic activity with the best SCs (effective area 0.16 cm2) showing up to 2.13% conversion efficiency under AM1.5 illumination. The photovoltaic characteristic of the solar cells was measured using a calibrated solar simulator with 100 mW/cm^2 irradiation (AM 1.5). The colloidal QDSC performance was primarily limited by a low fill factor of 0.45, which is believed to arise from charge transfer of photogenerated electrons to the aqueous electrolyte. This work was supported by the MATEPRO - NORTE-07-0124-FEDER-000037 and the European Commission through NanoCIS project (FP7/PIRSESGA-2010-269279), both of which are gratefully acknowledged.

Keywords: CdSe, quantum dot, solar cell, TOPO, Cu2S

Presenting author's email: anura@fisica.uminho.pt

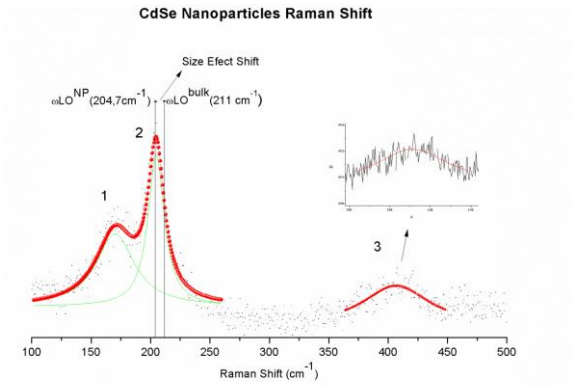

Figure 1: Ressonance Raman spectrum of CdSe nanoparticles (NP) deposited on glass, excited at laser wavelength 514 nm. (1)-TO (170.3 cm-1); (2)-LO (204.7 cm-1); (3)-2LO (408.8 cm-1).
Laser intensity of <9.32 kW/cm2 was used to minimize a possible local heating. Red and green depict the spectral deconvolution to the vibrational modes.
The inset shows the amplified Raman shift' at (3). LO phonon mode shift and asymmetric broadenings towards low-frequency (2,3) in comparision with Bulk CdSe are explained by the contribution of different phonon modes and are an indication of the phonon confinement effect, which is a consequence of the nano size of the CdSe particles. The presence of transverse modes at (1) is an evidence of the non spherical symmetry of the NP's.

References:

[1]..Prashant V. Kamat, (2008) Quantum Dot Solar Cells. Semiconductor Nanocrystals as Light Harvesters, *J. Phys. Chem. C*, *112* (48), 18737–18753
[3]. Chia-Hao M. Chuang, Patrick R. Brown, Vladimir Bulović and Moungi G. Bawendi (2014) Improved performance and stability in quantum dot solar cells through band alignment engineering, Nature Materials, **13**,796–801

Reduced graphene oxide on TiO_2 nanorods and nanotubes photo-anode for solar hydrogen evolution

Hyun Kim,[1] Bee Lyong Yang[1*]
[1]Kumoh National Institute of Technology, Laboratory of nanoelectric materials, Geongbuk, Korea

Abstract: The solar hydrogen evolution process via water splitting is a carbon free technology for next generation. Many reseachers and energy departments are expecting that minimum efficiency for commercialization is about ~10% of solar to hydrogen conversion efficiency (STH). However the world STH efficiency doesn't reach yet. Splitting water into hydrogen and oxygen has been occured by stages, i) absorption of light, ii) electron-hole excitation, iii) charge transfer to reactive sites, iv) redox reaction. Among these stages, charge transfer stage is most important to lead the redox reaction of water. Graphene has been considered a new approach to improve the charge transfer rate without direct or indirect recombination. In this work, we demonstrated that improved charge transfer and collection in PEC system by using a reduced graphene oxide sheets. Reduced graphene oxide sheets were chemically synthesized by improved Hummer's method. TiO_2 nanotubes and nanorods were synthesized by anodizing and hydrothermal method respectively. Subsequently, These TiO_2 photo-anodes were directly immersed into solution involving reduced graphene oxide. After several minutes in immersed state, the graphene oxide on TiO_2 nanotubes were chemically reduced by adding hydrazine solution as a reducing agent. The microstructural features of RGO/TiO_2 nanotubes photo-anode were investigated by FE-SEM, TEM, XRD, Raman spectroscopy. Furthermore solar hydrogen production test was characterized in the PEC cells Consequently graphene decorated TiO_2 nanotubes and nanorods were revealed superior photocatalytic activity because the graphene sheets led to increase the mobility of charge carriers and recombination time.

Keywords: Reduced graphene oxide(RGO), Titanium dioxide(TiO_2), Solar hydrogen evolution

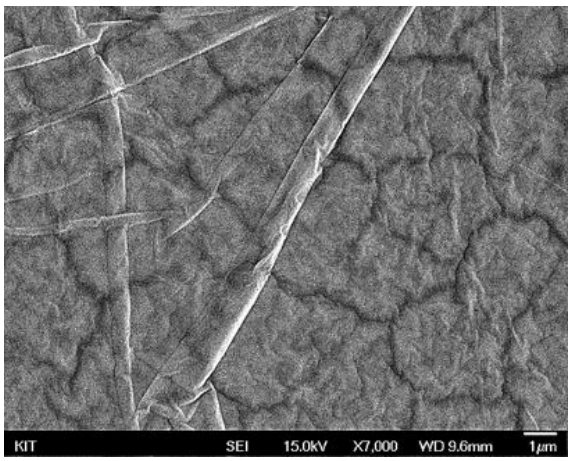

Figure 1: FE-SEM image of a graphene oxide coated TiO_2 nanorods.

References:

Ma, Y., Wang, X., Jia, Y., Chen, X., Han, H., Li, C. (2014) Titanium dioxide-based nanomaterials for photocatalytic fuel generations, Chem. Rev., 114, 9987-10043.

Te-Fu, Y., Jaroslav, C., Chih-Yung, C., Ching, C., Hsisheng, T. (2013) Roles of graphene oxide in photocatalytic water splitting, Mater. Today., 16, 78-84.

Daniela C, M., Dmitry V, K., Jacob M, B., Alexander, S., Zhengzong, S., Alexander, S., Lawrence B, A., Wei, L., James M, T. (2010) Improved synthesis of graphene oxide, ACS. NANO., 4, 4806-4814.

Silicon Nanowire as an Effective Absorber for Solar Cell Application: Fabrication and Numerical Simulation

M. K. Hossain,[1,*] B. Salhi,[1,*] A. W. Mukhaimer,[1] and F. A. Al-Sulaiman[1,2]
[1]Center of Research Excellence in Renewable Energy (CORERE), King Fahd University of Petroleum and Minerals (KFUPM), Dhahran 31261, Dhahran, Kingdom of Saudi Arabia
[2]Departmentof Mchnical Engineering, King Fahd University of Petroleum and Minerals (KFUPM), Dhahran 31261, Dhahran, Kingdom of Saudi Arabia

Abstract: Silicon nanowires (Si-NWs) have been considered widely as a perfect light absorber with strong evidence of enhanced optical functionalities. Here we report finite-difference time-domain simulations for Si-NWs to elucidate the key factors that determine enhanced light absorption, energy flow behavior, electric field profile and exciton generation rate distribution. To avoid further complexity, a single Si-NW of cylindrical shape was modelled on c-Si and optimized to elucidate the aforementioned characteristics. Light absorption and energy flow distribution confirmed that Si-NW facilitates to confine photon absorption of several orders of enhancement whereas the energy flow is also distributed along the wire itself. With reference to electric field and exciton generation distribution it was revealed that Si-NW possesses the sites of strongest field distributions compared to those of flat silicon wafer. To realize the potential of Si-NWs-based thin film solar cell, a simple process was adopted to acquire vertically aligned Si-NWs grown on c-Si wafer. Further topographic characterizations were conducted through SEM and TEM-coupled EDS.

Keywords: Fabrication, FDTD simulation, photovoltaic solar cell, Silicon nanowires.

One dimensional Si nanostructures, such as, Si nanowires (Si-NWs) have been emerged as an extremely attractive candidate due to their unique properties. Apart from low-cost, Si-NWs have strong optical absorption in the solar spectrum, i.e., less than 1% equivalent of Si materials in Si-NWs can achieve the same amount of absorption absorbed by traditional planar wafer-based PV devices. Si-NWs-based solar cells with radial p-n junctions offer a short collection length for charge carriers, thus allowing the use of lower-quality Si materials. Si-NWs can be produced with excellent electrical characteristics. These advantages may substantially reduce the production cost of Si-NW-based solar cells while retaining efficiencies competitive with planar multicrystalline Si solar cells.

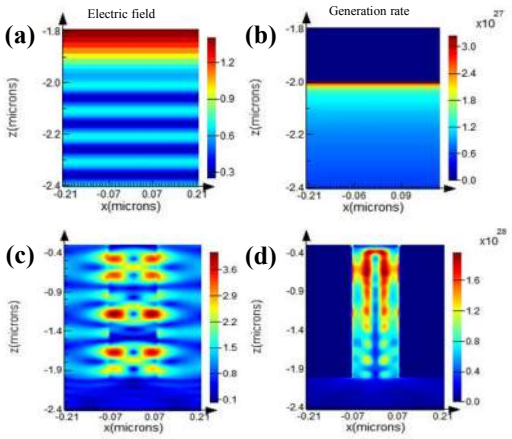

Fig. 1 Electric field and generation rate profile at 740 nm wavelength. (a) Fabry-Perot mode like electric field distribution in c-Si slab, (b) generation rate distribution in c-Si slab, (c) confined and enhanced electric field distribution in Si-NW on c-Si slab and (d) confined exciton generation rate distribution along the Si-NW length.

Vertically aligned Si-NWs were fabricated on c-Si wafer. The process was consisted of four simple steps, *viz.* i) ultrathin layer of Au coating on c-Si wafer, ii) sintering to turn the film into Au nanoparticles, ii) CVD to grow Au nanoparticles-assisted Si-NWs and iv) removal of Au nanoparticles. SEM and TEM measurements confirmed a variety of lengths (eg. few microns) and diameters (eg. 50 to 200 nm) of Si-NWs.

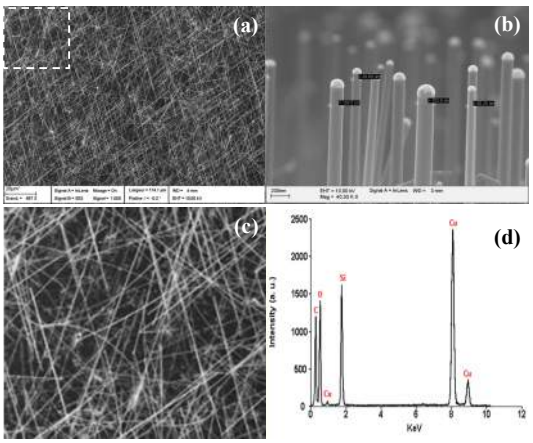

Fig. 2 SEM micrographs. (a) wide view of as-fabricated Si-NWs on c-Si wafer, (b) close-view of individual as-fabricated Si-NWs showing different dimensions in length and diameter, (c) Magnified images of the small area marked by white square in Fig. 2a and (d) TEM-coupled EDS to confirm the elemental composition of as-fabricated Si-NWs on c-Si wafer.

Details will be presented and explained in full report.

Acknowledgement: The authors are thankful to Center of Research Excellence in Renewable Energy (CoRERE), King Fahd University of Petroleum and Minerals, KSA.

Environmentally Friendly Design of Tailor-Made Nano-porous Polymeric Gas Adsorbents

Worood A. El-Mehalmey*, [1] Tarek Madkour[1] and Rasha A. Azzam[2]
[1]*Department of Chemistry, The American University in Cairo, New Cairo, Egypt*
[2]*Department of Chemistry, Helwan University, Ain-Helwan, Cairo, Egypt*

Abstract: More than 80% of the worldwide commercial energy supply is based on fossil fuels. The heavy use of fossil fuels as energy source has led to two major drawbacks. The first is environmentally related problem due to the large amounts of greenhouse gas (GHG) emissions, especially carbon dioxide (CO_2) whereas the second problem is related to the continual depletion of the fossil fuel resources. Eliminating the dependency on fossil fuel as a source of energy and searching for alternative sources for energy use such as hydrogen is, therefore, a crucial step. Conventionally, gases of a natural gas mix are separated using cryogenic distillation, which is an energy intensive process as well as a damaging one to the environment since it involves the consumption of large amount of fossil fuel to generate the required energy for the liquefaction and distillation processes. Hence, there is an urgent need for gas separation using a novel cost-effective material that consumes lower energy.(McKeown, Budd, & Book, 2007; Xu et al., 2014) A range of nanoporous polyimide polymers were synthesized using a two-step poly-condensation reactions as shown in Figure 1 of bis (carboxylic anhydride) with various aromatic diamines designed to investigate their effect on both the pore sizes and pore size distribution for gas storage application. This reaction ended with the formation of polymers of intrinsic micro-porosity (PIM), which are known to comprise rigid backbone due to their lack of rotational freedom along the polymeric backbone.(McKeown & Budd, 2010) The polymers exhibited high surface area as determined by nitrogen adsorption and high thermal stability as determined by TGA. The high surface area was further validated using molecular simulation techniques. Structural modifications of the diamines have resulted into a variety of nano-porous polymeric structures. The chemical structures were confirmed using FTIR, NMR and GPC techniques. BET isotherms of the resultant polymers were carried out to evaluate their physical characteristics. The results showed that the fractional free volume and the Connolly surface of the PIMs had greater values resulting from the inability of the rigid and contorted structures of the PIMs to pack space efficiently and thus creating interconnected nano-channels throughout the polymeric structures as shown in Figure 2.

Keywords: Carbon dioxide, Hydrogen, Polymers of Intrinsic Micro-porosity (PIMs), Two-step poly-condensation, interconnected nano-channels, gas adsorbents.

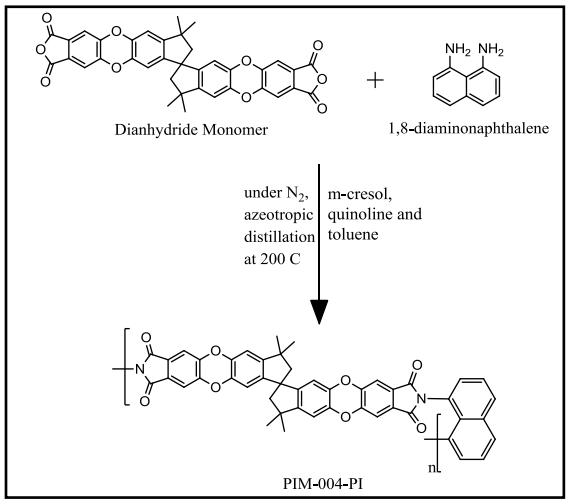

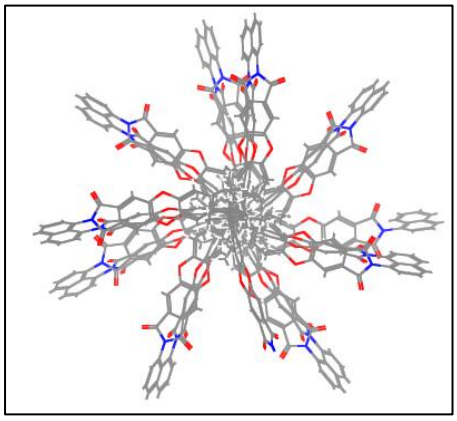

Figure 1 Synthesis of Nano-Porous Polyimide using Two-Step Poly-condensation.

Figure 2 PIM-004-PI Porous Structure.

References:

McKeown, N. B., & Budd, P. M. (2010). Exploitation of intrinsic microporosity in polymer-based materials. *Macromolecules*,*43*,5163–5176. doi:10.1021/ma1006396

McKeown, N. B., Budd, P. M., & Book, D. (2007). Microporous polymers as potential hydrogen storage materials. *Macromolecular Rapid Communications*, *28*, 995–1002. doi:10.1002/marc.200700054

Xu, G., Liang, F., Yang, Y., Hu, Y., Zhang, K., & Liu, W. (2014). An improved CO2 separation and purification system based on cryogenic separation and distillation theory. *Energies*, *7*, 3484–3502. doi:10.3390/en7053484

Silica-based nanocoating and LDHs sensors for enhancement of paperboard barrier properties

V. M. Dias[1*], A. Kuznetsova[2], I. Portugal[1], J. Tedim[2], A. A. Yaremchenko[2], D. V. Evtuguin[1]
[1]CICECO - Aveiro Institute of Materials, Department of Chemistry, University of Aveiro, Aveiro, Portugal
[2]CICECO - Aveiro Institute of Materials, Department of Materials and Ceramic Engineering, University of Aveiro, Aveiro, Portugal *e-mail: vania.dias09@gmail.com

Abstract: Conventional solutions to enhance paperboard barrier properties for packaging are limited essentially to film coating by synthetic polymers that hinder end-of-life disposal or recycling (Han *et al.*, 2010). Sol-gel methods are proven and convenient for organic-silica nanocoating since silica particles are generated *in situ* and randomly dispersed on the paper surface thus forming an impermeable interface between three-dimensional silica network and cellulose fibers (Han *et al.*, 2010; Sequeira *et al.*, 2007) Tetraethyl orthosilicate (TEOS) is often used as silica precursor, individually or mixed with other alkoxide-derived precursors. For instance, dimethyldiethoxysilane (DEDMS), 3-aminopropyltriethoxysilane (APTES) and octyltriethoxysilane (OTES) can be used to improve barrier properties due to their polarity. Similarly, Zn(2)-Al-NO_3 type layered double hydroxides (LDHs) can be added to the formulation and used as anion/water sensors (Tedim *et al.*, 2011). The silica-coated paperboard were characterized by scanning electron microscopy (SEM-EDS). Water vapor transmission rate (WVTR) was measured by the "desiccant method" (ASTM E 96-95, 1995) and oxygen permeation (J_{O_2}) measurements were performed using air in one side of paperboard and nitrogen flow on the other side and measuring p(O_2) in the N_2 flow (Yaremchenko *et al.*, 2007).

Keywords: Nanocoating, paperboard, silica-based formulations, layered double hydroxides, sol-gel process, barrier properties.

SEM images (Figure 1) of paperboard transversal cuts (delimited by dashed lines) reveal the position of silicon (red areas) on the side where the formulation was applied (ca. 2 g/m^2). Silica (red color) remains mostly at the outer surface.

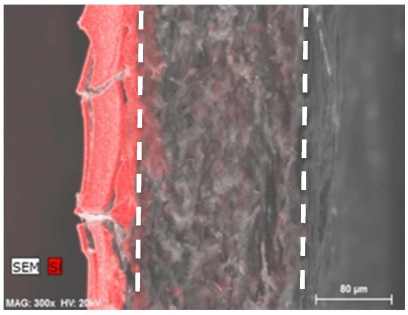

Figure 1: SEM image of TEOS_OTES formulation (2g/m^2) applied on the paperboard surface (left side).

Table 1. Barrier properties of paperboard before (uncoated) and after coating with various silica based formulations.

	WVTR (g m^{-2} day^{-1})	J_{O_2} (m^3 m^{-2} day^{-1})
Uncoated	548.83 ± 21.05	1.512
TEOS	300.20 ± 4.87	0.677
TEOS_LDHs	269.59 ± 3.25	1.037
TEOS_DEDMS	230.98 ± 3.33	0.562
TEOS_DEDMS_LDHs	199.25 ± 2.98	0.936
TEOS_APTES	221.96 ± 4.04	0.490
TEOS_APTES_LDHs	132.35 ± 2.95	0.778
TEOS_OTES	225.60 ± 3.54	2.578
TEOS_OTES_LDHs	131.37 ± 2.90	1.915

Generaly the incorporation of a secondary silica precursor improves barrier properties (WVTR and J_{O_2} decrease) (Table 1). For example, in comparison with the uncoated the TEOS_APTES coating decreased WVTR approximately 60% and J_{O_2} about 67%. The incorporation of LDHs caused an increase in J_{O_2} (ca. 60%) and diminished WVTR (ca. 10-40%) when compared with initial formulations. The best results were obtained with the formulation TEOS_APTES. Considering the anionexchange properties of LDHs they can act as nanosensors but also as water scavengers.

Conclusion: Silica coated paperboards exhibit good barrier properties when mixed silica alkoxide precursors are used. The incorporation of LDHs is very promising.

References:

Han, J., Salmieri, S., Le Tien, C., Lacroix, M. (2010), *J. Agric. Food Chem.*, 58, 3125–3131.

Sequeira, S., Evtuguin, D. V., Portugal, I., Esculcas, A. P. (2007), *Mater. Sci. Eng. C*, 27, 172–179.

Tedim, J., Kuznetsova, A., Salak, A. N., Montemor,F., Snihirova, D., Pilz, M., Zheludkevich, M. L., Ferreira, M.G.S. (2011), *Corros Sci*, 55, 1-4.

ASTM E 96-95, (1995) Annual Books of ASTM Standards, 552, 785–792.

Yaremchenko, A. A., Kharton, V. V., Avdeev, M., Shaula, A. L., Marques, F. M. B. (2007). *Solid State Ionics* 178, 1205–1217.

This work was developed in the scope of the project CICECO-Aveiro Institute of Materials (Ref. FCT UID /CTM /50011/2013), financed by EU funds of FP7 program (FP7-NMP-2011-LARGE-5 - NanoBarrier). Authors also thank the Prado Karton SA for the paperboard substrates.